Universidade de Aveiro Departamento de Química
Ano 2017

Marcelo Morais Rodrigues de Melo

VALORIZAÇÃO DE BIOMASSA VEGETAL ATRAVÉS DE EXTRAÇÃO COM CO_2 SUPERCRÍTICO: DO LABORATÓRIO À EXPLORAÇÃO

VALORIZATION OF VEGETAL BIOMASS THROUGH SUPERCRITICAL CO_2 EXTRACTION: FROM LAB TO EXPLOITATION

Universidade de Aveiro Departamento de Química
Ano 2017

Marcelo Morais Rodrigues de Melo

VALORIZAÇÃO DE BIOMASSA VEGETAL ATRAVÉS DE EXTRAÇÃO COM CO_2 SUPERCRÍTICO: DO LABORATÓRIO À EXPLORAÇÃO

VALORIZATION OF VEGETAL BIOMASS THROUGH SUPERCRITICAL CO_2 EXTRACTION: FROM LAB TO EXPLOITATION

Tese apresentada à Universidade de Aveiro para cumprimento dos requisitos necessários à obtenção do grau de Doutor em Engenharia Química, realizada sob a orientação científica do Doutor Carlos Manuel Santos Silva, Professor Auxiliar do Departamento de Química da Universidade de Aveiro, e do Doutor Armando Jorge Domingues Silvestre, Professor Associado do Departamento de Química da Universidade de Aveiro.

“When you wish upon a star
Makes no difference who you are”

Walt Disney theme

o júri

presidente

Doutor **Jorge Ribeiro Frade**, Professor Catedrático da Universidade de Aveiro

Doutor **Carlos Manuel Santos Silva**, Professor Auxiliar da Universidade de Aveiro (orientador)

Doutora **Maria Gabriela Bernardo-Gil**, Professora Associada com Agregação da Universidade de Lisboa

Doutor **Manuel Luís de Magalhães Nunes da Ponte**, Professor Catedrático da Universidade Nova de Lisboa

Doutora **Maria Arminda Costa Alves**, Professora Catedrática da Universidade do Porto

Doutor **José Miguel Loureiro**, Professor Associado com Agregação da Universidade do Porto

Doutor **Artur Manuel Soares da Silva**, Professor Catedrático da Universidade de Aveiro

Doutora **Maria Inês Purcell de Portugal Branco**, Professora Auxiliar da Universidade de Aveiro

agradecimentos

Ao meu orientador Carlos Manuel Silva, por ter sido o grande mentor deste doutoramento e percurso, pelas incontáveis horas dedicadas à expansão e consolidação do meu conhecimento, bem como pelo aconselhamento e contributos prestados em prol da potenciação do meu desempenho. Um tremendo obrigado, com amizade, respeito e estima.

Ao meu coorientador Armando Silvestre, por igualmente ter acreditado no meu potencial, me ter apoiado no que precisei, e por partilhar comigo o apreço por *biomassa* vegetal e animal, incluindo a de origem nipónica e comestível.

Aos vários colegas do grupo EgiChem de/com quem tanto recebi, conversei, almocei, partilhei, joguei, sorri, aprendi.

Aos colegas de investigação Rui Domingues, Umut Şen, Paulo Toledo, Pedro Martins, Hugo Barbosa, e Rui Silva, pelas parcerias de trabalho estabelecidas, as quais contribuíram para o documento e conhecimento aqui apresentados e para o contributo global que este possa dar para o tema da extração supercrítica e da valorização de biomassa vegetal.

* * *

Aos meus pais, João e Alice, pela possibilidade da vida, pelo mérito com que idealizaram e executaram a minha educação, e ainda pelos nobres valores e hábitos que me incutiram. Que este marco académico personifique a gratidão que vos tenho, e o sucesso do vosso empenho e estímulo para comigo.

Ao meu irmão Gonçalo, pelo companheirismo e partilha, pelo estímulo e alento, pelo ânimo que semeia na minha vida.

Aos meus avós paternos, Felisberto e Esmeralda, pela fraternidade e carinho incondicionais que me devotam desde que existo.

À Ana, por ter empaticamente persistido na minha vida desde os primórdios da formação em engenharia química, e muito em especial por ter confiado e acreditado que *juntos somos* (temos sido) *mais fortes*, e que é *preciso perder para depois se ganhar.*

* * *

A todos os que, não estando aqui individualizados, fizeram parte desta caminhada e da pessoa que sou.

palavras-chave Biomassa, Biorefinaria, CO_2, Extração supercrítica, Extratos vegetais, Valorização

resumo

A investigação no tema de extração com dióxido carbono supercrítico (SFE) de compostos de valor acrescentado a partir de biomassa vegetal tem sido fortemente impulsionada por duas motivações: a valorização de subprodutos e a biorefinaria.

Neste trabalho seis estágios diferentes da investigação neste campo são abordados: a caraterização preliminar de extratos, a otimização experimental, a medição de curvas cinéticas, a modelação das mesmas, estudos de escalabilidade (scale-up), e a análise tecno-económica. Para este efeito, selecionaram-se subprodutos e resíduos agroflorestais promissores, a saber: resíduos de café, folhas e ramos de jacinto de água, cortiça de carvalho turco, sementes de moringa, fruto gac, e casca de eucalipto, com especial ênfase neste último pela sua pertinência no contexto industrial português, nomeadamente para o setor da pasta e papel. O trabalho experimental focou-se em extratos crude e compostos bioativos com potencial para aplicações em cosmética e nutracêutica, tais como os ácidos triterpénicos (ácidos ursólico, oleanólico, betulínico), diterpenos (cafestol, kahweol, 16-*O*-methylcafestol), esteróis (estigmasterol, etc), friedelina, e licopeno.

- Casca de eucalipto *(Eucalyptus globulus)*: puro ou modificado com etanol, o SC-CO_2 foi capaz de remover ácidos triterpénicos, e a medição e modelação de curvas de extração em condições ótimas (200 bar, 40 ºC e 2.5-5.0 % m/m de etanol) apontaram o rácio entre o caudal e a massa de biomassa como o critério de scale-up apropriado para o processo. Seguindo este critério realizou-se com sucesso um scale-up experimental a três escalas: 0.5, 5.0, and 80 L.
- Cortiça de carvalho turco *(Quercus cerris)*: extratos crude contendo cerca de 35 % m/m de friedelina foram produzidos com sucesso por SFE e as curvas de extração foram modeladas. A seletividade para a friedelina pode atingir 2.5 através da correta seleção do tamanho de partícula, quantidade de cosolvente (etanol) e tempo de extração.
- Folhas e ramos de jacinto de água (*Eichhornia crassipes*): extratos ricos em estigmasterol foram obtidos para tempos de extração curtos (<1 h). As condições ótimas para o rendimento total de extração são 250–300 bar e 5.0 % m/m de etanol, enquanto que para os esteróis são 300 bar e 2.5 % m/m
- Resíduos de tomate (*Solanum lycopersicum*): tanto o dióxido de carbono como o etano podem ser usados como solvente supercrítico para produzir um óleo essencial que é rico em licopeno. A viabilidade da SFE foi demonstrada, e apesar de o etano conduzir a maior produtividade, mais investigação é necessária para definir qual dos solventes é preferível na globalidade.
- Fruta gac (*Momordica. cochinchinensis*): poderá ser uma promissora e economicamente viável fonte de carotenos, quando extraídos por SFE a 400 bar, 70-90 $\mathrm{kg_{CO_2}\,kg_{biomassa}^{-1}\,h^{-1}}$, durante 0.5-1.0 h.
- Sementes de moringa (*Moringa oleifera*): uma análise tecno-económica revelou que um processo integrado bem projetado e combinando SFE com destilação a vácuo permite a produção simultânea de um óleo essencial e de um extratos com uma concentração de esteróis de 89.4 %.
- Borras de café (*Coffea* spp.): o óleo produzido por SFE é até 4.1 vezes mais rico em diterpenos do que extratos obtidos com *n*-hexano, e um processo altamente rentável é esperado a nível comercial.

No cômputo geral, esta tese contribui para a sistematização de uma abordagem científica e técnica que promova a valorização industrial de biomassa vegetal através da tecnologia de extração supercrítica.

keywords Biomass, Biorefinery, CO_2, Supercritical extraction, Valorization, Vegetal extracts

abstract

The research on supercritical CO_2 extraction (SFE) of added value compounds from vegetal biomass has been strongly driven by by-products valorization and biorefinery motivations.

In this work, preliminary characterization of extracts, experimental optimization, measurement of kinetic curves, modeling, scale-up, and techno-economic analysis are covered. For this, several promising agro-forest by-products and residues were selected: spent coffee grounds, water hyacinth stalks and leaves, Turkish oak cork, moringa seed, tomato wastes, gac fruit, and eucalypt bark, with a strong emphasis on the latter due to its pertinence for the Portuguese industrial pulp and paper sector. Experimental work focused on bulk extracts and bioactive compounds with potential cosmetic and nutraceutical applications, such as essential oils, triterpenic acids (ursolic, oleanolic, and betulinic acids), diterpenes (cafestol, kahweol, 16-*O*-methylcafestol), sterols (e.g., stigmasterol), friedeline, and lycopene. The main results are:

- Eucalypt *(Eucalyptus globulus)* bark: whether pure or modified with ethanol, SC-CO_2 was able to remove triterpenic acids, and the measurement and modeling of extraction curves under optimum conditions (200 bar, 40 ºC and 2.5-5.0 wt.% of ethanol) pointed the ratio between solvent flow rate and biomass weight as the appropriate scale-up criterion of the process. With this criterion, a successful experimental scale-up was achieved at three scales: 0.5, 5.0, and 80 L.
- Turkish oak *(Quercus cerris)* cork: bulk extracts containing *ca*. 35 wt.% of friedeline were successfully produced by SFE and the extraction curves were modeled. The selectivity to friedeline can reach up to 2.5 through a correct selection of particle size, cosolvent (ethanol) amounts and extraction time.
- Water hyacinth (*Eichhornia crassipes*) leaves and stalks: stigmasterol enriched extracts were obtained for shorter times (<1 h). The optimized conditions for total extraction yield were 250–300 bar and 5.0 wt.% ethanol, while for sterols were 300 bar and 2.5 wt.%.
- Tomato (*Solanum lycopersicum*) wastes: both carbon dioxide and ethane can be used as supercritical solvents to produce an essential oil that is rich in lycopene. The viability of the SFE was demonstrated, but while ethane led to greater productivity, further research is needed to define which one is preferable on a global basis.
- Gac (*Momordica. cochinchinensis*) fruit: it may be a promising and economically viable source of carotenes when produced by SFE at 400 bar, 70-90 $\mathrm{kg_{CO_2}\,kg_{biomass}^{-1}\,h^{-1}}$, during 0.5-1.0 h.
- Moringa (*Moringa oleifera*) seeds: a techno-economic analysis unveiled that a well designed integrated process combining SFE and vacuum distillation allows the simultaneous production of an essential oil and a sterols enriched extract with 89.4 % concentration.
- Spent coffee (*Coffea* spp.) grounds: the oil produced by SFE is up to 4.1 times richer in diterpenes than *n*-hexane extracts, and a highly profitable process may be expected at commercial level.

In the whole, the presented thesis contributes to the systematization of a scientific and technical approach to foster the industrial valorization of vegetal biomass through SFE technology.

THESIS OUTLINE

Nomenclature

^{1}H NMR	nuclear magnetic resonance
a	specific surface area
AARD	average absolute relative deviation
ANOVA	analysis of variance
ATEX	equipment for potentially explosive atmospheres
BBD	Box-Behnken design
BIC	broken plus intact cells
BICM	broken plus intact cells model
BPR	backpressure regulator
c , C	concentration
ΔC_p	heat capacity change
ΔS	entropy change
CCD	Central composite design
CER	constant extraction rate
CRM	raw material cost
COL	labor cost
COM	cost of manufacturing
CUT	utility cost
CWT	waste treatment cost
CZE-HPLC	Capillary electrophoresis with high-performance liquid chromatography
D	debye units
D_b	bed diameter
DC	diffusion controlled
D_{12}	tracer diffusion coefficient
D_{eff}	effective diffusion coefficient
D_{ax}	axial dispersion
DSC	Differential scanning calorimetry
d_p	particle diameter
$\overline{d_p}$	mean particle diameter
DoE	design of experiments
EoS	equation of state
EtOH	ethanol
FA	fatty acids
FCI	investment cost

FAME	fatty acid methyl esters analysis
FER	falling extraction rate
FE-SEM	Field Emission Scanning Electron Microscopy
FM	Full model
g	grinding efficiency
GC-MS	gas chromatography – mass spectrometry
GC-FID	gas chromatography – flame ionization detector
GC-O	gas chromatography-olfactometry
GC-HRMS	gas chromatography - high resolution mass spectrometry
GRAS	Generally Recognized as Safe
h	axial coordinate
H	equilibrium partition coefficient
HPLC	High-performance liquid chromatography
HPLC-ELSD	High-performance liquid Chromatography with evaporative light scattering detector
HPLC-ESI-MS	High-performance liquid Chromatography with electrospray ionization and mass spectrometry
HPLC-FLD	High Performance liquid chromatography with postcolumn fluorescence derivatization
HPTLC	High-performance liquid layer chromatography
HPLC-PAD-MS	High-performance liquid Chromatography with pulsed amperometric detector and mass spectrometry
HRGC	High resolution gas chromatography
ICP-MS	Inductively coupled plasma mass spectrometry
IU	isoprene units
j	mass flux
k	convective mass transfer coefficient
k_d	desorption constant
L_b	length of the bed
LCAA	long chain aliphatic alcohols
LC-ESI	Liquid chromatography with electrospray ionization
LC-DAD	Liquid chromatography with diode array detection
LC-MS	Liquid chromatography - mass spectrometry
l	plate thickness
M	molecular weight
MeOH	methanol
N	flux
ND	not detected
OT	orthogonal test
P	pressure

Pe	Peclet dimensionless number
PR	Peng Robinson
Q	mass flow rate
r	radial coordinate
$\Re$	gas constant
R^2	coefficient of determination
Re	Reynolds dimensionless number
R^2_{adj}	adjusted coefficient of determination
R_{p}	particle radius
RT	retention time
RP-HPLC	reversed phase high-performance liquid chromatography
RSM	response surface methodology
Re	Reynolds number
S	bed cross-sectional area or entropy
Sc	Schmidt dimensionless number
ΔS	entropy change
SEM	Scanning Electron Microscopy
Sc	Schmidt number
SC	supercritical
SCG	spent coffee grounds
SC-CO_2	supercritical carbon dioxide
SCM	shrinking core model
SC-BICM	model bridging SCM and BICM
SFC	supercritical fluid chromatography
SFE	supercritical fluid extraction
Sh	Sherwood number
SLE	solid-liquid extraction
ST	sterols
t	Time
T	temperature
$T_{col\,bot}$	temperature at the bottom of the column
$T_{col\,top}$	temperature at the top of the column
TT	triterpenoids
TLC	thin layer chromatography
TMS	trimethylsilyl
TPC	thermo-chromatographic pulse
U	intersticial velocity
UPLC-MS	Ultra-performance liquid chromatography - mass spectrometry
V	Molar volume

V_{ex}	volumetric exhaustion degree
$V_{\text{extractor}}$	extractor volume
vol.	Volumetric or related to volume
v	velocity
x	Solid or fluid phase concentration
x_0	real value of the independent variable at the central point
X_0	concentration of the target species in the raw material
x_{k}	independent variable of DoE modeling
Δx_{k}	step change of x_{k}
X_{k}	codified value of the independent variable of DoE modeling
y	gas or supercritical phase concentration
w	mass or accentric factor
w'	mass in a oil free basis
	Greek letters
α	selectivity
ρ	density
ε	porosity
η	yield
δ	Hildebrand solubility parameter
ϕ	fugacity coefficient
μ	viscosity
	Subscript
β-sitost	relative to β-sistosterol
b	Bed
c	critical
cholest	relative to cholesterol
cosolv	relative to cosolvent
eb	at normal boiling point
dit	diterpenes
f,nf	relative to friedelin and non-friedelin molecules
f	Fluid
i	relative to species i
LDF	linear driving force
m	melting
Pi	at pressure i
pore	relative to the pore network
r	reduced
s	Solid

std	at standard conditions
stigm	stigmasterol
0	initial moment
	Superscript
*	equilibrium
f	fluid phase, or relative to friedelin
mix	mixture
sat	saturation
std	standard
SCF	supercritical fluid phase
solid	solid phase
total	relative to all the extract produced
∞	infinite dilution

LIST OF FIGURES

CHAPTER 3 – PRELIMINARY SFE & CHARACTERIZATION OF EXTRACTS

CHAPTER 4 – EXPERIMENTAL OPTIMIZATION

CHAPTER 8 – TECHNO-ECONOMIC ANALYSIS

LIST OF TABLES

CHAPTER 5 – MEASUREMENT OF EXTRACTION CURVES

CHAPTER 6 – KINETIC MODELING

1 MOTIVATION AND STRUCTURE OF THE THESIS

An important answer to environmental pollution and sustainability issues encompasses a transition to organic solvent-free products and processes [1]. This change of paradigm can only be fruitful if the new processes are reliable as well as technically and economically advantageous. Therefore, chemists and engineers should collaborate in the development of supporting know-how for such improvements.

The scientific community has been rather prolific in studies centered on the high pressure technology known as supercritical fluid extraction (SFE), which exploits thermodynamic and kinetic features of fluids above their critical points, with special emphasis on the use of carbon dioxide (CO_2) as solvent. Specifically, SFE has been exploited to retain the *natural* character of products after their processing/production stage and, simultaneously, avoid the presence of organic solvents as contaminants, thus increasing the market value of the final products [2]. This is not only true for food-related applications but also for cosmetics and even pharmaceuticals. As a result, in the last years SFE has been studied for the isolation of valuable extracts and/or components from a vast group of plant species. Despite the main motivation for SFE is the replacement of organic solvents by fluids bearing the so-called Generally Recognized as Safe (GRAS) standard [3], emphasis is rarely given to the fact that SFE may impart synergies and improvements to both processes and products in comparison to conventional solid-liquid extraction (SLE). Some of these advantages include: a more compact layout of SFE units with significant savings on machinery and space, wiser industrial process design, not only by means of integration but also by still weakly exploited coupling opportunities. It has been estimated that the number of industrial SFE plants with a total extraction volume of more than 500 L that are in operation in the world has surpassed the round number of 150 [4]. This is an acknowledgement of the global acceptance of SFE for industrial separation processes.

On the other hand, as the worldwide demand grows for many of the goods produced by beverages, food, and pulp and paper industries, the question of dealing with the consequent vegetable biomass residues becomes increasingly pertinent. The wastes in question typically arise from biomass pretreatment procedures (e.g. debarking, comminution, sieving) but also include the processed biomass that is functionally exhausted. The valorization of such residues is a likely strategy to unveil added-value opportunities that may justify further processing steps. A sound embodiment for the valorization of vegetal biomass is the biorefinery concept, which aims at an integration of processes and the launching of biobased products from biomass refining, with an incisive emphasis on green technologies.

This thesis arises from the described contexts, and intends to cover the stages between the preliminary identification of biomass potential and the scale-up of the SFE of vegetal matrices.

Based on the research work, it was possible to systematize the SFE research in six key stages: 1) Preliminary SFE + characterization of extracts; 2) Experimental optimization; 3) Measurement of extraction curves; 4) Kinetic modeling; 5) Scale-up; 6) Techno-economic analysis. These are schematized in Figure 1.1 in a sequenced order, as they are supposed to be carried out in series, rather than in parallel (e.g. scale-up coming after experimental optimization, or modeling coming after preliminary SFE assays).

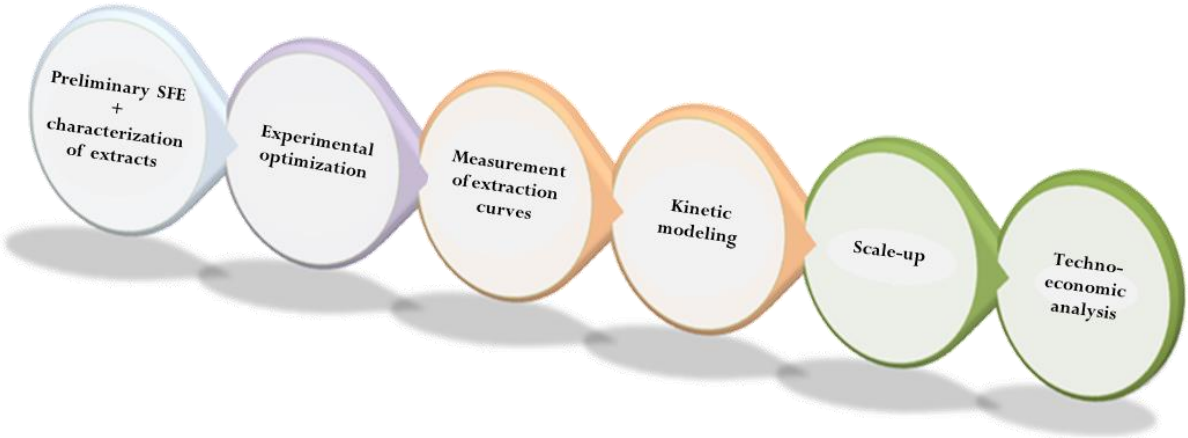

Figure 1.1 – Proposed systematization of the SFE research in six key stages, based on the analysis of the literature since 2000.

Globally, the thesis was structured in order to address and cover all these stages as structural divisions of the research on SFE of vegetal biomass. Despite possible casuistic nuances, these stages can be considered independent of the biomass-solvent pairs that are studied in particular. For this reason, seven vegetal species of interest were considered during the research work for this thesis, namely: coffee (*Coffea* spp.), water hyacinth (*Eichornia crassipes*), turkish oak (*Quercus cerris*), tomato (*Solanum lycopersicum* L.), gac (*Momordica cochinchinensis* Spreng), moringa seed (*Moringa oleifera* L.) and eucalypt (*Eucalyptus globulus*), with a strong emphasis on the latter due to its pertinence for the Portuguese pulp and paper industrial sector. These species were studied with special focus on different target compounds and families of extractives, such as triterpenic acids (found in eucalypt), diterpenes (coffee), sterols (water hyacinth and moringa), friedelin (Turkish oak), lycopene (tomato and gac), whose importance is emphasized in the introduction chapter of the thesis.

The matching of the different biomass sources and extractives with the research stages to systematize in this thesis is furnished in Table 1.1, which intends to be a guide to understand the information that is presented and cited in the successive chapters of this dissertation, namely the 10 scientific publications achieved during the course of this PhD.

Table 1.1 – Summary and systematization of the work accomplished during the PhD dissertation, including publications achieved on the different research stages on SFE.

Research Stage	Thesis Chapter	Studied Biomass	Target Extractives	Publications
Introduction	2	-	-	[5-7]
Preliminary SFE + characterization of extracts	3	Eucalypt	Triterpenic acids	[8]
Experimental optimization	4	Coffee Water hyacinth	Diterpenes Sterols	[9-10]
Measurement of extraction curves	5	Coffee Water hyacinth Turkish oak	Diterpenes Sterols Friedelin	[9, 11-12]
Kinetic modeling	6	Water hyacinth Turkish oak	Sterols Friedelin	[11-12]
Scale-up	7	Eucalypt	Triterpenic acids	[13]
Techno-economic analysis	8	Coffee Tomato Gac Moringa	Diterpenes Lycopene Lycopene Sterols	[9, 14-16]

REFERENCES

[1] J.H. Clark, Introduction to green chemistry, in: A. Proctor (Ed.) Alternatives to Conventional Food Processing, RSC, Cambridge, 2011.

[2] M. Perrut, Supercritical fluid applications: Industrial developments and economic issues, Industrial & Engineering Chemistry Research, 39 (2000) 4531-4535.

[3] G.A. Burdock, I.G. Carabin, Generally recognized as safe (GRAS): history and description, Toxicology Letters, 150 (2004) 3-18.

[4] J.W. King, Modern Supercritical Fluid Technology for Food Applications, Annual Review of Food Science and Technology, 5 (2014) 215-238.

[5] M.M.R. de Melo, A.J.D. Silvestre, C.M. Silva, Supercritical fluid extraction of vegetable matrices: Applications, trends and future perspectives of a convincing green technology, Journal of Supercritical Fluids, 92 (2014) 115-176.

[6] M.M.R. de Melo, R.M.A. Domingues, A.J.D. Silvestre, C.M. Silva, Extraction and purification of triterpenoids using supercritical fluids: From lab to exploitation, Mini-Reviews in Organic Chemistry, 11 (2014) 362-381.

[7] M.M.R. de Melo, I. Portugal, A.J.D. Silvestre, C.M. Silva, Environmentally benign supercritical fluid extraction, in: F. Pena-Pereira (Ed.) The Application of Green Solvents in Separation Processes, Elsevier, Amsterdam, 2017

[8] M.M.R. de Melo, E.L.G. Oliveira, A.J.D. Silvestre, C.M. Silva, Supercritical fluid extraction of triterpenic acids from *Eucalyptus globulus* bark, Journal of Supercritical Fluids, 70 (2012) 137-145.

[9] M.M.R. de Melo, H.M.A. Barbosa, C.P. Passos, C.M. Silva, Supercritical fluid extraction of spent coffee grounds: Measurement of extraction curves, oil characterization and economic analysis, Journal of Supercritical Fluids, 86 (2014) 150-159.

[10] P.F. Martins, M.M.R. de Melo, P. Sarmento, C.M. Silva, Supercritical fluid extraction of sterols from *Eichhornia crassipes* biomass using pure and modified carbon dioxide. Enhancement of stigmasterol yield and extract concentration, Journal of Supercritical Fluids, 107 (2016) 441-449.

[11] M.M.R. de Melo, P.F. Martins, A.J.D. Silvestre, P. Sarmento, C.M. Silva, Measurement and modeling of supercritical fluid extraction curves of Eichhornia crassipes for enhanced stigmasterol production: Mechanistic insights of the process, Separation and Purification Technology, 163 (2016) 189-198.

[12] M.M.R. de Melo, A. Şen, A.J.D. Silvestre, H. Pereira, C.M. Silva, Experimental and modeling study of supercritical CO_2 extraction of *Quercus cerris* cork: Influence of ethanol and particle size on extraction kinetics and selectivity to friedelin, Separation and Purification Technology, 187 (2017) 34-45.

[13] M.M.R. de Melo, R.M.A. Domingues, M. Sova, E. Lack, H. Seidlitz, F. Lang Jr, A.J.D. Silvestre, C.M. Silva, Scale-up studies of the supercritical fluid extraction of triterpenic acids from *Eucalyptus globulus* bark, Journal of Supercritical Fluids, 95 (2014) 44-50.

[14] A.F. Silva, M.M.R. de Melo, C.M. Silva, Supercritical solvent selection (CO_2 versus ethane) and optimization of operating conditions of the extraction of lycopene from tomato residues: Innovative analysis of extraction curves by a response surface methodology and cost of manufacturing hybrid approach, Journal of Supercritical Fluids, 95 (2014) 618-627.

[15] P.F. Martins, M.M.R. de Melo, C.M. Silva, Gac oil and carotenes production using supercritical CO_2: Sensitivity analysis and process optimization through a RSM–COM hybrid approach, Journal of Supercritical Fluids, 100 (2015) 97-104.

[16] P.F. Martins, M.M.R. de Melo, C.M. Silva, Techno-economic optimization of the subcritical fluid extraction of oil from *Moringa oleifera* seeds and subsequent production of a purified sterols fraction, Journal of Supercritical Fluids, 107 (2016) 682-689.

2 INTRODUCTION

This chapter is essentially based on a published review comprising a large compilation of almost 600 essays from 2000 to 2013, that allowed SFE indicators and trends to be unveiled [1]. It also includes parts of another review article on lab to exploitation SFE of triterpenes [2], and a book chapter devoted to the environmental benignity of SFE [3].

CHAPTER OUTLINE

In the period of 2000 to 2013, the extracts of more than 300 plant species have been studied using supercritical fluid extraction (SFE) technology. It is worth noting the major share of SFE research covers vegetable biomass [4-5]. While many extracts and pure components of these species are already in use for human nutrition and health purposes, others represent potentially new applications involving plants whose knowledge, in most of the cases, has been empirically established or still lacks scientific analysis.

The remarkable interest of scientific community on this technology has been driven by the great versatility of carbon dioxide, the most used solvent in supercritical state, whose properties can be tuned in order to provide extracts with desirable compositions (selectivity enhancements), while at the same time it ensures an innocuous separation process both to human health and to the environment. Other solvents (e.g. ethane, propane) have also been object of research but their use is not as widespread as carbon dioxide, and for this reason the emphasis of this review is on supercritical carbon dioxide (SC-CO_2).

In what concerns food related species, the great expansion of nutraceuticals market in recent years, as an emerging sector comprising the use of dietary substances for prevention of diseases [6], has been attracting the attention of researchers and food industry. In this context, SFE is advantageously positioned as a sustainable and safe extraction option for the preparation of plant extracts for supplements and nutrient enriched products in which, as Perrut anticipated in 2000 [7], the *natural* character of the preparation mode has a high marketing value. Besides those requisites, when SFE is applied to eatable raw materials as a pretreatment for removal of compounds (e.g. cleaning of rice), other advantages are also observed, such as enhancement of product shelf life and, eventually, the shortening of the cooking time [4]. In addition, research on this field has also explored the valorization of residues from main stream processes [8-9].

Considering the abundance of compounds that are prone to be found in supercritical extracts, it becomes pertinent to expose different possible focuses of SFE researchers for the vegetables under investigation. For this, it is convenient to divide biomass species based on usual extract classifications, namely edible oils (higher volume, lower value) and essential oils (higher value, lower volume).

The most abundant extracts from vegetable matrices are the edible oils, which are mostly constituted by mixtures of triacylglycerides obtained with high extraction yields from the following typical sources: palm, soybean, sunflower, rapeseed, peanut, cottonseed, coconut, olive, corn, and sesame species. An edible oil, like palm oil, may reach triacylglycerides concentrations around 95 % [10], and the use of SFE is many times devoted to other purposes than their bulk extraction. Instead, it is more commonly linked to attempts to enhance the concentration of valuable compounds existing in minor concentrations. In the whole, SFE works regarding these edible oils have focused on the following goals:

i) tentative replacement of organic solvents like *n*-hexane as extraction agents, avoiding thus the consequent environmental and human health hazards;
ii) enrichment of main stream oils with bioactive or other distinctive minor constituents. In this respect, one may mention several SFE works on palm [11-13], where β-carotene, squalene, α-tocopherol contents were evaluated;
iii) valorization of vegetable residues or by-products from main extraction processes in order to uptake available bioactive molecules. Several works on sunflower distillate [14-15], soybean distillate [16-17], olive pomace [18-19], and olive husk [20-21] are examples of this approach.
iv) valorization of non-explored vegetable parts that do not belong to the prime oil extraction process, such in the cases of SFE of sunflower leaves [22-24] and of olive leaves [25].

Essential oil is the general classification used for volatile oils that can be obtained by steam distillation of plants. This category of extracts has been the core area of the research on SFE of natural matrixes since 2000 because it includes valuable specialty oils. Although the extraction yields obtained through the employment of SC-CO_2 are quite flexible, it is common to establish essential oils as a group of natural extracts comprising up to 5 % of vegetal dry matter.

The presence of bioactive compounds makes essential oils interesting for numerous applications. With respect to their commercial relevance, they are widely applied in segments such as flavors, fragrances, food ingredients, nutraceuticals, phytopharmaceuticals and cosmetics. In this context, the research on SFE has mainly aimed at technical validation, in order to support its feasibility as an alternative process for applications where the desired green and/or healthy characters are required. Different approaches can be found in the literature regarding the SFE of essential oils:

i) for new or unusual plant species, SFE is sometimes used simply as an exploratory method that provides new extracts to be further characterized, purified or tested regarding their bioactivity or other distinctive features. Works involving *Ligusticum chuanxiong* [26] , *Cyperus rotundus* [27], *Cassia tora* [28] may be consulted in this respect.

ii) for species whose extracts and bioactive compounds are known, SFE advantages as an alternative technology are assessed in comparison to other methods, usually organic solvent extraction or steam distillation. Examples of this approach are found in the publications regarding yerba mansa (*Anemopsis californica*) [29], *Catharanthus roseus* [30], *Zataria multiflora* Boiss [31], thyme (*Thymus vulgaris* L) [32].

iii) concentration enhancement of bioactive or organolepsy related compounds in extracts by means of supercritical fractionation, multistage decompression, or combination of SFE with matrix pretreatments. Matrix pretreatment examples may be consulted in SFE works of grape seed [33-34], and turmeric (*Curcuma longa* L) [35], while fractionation examples may be consulted for SFE of cashew (*Anacardium occidentale* L.)

[36], origanum (*Origanum vulgare* L.) [37] and chamomile (*Matricaria chamomilla*) [38]. Multistage decompression can be found in the following works: SFE of laurel (*Laurus nobilis*) [39], sea buckthorn (*Hippophae rhamnoides* L.) [40] and rosemary (*Rosmarinus officinalis* L.) [41].

2.1 VEGETAL BIOMASS SOURCES

When overviewing the field of vegetable matrices extracts for a period larger than a decade, a vast group of species arises as issue of SFE research, hence revealing the strong interest and attention that supercritical fluids have conquered. A wide-ranging compilation of works in this field is presented in Table S1 (see supplementary material in the end of this chapter), sorted by the scientic names of plant species substrates. Information regarding the vegetable species, target molecules and operating conditions (pressure, temperature, solvent flow rate, and cosolvent content) are provided for each SFE publication, as well as the respective analytical techniques employed and complementary features about each work.

Among the vast group of species that have been studied under the scope of SFE, some have appeared in great number in literature since 2000. It is the case of grape (*Vitis vinifera* L.) [33, 42-63], tomato (*Solanum lycopersicum* L.) [64-73], thyme (*Thymus vulgaris* L.) [32, 74-81], eucalypt (*Eucalyptus* spp.) [82-90], coffee (*Coffea* spp.) [91-99], sunflower (*Heliantus annuus* L.) [14-15, 22-24, 100-101], flax (*Linum usitatissimum*) [102-106], rosemary (*Rosmarinus officinalis* L.) [41, 107-113], red pepper (*Capsicum anuum* L.) [114-119], and rice (*Oryza* variety) [120-126].

Moreover, a substantial number of dairy plant products has been object of SFE technology, such as, among others, apricot (*Prunus armeniaca* L.) [127-131], carrot (*Daucus carota* L.) [132-135], cashew (*Anacardium occidentale L.*) [36, 136-138], cocoa (*Theobroma cacao*) [139-141], garlic (*Allium sativum*) [142-145], ginger (*Zingiber officinale*) [146-150], ginseng (*Panax ginseng*) [151-154], laurel (*Laurus nobilis* L.) [39, 155-158], orange (*Citrus sinensis* L.) [159-163], oregano (*Origanum virens* L.) [164-168], pumpkin (*Cucurbita* spp.) [169-173], soybean [16-17, 174-177], turmeric (*Curcuma longa*) [35, 178-180], and wheat germ (*Triticum* spp.) [181-185].

Following a major trend of western pharmaceutical industry of integrating oriental folk medicine species that have been used for centuries in natural formulations for a myriad of health problems, extracts of a significant number of species used in those contexts have been prepared using SFE. Although many species are still to be recognized for their health/nutrition benefits by health authorities such as World Health Organization, others have seen their bioactivity confirmed, such as on the cases of *Acorus calamus* [186], *Andrographis paniculata* [187], *Azadirachta indica [188-191]*, *Curcuma longa* [35, 178-180, 192], *Cyperus rotundus [27], Ocimum gratissimum [193-197], Panax ginseng* [151-153], *Taxus baccata* [198]. Its application has been directed by the

interest to isolate and quantify phytopharmaceuticals existing in those extracts so that further pharmacological studies can then be carried out in order to confirm the respective bioactivities. An elucidating perspective on this research path was recently published for the case of triterpenoid compounds, either with respect to their extraction with SC-CO_2 [2], either in terms of the corresponding bioactivity studies that support their therapeutic potential [199].

Considering the representative number of works covered in this review, it is possible to depict some structural tendencies regarding the directions research has followed in this field, such as the characteristics of the biomass matrices that have been most studied. Accordingly, Figure 2.1 presents a statistical distribution of the vegetables matrices types mostly found on SFE publications. It becomes clear that supercritical fluids have been mainly applied to the extraction of seeds and leaves. Together, they represent 45 % of the plant fractions of all the works considered, being seeds the biggest fraction (28 %), and leaves only 17 %. They are followed by fruits (10 %), roots (7 %), flowers (5 %), rhizomes (3 %) and bark (2 %). On the other hand, parts such as stems, branches, and woods seem not to justify individual studies of SFE, being instead included only in cases where matrices comprise mixtures of components, such as aerial parts, which account for 9 % of the researched matrices. In addition, processed vegetables like pomace or husks represent 5 % of the 544 SFE publications considered in this review within 2000 and 2013.

In the following paragraphs, special emphasis is given to vegetal matrices that were studied within the scope of the PhD work, and which will appear repeatedly in the different chapters of the thesis:

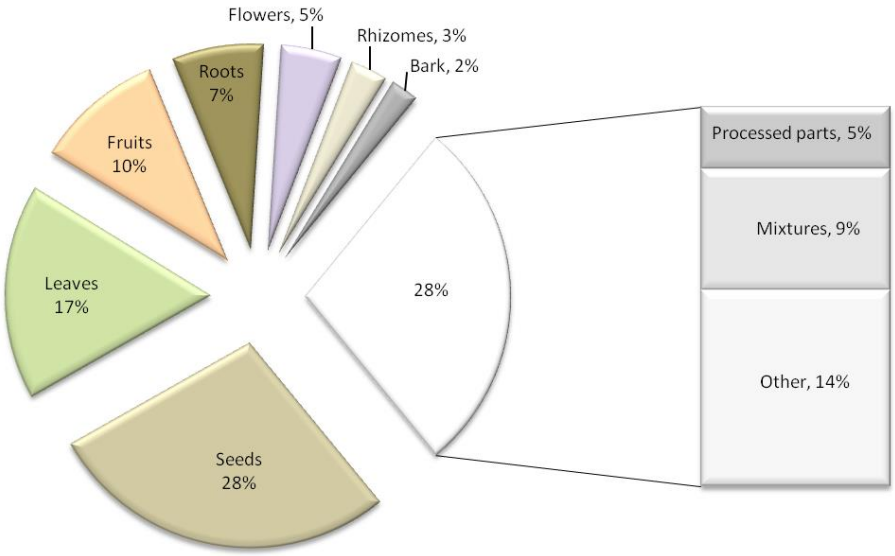

Figure 2.1 – Type of the biomass matrices used in SFE works along 2000-2013, for a total of 544 publications considered.

Eucalypt *(Eucalyptus globulus)* bark – Pulp and paper industry is one of the major industries of the agro-forestry sector. In the production of paper, the first step is to extract cellulose fibers from raw wood [200]. On arrival to the mill, the wood is debarked and the bark is burned for power generation.

Eucalyptus species are the most important fiber sources for pulp and paper production in southwestern Europe (Portugal and Spain) and south America (Brazil and Chile), where this sector has observed a fast growing during the last few years [201]. The total *Eucalyptus* planted area in Brazil, Chile, Portugal and Spain is around 5.7 million ha [202] and it was estimated that in 2010 they were producing together around 14.7 million ton of *Eucalyptus* spp. pulp, representing 81 % of the total *Eucalyptus* spp. wood pulp produced worldwide [203]. In the Portuguese context, *Eucalyptus globulus* is the dominant species in terms of pulp and paper production, and the third in terms of forest area, (about 672.000 ha, see Figure 2.2), representing nearly 31 % of the *E. globulus* area planted worldwide [204].

In a medium size pulp mill using *E. globulus* wood as feedstock and producing 5×10^5 tons of bleached pulp per year, about 1×10^5 tons of bark are produced [205] indicating that there is a possibility for upgrading this side stream if high value compounds are present in the bark (see Figure 2.2).

Figure 2.2 – *E. globulus* plantation (credit:[206]) and its bark (credit:[207]).

Spent coffee *(Coffea* spp.*)* grounds – Coffee, whose plant is depicted in Figure 2.3, is one of the most consumed beverages in the world and gives rise to around 6 million tons of spent coffee grounds (SCG) every year [208-209]. The large variability of SCG composition in terms of carbohydrates, proteins and phenolic compounds makes this residue a potential raw material for industrial processes [210-211]. Some years ago, SCG used to find application as animal feed or farming fertilizers, but recent studies showed its potential as a source of green energy like biofuel, and oil or isolated molecules for the pharmaceutical, cosmetic and food industries [98, 212-214]. In fact, SCG contain several human health related compounds, such as phenolics and

diterpenes, which have demonstrated bioactivities at antioxidant, anti-bacterial, antiviral, anti-inflammatory and anti-carcinogenic levels [215-217].

According to data from 2011, coffee market in Portugal involves an annual consumption of around 50 kton [218]. Considering what it represents for final consumer drinking habits, this value implies a large volume of waste being generated by food industry in consequence of processing this raw material. For instance, when considering soluble coffee, 2 to 4.5 tons of spent coffee grounds (SCG, see Figure 2.3) are generated per ton of soluble coffee produced [91, 208], with a moisture content around 80 % [91].

Whether in domestic or industrial contexts, SCG are a waste material that typically undergoes incineration and landfill disposal despite its toxicity due to caffeine, tannins and polyphenols content. In view of minimizing the environmental impact of this residue and to increase its market profitability, researchers have been studying SCG features and identifying potential applications [208, 219-221].

Figure 2.3 – Coffee plantation (credit:[222]) and spent coffee grounds (credit:[223]).

Turkish oak *(Quercus cerris)* cork – Cork is one of the plant tissues forming the barks of some trees species (see Figure 2.4). A great popularity of this natural material is already credited to the cork oak (*Quercus suber* L), whose transformation is responsible for a myriad a products such as cork stoppers, insulation, surfacing and paneling materials, engine joints, etc [224]. Nevertheless, the Turkey oak (*Quercus cerris*), illustrated in Figure 2.4, is also a potential important provider of cork that can be found in regions such as Eastern Europe and Minor Asia [225]. Since in countries like Turkey the bark of *Q. cerris* is not used except for fuel, the extraction of chemicals from this forest residue may offer opportunities towards its integrated utilization under the biorefinery concept.

The cork industry generates a large amount of powder and related by-products every year [226-227]. Additionally, certain trees like *Quercus cerris*, *Betula pendula*, *Quercus variabilis*, etc, contain

cork portions in their barks that are not industrially used [225, 228-229]. Cork contains approximately 2 % of triterpenoids, such as friedelin, betulin and β-sitosterol [230-231].

Figure 2.4 – Turkish oak forest (credit:[232]) and cork (credit:[233]).

Tomato *(Solanum lycopersicum* L.*)* wastes – In light of the research trend on the valorization of vegetable biomass through supercritical fluid extraction (SFE) technology, tomatois among the most representative raw materials that have been investigated with that pur pose [64-73, 234]. The pertinence of studying tomato is supported by the large volumes of industrial residues (exemplified in Figure 2.5) that are produced every year as a result of the vast application of this species in food industry (also depited in Figure 2.5), for products such as ketchup, sauces, etc. In fact, it is referred that tomato industrial wastes can represent up to 40 % of the initial raw material amounts processed [72].

According to data from 2011 [235], Portugal is the third greater producer of tomato in the European Union, with an annual production of 1.06 million tons, about half of Spain production, and nealy 1/5 of Italy's. In the world context, Portugal falls to the 5th position in the rank, standing behind Turkey and Iran.

Figure 2.5 – Tomato plantation (credit:[236]) and tomato wastes (credit:[237]).

Water hyacinth *(Eichhornia crassipes)* biomass – As an aquatic species original from the Amazon basin [238-239], it has been purposely introduced in other regions of the world where it spread uncontrollably (see a typical stand in Figure 2.6). As one of the most productive plants on earth, the annual biomass production of *E. crassipes* can be up to 140 tons of dry matter per hectare [240]. Such performance has led to the formation of vast monotypic stands in lakes, rivers and rice paddy fields, which raise problems at water quality level as well as the depletion of biological diversity [239, 241].

Figure 2.6 – Water hyacinth stand (credit:[242]) and its stalks and leaves (credit:[243]).

Gac *(Momordica cochinchinensis* Spreng*)* fruit – Is a traditional fruit from south Asia, mainly from Vietnam. Its aril (depicted in Figure 2.7) not only exhibits an interesting amount of oil (up to 44.4 wt.% [244]), but also a remarkable abundance of carotenoids like lycopene and β-carotene [245]. The latter are present in amounts five times greater than in tomatoes, and ten times greater than in carrots, respectively [246]. Due to the bioactive features of carotenoids, such as anti-carcinogenic, and antioxidant effects [245], the enhancement of their presence in the gac oil has triggered a remarkable interest in the scientific community. So far gac oil is usually obtained either by mechanical pressing or solid-liquid extraction using organic solvents, but the SFE has been recently tested and provided auspicious results for both a productive and green extraction process [244].

Figure 2.7 – Gac plantation (credit:[247]), and gac fruit aril (credit:[248]).

Moringa *(Moringa oleifera* L.*)* seed – Moringa oleifera is a plant native from northwestern India butcommonly found in many tropical areas (see Figure 2.8). Due to the high nutritive value, various parts of this plant are used as edible items, including animal fodder, in many locations [249-250]. Moringa is also exploitedas a source of wood for lumber industry. Also due to its composition, *M. oleifera* is also applied in medicinal and pharmacologicalproducts [251]. In this context, moringa seeds can be seen as a side product prone to bevalorized in an integrated biorefinery, without disturbing the mainindustrial stream.

Figure 2.8 – Moringa plantation (credit:[252]), and Moringa seed (credit: [253]).

2.2 EXTRACTIVES USING SC-CO_2

In view of the vast diversity of molecules found in natural matrices, vegetables are typically matter of research for more than one application. Depending on the species and plant component studied, SFE processes can be devoted to many naturally occurring compounds. Furthermore, SFE extracts obtained from vegetable matrices are typically mixtures of the following family of compounds: triglycerides, fatty acids, fatty alcohols, terpenoids, phytosterols, tocopherols, tocotrienols, and phenolics. Examples from each family are presented in Figure 2.9.

Triglycerides constitute the lion share of edible oils extracts. They are neutral lipids with a triesters structure of glycerol and fatty acids. Besides their important application for cooking purposes, it is known that their abundance in extracts lead to high quality biodiesel. Notwithstanding some examples of biodiesel production research from SFE extracts, namely from cardoon (*Cynara cardunculus* L.) [254]and *Jatropha curcas* L. [255], the number of publications covering this application was found to be very low.

The classification of triacylglycerides is usually achieved attending to the respective esterified fatty acids, but the free fatty acids are also a specific family of compounds that occur independently in SFE extracts. Moreover, in some cases, free fatty acids have been studied as

target compounds for extraction, such as in SFE of borage (*Borage officinalis* L.) [256], primrose (*Oenothera biennis L.*) [256], chinese star anise (*Illicium verum*) [257], palm (*Elaes guineensis*) [258], pine *(Pinus sylvestris L.) [259]*, pupunha (*Guilielma speciosa*) [260] and soybean (*Glycine* variety) [17]. These compounds are keystones for soaps, oleochemical esters, oils and lubricants [261] and in some cases their concentration may be helpful to control the quality of oils [257]. Since fatty acids oxidation can lead to aldehydes formation, and consequently odor problems, they can have a negative impact on products [259]. Therefore, depending on the studied case, fatty acids removal can be advantageous.

Regarding fatty alcohols it is known that they play an important industrial role as oleochemical solvents, plasticizers, and as surfactants in detergent formulations [261]. However due to the easiness they can be produced from fatty acids and from ethylene or other olefins, specific SFE approaches aiming at the extraction of these molecules tend not to be explored. These compounds are frequently found in leaves and seeds, and most frequently are waxy at room temperature [262]. For this reason extracts containing fatty alcohols may exhibit oil turbidity, a visual effect that can be considered inconvenient depending on the final application of the extract. No work specifically addressing SFE of fatty alcohols as target molecules is reported in Table S1.

A wide range of naturally occurring chemicals found in vegetable matrices belong to the terpenoids group, secondary metabolites whose role in plants is related to protection, pollination and growth mechanisms [263]. Terpenoids comprise chemical entities that have one or more isoprene units (IU) linked together and repositioned through cyclization, functionalization and arrangement. The extraction of these compounds has been one of the dominant objectives driving SFE research. Due to their diversity, it is common to classify these molecules according to the number IU, giving rise to different subgroups:

- monoterpenoids, with two IU, such as geraniol [264-265] or citronellol [266];
- sesquiterpenoids, three IU, like artemisin [267] or parthenolide [268];
- diterpenoids, with four IU, like cafestol [92, 99] and kahweol [92, 99];
- triterpernoids, with six IU, such as ursolic acid [84-86, 89] or squalene [17-18, 269-271];
- tetraterpenoids, with eight IU, like β-carotene [69-70, 127, 130-131, 133, 172, 258, 260, 272] or lycopene [64-67, 69-73, 273-275].

When considered from an end-user point of view, terpenoids affect the organoleptic perception of natural products, as they can have fragrant and colorant features. For instance, tetraterpenoids are typically responsible for the colors that many fruits and vegetables exhibit within red, brown and yellow tones. Nevertheless it is at flavor and fragrance levels that these compounds are more frequently investigated in view of food and cosmetic applications. For instance, terpenoids such as limonene, camphor, geraniol, 2-acetyl-1-pyrroline or labdanum are known for their scent and flavoring properties, and have been reported in SFE extracts [265] [276-285].

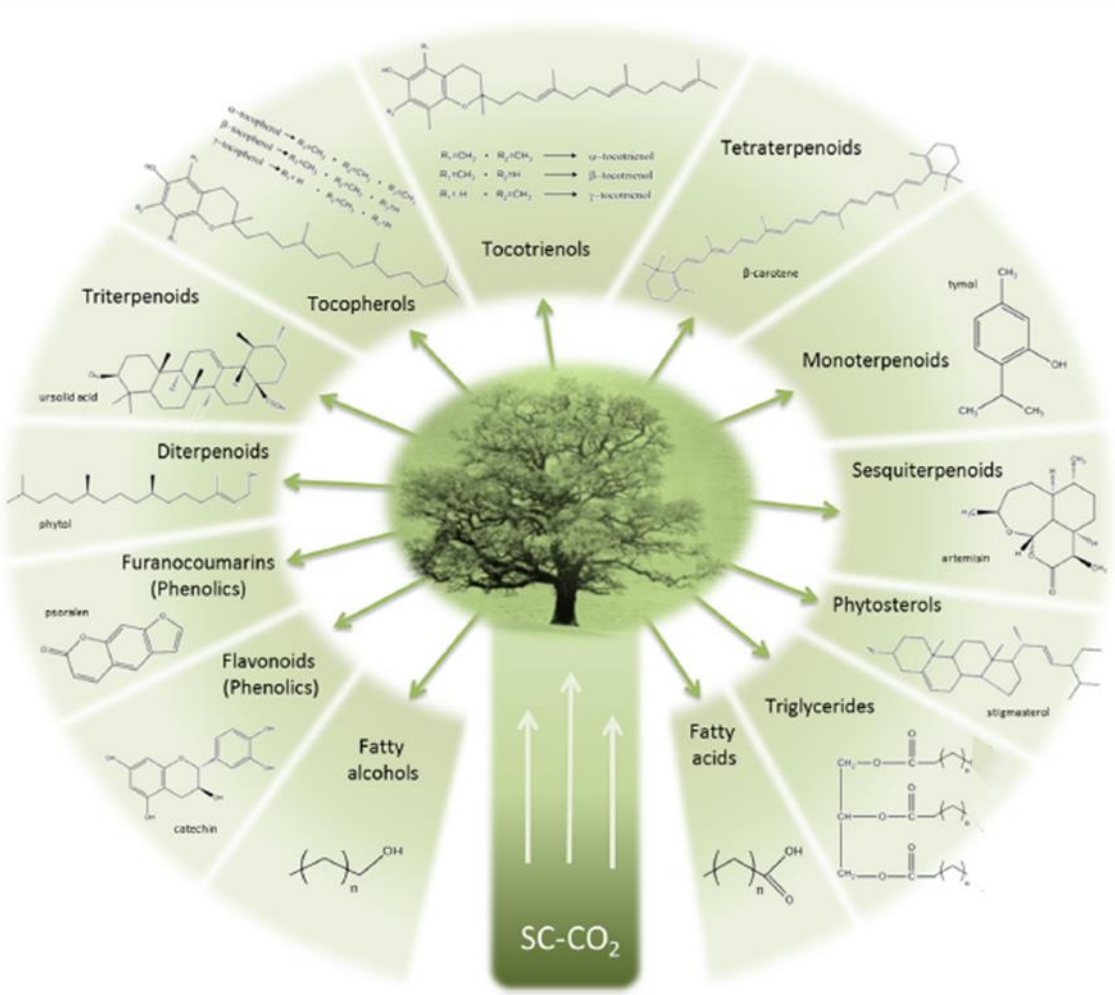

Figure 2.9 – Main families of compounds found in SFE vegetable extracts and examples from each one.

On the other hand, advantages may be taken from the protection functions played by these compounds when applied to human health. Several terpenoids have seen their bioactivity proved for many functions. For instance, triterpenic acids like ursolic, oleanolic, betulinic and betulonic acids exhibit a wide range of biological activities being recognized as promising compounds for the development of new multi-targeting bioactive agents [286-289].

Within the group of triterpenoids, phytosterols are a particular class of compounds that assume a special importance for human health purpose in view of reducing cholesterol intestinal absorption. The most representative phytosterols occurring in vegetable species are β-sitosterol, campesterol and stigmasterol, and many SFE publications have targeted them. These compounds have been found in extracts of amaranth (*Amaranthus* spp.) [290], corn (*Zea mays*) [291], eucalypt (*Eucalyptus globulus*) [83-86, 89], grape (*Vitis vinifera* L.) [45], jinxianlian (*Anoectochilus roxburghii*) [292], Kalahari melon (*Citrullus lanatus*) [293], mulberry (*Morus alba*)

[294], orange (*Citrus sinensis*) [162], pumpkin (*Curcurbita* spp.) [170], sea buckthorn (*Hippophae rhamnoides* L.) [295-296], soybean (Glycine *spp.*) [17], and sunflower (*Helianthus annuus* L.) [15].

Tocopherols and tocotrienols are specific families of compounds also found in many plant extracts. One of the most important molecules of this group is vitamin E (α – tocopherol), a powerful antioxidant whose deficient concentration in human organisms lead to chronic diseases [297]. The structural differences between the *-pherol* and *-trienol* derivatives are in the aliphatic side chains. While tocotrienols occurrence is restricted to fewer species, tocopherols are produced by all photosynthetic vegetables as part of their antioxidative system to cope with environmental stresses such as intense light, UV radiation and low temperatures [228]. The presence of these compounds in SFE articles has been reported in works with olive (*Olea europaea* L.) [19, 25], sea buckthorn (*Hippophae rhamnoides* L.) [272], soybean (Glycine *spp.*) [16-17], sunflower (*Helianthus annuus* L.) [15], and wheat (*Triticum* spp.) [181-183].

Phenolic compounds embody a vast group of molecules related to plants growth, development and defense. These compounds commonly exhibit an active organolepsy due to their contribution to color and taste of vegetable products. From a structural point of view, phenolics comprise an aromatic ring with one of more hydroxyl substituents, being the number and arrangement of the hydroxyl groups attached to the ring criteria of classification. Besides the most simpler phenolic structures (e.g. catechol, benzoic acid or gallic acid), high-molecular weight insoluble molecules are formed between phenolics and compounds of different nature, such as carbohydrates, proteins [298]. Depending on the vegetable species, extracts obtained by SFE can comprise substances from several phenolic groups like coumarins [299-300], cinnamic acids [300], quinones [77, 301-303], flavonoids [304-308], and lignans [104, 300].

In what concerns the extractives of the vegetal species studied during the PhD work, specific details are provided in the next paragraphs:

Triterpenic acids in Eucalypt bark – Freire *et al* [309] and Domingues *et al* [205] studied the composition of *Eucalyptus globulus* bark, the most used for papermaking in Portugal. Among the many compounds quantified by gas chromatography-mass spectrometry (GC-MS), several high-value triterpenic acids such as betulinic, betulonic, oleanolic and ursolic acids as well as the acetylated forms of the latter two were identified. These triterpenic acids (depicted in Table S1) are powerful antioxidants and have anti-inflammatory and anti-cancer activities [10-13], making them considerably valuable and their extraction from the low-value bark worthwhile in terms of the scale of the papermaking process. Some triterpenic acids have also been reported in extracts from different raw materials, such as birch [310], alder [311], greater plantain [312], sea buckthorn [313] and quince [314].

The same researchers [205, 309] reported also that the highest concentrations of extractives were found in the external part of *E. globulus* bark with about nine times the yield of the inner bark, despite the fraction of outer bark (1-3 mm) being much smaller than the inner bark (~10 mm). Also, triterpenoids are the major constituents of the outer bark extractives obtained by Soxhlet dichloromethane extraction, making this part of the bark more interesting for an industrial valorization of this low-value stream from papermaking process.

The solid-liquid extraction of such triterpenic acids from *Eucalyptus* bark using conventional solvents can be scaled-up to accommodate the high throughput necessary for the industrial process. However, this route, by itself, is not very selective for the compounds of interest. Moreover, increasing consumer awareness of the use of hazardous solvents by the chemical industry constitutes a driving force for the research of more environmentally friendly alternatives.

Diterpenes in spent coffee grounds – Almost all coffee production originates from the exploration of two species, *Coffea arabica* and *Coffea robusta,* yielding between 7 and 17 wt. % of oil [98, 214, 315]. The average lipid content of green *C. arabica* is higher than *C. robusta*, 15 % *vs.* 10 %, respectively [316]. In roasted coffee, oil is composed of fatty acids esterified with glycerol (triacylglycerols, around 78 wt.%) and diterpenes (around 15 wt.%), and only a small fraction is in sterol esters form [316-317].

Diterpenes belong to a group of compounds with important physiological activities, which also present beneficial effects to human health. Even though they are related with the increase of serum cholesterol, they manage to enhance glutathione S-transferase activity and to protect against benzo[a]pyrene and aflatoxin B1 – induced genotoxicity [318-320]. The main diterpenes found in SCG are cafestol, kahweol and 16-*O*-methylcafestol (see Table 2.1), which are mainly sterified by fatty acids such as palmitic (C16:0), stearic (C18:0), oleic (C18:1), linoleic (C18:2), α-linolenic (C18:3) and arachidic (C20:0) [321]. The total amount of these compounds in SCG depends on coffee species and on the brewing method [321-322]. For instance, in filtered coffee the kahweol levels range between 0.06 $\mathrm{mg\,L_{oil}^{-1}}$ to 2.66 $\mathrm{mg\,L_{oil}^{-1}}$, while cafestol levels are between 0.26 $\mathrm{mg\,L_{oil}^{-1}}$ and 5.30 $\mathrm{mg\,L_{oil}^{-1}}$. When dealing with *espresso* coffee, these levels are 1.2–8 and 4–16 $\mathrm{mg\,L_{oil}^{-1}}$, respectively [323]. Kurzrock *et al* [316] reported different levels on *espresso* coffee samples – 26 $\mathrm{mg\,L_{oil}^{-1}}$ for cafestol and 10 $\mathrm{mg\,L_{oil}^{-1}}$ for kahweol – when prepared from *C. arabica* species. Concerning SCG it has been reported that samples can lead to very distinct extraction yields and also to distinct extract composition values, that vary even within the same commercial brand [98, 219].

Table 2.1 – Target extractives of the thesis and respective biological features.

Extractive Family	Target Compound	Biological Features:
Triterpenic acids	Betulinic Acid ($C_{30}H_{48}O_3$) 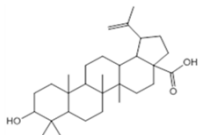	• anti-HIV[324] • anti-malarial [325-326] • anti-inflammatory [327-328] • anti-tumor [329-330] • anti-leishmanial [331] • anti-leukemia [289]
	Betulonic Acid ($C_{30}H_{46}O_3$) 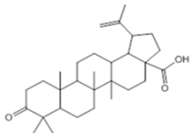	• anti-leishmanial [331] • anti-inflammatory [289] • anti-melanoma [289] • anti-viral [289]
	Ursolic Acid ($C_{30}H_{48}O_3$) 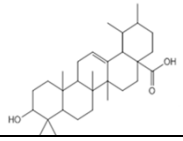	• anti-inflammatory [332] • anti-hyperlipidemic [332] • hepatoprotective [332]
	Oleanolic Acid ($C_{30}H_{48}O_3$) 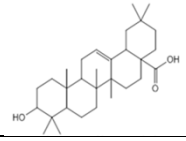	• anti-inflammatory [332] • anti-hyperlipidemic [332] • hepatoprotective [332]
Triterpenoid	Friedelin ($C_{30}H_{50}O$) 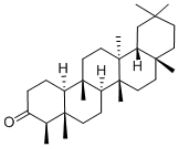	• analgesic [333] • anti-tumor [334] • anti-inflammatory [333], • anti-pyretic [333]
Tetraterpenoids	Lycopene ($C_{40}H_{56}$) 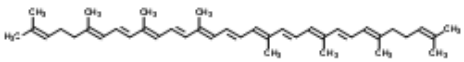	• natural pigment • anti-inflammatory [335] • anti-atherogenic [335]
Diterpenes	Cafestol ($C_{20}H_{28}O_3$) 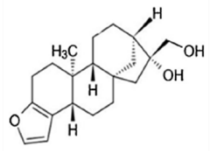	• anti-angiogenic[336] • anti-tumor [337] • anti-carcinogenic [217, 338] • analgesic [339] • anti-diabetes [340]
	Kawheol ($C_{20}H_{26}O_3$)	• anti-carcinogenic [217, 338] • analgesic [339]

	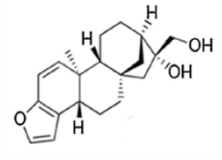	
	16-*O*-methylcafestol ($C_{20}H_{28}O_3$) 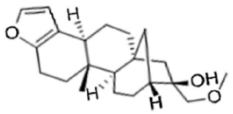	• anti-carcinogenic [217, 338]
Sterols	Stigmasterol ($C_{21}H_{30}O_3$) 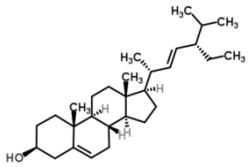	• synthesis precursor of hormones like progesterone, androgens, estrogens and corticoids [341]

Friedelin in Turkish oak cork – Cork contains approximately 2 % of triterpenoids, such as friedelin, betulin and β-sitosterol [230-231]. Many triterpenoids have been reported to possess biological activities [199]. In particular, friedelin (3-friedelanone, $C_{30}H_{50}O$) is a pentacyclic triterpene ketone first isolated from cork in the late 1700's by Chevreul [342], and it is the major component of dichloromethane and supercritical CO_2 extracts of cork [230-231, 342].

When working with *Q. suber* cork, Castola et al. [231] did not find significant differences in friedelin concentration between SFE and dichloromethane extracts. In their case, they ranged nearly around 20.4 wt.% (SFE) and 21.0 wt.% (Soxhlet extraction), i.e. the concentration ratio was ca. 0.97. This fact presents an advantage of the SFE of Q. *cerris* that may be exploited with interest for commercial application after careful optimization and economic evaluation of the process. As far as we know no sound commercial application has yet been established for friedelin, despite the evidences of its effective performance as anti-tumor [334], anti-inflammatory [333], analgesic [333], and antipyretic [333] agent. Furthermore, a method comprising conventional solid–liquid extraction followed by purification of friedelin has been patented for extracts from cork and cork-derived materials by Corticeira Amorim (a Portuguese cork industry company) [343], which is a signal of the commercial interest around thiscompound.

Lycopene in tomato wastes and gac fruit – The SFE work on tomato wastes has been driven by the interest and opportunity to exploit these residues as a source of lycopene, which is a carotenoid with remarkable red color that can be applied as a food additive. In addition lycopene exhibits antioxidant features and some studies suggest this molecule is linked to anti-carcinogenic and anti-atherogenic effects [335]. As a result, lycopene is a compound that currently raises interest to food, cosmetic and pharmaceutical industries.

From a technical point of view, a challenging aspect of the lycopene extraction through conventional methods relies on solubility problems: it is insoluble in water, but has large affinity to organic solvents such as chloroform and dichloromethane. These solvents not only motivate relevant concerns at toxicity and harmfulness levels, but their separation from the extracts can also be rather demanding [344].
In this context, tests using SFE technology have succeeded to circumvent the referred technical hurdles, particularly through the employment of carbon dioxide as supercritical solvent [67, 71, 73, 234].

Sterols in water hyacinth and moringa – The water content present in water hyacinth can attain values as high as 95 % of its weight. Moreover, organic matter comprises only 3.5 % of the raw weight, being able to reach a fraction higher than 75 % when in a dry basis [345]. The lipophilic and polar extractives of *E. crassipes* morphological parts (flower, leaves, stalks and roots) were only addressed recently, through the work of Silva et al. [346], who analyzed features such as extraction yields, chemical composition of extracts, and also antioxidant activity and total phenolics. In that study it was shown that, depending on the morphological part, sterols represented 19-23 wt.% of the extracts. Moreover, the major contribution was given by stigmasterol, whose individual concentrations reached up to 15 wt.% in the extracts of stalks and leaves, and 4437 $\mathrm{mg\,kg^{-1}_{biomass}}$ ([346]. However, other sterols such as β-sitosterol and campesterol (methylcholesterol) [346-347] may be cited.

As a result, a potential valorization strategy for water hyacinth may encompass its exploitation as a source of sterols (particularly stigmasterol), which are highly sought in view of their medicinal properties [348]. Stigmasterol is employed in several chemical processes designed to yield numerous synthetic and semi-synthetic compounds for pharmaceutical industry [349]. It acts as a precursor in the manufacture of synthetic progesterone, vitamin D3, as well as an intermediary in the biosynthesis of androgens, estrogens, and corticoids. Research has indicated that stigmasterol may be useful in the prevention of certain cancers (ovarian, prostate, breast, and colon cancers), cholesterol biosynthesis inhibition and offers a potential anti-osteoarthritic effect [350-351].

As for the moringa seed, the plant seed contains up to 40 % of the so-called ben oil, whose composition comprises high contents of oleic, behenic palmitic and stearic acids [352]. Due to the vast properties of this oil, it has a wide range potential applications: it can be used inthe cosmetic industry as an emulsifier, lubricant in the mechanicalindustry and even for medicinal purposes in the pharmaceutical business [251]. Moreover, ben oil can also be used as edible oil, sinceits fatty acids composition resembles that of olive oil [353].

2.3 SFE TECHNOLOGY

2.3.1 CO_2 AS A SUPERCRITICAL SOLVENT

A supercritical fluid (SFC) is a substance or mixture above its critical pressure and temperature. For a pragmatic appraisal of their interest, it is worth mentioning the typical orders of magnitude of some physicochemical properties of SCFs, particularly: density, that can be as low as 0.1 $\mathrm{g\,cm^{-3}}$ and reach liquid-like values of 0.85-0.95 $\mathrm{g\,cm^{-3}}$; viscosity, which is close to values of the respective gas state; and diffusivities, which may be up to two orders of magnitude greater than those of liquids [1, 354]. Furthermore, the solvent power of SCF can be tuned by small changes in the operational conditions (pressure and/or temperature), depending on the application and technical goal.

Bringing a fluid to supercritical conditions normally requires considerable heating and compression efforts. This is one of the constraints for a number of substances prone to be exploited as supercritical solvents in industrial processes, and responsible for the price of the industrial equipment and operational costs. Solvents usually considered for SFE applications include, among others, ethane, propane, ammonia, water, and carbon dioxide. However, CO_2 is generally preferred for research and industrial applications due to the milder $P - T$ conditions required to attain the supercritical region ($T_c = 31.1$ °C and $P_c = 73.8$ bar). In addition, it does not require explosion-proof apparatus (as those necessary to operate with supercritical propane and ethane), it is non-corrosive (in contrast to supercritical water), non-toxic and chemically inert [354]. Moreover, CO_2 has a practically null surface tension, which is advantageous to wet and penetrate easily most of the solid materials [84].

2.3.2 EXTRACTION PROCESS

A typical layout of an industrial SFE plant is depicted in Figure 2.10. It includes an extractor operating in a closed loop recycling system for carbon dioxide and a modifier. Semi-continuous operation has been reported to be simpler and almost as productive as continuous operation of SFE processes, thus being the preferable mode to operate [4]. In contrast, lab scale installations for research rarely contemplate CO_2 reutilization.

In a system like the one illustrated in Figure 2.10, pressurized carbon dioxide is kept in the liquid state in a storage tank (right side of the scheme). To initiate the process, liquid CO_2 is pumped, heated, mixed with cosolvent in the desired proportions, and fed to the extractor (already filled with the biomass). Then, a semi-continuous operation starts as supercritical solvent flows through the extractor bed, leaves the extractor with the dissolved solutes, and is depressurized by a backpressure regulator (BPR) valve. The solvent power of the resulting mixture is very low, consequently the extracts precipitate (in a collection vessel) with the

cosolvent, and the gaseous CO_2 can be recycled to a condenser and promptly reused or saved in a liquid CO_2 storage tank. Depending on the specificities of the process, the final expansion may be performed in a cascade mode allowing a fractional recovery of the extract in multiple collection vessels submitted to a stepwise pressure profile. An alternative to the layout of Figure 2.10 is depicted in Figure 2.11. Here the arrangement comprises three extractors in series for trim bed operation, where one extractor is brought offline periodically in order to substitute the exhausted biomass by fresh material.
The tendency to adopt green solvents is linked to the broader goal of sustainability in chemical processes. SFE can fulfill this objective by a thorough rethinking of the separation processes towards smaller, cleaner and more energy-efficient solutions, via process intensification as proposed by Stankiewicz and Moulijn [355].

SFE is typically compared to conventional SLE with organic solvents, which still stands as reference for industrial extraction processes. In this context, an apparent drawback of SFE is related to operation at high-pressure, which demands more expensive apparatus than for SLE (where operation is at atmospheric pressure or near). However, such appraisal is inadequate since it limits the scope of the analysis to a direct comparison between equipment.

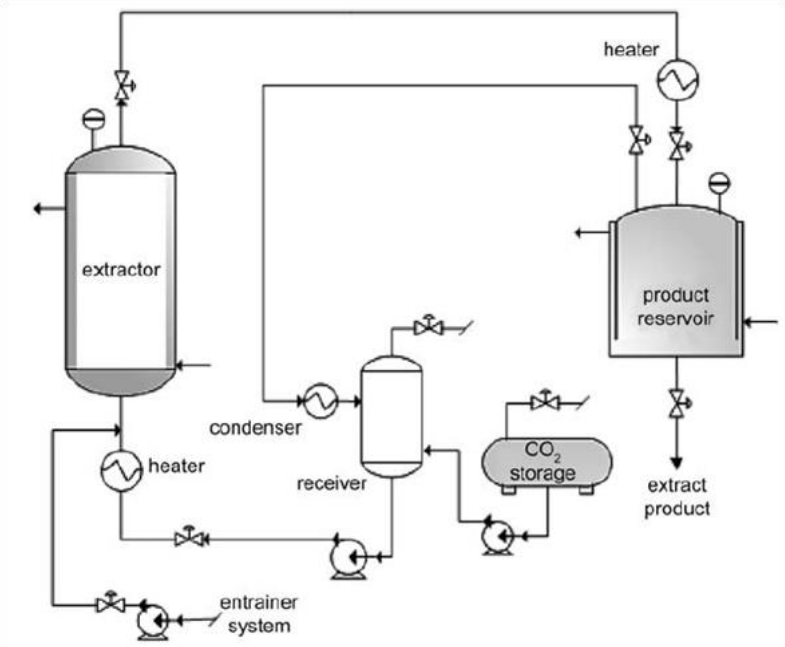

Figure 2.10 – Typical industrial layout of an industrial SFE process comprising a SCF and a cosolvent. Adapted from ref.[356].

In a broader perspective, SLE always demands subsequent separation units to recover the solvent, whereas a simple decompression is sufficient with supercritical fluids. If carefully inspected a SLE encompasses frequently a set of operations to: (1) obtain the extract from the solid matrix using an organic solvent; (2) separate the solvent from the extract and raffinate

streams, which is usually accomplished by distillation or evaporation/crystallization; and (3) avoid moisture accumulation in the recycled solvent (e.g. methanol, ethanol), since water may penalize solutes solubility.

The third step usually comprises a rectification unit and it may be mandatory to ensure the efficiency of step (1). Remarkably, in SFE steps (2) and (3) are not required for continuous recycling of the solvent, at least when a cosolvent is not present. Moreover, the operation of SFE units with pure SC-CO_2 does not tie the process to ATEX (equipment for potentially explosive atmospheres; from French: *Appareils destinés à être utilisés en ATmosphères EXplosibles*) directive requirements. Certification regarding explosive industrial atmosphere evidences how SFE can be a lower risk process than SLE, despite the high-pressure conditions involved in the former. In the whole, these remarks highlight how the option towards SFE should not be trapped in simplistic comparisons to conventional SLE. Leaving the above mentioned aspects out of consideration disturbs the fair appraisal of the advantages of SFE technology.

An enlightening example of SFE for intensification and integration of industrial processes can be found in the pulp and paper integrated biorefinery illustrated in Figure 2.12. Here, a SFE unit is introduced to remove bioactive extracts from byproducts (bark) produced in the pulp mill, without substantial loss of their calorific value [357]. Therefore, exhausted bark can be burned in the biomass boiler for energy recovery maximizing available resources. This SFE process has been studied in detail [83, 85, 205, 358-359] to produce extracts enriched in bioactive components from the bark and leaves of *Eucalyptus globulus*, the dominant species of the Portuguese pulp and paper industry.

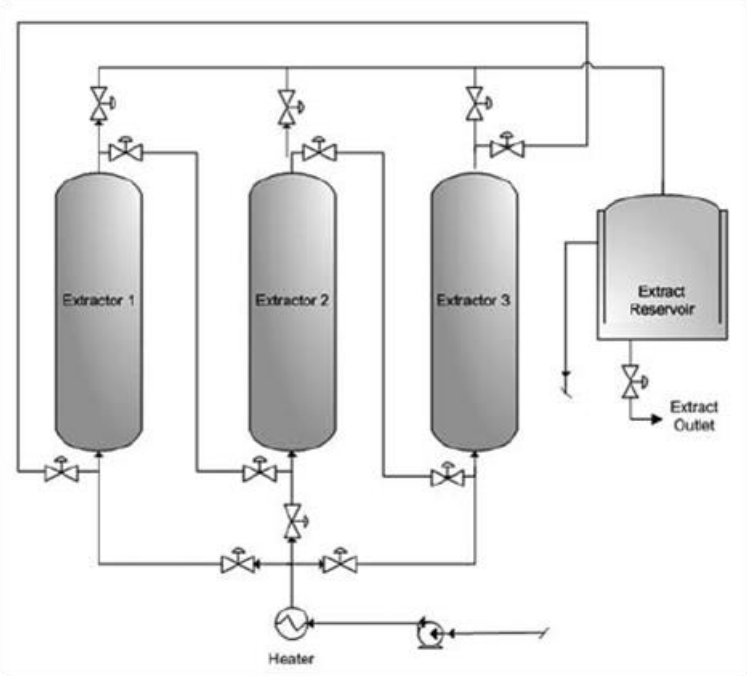

Figure 2.11 - Industrial layout of a SFE process comprising three extractors in series prepared for trim bed operation.

A similar approach has been reported by Albarelli et al. [360] for SFE of Annato seeds (source of bixin, a valuable natural colorant) within a sugarcane integrated biorefinery. Interestingly, in the sugarcane refinery a CO_2 stream is formed by enzymatic hydrolysis for second generation ethanol production. Hence, in this case, the supercritical solvent (and eventually ethanol as cosolvent) rather than the vegetal raw material is taken from the parent process. The synergies related to the consumption and production of utilities can be assumed to follow the same rational explained for the pulp mill integrated biorefinery (Figure 2.11), i.e. taking advantage of the calorific value of the residual biomass in a downstream biomass boiler.

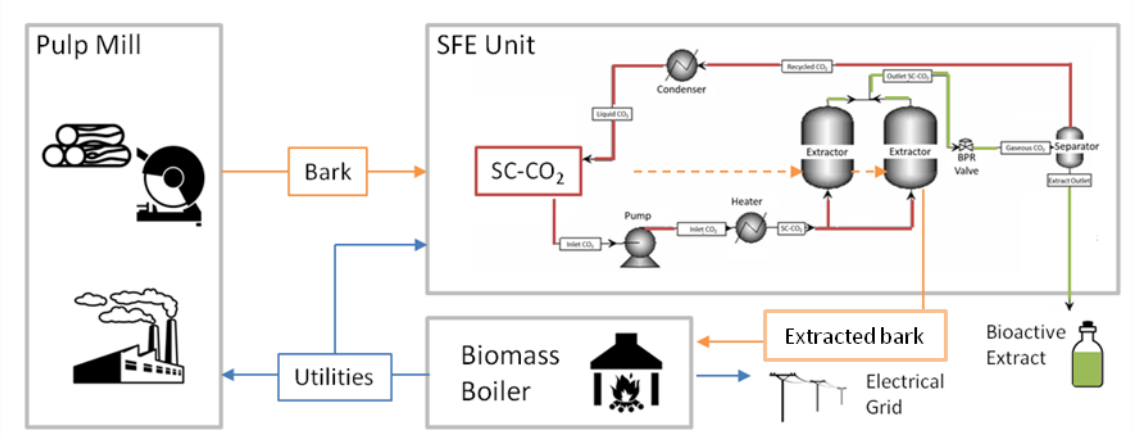

Figure 2.12 – Biorefinery concept for pulp mill with an integrated SFE unit.

2.3.3 OPERATING CONDITIONS

Pressure & Temperature - SFE is traditionally defined as a high pressure (P) technology and this variable is in fact of supreme importance for many technical and economic aspects of this process. The most direct property prone to be affected by pressure variations is density (ρ), which can be used to perceive how close SC-CO_2 reaches a liquid-like solvent power. When studying the influence of density on SFE behavior (intimately related to solvent power), pressure is a much preferable variable to tune its values as it offers considerably wider manipulation margins than temperature. In fact, while pressure usually ranges up to 8 or 10 times the usual minimum values investigated in experiments (c.a. 100 bar), temperature is many times restricted to a narrower window, i.e. up to 3 times the common low 40 °C.

Figure 2.13 presents a distribution of SFE operating conditions mostly found in literature (543 publications). For each work, the maximum and minimum densities studied were plotted in $P-T$ coordinates, being possible to observe that essays typically focus on pressures from 100 to 400 bar. Within this interval, and taking into account the temperature window considered, densities can range from 200 to 900 kg m^{-3}, as revealed by the density lines superimposed in Figure 2.13. The interdependence between pressure and density can be fully disclosed in this graph: for instance, a sensitive interrelation is visibile at low pressures (e.g. 100 bar), where

densities can oscillate up to 70 % from 40 °C to 100 °C, while at higher pressures (e.g. 400 bar) the corresponding oscillation only reaches a maximum of 20 %.

It is noticeable in Figure 2.13 that most works concentrate in temperature values within 40 to 60 °C, yet this accumulation is greater around the lower value. This trend reveals that researchers have been eager to explore the pressure impact on results at lower temperatures, probably due to the higher degree of density variation on this region but also owing to concerns regarding thermal degradation of extractable labile compounds, equipment limitations and costs policy.

The predilection to work at 40 °C implies that the opportunity to assess the impact of temperature on SFE processes at higher pressures (e.g., higher than 300 bar) is being much less considered. Since density suffers a lower degree of variation at higher pressures and kinetic variables exhibit weaker dependences on pressure in comparison to temperature, the interesting opportunity to study the influence of temperature via vapor pressure (solubility) and transport properties is being discarded. In this respect, Figure 2.14 presents, without loss of generality, the $P-T$ dependence of ursolic acid diffusivity (D_{12}) and solubility (y*) in SC-CO_2, and also of CO_2 density. Along the displayed ranges one can depict that diffusivity becomes favorable when approaching 200 bar and 100 °C while solubility exhibits a distinct trend, being its best pole around 500 bar and 100 °C. In fact, y*, D_{12} and density exhibit their maxima at distinct $P-T$ values. Considering that density is many times used as general (though simplistic) criterion to choose operating conditions or to support the discussion of experimental results, the elucidating example from Figure 2.14 stresses that the optimum $P-T$ conditions of a SFE process are those that best suit the trade-off between kinetics and equilibrium behaviors. In addition, results also show (see Figure 2.13) that researchers exhibit a preference to approach density variations through pressure manipulation rather than temperature.

Another fundamental variable is the selectivity of SC-CO_2 to distinct target molecules, which combines all previous dependences in a very competitive way. Taking into account that temperature influences similarly the vapor pressure of all extractable compounds, their distinct solubilization in the supercritical solvent becomes a matter of both temperature and pressure. Moreover, as the intermolecular interactions are the key factor of the separation, the role played by cosolvents is of great importance (topic discussed below).

Finally, the so-called tunable properties of supercritical solvents that contribute to the attractiveness of this technology, comprise, among other possibilities, the chance to play with temperature at near constant density regions (high pressure), but our compilation of works show that it is not being very explored by researchers in higher pressure experiments.

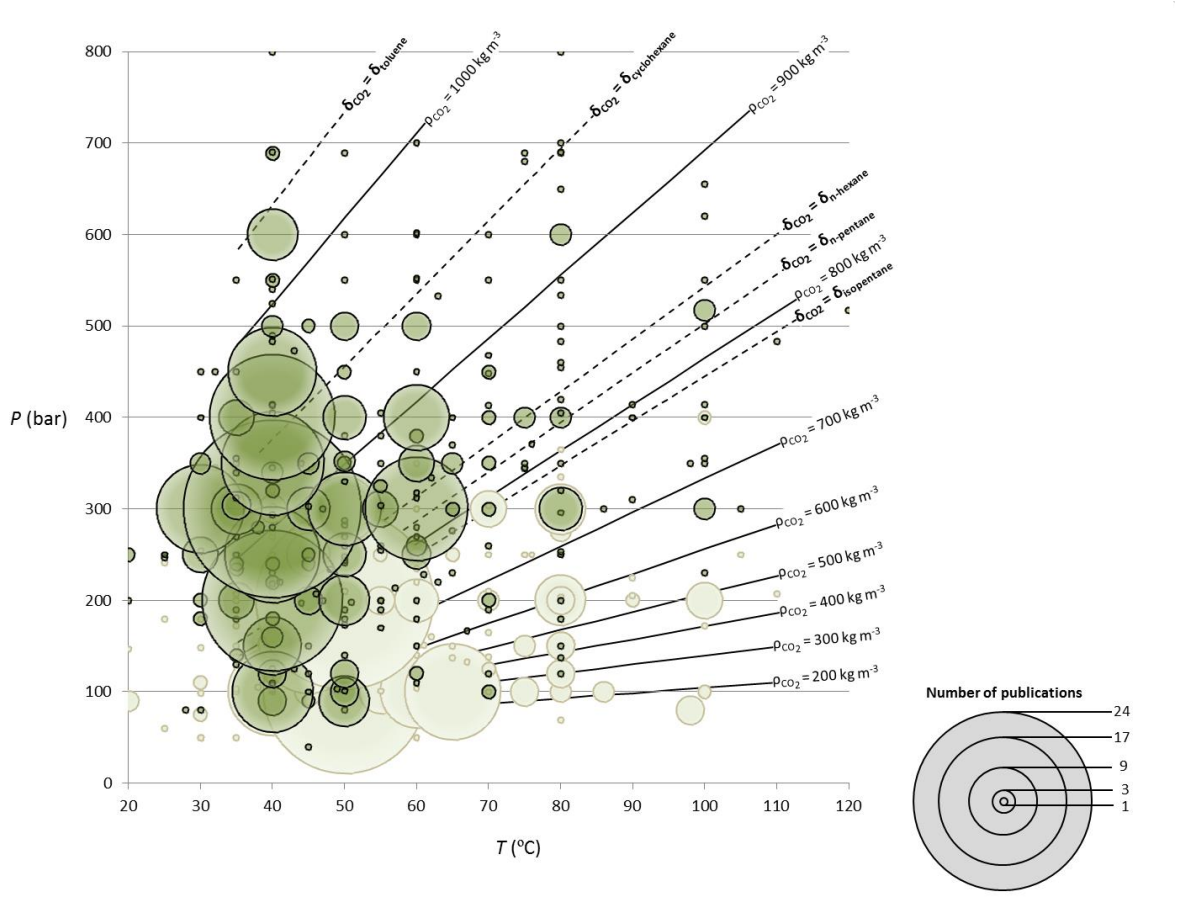

Figure 2.13 – Most common operating conditions for the SC-CO_2 extraction of vegetable matrices, for a total of 543 publications (Table S1). Darker clouds represent regions of higher CO_2 densities in each work, and lighter circles delimit the regions of lower CO_2 densities. Superimposed are lines of constant CO_2 density and Hildebrand solubility parameter.

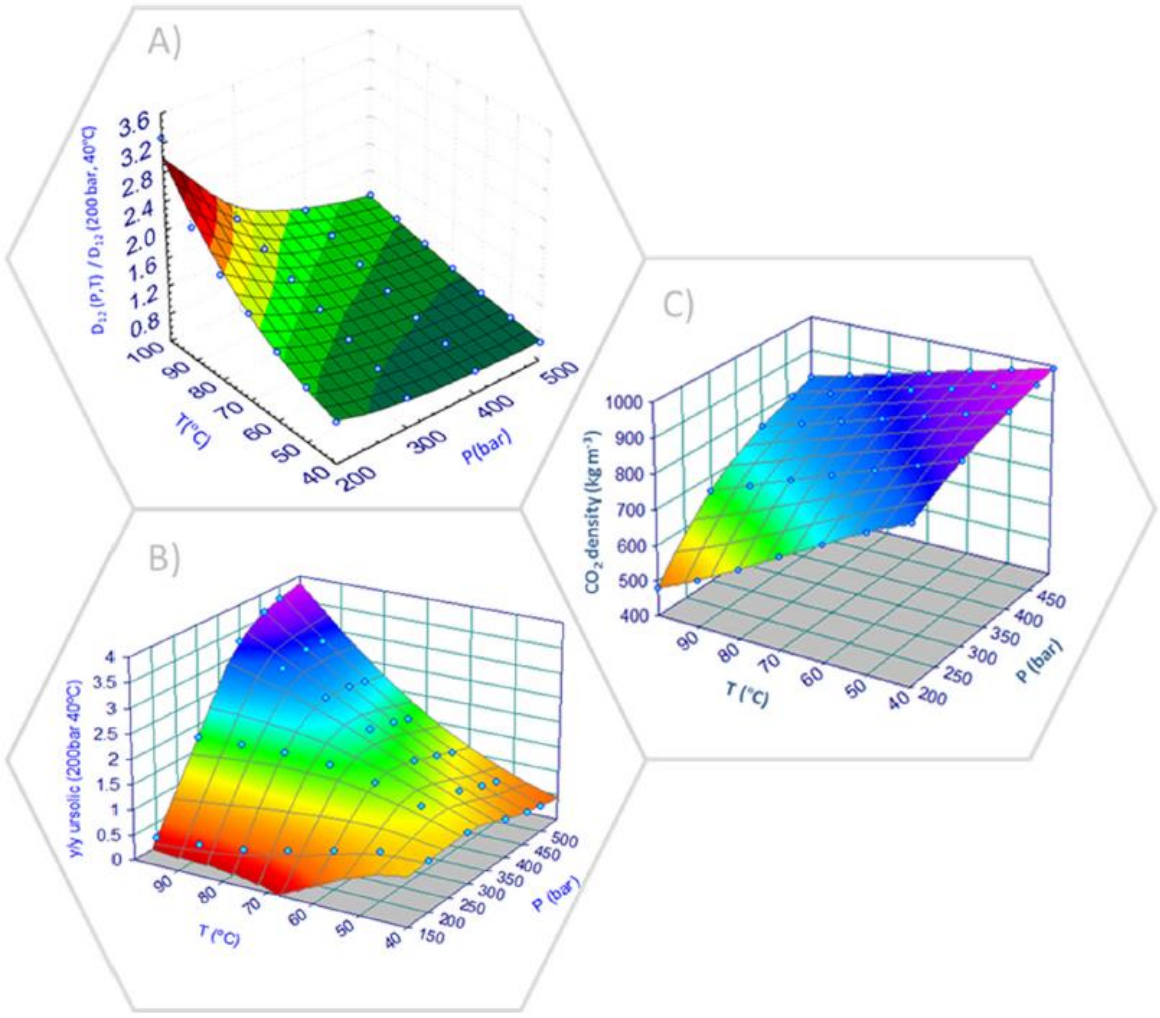

Figure 2.14 – Influence of pressure and temperature upon (A) ursolic acid diffusivity in CO_2, (B) ursolid acid solubility in CO_2, and (C) SC-CO_2 density. Data calculated from Wilke-Chang [361], Peng-Robinson [362], and Pitzer and Schreiber [363] equations.

Flow Rate - While P and T affect the thermodynamic (density and solutes solubility) and transport properties (viscosity and diffusivity), solvent velocity is an independent variable that influences directly the axial dispersion, the convective mass transfer coefficient, and the accumulation in the bulk under semi-continuous operation (i.e. supercritical phase). Therefore, it may be rationally incremented to enhance the extraction rate upon the reduction of the film resistance to mass transfer and bulk concentration. As the external film diffusion (here measured in terms of the convective coefficient, k_f) and the global driving force are increased, a positive effect on extraction yield is achieved.

When analyzing SFE results from the perspective of flow rate, the chief variable is the surface velocity or, equivalently, the interstitial velocity through the bed. A systematization of SFE works in terms of interstitial velocities is not feasible in this review due to lack of information about extractors and beds, but an illustrative picture can be provided based on the values of SC-

CO_2 flow rate per mass of bed reported in the compilation of Table S1. Considering that the final goal of scientific research on SFE is its commercial implementation, it would be positive if upcoming works on the field could provide more information regarding extractors and beds. In this sense, both academic and industry readers would benefit from richer data regarding bed length (L_b), bed diameter (D_b), bed porosity (ε_b) and particle size (d_p). This would allow a better disclosure and assessment of the hydrodynamics impact on experimental results. In addition, these data are also very useful to interpret scale-up experiments and approach industrial reality.

Figure 2.15 presents an analysis of 231 SFE works, where individual flow rates were combined with extraction time and graphed in $kg_{CO2}\ kg^{-1}_{raw\ material}$ units in abscissa. This study points out that 40 % of the works comprised a CO_2 usage ranging from 0 to 40 $kg_{CO2}\ kg^{-1}_{sample}$, and that the other 40 % are between 40 and 140 $kg_{CO2}\ kg^{-1}_{sample}$. Even though this information cannot be taken as a correct measurement of the extraction efficiency, it at least provides worthwhile hints of typical energy and utilities costs from pumps, heating and cooling steps that SFE processes always imply.

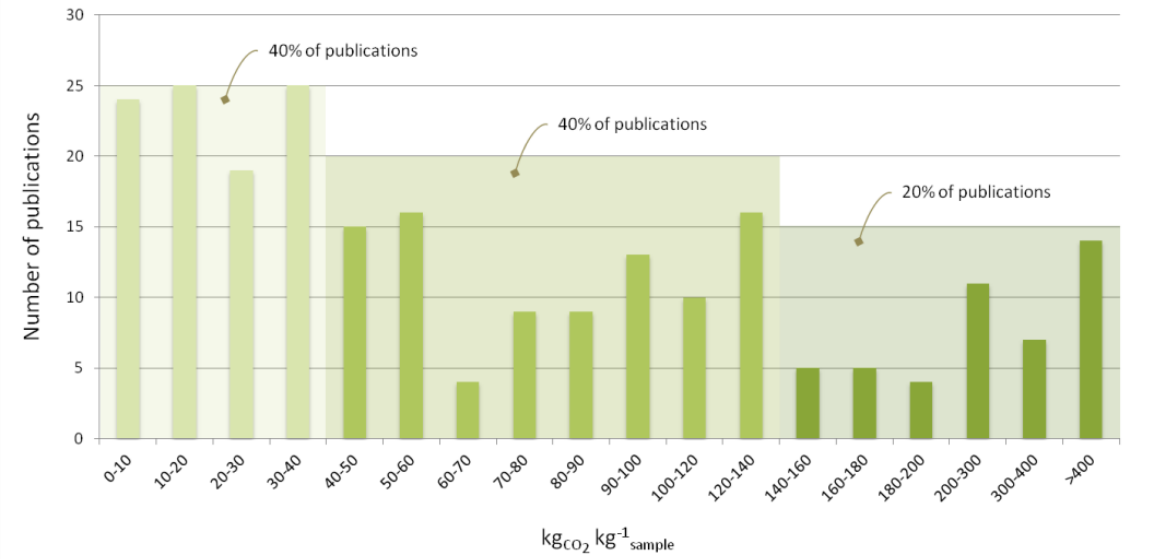

Figure 2.15 – Maximum amounts of SC-CO_2 used in the SFE of vegetables matrices for a total of 231 publications considered.

Some of the data of Figure 2.15 were taken from works where extraction curves were measured, leading to yields and concentration profiles along time or spent CO_2. Extraction curves are vital for the correct assessment of kinetic aspects as they allow the visualization of distinct extraction regimes (characterized by distinct extraction rates) and the inspection of the mechanisms that govern the separation in different moments.

If a low interstitial velocity (low flow rate) is chosen, the film resistance and/or the accumulation in the bulk may prevail over intraparticular diffusion and solubility issues, thus

diminishing the rate of extraction by itself. On the other hand, if the extractor is being run under very high interstitial velocity, the most representative sources of limitation may be therefore attributed to solubility and/or to intraparticle diffusion. Nonetheless, high velocities may also lead to a misuse of SC-CO_2 that will then be spent in excess at the expenses of non-optimized utility and energy costs. This aspect is important to increase the economic viability of a SFE unit.

Figure 2.16 illustrates an optimization of flow rate by graphing cumulative curves of total extraction yield of *E. globulus* bark measured at 200 bar, 40 °C, with 5 % (wt.) of ethanol, for different CO_2 flow rates [84]: 6, 12 and 14 g min^{-1}. When Q_{CO2} is doubled from 6 to 12 g min^{-1} a relevant enhancement of the extraction rate is observed. An additional increase to 14 g min^{-1} shows no further significant yield enhancement. As a result, it was considered that 12 g min^{-1} is an optimized value for SFE flow rate since it originates an interstitial velocity that maximizes the rate of extraction while simultaneously minimizes utilities and energy costs. This is an elucidative example of a rational selection of a flow rate value.

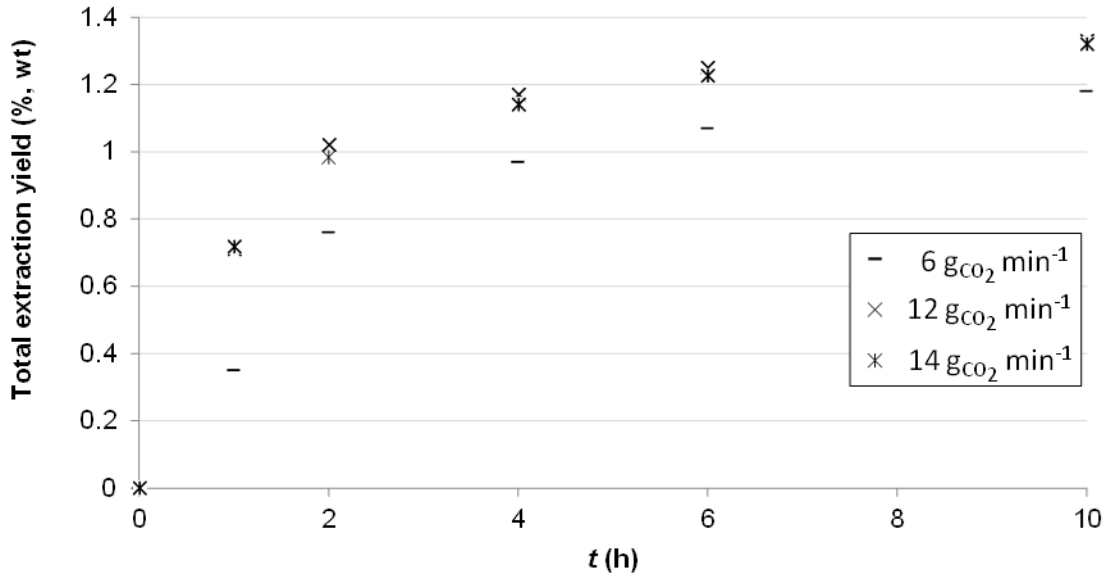

Figure 2.16 – Cumulative curves of total extraction yield of *E. globukus* bark at different CO_2 flow rates. Fixed conditions: 200 bar, 40 °C, 5 wt.% ethanol. Data taken from [84].

Cosolvent - With regard to the use of modifiers, Figure 2.17 shows a statistic of the most employed cosolvents. The chief reason for adding a second solvent to the supercritical phase relies on the tunable affinity to polar solutes that modified SC-CO_2 allows. This is the prime reason why 38 % of 441 publications reviewed in this work (that contain the necessary information) include at least one experimental assay with modified CO_2.

The application of cosolvents in SFE works has been unsurprisingly dominated by ethanol, which was selected in 53 % of the works involving entrainers (see Figure 2.17). Ethanol is an innocuous solvent both at human health and environmental levels (like SC-CO_2) and this is a strong advantage comparing to *n*-hexane or even methanol, particularly when SFE is devoted to applications in food, cosmetic or pharmaceutical industries. Besides the referred advantages, ethanol is substantially polar (1.69 D [361]) which means that the addition of small amounts may increase expressively the polarity of the supercritical solvent.

In addition, methanol comes second with a share of 21 %, and is followed by water and dichloromethane, with 5 % and 3 % each, respectively. Despite being more polar than ethanol, methanol raises hazard concerns to human health, a fact that discourages an extended use of it. In fact it is being progressively abandoned nowadays.

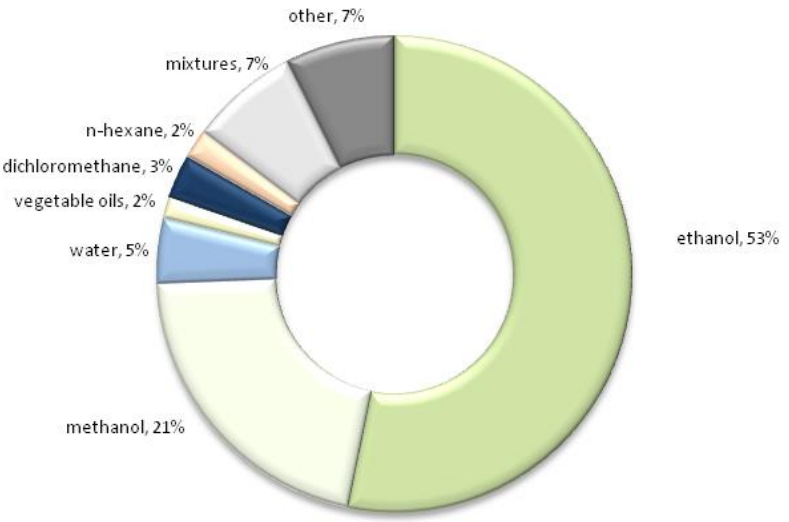

Figure 2.17 – Most employed cosolvents in SFE of vegetables matrices, based on 166 SFE publications of database.

A noteworthy aspect of SFE works with modified CO_2 is that they are implemented in two distinct ways: the more conventional procedure involves the mixing of the SC-CO_2 with the cosolvent in a fixed proportion along time, which requires a pump and independent feed line for each fluid, while the alternative is through the impregnation of the matrix with the cosolvent at the onset of the experiment, followed by the extraction with pure SC-CO_2. While the former approach is commonly characterized in terms of the modifier content in the supercritical mixture, the latter is usually described in term of the total quantity of cosolvent impregnated. To the best of our knowledge there are no works targeting a comparative study of the two techniques, reason why carefulness should be given when comparing works that employ distinct cosolvent addition procedures. Additionally, more accuracy is recommended when referring the concentration of cosolvent, particularly regarding whether mass, volume or molar basis is used to describe the addition percentages.

With respect to the impact of cosolvents on results, the typical approach involves the comparison between the modified SC-CO_2 and the pure SC-CO_2 results. This provides experimental arguments to check if the inclusion of a cosolvent in the process is worthwhile from the point of view of yields or extract concentrations enhancement. A less explored approach is the comparison of the impact of different cosolvents on results. In this respect, Table 2.2 presents experimental measurements concerning SFE of caraway (*Carum carvi* L.) seeds using eight different CO_2 modifiers under identical operating conditions [276]. The Hildebrand solubilities for each cosolvent (at 25 °C) are also given in Table 2.2 to highlight their different polarity. One of the objectives of the authors was to assess if modified SC-CO_2 could maximize the carvone concentration in caraway seed oil, which enhances the final quality of the product. The results from Table 2.2 reveal two important facts: modifiers failed to enhance carvone content in the oil as desired, but they did affect the extraction yields obtained. Despite the fact that the various supercritical mixtures provide higher extraction yields η (wt.%) in comparison to pure SC-CO_2, a negative correlation of 80 % was found between η and δ. Being negative, it means that from an extraction yield perspective the option towards the most polar cosolvent (methanol) is the less preferable (it only enhances yield results by 21 %). Less polar cosolvents such as chloroform or toluene increase the extraction yield in greater extents, 41 % and 33 %, respectively.

Table 2.2 – SFE results of caraway (*Carum carvi* L.) seeds using eight different CO_2 modifiers at 400 bar and 80 °C. Data taken from [276]. Correlation between extraction yield (η) or carvone concentration C in extracts and the Hildebrand solubility parameter (δ) of cosolvent.

Modifier 10 % (vol.)	$\delta_{cosolvent}$ @ 25 °C ($MPa^{0.5}$)	Extraction yield η (wt.%)	Carvone conc. C (wt.%)
n-hexane	3.6	3.23	57.53
Toluene	4.4	3.25	57.22
Chloroform	4.5	3.44	58.11
Acetone	4.6	3.3	57.89
Dichloromethane	4.9	3.24	57.16
Acetonitrile	5.8	2.91	57.11
Ethanol	6.3	2.85	57.89
Methanol	7.1	2.95	57.77
Pure CO_2	3.5	2.43	57.97
		R^2 (δ vs. η) = -80 %	R^2 (δ vs. C) = 18 %

The very weak correlation (18 %) between the modifier Hildebrand parameter and carvone concentration is a straightforward indicator of null selectivity provided by the different co-solvents in this case. However, one should bear in mind that the unexpected lack of selectivity observed in many systems may also be due to the extraction time, which in case of being too high can lead to a period of preferential solute extraction followed by the undistinguished

uptake of other compounds. In such situations extraction curves can provide richer information about cases of apparent lack of selectivity.

Another noteworthy aspect from Table 2.2 emerges from the comparison between the results achieved with pure SC-CO_2 (δ=3.5 $MPa^{0.5}$) and its modification with *n*-hexane (δ=3.6 $MPa^{0.5}$). Despite the close Hildebrand parameters values of the two molecules, results evidence that the modification leads to a global yield 1.33 times greater than when only CO_2 is employed. This example clearly expresses how supercritical fluid-solid systems that involve modified SC-CO_2 (for which there is a lack of equilibrium data and properties) and natural matrices (which typically comprise a mixture of solutes) are challenging media to be studied.

As far as water is concerned, the circumstances of working with this cosolvent are special given that most vegetable matrices typically exhibit natural moisture. This is the reason for the common preliminary drying stage before SFE takes place. However moisture content can only be typically reduced to a minimum level rather than completely removed from the matrix.

In cases where water can be technically employed with success as cosolvent, the drying stage can then be softer and optimized, leading to energy and utility savings. Besides these savings, water is obviously an inexpensive cosolvent to include in a SC-CO_2 process, being this a motive that fosters even more its potential inclusion in commercial SFE units. Nonetheless the economic advantages are only attractive if such SC-CO_2 modification leads to an enhancement that justifies this option. There are examples in literature attesting an effective enhancement brought about by water addition. It is the case of SFE of andrographolide from *Andrographis paniculata* Nees leaves [187] (see Figure 2.18) whose results reveal that water is able to increment the concentration of the target compound in supercritical extracts in a comparable degree of ethanol. According to this investigation, 15 % of water (the percentage basis is not mentioned) increases the concentration of andrographolide in extract from 61.6 % to 84.3 %. In a different application, it has been demonstrated that water favors a selective removal of caffeine from green tea in relation to the use of ethanol [364]. In the same study, the selectivity of water as cosolvent for caffeine extraction (in relation to epigallocatechin gallate) was shown to be 3.6 times greater than when ethanol was employed.

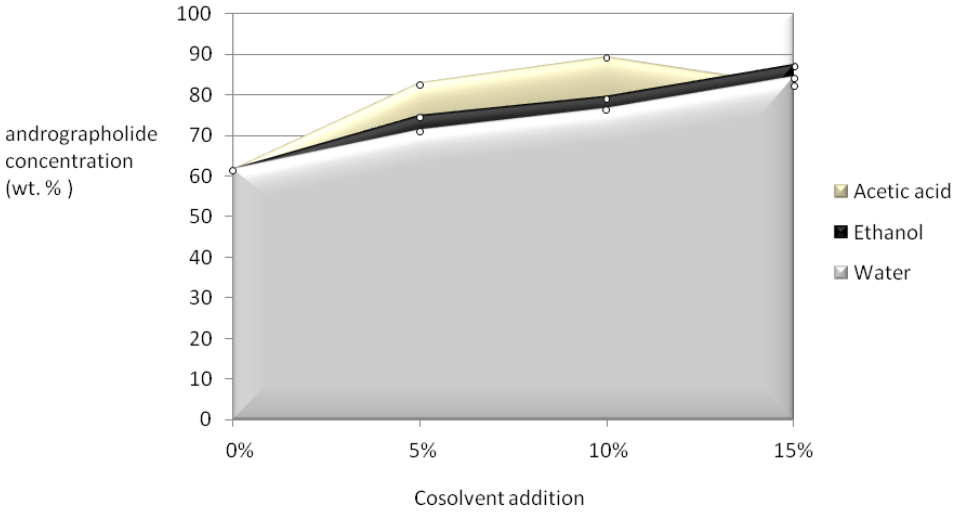

Figure 2.18 – Andrographolide concentration enhancement in SC-CO_2 extracts of *Andrographis paniculata* Nees leaves upon addition of three different modifiers (water, ethanol and acetic acid) at 240 bar and 70 °C. Data taken from reference [187].

2.5 SUPPLEMENTARY MATERIAL

Table S1 - Publications comprising SFE vegetable raw materials from 2000 to 2013, and their respective features.

Scientific Name	Common Name	Plant Part	Target	Extraction Yield (wt.%)	*P* (bar)	*T* (°C)	CO_2 & Co-Solvent	Analytical Technique	Other Features	Ref.
-	Berries	fruit	phenolic	1.4-5.20	80-300	60	EtOH	GC-MS	Antioxidant activity	[365]
-	Tea	seed		7-30	300-400	60-80	10-20 $L_{CO2}kg^{-1}_{sample}$ 0-15 % EtOH	Gravimetric	Soxhlet extraction Sonication ANOVA	[366]
-	Cuphea	seed		28.1	270	50	15 $kg_{CO2}\,kg^{-1}_{sample}$	GC	Acid value Gardner color FAME	[367]
Abutilon hybridum, Malvaviscus drummondii, Pavonia hastata, Pavonia. lasiopetala,Sida spinoza	*Hibiscus*	seed		11.4	534	80	20 $L_{CO2}kg^{-1}_{sample}$	FAME GC-FID	Soxhlet extraction	[368]
Achyrocline satureioides	Macela	flower		87-96	200-300	30-35	4-16 $kg_{CO2}\,kg^{-1}_{sample}$	GC-MS	Modeling	[369]
Acori graminei	-	rhizome	β-asarone	2.5-3.0	80-140	35-55	960 $L_{CO2}kg^{-1}_{sample}$	GC-MS	Hydrodistillation	[370]
Agrimonia eupatoria *Agrimonia procera*	-	leaf		0-4.3	150-350	35-42	1 % EtOH	HPLC		[371]
Alkanna tinctoria	-		alkannin		50-300	30-80	30 $kg_{CO2}\,kg^{-1}_{sample}$	HPLC	RSM DoE	[372]
Allium cepa L.	Onion	bulb	sulphur	0.6-2.5	100-300	45-65	29-41 $kg_{CO2}\,kg^{-1}_{sample}$	GC-MS	Pilot scale Two-step ecompression system Steam distillation Soxhlet extraction	[373]
Allium cepa L.	Onion	bulb		0.005-0.025	103-287	309-50	200-800 $L_{CO2}kg^{-1}_{sample}$	Gravimetric Analysis GC-MS	Adsorbent bed	[374]

Allium cepa L.	Onion	bulb		0.295-4.68	160-240	35-45	66-220 $L_{CO2}kg^{-1}$ sample	GC-MS	RSM DoE	[375]
Allium sativum	Garlic	bulb	3-vinyl-4H-1,2-dithiin	0.81	100	45-55	3 $L_{CO2}kg^{-1}$ sample	GC GC-MS	DoE RSM	[143]
Allium sativum	Garlic	flake	allicin	0.4-2.3	150-450	35-65	97 kg_{CO2} kg^{-1} sample	HPLC	Modeling	[144]
Allium sativum L.	Garlic	flake		0.6-1.0	140-400	35-60	1.8 kg_{CO2} kg^{-1} sample	HPLC		[145]
Allium sativum L.	Garlic	clove	Allicin		240	35		HPLC		[376]
Alnus glutinosa (L.) Gaertn	-	bark	betulin, betulinic acid, lupeol	1.5-3.8	300-450	40-60	0-10 % EtOH 5-45 kg_{CO2} kg^{-1} sample	TLC GC–MS LC–MS RP-HPLC	Soxhlet ext.	[377]
Aloe barbadensis Miller	*Aloe vera*	leaf		0.13-1.5	350-450	32-50	0-20 % (vol./w) MeOH	Gravimetric Analysis	DoE Antioxidant activity	[378]
Alpinia oxyphylla	-	seed		1.36-2.80	20-40	45-65			RSM DoE	[379]
Amaranthus caudatus	Amaranth	seed	tocopherols, fatty acids, sterols	3.4-8.3	200-400	40	5600 l_{CO2} kg^{-1} sample	HPLC GC GC-MS	Ultrasound extractions	[290]
Amaranthus caudatus	Amaranth	seed		4-6	200-400	40	5.6 L_{CO2} kg^{-1} sample	HPLC GC-FID	Organic solvent extraction Ultrasound extraction	[380]
Amaranthus caudatus	Amaranth	seed	squalene	0-6	150-250	40-70	4000 L_{CO2} kg^{-1} sample	HPLC	Particle size effect	[269]
Amaranthus cruentus	Amaranthus	bract		0.5-4.8	100-300	40-70	100 kg_{CO2} kg^{-1} sample	Gravimetric Analysis	Soxhlet extraction Solubility Flow rate effect Modeling	[381]
Amaranthus paniculatus	Amaranth	seed	squalene		110-280	60-100	1200-600 L_{CO2} kg^{-1} sample	HPTLC	Modeling DoE	[270]
Ammi majus	-	seed	furocoumarins		250-550	40-80	10 % EtOH 20-160 kg_{CO2} kg^{-1} sample	^{1}H NMR	SC Chromatography	[299]
Anacardium occidentale	Cashew		anacardic acid	0-60	300	40-60		HPLC	Modeling	[136]
Anacardium occidentale	Cashew	fruit	Cardanol		225-300	50	8-45 kg_{CO2} kg^{-1} sample	GC-MS	Cost Optimization	[138]
Anacardium occidentale	Cashew	fruit		1-23	200-300	40-60		GC-MS	Modeling Flow rates effect	[137]

									Thermal method comparison	
Anacardium occidentale L.	Cashew	shell		1.1-4	147-294	40-60	4-11 $L_{CO2}kg^{-1}$ sample	Gravimetric Analysis	Fractionation	[36]
Andrographis paniculata	Hempedu Bumi	leaf	andrographolide		80-240	40-70	0-15 % EtOH 0-15 % H_2O 0-15 % Acetic acid	SEM X-ray diffraction HPLC	Purification objective	[187]
Andrographis paniculata	Hempedu Bumi	leaf	andrographolide		100	40		HPLC TLC	Modeling Particle sizes effect	[382]
Anemopsis californica	Yerba mansa	leaf		5-6	355	100	28 $L_{CO2}\,kg^{-1}$ sample	GC-MS	Steam distillation	[29]
Angelica archangelica L.	Angelica	root			90-120	40-60		GC-MS	Hydrodistillation	[383]
Angelica dahurica	-			2-4	250-350	44-50	21818-43636 $l_{CO2}\,kg^{-1}$ sample (75% EtOH/25 % H_2O)	GC-MS	DoE	[384]
Angelica gigas NAKAI *Angelica sinensis* *Angelica acutiloba*	*Angelica*	rhizome		0.48	296	80	60 $L_{CO2}\,kg^{-1}$ sample	GC-MS	Solid-phase microextraction	[385]
Angelica sinensis (Oliv.) Diels (Umbelliferae)		root	ferulic acid	0.8-4.0	300-500	45-65	0-40 $kg_{CO2}\,kg^{-1}$ sample EtOH	HPLC	Particle sizes effect	[386]
Anoectochilus roxburghii	-	herb	phytosterols β-Sitosterol, stigmasterol		250	45	50 $L_{CO2}\,kg^{-1}$ sample H_2O	HPLC APCI MS	Soxhlet extraction DoE	[292]
Apium graveolens L.	Celery	seed		0-23	100-200	45	10-150 $kg_{CO2}\,kg^{-1}$ sample		Modeling	[387]
Arbutus unedo L.	Strawberry	fruit	phenols	6.29-25.3 % (phenols)	150-300	40-80	30 $kg_{CO2}\,kg^{-1}$ sample 0-20 % (w/w) EtOH		RSM DoE Antioxidant activity	[388]
*Arrabidaea chica (*Humb. Bonpl.)		leaf	anthocyanins	0-3.6	300	40	0-20 % EtOH 0-140 $kg_{CO2}\,kg^{-1}$ sample	HPLC	Fractionation Organic solvent extraction	[389]
Artemisia absinthium L.	Wormwood	leaf + flower		0.75-3.66	90-180	40-50	88-447 $kg_{CO2}\,kg^{-1}$ sample EtOH			[390]

Artemisia annua L.	*Wormwood*	leaf	artemisinin	0-7	75-400	30-50	0-400 $kg_{CO2}\,kg^{-1}_{sample}$	GC-FID	DoE Hydrodistillation Soxhlet extraction Modeling	[267]
Artemisia arborescens L. *Helichrysum splendidum* (Thunb.) Less		leaf		0.1-0.4	90	50	14 $kg_{CO2}\,kg^{-1}_{sample}$	GC-MS	Hydrodistillation	[391]
Artemisia capillaris T.	-	whole plant	capillarisin		173	50	7.5 wt.% ethyl-acetate		Bioactivity test DoE RSM	[392]
Artemisia sieberi	*Wormwood*	aerial parts	camphor	1.7-14.9	101-304	35-65	1.8-4.2 $L_{CO2}\,kg^{-1}_{sample}$	GC GC-MS	Hydrodistillation DoE	[280]
Atractylode lancea	-	root		2.3-10.3	150-250	40-60	22-62 $L_{CO2}\,kg^{-1}_{sample}$	GC-MS	DoE	[393]
Atractylodis macrocephalae	Baizhu	rhizome		3.67-6.76	150-450	40-60	54 $L_{CO2}\,kg^{-1}_{sample}$			[394]
Azadirachta indica	Neem	seed		5-85	100-260	30-55	4.7-26 $L_{CO2}kg^{-1}_{sample}$ 0-10 % MeOH	HPLC	d_p, Q effects	[189]
Azadirachta indica	Neem	seed		5-70	100-260	35-60	0-2.7 $L_{CO2}kg^{-1}_{sample}$	Gravimetric	d_p effect Modeling Q effects	[191]
Azadirachta indica	Neem	seed		0-85	100-260	35-60	2-186 $L_{CO2}kg^{-1}_{sample}$	Gravimetric Analysis	Modeling Effect of particle size	[190]
Azadirachta indica A. Juss	Neem	seed	nimbin	0-0.02	100-260	35-60	12-53 $kg_{CO2}\,kg^{-1}_{sample}$	HPLC		[188]
Baccharis dracunculifolia	Baccharis	leaf	DHCA, PHCA, p-coumaric acid, kaempferide	2.4-4.7	200-400	40-60	85 $kg_{CO2}\,kg^{-1}_{sample}$	HPLC	Soxhlet extraction	[395]
Baccharis dracunculifolia	Baccharis	branch and leaf	E)-nerolidol; spathulenol	0.38	90-120	40-60	3-40 $L_{CO2}\,kg^{-1}_{sample}$	GC GC-MS	ODS trap (n-hexane) Hydrodistillation	[396]
Baccharis trimera	Baccharis	branch and leaf		1.7-2.3	90	40-70	80 $L_{CO2}\,kg^{-1}_{sample}$	GC GC-MS	Modeling	[397]
Baccharis trimera	Baccharis	stem and leaf		0.3-2.0	100-300	30-40		GC-MS	Modeling Solvent extraction	[398]
Betula pendula Roth	Birch	leaf	amino acids		100-400	35-100	MeOH–H_2O–acetonitrile	HPLC-FLD	Soxhlet extraction	[399]

Bixa orelana L.	Annatto	seed	carotenoid bixin	1-45	200-300	50-60	100 $kg_{CO2}\,kg^{-1}{}_{sample}$ 5 % EtOH	Gravimetric Analysis	Modeling Flow rates effect Particle sizes effect	[400]
Bixa orelana L.	Annatto	seed	bixin		100-350	30-50		GC-FID	Modeling	[401]
Bixa orelana L.	Annatto	seed	bixin	1.4-3.5	200-400	40-60	35-482 $kg_{CO2}\,kg^{-1}{}_{sample}$	UV–vis spectrophotometer HPLC	Economic analysis Scale-up Modeling	[402]
Borage officinalis L.	Borage	seed	ϒ-linolenic acid	0-0.18	0-350	30-60	3750-15000 $L_{CO2}kg^{-1}{}_{sample}$	GC	Soxhlet extraction	[403]
Borage officinalis L.	Borage	seeds	fatty acids	0-30	200-300	40-60	0-130 $kg_{CO2}\,kg^{-1}{}_{sample}$	GC	Modeling Soxhlet extraction	[256]
Borago officinalis L.	Borage	seed	caprylic acid methyl ester	0.1-24.3	100-350	40	1-20 $kg_{CO2}\,kg^{-1}{}_{sample}$ 0-2 % EtOH	GC		[404]
Borago officinalis L.	Borage	seed		0-30	200-300	55	0-60 $kg_{CO2}\,kg^{-1}{}_{sample}$		Bed length effect Flow rate effect SEM	[405]
Borago officinalis L.	Borage	seed		9-57	150-250	30-60	1000 $L_{CO2}kg^{-1}{}_{sample}$	HPLC GC-MS	Soxhlet extraction	[406]
Brassica napus	Rapeseed	seed		5-12	300	40	10-130 $kg_{CO2}\,kg^{-1}{}_{sample}$	Gravimetric Analysis	Modeling	[407]
Brassica napus	Rapeseed	seed		7.7-28.1	200-300	40-60	6-26 $kg_{CO2}\,kg^{-1}{}_{sample}$	GC-MS	RSM Modeling Soxhlet extraction	[408]
Brassica napus	Rapeseed/ Sunflower/ Soybean	seed		18-47	517	100		Gravimetric Analysis	Solvent extraction Vortex extraction	[177]
Brassica napus L.	Canola	press cake	phenolics	2.1-10.3	300-500	40-60	10 % EtOH 61 $kg_{CO2}\,kg^{-1}{}_{sample}$	HPLC		[409]
Brassica oleracea	Broccoli	leaf	amino acids		100-250	50-80	20-35 % (vol.) MeOH	GC-MS	Solvent extraction	[410]
Bunium persicum Boiss.	Black cumim	seed	benzaldehyde		200	45	2 $L_{CO2}kg^{-1}{}_{sample}$	GC-MS	Hydrodistillation	[411]
Mespilus germanica L.	Medlar	seed	γ -terpinene							
Bupleurum falcatum	-	root	saikosaponins	9-18	300-400	40-50	2400 $L_{CO2}\,kg^{-1}{}_{sample}$	HPLC	DoE	[412]

							9 % (vol.) EtOH		Solvent Conc. effect	
Cajanus cajan	Pigeonpea	leaf	cajaninstilbene acid pinostrobin	0.2-1.3	200-400	40-70	EtOH	HPLC	Antioxidant activity DoE SEM RSM	[413]
Calendula officinalis	Marigold	flower	faradiol	5	500	50	105 $kg_{CO2}\,kg^{-1}$ sample	LPLC HPLC	Preparative HPLC	[414]
Calendula officinalis	Marigold	flower		0-2.6	120-200	20-40	0-30 $kg_{CO2}\,kg^{-1}$ sample	Gravimetric Analysis	Modeling	[415]
Calendula officinalis *Matricaria recutita*	Marigold Chamomile	flower		0-1.8	90-100	40-50	0-35 $kg_{CO2}\,kg^{-1}$ sample		Soxhlet extraction Hydrodistillation Modeling SEM Particle sizes effect	[416]
Calendula officinalis L.	Marigold	flower		3.8	100-200	20-40	50 $kg_{CO2}\,kg^{-1}$ sample	GC GC-MS	Modeling Solvent extraction	[417]
Calendulae flos *Crataegus* ssp. *Matricaria recutita* L.	Marigold Hawthorn Chamomile	flower	phenolic	0.5-5.5	300-689	50	0-16 $L_{CO2}kg^{-1}$ sample 0.5-20 % (vol.) EtOH	HPLC HPLC-PAD-MS GC		[418]
Camellia sinensis L.	Tea	seed		14.8-29 %	50-90	35-45	400-1800 $L_{CO2}kg^{-1}$ sample	HPLC	RSM DoE Antioxidant activity	[419]
Camellia sinensis L.	Tea (green)	leaf	caffeine		150-300	45-60	62.5-625 $L_{CO2}kg^{-1}$ sample	HPLC	Ultrasonic assisted Moisture effect DoE	[420]
Camellia sinensis L.	Tea (green)	leaf	epigallocatechin gallate		100-300	40-60	30-240 $L_{CO2}kg^{-1}$ sample	HPLC	Modeling Soxhlet extraction	[421]
Cannabis sativa L.	Hemp	seed		17.3-22.1	300-400	40-80	30-60 $kg_{CO2}\,kg^{-1}$ sample	GC-MS	Soxhlet	[422]
Cannabis sativa L.	Hemp	seed		10-21	250-350	40-60	19 $kg_{CO2}\,kg^{-1}$ sample	GC-FID	RSM DoE Particle sizes effect	[423]
Capsicum annuum L.	Red pepper	seed,	vitamin A and E	12.9 – 68.1 (A)	200-300	45-100	100 – 133 $L_{CO2}kg^{-1}$		Microencapsulatio	[424]

		fruit, stem		4.0-97 (E)			EtOH 13 vol.%		n	
Capsicum annuum L.	Paprika	fruit	carotenoid	81-85	300-500	60-80	2-70 $kg_{CO2}\,kg^{-1}_{sample}$	Spectrophotometry	Fractionation	[117]
Capsicum annuum L.	Paprika	fruit			450	50	15-47 $kg_{CO2}\,kg^{-1}_{sample}$		Soxhlet extraction Particle sizes study Modeling	[174]]
Capsicum annuum L.	Paprika	seed		0-10	200-400	40		GC-MS HPLC	Solvent extraction Soxhlet extraction	[118]
Capsicum annuum L.	Jalapeño	flake		0-0.11	120-320	40		HPLC	Modeling	[114]
Capsicum annuum L.	Red pepper	flake		1-55	320-540	40	0-160 $kg_{CO2}\,kg^{-1}_{sample}$	HPLC	Soxhlet extraction Micrograph Fractal analysis Pelletization Linear driving force model	[425]
Capsicum annuum L.	Red Pepper	fruit		0.7-2.2	100-500	40-60	0-370 $kg_{CO2}\,kg^{-1}_{sample}$	GC-MS GC-FID	SEM Use of biotic elicitor	[119]
Capsicum frutescens	Red pepper	fruit		1-6	162-230	40		Gravimetric Analysis	DoE RSM Rancimat test DSC Velocity effect	[426]
Capsicum frutescens L.	Red pepper	seed	capsaicinoids	15-90	162-218	40	7-168 $kg_{CO2}\,kg^{-1}_{sample}$	HPLC	Soxhlet extraction DoE RSM	[427]
Capsicum spp. *Piper nigrum* *Zingiber officinale*	Chili Black Pepper Ginger		piperine	4.1-12.0	300	40	0-30 $kg_{CO2}\,kg^{-1}_{sample}$	^{1}H NMR spectroscopy	Soxhlet ext.	[148]
Carthamus tinctorius	Safflower	seed		10-40	220-280	35-40	7-243 $kg_{CO2}\,kg^{-1}_{sample}$	GC-FID	Particle sizes effect Modeling Pilot scale	[428]
Carum carvi L.	Caraway	fruit	limonene carvone	1-9	70-400	80	0-3 % MeOH 0-3 % EtOH	GC-MS GC-FID	Harvest time effect	[276]

							0-3 % Acetone 0-3 % Acetonitrile 0-3 % Hexane 0-3 % Dichloromethane 0-3 % Chloroform 0-3 % Toluene	HPLC	Particle sizes effect	
Carum carvi L.	Caraway	seed	carvone limonene		50-80	28-60		FT-IR GC-FID	Analytical technique study	[429]
Carum carvi L.	Caraway	seed			90	50		GC-MS	Hydrodistillation	[430]
Carum copticum	*Carum*	seed		1.0-5.8	101-304	35-55	1-3.5 $L_{CO2}kg^{-1}$ sample	GC GC-MS	Hydrodistillation ANOVA	[431]
Cassia tora	Juemingzi	seed		0.27	250	45		GC-FID GC-MS		[28]
Catharanthus roseus	-	leaf	terpenoid indole alkaloids (Vindoline, catharanthine)		200-400	40-80	0.3-0.9 L_{CO2} kg^{-1} sample MeOH 2.2-6.6 % (vol.)	HPLC	DoE Soxhlet extraction Ultrasonic solid-liquid extraction Water extraction	[30]
Ceratonia siliqua L.	Carob tree			0-0.45 %	150-220	41-60		HPLC	Antioxidant activity DoE	[432]
Chamomilla recutita	Chamomile	flower		0.5-4.3	100-200	30-40	3 kg_{CO2} kg^{-1} sample	GC-MS GC	Modeling	[433]
Chamomilla recutita L. Rauschert	Chamomile	flower		1.9	90	40	92 kg_{CO2} kg^{-1} sample	HPLC GC	In-line inclusion	[434]
Chrysobalanus icaco	*Abajeru*	leaf	lupenol	0.95	105-200	40-80	58-148 L_{CO2} kg^{-1} sample	GC-DIC GC-MS	Soxhlet extraction Hydrodistillation	[435]
Cinnamomum zeylanicum	Cinnamon	bark	tyrosinase melanin		90-120	40-50		GC-MS	Soxhlet extraction Hydrodistillation	[436]
Cistus ladanifer L.	Roc Rose	leaf	labdanum	0.1-0.5	80-100	30-70	2-8 kg_{CO2} kg^{-1} sample	GC	Two-step decompression system	[285]
Citrullus lanatus	Watermelon	fruit	lycopene	0.001-0.004	207-414	70-90	90 $L_{CO2}kg^{-1}$ sample 10-15 % EtOH	HPLC		[275]
Citrullus lanatus *Hibiscus sabdarriffa* Lin	Kalahari melon	seed	tocopherols		200-400	40-80		HPLC	RSM DoE	[293]

Citrullus lanatus	Roselle Kalahari melon	seed	phytosterol	59.5-78.5	200-400	40-80	72 $L_{CO2}kg^{-1}$ sample	GC-FID	RSM DoE	[437]
Citrus depressa		fruit	nobiletin, tangeretin	0.4-1.6	200-400	40-80	32 $L_{CO2}kg^{-1}$ sample EtOH	HPLC	Particle sizes effect	[438]
Citrus grandis L. Osbeck	Pomelo	fruit	flavonoids	1.7-2.4	280-420	60-80	5-15 $L_{CO2}kg^{-1}$ sample	Gravimetric Analysis	Antioxidant activity RSM DoE Conventional solvent extraction	[308]
Citrus junos	Yuzu	seed		10-28	200-500	40-70		GC-FID	Soxhlet extraction	[439]
Citrus latifolia Tanaka	Lime	fruit	limonene	1.6-3.6	90-110	40-60	60-320 $L_{CO2}kg^{-1}$ sample	GC GC-MS	Hydrodistillation	[440]
Citrus maxima Merr		peel			276-345	40-50	3600 L_{CO2} kg^{-1} sample	HPLC		[441]
Citrus paradisi L. (variety Ruby Red)	Citrus plants	peel	naringin		78-108	40-95	5-15 % EtOH	HPLC	Maceration extraction Reflux extraction	[442]
Citrus paradisi Macf.	Grapefruit	seed	limonoids naringin	0.1-0.6	345-483	40-60	10-30 % EtOH 8.6 $L_{CO2}kg^{-1}$ sample	HPLC	DoE RSM Multistep extraction	[443]
Citrus sinensis	Korean orange	peel	perillyl alcohol	0-0.9	150-200	30-60		GC		[444]
Citrus sinensis	Korean orange	peel	perillyl Alcohol	0-4.4	200	50	84 kg_{CO2} kg^{-1} sample	GC	Pilot plant	[159]
Citrus sinensis	Orange	fruit		6-13	200	40	20-100 kg_{CO2} kg^{-1} sample	Gravimetric Analysis	Modeling Diatomaceous earth Scale-up	[161]
Citrus sinensis, C.limon C. reticulata	Cytrus	seed		0-2.41	85-490	40		GC-FID GC-EM	Organic solvent extraction Extractors effect Fractionation	[163]
Citrus sinensis. L Osbeck	Orange	pomace	L-limonene palmitic and oleic acids n-butyl	0.85-3	100-300	40-50	0-340 kg_{CO2} kg^{-1} sample EtOH (0.02-0.08 W/W)	GC-MS	Antioxidant capacity Ultrasound Soxhlet extraction	[162]

			benzenesulfonamide beta-sitosterol							
Citrus unshiu		press cake	carotenoids		172-448	70	0-20 % EtOH		RSM DoE	[445]
Cocos nucifera L.	Coconut	kernel		9.8-64.7	517	120	4 -10 $L_{CO2}kg^{-1}$ sample		Soxhlet extraction Diatomaceous earth	[446]
Coffea arabica	Coffee	husk/spent		0.5-9.7	100-300	40-60	101-189 $kg_{CO2}\,kg^{-1}$ sample 4-15 % (wt.)	HPLC	Modeling Soxhlet extraction Antioxidant activity	[91]
Coffea arabica *Coffea robusta*	Coffee	residue	kahweol cafestol 16-O-methylcafestol	0-12	140-190	40-70	91 $kg_{CO2}\,kg^{-1}$ sample	GC-FID	DoE RSM Soxhlet extraction	[447]
Coffea arabica *Coffea robusta*	Coffee	residue		15	190	40-55	85 $kg_{CO2}\,kg^{-1}$ sample	Gravimetric Analysis	Economic analysis Tryacylglicerides profile	[448]
Coffea arabica	Coffee	bean	cafestol, kahweol		235-380	60-90	62.5 $L_{CO2}kg^{-1}$ sample	HPLC	Soxhlet extraction DoE	[92]
Coffea arabica	Coffee	bean	caffeine	0-17	152-352	50-70	0-200 $kg_{CO2}\,kg^{-1}$ sample	HPLC		[449]
Coffea arabica	Coffee	beans			250-300	50-90			RSM DoE	[450]
Coffea arabica variety Mundo Novo	Coffee	bean			152-352	50-60	0-5 % (wt.) EtOH 0-5 % (wt.) isopropyl alcohol	HPLC		[93]
Coffea canephora var. Robusta	Robusta coffee	husks	caffeine	24-59)	200-300	60-100	35-197 $kg_{CO2}\,kg^{-1}$ sample	HPLC		[451]
Coffea spp.	Coffee	seed		4.2-19.4	150-350	40-60	90 $kg_{CO2}\,kg^{-1}$ sample	HRGC	Soxhlet ext. Modeling	[94]
Coix lachrymal-jobi	Adlay	seed		80-97	100-300	30-55	7.5-200 $L_{CO2}\,kg^{-1}$ sample	Gravimetric Analysis	Ultrasound assisted SFE Flow rate effect	[452]
Coix lachrymal-jobi L. var. Adlay	Adlay	seed		11.6-82.6	100-250	35-50	180 $L_{CO2}\,kg^{-1}$ sample	GC-MS	Ultrassound assisted SFE Particle size effect	[453]
Colchicum autumnale		seed	colchicine		247	25-40	0-7 % MeOH	HPLC	Organic solvent	[454]

L.									extraction Soxhlet extraction Sonication	
Commiphora myrrha *Acorus calamus*	Commiphora *Acorus*	exudates rhizomes	furanogermacranes	3.2-3.5	90	45-50		GC-MS	Hydrodistillation Steam distillation	[186]
Coptis chinensis	*Coptis chinensis*	rhizome	berberine	0.15-7.53	200-600	60	EtOH MeOH 1,2-Propanediol	HPLC	Soxhlet	[455]
Cordia verbenacea	-	leaf	β-caryophyllene	3-4	80-300	60	1-77 $kg_{CO2}\,kg^{-1}_{sample}$	GC-MS	Fractionation Soxhlet extraction Hydrodistillation Modeling	[456]
Cordia verbenácea D.C.	-	leaf			100-300	30-50	20-100 $kg_{CO2}\,kg^{-1}_{sample}$		Antitumor activity	[457]
Coriandrum sativum	Coriander	seed		0.8-2.0	116-280	38-58		Spectrophotometry	Hydrodistillation	[458]
Coriandrum sativum L.	Coriander	seed		0.05-0.6	90-150	40-50	47 $kg_{CO2}\,kg^{-1}_{sample}$	GC GC-MS	Particle size effect Hydrodistillation SEM	[459]
Coriandrum sativum L.	Coriander	seed		0-16.4	200-300	35	0-40 $kg_{CO2}\,kg^{-1}_{sample}$	GC	Organic solvent extraction	[460]
Corylus avellana *Juglans regia*	Hazel / Walnut	fruit		0.05-0.6	180-234	35-48	50-1500 $kg_{CO2}\,kg^{-1}_{sample}$	Gravimetric Analysis	Modeling	[461]
Corylus avellana L.	Hazel	fruit		60-80	180-234	35-48		Rancimat method HPLC GC	Solvent extraction DoE RSM	[462]
Corylus avellana L.	Hazel	fruit			150-600	40-60	0-127 $kg_{CO2}\,kg^{-1}_{sample}$	GC	Solubility measurements Modeling	[463]
Corylus avellana L.	Hazel	fruit		1-17	300-450	40-60	2-18 $kg_{CO2}\,kg^{-1}_{sample}$	Gravimetric Analysis	RSM DoE	[464]
Cratoxylum prunifolium Dyer		leaf	catechins		125-250	40-80	4.8 $L_{CO2}kg^{-1}_{sample}$	HPLC	DoE	[465]
Croton zehntneri Pax et Hoff		leaf		0-0.9	67-79	10-28	3 $kg_{CO2}\,kg^{-1}_{sample}$	GC	Modeling	[466]]
Cucumis melo Cantalupensis	Cantaloupe	seed	linoleic acid	22.7-30.4	600	40	270 $kg_{CO2}\,kg^{-1}_{sample}$	GC	Antioxidant activity	[467]

Cucumis melo reticulates									Soxhlet	
Cucurbita ficifolia	Fig leaf gourd	seed		40-43	180-200	35-45		GC	Modeling	[468]
Cucurbita ficifolia	Pumpkin	seed		86-93	180-200	35-45			Soxhlet extraction	[169]
Cucurbita maxima	Pumpkin	seed		6-30	151-344	35-75	300-1500 $L_{CO2}kg^{-1}$ sample	GC	DoE RSM	[[171]
Cucurbita moschata	Pumpkin	seed		10-98	250-300	55		GC-MS	Solvent extraction	[173]
Cucurbita ficifolia									Flow rates efffect	
Cucurbita moschata	Pumpkin	fruit	α-carotene, β-carotene lutein ester		250-371	40-76	150 $L_{CO2}kg^{-1}$ sample	HPLC	Solvent extraction DoE RSM	[172]
Cucurbita pepo convar. *citrullina*	Pumpkin	seed	spinasterol Δ7,22,25-stigmastatrienol	36.1	400	40	30 kg_{CO2} kg^{-1} sample	GC-MS	Solvent extraction	[170]
Cuminum cyminum L.	Cumin	seed	cuminaldehyde	1.7-3.5	550	100	513 kg_{CO2} kg^{-1} sample	GC-FID		[469]
Curcuma longa L.	Turmeric	rhizome	-	5-7	125-325	35-55	1.7-6.7 $L_{CO2}kg^{-1}$ sample	GC-MS	RSM DoE	[180]
Curcuma longa L.	Turmeric	rhizome	turmerone ar-turmerone	2-5	200-400	40-60	6-130 kg_{CO2} kg^{-1} sample	GC-MS	Steam distillation	[178]
Curcuma longa L.	Turmeric	rhizome		0-7	300	30	0-1 kg_{CO2} kg^{-1} sample 6.9-16.1 % EtOH/Isopropyl	GC-FID	Organic solvent extraction Soxhlet extraction Hydrodistillation	[179]
Curcuma longa L.	Turmeric	rhizome	curcuminoids	4.5-6.5	250-300	45-105		Spectrophotometry	Modeling Pilot plant Drying pretreatment	[192]
Curcuma longa L.	Turmeric	rhizome	curcuminoids	4.5-22.6	250-300	45	EtOH	Spectrophotometry HPLC GC	Soxhlet extraction Modeling Drying pretreatment	[35]
Cydonia oblonga Miller	Quince	seed			100-345	30-65	24 $L_{CO2}kg^{-1}$ sample 0.8-1.1 % (vol.) MEtOH	GC-MS	DoE RSM Ultrasound assisted extraction	[470]
Cymbopogon citratus	Lemongrass				80	50	19-144 $L_{CO2}kg^{-1}$ sample	GC-FID	Solvent extraction Steam distillation	[471]

							0-30 % Hexane 0-30 % Dichlorometane		Accelerated solvent extraction	
Cymbopogon citratus	Lemongrass	leaf		0.4-1.7	80-120	23-50	2.8-3.7 $kg_{CO2}\,kg^{-1}_{sample}$	GC-MS		[472]
Cynanchum paniculatum (Bge.) Kitag	-	root	paenol	0.1-6.0	100-200	45-55	0-2000 $L_{CO2}\,kg^{-1}_{sample}$	HPLC-PDA HSCCC	Particle size efffect DoE Ultrasonic extraction Steam distillation Soxhlet extraction Microwave-assisted extraction High-speed counter-current chromatography	[473]
Cynara cardunculus L.	Cardoon	seed		4.7-24	150-300	35-55	180 $kg_{CO2}\,kg^{-1}_{sample}$	TLC GC HPLC	Soxhlet extraction Biodiesel production	[254]
Cyperus rotundus	-	rhizome	α-cyperone	2.6	200	40		HPLC MS	Purification	[27]
Daucus carota L.	Carrot	root			276-551	40-70	0-5 % (w/w) Canola Oil 0-470 $kg_{CO2}\,kg^{-1}_{sample}$	HPLC	Solvent extraction Moisture effect Particle size effect Flow rate effect	[474]
Daucus carota L.	Carrot	root	carotenes	0.25	330	40	24 $kg_{CO2}\,kg^{-1}_{sample}$ EtOH	NMR HPLC GC	Pilot scale	[133]
Daucus carota L.	Carrot	root	carotenoids	1.5-2.5	276-551	40-70	2.5-5.0 % w/w Canola oil	HPLC	Particle sizes effect Solvent extraction ANOVA	[132]
Daucus carota L. subsp. *carota*	Carrot	umbels			90	40		GC-MS	Antifungal activity Hydrodistillation	[475]
Daucus carrota L., cultivar ''Chanteney"	Carrot	root	carotol		90-100	40-50	0-16 $kg_{CO2}\,kg^{-1}_{sample}$	GC-FID GC-MS	Antimicrobial activity Hydrodistillation	[476]

Diospyros kaki Thunb.	Persimmon	fruit	carotenoids	36	300	40-80	5-20 % EtOH $2.8x10^5$ $L_{CO2}kg^{-1}$ sample	HPLC	Particle size study	[477]
Diplotaenia cachrydifolia	-	aerial parts		0.3-2.5	101-304	35-75		GC-MS	RSM DoE	[478]
Diplotaenia cachrydifolia	-	aerial parts	dillapiole limonene α-calacorene	0.0-2.4	101-304	35-75	3-15 L_{CO2} kg^{-1} sample 0-3.8 % (vol.) MeOH	GC GC-MS	Artificial neural network	[479]
Dracocephalum moldavica L.	Moldavian dragonhead	herb	geraniol	1.3	450	40	5-18 kg_{CO2} kg^{-1} sample	GC-MS	Hydrodistillation Soxhlet extraction Solvent extraction Two-step decompression system	[264]
Drosera intermedia	-	plant	plumbagin	0.6	200	40	87 kg_{CO2} kg^{-1} sample	HPLC–DAD		[480]
Echinacea purpúrea - - -	Kava Saw Palmetto St. John's wort -	aerial parts fruit flower/stem root		2-3 2-12 10-12 3-8	250-300	40-60	0-20 kg_{CO2} kg^{-1} sample	HPLC		[481]
Ekebergia capensis	-	wood			405	80	2 % (mol) H_20	NMR	Uterotonic activity	[482]
Elaeis guineensis	Palm	kernel	triglycerides	80	207-483	40-80		GC	Fractionation Solubility analysis Micrograph	[483]
Elaeis guineensis	Palm	kernel cake		0-9.26	275-413	40-70	6.66-10 $l_{CO2}kg^{-1}$ sample		Particle sized effect ANOVA	[12]
Elaeis guineensis	Palm	fruit	oil	77.8	140-300	40-80		GC-FID	Soxhlet extraction	[484]
Elaes guineensis	Palm	Fiber	fatty acids carotene, Lipids	2.9-5.3	200-300	45-55	3-17 kg_{CO2} kg^{-1} sample	Spectrophotometry	Modeling	[11]
Elettaria cardamomum L.	Elettaria	seed		2-5	90-110	40-50	2-18 kg_{CO2} kg^{-1} sample	GC-MS	Hydrodistillation Particle sizes effect	[485]

Elettaria cardamomum Maton	Cardamom	seed			100-300	35-55	25 % (w/w) EtOH	HPLC GC-MS	Sub-critical propane extraction Solvent extraction	[486]
Ephedra sinica		aerial parts			136-340	40-80	0-10 % H_2O 0-10 % MeOH	GC	Organic solvent extraction	[487]
Equisetum giganteum L.	Horsetail	aerial parts		0-0.9	120-300	30-40	0-53 $kg_{CO2}\,kg^{-1}$ sample	GC GC-MS	Organic solvent extraction	[488]
Erythroxylum coca var. *coca*	Coca	leaf	cocaine		150-250	40-100	5-15 % (vol.) MeOH/H_2O (29:71)	GC-FID GC-MS	DoE RSM	[489]
Eucalyptus camaldulensis	Eucalypt	leaf	1,8-cineole	1.4-2.0	80-250	40-60	2500 $L_{CO2}kg^{-1}$ sample	GC-MS	Hidrodistillation	[88]
Eucalyptus camaldulensis var.*brevirostris*	*Eucalyptus*	leaf	gallic acid	12.0-16.6	400	70	15 % EtOH 200 $L_{CO2}kg^{-1}$ sample	RP-HPLC	Antioxidant activity Hydrodistillation	[490]
Eucalyptus citriodora *Melissa officinalis* *Monarda citriodora* *Cymbopogon citratus*	Lemon Lemongrass	leaf			138-414	40-60	100-240 $L_{CO2}kg^{-1}$ sample	GC GC-MS	Hydrodistillation MANOVA	[491]
Eucalyptus globulus	Eucalypt	bark	betulinic acid betulonic acid oleanolic acid ursolic acid 3-acetyloleanolic acid 3-acetylursolic acid β-sitosterol	0.0-1.3	100-200	40-60	80 $kg_{CO2}\,kg^{-1}$ sample	GC-MS	Soxhlet extraction Kinetic and equilibrium properties calculation	[83]
Eucalyptus globulus	Eucalypt	bark	Phenolic	0.28-0.51	300	50-70	45 $l_{CO2}kg^{-1}$ sample EtOH (15-20 % w/w)	HPLC-UV ESI-MS	Antioxidant activity DoE RSM	[90]
Eucalyptus globulus	Eucalypt	bark	betulinic acid betulonic,acid oleanolic acid ursolic acid 3-acetyloleanolic acid		120-200	40-60	5-51 $kg_{CO2}\,kg^{-1}$ sample 0-5 % (wt.) EtOH	GC-MS	Modeling	[84]

			3-acetylursolic acid β-sitosterol							
Eucalyptus globulus	Eucalypt	bark	betulinic acid betulonic,acid oleanolic acid ursolic acid 3-acetyloleanolic acid 3-acetylursolic acid β-sitosterol	0.5-1.7	100-200	40	8-110 $kg_{CO2}\,kg^{-1}_{sample}$ 0-8 % (wt.) EtOH	GC-MS	Soxhlet extraction Fractionation	[492]
Eucalyptus globulus	Eucalypt	bark	betulinic acid betulonic,acid oleanolic acid ursolic acid 3-acetyloleanolic acid 3-acetylursolic acid β-sitosterol	0.04-1.2	100-200	40-60	31 $kg_{CO2}\,kg^{-1}_{sample}$ 0-5 % (wt.) EtOH	GC-MS	DoE	[85]
Eucalyptus grandis *Eucalyptus globulus*	Eucalypt	bark	methyl morolate		200	60	5-51 $kg_{CO2}\,kg^{-1}_{sample}$	GC-MS NMR	Soxhlet extraction	[89]
Eucalyptus spathulata *Eucalyptus microtheca*	*Eucalyptus*	leaf			100-300	45-55	MeOH	GC-FID	Hydrodistillation	[82]
Eucalyptus tereticornis - *Zingiber officinale* Roscoe	Eucalyptus Clove Ginger	bud leaf rhizome		0.8-11	67-250	15-40	2.5 $kg_{CO2}\,kg^{-1}_{sample}$	GC-MS	Modeling Solubility measurement Flow rate study	[493]
Eucommia ulmoides	-	seed	aucubin	0.6-2.0	180-300	45-330	400 $L_{CO2}kg^{-1}_{sample}$ 0-3 % (vol.)H_2O - EtOH 0-3 % (vol.)H_2O 0-3 % (vol.)MeOH 0-3 % (vol.) EtOH 0-3 % (vol.) H_2O -	HPLC	Soxhlet extraction	[494]

							MeOH 0-3 % (vol.) H_2O-EtOH			
Eugenia caryophillus	Clove	bud			66-150	15-50		Gravimetric Analysis	Modeling – Genetic algorithm Scale-up	[495]
Eugenia caryophillus *Vetiveria zizanioides* (L.) Nash ex Small	Clove Vetiver	bud root		5.8-13.3	100-200	35-40	4-36 $kg_{CO2}\,kg^{-1}_{sample}$	Gravimetric	Modeling Extractor geometry study Flow rates effect Scale-up	[496]
Eugenia caryophyllata	-	bud	eugenol	17.1	300	50		HPLC	SFC	[497]
Eugenia caryophyllata Thunb.	Clove	bud	eugenol	18-23	100-300	30-50	16000 $L_{CO2}kg^{-1}_{sample}$	GC GC-MS	Hidrodistillation Soxhlet extraction Particle sizes effect DoE	[498]
Eugenia uniflora L	Brazilian cherry	fruit	sesquiterpenes ketones	0.42 % to 0.56 % (extracts flavour	150-250	40-60	36 $kg_{CO2}\,kg^{-1}_{sample}$	GC-MS	ANOVA PCA FDA	[499]
Euphorbia rigida	Euphorbia	leaf +stalk	hydrocarbons	8.6	400	50	0.6 $kg_{CO2}\,kg^{-1}_{sample}$ 0-10 % MEtOH	GC-FID GC-MS	Soxhlet extraction	[500]
Evodia rutaecarpa	-	fruit	evodiamine rutaecarpine	0.6-6.5	200-400	50-70	180000 $L_{CO2}\,kg^{-1}_{sample}$ 16 % (vol.) MeOH	HPLC	Soxhlet extraction	[501]
Ferula assa-foetida	-			0.8-5.5	101-303	45-65	1.5-4.7 $L_{CO2}\,kg^{-1}_{sample}$ 4.8 % (vol.) MeOH	GC GC-MS	Hydrodistillation	[502]
Ferulago Angulata	-	aerial parts		0.05-0.82	90-190	35-55				[503]
Foeniculum vulgare	Fennel	seed			120	40		GC-MS	Coupled distillation	[75]
Thymus vulgaris	Thyme	leaf						GC-O		
Foeniculum vulgare	Fennel	seed	(*E*)-anethol	-	200-350	45-55	3.6-5.4 $L_{CO2}kg^{-1}_{sample}$ 0-5 % MEtOH	GC-MS	Hydrodistillation	[108]
Foeniculum vulgare	Fennel	seed		2-13	100-300	30-40	0-449 $kg_{CO2}\,kg^{-1}_{sample}$	GC TLC	Hydrodistillation Modeling	[504]
Foeniculum vulgare	Fennel	fruit		0-98	90-100	40-50	35-106 $kg_{CO2}\,kg^{-1}_{sample}$	GC GC-MS Gravimetric	Two-step decompression Hydrodistillation	[505]

Foeniculum vulgare Mill	Fennel	seed		1.5-5.5	80-150	40-57	36-285 $kg_{CO2}\,kg^{-1}{}_{sample}$	Analysis GC GC-MS	Hydrodistillation	[506]
Garcinia mangostana L.	Mangosteen	fruit	xanthones	0.23-6.5	200-300	40-60	100-300 $kg_{CO2}\,kg^{-1}{}_{sample}$	HPLC	RSM DoE Antioxidant activity	[507]
Garcinia mangostana L.	Mangosteen	fruit	xanthones	5.37-15.14	180-380	40-60	EtOH (5 % w/w)	HPLC- ESI/MS	DPPH	[508]
Ginkgo biloba	*Ginkgo biloba*	leaf	flavonoids	0-0.24	100-300	35-65	6-16 $L_{CO2}kg^{-1}{}_{sample}$ 60 % (vol./w) EtOH	UV-vis spectrophotometry	SEM	[306]
Ginko biloba	*Ginko biloba*	leaf	flavonoids terpenoids	0.0-2.3	100-300	50-80	1-10 % EtOH	HPLC	DoE EtOH preextraction	[509]
Ginko biloba	*Ginko biloba*	leaf	terpene lactone flavoinoids	4.5-11.4	242-312	60-120	5-24 % (mol) EtOH	HPLC	Soxhlet extraction	[510]
Ginko biloba	*Ginko biloba*	leaf	bilobalide ginkolides		204-340	40-80	5-20 % (vol.) MeOH 16/4 % (vol.) MeOH/ H_2O	HPLC-ESI-MS	Organic solvent extraction	[511]
Glycine variety	Soybean	distillate	fatty acids, tocopherols, sterols, squalene	32-65	241-310	50-90		RP-HPLC		[17]
Glycine variety	Soybean	flakes	lecithin		655	80	6.7 $l_{CO2}\,kg^{-1}{}_{sample}$ 15 % EtOH	HPLC	SCF Fractionation	[176]
Glycine variety	Soybean	distillate	tocopherols	-	110-318	50-60	(1-4.7) x 10^{-4} $L_{CO2}\,L^{-1}{}_{sample}$	GC	ODS traps	[512]
Glycine variety	Soybean	bean		2-19	300-500	40-60	18-20 $kg_{CO2}\,kg^{-1}{}_{sample}$	Gravimetric Analysis	Particle sizes effect Modeling Scale-up	[174]
Glycine variety	Soybean	bean	triglycerides	0-7	100-300	40-50	814.5 $L_{CO2}kg^{-1}{}_{sample}$	HPLC	RSM DoE	[175]
Glycyrrhiza uralensis Fisch	Glycyrrhiza	root		1.2-2.8	150-350	40-60	6-14 $kg_{CO2}\,kg^{-1}{}_{sample}$	GC-MS	Antibacterial activity	[513]
Gossypium spp.	Cotton	seed	gossypol	2.1-43.1	350-550	60-80	1200-3600 $L_{CO2}kg^{-1}{}_{sample}$		RSM DoE	[514]
Guaicum Bulnesia	-	wood		0.7	120	80		GC-MS	Hydrostillation	[515]
Guilielma speciosa	Pupunha	fruit	fatty Acids	13	250-300	50-45	65-93 $kg_{CO2}\,kg^{-1}$	GC	Modeling	[260]

			carotenes							
Helianthus annuus L.	Sunflower	seed		0-90	250	40	0-650 $kg_{CO2}\,kg^{-1}_{sample}$	HPLC	Modeling Two-step decompression system	[100]
Helianthus annuus L.	Sunflower	distillate	polyphenol	20-100	200-700	40-80	6-119 $kg_{CO2}\,kg^{-1}_{sample}$	Gravimetric Analysis	Three-step SFE extraction Soxhlet extraction Modeling	[14]
Helianthus annuus L.	Sunflower	distillate	tocopherols phytosterols	20-100	150-230	65		HPLC-UV/Vis HPLC-ELSD GC	Pilot-scale	[516]
Helianthus annuus L.	Sunflower	leaf	allelopathic compounds	0-2	100-500	35-50	5 % MeOH 5 % DSMO 5 % H_2O		DoE Cluster Analysis	[24]
Helianthus annuus L.	Sunflower	leaf	allelopathic compounds	0.2-1.6	380	50	42-126 $kg_{CO2}\,kg^{-1}_{sample}$ 3.8-4.7 % H_2O		Pilot scale Flow rates effect Cluster Analysis Biological activity	[22]
Helianthus annuus L.	Sunflower	leaf	allelopathic compounds	0.1-1.2	300-500	50	2-126 $kg_{CO2}\,kg^{-1}_{sample}$	Gravimetric Analysis	Cluster Analysis Pilot scale	[23]
Helianthus annuus L.	Sunflower	seed		0-95	200-600	40-80	425 $kg_{CO2}\,kg^{-1}_{sample}$	Gravimetric Analysis	Modeling Flow rates study Particle sizes study	[101]
Helichrysum italicum	-	flower		0-4.5	100 - 200	40-60	36 $kg_{CO2}\,kg^{-1}_{sample}$	GC-MS GC-FID		[515]
Hemerocallis disticha	Daylily flowers	flower	lutein zeaxanthin	4.86-8.12	300-600	50-95		HPLC	Antioxidant activity	[517]
Hibiscus cannabinus	Kenaf	seed		0.5-20	200-600	40-80	0-38 $kg_{CO2}\,kg^{-1}_{sample}$	Gravimetric Analysis	Soxhlet extraction Ultra-sonic assisted solvent extraction	[518]
Hibiscus cannabinus L	Kenaf	seed			400-600	40-80	38 $kg_{CO2}\,kg^{-1}_{sample}$			[519]
Hippophae rhamnoides L	Seabuckthorn	fruit	tocopherol carotene		150-350	35-55	2.4 $kg_{CO2}\,kg^{-1}_{sample}$ 0-30 % (vol./w)	GC-MS HPLC	DoE Soxhlet extraction	[272]

							mEtOH 0-30 % (vol./w) EtOH 0-30 % (vol./w) 2-Propanol		Antioxidant activity RSM	
Hippophae rhamnoides L.	Sea buckthorn	fruit	β-sitosterol	9.9-10.9	150-600	40-80	0-137 $kg_{CO2}\,kg^{-1}_{sample}$	HPLC	Solvent extraction Soxhlet extraction	[295]
Hippophae rhamnoides L.	Sea buckthorn	seed		0.1-2.9	150-300	30-45	267 $L_{CO2}kg^{-1}_{sample}$	Gravimetric Analysis	2-step decompression Particle sizes effect	[40]
Hippophae rhamnoides L.	Sea buckthorn	seed		1-6	200-300	35-40		GC	Particle sizes effect Organic solvent extraction	[520]
Hippophae rhamnoides L.	Sea buckthorn	fruit	β-sitosterol	1-11	150-600	40-80	0-140 $kg_{CO2}\,kg^{-1}_{sample}$	HPLC	Modeling	[296]
Hippophae rhamnoids L.	Seabuckthorn	seed		2.48-9.28 7.60-9.68	100-400	45-75	24 $kg_{CO2}\,kg^{-1}_{sample}$ EtOH, MeOH, 2-propanol	HPLC	DoE RSM Antioxidant activity	[521] [522]
Hordeum vulgare L. *Zea mays*	Malt Corn	seed		1.1-1.4	650	60-100		Gravimetric	Soxhlet ext.	[523]
Hordeum vulgare L. var. Robur	Barley		tocochromanols	4.0-4.7	200-450	40	30 $L_{CO2}kg^{-1}_{sample}$	TLC HPLC	Fractionation Soxhlet extraction Folch method	[524]
Hordeum vulgare L.	Brewer's Spent Grain		tocopherol	0.2-1.7	100-350	40-80	66-400 $L_{CO2}kg^{-1}_{sample}$	HPLC	Economic analysis	[525]
Hylocereus undatus	White pitaya	seed		5.54	250	40		GC-MS	Soxhlet extraction Microwave-assistant extraction Aqueous enzymatic extraction	[526]
Hypericum carinatum:	-	flower	phloroglucinol, benzophenone	1.05-3.04	90/120/150/200	40-60	76 $kg_{CO2}\,kg^{-1}_{sample}$	HPLC	ANOVA	[527]

			derivatives		(sequence)					
Hypericum perforatum	St. John's		hyperforin,		80	30	EtOH/acetic acid			[528]
Ginkgo biloba	wort	leaf	dhyperforin				(9:1)			
	Ginko biloba		bilobalide,		350	100				
			ginkgolide A, B,							
			Q							
Hypericum perforatum	*St. John's*			1-4	100-350	40	2675 $L_{CO2}kg^{-1}$ sample	GC-MS	Steam distillation	[529]
L.	*Wort*								Particle sizes	
									effect	
Hypericum perforatum	*St. John's*			0-4.8	100-200	40-50	45 $kg_{CO2}\,kg^{-1}$ sample		Modeling	[369]
L.	*Wort*								Optimization	
Hyssopus officinalis	Hyssop	leaf	terpinen-4-ol	1.0-2.3	90-100	40-50	0.2-8 $kg_{CO2}\,kg^{-1}$ sample	GC-FID	Hydrodistillation	[530]
		+flower	1,8-cineol						Modeling	
									SEM	
Hyssopus officinalis	Hyssop	root		0.1-2.9	100-350	45-75	0.0-6.0 % (vol.)	GC	DoE	[531]
							MeOH	GC-MS	Hydrodistiilation	
Ilex paraguariensis	Yerba mate	leaf	methylxantines	0-3.79	120-200	40-70		HPLC		[532]
			caffeine							
Illicium verum	Chinese star	seed	fatty acids	6.80-23.72	100-300	30-50	(0-15 %) (vol.) EtOH	HPLC	RSM	[257]
	anise								DoE	
Inula viscosa (L.) Aiton	-	leaf	sesquiterpene	0.65	90	50		GC-MS	Hydrodistillation	[533]
Inula graveolens (L.)			lactones,						2-step	
Desf			sesquiterpene						decompression	
			acids and							
			flavonoids							
Jatropha curcas	-	seed	triglycerides	14.4-48.9	250-350	40-60		GC	RSM	[255]
									Soxhlet extraction	
Juglans regia L	Walnut	fruit		0-95	180-234	35-48	0-550 $kg_{CO2}\,kg^{-1}$ sample	HPLC	Soxhlet extraction	[534]
									Rancimat method	
Juglans regia L.	Walnut			68.2	689	85	70 $L_{CO2}kg^{-1}$ sample	Gravimetric	Subcritical solvent extractions	[535]
Juniperus communis L.	Juniper	fruit		0.2-0.4	90-200	40	30 $kg_{CO2}\,kg^{-1}$ sample	GC-FID	Hydrodistillation	[536]
								GC-MS		
Juniperus communis L.	Juniperus	fruit		4.5-12.5	90-125	40-50	6-18 $kg_{CO2}\,kg^{-1}$ sample	GC	Hydrodistillation	[537]
								GC-MS		
Juniperus communis L.	Juniper	fruit		0.1-4	80-100	40	1-80 $kg_{CO2}\,kg^{-1}$ sample	GC-MS	Steam distillation	[538]
								GC-FID		
Juniperus communis L.	Juniper	fruit		0.2-0.5	90-200	40	30 $kg_{CO2}\,kg^{-1}$ sample	GC-FID	Hydrodistillation	[539]

								GC-MS	Particle sizes effect	
Juniperus communis L.	*Juniperus*	leaf			200-350	45-55	0-5 % MeOH	GC-MS GC-FID	Hydrodistillation	[540]
Juniperus oxycedrus L.	*Juniperus*	leaf + fruit		0-15	80-100	50		GC-MS	2-step decompression Hydrodistillation Antiviral activity test	[541]
Juniperus virginiana L.	Cedarwood	wood	-	4.5-10.4	103-689	40-100	20.8 $L_{CO2}kg^{-1}$ sample	GC	Steam distillation	[542]
Juniperus Virginiana L.	Cedarwood	wood	cedrol cedrene	2.5-3.9	414	100	909-7273 $L_{CO2}kg^{-1}$ sample	GC	Water extraction	[543]
L. Stoechas subspecies C. Boiss	Lavender	flower	-	1.2	80-140	35-50	10-40 $kg_{CO2}kg^{-1}$ sample	GC	Modeling	[544]
Laurus nobilis	Bay Basil Coriander Dill Spearmint Marjoram Peppermint Oregano Parsley Rosemary Sage Thyme	leaf	tocopherol		101-405	40		HPLC	Algae extraction	[545]
Laurus nobilis L.	Laurel	leaf	monoterpenes, oxygenated derivates	1.37	100	40	17 kg_{CO2} kg^{-1} sample	GC-FID GC-M		[156]
Laurus nobilis L.	Laurel	leaf	1,8-cineole	0.82	90	50	21 kg_{CO2} kg^{-1} sample	GC-MS	Hydrodistillation 2-step decompression system	[39]
Laurus nobilis L.	Daphne	seed		0-28	340	35-75	0-15 $L_{CO2}kg^{-1}$ sample	HPLC		[546]
Laurus nobilis L.		fruit		0.9	90-250	40		HPLC	Hydrodistillation	[547]
Lavandula angustifolia	Lavender	flower		5.5-9.8	73-207	46-53	1-12 $L_{CO2}kg^{-1}$ sample	GC-MS	RSM DoE	[548]

Lavandula angustifolia	Lavender	flower	linalyl acetate	77-95	80-120	45-55		GC-FID	Antioxidant activity DoE	[549]
Lavandula hybrida	Lavandin	flower	linalool linalyl acetate camphor 1,8-cineole	79.4-99.0	10-130	35-95	0.1-0.93 $L_{CO_2}kg^{-1}$ sample	GC-FID	Periodic static-dynamic procedure RSM DoE Soxhlet extraction	[550]
Lavandula stoechas L. ssp. *cariensis* (Boiss.) Rozeira		flower							RSM DoE Solvent extraction	[551]
Lavandula viridis L'Hér	-	aerial parts	camphor	12.2-12.7	120-180	40		GC–FID GC–IT–MS	Hydrodistillation Fractionation Antioxidant activity	[281]
Lepidium apetalum	-	seed		11.79 - 35.56	200-300	50-70	375 $L_{CO_2}kg^{-1}$ sample	GC-MS	DoE RSM Antioxidant activity	[552]
Levisticum officinale Koch. *Apium graveolens* L.	Lovage Celery	seed leaf root		1.6-2.2	200-350	40	100-200 $kg_{CO_2}kg^{-1}$ sample	GC-MS	Extractor size study	[553]
Ligusticum Chuanxiong	*Ligusticum*	root		0-5	200-350	55-70	8-80 $L_{CO_2}kg^{-1}$ sample	GC-MS		[554]
Lingusticum chuanxiong	-		ligustilide butylidenephalide	0-3.85	350	70	16 $L_{CO_2}kg^{-1}$ sample	GC-MS (SIM)		[26]
Linum usitatissimum	Flax	waste	policosanols	7.4	552	60	1-10 % (vol.) EtOH 60 $L_{CO_2}kg^{-1}$ sample	GC-MS	Organic solvent extraction	[105]
Linum usitatissimum	Flax	seed		35.7-41.0	413-620	100	$(0.6\text{-}1.2) \times 10^5$ $L_{CO_2}kg^{-1}$ sample 0-1 $L_{EtOH}kg^{-1}$ sample	GC-FID	RSM Soxhlet extraction Particle sizes effect	[555]
Linum usitatissimum	Flax	seed		21-25	210-550	50-70	10-210 $kg_{CO_2}kg^{-1}$ sample	HPLC GC-FID	Soxhlet extraction	[103]
Linum usitatissimum	Flax	seed	lignans	1.4-2.7	350-450	40-60	163 $kg_{CO_2}kg^{-1}$ sample	HPLC	RSM DoE	[104]

Linum usitatissimum	Flax	straw	wax	0.52-1.23	200-400	40-70		GC-MS	RSM DoE	[102]
Linum usitatissimum	Flax	seed		10-40	300-500	50-70	2- 72 $kg_{CO2}\,kg^{-1}{}_{sample}$	Gravimetric Analysis	Particle sizes effect Flow rates effect RSM DoE	[106]
Linum usitatissimum L.	Linseed	seed		8.6-28.8	250	50	0-5 % (vol.) EtOH		Economic analysis Modeling	[556]
Linum usitatissimum/ *Brassica rapa*/ *Brassica napus*/ *Brassica juncea*/ *Sinapis alba*	Flax/ solin/ canola/ mustard	seed		21-49	517	100	7.5-132 $L_{CO2}kg^{-1}{}_{sample}$ 0-15 % EtOH	GC	Reference method extraction	[557]
Lippia alba	Lippia	leaf	limonene carvone	0.2-5.7	80-120	40-50	51-654 $kg_{CO2}\,kg^{-1}{}_{sample}$	GC	Hydrodistillation Solvent extraction Soxhlet extraction SEM	[279]
Lippia alba Mill.	-	leaf/stem	carvone					GC-MS	Hydrodistillation Simultaneous distillation Microwave-assisted Hydrodistillation Antioxidant activity	[558]
Lippia dulcis Trev.	Lippia	leaf + flower		1.6-3.2	100-140	45-50	23 $kg_{CO2}\,kg^{-1}{}_{sample}$	GC-MS, LCMS HPLC	Hydrodistillation	[559]
Lippia sidoides	Lippia	leaf	thymol	1.2-1.8	67-79	10-25	2 $kg_{CO2}\,kg^{-1}{}_{sample}$	GC-MS	Steam distillation Solvent extraction Modeling	[560]
Lycopersicum esculentum	Tomato	pulp/fruit	lycopene	72.5-80.0	400	60	21-51 $kg_{CO2}\,kg^{-1}{}_{sample}$	HPLC	Mixture of raw materials	[273]
Corylus avellana	Hazelnut									
Macadamia integrifolia	Macadamia	fruit		0-0.65	100-180	40-80	53 $L_{CO2}kg^{-1}{}_{sample}$	GC	Modeling	[561]
Majorana hortensis Moench	Marjoram	leaf		1.4	200	50	80 $l_{CO2}\,kg^{-1}{}_{sample}$	GC-MS	Hydrodistillation	[278]

Mangifera indica L.	*Mango*	leaf	mangiferin quercetin		100-400	35-75	240 kg_{CO2} kg^{-1} $_{sample}$ 0-20 % EtOH 0-20 % MEtOH	HPLC	Antioxidant activity Hydrodistillation	[562]
Marchantia convoluta				0.8-4.7	50-200	35-65	1.8-5.3 $L_{CO2}kg^{-1}$ $_{sample}$	GC-MS	Organic solvent extraction	[563]
Marchantia convoluta		whole plant		0.7-4.7	50-200	35-65	6 $L_{CO2}kg^{-1}$ $_{sample}$ MeOH	GC-MS		[564]
Matricaria chamomilla	Chamomile	flower	matricine chamazulene α-bisabolol	2-4	100-250	30-40		GC-MS HPLC	Soxhlet extraction Steam distillation Scale-up Fractionation	[38]
Matricaria recutita	Chamomile	flower			240	40		GC-MS	Modeling	[565]
Maydis stigma	-	flower	flavonoids		250-450	40-60	EtOH 4000 L_{CO2} kg^{-1} $_{sample}$	UV-Vis Spectrophotometry	DoE	[304]
Maytenus aquifolium Martius (Celastraceae)		Leaf		1.0-6.6	101	50	0-10 % (vol.) pentane 0-20 % (vol.) pentane 0-10 % (vol.) EtOH 0-10 % (vol.) MeOH	HRGC-FID	Soxhlet extraction Maceration/Sonication extraction	[566]
Maytenus ilicifolia		leaf			100-250	20-40		GC-MS	Particle sizes study	[567]
Melaleuca cajuputi	-	leaf	Sesquiterpenes, oxygenated derivatives	1.6-4.2	83-197	44-86		GC-FID GC-M	Organic solvent extraction Anova	[568]
Melissa officinalis	Lemon balm	aerial parts	gallic acid, protocatechuic acid, *p*-hydroxybenzoic acid vanillic acid, syringic acid		100-300	40-80	MeOH	HPLC	Soxhlet extraction Organic solvent extraction	[569]
Melissa officinalis, L.	Lemon balm	leaf	phenols	2-30	100-180	35-40			Rancimat method	[570]
Mentha pulegium	Pennyroyal	leaf +		10-98	100	50	50-100 kg_{CO2} kg^{-1}	Gravimetric	Steam distillation	[571]

Mentha pulegium L.	Pennyroyal	flower aerial parts	pulegone menthone		100-200	35-55	1-5 $kg_{CO2}\,kg^{-1}_{sample}$ 0-53 % MEtOH	GC-MS	Modeling Hydrodistillation	[572]
Mentha spicata Salvia desoleana	Sage/Mint	leaf			90	50		GC-MS	Fractionation Hydrodistillation	[573]
Mentha spicata	Spearmint	leaf	carvone limonene	0-0.32	69-103	39-49	22-88 $kg_{CO2}\,kg^{-1}_{sample}$	Gravimetric Analysis	Modeling	[574]
Mentha spicata	Spearmint	flake		1.3-2.9	100-300	40-50	15-20 % w/w EtOH 60 $kg_{CO2}\,kg^{-1}_{sample}$	GC-MS	Hydrodistillation Soxhlet extraction Antioxidant activity	[575]
Mentha spicata L.	Spearmint	leaves		0.25-1.82	90-170	35-55		Gravimetric Analysis	DoE Particle size effect	[576]
Mentha spicata L.	Spearmint	leaves	catechin, epicatechin, rutin, luteolin, myricetin, apigenin and naringenin	3.0-6.9	100-300	40-60	30 $kg_{CO2}\,kg^{-1}_{sample}$	HPLC	RSM DoE	[577]
Microula sikkimensis	-	seed		27-35	210-270	35-55	6.8-18.4 $L_{CO2}\,kg^{-1}_{sample}$	GC	DoE	[578]
Mikania glomerata Spreng	Guaco	leaf	coumarin		100	70		HPLC-UV	Maceration Ultrasound Infusion	[579]
Momordica charantia L.	-	fruit	flavonoids	1.2-1.5	250-350	30-50	555-1000 $L_{CO2}\,kg^{-1}_{sample}$ EtOH		DoE RSM Antioxidant activity	[305]
Morinda citrifolia	Noni	leaf + stem	phenolic compounds	0.2-2.0	103-241	25-50		Gravimetric Analysis	Antioxidant activity	[580]
Moringa oleifera	-	kernel	oil	6.71-36.13	150-300	35-60	(0-15 % w/w) EtOH	GC	RSM DoE	[581]
Morus alba	Mulberry	leaf and bark	β-sitosterol	0.3-2.0	200-450	40	0-60 $kg_{CO2}\,kg^{-1}_{sample}$	GC–FID GC–MS	Organic Solvent Extraction Soxhlet extraction	[294]
Myristica fragrans	Nutmeg	seed	terpenes	2-4	150-200	40-50		GC-MS	Modeling Particle sizes effect	[582]

Myristica fragrans	Nutmeg	fruit	2-alkylcyclobutanones		151-253	80	80 $L_{CO2}kg^{-1}$ sample	GC-MS GC-HRMS		[583]
Myrtus communis L.	-	leaf	oil	0.5-6.3	100-350		0.24 $L_{CO2}\,kg^{-1}$ sample MeOH	GC-MS GC-FID HPLC	RSM DoE Anova	[584]
Nepatia cataria	Catnip	leaf, stem, bud	nepetalactone	4.6-5.7	413	40		TLC		[585]
Nepeta persica	-	aerial parts	nepetalactone	0.22-8.9	100-355	35-75	12 $L_{CO2}\,kg^{-1}$ sample 0-6 % (vol.) MeOH	GC-FID GC-MS	Steam distillation DoE	[586]
Nicotiana spp	Tobacco	leaf	solanesol		80-250	25-60		GC-MS		[587]
Nicotiana tabacum L.	*Tobacco*	leaf	nicotine, neophytadiene	0.4-1.0	100-300	40		GC-MS		[588]
Nigella damascena	*Nigella*	seed		10.6-50.0	150-350	40	0-1 % EtOH	GC GC-MS	Soxhlet extraction 2-step decompression system	[589]
Nigella sativa L.	Black Cumin	seed	thymoquinone	0.2-0.3	150-200	35-45		GC HPLC	DoE Neural networks Pseudohomogeneous model	[301]
Nigella sativa L.	Black Cumin	seed		14-28	200-500	40	68 $L_{CO2}kg^{-1}$ sample	UV-Vis spectrophotometry	Antioxidant activity	[590]
Nigella sativa L.	Black Cumin	seed		0.8-31.7	200-300	40-70	60 $L_{CO2}kg^{-1}$ sample	HPLC	Soxhlet extraction	[591]
Nigella sativa L.	Black Cumin	seed	thymoquinone		150-350	40-50	90-120 $kg_{CO2}\,kg^{-1}$ sample 0.3 $L_{EtOH}\,kg^{-1}{}_{CO2}$		Antioxidant DoE	[302]
Ocimum basilicum	Basil	seedling		5-23	100-300	30-50	0.3-0.5 $kg_{CO2}\,kg^{-1}$ sample 1-20 % H_2O	GC-MS ESI-MS	Economic analysis	[195]
Ocimum basilicum	Ocimum basilicum	seed		1.08-1.95	99-243.7	25-50	36 $kg_{CO2}\,kg^{-1}$ sample	GC-MS	Oil characterization	[194]
Ocimum gratissimum L.	*Clove basil*	leaf		0.91-1.79	100-300	40		GC-FID	Fertilizer dosage effect Harvesting time effect	[196]
Ocimum gratissimum	*Ocimum*	leaf	eugenol	0.1-2.1	70	33		GC-MS	Hydrodistillation	[193]

L. / Ocimum micranthum Willd / Ocimum selloi Benth									Steam distillation	
Oenothera biennis L.	Primrose	seed	fatty acids	21	200-300	40-60	155 $kg_{CO2}\,kg^{-1}{}_{sample}$	GC	Soxhlet extraction Modeling	[592]
Olea europaea L.	Olive	husk		4-75	100-300	40-60	6000-9000 $L_{CO2}kg^{-1}{}_{sample}$	Gravimetric Analysis	Soxhlet extraction RSM DoE	[25]
Olea europaea L.	Olive	husk		64-80	75-350	40-60	8400-36000 $L_{CO2}kg^{-1}{}_{sample}$ 0-1 % EtOH	HPLC	RSM DoE Fractionation	[593]
Olea europaea L.	Olive	leaf	tocopherol	4-38	250-450	40-60	200-600 $L_{CO2}kg^{-1}{}_{sample}$	HPLC	Soxhlet extraction	[594]
Olea europaea L.	Olive	pomace	tocopherols	-	350	50		SFC GC-MS	Fractionation	[19]
Olea europaea L.	Olive	pomace	squalene	0-3	75-125	33-43	5-17 $kg_{CO2}\,kg^{-1}{}_{sample}$	GC-FID	DoE RSM Solubility	[18]
Olea europaea L.	Olive	leaf	oleuropein		100-300	50-100	72000 $L_{CO2}kg^{-1}{}_{sample}$ 0-20 % (vol.) EtOH 0-20 % MeOH 0-20 % H_2O	HPLC LC-ESI		[595]
Ophiopogon japonicus	-	root	6-aldehydo-isoophiopogonone A, 6-formyl-isoophiopogonanone A	0.1-0.3	150-350	55-65	50 $L_{CO2}kg^{-1}{}_{sample}$ Methanol	HPLC ESI-MS NMR	DoE	[596]
Opuntia dillenii	Pear bush	seed		4.2-6.0	250-400	65-50	13-133 $kg_{CO2}\,kg^{-1}{}_{sample}$	GC-MS	Antioxidant activity DoE RSM	[597]
Origanum majorana	Marjoram	leaf and top		0-20	100-400	40-60		HPLC	Organic solvent extraction Rancimat method DoE RSM	[598]

Origanum majorana	Marjoram	aerial parts		3.8	450	50	29 $kg_{CO2}\,kg^{-1}_{sample}$	GC GC-MS	Soxhlet extraction Antimicrobial tests	[599]
Origanum virens L.	Oregano	flower		5-95	50-300	27-47	0-55 $kg_{CO2}\,kg^{-1}_{sample}$	GC	Hydrodistillation	[167]
Origanum virens L.	Oregano	bract		50-80	70-200	27-47	33-100 $kg_{CO2}\,kg^{-1}_{sample}$	Gravimetric Analysis	Modeling Effect of particle size Scanning electron micrograph	[168]
Origanum vulgare L. *Thymus zygis* *Salvia officinalis* *Rosmarinus officinalis*	Oregano Thyme Sage Rosemary	leaf		0.9-3.2	300	40	20 $kg_{CO2}\,kg^{-1}_{sample}$	HPLC GC-MS	Pilot scale Two-step decompression	[165]
Origanum vulgare L.	Oregano	leaf		0.1-15.3	150-300	40-60	0-7 % EtOH	LC-MS LC-DAD	Pilot scale	[164]
Origanum vulgare L.	Oregano				150	40	7 % EtOH	GC-MS	Pilot scale Antimicrobial activity	[166]
Oriza spp.	Rice	bran		-	205-320	45-80	7854 $L_{CO2}kg^{-1}_{sample}$	HPLC	Fractionation Deacidification Likens–Nickerson extraction	[126]
Oriza spp.	Rice	bran	lipids, γ-oryzanol	-	680	30-75	29-41 $kg_{CO2}\,kg^{-1}_{sample}$	HPLC	Solvent extraction	[125]
Oriza spp.	Rice	bran		0-25	345-689	40-80	0-18 $kg_{CO2}\,kg^{-1}_{sample}$	Gravimetric HPLC	Soxhlet extraction Solubility analysis	[123]
Oriza spp.	Rice	bran	γ-oryzanols	18.1	300	40	78 $kg_{CO2}\,kg^{-1}_{sample}$	GC	Soxhlet extraction	[124]
Oryza sativa L.	Rice	bran	aroma		120	50	20-40 $L_{CO2}kg^{-1}_{sample}$	GC-MS	Cooking stage	[120]
Oryza sativa L.	Rice	bran		0-20	100-400	50-60	3-79 $kg_{CO2}\,kg^{-1}_{sample}$	GC-FID	Deacidification Pilot scale Particle sizes effect Economic study	[121]
Oryza sativa L.	Rice	bran	niosomes	11.2	200	40	10-35 % (w/v) EtOH	HPLC TPC	Soxhlet extraction Modeling Biological activity	[122]

Panax ginseng	Ginseng	root		1.1-10.7	104-312	35-60	6250 $L_{CO2}kg^{-1}$ sample 0-6 % EtOH	HPLC	Soxhlet extraction Ultrasonic extraction	[600]
Panax ginseng	Ginseng		ginsenosides		240	45	10-80 $L_{CO2}kg^{-1}$ sample bis(2-ethylhexyl) sodium sulfosuccinate/EtOH	Gravimetric	Ultra-sound assisted SFE Reverse microemulsion	[154]
Panax quinquefolium	American ginseng	root	ginsenoside		300	50	3 % (vol.) EtOH	HPLC	Ultra High pressure extraction Soxhlet extraction Ultrasound-assisted extraction Microwave-assisted extraction	[151]
Panax quinquefolius	Ginseng	root	ginsenosides	20-40	207-483	110	11-31 % (mol) MetOH DMSO	HPLC LC-MS	Soxhlet extraction	[152]
Pandanus amaryllifolius Roxb.	Pandan	leaf	2-acetyl-1-pyrroline	0-1	200	50	7200 $L_{CO2}kg^{-1}$ sample	GC-MS GC-FID	SEM	[283]
Pandanus amaryllifolius Roxb.	Pandanus	leaf	2-acetyl-1-pyrroline	-	120-455	40-80	20-40 $L_{CO2}kg^{-1}$ sample	GC-MS	Organic solvent extraction Steam distillation	[284]
Panicum miliaceum (L.)	Millet	bran	-	-	300-500	40-60	4-44 $kg_{CO2}\,kg^{-1}$ sample	HPTLC GC HPLC ICP-MS	Soxhlet extraction Three-step decompression	[601]
Papaver Somniferum L.	Poppy	seed		15.8-38.7	210-550	50-70	5-105 $kg_{CO2}\,kg^{-1}$ sample	GC		[602]
Patrinia villosa Juss	-			0.3-2.0	150-350	45-65	MEtOH 10-20 % (vol.)	GC-MS	DoE	[603]
Paullinia cupana	Guaraná	seed	caffeine	0-4	100-400	40-70	0-400 $kg_{CO2}\,kg^{-1}$ sample	HPLC		[604]
Pelargonium graveolens	Geranium	root	geraniol	0.2-3.8	100-300	40-70	35 $kg_{CO2}\,kg^{-1}$ sample	GC-MS	Steam distillation	[265]
Pelargonium graveolens	*Geranium*	root	citronellol		80-160	40-100	1-40 $kg_{CO2}\,kg^{-1}$ sample	GC-MS	Particle size effect Hydrodistillation Solvent Extraction	[266]

Perovskia atriplicifolia Benth.	Perovskia	aerial parts			100-300	45-65	0-5 % MEtOH 0-5 % EtOH 0-5 % Dicloromethane 0-5 % n-hexane	GC GC-MS	Steam distillation	[277]
Persea americana	Avocado	fruit		59.56-62.87	420-450	40-45	7-8 $\times 10^{-2}$ $L_{CO2}\,kg^{-1}_{sample}$			[605]
Persea indica	-	brach	ryanodanes	0.4-1.13	100-200	40-50		HPLC GC-MS	Modeling Organic solvent extraction	[606]
Petroselinum sativum Hoffm.	Parsley	seed		1-31	100-150	35-45	1-300 $kg_{CO2}\,kg^{-1}_{sample}$	GC	Hydrodistillation Modeling	[607]
Peumus boldus M.	Boldo Oregano	leaf branch	oil	0.4-3.1	100	40	6 $kg_{CO2}\,kg^{-1}_{sample}$		Matrix pretreatment	[608]
Peumus boldus M.	Boldo	bark	boldine	1.6-2.9	400-600	40-60	113 $kg_{CO2}\,kg^{-1}_{sample}$	HPLC	Antioxidant activity Solvent extraction	[609]
Peumus boldus M.	Boldo	leaf		0.5-2.9	60-450	30-60	15-634 $kg_{CO2}\,kg^{-1}_{sample}$ 0-10 % EtOH	HPLC GC-FID GC-MS	Hot pressurized water extraction Soxhlet extraction	[610]
Pfaffia glomerata *Pfaffia glomerata*	Brazilian Ginseng	root	β -Ecdysone	0.18-0.56 (dry bases)	100-300	30-50	19 $kg_{CO2}\,kg^{-1}_{sample}$ EtOH	TLC HPLC	Antioxidant activity	[611]
Phyllanthus emblica	Emblica	fruit	phenolic compounds	1.1-2.5	150-250	5-55	2-11 % (vol.)MeOH	GC-MS	Organic solvent extraction DoE Antimicrobial activity Antioxidant activity	[612]
Physalis peruviana	Physalis	leaf	flavonoids phenols	3.6-15.5	400	60	0-5 % EtOH		Hydrodistillation Solvent extraction	[307]
Picea abies	Spruce	bark		2.5-3.3	260	70	16 $kg_{CO2}\,kg^{-1}_{sample}$	NMR HPLC-DAD-MS/MS	Solvent extraction	[613]
Pimpinella anisum L	Aniseed	seed		3.1-10.7	80-180	30	0-0.4 $kg_{CO2}\,kg^{-1}_{sample}$	GC-MS TLC	Modeling	[614]
Pimpinella anisum L	Aniseed	seed			80-180	30	0.2-2.9 $kg_{CO2}\,kg^{-1}$	Gravimetric	Neural networks	[614]

Pinus brutia	Pine	bark	catechins epicatechin		200-800	27-80	0-3 % w/w EtOH	Analysis HPLC	Pilot scale Sonication	[615]
Pinus pinaster		wood	phenolics	0.3-2.1	100-250	30-50	0-20 % (wt.) EtOH	GC-FID		[616]
Pinus sylvestris L.	Pine	sawdust	fatty and resin acids	0.1-1.6	74-250	40-60	0-10 % w/w EtOH	GC-MS	Soxhlet extractions	[259]
Piper amalago	-	root			125-250	40-60	2300 $L_{CO2}\,kg^{-1}$ sample	HPLC	Compressed gas extraction	[617]
Piper nigrum	Pepper	seed			160-260	35-50		Gravimetric Analysis	Particle sizes effect	[618]
Piper nigrum L.	Black pepper	fruit		0-12	90-150	40-50	0-340 $kg_{CO2}\,kg^{-1}$ sample	GC-MS	Flow rates effect Modeling	[619]
Pistachia vera	Pistachio	seed	phenolic		100-350	45-65	0-15 % MeOH	Gravimetric Analysis	Organic solvent extraction Ultrasonic aided extraction Antioxidant activity	[620]
Pistacia lentiscus L.	Pistachio	berry + leaf		0.45	90-200	50		GC-MS	Hydrodistillation Two-step decompression system	[621]
Pistacia vera L.	Pistachio	seed			10-150	40-80	EtOH n-hexane	GC-FID	DoE RSM Soxhlet extraction	[622]
Plukenetia volubilis	Sacha inchi	seed	omega-3	41.9-50.1	300-400	40-60	130 $kg_{CO2}\,kg^{-1}$ sample	GC	Solvent extraction Modeling Particle sizes effect	[623]
Prunus amygdalus	Almond	seed + kernel		15-65	330	50	15-73 $kg_{CO2}\,kg^{-1}$ sample	HPLC	Soxhlet extraction Cold Pressing Multifactor analysis of variance	[624]
Prunus armeniaca L	Apricot	bagasse	β-carotene	3-6	304-507	40-60	8-87 $L_{CO2}\,kg^{-1}$ sample	Spectrophotometry	Micrograph Modeling	[131]

Prunus armeniaca L.	Apricot	pomace	β-carotene	1-8	304-507	40-60	5-150 $L_{CO2}\,kg^{-1}{}_{sample}$	Spectrophotometry HPLC	Solvent extraction Particle sizes effect Flow rates effect	[127]
Prunus armeniaca L.	Apricot	kernel		5-42	300-600	40-70	0-50 $kg_{CO2}\,kg^{-1}{}_{sample}$ 0-3 % EtOH	SEM Gravimetric Analysis	Particle sizes effect Modeling	[129]
Prunus armeniaca L.	Apricot	kernel		4-22	300-450	40-60	6-12 $kg_{CO2}\,kg^{-1}{}_{sample}$ 0-3 % EtOH	GC	RSM	[128]
Prunus armeniaca L.	Apricot	pomace	β-carotene	3-9	133-473	43-77	10-90 $L_{CO2}\,kg^{-1}{}_{sample}$ 2-28 % EtOH	HPLC	RSM Static extraction	[130]
Prunus avium L.	Cherry	pomace			50-200	20-60	20-40 $L_{CO2}kg^{-1}{}_{sample}$ 0-20 % (wt.) EtOH		Antioxidant activity RSM DoE	[625]
Prunus avium L.	Cherry	fruit		0.5	250	50		TLC HPLC	Solvent extraction Fractionation Solvent extraction	[626]
Prunus avium L.	Cherry	seed		2-8	180-220	40-60		GC	Hexane extraction RSM	[627]
Prunus persica	Peach	kernel		1-18	150-250	40	123 -386 $kg_{CO2}\,kg^{-1}{}_{sample}$	Gravimetric Analysis	Modeling Particle sizes effect Scale-up	[628]
Prunus persica	Peach	seed		0-30	150-198	40-51	0-140 $kg_{CO2}\,kg^{-1}{}_{sample}$ 2.5-5.0 % mol/mol EtOH	GC-MS	Flow rates effect Extractor geometry effect	[629]
Prunus persica	Peach	kernel		3.8-24	100-300	50-70	(2-5 %)(w/w) EtOH			[630]
Prunus spp.	Almond	seed		2-98	350-550	35-50	10-60 $kg_{CO2}\,kg^{-1}{}_{sample}$	HPLC	Particle size effect Solvent extraction Three-step decompression system	[631]
Prunus spp.	Almond	seed		0-17	200-320	40-60	23-35 $kg_{CO2}\,kg^{-1}{}_{sample}$		Ultrasound assisted	[632]
Psidium guajava	Guava	leaf		1.3-3.9	100-300	86-54	0-6 kg/kg	TLC GC-MS	Modeling Soxhlet extraction	[633]

Psoralea corylitolia L.	Fructus Psoraleae	seed	psoralen isopsoralen	5.0-9.8	260-340	40-60	1200 $L_{CO2}kg^{-1}$ sample	HPLC	Ultrassound extraction Hydrodistillation DoE Particle sizes effect	[634]
Pteris semipinnata L.	-	aerial parts	ent-11a-hydroxy-15-oxo-kaur-16-en-19-oic-acid	0.00-0.05	300	55	53-266 $kg_{CO2}\,kg^{-1}$ sample 0-15 % EtOH	HPLC	Pilot scale	[635]
Pueraria lobata	-	root	puerarin daidzein rutin	0.2-2.0	150-250	40-60	750 $L_{CO2}kg^{-1}$ sample EtOH 0.3-0.6 % (vol.)	Gravimetric Analysis	RSM DoE	[636]
Pueraria lobata	-	root	*puerarin*	0.4-0.6	100-300	40-60	1-2.3 $kg_{CO2}\,kg^{-1}$ sample 46-63 w/w EtOH	HPLC		[637]
Punica granatum	Pomegranate	seed		0.7-12.8	132-468	33-70	80-192 $L_{CO2}kg^{-1}$ sample	HPLC	RSM DoE Flow rates effect Soxhlet extraction	[638]
Quercus urfassea L. *Quercus suber L.*	Oak	fruit			180	40		FAME HPLC TLC	Soxhlet extraction	[639]
Quercus suber L.	Oak	cork	triterpenes	6	200-250	50	96 $kg_{CO2}\,kg^{-1}$ sample	^{13}C NMR	Organic solvent extraction	[640]
Rhodiola rosea	*R. rosea*	herb	rosavin	18-21	200	70-80	324-540 $kg_{CO2}\,kg^{-1}$ sample 10 % H_2O	HPLC		[641]
Rosa aff. Rubiginosa	Rose hip	seed		4.7-7.1	300-500	40-60	3 $kg_{CO2}\,kg^{-1}$ sample	Spectrophotometry Gravimetric	Soxhlet extraction RSM DoE	[642]
Rosa aff. Rubiginosa	Rose hip	seed		0-0.35	300	40	0-60 $kg_{CO2}\,kg^{-1}$ sample	Gravimetric	Micrograph	[643]
Rosa aff. Rubiginosa	Rosehip	seed		0-7.5	300-400	40-50	9.2-83 $kg_{CO2}\,kg^{-1}$ sample	Gravimetric	Two-stage model	[644]
Rosa canina L.	Rose hip	seed		5.72	250	30	0.4-1.6 $kg_{CO2}\,kg^{-1}$ sample	Gravimetric	Soxhlet extraction Ultrasound water bath Microwave	[645]

									extraction Subcritical fluid extraction ANOVA	
Rosa Mosqueta; Rosa Aff. Rubiginosa	Rose hip	seed		100 % Soxhlet	300-700	60	27-54 $kg_{CO2}\,kg^{-1}_{sample}$	-	Matrix pretreatment effect	[646]
Rosa spp.	Hiprose	seed		0-7.4	103-689	40-70	2-20 $kg_{CO2}\,kg^{-1}_{sample}$	Gravimetric	SEM Modeling	[647]
Rosmarinus officinalis	Rosemary	leaf			90-400	40-60	2.5 $L_{CO2}kg^{-1}_{sample}$	SFC-FID		[113]
Rosmarinus officinalis	Rosemary	leaf		1-5	100-300	30-40	2-45 $kg_{CO2}\,kg^{-1}_{sample}$	GC Spectrophotometry TLC	Hydrodistillation Solvent extraction Modeling	[648]
Rosmarinus officinalis	Rosemary	leaf			100-180	40-60	EtOH 0-3 wt.% 0-25 $kg_{CO2}\,kg^{-1}_{sample}$	Gravimetric Analysis	Particle sizes effect Flow rates effect 2-stage separation Modeling	[107]
Rosmarinus officinalis *Foeniculum vulgare* *Pimpinella anisum*	Rosemary / fennel / anise	leaf seed leaf		0.1-3.5	100-350	30-40		Gravimetric Analysis	Steam distillation Economic analysis	[112]
Rosmarinus officinalis	Rosemary	leaf	phenols	0.5-3.1	100-400	40	36 $kg_{CO2}\,kg^{-1}_{sample}$ 0-7 % EtOH	UPLC-MS	Antioxidant activity	[109]
Rosmarinus officinalis	Rosemary	leaf	various	1	100-205	40-55	0-5 % EtOH	GC-MS	Antioxidant activity Three steps sequential	[110]
Rosmarinus officinalis L.	Rosemary	leaf	carnosic acid, rosmanol, carnosol	-	300-350	40-60	0-2 % EtOH	RP-HPLC MEC	Two-step decompression	[41]
Rosmarinus officinalis L.	Rosemary	leaf	1,8-cineole		250	60	3 $L_{CO2}kg^{-1}_{sample}$	GC-FID GC-MS	Organic solvent extraction Microwave assisted Hydrodistillation	[111]
Rosmarinus officinalis	Rosemary	leaf		-	300-350	40-60	0-2 % EtOH	HPLC	Pilot scale	[41]

L.									Fractionation	
Salvia lavandulifolia	Spanish sage	leaf / flower		1.2-1.8	90-100	40-50	4-165 $kg_{CO2}\,kg^{-1}_{sample}$	GC-MS	Hydrodistillation Modeling Flow rates study Particle size study	[649]
Salvia miltiorrhiza	Danshen	root	tanshinones	0-5	200-400	40-60	13-75 $L_{CO2}kg^{-1}_{sample}$	HPLC	DoE	[650]
Salvia officinalis L.	Sage			12-46	250-350	40	20 $kg_{CO2}\,kg^{-1}_{sample}$ 0-2 % EtOH	Gravimetric Analysis	3-step decompression Antioxidant activity test	[651]
Salvia officinalis L. *Ocimum basilicum* *Origanum vulgare* *Levisticum officinale*	Sage Basil Oregano Lovage	leaf + flower		0.2-1.5	172-255	55	0-7.5 % EtOH	GC	Antimicrobial activity Hydrodistillation	[197]
Santalum álbum *Boswellia carterii*	Santalum album *Boswellia carterii*	wood *(resin)*		1.3-6.5	90-120	45-60	120 $kg_{CO2}\,kg^{-1}_{sample}$	GC-MS	Hydrodistillation	[652]
Santolina chamaecyparissus	-	flower		0.1-1.4	80-90	40-50	21 $kg_{CO2}\,kg^{-1}_{sample}$	GC GC-MS	Hydrodistillation SEM Particle size effect Flow rate effect	[653]
Santolina insularis	-	aerial parts		2	80-120	45-70		GC-MS	2-step decompression Hidrodistillation Cytotoxic and antimicrobial activity	[654]
Satureja hortensis	Savoury	aerial parts	terpinene thymol carvacrol	5.9-8.7	303-405	55-75	5-10 % (vol.) EtOH	GC-MS GC-FID	Two steps of DoE RSM Hydrodistillation	[655]
Satureja hortensis L.	Savoury		carnosol carnosic acid rosmarinic acid	0.87-6.42	300-450	40	7 $kg_{CO2}\,kg^{-1}_{sample}$ EtOH (5-15 % w/w)	GC-FID HPLC	Antioxidant activity Organic solvent extraction	[656]
Satureja montana	Savoury	aerial parts		0.9-1.4	90-250	40	40 $kg_{CO2}\,kg^{-1}_{sample}$	GC	Hydrodistillation Soxhlet extraction Antioxidant	[657]

									activity	
Satureja montana	Savory	herb	thymoquinone	0.9-1.6	90-100	40-50	44 $kg_{CO2}\,kg^{-1}{}_{sample}$	GC GC-MS	Hydrodistillation SEM Particle size effect Flow rate effect	[303]
Schinus molle L.	Schinus	leaf		0.4-0.7	90	50		GC-MS	Hydrodistillation Steam distillation	[658]
Schisandra chinensis	-	fruit		18.5	250	50	250 $L_{CO2}kg^{-1}{}_{sample}$	GC-MS	2-step decompression Steam distillation Soxhlet extraction Ultrasonic extraction	[659]
Schisandra chinensis	-	stem + leaf	lignan cinnamic acid	0.2-1.3	200-270	40-60	10-74 $kg_{CO2}\,kg^{-1}{}_{sample}$	RP-HPLC	Modeling	[300]
Scutellaria baicalensis	-	*root*	baicalin	0.1-8.3	200-400	40-60	0.4 % (vol.) MeOH 0.4 % (vol.) EtOH 0.4 % (vol.) 1,2-Propanediol	HPLC	DoE Soxhlet extraction	[660]
Sesamum indicum L.	Black Sesame	seed		41-52	200-400	35-85	225-300 $L_{CO2}kg^{-1}{}_{sample}$	Spectrophotometry	Solvent extraction	[661]
Seseli bocconi Guss	Seseli bocconi Guss	leaf		0.13-0.60	90	50		GC-MS	Hydrodistillation	[662]
Silybum marianum	*Silybum*	*seed*	vitamin E	5-25	100-300	5-80	65-82 $kg_{CO2}\,kg^{-1}{}_{sample}$	HPLC	Soxhlet extraction Acid value test Modeling	[663]
Simmondsia chinensis	Jojoba	seed		10-52	300-600	70-90	2-49 $kg_{CO2}\,kg^{-1}{}_{sample}$ 0-10 % Hexane	Gravimetric Analysis	Solvent extraction Flow rates effect Particle sizes effect	[664]
Sinomenium acutum (Thumb) Rehd et Wils	-	stem	sinomenine	0.01-0.70	200-600	40-60	15000 $L_{CO2}kg^{-1}{}_{sample}$ MeOH	HPLC		[665]
Solanum lycopersicum L.	Tomato	skin	lycopene		335-450	45-70	3-40 $kg_{CO2}\,kg^{-1}{}_{sample}$ 0-20 % Hazelnut oil	HPLC Spectrophotometry	Particle size effect	[65]
Solanum lycopersicum	Tomato	fruit		0.03-0.07	250-350	45-75	5-15 % EtOH/ H_2O	HPLC	Cluster analysis	[68]

L.							/Canola Oil			
Solanum lycopersicum L.	Tomato	fruit	lycopene	0.001-0.002	250-450	40-70	21 $L_{CO2}kg^{-1}$ sample	HPLC	DoE RSM	[73]
Solanum lycopersicum L.	Tomato	fruit	lycopene		200-400	40-100		HPLC	DoE ANOVA RSM	[64]
Solanum lycopersicum L.	Tomato	waste	trans-Lycopene	0-0.03	300	40-80	220 kg_{CO2} kg^{-1} sample	HPLC	Particle size study Flow rate study	[71]
Solanum lycopersicum L.	Tomato	waste	lycopene	0.001-0.004	300-460	40-80		HPLC	Solvent Extraction RSM DoE Modeling	[66]
Solanum lycopersicum L.	Tomato	fruit	lycopene		200-500	40-100		HPLC UV-Vis	Modeling Soxhlet extraction	[67]
Solanum lycopersicum L.	Tomato	Waste	Lipids Lycopene β-carotene		250-300	60-80	130 kg_{CO2} kg^{-1} sample	Gravimetric HPLC	Particle sizes effect Solvent extraction	[70]
Solanum lycopersicum L.	Tomato	pomace	lycopene		365-533	47-63	71-773 $L_{CO2}kg^{-1}$ sample	HPLC	Antioxidant activity RSM DoE Soxhlet extraction Pretreatment effect	[274]
Solanum lycopersicum L.	Tomato	fruit	lycopene β-carotene		400	40-70	0-5 wt.% EtOH 0-5 wt.% Canola oil	HPLC	Soxhlet extraction	[69]
Solanum lycopersicum L.	Tomato	fruit and seed	lycopene		200-400	70-90	7-180 $L_{CO2}kg^{-1}$ sample	GC-MS GC-FID HPLC	Modeling	[72]
Sophora flavescens	-	root	quinolizidine alkaloids oxymatrine matrine	0.3-0.5	200-300	45-55	2-4 % (3/4 EtOH + ¼ H_2O)	HPLC TLC	Scale-up DoE	[666]
Spilanthes acmella var oleracea	*Jambú*	flower leaf stem	spilanthol	1.2-4.8	250	50		GC	Hydrodistillation Organic Solvent extraction	[667]

									Antioxidant activity Anti-inflammatory activity	
Stevia rebaudiana	-	leaf	stevioside rebaudioside A		150-350	40-80	0-20 % EtOH-H_2O	HPLC-UV	Solvent extraction RSM DoE	[668]
Stevia rebaudiana Bertoni	Stevia	leaf		0-1.2	200-250	30	35 $kg_{CO2}\,kg^{-1}$ sample	GC-FID GC-MS TLC HPLC	Modeling	[669]
Syzygium aromaticum L.	Clove	Bud			90-120	50	8-42 $kg_{CO2}\,kg^{-1}$ sample		Modeling	[670]
Tagetes erecta	Marigold	flower	lutein esters	0.4-0.7	175-325	45-55	150-300 $kg_{CO2}\,kg^{-1}$ sample	Spectrophotometer	Ultrasound assisted Modeling Particle sizes effect	[671]
Tanacetum cinerariifolium (Trevir) Sch. Bip. *Glebionis 73urfasse73* (L.) Spach *Glebionis segetum* (L.) Fourr *Plagius flosculosus* (L.) Alavi and Heywood	Chrysanthemums	flower	pyrethrins		90-300	40-50		GC-MS	Hydrodistillation Cytotoxic activity Antiviral activity	[672]
Tanacetum parthenium	Feverfew	flower	parthenolide	2-9	200-800	40-80	19-33 $kg_{CO2}\,kg^{-1}$ sample	HPLC	Pilot scale 2-step decompression	[268]
Tanacetum parthenium	Feverfew	seed	parthenolide					HPLC SFC Densitometry		[673]
Taraxacum officinale Weber et Wiggers	Dandelian	leaf	β-amyrin β-sitosterol	1.5-4	150-450	35-65	35-53 $kg_{CO2}\,kg^{-1}$ sample		DoE RSM Organic solvent extraction	[674]
Taxus baccata	*Yew*	needle	10-		100-400	65-75	8-50 $L_{CO2}kg^{-1}$ sample	HPLC	Soxhlet extraction	[198]

			deacetylbaccatin III				10 % MeOH			
Terminalia catappa	-	leaf and seed	squalene	7-18	138-275	40	45 $L_{CO2}kg^{-1}$ sample	GC-MS HPLC	Antioxidant activity	[271]
Theobroma cacao	Cocoa	seed		52-92	350	60	25 % EtOH	HPLC Gravimetric Analysis	Fermentation level effect Roasting time effect	[141]
Theobroma cacao	Cocoa	bean		3-13	152-248	50	4-23 $kg_{CO2}\,kg^{-1}$ sample	GC	Supercritical ethane	[139]
Theobroma cacao	Cocoa	beans	caffeine theobromine		200-400	50	0-750 $kg_{CO2}\,kg^{-1}$ sample	HPLC	Ethane extraction	[140]
Theobroma grandiflorum	Cupuacu	seed		5-60	248-352	50-70	0-140 $kg_{CO2}\,kg^{-1}$ sample	HPLC	Supercritical ethane extraction Modeling	[675]
Thymbra spicata	*Thymbra*	leaf and branch		0.67	80-120	40-60		GC-MS	RSM DoE Steam distillation	[676]
Thymus vulgaris	Thyme	Flower + leaf	thymol, carvacrol	0.7-1.9	200	40	8-30 $L_{CO2}kg^{-1}$ sample	Gravimetric Analysis	Modeling	[74]
Thymus vulgaris L.	Thyme			5-50	100	40	5-14 $kg_{CO2}\,kg^{-1}$ sample	HPLC GC-MS	Steam distillation Modeling	[677]
Thymus vulgaris	Thyme	flower	P-cymene y-terpinene linalool thymoquinone	1-12	90-100	40	28-52 $kg_{CO2}\,kg^{-1}$ sample	GC	Hydrodistillation Soxhlet extraction Antioxidant activity	[77]
Thymus vulgaris	Thyme	leaf		1.15	100	40	94 $kg_{CO2}\,kg^{-1}$ sample		Modeling Conventional solvent extraction Ultrassound assisted extraction Soxhlet extraction Pilot scale	[678]
Thymus vulgaris L.	Thyme		phenolic	0.6-4.0	80-400	40	4886 $L_{CO2}kg^{-1}$ sample	GC-MS HPLC	Steam distillation Soxhlet extraction	[32]
Thymus vulgaris L.	Thyme	leaf		4.9	400	60			Pilot scale Soxhlet extraction	[81]
Thymus vulgaris L.	Thyme	leaf	thymol,	3.3-4.7		40		GC-MS		[76]

					150-400					
Thymus zygis L.	Thyme	leaf		1.2	100-150	40		GC GC-MS	Hydrodistillation Sensorial analysis	[78]
Thymus zygis L. subsp. Sylvestris	Thyme	aerial parts		0-11	80-214	30-57	2-118 $kg_{CO2}\,kg^{-1}_{sample}$	GC GC-MS	RSM DoE	[79]
Torresea cearensis	Emburana	seed	coumarin		85-240	35-50	0-21 $kg_{CO2}\,kg^{-1}_{sample}$	HPLC	Steam distillation Flow rates effect Particle sizes effect	[679]
Tribulus 75urfasse7575 L.	-	fruit	diosgenin	17.4	100-300	35-55		HPLC Gravimetric Analysis	RSM DoE Soxhlet extraction	[680]
Trifolium pratense	Red clover	leaf	isoflavones		100-400	35-75	5 % (vol.) (14:1) $MeOH/H_2O$	HPLC/MS		[681]
Trifolium pretense L.	Red clover	root			137	80	n-hexane	GC-MS		[682]
Trigonella foenum-graecum L.	-	seed	oil	2.33-4.08	200-300	45-50		HPLC-FLD-MS	Antioxidant activity RSM DoE Soxhlet extraction	[683]
Tripterygium wilfordii	-	root	tripterine	0.37	100-300	40-70	Acetone EtOH Ethyl acetate n-butanol	HPLC	Soxhlet extraction	[684]
Triticum spp.	Wheat	flour	lipids	0.6-1.4	172-517	60-100	0-19 % EtOH	TLC	Soxhlet extraction Butt extraction	[184]
Triticum spp.	Wheat	germ	tocopherols	7.3-8.0	50-300	10-60		GC HPLC	Soxhlet extraction Physicochemical characterization	[183]
Triticum spp.	Wheat	germ		50-92	250-380	55	369 $L_{CO2}kg^{-1}_{sample}$	Gravimetric Analysis HPLC	Soxhlet extraction	[185]
Triticum spp.	Wheat	germ	α-tocopherol	14-21	400-550	40-80	20-80 $kg_{CO2}\,kg^{-1}_{sample}$	GC HPLC	Organic solvent extraction Pilot Scale	[181]
Triticum spp.	Wheat	germ	tocopherol	0.5-9.5	148-602	40-60	10-60 $kg_{CO2}\,kg^{-1}_{sample}$	HPLC	DoE RSM	[182]

									Antioxidant activity	
Triticum spp.	Wheat	bran			100-300	40-60			Antioxidant activity	[685]
									Conventional solvent extraction	
Undaria pinnatifida	Seaweed	aerial parts			230	100	16.7 $L_{CO2}kg^{-1}$ $_{sample}$ MeOH	GC-FID	Soxhlet extraction	[686]
Valeriana officinalis L.	Valerian	root	valerenic acid	0.2-2.0	100-200	40-70	0-5 % EtOH 0-5 % MeOH	HPLC		[687]
Valeriana officinalis L.	Valerian	root		0.1-2.5	100-200	40-50	1-32 $kg_{CO2}kg^{-1}$ $_{sample}$	GC-FID GC-MS	Modeling SEM analysis	[688]
Valeriana officinalis L.	Valerian	Root	valerenic acids	1.8-4.9	152-228	37-61	4-12 $L_{CO2}kg^{-1}$ $_{sample}$	GC GC-MS	Mixture design	[689]
Valeriana officinalis var. latifolia	Valerian	root		0.8-1.9	250-400	35-65		GC-MS	Hydrodistillation	[690]
Vernonia galamensis L.	iron weed	*seed*	vernolic acid	20-40	138-690	40-80	20000-50000 $L_{CO2}kg^{-1}$ $_{sample}$	Gravimetric Analysis	Deacidification	[691]
Vetiveria zizanioides (L.) Nash ex Small	Vetiver	root	khusimol, zizanoic acid	3.2	200	40	0-15 % EtOH 8 $kg_{CO2}kg^{-1}$ $_{sample}$	GC-FID GC GC-MS GC-FID	Hydrodistillation Sensory evaluation	[692]
Vetiveria zizanioides L.	Vetiver	root		3.90-4.35	300	40	7-33 $kg_{CO2}kg^{-1}$ $_{sample}$	HPLC	Pilot plant	[693]
Vetiveria zizanioides L.	Vetiver	root		0.46-1.38	100-220	40-63	2-40 $kg_{CO2}kg^{-1}$ $_{sample}$	GC-MS	Antioxidant activity RSM DoE	[694]
Vetiveria zizanioides L.	Vetiver	root		2.0-3.5	200	40	162 $kg_{CO2}kg^{-1}$ $_{sample}$	GC-FID	Hydrodistillation Soxhlet extraction Phase equilibrium study	[695]
Vetiveria zizanioides L.	Vetiver	grass		0-6	100-190	40-50	40 $L_{CO2}kg^{-1}$ $_{sample}$	GS-MS	Modeling Economic analysis RSM DoE	[693]
Vetiveria zizanioides L.	Vetiver	root		3.4-4.7	100-300	40	Etanol (5-15 % (vol.) 0-10 % (vol.) EtOH 81-108 $kg_{CO2}kg^{-1}$	TLC GC	Hydrodistillation Kinetics study	[696]

Vitex agnus castus	Chaste tree	fruit		6.4	100-450	40-60	22-39 $kg_{CO2}\,kg^{-1}_{sample}$	TLC TLC-densitometry GC HPLC	Soxhlet extraction DoE RSM	[697]
Vitis 77urfasse L.	Grape	seed	tryacylglicerides	11.5	180-220	40-50	90 $kg_{CO2}\,kg^{-1}_{sample}$	GC-FID	Antioxidant activity	[59]
Vitis 77urfasse L.	Grape	seed		0-16	160-200	40	0-10 $kg_{CO2}\,kg^{-1}_{sample}$	GC-FID	Matrix enzymatic pretreatment	[33]
Vitis labrusca B.	Grape	seed	gallic acid protocatechuic acid phydroxybenzoic acid	5.7-12.3	137-167	67-76	5-8 % EtOH	HPLC	RSM DoE Antiradical activity	[54]
Vitis spp.	Grape	pomace	anthocyanins	0.02-1.2	150-300	40	28-66 % EtOH	HPLC	Fractionation	[62]
Vitis spp.	Grape	seed		0-12	280-550	40	0-24 $kg_{CO2}\,kg^{-1}_{sample}$		Extractor volume study Modeling Solubility	[52]
Vitis vinifera	Grape	seed		8-16	250	80	41 $kg_{CO2}\,kg^{-1}_{sample}$	GC-MS HPLC	Species varieties comparison	[42]
Vitis vinifera	Grape	fruit	glycosides			40-60	5-20 % MeOH	GC	DoE Sand bed Diatomaceous earth	[58]
Vitis vinifera	Grape	marc	polyphenols		270-350	40-50	150-200 $L_{CO2}kg^{-1}_{sample}$ 0-25 % MeOH	HPLC	Diatomaceous earth	[698]
Vitis vinifera	Grape	skin	resveratrol		80-150	40	5-15 % EtOH	HPLC		[699]
Vitis vinifera	Grape	marc	polyphenols			50	10 % H_2O	Amperometric Detection	Species variety effect	[57]
Vitis vinifera	Grape	marc	polyphenols		350	50	45-180 $L_{CO2}kg^{-1}_{sample}$ 0-7 % MeOH	Electrophoresis	Biological activity Diatomaceous earth	[56]
Vitis vinifera	Grape	pomace	phenolics		150	40	10-20 % (wt.) EtOH 4 $kg_{CO2}\,kg^{-1}_{sample}$	GC-MS	Antioxidant activity Soxhlet extraction	[49]

Vitis vinifera	Grape	seed			250	40	0-130 $kg_{CO2}\,kg^{-1}_{sample}$ 0-10 % (wt.) EtOH	GC-FID		[48]
Vitis vinifera	Grape	seed		0.1-7.9	60-254	30-60	40 $L_{CO2}kg^{-1}_{sample}$	GC	Propane extraction	[700]
Vitis vinifera L.	Grape	pomace	phenol	2.8-28.9	80-350	98-50	0-8 % EtOH	HPLC	Solid-liquid extraction	[60]
Vitis vinifera L.	Grape	seed	phenolic	0-0.15	200-300	40	0-15 % EtOH 0-15 % MetOH	HPLC-MS	Solubility tests	[55]
Vitis vinifera L.	Grape	seed		2.5-6.2	300-400	35-40	6 $L_{CO2}kg^{-1}_{sample}$ 0-10 % EtOH	HPLC–ELSD	DoE Scale-up	[46]
Vitis vinifera L.	Grape	seed		9.1-10	655	80	24 $L_{CO2}kg^{-1}_{sample}$ 0-40 % MetOH	HPLC-UV SFC-UV HPLC-MS	Fractionation	[44]
Vitis vinifera L.	Grape	pomace	phytosterols	6.6-11.2	370	65	2-123 $kg_{CO2}\,kg^{-1}_{sample}$	GC-MS GC-FID HPLC	Solvent extraction	[701]
Vitis vinifera L.	Grape	fruit/seed	polyphenols	0.01-0.03	200-500	45	7-67 $kg_{CO2}\,kg^{-1}_{sample}$ 4 % wt EtOH	UV–vis spectrophotometer		[702]
Vitis vinifera L.	Grape	skin	(+)-catechin, (–)-epicatechin, quercetin, rutin		100-300	60	10-50 $L_{CO2}kg^{-1}_{sample}$ 5-25 % (vol.) EtOH	HPLC		[47]
Vitis vinifera L.	Grape	seed		13.42	350	40	13 $kg_{CO2}\,kg^{-1}_{sample}$		Scale-up Economic analysis	[61]
Vitis vinifera L.	Grape	Seed			250-300	30-50		HPLC		[63]
Xanthoceras sorbifolia Bunge	Yellow Horn	seed		40-61	165-334	28-62	20-100 $kg_{CO2}\,kg^{-1}_{sample}$	GC-MS	DoE Particle sizes effect Soxhlet extraction Flow rates effect Anti-oxidant activity RSM	[703]

Zanthoxylum bungeanum	-	seed		2.3-4.1	200-400	50-80	0-15 % EtOH	HPLC-FLD-MS	RSM Antioxidant activity	[704]
Zataria multiflora Boiss	Zataria		thymol; l-terpinene; r-cymene		101-304	35-55	1-5 $L_{CO2}kg^{-1}$ $_{sample}$ MeOH	HPLC GC GC-MS	Steam distillation	[705]
Zea mays	Corn	germ			210-525	40-86	100-300 $kg_{CO2}\,kg^{-1}$ $_{sample}$	HPLC GC-FID	Modeling	[706]
Zea mays	Corn	bran	phytosterols	96	345-690	40-80	60-120 $L_{CO2}kg^{-1}$ $_{sample}$ 0-15 % EtOH	SFC		[291]
Zingiber corallinum Hance	-	rhizome		2.8-9.1	20-150	30-60	5-8 $L_{CO2}kg^{-1}$ $_{sample}$	GC-MS	Steam distillation DoE	[707]
Zingiber officinale	Ginger	rhizome	gingerol		160	40			Ultrasound Particle size effect FE-SEM	[150]
Zingiber officinale	Ginger	rhizome	gingerol	1.9-2.7	200-250	25-35	158 $kg_{CO2}\,kg^{-1}$ $_{sample}$ 0-1.2 %EtOH 0-1.2 % Isopropyl Alcohol	GC-MS GC-FID	DoE Modeling	[146]
Zingiber officinale Rosco	Ginger	rhizome		0-90	150-250	20-40	0-10 $kg_{CO2}\,kg^{-1}$ $_{sample}$	GC-MS	Modeling	[147]
Zingiber oficinale	Ginger	rhyzome				40	30 L kg	GC-MS	Drying effect	[149]

2.5 REFERENCES

[1] M.M.R. de Melo, A.J.D. Silvestre, C.M. Silva, Supercritical fluid extraction of vegetable matrices: Applications, trends and future perspectives of a convincing green technology, Journal of Supercritical Fluids 92(0) (2014) 115-176.

[2] M.M.R. de Melo, R.M.A. Domingues, A.J.D. Silvestre, C.M. Silva, Extraction and Purification of Triterpenoids using Supercritical Fluids: From Lab to Exploitation, Mini-Reviews in Organic Chemistry 11(3) (2014) 362-381.

[3] M.M.R. de Melo, I. Portugal, A.J.D. Silvestre, C.M. Silva, Environmentally benign supercritical fluid extraction, in: F. Pena-Pereira (Ed.), The Application of Green Solvents in Separation Processes, Elsevier, Amsterdam, 2017

[4] G. Brunner, Applications of Supercritical Fluids, in: J.M. Prausnitz, M.F. Doherty, R.A. Segalman (Eds.), Annual Review of Chemical and Biomolecular Engineering, Vol 12010, pp. 321-342.

[5] B.A.S. Machado, C.G. Pereira, S.B. Nunes, F.F. Padilha, M.A. Umsza-Guez, Supercritical Fluid Extraction Using CO2: Main Applications and Future Perspectives, Separation Science and Technology 48(18) (2013) 2741-2760.

[6] R.R. Chaudhury, U.M. Rafei, Traditional Medicine in Asia, Stylus Pub Llc2002.

[7] M. Perrut, Supercritical fluid applications: Industrial developments and economic issues, Industrial & Engineering Chemistry Research 39(12) (2000) 4531-4535.

[8] M.M.R. de Melo, A.J.D. Silvestre, C.M. Silva, Supercritical fluid extraction of oil and bioactive compounds from grape residues: experimental optimization, modeling and economic evaluation, in: J.S. Câmara (Ed.), Grapes: Production, Phenolic Composition and Potential Biomedical Effects, Nova Publisher2014.

[9] M.M.R. de Melo, A.J.D. Silvestre, C.M. Silva, Enhanced technologies for thevalorization of waste and side vegetable products using supercritical fluids, Recent Research Developments in Chemical Engineering 7 (2014) 19-32.

[10] M.J.H. Akanda, M.Z.I. Sarker, S. Ferdosh, M.Y.A. Manap, N.N.N. Ab Rahman, M.O. Ab Kadir, Applications of Supercritical Fluid Extraction (SFE) of Palm Oil and Oil from Natural Sources, Molecules 17(2) (2012) 1764-1794.

[11] L.F. de Franca, M.A.A. Meireles, Modeling the extraction of carotene and lipids from pressed palm oil (*Elaes guineensis*) fibers using supercritical CO_2, Journal of Supercritical Fluids 18(1) (2000) 35-47.

[12] H.L.N. Lau, Y.M. Choo, A.N. Ma, C.H. Chuah, Characterization and supercritical carbon dioxide extraction of palm oil (*Elaeis guineensis*), Journal of Food Lipids 13(2) (2006) 210-221.

[13] R. Davarnejad, K.M. Kassim, A. Zainal, S.A. Sata, Supercritical fluid extraction of beta-carotene from crude palm oil using CO(2), Journal of Food Engineering 89(4) (2008) 472-478.

[14] G. Andrich, S. Balzini, A. Zinnai, V. De Vitis, S. Silvestri, F. Venturi, R. Fiorentini, Supercritical fluid extraction in sunflower seed technology, European Journal of Lipid Science and Technology 103(3) (2001) 151-157.

[15] L. Vazquez, C.F. Torres, T. Fornari, N. Grigelmo, F.J. Senorans, G. Reglero, Supercritical fluid extract ion of minor lipids from pretreated sunflower oil deodorizer distillates, European Journal of Lipid Science and Technology 108(8) (2006) 659-665.

[16] J.M.D. Araujo, A.P.N. Nicolino, C. Blatt, Utilization of supercritical carbon dioxide for concentration of tocopherols from soybean oil deodorizer distillate, Pesqui Agropecu Bras 35(1) (2000) 201-205.

[17] C.M.J. Chang, Y.F. Chang, H.Z. Lee, J.Q. Lin, P.W. Yang, Supercritical carbon dioxide extraction of high-value substances from soybean oil deodorizer distillate, Industrial & Engineering Chemistry Research 39(12) (2000) 4521-4525.

[18] S. Stavroulias, C. Panayiotou, Determination of optimum conditions for the extraction of squalene from olive pomace with supercritical CO_2, Chem Biochem Eng Q 19(4) (2005) 373-381.

[19] E. Ibanez, J. Palacios, F.J. Senorans, G. Santa-Maria, J. Tabera, G. Reglero, Isolation and separation of tocopherols from olive by-products with supercritical fluids, Journal of the American Oil Chemists Society 77(2) (2000) 187-190.

[20] A. de Lucas, J. Rincon, I. Gracia, Influence of operation variables on quality parameters of olive husk oil extracted with CO_2: Three-step sequential extraction, J Am Oil Chem Soc 80(2) (2003) 181-188.

[21] A. de Lucas, J. Rincon, I. Gracia, Influence of operating variables on yield and quality parameters of olive husk oil extracted with supercritical carbon dioxide, Journal of the American Oil Chemists Society 79(3) (2002) 237-243.

[22] L. Casas, C. Mantell, M. Rodriguez, A. Torres, F.A. Macias, E.J.M. de la Ossa, Supercritical fluid extraction of bioactive compounds from sunflower leaves with carbon dioxide and water on a pilot plant scale, Journal of Supercritical Fluids 45(1) (2008) 37-42.

[23] L. Casas, C. Mantell, M. Rodriguez, A. Torres, F.A. Macias, E.J.M. de La Ossa, SFE kinetics of bioactive compounds from Helianthus annuus L., Journal of Separation Science 32(9) (2009) 1445-1453.

[24] L. Casas, C. Mantell, M. Rodriguez, A. Torres, F.A. Macias, E.M. de la Ossa, Effect of the addition of cosolvent on the supercritical fluid extraction of bioactive compounds from *Helianthus annuus* L., Journal of Supercritical Fluids 41(1) (2007) 43-49.

[25] A. de Lucas, E.M. de la Ossa, J. Rincon, M.A. Blanco, I. Gracia, Supercritical fluid extraction of tocopherol concentrates from olive tree leaves, Journal of Supercritical Fluids 22(3) (2002) 221-228.

[26] Q.H. Chen, P. Li, B. Li, H.D. Yang, X.L. Li, F.C. Chen, A GC-MS-SIM simultaneous determination of ligustilide and butylidenephthalide from *Ligusticum chuanxiong* using SFE, Chromatographia 72(9-10) (2010) 963-967.

[27] X.G. Shi, X. Wang, D.J. Wang, Y.L. Geng, J.H. Liu, Separation and purification of -cyperone from *Cyperus rotundus* with supercritical fluid extraction and high-speed counter-current chromatography, Separation Science and Technology 44(3) (2009) 712-721.

[28] Y. Zhang, D. Wei, S. Guo, X. Zhang, M. Wang, F. Chen, Chemical components and antioxidant activity of the volatile oil from *Cassia tora* L. seed prepared by supercritical fluid extraction, Journal of Food Lipids 14(4) (2007) 411-423.

[29] A.L. Medina, M.E. Lucero, F.O. Holguin, R.E. Estell, J.J. Posakony, J. Simon, M.A. O'Connell, Composition and antimicrobial activity of *Anemopsis californica* leaf oil, Journal of Agricultural and Food Chemistry 53(22) (2005) 8694-8698.

[30] A. Verma, K. Hartonen, M.L. Riekkola, Optimisation of supercritical fluid extraction of indole alkaloids from *Catharanthus roseus* using experimental design methodology-comparison with other extraction techniques, Phytochemical Analysis 19(1) (2008) 52-63.

[31] H. Ebrahimzadeh, Y. Yamini, F. Sefidkon, D. Chaloosi, S.M. Pourmortazavi, Chemical composition of the essential oil and super critical CO2 extracts of Zataria multiflora Boiss, Food Chemistry 83(3) (2003) 357-361.

[32] Z. Zekovic, Z. Lepojevic, D. Vujic, Supercritical extraction of thyme (Thymus vulgaris L.), Chromatographia 51(3-4) (2000) 175-179.

[33] C.P. Passos, R.M. Silva, F.A. Da Silva, M.A. Coimbra, C.M. Silva, Enhancement of the supercritical fluid extraction of grape seed oil by using enzymatically pre-treated seed, Journal of Supercritical Fluids 48(3) (2009) 225-229.

[34] C.P. Passos, M.A. Coimbra, F.A. Da Silva, C.M. Silva, Modelling the supercritical fluid extraction of edible oils and analysis of the effect of enzymatic pre-treatments of seed upon model parameters, Chemical Engineering Research and Design 89(7) (2011) 1118-1125.

[35] A.L. Chassagnez-Mendez, N.T. Machado, M.E. Araujo, J.G. Maia, M.A.A. Meireles, Supercritical CO_2 extraction of curcumins and essential oil from the rhizomes of turmeric (*Curcuma longa* L.), Industrial & Engineering Chemistry Research 39(12) (2000) 4729-4733.

[36] R.L. Smith, R.M. Malaluan, W.B. Setianto, H. Inomata, K. Arai, Separation of cashew (*Anacardium occidentale* L.) nut shell liquid with supercritical carbon dioxide, Bioresource Technology 88(1) (2003) 1-7.

[37] H. Kubat, U. Akman, O. Hortacsu, Semi-batch packed-column deterpenation of origanum oil by dense carbon dioxide, Chemical Engineering and Processing 40(1) (2001) 19-32.

[38] P. Kotnik, M. Skerget, Z. Knez, Supercritical fluid extraction of chamomile flower heads: Comparison with conventional extraction, kinetics and scale-up, Journal of Supercritical Fluids 43(2) (2007) 192-198.

[39] A. Caredda, B. Marongiu, S. Porcedda, C. Soro, Supercritical carbon dioxide extraction and characterization of *Laurus nobilis* essential oil, Journal of Agricultural and Food Chemistry 50(6) (2002) 1492-1496.

[40] J.Z. Yin, X.W. Sun, X.W. Ding, H.H. Liang, Modeling of supercritical fluid extraction from *Hippophae rhamnoides* L. seeds, Separation Science and Technology 38(16) (2003) 4041-4055.

[41] F.J. Senorans, E. Ibanez, S. Cavero, J. Tabera, G. Reglero, Liquid chromatographic-mass spectrometric analysis of supercritical-fluid extracts of rosemary plants, J Chromatogr A 870(1-2) (2000) 491-499.

[42] F. Agostini, R.A. Bertussi, G. Agostini, A.C. Atti dos Santos, M. Rossato, R. Vanderlinde, Supercritical extraction from vinification residues: Fatty Acids, α-tocopherol, and phenolic compounds in the oil seeds from different varieties of grape, The Scientific World Journal 2012 (2012) 9.

[43] L. Arce, A.G. Lista, A. Ríos, M. Valcárcel, Screening of polyphenols in grape mark by online supercritical fluid extraction - flow through sensor, Analytical Letters 34(9) (2001) 1461-1476.

[44] M. Ashraf-Khorassani, L.T. Taylor, Sequential fractionation of grape seeds into oils, polyphenols, and procyanidins via a single system employing CO2-based fluids, Journal of Agricultural and Food Chemistry 52(9) (2004) 2440-2444.

[45] T.H.J. Beveridge, B. Girard, T. Kopp, J.C.G. Drover, Yield and composition of grape seed oils extracted by supercritical carbon dioxide and petroleum ether: Varietal effects, Journal of Agricultural and Food Chemistry 53(5) (2005) 1799-1804.

[46] X.L. Cao, Y.C. Ito, Supercritical fluid extraction of grape seed oil and subsequent separation of free fatty acids by high-speed counter-current chromatography, J Chromatogr A 1021(1-2) (2003) 117-124.

[47] A. Chafer, M.C. Pascual-Martí, A. Salvador, A. Berna, Supercritical fluid extraction and HPLC determination of relevant polyphenolic compounds in grape skin, J Sep Sci 28(16) (2005) 2050-2056.

[48] T.L. Da Silva, E.C. Bernardo, B. Nobre, R.L. Mendes, A. Reis, Extraction of Victoria and Red Globe grape seed oils using supercritical carbon dioxide with and without ethanol, Journal of Food Lipids 15(3) (2008) 356-369.

[49] L. de Campos, F.V. Leimann, R.C. Pedrosa, S.R.S. Ferreira, Free radical scavenging of grape pomace extracts from Cabernet sauvingnon (*Vitis vinifera*), Bioresource Technol 99(17) (2008) 8413-8420.

[50] L.D.S. Freitas, J.V. De Oliveira, C. Dariva, R.A. Jacques, E.B. Caramao, Extraction of grape seed oil using compressed carbon dioxide and propane: Extraction yields and characterization of free glycerol compounds, J Agr Food Chem 56(8) (2008) 2558-2564.

[51] L.D. Freitas, R.A. Jacques, M.F. Richter, A.L. da Silva, E.B. Caramao, Pressurized liquid extraction of vitamin E from Brazilian grape seed oil, Journal of Chromatography A 1200(1) (2008) 80-83.

[52] L. Fiori, Grape seed oil supercritical extraction kinetic and solubility data: Critical approach and modeling, Journal of Supercritical Fluids 43(1) (2007) 43-54.

[53] L. Fiori, D. de Faveri, A.A. Casazza, P. Perego, Grape by-products: extraction of polyphenolic compounds using supercritical CO2 and liquid organic solvent - a preliminary investigation Subproductos de la uva: extraccion de compuestos polifenolicos usando CO2 supercritico y disolventes organicos liquidos - una investigacion preliminar, Cyta-Journal of Food 7(3) (2009) 163-171.

[54] K. Ghafoor, F.Y. AL-Juhaimi, Y.H. Choi, Supercritical Fluid Extraction of Phenolic Compounds and Antioxidants from Grape (Vitis labrusca B.) Seeds, Plant Foods for Human Nutrition 67(4) (2012) 407-414.

[55] R. Murga, R. Ruiz, S. Beltran, J.L. Cabezas, Extraction of natural complex phenols and tannins from grape seeds by using supercritical mixtures of carbon dioxide and alcohol, Journal of Agricultural and Food Chemistry 48(8) (2000) 3408-3412.

[56] B. Palenzuela, L. Arce, A. Macho, E. Munoz, A. Rios, M. Valcarcel, Bioguided extraction of polyphenols from grape marc by using an alternative supercritical-fluid extraction method based on a liquid solvent trap, Analytical and Bioanalytical Chemistry 378(8) (2004) 2021-2027.

[57] B. Palenzuela, R. Rodriguez-Amaro, A. Rios, M. Valcarcel, Screening of polyphenols in grape marc by online supercritical fluid extraction - Amperometric detection with a PVC-graphite composite electrode, Electroanalysis 14(19-20) (2002) 1427-1432.

[58] M. Palma, L.T. Taylor, B.W. Zoecklein, L.S. Douglas, Supercritical fluid extraction of grape glycosides, Journal of Agricultural and Food Chemistry 48(3) (2000) 775-779.

[59] C.P. Passos, R.M. Silva, F.A. Da Silva, M.A. Coimbra, C.M. Silva, Supercritical fluid extraction of grape seed (*Vitis vinifera* L.) oil. Effect of the operating conditions upon oil composition and antioxidant capacity, Chem Eng J 160(2) (2010) 634-640.

[60] M. Pinelo, A. Ruiz-Rodriguez, J. Sineiro, F.J. Senorans, G. Reglero, M.J. Nunez, Supercritical fluid and solid-liquid extraction of phenolic antioxidants from grape pomace: a comparative study, European Food Research and Technology 226(1-2) (2007) 199-205.

[61] J.M. Prado, I. Dalmolin, N.D.D. Carareto, R.C. Basso, A.J.A. Meirelles, J.V. Oliveira, E.A.C. Batista, M.A.A. Meireles, Supercritical fluid extraction of grape seed: Process scale-up, extract chemical composition and economic evaluation, Journal of Food Engineering 109(2) (2012) 249-257.

[62] T. Vatai, M. Skerget, Z. Knez, Extraction of phenolic compounds from elder berry and different grape marc varieties using organic solvents and/or supercritical carbon dioxide, J Food Eng 90(2) (2009) 246-254.

[63] E.E. Yilmaz, E.B. Ozvural, H. Vural, Extraction and identification of proanthocyanidins from grape seed (*Vitis vinifera*) using supercritical carbon dioxide, Journal of Supercritical Fluids 55(3) (2011) 924-928.

[64] C. Yi, J. Shi, S.J. Xue, Y.M. Jiang, D. Li, Effects of supercritical fluid extraction parameters on lycopene yield and antioxidant activity, Food Chem 113(4) (2009) 1088-1094.

[65] G. Vasapollo, L. Longo, L. Rescio, L. Ciurlia, Innovative supercritical CO_2 extraction of lycopene from tomato in the presence of vegetable oil as co-solvent, Journal of Supercritical Fluids 29(1-2) (2004) 87-96.

[66] E. Vági, B. Simándi, K.P. Vásárhelyiné, H. Daood, Á. Kéry, F. Doleschall, B. Nagy, Supercritical carbon dioxide extraction of carotenoids, tocopherols and sitosterols from industrial tomato by-products, Journal of Supercritical Fluids 40(2) (2007) 218-226.

[67] U. Topal, M. Sasaki, M. Goto, K. Hayakawa, Extraction of lycopene from tomato skin with supercritical carbon dioxide: Effect of operating conditions and solubility analysis, J Agr Food Chem 54(15) (2006) 5604-5610.

[68] J. Shi, C. Yi, S.J. Xue, Y.M. Jiang, Y. Ma, D. Li, Effects of modifiers on the profile of lycopene extracted from tomato skins by supercritical CO_2, J Food Eng 93(4) (2009) 431-436.

[69] M.D.A. Saldaña, F. Temelli, S.E. Guigard, B. Tomberli, C.G. Gray, Apparent solubility of lycopene and β-carotene in supercritical CO_2, CO_2+ethanol and CO_2+canola oil using dynamic extraction of tomatoes, J Food Eng 99(1) (2010) 1-8.

[70] E. Sabio, M. Lozano, V. Montero de Espinosa, R.L. Mendes, A.P. Pereira, A.F. Palavra, J.A. Coelho, Lycopene and β-carotene extraction from tomato processing waste using supercritical CO_2, Industrial & Engineering Chemistry Research 42(25) (2003) 6641-6646.

[71] B.P. Nobre, A.F. Palavra, F.L.P. Pessoa, R.L. Mendes, Supercritical CO_2 extraction of trans-lycopene from Portuguese tomato industrial waste, Food Chemistry 116(3) (2009) 680-685.

[72] S. Machmudah, Zakaria, S. Winardi, M. Sasaki, M. Goto, N. Kusumoto, K. Hayakawa, Lycopene extraction from tomato peel by-product containing tomato seed using supercritical carbon dioxide, J Food Eng 108(2) (2012) 290-296.

[73] L.S. Kassama, J. Shi, G.S. Mittal, Optimization of supercritical fluid extraction of lycopene from tomato skin with central composite rotatable design model, Sep Purif Technol 60(3) (2008) 278-284.

[74] S.A.B.V. de Melo, G.M.N. Costa, R. Garau, A. Casula, B. Pittau, Supercritical CO2 extraction of essential oils from Thymus vulgaris, Brazilian Journal of Chemical Engineering 17(3) (2000) 367-371.

[75] M.C. Diaz-Maroto, I.J. Diaz-Maroto, E. Sanchez-Palomo, M.S. Perez-Coello, Volatile components and key odorants of fennel (*Foeniculum vulgare* Mill.) and thyme (*Thymus vulgaris* L.) oil extracts obtained by simultaneous distillation-extraction and supercritical fluid extraction, Journal of Agricultural and Food Chemistry 53(13) (2005) 5385-5389.

[76] M.R. Garcia-Risco, G. Vicente, G. Reglero, T. Fornari, Fractionation of thyme (*Thymus vulgaris* L.) by supercritical fluid extraction and chromatography, Journal of Supercritical Fluids 55(3) (2011) 949-954.

[77] C. Grosso, A.C. Figueiredo, J. Burillo, A.M. Mainar, J.S. Urieta, J.G. Barroso, J.A. Coelho, A.M.F. Palavra, Composition and antioxidant activity of *Thymus vulgaris* volatiles:

Comparison between supercritical fluid extraction and hydrodistillation, J Sep Sci 33(14) (2010) 2211-2218.

[78] M. Moldao-Martins, M.G. Bernardo-Gil, M.L.B. da Costa, Sensory and chemical evaluation of Thymus zygis L. essential oil and compressed CO2 extracts, European Food Research and Technology 214(3) (2002) 207-211.

[79] M. Moldao-Martins, A. Palavra, M.L.B. da Costa, M.G. Bernardo-Gil, Supercritical CO2 extraction of Thymus zygis L. subsp sylvestris aroma, Journal of Supercritical Fluids 18(1) (2000) 25-34.

[80] S.S. Petrovic, J. Ivanovic, S. Milovanovic, I. Zizovic, Comparative analyses of the diffusion coefficients from thyme for different extraction processes, Journal of the Serbian Chemical Society 77(6) (2012) 799-813.

[81] B. Simandi, V. Hajdu, K. Peredi, B. Czukor, A. Nobik-Kovacs, A. Kery, Antioxidant activity of pilot-plant alcoholic and supercritical carbon dioxide extracts of thyme, Eur J Lipid Sci Tech 103(6) (2001) 355-358.

[82] F. Ashtiani, F. Sefidkon, Y. Yamini, K. Khajeh, Supercritical carbon dioxide extraction of volatile components from two eucalyptus species (*E. spathulata* and *E. microtheca*), Journal of Essential Oil Bearing Plants 10(3) (2007) 198-208.

[83] M.M.R. de Melo, E.L.G. Oliveira, A.J.D. Silvestre, C.M. Silva, Supercritical fluid extraction of triterpenic acids from *Eucalyptus globulus* bark, Journal of Supercritical Fluids 70 (2012) 137-145.

[84] R.M.A. Domingues, M.M.R. de Melo, C.P. Neto, A.J.D. Silvestre, C.M. Silva, Measurement and modeling of supercritical fluid extraction curves of *Eucalyptus globulus* bark: Influence of the operating conditions upon yields and extract composition, Journal of Supercritical Fluids 72 (2012) 176-185.

[85] R.M.A. Domingues, M.M.R. de Melo, E.L.G. Oliveira, C.P. Neto, A.J.D. Silvestre, C.M. Silva, Optimization of the supercritical fluid extraction of triterpenic acids from *Eucalyptus globulus* bark using experimental design, Journal of Supercritical Fluids 74 (2013) 105-114.

[86] R.M.A. Domingues, E.L.G. Oliveira, C.S.R. Freire, R.M. Couto, P.C. Simões, C.P. Neto, A.J.D. Silvestre, C.M. Silva, Supercritical fluid extraction of *Eucalyptus globulus* bark – a promising approach for triterpenoids production, International Journal of Molecular Sciences *13(6),* (2012) *7648-7662*.

[87] A.H. El-Ghorab, K.F. El-Massry, F. Marx, H.M. Fadel, Antioxidant activity of Egyptian *Eucalyptus camaldulensis* var. *brevirostris* leaf extracts, Nahrung-Food 47(1) (2003) 41-45.

[88] J.D. Francisco, E.P. Jarvenpaa, R. Huopalahti, B. Sivik, Comparison of *Eucalyptus camaldulensis* Dehn. Oils from mozambique as obtained by hydrodistillation and supercritical carbon dioxide extraction., Journal of Agricultural and Food Chemistry 49(5) (2001) 2339-2342.

[89] D.J.S. Patinha, R.M.A. Domingues, J.J. Villaverde, A.M.S. Silva, C.M. Silva, C.S.R. Freire, C. Pascoal Neto, A.J.D. Silvestre, Lipophilic extractives from the bark of

Eucalyptus grandis x globulus, a rich source of methyl morolate: Selective extraction with supercritical CO_2, Industrial Crops and Products 43 (2013) 340-348.

[90] S.A.O. Santos, J.J. Villaverde, C.M. Silva, C.P. Neto, A.J.D. Silvestre, Supercritical fluid extraction of phenolic compounds from *Eucalyptus globulus* Labill bark, Journal of Supercritical Fluids 71 (2012) 71-79.

[91] K.S. Andrade, R.T. Goncalvez, M. Maraschin, R.M. Ribeiro-do-Valle, J. Martinez, S.R.S. Ferreira, Supercritical fluid extraction from spent coffee grounds and coffee husks: Antioxidant activity and effect of operational variables on extract composition, Talanta 88 (2012) 544-552.

[92] J.M.A. Araujo, D. Sandi, Extraction of coffee diterpenes and coffee oil using supercritical carbon dioxide, Food Chemistry 101(3) (2006) 1087-1094.

[93] Á.B.A.d. Azevedo, T.G. Kieckbusch, A.K. Tashima, R.S. Mohamed, P. Mazzafera, S.A.B.V.d. Melo, Supercritical CO_2 recovery of caffeine from green coffee oil: new experimental solubility data and modeling, Química Nova 31 (2008) 1319-1323.

[94] R.M. Couto, J. Fernandes, M.D.R.G. da Silva, P.C. Simoes, Supercritical fluid extraction of lipids from spent coffee grounds, Journal of Supercritical Fluids 51(2) (2009) 159-166.

[95] A.B.A. de Azevedo, P. Mazzafera, R.S. Mohamed, S. de Melo, T.G. Kieckbusch, Extraction of caffeine, chlorogenic acids and lipids from green coffee beans using supercritical carbon dioxide and co-solvents, Brazilian Journal of Chemical Engineering 25(3) (2008) 543-552.

[96] A.L. Oliveira, S.S. Silva, M.A.P. Da Silva, M.N. Eberlin, F.A. Cabral, Sensory and yield response surface analysis of supercritical CO_2 extracted aromatic oil from roasted coffee, Journal of Food Science and Technology-Mysore 38(1) (2001) 38-42.

[97] J. Tello, M. Viguera, L. Calvo, Extraction of caffeine from Robusta coffee (*Coffea canephora* var. Robusta) husks using supercritical carbon dioxide, The Journal of Supercritical Fluids 59(0) (2011) 53-60.

[98] M.M.R. de Melo, H.M.A. Barbosa, C.P. Passos, C.M. Silva, Supercritical fluid extraction of spent coffee grounds: Measurement of extraction curves, oil characterization and economic analysis, Journal of Supercritical Fluids 86(0) (2014) 150-159.

[99] H.M.A. Barbosa, M.M.R. de Melo, M.A. Coimbra, C.P. Passos, C.M. Silva, Optimization of the supercritical fluid coextraction of oil and diterpenes from spent coffee grounds using experimental design and response surface methodology, Journal of Supercritical Fluids 85(0) (2014) 165-172.

[100] H.K. Kiriamiti, E. Rascol, A. Marty, J.S. Condoret, Extraction rates of oil from high oleic sunflower seeds with supercritical carbon dioxide, Chemical Engineering and Processing 41(8) (2002) 711-718.

[101] U. Salgin, O. Doker, A. Calimli, Extraction of sunflower oil with supercritical CO_2: Experiments and modeling, Journal of Supercritical Fluids 38(3) (2006) 326-331.

[102] Y. Athukorala, G. Mazza, Optimization of extraction of wax from flax straw by supercritical carbon dioxide, Separation Science and Technology 46(2) (2011) 247-253.

[103] B. Bozan, F. Temelli, Supercritical CO_2 extraction of flaxseed, Journal of the American Oil Chemists Society 79(3) (2002) 231-235.

[104] L.M. Comin, F. Temelli, M.A. Saldana, Supercritical CO_2 extraction of flax lignans, J Am Oil Chem Soc 88(5) (2011) 707-715.

[105] W.H. Morrison, R. Holser, D.E. Akin, Cuticular wax from flax processing waste with hexane and super critical carbon dioxide extractions, Industrial Crops and Products 24(2) (2006) 119-122.

[106] S.G. Ozkal, Response surface analysis and modeling of flaxseed oil yield in supercritical carbon dioxide, Journal of the American Oil Chemists Society 86(11) (2009) 1129-1135.

[107] O. Bensebia, D. Barth, B. Bensebia, A. Dahmani, Supercritical CO2 extraction of rosemary: Effect of extraction parameters and modelling, Journal of Supercritical Fluids 49(2) (2009) 161-166.

[108] L.S. Moura, R.N. Carvalho, M.B. Stefanini, L.C. Ming, M.A.A. Meireles, Supercritical fluid extraction from fennel (*Foeniculum vulgare*): global yield, composition and kinetic data, Journal of Supercritical Fluids 35(3) (2005) 212-219.

[109] M. Herrero, M. Plaza, A. Cifuentes, E. Ibanez, Green processes for the extraction of bioactives from rosemary: Chemical and functional characterization via ultra-performance liquid chromatography-tandem mass spectrometry and in-vitro assays, J Chromatogr A 1217(16) (2010) 2512-2520.

[110] S. Irmak, K. Solakyildirim, A. Hesenov, O. Erbatur, Study on the stability of supercritical fluid extracted rosemary (*Rosmarinus offcinalis* L.) essential oil, Journal of Analytical Chemistry 65(9) (2010) 899-906.

[111] M. Lo Presti, S. Ragusa, A. Trozzi, P. Dugo, F. Visinoni, A. Fazio, G. Dugo, L. Mondello, A comparison between different techniques for the isolation of rosemary essential oil, Journal of Separation Science 28(3) (2005) 273-280.

[112] C.G. Pereira, M.A.A. Meireles, Economic analysis of rosemary, fennel and anise essential oils obtained by supercritical fluid extraction, Flavour and Fragrance Journal 22(5) (2007) 407-413.

[113] P. Ramirez, F.J. Senorans, E. Ibanez, G. Reglero, Separation of rosemary antioxidant compounds by supercritical fluid chromatography on coated packed capillary columns, Journal of Chromatography A 1057(1-2) (2004) 241-245.

[114] J.M. del Valle, M. Jimenez, J.C. de la Fuente, Extraction kinetics of pre-pelletized Jalapeno peppers with supercritical CO_2, Journal of Supercritical Fluids 25(1) (2003) 33-44.

[115] B. Nagy, B. Simandi, Effects of particle size distribution, moisture content, and initial oil content on the supercritical fluid extraction of paprika, Journal of Supercritical Fluids 46(3) (2008) 293-298.

[116] A. Romo-Hualde, A.I. Yetano-Cunchillos, C. Gonzalez-Ferrero, M.J. Saiz-Abajo, C.J. Gonzalez-Navarro, Supercritical fluid extraction and microencapsulation of bioactive

compounds from red pepper (*Capsicum annum* L.) by-products, Food Chemistry 133(3) (2012) 1045-1049.

[117] A. Ambrogi, D.A. Cardarelli, R. Eggers, Fractional extraction of paprika using supercritical carbon dioxide and on-line determination of carotenoids, Journal of Food Science 67(9) (2002) 3236-3241.

[118] A. Tepic, Z. Zekovic, S. Kravic, A. Mandic, Pigment content and fatty acid composition of paprika oleoresins obtained by conventional and supercritical carbon dioxide extraction, Cyta-Journal of Food 7(2) (2009) 95-102.

[119] U. Salgin, A.S. Ustun, U. Mehmetoglu, A. Calimli, Supercritical CO_2 extraction of accumulated capsidiol from biotic elicitor-activated *Capsicum annuum* L fruit tissues, Journal of Chemical Technology and Biotechnology 80(2) (2005) 124-132.

[120] P. Bhattacharjee, T.V. Ranganathan, R.S. Singhal, P.R. Kulkarni, Comparative aroma profiles using supercritical carbon dioxide and Likens-Nickerson extraction from a commercial brand of Basmati rice, J Sci Food Agr 83(9) (2003) 880-883.

[121] L. Danielski, C. Zetzl, H. Hense, G. Brunner, A process line for the production of raffinated rice oil from rice bran, Journal of Supercritical Fluids 34(2) (2005) 133-141.

[122] A. Manosroi, W. Ruksiriwanich, M. Abe, H. Sakai, W. Manosroi, J. Manosroi, Biological activities of the rice bran extract and physical characteristics of its entrapment in niosomes by supercritical carbon dioxide fluid, Journal of Supercritical Fluids 54(2) (2010) 137-144.

[123] G. Perretti, E. Miniati, L. Montanari, P. Fantozzi, Improving the value of rice by-products by SFE, Journal of Supercritical Fluids 26(1) (2003) 63-71.

[124] C.H. Wang, C.R. Chen, J.J. Wu, L.Y. Wang, C.M.J. Chang, W.J. Ho, Designing supercritical carbon dioxide extraction of rice bran oil that contain oryzanols using response surface methodology, Journal of Separation Science 31(8) (2008) 1399-1407.

[125] Z.M. Xu, J.S. Godber, Comparison of supercritical fluid and solvent extraction methods in extracting gamma-oryzanol from rice bran, J Am Oil Chem Soc 77(5) (2000) 547-551.

[126] N.T. Dunford, J.W. King, Phytosterol enrichment of rice bran oil by a supercritical carbon dioxide fractionation technique, Journal of Food Science 65(8) (2000) 1395-1399.

[127] I.S. Sanal, A. Guvenc, U. Salgin, U. Mehmetoglu, A. Calimli, Recycling of apricot pomace by supercritical CO2 extraction, Journal of Supercritical Fluids 32(1-3) (2004) 221-230.

[128] S.G. Ozkal, M.E. Yener, L. Bayindirli, Response surfaces of apricot kernel oil yield in supercritical carbon dioxide, Lwt-Food Sci Technol 38(6) (2005) 611-616.

[129] S.G. Ozkal, M.E. Yener, L. Bayindirli, Mass transfer modeling of apricot kernel oil extraction with supercritical carbon dioxide, Journal of Supercritical Fluids 35(2) (2005) 119-127.

[130] I.S. Sanal, E. Bayraktar, U.U. Mehmetoglu, A. Calimli, Determination of optimum conditions for SC-(CO_2 plus ethanol) extraction of beta-carotene from apricot pomace

using response surface methodology, Journal of Supercritical Fluids 34(3) (2005) 331-338.

[131] O. Doker, U. Salgin, I. Sanal, U. Mehmetoglu, A. Calimli, Modeling of extraction of beta-carotene from apricot bagasse using supercritical CO2 in packed bed extractor, Journal of Supercritical Fluids 28(1) (2004) 11-19.

[132] M. Sun, F. Temelli, Supercritical carbon dioxide extraction of carotenoids from carrot using canola oil as a continuous co-solvent, Journal of Supercritical Fluids 37(3) (2006) 397-408.

[133] A. Ranalli, S. Contento, L. Lucera, G. Pavone, G. Di Giacomo, L. Aloisio, C. Di Gregorio, A. Mucci, I. Kourtikakis, Characterization of carrot root oil arising from supercritical fluid carbon dioxide extraction, Journal of Agricultural and Food Chemistry 52(15) (2004) 4795-4801.

[134] S.B. Glisic, D.R. Misic, M.D. Stamenic, I.T. Zizovic, R.M. Asanin, D.U. Skala, Supercritical carbon dioxide extraction of carrot fruit essential oil: Chemical composition and antimicrobial activity, Food Chemistry 105(1) (2007) 346-352.

[135] A. Maxia, B. Marongiu, A. Piras, S. Porcedda, E. Tuveri, M.J. Goncalves, C. Cavaleiro, L. Salgueiro, Chemical characterization and biological activity of essential oils from Daucus carota L. subsp carota growing wild on the Mediterranean coast and on the Atlantic coast, Fitoterapia 80(1) (2009) 57-61.

[136] W.B. Setianto, S. Yoshikawa, R.L. Smith, H. Inomata, L.J. Florusse, C.J. Peters, Pressure profile separation of phenolic liquid compounds from cashew (*Anacardium occidentale*) shell with supercritical carbon dioxide and aspects of its phase equilibria, Journal of Supercritical Fluids 48(3) (2009) 203-210.

[137] R.N. Patel, S. Bandyopadhyay, A. Ganesh, Extraction of cashew (*Anacardium occidentale*) nut shell liquid using supercritical carbon dioxide, Bioresource Technology 97(6) (2006) 847-853.

[138] R.N. Patel, S. Bandyopadhyay, A. Ganesh, Economic appraisal of supercritical fluid extraction of refined cashew nut shell liquid, Journal of Chromatography A 1124(1-2) (2006) 130-138.

[139] M.D.A. Saldana, R.S. Mohamed, P. Mazzafera, Extraction of cocoa butter from Brazilian cocoa beans using supercritical CO_2 and ethane, Fluid Phase Equilibria 194 (2002) 885-894.

[140] R.S. Mohamed, M.D.A. Saldana, P. Mazzafera, C. Zetzl, G. Brunner, Extraction of caffeine, theobromine, and cocoa butter from Brazilian cocoa beans using supercritical CO_2 and ethane, Ind Eng Chem Res 41(26) (2002) 6751-6758.

[141] E.K. Asep, S. Jinap, T.J. Tan, A.R. Russly, S. Harcharan, S.A.H. Nazimah, The effects of particle size, fermentation and roasting of cocoa nibs on supercritical fluid extraction of cocoa butter, Journal of Food Engineering 85(3) (2008) 450-458.

[142] M.E. Rybak, E.M. Calvey, J.M. Harnly, Quantitative determination of allicin in garlic: Supercritical fluid extraction and standard addition of alliin, J Agr Food Chem 52(4) (2004) 682-687.

[143] R. Li, W.-c. Chen, W.-p. Wang, W.-y. Tian, X.-g. Zhang, Extraction of essential oils from garlic (*Allium sativum*) using ligarine as solvent and its immunity activity in gastric cancer rat, Medicinal Chemistry Research 19(9) (2010) 1092-1105.

[144] J.M. del Valle, V. Glatzel, J.L. Martinez, Supercritical CO_2 extraction of allicin from garlic flakes: Screening and kinetic studies, Food Research International 45(1) (2012) 216-224.

[145] J.M. Del Valle, C. Mena, M. Budinich, Extraction of garlic with supercritical CO_2 and conventional organic solvents, Brazilian Journal of Chemical Engineering 25(3) (2008) 535-542.

[146] K.C. Zancan, M.O.M. Marques, A.J. Petenate, M.A.M. Meireles, Extraction of ginger (Zingiber officinale Roscoe) oleoresin with CO2 and co-solvents: a study of the antioxidant action of the extracts, Journal of Supercritical Fluids 24(1) (2002) 57-76.

[147] J. Martinez, A.R. Monteiro, P.T.V. Rosa, M.O.M. Marques, M.A.A. Meireles, Multicomponent model to describe extraction of ginger oleoresin with supercritical carbon dioxide, Ind Eng Chem Res 42(5) (2003) 1057-1063.

[148] O.J. Catchpole, J.B. Grey, N.B. Perry, E.J. Burgess, W.A. Redmond, N.G. Porter, Extraction of chill, black pepper, and ginger with near-critical CO_2, propane, and dimethyl ether: Analysis of the extracts by quantitative nuclear magnetic resonance, Journal of Agricultural and Food Chemistry 51(17) (2003) 4853-4860.

[149] J.P. Bartley, A.L. Jacobs, Effects of drying on flavour compounds in Australian-grown ginger (*Zingiber officinale*), J Sci Food Agr 80(2) (2000) 209-215.

[150] S. Balachandran, S.E. Kentish, R. Mawson, M. Ashokkumar, Ultrasonic enhancement of the supercritical extraction from ginger, Ultrasonics Sonochemistry 13(6) (2006) 471-479.

[151] S.Q. Zhang, R.Z. Chen, H. Wu, C.Z. Wang, Ginsenoside extraction from *Panax quinquefolium* L. (American ginseng) root by using ultrahigh pressure, J Pharmaceut Biomed 41(1) (2006) 57-63.

[152] J.A. Wood, M.A. Bernards, W.K. Wan, P.A. Charpentier, Extraction of ginsenosides from North American ginseng using modified supercritical carbon dioxide, Journal of Supercritical Fluids 39(1) (2006) 40-47.

[153] H.C. Wang, C.R. Chen, C.M.J. Chang, Carbon dioxide extraction of ginseng root hair oil and ginsenosides, Food Chem 72(4) (2001) 505-509.

[154] D.L. Luo, T.Q. Qiu, Q. Lu, Ultrasound-assisted extraction of ginsenosides in supercritical CO_2 reverse microemulsions, J Sci Food Agr 87(3) (2007) 431-436.

[155] H. Marzouki, A. Piras, B. Marongiu, A. Rosa, M.A. Dessi, Extraction and separation of volatile and fixed oils from berries of *Laurus nobilis* L. by supercritical CO_2, Molecules 13(8) (2008) 1702-1711.

[156] J. Ivanovic, D. Misic, M. Ristic, O. Pesic, I. Zizovic, Supercritical CO_2 extract and essential oil of bay (*Laurus nobilis* L.) - chemical composition and antibacterial activity, Journal of the Serbian Chemical Society 75(3) (2010) 395-404.

[157] S.H. Beis, N.T. Dunford, Supercritical fluid extraction of daphne (Laurus nobilis L.) seed oil, J Am Oil Chem Soc 83(11) (2006) 953-957.

[158] D.J.M. Gomez-Coronado, E. Ibanez, F.J. Ruperez, C. Barbas, Tocopherol measurement in edible products of vegetable origin, Journal of Chromatography A 1054(1-2) (2004) 227-233.

[159] Y.W. Lee, C.H. Lee, J.D. Kim, Y.Y. Lee, K.H. Row, Extraction of perillyl alcohol in Korean orange peel by supercritical CO_2, Separation Science and Technology 35(7) (2000) 1069-1076.

[160] C.H. Lee, K.H. Row, Y.W. Lee, J.D. Kim, Y.Y. Lee, Supercritical fluid extraction of perillyl alcohol in Korean orange peel, Journal of Liquid Chromatography & Related Technologies 24(13) (2001) 1987-1996.

[161] A. Berna, A. Tarrega, M. Blasco, S. Subirats, Supercritical CO_2 extraction of essential oil from orange peel; effect of the height of the bed, Journal of Supercritical Fluids 18(3) (2000) 227-237.

[162] P. Benelli, C.A.S. Riehl, A. Smania, E.F.A. Smania, S.R.S. Ferreira, Bioactive extracts of orange (*Citrus sinensis* L. Osbeck) pomace obtained by SFE and low pressure techniques: Mathematical modeling and extract composition, Journal of Supercritical Fluids 55(1) (2010) 132-141.

[163] J.B. Fernandes, V. David, P.H. Facchini, M.F.D.F. da Silva, E. Rodrigues, P.C. Vieira, M.S. Galhiane, F.C. Pagnocca, O.C. Bueno, M.J. Hebling, S.R. Victor, A.M.R. dos Santos, Citrus seed oils extractions and their activity against leaf cutting ant *Atta sexdens* and its symbiotic fungus, Quimica Nova 25(6B) (2002) 1091-1095.

[164] S. Cavero, M.R. Garcia-Risco, F.R. Marin, L. Jaime, S. Santoyo, F.J. Senorans, G. Reglero, E. Ibanez, Supercritical fluid extraction of antioxidant compounds from oregano - Chemical and functional characterization via LC-MS and in vitro assays, Journal of Supercritical Fluids 38(1) (2006) 62-69.

[165] T. Fornari, A. Ruiz-Rodriguez, G. Vicente, E. Vazquez, M.R. Garcia-Risco, G. Reglero, Kinetic study of the supercritical CO_2 extraction of different plants from Lamiaceae family, Journal of Supercritical Fluids 64 (2012) 1-8.

[166] S. Santoyo, S. Cavero, L. Jaime, E. Ibanez, F.J. Senorans, G. Reglero, Supercritical carbon dioxide extraction of compounds with antimicrobial activity from *Origanum vulgare* L.: Determination of optimal extraction parameters, Journal of Food Protection 69(2) (2006) 369-375.

[167] F. Gaspar, Extraction of essential oils and cuticular waxes with compressed CO_2: Effect of extraction pressure and temperature, Ind Eng Chem Res 41(10) (2002) 2497-2503.

[168] F. Gaspar, T. Lu, R. Santos, B. Al-Duri, Modelling the extraction of essential oils with compressed carbon dioxide, Journal of Supercritical Fluids 25(3) (2003) 247-260.

[169] M.G. Bernardo-Gil, L.M.C. Lopes, Supercritical fluid extraction of *Cucurbita ficifolia* seed oil, European Food Research and Technology 219(6) (2004) 593-597.

[170] N. Hrabovski, S. Sinadinovic-Fiser, B. Nikolovski, M. Sovilj, O. Borota, Phytosterols in pumpkin seed oil extracted by organic solvents and supercritical CO_2, Eur J Lipid Sci Tech 114(10) (2012) 1204-1211.

[171] P. Mitra, H.S. Ramaswamy, K.S. Chang, Pumpkin (*Cucurbita maxima*) seed oil extraction using supercritical carbon dioxide and physicochemical properties of the oil, Journal of Food Engineering 95(1) (2009) 208-213.

[172] J. Shi, C. Yi, X. Ye, S. Xue, Y. Jiang, Y. Ma, D. Liu, Effects of supercritical CO_2 fluid parameters on chemical composition and yield of carotenoids extracted from pumpkin, LWT - Food Science and Technology 43(1) (2010) 39-44.

[173] W.L. Yu, Y.P. Zhao, J.J. Chen, B. Shu, Comparison of two kinds of pumpkin seed oils obtained by supercritical CO2 extraction, European Journal of Lipid Science and Technology 106(6) (2004) 355-358.

[174] S. Jokic, B. Nagy, Z. Zekovic, S. Vidovic, M. Bilic, D. Velic, B. Simandi, Effects of supercritical CO_2 extraction parameters on soybean oil yield, Food and Bioproducts Processing 90(C4) (2012) 693-699.

[175] S. Jokic, Z. Zekovic, S. Vidovic, R. Sudar, I. Nemet, M. Bilic, D. Velic, Supercritical CO_2 extraction of soybean oil: process optimisation and triacylglycerol composition, International Journal of Food Science and Technology 45(9) (2010) 1939-1946.

[176] S.L. Taylor, J.W. King, L. Montanari, P. Fantozzi, M.A. Blanco, Enrichment and fractionation of phospholipid concentrates by supercritical fluid extraction and chromatography, Italian Journal of Food Science 12(1) (2000) 65-76.

[177] B. Matthaus, L. Bruhl, Comparison of different methods for the determination of the oil content in oilseeds, Journal of the American Oil Chemists Society 78(1) (2001) 95-102.

[178] B. Gopalan, M. Goto, A. Kodama, T. Hirose, Supercritical carbon dioxide extraction of turmeric (Curcuma longa), Journal of Agricultural and Food Chemistry 48(6) (2000) 2189-2192.

[179] M.E.M. Braga, P.F. Leal, J.E. Carvalho, M.A.A. Meireles, Comparison of yield, composition, and antioxidant activity of turmeric (Curcuma longa L.) extracts obtained using various techniques, Journal of Agricultural and Food Chemistry 51(22) (2003) 6604-6611.

[180] G. Began, M. Goto, A. Kodama, T. Hirose, Response surfaces of total oil yield of turmeric (*Curcuma longa*) in supercritical carbon dioxide, Food Research International 33(5) (2000) 341-345.

[181] M. Eisenmenger, N.T. Dunford, F. Eller, S. Taylor, J. Martinez, Pilot-scale supercritical carbon dioxide extraction and fractionation of wheat germ oil, J Am Oil Chem Soc 83(10) (2006) 863-868.

[182] N. Gelmez, N.S. Kincal, M.E. Yener, Optimization of supercritical carbon dioxide extraction of antioxidants from roasted wheat germ based on yield, total phenolic and

tocopherol contents, and antioxidant activities of the extracts, Journal of Supercritical Fluids 48(3) (2009) 217-224.

[183] A.M. Gomez, E.M. de la Ossa, Quality of wheat germ oil extracted by liquid and supercritical carbon dioxide, Journal of the American Oil Chemists Society 77(9) (2000) 969-974.

[184] J.D. Hubbard, J.M. Downing, M.S. Ram, O.K. Chung, Lipid extraction from wheat flour using supercritical fluid extraction, Cereal Chem 81(6) (2004) 693-698.

[185] G. Panfili, L. Cinquanta, A. Fratianni, R. Cubadda, Extraction of wheat germ oil by supercritical CO_2: Oil and defatted cake characterization, J Am Oil Chem Soc 80(2) (2003) 157-161.

[186] B. Marongiu, A. Piras, S. Porcedda, A. Scorciapino, Chemical composition of the essential oil and supercritical CO_2 extract of *Commiphora myrrha* (Nees) Engl. and of *Acorus calamus* L., J Agr Food Chem 53(20) (2005) 7939-7943.

[187] K.X. Chen, W.H. Yin, Effects of entrainers on the purity of andrographolide extracted from andrographolide raw material by SC-CO_2, Separation and Purification Technology 70(2) (2009) 207-211.

[188] P. Tonthubthimthong, S. Chuaprasert, P. Douglas, W. Luewisutthichat, Supercritical CO_2 extraction of nimbin from neem seeds - an experimental study, J Food Eng 47(4) (2001) 289-293.

[189] P. Tonthubthimthong, P.L. Douglas, S. Douglas, W. Leuwisutthichat, W. Teppaitoon, L. Pengsopa, Extraction of nimbin from neem seeds using supercritical CO_2 and a supercritical CO_2-methanol mixture, Journal of Supercritical Fluids 30(3) (2004) 287-301.

[190] D. Mongkholkhajornsilp, S. Douglas, P.L. Douglas, A. Elkamel, W. Teppaitoon, S. Pongamphai, Supercritical CO_2 extraction of nimbin from neem seeds - a modelling study, J Food Eng 71(4) (2005) 331-340.

[191] A. Ajchariyapagorn, T. Kumhom, S. Pongamphai, S. Douglas, P.L. Douglas, W. Teppaitoon, Predicting the extraction yield of nimbin from neem seeds in supercritical CO_2 using group contribution methods, equations of state and a shrinking core extraction model, Journal of Supercritical Fluids 51(1) (2009) 36-42.

[192] A.L. Chassagnez-Mendez, N.C.F. Correa, L.F. Franca, N.T. Machado, M.E. Araujo, A mass transfer model applied to the supercritical extraction with CO_2 of curcumins from turmeric rhizomes (*Curcuma longa* L), Braz J Chem Eng 17(3) (2000) 315-322.

[193] M.G.D. Silva, F.J.D. Matos, P.R.O. Lopes, F.O. Silva, M.T. Holanda, Composition of essential oils from three *Ocimum* species obtained by steam and microwave distillation and supercritical CO_2 extraction, Arkivoc (2004) 66-71.

[194] M. Mazutti, B. Beledelli, A.J. Mossi, R.L. Cansian, C. Dariva, J.V.d. Oliveira, N. Paroul, Caracterização química de extratos de *Ocimum basilicum* L. obtidos através de extração com CO_2 a altas pressões, Química Nova 29 (2006) 1198-1202.

[195] P.F. Leal, N.B. Maia, Q.A.C. Carmello, R.R. Catharino, M.N. Eberlin, M.A.A. Meireles, Sweet Basil (*Ocimum basilicum*) extracts obtained by supercritical fluid extraction (SFE): Global yields, chemical composition, antioxidant activity, and estimation of the cost of manufacturing, Food Bioprocess Tech 1(4) (2007) 326.

[196] P.F. Leal, F.C.M. Chaves, L.C. Ming, A.J. Petenate, M.A.A. Meireles, Global yields, chemical compositions and antioxidant activities of clove basil (*Ocimum gratissimum* L.) extracts obtained by supercritical fluid extraction, Journal of Food Process Engineering 29(5) (2006) 547-559.

[197] A. Menaker, M. Kravets, M. Koel, A. Orav, Identification and characterization of supercritical fluid extracts from herbs, Comptes Rendus Chimie 7(6–7) (2004) 629-633.

[198] B. Kayan, A.M. Gizir, Co-solvent-modified supercritical carbon dioxide extraction of 10-deacetylbaccatin III from needles of *Taxus baccata* L, Separation Science and Technology 44(9) (2009) 2004-2021.

[199] R.M.A. Domingues, A.R. Guerra, M. Duarte, C.S.R. Freire, C.P. Neto, C.M.S. Silva, A.J.D. Silvestre, Bioactive triterpenic acids: From agroforestry biomass residues to promising therapeutic tools, Mini-Reviews in Organic Chemistry 11(3) (2014) 382-399.

[200] R. Patt, O. Kordsachia, R. Süttinger, Y. Ohtani, J.F. Hoesch, P. Ehrler, R. Eichinger, H. Holik, U. Hamm, P. Rohmann, P. Mummenhoff, E. Petermann, R.F. Miller, D. Frank, R. Wilken, H.L. Baumgarten, G.-H. Rentrop, Pulp and Paper, Ulmann's Encyclopedia of Industrial Chemistry, Wiley-VCH Verlag GmbH & Co.2000.

[201] CELPA, Statistical bulletin 2007, (2008).

[202] G.I. Trabado, Wilstermann, D., *Eucalyptus universalis*. Global Cultivated Eucalypt Forest Map 2008, 2008.

[203] BRACELPA, Brazilian pulp and paper industry performance, 2009.

[204] B.M. Potts, Vaillancourt, R.E., Jordan, G., Dutkowski, G., Silva, J., McKinnon, G., Steane, D., Volker, P., Lopez, G., Apiolaza, L., Li, L.N., Marques, C., Borralho, N., Exploration of the *Eucalyptus globulus* gene pool., in: N. Borralho, Pereira, J.S., Marques, C., Coutinho, J., Madeira, M., Tomé, M. (Ed.) Eucalyptus in a Changing World, Aveiro, Portugal, 2004.

[205] R.M.A. Domingues, G.D.A. Sousa, C.S.R. Freire, A.J.D. Silvestre, C.P. Neto, *Eucalyptus globulus* biomass residues from pulping industry as a source of high value triterpenic compounds, Industrial Crops and Products 31(1) (2010) 65-70.

[206] Florabank website - *Eucalyptus globulus*, Accessed in December 2016, http://www.florabank.org.au.).

[207] Simply Fresh Purely Natural, Accessed in December 2016, http://www.simplyfreshpurelynatural.com/.).

[208] S.I. Mussatto, E.M.S. Machado, S. Martins, J.A. Teixeira, Production, composition, and application of coffee and its industrial residues, Food Bioprocess Tech 4(5) (2011) 661-672.

[209] T. Tokimoto, N. Kawasaki, T. Nakamura, J. Akutagawa, S. Tanada, Removal of lead ions in drinking water by coffee grounds as vegetable biomass, J Colloid Interf Sci 281(1) (2005) 56-61.

[210] S.I. Mussatto, L.M. Carneiro, J.P.A. Silva, I.C. Roberto, J.A. Teixeira, A study on chemical constituents and sugars extraction from spent coffee grounds, Carbohyd Polym 83(2) (2011) 368-374.

[211] C.P. Passos, M.A. Coimbra, Microwave superheated water extraction of polysaccharides from spent coffee grounds, Carbohyd Polym 94(1) (2013) 626-633.

[212] N. Kondamudi, S.K. Mohapatra, M. Misra, Spent coffee grounds as a versatile source of green energy, J Agr Food Chem 56(24) (2008) 11757-11760.

[213] A.L. de Souza, R. Garcia, F.S. Bernardino, F.C. Rocha, S.D. Valadares, O.G. Pereira, A.J.V. Pires, Coffee hulls in the diet of sheep: Intake and apparent digestibility, Rev Bras Zootecn 33(6) (2004) 2170-2176.

[214] R.M. Couto, J. Fernandes, M.D.R.G. da Silva, P.C. Simões, Supercritical fluid extraction of lipids from spent coffee grounds, Journal of Supercritical Fluids 51(2) (2009) 159-166.

[215] A.L. de Souza, R. Garcia, L. Cabral', F.S. Bernardino, J.T. Zervoudakis, F.C. Rocha, R.F.D. Valadares, Coffee hulls in diets of dairy cows: Nitrogenous compounds balance, Poultry Sci 83 (2004) 51-51.

[216] E.S. Dias, E.M.S. Koshikumo, R.F. Schwan, R. da Silva, Cultivation of the mushroom *Pleutoruss sajor-caju* in different agricultural residues, Cienc Agrotec 27(6) (2003) 1363-1369.

[217] C. Cavin, D. Holzhaeuser, G. Scharf, A. Constable, W.W. Huber, B. Schilter, Cafestol and kahweol, two coffee specific diterpenes with anticarcinogenic activity, Food and Chemical Toxicology 40(8) (2002) 1155-1163.

[218] International Coffee Organization, Statistics - Country Datasheets, December 2013, Available from: http://www.ico.org/profiles e.asp?section=Statistics[

[219] R. Cruz, M.M. Cardoso, L. Fernandes, M. Oliveira, E. Mendes, P. Baptista, S. Morais, S. Casal, Espresso coffee residues: A valuable source of unextracted compounds, J Agr Food Chem 60(32) (2012) 7777-7784.

[220] P.S. Murthy, M. Madhava Naidu, Sustainable management of coffee industry by-products and value addition—A review, Resources, Conservation and Recycling 66 (2012) 45-58.

[221] H. Ribeiro, J. Marto, S. Raposo, M. Agapito, V. Isaac, B.G. Chiari, P.F. Lisboa, A. Paiva, S. Barreiros, P. Simões, From coffee industry waste materials to skin-friendly products with improved skin fat levels, Eur J Lipid Sci Tech 115(3) (2013) 330-336.

[222] The Edible, Accessed in December 2016, https://camedillus.wordpress.com/.).

[223] Donegal Daily, Accessed in December 2016, http://www.donegaldaily.com/.).

[224] H. Pereira, Cork: Biology Production and Uses, Elsevier Science B.V. , Amsterdam, 2007.

[225] A. Şen, I. Miranda, S. Santos, J. Graça, H. Pereira, The chemical composition of cork and phloem in the rhytidome of *Quercus cerris* bark, Industrial Crops and Products 31(2) (2010) 417-422.

[226] L. Gil, Cork powder waste: An overview, Biomass & Bioenergy 13(1-2) (1997) 59-61.

[227] C. Moiteiro, M.J.M. Curto, N. Mohamed, M. Bailen, R. Martinez-Diaz, A. Gonzalez-Coloma, Biovalorization of friedelane triterpenes derived from cork processing industry byproducts, J Agr Food Chem 54(10) (2006) 3566-3571.

[228] A.V. Marques, H. Pereira, Lignin monomeric composition of corks from the barks of Betula pendula, Quercus suber and Quercus cerris determined by Py-GC-MS/FID, Journal of Analytical and Applied Pyrolysis 100 (2013) 88-94.

[229] I. Miranda, J. Gominho, H. Pereira, Cellular structure and chemical composition of cork from the Chinese cork oak (*Quercus variabilis*), Journal of Wood Science 59(1) (2013) 1-9.

[230] V. Castola, A. Bighelli, S. Rezzi, G. Melloni, S. Gladiali, J.M. Desjobert, J. Casanova, Composition and chemical variability of the triterpene fraction of dichloromethane extracts of cork (*Quercus suber* L.), Industrial Crops and Products 15(1) (2002) 15-22.

[231] V. Castola, B. Marongiu, A. Bighelli, C. Floris, A. Lai, J. Casanova, Extractives of cork (*Quercus suber* L.): chemical composition of dichloromethane and supercritical CO_2 extracts, Industrial Crops and Products 21(1) (2005) 65-69.

[232] Bulgarian Academy of Sciences & Ministry of Environment and Water, Red Data Book of the Republic of Bulgaria Digital edition, Accessed in December 2016, http://e-ecodb.bas.bg/rdb/en/vol3/18g1.html.).

[233] Cork Link, Accessed in December 2016, http://www.corklink.com/.).

[234] B.P. Nobre, L. Gouveia, P.G.S. Matos, A.F. Cristino, A.F. Palavra, R.L. Mendes, Supercritical extraction of lycopene from tomato industrial wastes with ethane, Molecules 17(7) (2012) 8397.

[235] IBERSEM, A cultura do tomate de indústria em Portugal, 5º Congresso brasileiro de tomate industrial - Feira de produtos e negócios, 2011.

[236] Verde Azurro, Caldo, Confagricoltura Toscana: "Emergenza pomodoro, riduzioni fino al 30%", Accessed in December 2016, http://www.verdeazzurronotizie.it/.).

[237] A. Cleantech, Accessed in December 2016, http://www.azocleantech.com/.).

[238] S.C.H. Barrett, I.W. Forno, Style morph distrivution in new worl populations of *Eichhornia crassipes* (Mart) Solms-Laubach (water hyacinth), Aquatic Botany 13(3) (1982) 299-306.

[239] C.M. Laranjeira, G. Nadais, *Eichhornia crassipes* control in the largest Portuguese natural freshwater lagoon, EPPO Bulletin 38(3) (2008) 487-495.

[240] M.Y. Harun, A.B.D. Radiah, Z.Z. Abidin, R. Yunus, Effect of physical pretreatment on dilute acid hydrolysis of water hyacinth (*Eichhornia crassipes*), Bioresource Technol 102(8) (2011) 5193-5199.

[241] C.C. Gunnarsson, C.M. Petersen, Water hyacinths as a resource in agriculture and energy production: A literature review, Waste Management 27(1) (2007) 117-129.

[242] Full Service Aquatics, Accessed in December 2016, http://fullserviceaquatics.com/.).

[243] School of Forest & Conservation - University of Florida, Accessed in December 2016, http://www.sfrc.ufl.edu/.

[244] H.P. Tai, K.P.T. Kim, Supercritical carbon dioxide extraction of Gac oil, Journal of Supercritical Fluids 95 (2014) 567-571.

[245] J. Kubola, N. Meeso, S. Siriamornpun, Lycopene and beta carotene concentration in aril oil of gac (*Momordica cochinchinensis* Spreng) as influenced by aril-drying process and solvents extraction, Food Res Int 50(2) (2013) 664-669.

[246] L.T. Vuong, Underutilized β-carotene–rich crops of Vietnam, Food and Nutrition Bulletin 21(2) (2000) 173-181.

[247] Biscara Tentang Tumbuhan, Gac Fruit @ Buah Gac, Accessed in December 2016, http://fazlisyam.com/2016/03/gac-fruit-buah-gac/.).

[248] Zishan Agro, Gac Fruit in Bangladesh, Accessed in 2016, http://www.zishanagro.com/seed-links/gac-fruit-in-bangladesh/.

[249] S.M. Abdulkarim, K. Long, O.M. Lai, S.K.S. Muhammad, H.M. Ghazali, Some physico-chemical properties of *Moringa oleifera* seed oil extracted using solvent and aqueous enzymatic methods, Food Chem 93(2) (2005) 253-263.

[250] F. Anwar, M.I. Bhanger, Analytical Characterization of *Moringa oleifera* Seed Oil Grown in Temperate Regions of Pakistan, J Agr Food Chem 51(22) (2003) 6558-6563.

[251] S. Mani, S. Jaya, R. Vadivambal, Optimization of Solvent Extraction of Moringa (*Moringa Oleifera*) Seed Kernel Oil Using Response Surface Methodology, Food Bioprod Process 85(4) (2007) 328-335.

[252] Crops for the Future, Drumstick tree (Moringa oleifera), Accessed in 2017, https://commons.wikimedia.org/wiki/File:Drumstick_tree_(Moringa_oleifera).jpg.

[253] L. Allorge, Seeds of Moringa oleifera from Martinique, France, Accessed in 2017, https://commons.wikimedia.org/wiki/File:Seeds_of_Moringa_oleifera.jpg.

[254] A.M.R.C. Alexandre, A.M.A. Dias, I.J. Seabra, A.A.T.G. Portugal, H.C. de Sousa, M.E.M. Braga, Biodiesel obtained from supercritical carbon dioxide oil of *Cynara cardunculus* L., Journal of Supercritical Fluids 68 (2012) 52-63.

[255] W.H. Chen, C.H. Chen, C.M.J. Chang, Y.H. Chiu, D. Hsiang, Supercritical carbon dioxide extraction of triglycerides from *Jatropha curcas* L. seeds, Journal of Supercritical Fluids 51(2) (2009) 174-180.

[256] P. Kotnik, M. Skerget, Z. Knez, Kinetics of supercritical carbon dioxide extraction of borage and evening primrose seed oil, Eur J Lipid Sci Tech 108(7) (2006) 569-576.

[257] G.L. Li, Z.W. Sun, L.A. Xia, J.Y. Shi, Y.J. Liu, Y.R. Suo, J.M. You, Supercritical CO_2 oil extraction from Chinese star anise seed and simultaneous compositional analysis using HPLC by fluorescence detection and online atmospheric CI-MS identification, J Sci Food Agr 90(11) (2010) 1905-1913.

[258] L.F. de França, M.A.A. Meireles, Modeling the extraction of carotene and lipids from pressed palm oil (*Elaes guineensis*) fibers using supercritical CO_2, Journal of Supercritical Fluids 18(1) (2000) 35-47.

[259] M. Arshadi, A.J. Hunt, J.H. Clark, Supercritical fluid extraction (SFE) as an effective tool in reducing auto-oxidation of dried pine sawdust for power generation, RSC Advances 2(5) (2012) 1806-1809.

[260] M.E. Araújo, N.T. Machado, L.F. Franca, M.A.A. Meireles, Supercritical extraction of pupunha (*Guilielma speciosa*) oil in a fixed bed using carbon dioxide, Braz J Chem Eng 17(3) (2000) 297-306.

[261] K. Hill, R. Höfer, Natural fats and oils, in: R. Höfer (Ed.), Sustainable solutions for modern economies, RSC, Cambridge, 2009.

[262] H. Belitz, W. Grosch, Food Chemistry, Second ed., Springer1999.

[263] R. Arroo, Eberhard Breitmaier. Terpenes—flavors, fragrances, pharmaca, pheromones. Wiley-VCH, 2006, 214 pp ISBN 3-527-31786-4, Applied Organometallic Chemistry 21(5) (2007) 377-377.

[264] A.Z. Kakasy, E. Lemberkovics, B. Simandi, L. Lelik, E. Hethelyi, I. Antal, E. Szoke, Comparative study of traditional essential oil and supercritical fluid extracts of Moldavian dragonhead (*Dracocephalum moldavica* L.), Flavour and Fragrance Journal 21(4) (2006) 598-603.

[265] A. Peterson, S. Machmudah, B.C. Roy, M. Goto, M. Sasaki, T. Hirose, Extraction of essential oil from geranium (*Pelargonium graveolens*) with supercritical carbon dioxide, Journal of Chemical Technology & Biotechnology 81(2) (2006) 167-172.

[266] P.B. Gomes, V.G. Mata, A.E. Rodrigues, Production of rose geranium oil using supercritical fluid extraction, The Journal of Supercritical Fluids 41(1) (2007) 50-60.

[267] S. Quispe-Condori, D. Sanchez, M.A. Foglio, P.T.V. Rosa, C. Zetzl, G. Brunner, M.A.A. Meireles, Global yield isotherms and kinetic of artemisinin extraction from *Artemisia annua* L leaves using supercritical carbon dioxide, Journal of Supercritical Fluids 36(1) (2005) 40-48.

[268] L. Čretnik, M. Škerget, Ž. Knez, Separation of parthenolide from feverfew: performance of conventional and high-pressure extraction techniques, Sep Purif Technol 41(1) (2005) 13-20.

[269] H.P. He, H. Corke, J.G. Cai, Supercritical carbon dioxide extraction of oil and squalene from *Amaranthus* grain, Journal of Agricultural and Food Chemistry 51(27) (2003) 7921-7925.

[270] P. Bhattacharjee, D. Chatterjee, R.S. Singhal, Supercritical Carbon Dioxide Extraction of Squalene from *Amaranthus paniculatus*: Experiments and Process Characterization, Food and Bioprocess Technology 5(6) (2012) 2506-2521.

[271] T.-F. Ko, Y.-M. Weng, R.Y.Y. Chiou, Squalene content and antioxidant activity of *Terminalia catappa* leaves and seeds, J Agr Food Chem 50(19) (2002) 5343-5348.

[272] L.D. Kagliwal, A.S. Pol, S.C. Patil, R.S. Singhal, V.B. Patravale, Antioxidant-rich extract from dehydrated seabuckthorn berries by supercritical carbon dioxide extraction, Food Bioprocess Tech 5(7) (2012) 2768-2776.

[273] L. Ciurlia, M. Bleve, L. Rescio, Supercritical carbon dioxide co-extraction of tomatoes (*Lycopersicum esculentum* L.) and hazelnuts (*Corylus avellana* L.): A new procedure in obtaining a source of natural lycopene, Journal of Supercritical Fluids 49(3) (2009) 338-344.

[274] W. Huang, Z. Li, H. Niu, D. Li, J. Zhang, Optimization of operating parameters for supercritical carbon dioxide extraction of lycopene by response surface methodology, J Food Eng 89(3) (2008) 298-302.

[275] L.S.V. Katherine, C.C. Edgar, W.K. Jerry, R.H. Luke, C.D. Julie, Extraction conditions affecting supercritical fluid extraction (SFE) of lycopene from watermelon, Bioresource Technology 99(16) (2008) 7835-7841.

[276] J. Sedlakova, B. Kocourkova, L. Lojkova, V. Kuban, Determination of essential oil content in caraway (*Carum carvi* L.) species by means of supercritical fluid extraction, Plant Soil Environ 49(6) (2003) 277-282.

[277] S.M. Pourmortazavi, F. Sefidkon, S.G. Hosseini, Supercritical carbon dioxide extraction of essential oils from *Perovskia atriplicifolia* Benth, J Agr Food Chem 51(18) (2003) 5414-5419.

[278] A.H. El-Ghorab, A.F. Mansour, K.F. El-Massry, Effect of extraction methods on the chemical composition and antioxidant activity of Egyptian marjoram (*Majorana hortensis* Moench), Flavour and Fragrance Journal 19(1) (2004) 54-61.

[279] M.E.M. Braga, P.A.D. Ehlert, L.C. Ming, M.A.A. Meireles, Supercritical fluid extraction from *Lippia alba*: global yields, kinetic data, and extract chemical composition, Journal of Supercritical Fluids 34(2) (2005) 149-156.

[280] E. Ghasemi, Y. Yamini, N. Bahramifar, F. Sefidkon, Comparative analysis of the oil and supercritical CO_2 extract of *Artemisia sieberi*, J Food Eng 79(1) (2007) 306-311.

[281] P. Costa, C. Grosso, S. Goncalves, P.B. Andrade, P. Valentao, M.G. Bernardo-Gil, A. Romano, Supercritical fluid extraction and hydrodistillation for the recovery of bioactive compounds from *Lavandula viridis* L'Her, Food Chem 135(1) (2012) 112-121.

[282] D. Ehlers, T. Nguyen, K.W. Quirin, D. Gerard, Analysis of essential basil oils –CO_2 extracts and steam-distilled oils, Deutsche Lebensmittel-Rundschau 97(7) (2001) 245-250.

[283] F. Yahya, T. Lu, R.C.D. Santos, P.J. Fryer, S. Bakalis, Supercritical carbon dioxide and solvent extraction of 2-acetyl-1-pyrroline from Pandan leaf: The effect of pre-treatment, The Journal of Supercritical Fluids 55(1) (2010) 200-207.

[284] P. Bhattacharjee, A. Kshirsagar, R.S. Singhal, Supercritical carbon dioxide extraction of 2-acetyl-1-pyrroline from *Pandanus amaryllifolius* Roxb, Food Chem 91(2) (2005) 255-259.

[285] J. Rincon, A. De Lucas, I. Garcia, Isolation of rock rose essential oil using supercritical CO_2 extraction, Separation Science and Technology 35(16) (2000) 2745-2763.

[286] P. Dzubak, M. Hajduch, D. Vydra, A. Hustova, M. Kvasnica, D. Biedermann, L. Markova, M. Urban, J. Sarek, Pharmacological activities of natural triterpenoids and their therapeutic implications, Natural Product Reports 23(3) (2006) 394-411.

[287] M.N. Laszczyk, Pentacyclic triterpenes of the lupane, oleanane and ursane group as tools in cancer therapy, Planta Med 75(15) (2009) 1549-1560.

[288] N. Sultana, A. Ata, Oleanolic acid and related derivatives as medicinally important compounds, Journal of Enzyme Inhibition and Medicinal Chemistry 23(6) (2008) 739-756.

[289] Y. Perumal, S. Dharmarajan, Betulinic acid and its derivatives: A review on their biological properties, Current Medicinal Chemistry 12(6) (2005) 657-666.

[290] R. Bruni, A. Medici, A. Guerrini, S. Scalia, F. Poli, M. Muzzoli, G. Sacchetti, Wild *Amaranthus caudatus* seed oil, a nutraceutical resource from Ecuadorian flora, Journal of Agricultural and Food Chemistry 49(11) (2001) 5455-5460.

[291] S.L. Taylor, J.W. King, Preparative-scale supercritical fluid extraction/supercritical fluid chromatography of corn bran, Journal of the American Oil Chemists' Society 79(11) (2002) 1133-1136.

[292] L.Y. Huang, T.H. Zhong, T.W. Chen, Z. Ye, G.N. Chen, Identification of beta-sitosterol, stigmasterol and ergosterin in *A. roxburghii* using supercritical fluid extraction followed by liquid chromatography/atmospheric pressure chemical ioneization ion trap mass spectrometry, Rapid Commun Mass Sp 21(18) (2007) 3024-3032.

[293] K.L. Nyam, C.P. Tan, R. Karim, O.M. Lai, K. Long, Y.B.C. Man, Extraction of tocopherol-enriched oils from Kalahari melon and roselle seeds by supercritical fluid extraction (SFE-CO2), Food Chemistry 119(3) (2010) 1278-1283.

[294] A. Boszormenyi, S. Szarka, E. Hethelyi, I. Gyurjan, M. Laszlo, B. Simandi, E. Szoke, E. Lemberkovics, Triterpenes in Traditional and Supercritical-Fluid Extracts of *Morus alba* Leaf and Stem Bark, Acta Chromatographica 21(4) (2009) 659-669.

[295] M. Sajfrtová, I. Ličková, M. Wimmerová, H. Sovová, Z. Wimmer, β-Sitosterol: Supercritical carbon dioxide extraction from Sea Buckthorn (*Hippophae rhamnoides* L.) seeds, International Journal of Molecular Sciences 11(4) (2010) 1842-1850.

[296] H. Sovová, A.A. Galushko, R.P. Stateva, K. Rochová, M. Sajfrtová, M. Bártlová, Supercritical fluid extraction of minor components of vegetable oils: β-Sitosterol, J Food Eng 101(2) (2010) 201-209.

[297] V.R. Preedy, R.R. Watson, The encyclopedia of vitamin E, CABI, Oxon, 2007.

[298] M. Waksmundzka-Hajnos, J. Sherma, High Performance Liquid Chromatogra-phy in Phytochemical Analysis, , Taylor & Francis, Boca Raton, 2010.

[299] O.I. Pokrovskii, A.A. Markoliya, F.D. Lepeshkin, I.V. Kuvykin, O.O. Parenago, S.A. Gonchukov, Extraction of linear furocoumarins from *Ammi majus* seeds by means of

supercritical fluid extraction and supercritical fluid chromatography, Russ J Phys Chem B+ 3(8) (2009) 1165-1171.

[300] H. Sovová, L. Opletal, M. Bártlová, M. Sajfrtová, M. Křenková, Supercritical fluid extraction of lignans and cinnamic acid from *Schisandra chinensis*, The Journal of Supercritical Fluids 42(1) (2007) 88-95.

[301] M. Fullana, F. Trabelsi, F. Recasens, Use of neural net computing for statistical and kinetic modelling and simulation of supercritical fluid extractors, Chem Eng Sci 55(1) (2000) 79-95.

[302] Z. Solati, B.S. Baharin, H. Bagheri, Supercritical carbon dioxide (SC-CO_2) extraction of *Nigella sativa* L. oil using full factorial design, Industrial Crops and Products 36(1) (2012) 519-523.

[303] C. Grosso, A.C. Figueiredo, J. Burillo, A.M. Mainar, J.S. Urieta, J.G. Barroso, J.A. Coelho, A.M.F. Palavra, Enrichment of the thymoquinone content in volatile oil from *Satureja montana* using supercritical fluid extraction, J Sep Sci 32(2) (2009) 328-334.

[304] J. Liu, S.Y. Lin, Z.Z. Wang, C.N. Wang, E.L. Wang, Y. Zhang, J.B. Liu, Supercritical fluid extraction of flavonoids from *Maydis stigma* and its nitrite-scavenging ability, Food and Bioproducts Processing 89(C4) (2011) 333-339.

[305] B. Shan, J.H. Xie, J.H. Zhu, Y. Peng, Ethanol modified supercritical carbon dioxide extraction of flavonoids from *Momordica charantia* L. and its antioxidant activity, Food and Bioproducts Processing 90(C3) (2012) 579-587.

[306] S.-F. Miao, J.-P. Yu, Z. Du, Y.-X. Guan, S.-J. Yao, Z.-Q. Zhu, Supercritical fluid extraction and micronization of *Ginkgo f*lavonoids from *Ginkgo biloba* Leaves, Industrial & Engineering Chemistry Research 49(11) (2010) 5461-5466.

[307] S.J. Wu, J.Y. Tsai, S.P. Chang, D.L. Lin, S.S. Wang, S.N. Huang, L.T. Ng, Supercritical carbon dioxide extract exhibits enhanced antioxidant and anti-inflammatory activities of *Physalis peruviana*, Journal of Ethnopharmacology 108(3) (2006) 407-413.

[308] J.Z. He, P. Shao, J.H. Liu, Q.M. Ru, Supercritical carbon dioxide extraction of flavonoids from Pomelo (*Citrus grandis* (L.) Osbeck) peel and their antioxidant activity, International Journal of Molecular Sciences 13(10) (2012) 13065-13078.

[309] C.S.R. Freire, A.J.D. Silvestre, C.P. Neto, J.A.S. Cavaleiro, Lipophilic extractives of the inner and outer barks of *Eucalyptus globulus*, Holzforschung 56(4) (2002) 372–379.

[310] Z. Yu-hong, Y. Tao, W. Yang, Extraction of betulin from bark of *Betula platyphylla* by supercritical carbon dioxide extraction, Journal of Forestry Research 14(3) (2003) 202-204.

[311] A. Felfoldi-Gava, S. Szarka, B. Simandi, B. Blazics, B. Simon, A. Kery, Supercritical fluid extraction of *Alnus glutinosa* (L.) Gaertn., Journal of Supercritical Fluids 61 (2012) 55-61.

[312] M. Tarvainen, J.P. Suomela, H. Kallio, B.R. Yang, Triterpene acids in *Plantago major*: Identification, quantification and comparison of different extraction methods, Chromatographia 71(3-4) (2010) 279-284.

[313] D. Cossuta, B. Simandi, J. Hohmann, F. Doleschall, T. Keve, Supercritical carbon dioxide extraction of sea buckthorn (*Hippophae rhamnoides* L.) pomace, J Sci Food Agr 87(13) (2007) 2472-2481.

[314] P. Lorenz, M. Berger, J. Bertrams, K. Wende, K. Wenzel, U. Lindequist, U. Meyer, F.C. Stintzing, Natural wax constituents of a supercritical fluid CO_2 extract from quince (*Cydonia oblonga* Mill.) pomace, Analytical and Bioanalytical Chemistry 391(2) (2008) 633-646.

[315] K. Speer, I. Kölling-Speer, The lipid fraction of the coffee bean, Brazilian Journal of Plant Physiology 18 (2006) 201-216.

[316] T. Kurzrock, K. Speer, Diterpenes and diterpene esters in coffee, Food Rev Int 17(4) (2001) 433-450.

[317] H. Belitz, W. Grosch, P. Schieberle, Food Chemistry, 4th ed., Springer, Berlin, 2009.

[318] J.A. Suarez, P.A. Beaton, C.A. Luengo, F.F. Felfli, Coffee husk briquettes: A new renewable energy source, Energ Source 25(10) (2003) 961-967.

[319] D.M. Elston, J. Meffert, Photo quiz - What is your diagnosis? Fordyce spots, Cutis 68(1) (2001) 24-+.

[320] L. Epstein, S. Bassein, Pesticide applications of copper on perennial crops in California, 1993 to 1998, J Environ Qual 30(5) (2001) 1844-1847.

[321] H.D. Ly, S. Howard, K. Shum, S.M. He, A. Zhu, S.G. Withers, The synthesis, testing and use of 5-fluoro-alpha-D-galactosyl fluoride to trap an intermediate on green coffee bean alpha-galactosidase and identify the catalytic nucleophile, Carbohyd Res 329(3) (2000) 539-547.

[322] H.P. Singh, D.R. Batish, R.K. Kohli, Autotoxicity: Concept, organisms, and ecological significance, Crit Rev Plant Sci 18(6) (1999) 757-772.

[323] J.A. Silva, N. Borges, A. Santos, A. Alves, Method validation for cafestol and kahweol quantification in coffee brews by HPLC-DAD, Food Anal Method 5(6) (2012) 1404-1410.

[324] F. Hashimoto, Y. Kashiwada, L.M. Cosentino, C.-H. Chen, P.E. Garrett, K.-H. Lee, Anti-AIDS agents—XXVII. Synthesis and anti-HIV activity of betulinic acid and dihydrobetulinic acid derivatives, Bioorganic & Medicinal Chemistry 5(12) (1997) 2133-2143.

[325] G. Bringmann, W. Saeb, L.A. Assi, G. François, A.S. Sankara Narayanan, K. Peters, E.-M. Peters, Betulinic Acid: Isolation from *Triphyophyllum peltatum* and *Ancistrocladus heyneanus*, antimalarial activity, and crystal structure of the benzyl ester, Planta Med 63(03) (1997) 255-257.

[326] J.C.P. Steele, D.C. Warhurst, G.C. Kirby, M.S.J. Simmonds, In vitro and In vivo evaluation of betulinic acid as an antimalarial, Phytotherapy Research 13(2) (1999) 115-119.

[327] P.K. Mukherjee, K. Saha, J. Das, M. Pal, B.P. Saha, Studies on the anti-inflammatory activity of rhizomes of *Nelumbo nucifera*, Planta Med 63(04) (1997) 367-369.

[328] M. del Carmen Recio, R.M. Giner, S. Máñez, J. Gueho, H.R. Julien, K. Hostettmann, J.L. Ríos, Investigations on the steroidal anti-inflammatory activity of triterpenoids from *Diospyros leucomelas*, Planta Med 61(01) (1995) 9-12.

[329] E. Pisha, H. Chai, I.-S. Lee, T.E. Chagwedera, N.R. Farnsworth, G.A. Cordell, C.W.W. Beecher, H.H.S. Fong, A.D. Kinghorn, D.M. Brown, M.C. Wani, M.E. Wall, T.J. Hieken, T.K. Das Gupta, J.M. Pezzuto, Discovery of betulinic acid as a selective inhibitor of human melanoma that functions by induction of apoptosis, Nat Med 1(10) (1995) 1046-1051.

[330] A.R. Chowdhury, S. Mandal, B. Mittra, S. Sharma, S. Mukhopadhyay, H.K. Majumder, Betulinic acid, a potent inhibitor of eukaryotic topoisomerase. I.Identification of the inhibitory step, the major functional group responsible and development of more potent derivatives Medical Science Monitor 8 (2002) BR254-BR265.

[331] S. Alakurtti, P. Bergstrom, N. Sacerdoti-Sierra, C.L. Jaffe, J. Yli-Kauhaluoma, Anti-leishmanial activity of betulin derivatives, Journal of Antibiotics 63(3) (2010) 123-126.

[332] J. Liu, Pharmacology of oleanolic acid and ursolic acid, Journal of Ethnopharmacology 49(2) (1995) 57-68.

[333] P. Antonisamy, V. Duraipandiyan, S. Ignacimuthu, Anti-inflammatory, analgesic and antipyretic effects of friedelin isolated from Azima tetracantha Lam. in mouse and rat models, Journal of Pharmacy and Pharmacology 63(8) (2011) 1070-1077.

[334] B. Lu, L. Liu, X. Zhen, X. Wu, Y. Zhang, Anti-tumor activity of Triterpenoid-rich extract from bamboo shavings (*Caulis bamfusae* in Taeniam), African Journal of Biotechnology 9(38) (2010) 6430-6436.

[335] A.O. Omoni, R.E. Aluko, The anti-carcinogenic and anti-atherogenic effects of lycopene: a review, Trends in Food Science & Technology 16(8) (2005) 344-350.

[336] M. Moeenfard, A. Cortez, V. Machado, R. Costa, C. Luís, P. Coelho, R. Soares, A. Alves, N. Borges, A. Santos, Anti-angiogenic properties of cafestol and kahweol palmitate diterpene esters, Journal of Cellular Biochemistry 117(12) (2016) 2748-2756.

[337] K.J. Lee, H.G. Jeong, Protective effects of kahweol and cafestol against hydrogen peroxide-induced oxidative stress and DNA damage, Toxicology Letters 173(2) (2007) 80-87.

[338] C. Cavin, C. Bezencon, G. Guignard, B. Schilter, Coffee diterpenes prevent benzo a pyrene genotoxicity in rat and human culture systems, Biochem. Biophys. Res. Commun. 306(2) (2003) 488-495.

[339] L.S. Guzzo, M.G.M.e. Castor, A.d.C. Perez, I.D.G. Duarte, T.R.L. Romero, Natural diterpenes from coffee, cafestol, and kahweol induce peripheral antinoceception by adrenergic system interaction, Planta Med 82(01/02) (2016) 106-112.

[340] F.B. Mellbye, P.B. Jeppesen, K. Hermansen, S. Gregersen, Cafestol, a bioactive substance in coffee, stimulates insulin secretion and increases glucose uptake in muscle cells: Studies in vitro, Journal of Natural Products 78(10) (2015) 2447-2451.

[341] N. Kaur, J. Chaudhary, A. Jain, L. Kishore, Stigmasterol: A comprehensive review, International Journal of Pharmaceutical Sciences and Research 2 (2011) 2259-2265.

[342] M. Guillemonat, A. , État de nos connaissances sur la chimie de liège, Bulletin de la Société Chimique de France, 1942.

[343] R.A.R. Pires, S.P.A.S.E., J.A.M. Martins, Chagas, R.L.G. Reis, Extraction and purification of friedelin, EP2070906A1, (2009).

[344] M.H. Zuknik, N.A. Nik Norulaini, A.K. Mohd Omar, Supercritical carbon dioxide extraction of lycopene: A review, J Food Eng 112(4) (2012) 253-262.

[345] S. Rezania, M. Ponraj, M.F.M. Din, A.R. Songip, F.M. Sairan, S. Chelliapan, The diverse applications of water hyacinth with main focus on sustainable energy and production for new era: An overview, Renewable and Sustainable Energy Reviews 41 (2015) 943-954.

[346] R.P. Silva, M.M.R. de Melo, A.J.D. Silvestre, C.M. Silva, Polar and lipophilic extracts characterization of roots, stalks, leaves and flowers of water hyacinth (*Eichhornia crassipes*), and insights for its future valorization, Industrial Crops and Products 76 (2015) 1033-1038.

[347] P.S. Pião, L.M.X. Lopes, I.R. Nascimento, Esteróides e um nucleosídeo da macrófita fitoremediadora *Eicchornia crassipes* (Pontederiaceae), Araraquara, 2010.

[348] P. Fernandes, J.M.S. Cabral, Phytosterols: Applications and recovery methods, Bioresource Technol 98(12) (2007) 2335-2350.

[349] N. Kaur, J. Chaudhary, A. Jain, L. Kishore, Stigmasterol: a comprehensive review, Int. J. Pharm. Sci. Res. 2, 2259–2265. (2011).

[350] A.B. Awad, C.S. Fink, Phytosterols as anticancer dietary components: Evidence and mechanism of action, The Journal of Nutrition 130(9) (2000) 2127-2130.

[351] O. Gabay, C. Sanchez, C. Salvat, F. Chevy, M. Breton, G. Nourissat, C. Wolf, C. Jacques, F. Berenbaum, Stigmasterol: a phytosterol with potential anti-osteoarthritic properties, Osteoarthritis and Cartilage 18(1) (2010) 106-116.

[352] S. Zhao, D. Zhang, An experimental investigation into the solubility of *Moringa oleifera* oil in supercritical carbon dioxide, J Food Eng 138 (2014) 1-10.

[353] J. Tsaknis, S. Lalas, V. Gergis, V. Spiliotis, A total characterization of *Moringa oleifera* Malawi seed oil, La Rivista Italiana Delle Sostanze Grasse LXXV (1998).

[354] M. Mukhopadhyay, Natural extracts using supercritical carbon dioxide, USA, CRC Press2000.

[355] A.I. Stankiewicz, J.A. Moulijn, Process intensification: Transforming chemical engineering, Chemical Engineering Progress 96(1) (2000) 22-34.

[356] P. Krasutsky, R. Carlson, V. Nesterenko, I. Kolomitsyn, C. Edwardson, Birch bark processing and the isolation of natural
products from birch bark, WO 2001010885., 2001.

[357] R.M.A. Domingues, D.J.S. Patinha, G.D.A. Sousa, J.J. Villaverde, C.M. Silva, C.S.R. Freire, A.J.D. Silvestre, C. Pascoal Neto, *Eucalyptus* biomass residues from agro-forest

and pulping industries as sources of high-value triterpenic compounds, Cellulose Chemistry and Technology 45(7-8) (2011) 475-481.

[358] M.M.R. de Melo, R.M.A. Domingues, M. Sova, E. Lack, H. Seidlitz, F. Lang Jr, A.J.D. Silvestre, C.M. Silva, Scale-up studies of the supercritical fluid extraction of triterpenic acids from Eucalyptus globulus bark, The Journal of Supercritical Fluids 95 (2014) 44-50.

[359] V.H. Rodrigues, M.M.R. de Melo, I. Portugal, C.M. Silva, Supercritical fluid extraction of *Eucalyptus globulus* leaves. Experimental and modelling studies of the influence of operating conditions and biomass pretreatment upon yields and kinetics, Sep Purif Technol 191(Supplement C) (2018) 173-181.

[360] J.Q. Albarelli, D.T. Santos, M.J. Cocero, M.A.A. Meireles, Economic analysis of an integrated annatto seeds-sugarcane biorefinery using supercritical CO_2 extraction as a first step, Materials 9 (6) (2016).

[361] R.C. Reid, J.M. Prausnitz, B.E. Poling, The Properties of Gases & Liquids, 5th ed., McGraw-Hill Professional, New York, 2001.

[362] J.R. Elliott, C.T. Lira, Introductory Chemical Engineering Thermodynamics, Prentice Hall, New York, 2012.

[363] K.S. Pitzer, D.R. Schreiber, Improving equation-of-state accuracy in the critical region - Equations for carbon-dioxide and neopentane as examples, Fluid Phase Equilibria 41(1-2) (1988) 1-17.

[364] W.-J. Kim, J.-D. Kim, J. Kim, S.-G. Oh, Y.-W. Lee, Selective caffeine removal from green tea using supercritical carbon dioxide extraction, J Food Eng 89(3) (2008) 303-309.

[365] L.E. Laroze, B. Díaz-Reinoso, A. Moure, M.E. Zúñiga, H. Domínguez, Extraction of antioxidants from several berries pressing wastes using conventional and supercritical solvents, European Food Research and Technology 231(5) (2010) 669-677.

[366] A. Rajaei, M. Barzegar, Y. Yamini, Supercritical fluid extraction of tea seed oil and its comparison with solvent extraction, European Food Research and Technology 220(3-4) (2005) 401-405.

[367] F.J. Eller, S.C. Cermak, S.L. Taylor, Supercritical carbon dioxide extraction of cuphea seed oil, Industrial Crops and Products 33(2) (2011) 554-557.

[368] R.A. Holser, G. Bost, Hybrid hibiscus seed oil compositions, Journal of the American Oil Chemists Society 81(8) (2004) 795-797.

[369] T. Hatami, R.N. Cavalcanti, T.M. Takeuchi, M.A.A. Meireles, Supercritical fluid extraction of bioactive compounds from Macela (*Achyrocline satureioides*) flowers: Kinetic, experiments and modeling, The Journal of Supercritical Fluids 65(0) (2012) 71-77.

[370] J. Dai, C. Ha, M. Shen, Systematic study of β-asarone-rich volatile oil from *Acori graminei* rhizoma by off-line supercritical CO_2 extraction–gas chromatography–mass spectrometry, Journal of Separation Science 31(4) (2008) 714-720.

[371] P.R. Venskutonis, M. Škėmaitė, B. Sivik, Assessment of radical scavenging capacity of *Agrimonia* extracts isolated by supercritical carbon dioxide, The Journal of Supercritical Fluids 45(2) (2008) 231-237.

[372] I.H. Akgun, A. Erkucuk, M. Pilavtepe, O. Yesil-Celiktas, Optimization of total alkannin yields of *Alkanna tinctoria* by using sub- and supercritical carbon dioxide extraction, Journal of Supercritical Fluids 57(1) (2011) 31-37.

[373] B. Simandi, A. Sass-Kiss, B. Czukor, A. Deak, A. Prechl, A. Csordas, J. Sawinsky, Pilot-scale extraction and fractional separation of onion oleoresin using supercritical carbon dioxide, Journal of Food Engineering 46(3) (2000) 183-188.

[374] C. Saengcharoenrat, D.E. Guyer, Effects of supercritical carbon dioxide conditions on onion oil desorption, Journal of Food Engineering 63(1) (2004) 33-37.

[375] C.L. Ye, Y.F. Lai, Supercritical CO_2 extraction optimization of onion oil using response surface methodology, Chemical Engineering & Technology 35(4) (2012) 646-652.

[376] M.E. Rybak, E.M. Calvey, J.M. Harnly, Quantitative determination of allicin in garlic: Supercritical fluid extraction and standard addition of alliin, Journal of Agricultural and Food Chemistry 52(4) (2004) 682-687.

[377] A. Felföldi-Gáva, S. Szarka, B. Simándi, B. Blazics, B. Simon, Á. Kéry, Supercritical fluid extraction of *Alnus glutinosa* (L.) Gaertn, The Journal of Supercritical Fluids 61 (2012) 55-61.

[378] Q.H. Hu, Y. Hu, J. Xu, Free radical-scavenging activity of Aloe vera (*Aloe barbadensis* Miller) extracts by supercritical carbon dioxide extraction, Food Chemistry 91(1) (2005) 85-90.

[379] H.Y. Ju, K.C. Huang, J.H. Chen, Y.C. Liu, C.M.J. Chang, C.C. Lee, C. Chang, C.J. Shieh, Optimization of the extraction of *Alpinia oxyphylla* essence oil in supercritical carbon dioxide, Journal of the American Oil Chemists Society 87(9) (2010) 1063-1070.

[380] R. Bruni, A. Guerrini, S. Scalia, C. Romagnoli, G. Sacchetti, Rapid techniques for the extraction of vitamin E isomers from *Amaranthus caudatus* seeds: Ultrasonic and supercritical fluid extraction, Phytochemical Analysis 13(5) (2002) 257-261.

[381] D. Westerman, R.C.D. Santos, J.A. Bosley, J.S. Rogers, B. Al-Duri, Extraction of Amaranth seed oil by supercritical carbon dioxide, Journal of Supercritical Fluids 37(1) (2006) 38-52.

[382] A.C. Kumoro, M. Hasan, Modeling of supercritical carbon dioxide extraction of andrographolide from *Andrographis paniculata* leaves, Chemical Engineering Communications 195(1) (2008) 72-80.

[383] N. Paroul, L. Rota, C. Frizzo, A.C. Atti dos Santos, P. Moyna, A.E. Gower, L.A. Serafini, E. Cassel, Chemical composition of the volatiles of Angelica *r*oot obtained by hydrodistillation and supercritical CO_2 Extraction, Journal of Essential Oil Research 14(4) (2002) 282-285.

[384] Q.H. Chen, P. Li, J. He, Z. Zhang, J. Liu, Supercritical fluid extraction for identification and determination of volatile metabolites from *Angelica dahurica* by GC-MS, Journal of Separation Science 31(18) (2008) 3218-3224.

[385] M.R. Kim, A.M. Abd El-Aty, J.H. Choi, K.B. Lee, J.H. Shim, Identification of volatile components in *Angelica* species using supercritical-CO_2 fluid extraction and solid phase microextraction coupled to gas chromatography-mass spectrometry, Biomedical Chromatography 20(11) (2006) 1267-1273.

[386] Y. Sun, S. Li, H. Song, S. Tian, Extraction of ferulic acid from *Angelica sinensis* with supercritical CO_2, Natural Product Research 20(9) (2006) 835-841.

[387] I. Papamichail, V. Louli, K. Magoulas, Supercritical fluid extraction of celery seed oil, Journal of Supercritical Fluids 18(3) (2000) 213-226.

[388] S. Akay, I. Alpak, O. Yesil-Celiktas, Effects of process parameters on supercritical CO_2 extraction of total phenols from strawberry (*Arbutus unedo* L.) fruits: An optimization study, Journal of Separation Science 34(15) (2011) 1925-1931.

[389] J.T. Paula, L.C. Paviani, M.A. Foglio, I.M.O. Sousa, F.A. Cabral, Extraction of anthocyanins from *Arrabidaea chica* in fixed bed using CO_2 and CO_2/ethanol/water mixtures as solvents, The Journal of Supercritical Fluids 81 (2013) 33-41.

[390] L. Martín, A.M. Mainar, A. González-Coloma, J. Burillo, J.S. Urieta, Supercritical fluid extraction of wormwood (*Artemisia absinthium* L.), The Journal of Supercritical Fluids 56(1) (2011) 64-71.

[391] B. Marongiu, A. Piras, S. Porcedda, Comparative analysis of the oil and supercritical CO_2 extract of *Artemisia arborescens* L. and *Helichrysum splendidum* (Thunb.) Less, Natural Product Research 20(5) (2006) 421-428.

[392] C.-C. Yang, M.-R. Lee, S.-L. Hsu, C.-M.J. Chang, Supercritical fluids extraction of capillarisin from *Artemisia capillaris* and its inhibition of in vitro growth of hepatoma cells, The Journal of Supercritical Fluids 42(1) (2007) 96-103.

[393] Q.H. Chen, P. Li, H.D. Yang, X.L. Li, J. Zhu, F.C. Chen, Identification of volatile compounds of *Atractylode lancea* Rhizoma using supercritical fluid extraction and GC-MS, Journal of Separation Science 32(18) (2009) 3152-3156.

[394] Z. Huang, M.-J. Yang, S.-F. Liu, Q. Ma, Supercritical carbon dioxide extraction of Baizhu: Experiments and modeling, The Journal of Supercritical Fluids 58(1) (2011) 31-39.

[395] C.R. Piantino, F.W.B. Aquino, L.A. Follegatti-Romero, F.A. Cabral, Supercritical CO_2 extraction of phenolic compounds from *Baccharis dracunculifolia*, The Journal of Supercritical Fluids 47(2) (2008) 209-214.

[396] E. Cassel, C.D. Frizzo, R. Vanderlinde, L. Atti-Serafini, D. Lorenzo, E. Dellacassa, Extraction of *Baccharis* oil by supercritical CO_2, Industrial & Engineering Chemistry Research 39(12) (2000) 4803-4805.

[397] R.M.F. Vargas, E. Cassel, G.M.F. Gomes, L.G.S. Longhi, L. Atti-Serafini, A.C. Atti-Santos, Supercritical extraction of carqueja essential oil: Experiments and modeling, Brazilian Journal of Chemical Engineering 23(3) (2006) 375-382.

[398] D.C.M.N. Silva, L.F.V. Bresciani, R.L. Dalagnol, L. Danielski, R.A. Yunes, S.R.S. Ferreira, Supercritical fluid extraction of carqueja (*Baccharis trimera*) oil: Process parameters and composition profiles, Food and Bioproducts Processing 87(C4) (2009) 317-326.

[399] B. Klejdus, L. Lojkova, E. Kula, I. Buchta, P. Hrdlicka, V. Kuban, Supercritical fluid extraction of amino acids from birch (*Betula pendula* Roth) leaves and their liquid chromatographic determination with fluorimetric detection, Journal of Separation Science 31(8) (2008) 1363-1373.

[400] B.P. Nobre, R.L. Mendes, E.M. Queiroz, F.L.P. Pessoa, J.P. Coelho, A.F. Palavra, Supercritical carbon dioxide extraction of pigments from *Bixa orellana* seeds (experiments and modeling), Brazilian Journal of Chemical Engineering 23(2) (2006) 251-258.

[401] G.F. Silva, F.M.C. Gamarra, A.L. Oliveira, F.A. Cabral, Extraction of bixin from annatto seeds using supercritical carbon dioxide, Brazilian Journal of Chemical Engineering 25(2) (2008) 419-426.

[402] C.L.C. Albuquerque, M.A.A. Meireles, Defatting of annatto seeds using supercritical carbon dioxide as a pretreatment for the production of bixin: Experimental, modeling and economic evaluation of the process, Journal of Supercritical Fluids 66 (2012) 86-95.

[403] A.M. Gomez, E.M. de la Ossa, Quality of borage seed oil extracted by liquid and supercritical carbon dioxide, Chemical Engineering Journal 88(1-3) (2002) 103-109.

[404] E. Dauksas, P.R. Venskutonis, B. Sivik, Supercritical fluid extraction of borage (*Borago officinalis* L.) seeds with pure CO_2 and its mixture with caprylic acid methyl ester, Journal of Supercritical Fluids 22(3) (2002) 211-219.

[405] T. Lu, F. Gaspar, R. Marriott, S. Mellor, C. Watkinson, B. Al-Duri, J. Seville, R. Santos, Extraction of borage seed oil by compressed CO_2: Effect of extraction parameters and modelling, The Journal of Supercritical Fluids 41(1) (2007) 68-73.

[406] C. Soto, E. Conde, A. Moure, M.E. Zúñiga, H. Domínguez, Supercritical extraction of borage seed oil coupled to conventional solvent extraction of antioxidants, European Journal of Lipid Science and Technology 110(11) (2008) 1035-1044.

[407] J.C. Germain, J.M. del Valle, J.C. de la Fuente, Natural convection retards supercritical CO_2 extraction of essential oils and lipids from vegetable substrates, Industrial & Engineering Chemistry Research 44(8) (2005) 2879-2886.

[408] M. Cvjetko, S. Jokic, Z. Lepojevic, S. Vidovic, B. Maric, I.R. Redovnikovic, Optimization of the supercritical CO_2 extraction of oil from rapeseed using response surface methodology, Food Technology and Biotechnology 50(2) (2012) 208-215.

[409] H. Li, J. Wu, C.B. Rempel, U. Thiyam, Effect of operating parameters on oil and phenolic extraction using supercritical CO_2, Journal of the American Oil Chemists' Society 87(9) (2010) 1081-1089.

[410] E. Arnáiz, J. Bernal, M.T. Martín, M.J. Nozal, J.L. Bernal, L. Toribio, Supercritical fluid extraction of free amino acids from broccoli leaves, Journal of Chromatography A 1250 (2012) 49-53.

[411] S.M. Pourmortazavi, M. Ghadiri, S.S. Hajimirsadeghi, Supercritical fluid extraction of volatile components from *Bunium persicum* Boiss. (black cumin) and *Mespilus germanica* L. (medlar) seeds, Journal of Food Composition and Analysis 18(5) (2005) 439-446.

[412] Y. Sun, L. Wei, J. Wang, J. Bi, Z. Liu, Y. Wang, Z. Guo, Optimization of supercritical fluid extraction of saikosaponins from *Bupleurum falcatum* with orthogonal array design, Journal of Separation Science 33(8) (2010) 1161-1166.

[413] Y. Kong, Y.J. Fu, Y.G. Zu, W. Liu, W. Wang, X. Hua, M. Yang, Ethanol modified supercritical fluid extraction and antioxidant activity of cajaninstilbene acid and pinostrobin from pigeonpea [*Cajanus cajan* (L.) Millsp.] leaves, Food Chemistry 117(1) (2009) 152-159.

[414] M. Hamburger, S. Adler, D. Baumann, A. Förg, B. Weinreich, Preparative purification of the major anti-inflammatory triterpenoid esters from Marigold (*Calendula officinalis*), Fitoterapia 74(4) (2003) 328-338.

[415] L.M.A.S. Campos, E.M.Z. Michielin, L. Danielski, S.R.S. Ferreira, Experimental data and modeling the supercritical fluid extraction of marigold (*Calendula officinalis*) oleoresin, Journal of Supercritical Fluids 34(2) (2005) 163-170.

[416] I. Zizovic, M. Stamenic, A. Orlovic, D. Skala, Supercritical carbon dioxide extraction of essential oils from plants with secretory ducts: Mathematical modelling on the micro-scale, Journal of Supercritical Fluids 39(3) (2007) 338-346.

[417] L. Danielski, L.M.A.S. Campos, L.F.V. Bresciani, H. Hense, R.A. Yunes, S.R.S. Ferreira, Marigold (*Calendula officinalis* L.) oleoresin: Solubility in SC-CO2 and composition profile, Chemical Engineering and Processing: Process Intensification 46(2) (2007) 99-106.

[418] M. Hamburger, D. Baumann, S. Adler, Supercritical carbon dioxide extraction of selected medicinal plants—effects of high pressure and added ethanol on yield of extracted substances, Phytochemical Analysis 15(1) (2004) 46-54.

[419] Y.F. Wang, D. Sun, H. Chen, L.S. Qian, P. Xu, Fatty acid composition and antioxidant activity of tea (*Camellia sinensis* L.) seed oil extracted by optimized supercritical carbon dioxide, International Journal of Molecular Sciences 12(11) (2011) 7708-7719.

[420] W.-Q. Tang, D.-C. Li, Y.-X. Lv, J.-G. Jiang, Extraction and removal of caffeine from green tea by ultrasonic-enhanced supercritical fluid, Journal of Food Science 75(4) (2010) C363-C368.

[421] S.M. Ghoreishi, E. Heidari, Extraction of epigallocatechin gallate from green tea via modified supercritical CO_2: Experimental, modeling and optimization, The Journal of Supercritical Fluids 72(0) (2012) 36-45.

[422] C. Da Porto, D. Decorti, F. Tubaro, Fatty acid composition and oxidation stability of hemp (*Cannabis sativa* L.) seed oil extracted by supercritical carbon dioxide, Industrial Crops and Products 36(1) (2012) 401-404.

[423] C. Da Porto, D. Voinovich, D. Decorti, A. Natolino, Response surface optimization of hemp seed (*Cannabis sativa* L.) oil yield and oxidation stability by supercritical carbon dioxide extraction, Journal of Supercritical Fluids 68 (2012) 45-51.

[424] A. Romo-Hualde, A.I. Yetano-Cunchillos, C. González-Ferrero, M.J. Sáiz-Abajo, C.J. González-Navarro, Supercritical fluid extraction and microencapsulation of bioactive compounds from red pepper (*Capsicum annum* L.) by-products, Food Chemistry 133(3) (2012) 1045-1049.

[425] E. Uquiche, J.M. del Valle, J. Ortiz, Supercritical carbon dioxide extraction of red pepper (*Capsicum annuum* L.) oleoresin, Journal of Food Engineering 65(1) (2004) 55-66.

[426] A.F. Gouveia, C. Duarte, M.L.B. da Costa, M.G. Bernardo-Gil, M. Moldao-Martins, Oxidative stability of olive oil flavoured by *Capsicum frutescens* supercritical fluid extracts, European Journal of Lipid Science and Technology 108(5) (2006) 421-428.

[427] C. Duarte, M. Moldao-Martins, A.F. Gouveia, S. Beirao da Costa, A.E. Leitao, M.G. Bernardo-Gil, Supercritical fluid extraction of red pepper (*Capsicum frutescens* L.), Journal of Supercritical Fluids 30(2) (2004) 155-161.

[428] X.J. Han, L.M. Cheng, R. Zhang, J.C. Bi, Extraction of safflower seed oil by supercritical CO_2, Journal of Food Engineering 92(4) (2009) 370-376.

[429] M. Ahro, M. Hakala, J. Sihvonen, J. Kauppinen, H. Kallio, Low-resolution gas-phase FT-IR method for the determination of the limonene/carvone ratio in supercritical CO_2-extracted caraway fruit oils, Journal of Agricultural and Food Chemistry 49(7) (2001) 3140-3144.

[430] M. Cabizza, G. Cherchi, B. Marongiu, S. Porcedda, M. Satta, A. Stassi, Isolation of a volatile concentrate of caraway seed, Journal of Essential Oil Research 13(5) (2001) 371-375.

[431] M. Khajeh, Y. Yamini, F. Sefidkon, N. Bahramifar, Comparison of essential oil composition of *Carum copticum* obtained by supercritical carbon dioxide extraction and hydrodistillation methods, Food Chemistry 86(4) (2004) 587-591.

[432] M.G. Bernardo-Gil, R. Roque, L.B. Roseiro, L.C. Duarte, F. Girio, P. Esteves, Supercritical extraction of carob kibbles (*Ceratonia siliqua* L.), Journal of Supercritical Fluids 59 (2011) 36-42.

[433] N.P. Povh, M.O.M. Marques, M.A.A. Meireles, Supercritical CO_2 extraction of essential oil and oleoresin from chamomile (*Chamomilla recutita* [L.] Rauschert), Journal of Supercritical Fluids 21(3) (2001) 245-256.

[434] C.S. Kaiser, H. Rompp, P.C. Schmidt, Supercritical carbon dioxide extraction of chamomile flowers: Extraction efficiency, stability, and in-line inclusion of chamomile-carbon dioxide extract in beta-cyclodextrin, Phytochemical Analysis 15(4) (2004) 249-256.

[435] C.E. Vargas, M.F. Mendes, D.A. Azevedo, F.L.P. Pessoa, A.C. Uller, Extraction of the essential oil of abajeru (*Chrysobalanus icaco*) using supercritical CO_2, The Journal of Supercritical Fluids 54(2) (2010) 171-177.

[436] B. Marongiu, A. Piras, S. Porcedda, E. Tuveri, E. Sanjust, M. Meli, F. Sollai, P. Zucca, A. Rescigno, Supercritical CO_2 extract of *Cinnamomum zeylanicum*: Chemical characterization and antityrosinase activity, Journal of Agricultural and Food Chemistry 55(24) (2007) 10022-10027.

[437] K.L. Nyam, C.P. Tan, O.M. Lai, K. Long, Y.B.C. Man, Optimization of supercritical CO_2 extraction of phytosterol-enriched oil from Kalahari melon seeds, Food and Bioprocess Technology 4(8) (2011) 1432-1441.

[438] Y.-H. Lee, A.L. Charles, H.-F. Kung, C.-T. Ho, T.-C. Huang, Extraction of nobiletin and tangeretin from *Citrus depressa* Hayata by supercritical carbon dioxide with ethanol as modifier, Industrial Crops and Products 31(1) (2010) 59-64.

[439] H. Ueno, M. Tanaka, S. Machmudah, M. Sasaki, M. Goto, Supercritical carbon dioxide extraction of valuable compounds from *Citrus junos* seed, Food and Bioprocess Technology 1(4) (2008) 357-363.

[440] A.C. Atti-Santos, M. Rossato, L.A. Serafini, E. Cassel, P. Moyna, Extraction of essential oils from lime (*Citrus latifolia* Tanaka) by hydrodistillation and supercritical carbon dioxide, Brazilian Archives of Biology and Technology 48(1) (2005) 155-160.

[441] W.-Y. Teng, C.-C. Chen, R.-S. Chung, HPLC comparison of supercritical fluid extraction and solvent extraction of coumarins from the peel of *Citrus maxima* fruit, Phytochemical Analysis 16(6) (2005) 459-462.

[442] A.N. Giannuzzo, H.J. Boggetti, M.A. Nazareno, H.T. Mishima, Supercritical fluid extraction of naringin from the peel of *Citrus paradisi*, Phytochemical Analysis 14(4) (2003) 221-223.

[443] J. Yu, D.V. Dandekar, R.T. Toledo, R.K. Singh, B.S. Patil, Supercritical fluid extraction of limonoids and naringin from grapefruit (*Citrus paradisi* Macf.) seeds, Food Chemistry 105(3) (2007) 1026-1031.

[444] C.H. Lee, K.H. Row, Y.-W. Lee, J.-D. Kim, Y.Y. Lee, Supercritical fluid extraction of perillyl alcohol in Korean orange peel, Journal of Liquid Chromatography & Related Technologies 24(13) (2001) 1987-1996.

[445] S. Lim, S.K. Jung, M.K. Jwa, Extraction of carotenoids from *Citrus unshiu* press cake by supercritical carbon dioxide, Food Sci Biotechnol 12 (2003) 513 - 520.

[446] C. Asis, R. Baroy, S. Bendijo, S.L. Hansen, V. Nacion, J. Tolimao, Supercritical fluid extraction to determine the oil content in copra and extracted meal, Journal of the American Oil Chemists' Society 83(1) (2006) 11-14.

[447] H.M.A. Barbosa, M.M.R. de Melo, M.A. Coimbra, C.P. Passos, C.M. Silva, Optimization of the supercritical fluid coextraction of oil and diterpenes from spent coffee grounds using experimental design and response surface methodology, The Journal of Supercritical Fluids 85 (2014) 165-172.

[448] M.M.R. de Melo, H.M.A. Barbosa, C.P. Passos, C.M. Silva, Supercritical fluid extraction of spent coffee grounds: Measurement of extraction curves, oil characterization and economic analysis, The Journal of Supercritical Fluids 86 (2014) 150-159.

[449] A.B.A. De Azevedo, P. Mazzafera, R.S. Mohamed, S.A.B. Vieira De Melo, T.G. Kieckbusch, Extraction of caffeine, chlorogenic acids and lipids from green coffee beans using supercritical carbon dioxide and co-solvents, Brazilian Journal of Chemical Engineering 25(3) (2008) 543-552.

[450] A.L. Oliveira, S.S. Silva, M.A.P. Da Silva, M.N. Eberlin, F.A. Cabral, Sensory and yield response surface analysis of supercritical CO_2 extracted aromatic oil from roasted coffee, Journal of Food Science and Technology 38(1) (2001) 38-42.

[451] J. Tello, M. Viguera, L. Calvo, Extraction of caffeine from Robusta coffee (*Coffea canephora* var. Robusta) husks using supercritical carbon dioxide, The Journal of Supercritical Fluids 59 (2011) 53-60.

[452] A.J. Hu, S.N. Zhao, H.H. Liang, T.Q. Qiu, G.H. Chen, Ultrasound assisted supercritical fluid extraction of oil and coixenolide from Adlay seed, Ultrasonics Sonochemistry 14(2) (2007) 219-224.

[453] A. Hu, Z. Zhang, J. Zheng, Y. Wang, Q. Chen, R. Liu, X. Liu, S. Zhang, Optimizations and comparison of two supercritical extractions of adlay oil, Innovative Food Science & Emerging Technologies 13 (2012) 128-133.

[454] E. Ellington, J. Bastida, F. Viladomat, C. Codina, Supercritical carbon dioxide extraction of colchicine and related alkaloids from seeds of *Colchicum autumnale* L, Phytochemical Analysis 14(3) (2003) 164-169.

[455] B. Liu, W.J. Li, Y.L. Chang, W.H. Dong, L. Ni, Extraction of berberine from rhizome of *Coptis chinensis* Franch using supercritical fluid extraction, Journal of Pharmaceutical and Biomedical Analysis 41(3) (2006) 1056-1060.

[456] S. Quispe-Condori, M.A. Foglio, P.T.V. Rosa, M.A.A. Meireles, Obtaining beta-caryophyllene from *Cordia verbenacea* de Candolle by supercritical fluid extraction, Journal of Supercritical Fluids 46(1) (2008) 27-32.

[457] E.B. Parisotto, E.M.Z. Michielin, F. Biscaro, S.R.S. Ferreira, D.W. Filho, R.C. Pedrosa, The antitumor activity of extracts from *Cordia verbenacea* D.C. obtained by supercritical fluid extraction, The Journal of Supercritical Fluids 61 (2012) 101-107.

[458] B. Yepez, M. Espinosa, S. Lopez, G. Bolanos, Producing antioxidant fractions from herbaceous matrices by supercritical fluid extraction, Fluid Phase Equilibria 194 (2002) 879-884.

[459] C. Grosso, V. Ferraro, A.C. Figueiredo, J.G. Barroso, J.A. Coelho, A.M. Palavra, Supercritical carbon dioxide extraction of volatile oil from Italian coriander seeds, Food Chemistry 111(1) (2008) 197-203.

[460] V. Illés, H.G. Daood, S. Perneczki, L. Szokonya, M. Then, Extraction of coriander seed oil by CO_2 and propane at super- and subcritical conditions, The Journal of Supercritical Fluids 17(2) (2000) 177-186.

[461] M.G. Bernardo-Gil, M. Casquilho, Modeling the supercritical fluid extraction of hazelnut and walnut oils, Aiche Journal 53(11) (2007) 2980-2985.

[462] M.G. Bernardo-Gil, J. Grenha, J. Santos, P. Cardoso, Supercritical fluid extraction and characterisation of oil from hazelnut, European Journal of Lipid Science and Technology 104(7) (2002) 402-409.

[463] S.G. Ozkal, U. Salgin, M.E. Yener, Supercritical carbon dioxide extraction of hazelnut oil, Journal of Food Engineering 69(2) (2005) 217-223.

[464] S.G. Ozkal, M.E. Yener, U. Salgin, U. Mehmetoglu, Response surfaces of hazelnut oil yield in supercritical carbon dioxide, European Food Research and Technology 220(1) (2005) 74-78.

[465] X.L. Cao, Y. Tian, T.Y. Zhang, Y. Ito, Supercritical fluid extraction of catechins from *Cratoxylum prunifolium* Dyer and subsequent purification by high-speed counter-current chromatography, Journal of Chromatography A 898(1) (2000) 75-81.

[466] E. Sousa, J. Martinez, O. Chiavone, P.T.V. Rosa, T. Domingos, M.A.A. Meireles, Extraction of volatile oil from *Croton zehntneri* Pax et Hoff with pressurized CO_2: solubility, composition and kinetics, Journal of Food Engineering 69(3) (2005) 325-333.

[467] M. Ismail, A. Mariod, G. Bagalkotkar, H.S. Ling, Fatty acid composition and antioxidant activity of oils from two cultivars of Cantaloupe extracted by supercritical fluid extraction, Grasas Y Aceites 61(1) (2010) 37-44.

[468] M.G. Bernardo-Gil, M. Casquilho, M.M. Esquivel, M.A. Ribeiro, Supercritical fluid extraction of fig leaf gourd seeds oil: Fatty acids composition and extraction kinetics, Journal of Supercritical Fluids 49(1) (2009) 32-36.

[469] D.L. Heikes, B. Scott, N.A. Gorzovalitis, Quantitation of volatile oils in ground cumin by supercritical fluid extraction and gas chromatography with flame ionization detection, Journal of Aoac International 84(4) (2001) 1130-1134.

[470] B. Daneshvand, K.M. Ara, F. Raofie, Comparison of supercritical fluid extraction and ultrasound-assisted extraction of fatty acids from quince (*Cydonia oblonga* Miller) seed using response surface methodology and central composite design, Journal of Chromatography A 1252 (2012) 1-7.

[471] B.T. Schaneberg, I.A. Khan, Comparison of extraction methods for marker compounds in the essential oil of lemon grass by GC, Journal of Agricultural and Food Chemistry 50(6) (2002) 1345-1349.

[472] L.H.C. Carlson, R.A.F. Machado, C.B. Spricigo, L.K. Pereira, A. Bolzan, Extraction of lemongrass essential oil with dense carbon dioxide, Journal of Supercritical Fluids 21(1) (2001) 33-39.

[473] Y.S. Sun, Z.B. Liu, J.H. Wang, W. Tian, H.Y. Zhou, L.X. Zhu, C.L. Zhang, Supercritical fluid extraction of paeonol from *Cynanchum paniculatum* (Bge.) Kitag. and subsequent isolation by high-speed counter-current chromatography coupled with high-performance liquid chromatography-photodiode array detector, Separation and Purification Technology 64(2) (2008) 221-226.

[474] M. Takahashi, H. Watanabe, J. Kikkawa, M. Ota, M. Watanabe, Y. Sato, H. Inomata, N. Sato, Carotenoids extraction from Japanese persimmon (Hachiyakaki) peels by supercritical CO_2 with ethanol, Analytical Sciences 22(11) (2006) 1441-1447.

[475] A. Maxia, B. Marongiu, A. Piras, S. Porcedda, E. Tuveri, M.J. Gonçalves, C. Cavaleiro, L. Salgueiro, Chemical characterization and biological activity of essential oils from *Daucus carota* L. subsp. carota growing wild on the Mediterranean coast and on the Atlantic coast, Fitoterapia 80(1) (2009) 57-61.

[476] S.B. Glišić, D.R. Mišić, M.D. Stamenić, I.T. Zizovic, R.M. Ašanin, D.U. Skala, Supercritical carbon dioxide extraction of carrot fruit essential oil: Chemical composition and antimicrobial activity, Food Chemistry 105(1) (2007) 346-352.

[477] M. Khajeh, Optimisation of supercritical fluid extraction of essential oil components of *Diplotaenia cachrydifolia*: Box-Behnken design, Natural Product Research 26(20) (2012) 1926-1930.

[478] M. Khajeh, M.G. Moghaddam, M. Shakeri, Application of artificial neural network in predicting the extraction yield of essential oils of *Diplotaenia cachrydifolia* by supercritical fluid extraction, The Journal of Supercritical Fluids 69 (2012) 91-96.

[479] T. Grevenstuk, S. Gonçalves, J.M.F. Nogueira, M.G. Bernardo-Gil, A. Romano, Recovery of high purity plumbagin from *Drosera intermedia*, Industrial Crops and Products 35(1) (2012) 257-260.

[480] O.J. Catchpole, N.B. Perry, B.M.T. da Silva, J.B. Grey, B.M. Smallfield, Supercritical extraction of herbs I: Saw Palmetto, St John's Wort, Kava Root, and Echinacea, The Journal of Supercritical Fluids 22(2) (2002) 129-138.

[481] V. Sewram, M.W. Raynor, D.A. Mulholland, D.M. Raidoo, The uterotonic activity of compounds isolated from the supercritical fluid extract of *Ekebergia capensis*, Journal of Pharmaceutical and Biomedical Analysis 24(1) (2000) 133-145.

[482] M.N. Hassan, N.N.A. Rahman, M.H. Ibrahim, A.K.M. Omar, Simple fractionation through the supercritical carbon dioxide extraction of palm kernel oil, Separation and Purification Technology 19(1-2) (2000) 113-120.

[483] N.N.A. Rahman, S.S. Al-Rawi, A.H. Ibrahim, M.M. Ben Nama, M.O. Ab Kadir, Supercritical carbon dioxide extraction of the residual oil from palm kernel cake, Journal of Food Engineering 108(1) (2012) 166-170.

[484] B. Marongiu, A. Piras, S. Porcedda, Comparative analysis of the oil and supercritical CO_2 extract of *Elettaria cardamomum* (L.) maton, Journal of Agricultural and Food Chemistry 52(20) (2004) 6278-6282.

[485] S. Hamdan, H.G. Daood, M. Toth-Markus, V. Illés, Extraction of cardamom oil by supercritical carbon dioxide and sub-critical propane, Journal of Supercritical Fluids 44(1) (2008) 25-30.

[486] J.Y. Kim, K.-P. Yoo, Effects of basic modifiers on sfe efficiencies of ephedrine derivatives from plant matrix, Korean Journal of Chemical Engineering 17(6) (2000) 672-677.

[487] E.M.Z. Michielin, L.F.V. Bresciani, L. Danielski, R.A. Yunes, S.R.S. Ferreira, Composition profile of horsetail (*Equisetum giganteum* L.) oleoresin: comparing SFE and organic solvents extraction, Journal of Supercritical Fluids 33(2) (2005) 131-138.

[488] A. Brachet, P. Christen, J.Y. Gauvrit, R. Longeray, P. Lanteri, J.L. Veuthey, Experimental design in supercritical fluid extraction of cocaine from coca leaves, Journal of Biochemical and Biophysical Methods 43(1-3) (2000) 353-366.

[489] N.L. Rozzi, W. Phippen, J.E. Simon, R.K. Singh, Supercritical fluid extraction of essential oil components from lemon-scented botanicals, Lebensmittel-Wissenschaft Und-Technologie-Food Science and Technology 35(4) (2002) 319-324.

[490] A.H. El-Ghorab, K.F. El-Massry, F. Marx, H.M. Fadel, Antioxidant activity of Egyptian *Eucalyptus camaldulensisvar*. brevirostrisleaf extracts, Food / Nahrung 47(1) (2003) 41-45.

[491] V.M. Rodrigues, E. Sousa, A.R. Monteiro, O. Chiavone-Filho, M.O.M. Marques, M.A.A. Meireles, Determination of the solubility of extracts from vegetable raw material in pressurized CO_2: a pseudo-ternary mixture formed by cellulosic structure plus solute plus solvent, Journal of Supercritical Fluids 22(1) (2002) 21-36.

[492] R.M.A. Domingues, E.L.G. Oliveira, C.S.R. Freire, R.M. Couto, P.C. Simoes, C.P. Neto, A.J.D. Silvestre, C.M. Silva, Supercritical fluid extraction of *Eucalyptus globulus b*ark - A promising approach for triterpenoid production, International Journal of Molecular Sciences 13(6) (2012) 7648-7662.

[493] H. Li, J.Y. Hu, H. Ouyang, Y.N. Li, H. Shi, C.J. Ma, Y.K. Zhang, Extraction of aucubin from seeds of *Eucommia ulmoides* Oliv. using supercritical carbon dioxide, Journal of Aoac International 92(1) (2009) 103-110.

[494] T. Hatami, M.A.A. Meireles, G. Zahedi, Mathematical modeling and genetic algorithm optimization of clove oil extraction with supercritical carbon dioxide, The Journal of Supercritical Fluids 51(3) (2010) 331-338.

[495] J. Martínez, P.T.V. Rosa, M.A.A. Meireles, Extraction of clove and vetiver oils with supercritical carbon dioxide: modeling and simulation, , Open Chemical Engineering Journal 1-7 (2007).

[496] Y. Geng, J. Liu, R. Lv, J. Yuan, Y. Lin, X. Wang, An efficient method for extraction, separation and purification of eugenol from *Eugenia caryophyllata* by supercritical fluid extraction and high-speed counter-current chromatography, Separation and Purification Technology 57(2) (2007) 237-241.

[497] W. Guan, S. Li, R. Yan, S. Tang, C. Quan, Comparison of essential oils of clove buds extracted with supercritical carbon dioxide and other three traditional extraction methods, Food Chemistry 101(4) (2007) 1558-1564.

[498] F.S. Malaman, L.A.B. Moraes, C. West, N.J. Ferreira, A.L. Oliveira, Supercritical fluid extracts from the Brazilian cherry (*Eugenia uniflora* L.): Relationship between the extracted compounds and the characteristic flavour intensity of the fruit, Food Chemistry 124(1) (2011) 85-92.

[499] A. Ozcan, A.S. Ozcan, Supercritical fluid extraction of *Euphorbia rigida*, Hrc-Journal of High Resolution Chromatography 23(5) (2000) 397-400.

[500] B. Liu, F. Guo, Y. Chang, H. Jiang, Q. Wang, Optimization of extraction of evodiamine and rutaecarpine from fruit of *Evodia rutaecarpa* using modified supercritical CO_2, Journal of Chromatography A 1217(50) (2010) 7833-7839.

[501] M. Khajeh, Y. Yamini, N. Bahramifar, F. Sefidkon, M. Reza Pirmoradei, Comparison of essential oils compositions of *Ferula assa-foetida* obtained by supercritical carbon dioxide extraction and hydrodistillation methods, Food Chemistry 91(4) (2005) 639-644.

[502] G. Sodeifian, K. Ansari, Optimization of *Ferulago angulata* oil extraction with supercritical carbon dioxide, The Journal of Supercritical Fluids 57(1) (2011) 38-43.

[503] Y. Yamini, F. Sefidkon, S.M. Pourmortazavi, Comparison of essential oil composition of Iranian fennel (*Foeniculum vulgare*) obtained by supercritical carbon dioxide extraction and hydrodistillation methods, Flavour and Fragrance Journal 17(5) (2002) 345-348.

[504] J.A.P. Coelho, A.P. Pereira, R.L. Mendes, A.M.F. Palavra, Supercritical carbon dioxide extraction of *Foeniculum vulgare* volatile oil, Flavour and Fragrance Journal 18(4) (2003) 316-319.

[505] B. Damjanovic, Z. Lepojevic, V. Zivkovic, A. Tolic, Extraction of fennel (*Foeniculum vulgare* Mill.) seeds with supercritical CO_2: Comparison with hydrodistillation, Food Chemistry 92(1) (2005) 143-149.

[506] A.S. Zarena, B. Manohar, K. Udaya Sankar, Optimization of supercritical carbon dioxide extraction of xanthones from mangosteen pericarp by response surface methodology, Food and Bioprocess Technology 5(4) (2012) 1181-1188.

[507] A.S. Zarena, N.M. Sachindra, K.U. Sankar, Optimisation of ethanol modified supercritical carbon dioxide on the extract yield and antioxidant activity from *Garcinia mangostana* L., Food Chemistry 130(1) (2012) 203-208.

[508] C. Yang, Y.R. Xu, W.X. Yao, Extraction of pharmaceutical components from *Ginkgo biloba* leaves using supercritical carbon dioxide, Journal of Agricultural and Food Chemistry 50(4) (2002) 846-849.

[509] K.-L. Chiu, Y.-C. Cheng, J.-H. Chen, C.J. Chang, P.-W. Yang, Supercritical fluids extraction of *Ginkgo* ginkgolides and flavonoids, The Journal of Supercritical Fluids 24(1) (2002) 77-87.

[510] Y.H. Choi, J. Kim, K.-P. Yoo, Supercritical-fluid extraction of bilobalide and ginkgolides from *Ginkgo biloba* leaves by use of a mixture of carbon dioxide, methanol, and water, Chromatographia 56(11) (2002) 753-757.

[511] Y.J. Fu, W. Wang, Y.G. Zu, Q.Y. Li, X.N. Liu, Study on volatile components of seed oil from *Glycyrrhiza uralensis* Fisch by supercritical carbon dioxide extraction-gas chromatography-mass spectrometry, Chinese Journal of Analytical Chemistry 33(4) (2005) 498-500.

[512] J.M.D. Araújo, A.P.N. Nicolino, C. Blatt, Utilization of supercritical carbon dioxide for concentration of tocopherols from soybean oil deodorizer distillate, Pesquisa Agropecuaria Brasileira 35(1) (2000) 201-205.

[513] P. Bhattacharjee, R.S. Singhal, S.R. Tiwari, Supercritical carbon dioxide extraction of cottonseed oil, Journal of Food Engineering 79(3) (2007) 892-898.

[514] B. Marongiu, A. Piras, S. Porcedda, E. Tuveri, Isolation of *Guaiacum bulnesia* volatile oil by supercritical carbon dioxide extraction, Journal of Essential Oil Bearing Plants 10(3) (2007) 221-228.

[515] J. Ivanovic, M. Ristic, D. Skala, Supercritical CO_2 extraction of *Helichrysum italicum*: Influence of CO_2 density and moisture content of plant material, The Journal of Supercritical Fluids 57(2) (2011) 129-136.

[516] L. Vazquez, C.F. Torres, T. Fornari, N. Grigelmo, F.J. Senorans, G. Reglero, Supercritical fluid extraction of minor lipids from pretreated sunflower oil deodorizer distillates, European Journal of Lipid Science and Technology 108(8) (2006) 659-665.

[517] Y.-W. Hsu, C.-F. Tsai, W.-K. Chen, Y.-C. Ho, F.-J. Lu, Determination of lutein and zeaxanthin and antioxidant capacity of supercritical carbon dioxide extract from daylily (*Hemerocallis disticha*), Food Chemistry 129(4) (2011) 1813-1818.

[518] K.W. Chan, M. Ismail, Supercritical carbon dioxide fluid extraction of *Hibiscus cannabinus* L. seed oil: A potential solvent-free and high antioxidative edible oil, Food Chemistry 114(3) (2009) 970-975.

[519] A.A. Mariod, B. Matthäus, M. Ismail, Comparison of supercritical fluid and hexane extraction methods in extracting Kenaf (*Hibiscus cannabinus*) seed oil lipids, Journal of the American Oil Chemists' Society 88(7) (2011) 931-935.

[520] J.Z. Yin, A.Q. Wang, W. Wei, Y. Liu, W.H. Shi, Analysis of the operation conditions for supercritical fluid extraction of seed oil, Separation and Purification Technology 43(2) (2005) 163-167.

[521] L.D. Kagliwal, S.C. Patil, A.S. Pol, R.S. Singhal, V.B. Patravale, Separation of bioactives from seabuckthorn seeds by supercritical carbon dioxide extraction methodology through solubility parameter approach, Separation and Purification Technology 80(3) (2011) 533-540.

[522] T.H.J. Beveridge, M. Cliff, P. Sigmund, Supercritical carbon dioxide percolation of sea buckthorn press juice, Journal of Food Quality 27(1) (2004) 41-54.

[523] E. Bravi, G. Perretti, L. Montanari, F. Favati, P. Fantozzi, Supercritical fluid extraction for quality control in beer industry, Journal of Supercritical Fluids 42(3) (2007) 342-346.

[524] A. Fratianni, M. Caboni, M. Irano, G. Panfili, A critical comparison between traditional methods and supercritical carbon dioxide extraction for the determination of tocochromanols in cereals, European Food Research and Technology 215(4) (2002) 353-358.

[525] M.P. Fernandez, J.F. Rodriguez, M.T. Garcia, A. de Lucas, I. Gracia, Application of supercritical fluid extraction to brewer's spent grain management, Industrial & Engineering Chemistry Research 47(5) (2008) 1614-1619.

[526] H.M. Rui, L.Y. Zhang, Z.W. Li, Y.L. Pan, Extraction and characteristics of seed kernel oil from white pitaya, Journal of Food Engineering 93(4) (2009) 482-486.

[527] F.M.C. Barros, F.C. Silva, J.M. Nunes, R.M.F. Vargas, E. Cassel, G.L. von Poser, Supercritical extraction of phloroglucinol and benzophenone derivatives from *Hypericum carinatum*: Quantification and mathematical modeling, Journal of Separation Science 34(21) (2011) 3107-3113.

[528] M. Mannila, Q. Lang, C.M. Wai, Y. Cui, C.Y.W. Ang, Supercritical fluid extraction of bioactive components from St. John's Wort (*Hypericum perforatum* L.) and *Ginkgo biloba*, Supercritical Carbon Dioxide, American Chemical Society2003, pp. 130-144.

[529] A. Smelcerovic, Z. Lepojevic, S. Djordjevic, Sub-and supercritical CO_2-extraction of *Hypericum perforatum* L., Chemical Engineering & Technology 27(12) (2004) 1327-1329.

[530] E. Langa, J. Cacho, A.M.F. Palavra, J. Burillo, A.M. Mainar, J.S. Urieta, The evolution of hyssop oil composition in the supercritical extraction curve: Modelling of the oil extraction process, Journal of Supercritical Fluids 49(1) (2009) 37-44.

[531] H. Kazazi, K. Rezaei, S.J. Ghotb-Sharif, Z. Emam-Djomeh, Y. Yamini, Supercriticial fluid extraction of flavors and fragrances from *Hyssopus officinalis* L. cultivated in Iran, Food Chemistry 105(2) (2007) 805-811.

[532] E. Cassel, R.M.F. Vargas, G.W. Brun, D.E. Almeida, L. Cogoi, G. Ferraro, R. Filip, Supercritical fluid extraction of alkaloids from *Ilex paraguariensis* St. Hil, Journal of Food Engineering 100(4) (2010) 656-661.

[533] B. Marongiu, A. Piras, F. Pani, S. Porcedda, M. Ballero, Extraction, separation and isolation of essential oils from natural matrices by supercritical CO_2, Flavour and Fragrance Journal 18(6) (2003) 505-509.

[534] R. Oliveira, M.F. Rodrigues, M.G. Bernardo-Gil, Characterization and supercritical carbon dioxide extraction of walnut oil, Journal of the American Oil Chemists Society 79(3) (2002) 225-230.

[535] T.D. Crowe, T.W. Crowe, L.A. Johnson, P.J. White, Impact of extraction method on yield of lipid oxidation products from oxidized and unoxidized walnuts, Journal of the American Oil Chemists Society 79(5) (2002) 453-456.

[536] B.M. Damjanovic, D. Skala, D. Petrovic-Djakov, J. Baras, A comparison between the oil, hexane extract and Supercritical carbon dioxide extract of *Juniperus communis* L., Journal of Essential Oil Research 15(2) (2003) 90-92.

[537] P. Chatzopoulou, A. de Haan, S.T. Katsiotis, Investigation on the supercritical CO_2 extraction of the volatile constituents from Juniperus communis obtained under different treatments of the "berries" (cones), Planta Medica 68(9) (2002) 827-831.

[538] B. Barjaktarovic, M. Sovilj, Z. Knez, Chemical composition of *Juniperus communis* L. fruits supercritical CO_2 extracts: Dependence on pressure and extraction time, Journal of Agricultural and Food Chemistry 53(7) (2005) 2630-2636.

[539] B. Damjanovic, D. Skala, J. Baras, D. Petrovic-Djakov, Isolation of essential oil and supercritical carbon dioxide extract of *Juniperus communis* L. fruits from Montenegro, Flavour and Fragrance Journal 21(6) (2006) 875-880.

[540] S.M. Pourmortazavi, P. Baghaee, M.A. Mirhosseini, Extraction of volatile compounds from *Juniperus communis* L. leaves with supercritical fluid carbon dioxide: comparison with hydrodistillation, Flavour and Fragrance Journal 19(5) (2004) 417-420.

[541] B. Marongiu, S. Porcedda, A. Caredda, B. De Gioannis, L. Vargiu, P. La Colla, Extraction of *Juniperus oxycedrus* ssp *oxycedrus* essential oil by supercritical carbon dioxide: influence of some process parameters and biological activity, Flavour and Fragrance Journal 18(5) (2003) 390-397.

[542] F.J. Eller, J.W. King, Supercritical carbon dioxide extraction of cedarwood oil: a study of extraction parameters and oil characteristics, Phytochemical Analysis 11(4) (2000) 226-231.

[543] F.J. Eller, S.L. Taylor, Pressurized fluids for extraction of cedarwood oil from *Juniperus virginianna*, Journal of Agricultural and Food Chemistry 52(8) (2004) 2335-2338.

[544] M. Akgun, N.A. Akgun, S. Dincer, Extraction and modeling of lavender flower essential oil using supercritical carbon dioxide, Industrial & Engineering Chemistry Research 39(2) (2000) 473-477.

[545] D.J.M. Gómez-Coronado, E. Ibañez, F.J. Rupérez, C. Barbas, Tocopherol measurement in edible products of vegetable origin, Journal of Chromatography A 1054(1–2) (2004) 227-233.

[546] S.H. Beis, N.T. Dunford, Supercritical fluid extraction of daphne (*Laurus nobilis* L.) seed oil, Journal of the American Oil Chemists' Society 83(11) (2006) 953-957.

[547] H. Marzouki, A. Piras, B. Marongiu, A. Rosa, M. Dessì, Extraction and separation of volatile and fixed oils from berries of *Laurus nobilis* L. by supercritical CO_2, Molecules 13(8) (2008) 1702.

[548] L.T. Danh, D.A.T. Ngo, T.N.H. Le, J. Zhao, R. Mammucari, N. Foster, Antioxidant activity, yield and chemical composition of lavender essential oil extracted by supercritical CO_2, Journal of Supercritical Fluids 70 (2012) 27-34.

[549] S.M. Ghoreishi, H. Kamali, H.S. Ghaziaskar, A.A. Dadkhah, Optimization of supercritical extraction of linalyl acetate from lavender via Box-Behnken design, Chemical Engineering & Technology 35(9) (2012) 1641-1648.

[550] H. Kamali, M.R. Jalilvand, N. Aminimoghadamfarouj, Pressurized fluid extraction of essential oil from *Lavandula hybrida* using a modified supercritical fluid extractor and a central composite design for optimization, Journal of Separation Science 35(12) (2012) 1479-1485.

[551] N.A. Akgün, M. Akgün, S. Dinçer, A. Akgerman, Supercritical fluid extraction of *Lavandula stoechas* L. ssp. *cariensis* (Boiss.) Rozeira, Journal of Essential Oil Research 13(3) (2001) 143-148.

[552] W. Xu, K.D. Chu, H. Li, L.D. Chen, Y.Q. Zhang, X.C. Tang, Extraction of *Lepidium apetalum* seed oil using supercritical carbon dioxide and anti-oxidant activity of the extracted oil, Molecules 16(12) (2011) 10029-10045.

[553] E. Daukšas, P. Rimantas Venskutonis, B. Sivik, T. Nillson, Effect of fast CO_2 pressure changes on the yield of lovage (*Levisticum officinale* Koch.) and celery (*Apium graveolens* L.) extracts, The Journal of Supercritical Fluids 22(3) (2002) 201-210.

[554] Y.Y. Sun, S.F. Li, Measurement and correlation of the solubility of Ligusticum Chuanxiong oil in supercritical CO_2, Chinese Journal of Chemical Engineering 13(6) (2005) 796-799.

[555] D.S. Ivanov, R.R. Čolović, J.D. Lević, S.A. Sredanović, Optimization of supercritical fluid extraction of linseed oil using RSM, European Journal of Lipid Science and Technology 114(7) (2012) 807-815.

[556] E.L. Galvao, J. Martinez, H.N. Maia De Oliveira, E.M. Bittencourt Dutra De Sousa, Supercritical extraction of linseed oil: Economical viability and modeling extraction curves, Chemical Engineering Communications 200(2) (2013) 205-221.

[557] V.J. Barthet, J.K. Daun, An evaluation of supercritical fluid extraction as an analytical tool to determine fat in canola, flax, solin, and mustard, Journal of the American Oil Chemists Society 79(3) (2002) 245-251.

[558] E.E. Stashenko, B.E. Jaramillo, J.R. Martínez, Comparison of different extraction methods for the analysis of volatile secondary metabolites of *Lippia alba* (Mill.) N.E. Brown, grown in Colombia, and evaluation of its in vitro antioxidant activity, Journal of Chromatography A 1025(1) (2004) 93-103.

[559] P.F. de Oliveira, R.A.F. Machado, A. Bolzan, D. Barth, Supercritical fluid extraction of hernandulcin from *Lippia dulcis* Trev, The Journal of Supercritical Fluids 63 (2012) 161-168.

[560] E.M.B.D. Sousa, O. Chiavone, M.T. Moreno, D.N. Silva, M.O.M. Marques, M.A.A. Meireles, Experimental results for the extraction of essential oil from *Lippia sidoides* Cham. using pressurized carbon dioxide, Brazilian Journal of Chemical Engineering 19(2) (2002) 229-241.

[561] C.F. Silva, M.F. Mendes, F.L.P. Pessoa, E.M. Queiroz, Supercritical carbon dioxide extraction of macadamia (*Macadamia integrifolia*) nut oil: Experiments and modeling, Brazilian Journal of Chemical Engineering 25(1) (2008) 175-181.

[562] M.T. Fernández-Ponce, L. Casas, C. Mantell, M. Rodríguez, E. Martínez de la Ossa, Extraction of antioxidant compounds from different varieties of *Mangifera indica* leaves using green technologies, The Journal of Supercritical Fluids 72 (2012) 168-175.

[563] H. Cao, J.B. Xiao, M. Xu, Comparison of volatile components of *Marchantia convoluta* obtained by supercritical carbon dioxide extraction and petrol ether extraction, Journal of Food Composition and Analysis 20(1) (2007) 45-51.

[564] J.B. Xiao, J.W. Chen, M. Xu, Supercritical fluid CO_2 extraction of essential oil from *Marchantia convoluta*: global yields and extract chemical composition, 2007.

[565] Z.P. Zekovic, Chamomile ligulate flowers in supercritical CO_2-extraction, Journal of Essential Oil Research 12(1) (2000) 85-93.

[566] E.C. de Vasconcelos, J.H.Y. Vilegas, F.M. Lanças, Comparison of extraction and clean-up methods for the analysis of friedelan-3-ol and friedelin from leaves of *Maytenus aquifolium* Martius (Celastraceae), Phytochemical Analysis 11(4) (2000) 247-250.

[567] A.J. Mossi, R.L. Cansian, A.Z. Carvalho, C. Dariva, J. Vladimir Oliveira, M. Mazutti, I.N. Filho, S. Echeverrigaray, Extraction and characterization of volatile compounds in *Maytenus ilicifolia*, using high-pressure CO_2, Fitoterapia 75(2) (2004) 168-178.

[568] S.M. Jajaei, W.R.W. Daud, M. Markom, Z. Zakaria, M.L. Presti, R. Costa, L. Mondello, L. Santi, Extraction of *Melaleuca cajuputi* using supercritical fluid extraction and solvent extraction, Journal of Essential Oil Research 22(3) (2010) 205-210.

[569] G. Karasova, J. Lehotay, E. Klodzinska, R. Gadzala-Kopciuch, B. Buszewski, Comparison of several extraction methods for the isolation of benzoic acid derivatives from *Melissa officinalis*, Journal of Liquid Chromatography & Related Technologies 29(11) (2006) 1633-1644.

[570] M.A. Ribeiro, M.G. Bernardo-Gil, M.M. Esquivel, *Melissa officinalis* L.: study of antioxidant activity in supercritical residues, Journal of Supercritical Fluids 21(1) (2001) 51-60.

[571] E.M.C. Reis-Vasco, J.A.P. Coelho, A.M.F. Palavra, C. Marrone, E. Reverchon, Mathematical modelling and simulation of pennyroyal essential oil supercritical extraction, Chemical Engineering Science 55(15) (2000) 2917-2922.

[572] N. Aghel, Y. Yamini, A. Hadjiakhoondi, S.M. Pourmortazavi, Supercritical carbon dioxide extraction of *Mentha pulegium* L. essential oil, Talanta 62(2) (2004) 407-411.

[573] B. Marongiu, S. Porcedda, G. Della Porta, E. Reverchon, Extraction and isolation of *Salvia desoleana* and *Mentha spicata* subsp *insularis* essential oils by supercritical CO2, Flavour and Fragrance Journal 16(5) (2001) 384-388.

[574] K.H. Kim, J. Hong, A mass transfer model for super- and near-critical CO_2 extraction of spearmint leaf oil, Separation Science and Technology 37(10) (2002) 2271-2288.

[575] P.P. Almeida, N. Mezzomo, S.R.S. Ferreira, Extraction of *Mentha spicata* L. volatile compounds: Evaluation of process parameters and extract composition, Food and Bioprocess Technology 5(2) (2012) 548-559.

[576] K. Ansari, I. Goodarznia, Optimization of supercritical carbon dioxide extraction of essential oil from spearmint (*Mentha spicata* L.) leaves by using Taguchi methodology, Journal of Supercritical Fluids 67 (2012) 123-130.

[577] M. Bimakr, R.A. Rahman, A. Ganjloo, F.S. Taip, L.M. Salleh, M.Z.I. Sarker, Optimization of supercritical carbon dioxide extraction of bioactive flavonoid compounds from spearmint (*Mentha spicata* L.) leaves by using response surface methodology, Food and Bioprocess Technology 5(3) (2012) 912-920.

[578] S. Lina, R. Fei, Z. Xudong, D. Yangong, H. Fa, Supercritical carbon dioxide extraction of *Microula sikkimensis* seed oil, Journal of the American Oil Chemists' Society 87(10) (2010) 1221-1226.

[579] R.M.S. Celeghini, J.H.Y. Vilegas, F.M. Lanças, Extraction and quantitative HPLC analysis of coumarin in hydroalcoholic: Extracts of *Mikania glomerata* Spreng. ("guaco") leaves, Journal of the Brazilian Chemical Society 12(6) (2001) 706-709.

[580] C.H. Chen, T.P. Lin, Y.L. Chung, C.K. Lee, D.B. Yeh, S.Y. Chen, Determination of antioxidative properties of *Morinda citrifolia* using near supercritical fluid extraction, Journal of Food and Drug Analysis 17(5) (2009) 333-341.

[581] H.N. Nguyen, P.A.D. Gaspillo, J.B. Maridable, R.M. Malaluan, H. Hinode, C. Salim, H.K.P. Huynh, Extraction of oil from *Moringa oleifera* kernels using supercritical carbon dioxide with ethanol for pretreatment: Optimization of the extraction process, Chemical Engineering and Processing 50(11-12) (2011) 1207-1213.

[582] S. Machmudah, A. Sulaswatty, M. Sasaki, M. Goto, T. Hirose, Supercritical CO_2 extraction of nutmeg oil: Experiments and modeling, Journal of Supercritical Fluids 39(1) (2006) 30-39.

[583] T.-q. Chen, J.-g. Wu, Y.-b. Wu, H.-y. Wang, F.-h. Mao, J.-z. Wu, Supercritical fluid CO_2 extraction, simultaneous determination of total sterols in the spore lipids of *Ganoderma lucidum* by GC-MS/SIM methods, Chemistry of Natural Compounds 48(4) (2012) 657-658.

[584] E. Ghasemi, F. Raofie, N.M. Najafi, Application of response surface methodology and central composite design for the optimisation of supercritical fluid extraction of essential oils from *Myrtus communis* L. leaves, Food Chemistry 126(3) (2011) 1449-1453.

[585] J.P. Louey, H. Shaeffer, N. Petersen, D. Salotti, Oil of catnip by supercritical fluid extraction., Abstracts of Papers of the American Chemical Society 221 (2001) U215-U215.

[586] M. Khajeh, Y. Yamini, S. Shariati, Comparison of essential oils compositions of *Nepeta persica* obtained by supercritical carbon dioxide extraction and steam distillation methods, Food and Bioproducts Processing 88(2–3) (2010) 227-232.

[587] A. Ruiz-Rodriguez, M.R. Bronze, M.N. da Ponte, Supercritical fluid extraction of tobacco leaves: A preliminary study on the extraction of solanesol, Journal of Supercritical Fluids 45(2) (2008) 171-176.

[588] N. Radulovic, G. Stojanovic, R. Palic, S. Alagic, Chemical composition of the ether and ethyl acetate extracts of Serbian selected tobacco types: Yaka, Prilep and Otlja, Journal of Essential Oil Research 18(5) (2006) 562-565.

[589] E. Dauksas, P.R. Venskutonis, B. Sivik, Comparison of oil from *Nigella damascena* seed recovered by pressing, conventional solvent extraction and carbon dioxide extraction, Journal of Food Science 67(3) (2002) 1021-1024.

[590] S. Machmudah, Y. Shiramizu, M. Goto, M. Sasaki, T. Hirose, Extraction of *Nigella sativa* L. using supercritical CO_2: A study of antioxidant activity of the extract, Separation Science and Technology 40(6) (2005) 1267-1275.

[591] M.V. Rao, A.H. Al-Marzouqi, F.S. Kaneez, S.S. Ashraf, A. Adem, Comparative evaluation of SFE and solvent extraction methods on the yield and composition of black seeds (*Nigella Sativa*), Journal of Liquid Chromatography & Related Technologies 30(17) (2007) 2545-2555.

[592] P. Kotnik, M. Škerget, Ž. Knez, Kinetics of supercritical carbon dioxide extraction of borage and evening primrose seed oil, Eur J Lipid Sci Tech 108(7) (2006) 569-576.

[593] A. de Lucas, J. Rincón, I. Gracia, Influence of operation variables on quality parameters of olive husk oil extracted with CO_2: Three-step sequential extraction, Journal of the American Oil Chemists' Society 80(2) (2003) 181-188.

[594] A. de Lucas, J. Rincón, I. Gracia, Influence of operating variables on yield and quality parameters of olive husk oil extracted with supercritical carbon dioxide, Journal of the American Oil Chemists' Society 79(3) (2002) 237-243.

[595] S. Şahin, M. Bilgin, M.U. Dramur, Investigation of oleuropein content in olive leaf extract obtained by supercritical fluid extraction and Soxhlet methods, Separation Science and Technology 46(11) (2011) 1829-1837.

[596] C. Ma, G. Li, J. Zhang, Q. Zheng, X. Fan, Z. Wang, An efficient combination of supercritical fluid extraction and high-speed counter-current chromatography to extract and purify homoisoflavonoids from *Ophiopogon japonicus* (Thunb.) Ker-Gawler, J Sep Sci 32(11) (2009) 1949-1956.

[597] W. Liu, Y.-J. Fu, Y.-G. Zu, M.-H. Tong, N. Wu, X.-L. Liu, S. Zhang, Supercritical carbon dioxide extraction of seed oil from *Opuntia dillenii* Haw. and its antioxidant activity, Food Chem 114(1) (2009) 334-339.

[598] E. Vági, E. Rapavi, M. Hadolin, K. Vásárhelyiné Perédi, A. Balázs, A. Blázovics, B. Simándi, Phenolic and triterpenoid antioxidants from *Origanum majorana* L. herb and extracts obtained with different solvents, J Agr Food Chem 53(1) (2005) 17-21.

[599] E. Vági, B. Simándi, Á. Suhajda, É. Héthelyi, Essential oil composition and antimicrobial activity of *Origanum majorana* L. extracts obtained with ethyl alcohol and supercritical carbon dioxide, Food Res Int 38(1) (2005) 51-57.

[600] H.-C. Wang, C.-R. Chen, C.J. Chang, Carbon dioxide extraction of ginseng root hair oil and ginsenosides, Food Chem 72(4) (2001) 505-509.

[601] C. Devittori, D. Gumy, A. Kusy, L. Colarow, C. Bertoli, P. Lambelet, Supercritical fluid extraction of oil from millet bran, Journal of the American Oil Chemists' Society 77(6) (2000) 573.

[602] B. Bozan, F. Temelli, Extraction of Poppy Seed Oil Using Supercritical CO_2, J Food Sci 68(2) (2003) 422-426.

[603] Y. Xie, J. Peng, G. Fan, Y. Wu, Chemical composition and antioxidant activity of volatiles from *Patrinia Villosa* Juss obtained by optimized supercritical fluid extraction, J Pharmaceut Biomed 48(3) (2008) 796-801.

[604] M.D.A. Saldaña, C. Zetzl, R.S. Mohamed, G. Brunner, Decaffeination of guaraná seeds in a microextraction column using water-saturated CO_2, The Journal of Supercritical Fluids 22(2) (2002) 119-127.

[605] M. Reddy, R. Moodley, S.B. Jonnalagadda, Fatty acid profile and elemental content of avocado (*Persea americana* Mill.) oil –effect of extraction methods, Journal of Environmental Science and Health, Part B 47(6) (2012) 529-537.

[606] L. Martín, A. González-Coloma, C.E. Díaz, A.M. Mainar, J.S. Urieta, Supercritical CO_2 extraction of *Persea indica*: Effect of extraction parameters, modelling and bioactivity of its extracts, The Journal of Supercritical Fluids 57(2) (2011) 120-128.

[607] V. Louli, G. Folas, E. Voutsas, K. Magoulas, Extraction of parsley seed oil by supercritical CO_2, The Journal of Supercritical Fluids 30(2) (2004) 163-174.

[608] E. Uquiche, E. Huerta, A. Sandoval, J.M. del Valle, Effect of boldo (*Peumus boldus* M.) pretreatment on kinetics of supercritical CO_2 extraction of essential oil, J Food Eng 109(2) (2012) 230-237.

[609] J.M. del Valle, C. Godoy, M. Asencio, J.M. Aguilera, Recovery of antioxidants from boldo (*Peumus boldus* M.) by conventional and supercritical CO_2 extraction, Food Res Int 37(7) (2004) 695-702.

[610] J.M. del Valle, T. Rogalinski, C. Zetzl, G. Brunner, Extraction of boldo (*Peumus boldus* M.) leaves with supercritical CO_2 and hot pressurized water, Food Res Int 38(2) (2005) 203-213.

[611] P.F. Leal, M.B. Kfouri, F.C. Alexandre, F.H.R. Fagundes, J.M. Prado, M.H. Toyama, M.A.A. Meireles, Brazilian Ginseng extraction via LPSE and SFE: Global yields, extraction kinetics, chemical composition and antioxidant activity, The Journal of Supercritical Fluids 54(1) (2010) 38-45.

[612] X. Liu, M. Zhao, J. Wang, W.E.I. Luo, Antimicrobial and antioxidant activity of emblica extracts obtained by supercritical carbon dioxide extraction and methanol extraction, Journal of Food Biochemistry 33(3) (2009) 307-330.

[613] M. Co, A. Fagerlund, L. Engman, K. Sunnerheim, P.J.R. Sjöberg, C. Turner, Extraction of antioxidants from spruce (*Picea abies*) bark using eco-friendly solvents, Phytochem Analysis 23(1) (2012) 1-11.

[614] V.M. Rodrigues, P.T.V. Rosa, M.O.M. Marques, A.J. Petenate, M.A.A. Meireles, Supercritical extraction of essential oil from aniseed (*Pimpinella anisum* L) using CO_2: Solubility, kinetics, and composition data, J Agr Food Chem 51(6) (2003) 1518-1523.

[615] O. Yesil-Celiktas, F. Otto, S. Gruener, H. Parlar, Determination of extractability of pine bark using supercritical CO_2 extraction and different solvents: optimization and prediction, J Agr Food Chem 57(2) (2009) 341-347.

[616] E. Conde, J. Hemming, A. Smeds, B.D. Reinoso, A. Moure, S. Willför, H. Domínguez, J.C. Parajó, Extraction of low-molar-mass phenolics and lipophilic compounds from *Pinus pinaster* wood with compressed CO_2, The Journal of Supercritical Fluids 81 (2013) 193-199.

[617] V.d.S. Carrara, L.Z. Serra, L. Cardozo-Filho, E.F. Cunha-Júnior, E.C. Torres-Santos, D.A.G. Cortez, HPLC analysis of supercritical carbon dioxide and compressed propane extracts from *Piper amalago* L. with antileishmanial activity, Molecules 17(1) (2012) 15.

[618] Z.Y. Li, X.W. Liu, S.H. Chen, X.D. Zhang, Y.J. Xia, Y. Wei, F. Xiao, An experimental and simulating study of supercritical CO_2 extraction for pepper oil, Chem Eng Process 45(4) (2006) 264-267.

[619] C. Perakis, V. Louli, K. Magoulas, Supercritical fluid extraction of black pepper oil, J Food Eng 71(4) (2005) 386-393.

[620] A.H. Goli, M. Barzegar, M.A. Sahari, Antioxidant activity and total phenolic compounds of pistachio (*Pistachia vera*) hull extracts, Food Chem 92(3) (2005) 521-525.

[621] R. Congiu, D. Falconieri, B. Marongiu, A. Piras, S. Porcedda, Extraction and isolation of *Pistacia lentiscus* L. essential oil by supercritical CO2, Flavour Frag J 17(4) (2002) 239-244.

[622] A. Sheibani, H.S. Ghaziaskar, Pressurized fluid extraction of pistachio oil using a modified supercritical fluid extractor and factorial design for optimization, LWT - Food Science and Technology 41(8) (2008) 1472-1477.

[623] L.A. Follegatti-Romero, C.R. Piantino, R. Grimaldi, F.A. Cabral, Supercritical CO_2 extraction of omega-3 rich oil from Sacha inchi (*Plukenetia volubilis* L.) seeds, The Journal of Supercritical Fluids 49(3) (2009) 323-329.

[624] A. Femenia, M. García-Marín, S. Simal, C. Rosselló, M. Blasco, Effects of supercritical carbon dioxide (SC-CO_2) oil extraction on the cell wall composition of almond fruits, J Agr Food Chem 49(12) (2001) 5828-5834.

[625] İ.H. Adil, M.E. Yener, A. Bayındırlı, Extraction of total phenolics of sour cherry pomace by high pressure solvent and subcritical Fluid and determination of the antioxidant activities of the extracts, Separation Science and Technology 43(5) (2008) 1091-1110.

[626] A.T. Serra, I.J. Seabra, M.E.M. Braga, M.R. Bronze, H.C. de Sousa, C.M.M. Duarte, Processing cherries (*Prunus avium*) using supercritical fluid technology. Part 1: Recovery of extract fractions rich in bioactive compounds, The Journal of Supercritical Fluids 55(1) (2010) 184-191.

[627] G. Bernardo-Gil, C. Oneto, P. Antunes, M.F. Rodrigues, J.M. Empis, Extraction of lipids from cherry seed oil using supercritical carbon dioxide, Eur Food Res Technol 212(2) (2001) 170-174.

[628] N. Mezzomo, J. Martínez, S.R.S. Ferreira, Supercritical fluid extraction of peach (*Prunus persica*) almond oil: Kinetics, mathematical modeling and scale-up, Journal of Supercritical Fluids 51(1) (2009) 10-16.

[629] Y. Sánchez-Vicente, A. Cabañas, J.A.R. Renuncio, C. Pando, Supercritical fluid extraction of peach (*Prunus persica*) seed oil using carbon dioxide and ethanol, The Journal of Supercritical Fluids 49(2) (2009) 167-173.

[630] N. Mezzomo, B.R. Mileo, M.T. Friedrich, J. Martínez, S.R.S. Ferreira, Supercritical fluid extraction of peach (*Prunus persica*) almond oil: Process yield and extract composition, Bioresource Technol 101(14) (2010) 5622-5632.

[631] L. Leo, L. Rescio, L. Ciurlia, G. Zacheo, Supercritical carbon dioxide extraction of oil and α-tocopherol from almond seeds, J Sci Food Agr 85(13) (2005) 2167-2174.

[632] E. Riera, A. Blanco, J. García, J. Benedito, A. Mulet, J.A. Gallego-Juárez, M. Blasco, High-power ultrasonic system for the enhancement of mass transfer in supercritical CO2 extraction processes, Ultrasonics 50(2) (2010) 306-309.

[633] P.M. Moura, G.H.C. Prado, M.A.A. Meireles, C.G. Pereira, Supercritical fluid extraction from guava (*Psidium guajava*) leaves: Global yield, composition and kinetic data, The Journal of Supercritical Fluids 62 (2012) 116-122.

[634] X. Wang, C. Li, Y. Wang, T.-X. Cai, *n*-Heptane isomerization over mesoporous MoOx and Ni–MoOx catalysts, Catalysis Today 93–95 (2004) 135-140.

[635] Y. Lu, B. Zhu, K. Wu, Z. Gou, L. Li, G.G. Chen, L. Cui, N. Liang, Analysis of operation conditions for a pilot-scale supercritical CO_2 extraction of diterpenoid from *Pteris semipinnata* L, Asia-Pacific Journal of Chemical Engineering 7(5) (2012) 777-782.

[636] L. Wang, B. Yang, X. Du, C. Yi, Optimisation of supercritical fluid extraction of flavonoids from *Pueraria lobata*, Food Chem 108(2) (2008) 737-741.

[637] L. Wang, B.A.O. Yang, X. Du, Investigation of supercritical fluid extraction of puerarin from *Pueraria lobata*, Journal of Food Process Engineering 32(5) (2009) 682-691.

[638] G. Liu, X. Xu, Q. Hao, Y. Gao, Supercritical CO_2 extraction optimization of pomegranate (*Punica granatum* L.) seed oil using response surface methodology, LWT - Food Science and Technology 42(9) (2009) 1491-1495.

[639] I.M.G. Lopes, M.G. Bernardo-Gil, Characterisation of acorn oils extracted by hexane and by supercritical carbon dioxide, Eur J Lipid Sci Tech 107(1) (2005) 12-19.

[640] V. Castola, B. Marongiu, A. Bighelli, C. Floris, A. Laï, J. Casanova, Extractives of cork (*Quercus suber* L.): chemical composition of dichloromethane and supercritical CO_2 extracts, Industrial Crops and Products 21(1) (2005) 65-69.

[641] P. Iheozor-Ejiofor, E.S. Dey, Extraction of rosavin from *Rhodiola rosea* root using supercritical carbon dioxide with water, The Journal of Supercritical Fluids 50(1) (2009) 29-32.

[642] J.M. Del Valle, S. Bello, J. Thiel, A. Allen, L. Chordia, Comparison of conventional and supercritical CO_2-extracted rosehip oil, Braz J Chem Eng 17(3) (2000) 335-348.

[643] J.M. del Valle, E.L. Uquiche, Particle size effects on supercritical CO_2 extraction of oil-containing seeds, Journal of the American Oil Chemists' Society 79(12) (2002) 1261-1266.

[644] J.M. del Valle, O. Rivera, M. Mattea, L. Ruetsch, J. Daghero, A. Flores, Supercritical CO_2 processing of pretreated rosehip seeds: effect of process scale on oil extraction kinetics, The Journal of Supercritical Fluids 31(2) (2004) 159-174.

[645] K. Szentmihályi, P. Vinkler, B. Lakatos, V. Illés, M. Then, Rose hip (*Rosa canina* L.) oil obtained from waste hip seeds by different extraction methods, Bioresource Technol 82(2) (2002) 195-201.

[646] R. Eggers, A. Ambrogi, J. Von Schnitzler, Special features of SCF solid extraction of natural products: Deoiling of wheat gluten and extraction of rose hip oil, Braz J Chem Eng 17(3) (2000) 329-334.

[647] E. Reverchon, A. Kaziunas, C. Marrone, Supercritical CO_2 extraction of hiprose seed oil: experiments and mathematical modelling, Chem Eng Sci 55(12) (2000) 2195-2201.

[648] R.N. Carvalho Jr, L.S. Moura, P.T.V. Rosa, M.A.A. Meireles, Supercritical fluid extraction from rosemary (*Rosmarinus officinalis*): Kinetic data, extract's global yield, composition, and antioxidant activity, The Journal of Supercritical Fluids 35(3) (2005) 197-204.

[649] E. Langa, G.D. Porta, A.M.F. Palavra, J.S. Urieta, A.M. Mainar, Supercritical fluid extraction of Spanish sage essential oil: Optimization of the process parameters and modelling, The Journal of Supercritical Fluids 49(2) (2009) 174-181.

[650] L. Wang, Y. Song, Y. Cheng, X. Liu, Orthogonal array design for the optimization of supercritical fluid extraction of tanshinones from Danshen, J Sep Sci 31(2) (2008) 321-328.

[651] E. Daukšas, P.R. Venskutonis, V. Povilaityte, B. Sivik, Rapid screening of antioxidant activity of sage (*Salvia officinalis* L.) extracts obtained by supercritical carbon dioxide at different extraction conditions, Food / Nahrung 45(5) (2001) 338-341.

[652] B. Marongiu, A. Piras, S. Porcedda, E. Tuveri, Extraction of *Santalum album* and *Boswellia carterii* Birdw. volatile oil by supercritical carbon dioxide: influence of some process parameters, Flavour Frag J 21(4) (2006) 718-724.

[653] C. Grosso, A.C. Figueiredo, J. Burillo, A.M. Mainar, J.S. Urieta, J.G. Barroso, J.A. Coelho, A.M.F. Palavra, Supercritical fluid extraction of the volatile oil from *Santolina chamaecyparissus*, J Sep Sci 32(18) (2009) 3215-3222.

[654] G. Cherchi, D. Deidda, B.D. Gioannis, B. Marongiu, R. Pompei, S. Porcedda, Extraction of *Santolina insularis* essential oil by supercritical carbon dioxide: influence of some process parameters and biological activity, Flavour Frag J 16(1) (2001) 35-43.

[655] M. Khajeh, Optimization of process variables for essential oil components from *Satureja hortensis* by supercritical fluid extraction using Box-Behnken experimental design, The Journal of Supercritical Fluids 55(3) (2011) 944-948.

[656] S. Plánder, L. Gontaru, B. Blazics, K. Veres, Á. Kéry, S. Kareth, B. Simándi, Major antioxidant constituents from *Satureja hortensis* L. extracts obtained with different solvents, Eur J Lipid Sci Tech 114(7) (2012) 772-779.

[657] C. Grosso, A.C. Oliveira, A.M. Mainar, J.S. Urieta, J.G. Barroso, A.M.F. Palavra, Antioxidant activities of the supercritical and conventional*Satureja montana*extracts, J Food Sci 74(9) (2009) C713-C717.

[658] B. Marongiu, A.P.S. Porcedda, R. Casu, P. Pierucci, Chemical composition of the oil and supercritical CO_2 extract of *Schinus molle* L, Flavour Frag J 19(6) (2004) 554-558.

[659] L. Wang, Y. Chen, Y. Song, Y. Chen, X. Liu, GC-MS of volatile components of *Schisandra chinensis* obtained by supercritical fluid and conventional extraction, J Sep Sci 31(18) (2008) 3238-3245.

[660] Y. Chang, B. Liu, B. Shen, Orthogonal array design for the optimization of supercritical fluid extraction of baicalin from roots of *Scutellaria baicalensis* Georgi, J Sep Sci 30(10) (2007) 1568-1574.

[661] Q. Hu, J. Xu, S. Chen, F. Yang, Antioxidant activity of extracts of black sesame seed (*Sesamum indicum* L.) by supercritical carbon dioxide extraction, J Agr Food Chem 52(4) (2004) 943-947.

[662] B. Marongiu, A. Piras, S. Porcedda, E. Tuveri, A. Maxia, Isolation of *Seseli bocconi* Guss., subsp. praecox Gamisans (Apiaceae) volatile oil by supercritical carbon dioxide extraction, Natural Product Research 20(9) (2006) 820-826.

[663] M. Hadolin, M. Skerget, Z.e. Knez, D. Bauman, High pressure extraction of vitamin E-rich oil from *Silybum marianum*, Food Chem 74(3) (2001) 355-364.

[664] U. Salgin, A. Çalimli, B. Zühtü Uysal, Supercritical fluid extraction of jojoba oil, Journal of the American Oil Chemists' Society 81(3) (2004) 293-296.

[665] B. Liu, H. Jiang, B. Shen, Y. Chang, Supercritical fluid extraction of sinomenine from *Sinomenium acutum* (Thumb) Rehd et Wils, J Chromatogr A 1075(1–2) (2005) 213-215.

[666] J.Y. Ling, G.Y. Zhang, Z.J. Cui, C.K. Zhang, Supercritical fluid extraction of quinolizidine alkaloids from *Sophora flavescens* Ait. and purification by high-speed counter-current chromatography, J Chromatogr A 1145(1–2) (2007) 123-127.

[667] A.M.A. Dias, P. Santos, I.J. Seabra, R.N.C. Júnior, M.E.M. Braga, H.C. de Sousa, Spilanthol from *Spilanthes acmella* flowers, leaves and stems obtained by selective supercritical carbon dioxide extraction, The Journal of Supercritical Fluids 61 (2012) 62-70.

[668] A. Erkucuk, I.H. Akgun, O. Yesil-Celiktas, Supercritical CO_2 extraction of glycosides from *Stevia rebaudiana* leaves: Identification and optimization, The Journal of Supercritical Fluids 51(1) (2009) 29-35.

[669] S.K. Yoda, M.O.M. Marques, A.J. Petenate, M.A.A. Meireles, Supercritical fluid extraction from *Stevia rebaudiana* Bertoni using CO_2 and CO_2+water: extraction kinetics and identification of extracted components, J Food Eng 57(2) (2003) 125-134.

[670] L. Ruetsch, J. Daghero, M. Mattea, Supercritical extraction of solid matrices. Model formulation and experiments, Latin American Applied Research 33(2) (2003) 103-107.

[671] Y. Gao, B. Nagy, X. Liu, B. Simándi, Q. Wang, Supercritical CO_2 extraction of lutein esters from marigold (*Tagetes erecta* L.) enhanced by ultrasound, The Journal of Supercritical Fluids 49(3) (2009) 345-350.

[672] B. Marongiu, A. Piras, S. Porcedda, E. Tuveri, S. Laconi, D. Deidda, A. Maxia, Chemical and biological comparisons on supercritical extracts of *Tanacetum cinerariifolium* (Trevir) Sch. Bip. with three related species of *chrysanthemums* of Sardinia (Italy), Natural Product Research 23(2) (2009) 190-199.

[673] M. Kaplan, M.R. Simmonds, G. Davidson, Comparison of supercritical fluid and solvent extraction of feverfew (*Tanacetum parthenium*), Turkish Journal of Chemistry 26(4) (2002) 473-480.

[674] B. Simándi, S.T. Kristo, Á. Kéry, L.K. Selmeczi, I. Kmecz, S. Kemény, Supercritical fluid extraction of dandelion leaves, The Journal of Supercritical Fluids 23(2) (2002) 135-142.

[675] A.A. de Azevedo, U. Kopcak, R. Mohamed, Extraction of fat from fermented Cupuaçu seeds with supercritical solvents, Journal of Supercritical Fluids 27(2) (2003) 223-237.

[676] S. Sonsuzer, S. Sahin, L. Yilmaz, Optimization of supercritical CO_2 extraction of *Thymbra spicata* oil, The Journal of Supercritical Fluids 30(2) (2004) 189-199.

[677] Z. Zeković, Ž. Lepojević, A. Tolić, Modeling of the thyme-supercritical carbon dioxide extraction system. I. The influence of carbon dioxide flow rate and grinding degree of thyme, Separation Science and Technology 36(15) (2001) 3459-3472.

[678] P.S. Slobodan, I. Jasna, M. Stoja, I. Z., Comparative analyses of diffusion coefficients for different extraction processes from thyme, J Serb Chem Soc 7(6) (2012) 799-813.

[679] R.F. Rodrigues, A.K. Tashima, R.M.S. Pereira, R.S. Mohamed, F.A. Cabral, Coumarin solubility and extraction from emburana (*Torresea cearensis*) seeds with supercritical carbon dioxide, Journal of Supercritical Fluids 43(3) (2008) 375-382.

[680] S.M. Ghoreishi, E. Bataghva, A.A. Dadkhah, Response surface optimization of essential oil and diosgenin extraction from *Tribulus terrestris* via supercritical fluid technology, Chem. Eng. Technol. 35(1) (2012) 133-141.

[681] B. Klejdus, L. Lojková, O. Lapčík, R. Koblovská, J. Moravcová, V. Kubáň, Supercritical fluid extraction of isoflavones from biological samples with ultra-fast high-performance liquid chromatography/mass spectrometry, J Sep Sci 28(12) (2005) 1334-1346.

[682] T. Tapia, F. Perich, F. Pardo, G. Palma, A. Quiroz, Identification of volatiles from differently aged red clover (*Trifolium pratense*) root extracts and behavioural responses of clover root borer (*Hylastinus obscurus*) (Marsham) (Coleoptera: Scolytidae) to them, Biochemical Systematics and Ecology 35(2) (2007) 61-67.

[683] R. Yang, H. Wang, N. Jing, C. Ding, Y. Suo, J. You, *Trigonella foenum-graecum* L. seed oil obtained by supercritical CO_2 extraction, Journal of the American Oil Chemists' Society 89(12) (2012) 2269-2278.

[684] H. Li, S. Li, Y. Zhang, H. Duan, New supercritical fluid extraction treatment method for determination of tripterine in *Tripterygium wilfordii* Hook. F, Journal of Liquid Chromatography & Related Technologies 31(10) (2008) 1422-1433.

[685] G.-W. Jung, H.-M. Kang, B.-S. Chun, Characterization of wheat bran oil obtained by supercritical carbon dioxide and hexane extraction, Journal of Industrial and Engineering Chemistry 18(1) (2012) 360-363.

[686] M.O. Punín Crespo, M.A. Lage Yusty, Comparison of supercritical fluid extraction and Soxhlet extraction for the determination of aliphatic hydrocarbons in seaweed samples, Ecotoxicology and Environmental Safety 64(3) (2006) 400-405.

[687] D. Shohet, R.B.H. Wills, Characteristics of extracted valerenic acids from valerian (*Valeriana officinalis*) root by supercritical fluid extraction using carbon Dioxide, International Journal of Food Properties 9(2) (2006) 325-329.

[688] I. Zizovic, M. Stamenić, J. Ivanović, A. Orlović, M. Ristić, S. Djordjević, S.D. Petrović, D. Skala, Supercritical carbon dioxide extraction of sesquiterpenes from valerian root, The Journal of Supercritical Fluids 43(2) (2007) 249-258.

[689] A. Safaralie, S. Fatemi, A. Salimi, Experimental design on supercritical extraction of essential oil from valerian roots and study of optimal conditions, Food Bioprod Process 88(2–3) (2010) 312-318.

[690] B. Huang, L. Qin, Q. Chu, Q. Zhang, L. Gao, H. Zheng, Comparison of headspace SPME with hydrodistillation and SFE for analysis of the volatile components of the roots of *Valeriana officinalis* var. *latifolia*, Chromatographia 69(5) (2008) 489.

[691] J.W. King, A. Mohamed, S.L. Taylor, T. Mebrahtu, C. Paul, Supercritical fluid extraction of *Vernonia galamensis* seeds, Industrial Crops and Products 14(3) (2001) 241-249.

[692] J. Martinez, P.T.V. Rosa, C. Menut, A. Leydet, P. Brat, D. Pallet, M.A.A. Meireles, Valorization of Brazilian vetiver (*Vetiveria zizanioides* (L.) Nash ex Small) oil, J Agr Food Chem 52(21) (2004) 6578-6584.

[693] L.T. Danh, P. Truong, R. Mammucari, N. Foster, Extraction of vetiver essential oil by ethanol-modified supercritical carbon dioxide, Chem Eng J 165(1) (2010) 26-34.

[694] L.T. Danh, R. Mammucari, P. Truong, N. Foster, Response surface method applied to supercritical carbon dioxide extraction of *Vetiveria zizanioides* essential oil, Chem Eng J 155(3) (2009) 617-626.

[695] T.M. Takeuchi, P.F. Leal, R. Favareto, L. Cardozo-Filho, M.L. Corazza, P.T.V. Rosa, M.A.A. Meireles, Study of the phase equilibrium formed inside the flash tank used at the separation step of a supercritical fluid extraction unit, The Journal of Supercritical Fluids 43(3) (2008) 447-459.

[696] E. Talansier, M.E.M. Braga, P.T.V. Rosa, D. Paolucci-Jeanjean, M.A.A. Meireles, Supercritical fluid extraction of vetiver roots: A study of SFE kinetics, The Journal of Supercritical Fluids 47(2) (2008) 200-208.

[697] D. Cossuta, B. Simándi, E. Vági, J. Hohmann, A. Prechl, É. Lemberkovics, Á. Kéry, T. Keve, Supercritical fluid extraction of *Vitex agnus* castus fruit, The Journal of Supercritical Fluids 47(2) (2008) 188-194.

[698] L. Arce, A.G. Lista, A. Ríos, M. Valcárcel, Screening of polyphenols in grape marc by online supercritical fluid extraction-flow through sensor, Analytical Letters 34(9) (2001) 1461-1476.

[699] M.C. Pascual-Martí, A. Salvador, A. Chafer, A. Berna, Supercritical fluid extraction of resveratrol from grape skin of *Vitis vinifera* and determination by HPLC, Talanta 54(4) (2001) 735-740.

[700] L. dos Santos Freitas, J.V. de Oliveira, C. Dariva, R.A. Jacques, E.B. Caramão, Extraction of grape seed oil using compressed carbon dioxide and propane: Extraction yields and characterization of free glycerol compounds, J Agr Food Chem 56(8) (2008) 2558-2564.

[701] T.H.J. Beveridge, B. Girard, T. Kopp, J.C.G. Drover, Yield and composition of grape seed oils extracted by supercritical carbon dioxide and petroleum ether: Varietal effects, J Agr Food Chem 53(5) (2005) 1799-1804.

[702] L. Fiori, D. de Faveri, A.A. Casazza, P. Perego, Grape by-products: extraction of polyphenolic compounds using supercritical CO_2 and liquid organic solvent - a preliminary investigation, Cyta-J Food 7(3) (2009) 163-171.

[703] S. Zhang, Y.-G. Zu, Y.-J. Fu, M. Luo, W. Liu, J. Li, T. Efferth, Supercritical carbon dioxide extraction of seed oil from yellow horn (*Xanthoceras sorbifolia* Bunge.) and its anti-oxidant activity, Bioresource Technol 101(7) (2010) 2537-2544.

[704] L. Xia, J. You, G. Li, Z. Sun, Y. Suo, Compositional and antioxidant activity analysis of *Zanthoxylum bungeanum* seed oil obtained by supercritical CO_2 fluid extraction, Journal of the American Oil Chemists' Society 88(1) (2011) 23-32.

[705] H. Ebrahimzadeh, Y. Yamini, F. Sefidkon, M. Chaloosi, S.M. Pourmortazavi, Chemical composition of the essential oil and supercritical CO_2 extracts of *Zataria multiflora* Boiss, Food Chem 83(3) (2003) 357-361.

[706] S. Rebolleda, N. Rubio, S. Beltrán, M.T. Sanz, M.L. González-Sanjosé, Supercritical fluid extraction of corn germ oil: Study of the influence of process parameters on the extraction yield and oil quality, Journal of Supercritical Fluids 72 (2012) 270-277.

[707] Y. Zhannan, L. Shiqiong, P. Quancai, Z. Chao, Y. Zhengwen, GC-MS analysis of the essential oil of coral ginger (*Zingiber corallinum* Hance) rhizome obtained by supercritical fluid extraction and steam distillation extraction, Chromatographia 69(7) (2009) 785.

3 PRELIMINARY SFE & CHARACTERIZATION OF EXTRACTS

This chapter is based on a published article on SFE of Eucalyptus globulus deciduous bark [1]. *In brief, the extraction of Eucalyptus globulus deciduous bark with supercritical carbon dioxide was carried out at several pressures and temperatures in order to analyze their preliminary effect upon extraction yield and composition of final extracts. These were characterized in detail by GC-MS to determine the concentration of the most important families of compounds found, namely fatty acids, aliphatic alcohols, sterols and triterpenoids. Special attention is devoted to the triterpenic acids (TTA). The results are compared with those obtained by Soxhlet extraction with dichloromethane, and discussed taking into account theoretical calculations.*

CHAPTER OUTLINE

3.1 INTRODUCTION

In the last decade, supercritical fluid extraction (SFE) with carbon dioxide has been researched with very encouraging success to obtain crude extracts from vegetable biomass. In general, this high-pressure technology deals firstly with a combination of the operating pressure (P) and temperature (T) so that an optimized extraction yield (high and/or selective) is achieved within the supercritical state window. For this, the density, viscosity, and polarity of the solvent may be manipulated with advantage, as well as diffusivities and solubility. Recent reviews [2-4] report the great activity on the field in terms of experimental and modeling work, and the large number of vegetable species that have been studied with this separation technology.

Since SFE is an emergent separation technology in an industrial panorama still dominated by extractions with organic solvents (in particular hexane and dichloromethane), its achievements are typically contrasted with the existing methods. Accordingly, Soxhlet extractions are common practice to analyze SFE results, and several works report them [1, 5-23]. In general, given the range of operating conditions that SFE experiments may cover, a typical situation consists in the distribution of SFE yield results below, nearby or even greater than those achieved by Soxhlet [10, 15, 22]. Contrarily to Soxhlet extractions, whose results are relatively unalterable for a fixed matrix and solvent, the supercritical solvent power is always function of, at least, the chosen pressure, temperature, and cosolvent content. Taking this into account, some of the works that led to yields lower than Soxhlet extraction may evidence a non-optimized choice of operating conditions [5, 7, 9, 12]. On the other hand, even after optimization, Soxhlet yield results may prevail higher than SFE values [6, 16, 24]. Lab equipment limitations play a significant role in SFE results, particularly yields. Nevertheless, as referred before, yield is not the only variable to consider, and it is worth noting that supercritical extracts can exhibit much higher concentrations of target compounds [6, 14] despite lower extraction yields. For this reason, carefulness is recommended when comparing SFE with conventional extraction technologies.

In this chapter, the SFE of *E. globulus* bark, a vegetable waste of the Portuguese pulp and paper industry, is presented in detail. Several assays were carried out with carbon dioxide at 100, 140 and 200 bar, and 40, 50 and 60 °C, and the extracts were analyzed by gas chromatography – mass spectrometry (GC–MS). The results are compared with those obtained by Soxhlet with dichloromethane, and the influence of the operating conditions upon the global yield and the individual yields of the triterpenic acids (TTA) are discussed in detail.

3.2 EXPERIMENTAL SECTION

3.2.1 MATERIALS

The deciduous bark was both peeled from the *E. globulus* trees and collected from the ground near to the trees in a clone plantation located in the district of Aveiro, Portugal. Deciduous bark from *E. globulus* was used in this work since its composition is roughly the same as the external bark and is available in larger quantities in the clone plantation. The bark was milled and then dried in an oven at 40 ºC during approximately 72 h, reaching final moisture content between 2 and 5 %. The bark was stored in hermetically sealed bags until use. CO_2 was purchased from Praxair, Portugal. Other reagents were analytical grade existing in the lab.

3.2.2 SOXHLET EXTRACTION

For comparison purposes, an extract of *E. globulus* deciduous bark was obtained by Soxhlet extraction. An amount of ~27 g of deciduous bark was placed inside the Soxhlet apparatus and treated with 300 mL of analytical grade dichloromethane for 7 h. At the end the solvent was evaporated to dryness and the extract was weighed and analyzed by GC-MS.

3.2.3 SUPERCRITICAL FLUID EXTRACTION

Supercritical extraction experiments were performed in a 0.5 L capacity Spe-ed™ apparatus (Applied Separations), whose flowsheet is shown in Figure 3.1 [24-25]. Overall, the liquid CO_2 is pressurized by a cooled liquid pump to the desired extraction pressure, followed by a heating stage where it is heated to the extraction temperature. After attaining the supercritical state, the solvent flows upwards through the extractor where the biomass was previously placed. The effluent is then depressurized through a heated back pressure regulator valve (BPR), and bubbled in a trap containing ethanol to capture the extract for subsequent yield quantification and characterization. Finally, the spent CO_2 is vented to the atmosphere. Regarding the SFE assays with modifiers, the addition of cosolvent (ethanol) is accomplished by a liquid pump (LabAlliance Model 1500) coupled to the CO_2 line between the mass flow meter and the heating vessel. The total mass of extract was determined gravimetrically.

A constant CO_2 mass flow rate of 6 g min^{-1} was used in all extractions during 6 h, totalizing 2.2 kg of spent carbon dioxide. Table 3.1 lists the remaining experimental conditions, specifically CO_2 temperature, T, pressure, P, and mass of dry bark used in the extraction.

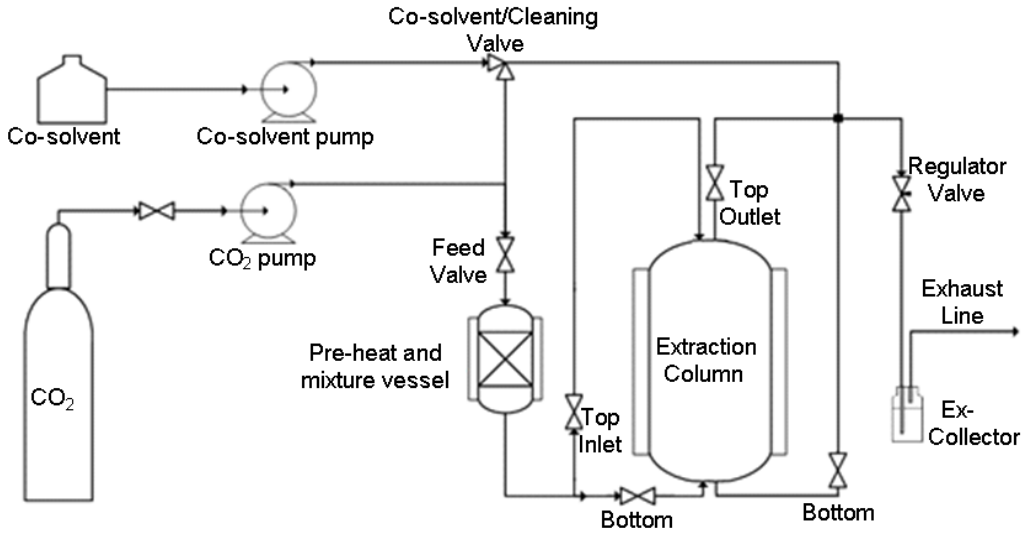

Figure 3.1 – Scheme of the supercritical fluid extraction unit. Retrieved from [24].

Table 3.1 – Experimental conditions employed for the supercritical extraction of *E. globulus* deciduous bark. Solvent flow rate (6 g min^{-1}) and extraction time (6 h) were fixed.

Run	*T* (ºC)	*P* (bar)	Mass of dry bark (g)
3.1	40	100	70.9421
3.2	40	140	78.9590
3.3	40	200	70.5335
3.4	50	100	79.3151
3.5	50	140	75.9773
3.6	50	200	75.9640
3.7	60	100	76.1820
3.8	60	140	76.6288
3.9	60	200	71.9807

3.2.4 ANALYSIS OF EXTRACTS

Extracts were analyzed by GC-MS. About 20 mg of each dried extract were trimethylsilylated according to the literature [26-27]. Two aliquots of each extract were analyzed. Each aliquot was injected in triplicate. The presented results are the average of the concordant values obtained for each run (less than 5 % variation between injections of the same aliquot and between aliquots of the same sample). GC–MS analyses were performed using tetracosane as internal standard, in a Trace Gas Chromatograph 2000 Series equipped with a Finnigan Trace MS mass spectrometer, using helium as carrier gas (35 cm s^{-1}), equipped with a DB-1 J&W capillary column (30 m × 0.32 mm i.d., 0.25 μm film thickness). The chromatographic conditions were as follows: initial temperature: 80 ºC for 5 min; temperature rate: 4 ºC min^{-1}; final temperature: 285 ºC for 10 min; injector temperature: 250 ºC; transfer-line temperature:

290 °C; split ratio: 1:50. The MS was operated in the electron impact mode with electron impact energy of 70 eV and data collected at a rate of 1 scan s^{-1} over a range of m/z of 33–750. The ion source was maintained at 250 °C.

3.3 RESULTS AND DISCUSSION

3.3.1 SOXHLET EXTRACTION

The major compound families present and identified in the dichloromethane extracts of the *E. globulus* deciduous bark are fatty acids (FA), long chain aliphatic alcohols (LCAA), sterols (ST) and triterpenoids (TT). A typical GC-MS chromatogram of the extracts obtained in this essay is illustrated in Figure 3.2, where two distinct sections have been delimited: the first one comprises the retention time (RT) range where FA, LCAA and ST can be found, while the second corresponds to TT region. Among these families, the most valuable components are triterpenoids and particularly triterpenic acids. The total yield of the dichloromethane extract was 1.3 % of the dry weight of bark sample, with the TT fraction representing 53.61 wt.% of the extract. This value is considered the maximum yield that can be obtained from the deciduous bark samples and as the reference value for the SFE extraction studies.

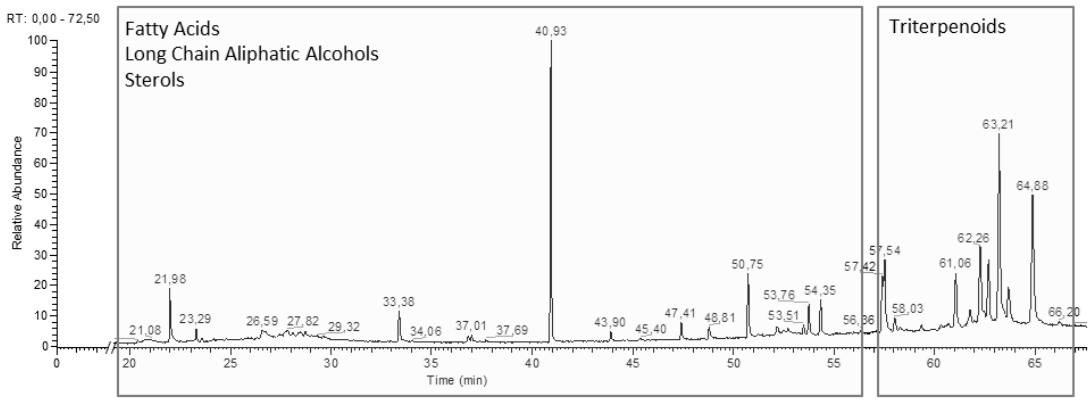

Figure 3.2 – GC-MS chromatogram of a dichloromethane extract of *E. globulus* deciduous bark. The two regions were delimited according to the major families found: fatty acids, long chain aliphatic alcohols and sterols *versus* triterpenoids. Peak at 40.93 min is the internal standard.

Table 3.2 presents the identified compounds from each family found in the Soxhlet extract. Among the triterpenoids of the extract, the triterpenic acids are the main group as they account for nearly 86 wt.% of the total TT fraction. Ursolic and 3-acetylursolic acids are the most abundant molecules of that group, totalizing 52 % of the TT obtained. With regard to the FA fraction, it represents 4 wt.% and comprises eight identified compounds, where palmitic, tetracosanoic and hexacosanoic acids are the most representative ones. Moreover, approximately 7 wt.% of the total extract is constituted of long chain aliphatic alcohols, mostly hexacosan-1-ol and octacosan-1-ol. In turn, sterols fraction weighs practically as much as fatty

acids in the total extract (4.24 % *vs.* 3.92 %) and β-sitosterol represents almost the totality of the mass of this group (4.05 % *vs.* 4.24 %). Finally, 24.10 wt.% of the extract was not detected by GC-MS, and 6.88 wt.% of the detected extract was not identified.

Table 3.2 – Major components and families present in the dichloromethane extract of *E. globulus* bark. Data corresponds to Figure 3.2.

Peak	RT (min)	Compound	Family†	(mg/kg$_{sample}$)	Content (%)
1	28.69	Tetradecanoic acid	FA	21.4	0.16
2	33.38	Palmitic acid	FA	107.6	0.82
3	36.79	Linoleic acid	FA	33.2	0.25
4	36.98	Oleic acid	FA	35.6	0.27
5	37.69	Octadecanoic acid	FA	14.7	0.11
6	43.91	Docosan-1-ol	LCAA	51.8	0.39
7	45.36	Docosanoic acid	FA	36.2	0.28
8	47.44	Tetracosan-1-ol	LCAA	101.6	0.77
9	48.82	Tetracosanoic acid	FA	152.9	1.16
10	50.76	Hexacosan-1-ol	LCAA	444.7	3.39
11	52.19	Hexacosanoic acid	FA	113.3	0.86
12	52.51	Heptacosan-1-ol	LCAA	39.1	0.30
13	53.74	α-tocopherol	-	14.6	0.11
14	54.38	Octacosan-1-ol	LCAA	299.5	2.28
15	56.37	Stigmasterol	ST	24.7	0.19
16	57.46	β-Amirine	TT	384.9	2.93
17	57.57	β-Sitosterol	ST	532.3	4.05
18	58.07	α-Amirine	TT	98.5	0.75
19	61.10	Betulonic acid	TT	665.7	5.07
20	62.32	Oleanolic acid	TT	760.5	5.79
21	62.75	Betulinic acid	TT	691.7	5.27
22	63.31	Ursolic acid	TT	2215.3	16.87
23	63.77	3-Acetyloleanolic acid	TT	482.5	3.67
24	65.01	3-Acetylursolic acid	TT	1742.5	13.27
Totals per family					
Fatty Acids (FA)				514.9	3.92
Long Chain Aliphatic Alcohols (LCAA)				936.7	7.13
Sterols (ST)				557.0	4.24
Triterpenoids (TT)				7634.6	58.13
Other Compounds				325.7	2.48
Not Detected (ND)				3165.3	24.10
Total				13134.4	100

†LCAA= long chain aliphatic alcohols; FA= fatty acids; ST= sterols; TT= triterpenoids

3.3.2 CALCULATION OF EQUILIBRIUM AND KINETIC PROPERTIES

In this section, the estimation of equilibrium and kinetic properties and variables of interest to interpret and understand our experimental results are focused. Despite being a process with

considerable variability concerning its operating conditions and the composition and structure of the raw material under study, the discussion of the SFE of triterpenoids from *E. globulus* bark may be enriched with a theoretical approach to the extraction results. Accordingly, the following properties and variables were selected and estimated: the density (ρ), viscosity (μ), and Hildebrand solubility parameter of CO_2 (δ), the solubilities (y_i^*) of pure ursolic and 3-acetylursolic acids in supercritical CO_2 (these molecules were chosen as key compounds, due to their abundance in the bark), and the convective mass transfer coefficient in the extractor (k_f).

The density of carbon dioxide was determined from the relationship proposed by Pitzer and Schreiber [28], which provides accurate results very near the critical point. This equation is related to the earlier works of Haar-Gallagher-Kell [29] on water. In Table 3.3 the density values for the conditions of this work are listed. In the range of 100 to 200 bar, the densities exhibit large variations at 60 °C (149.8 %) and 50 °C (103.7 %), while just 33.4 % at 40 °C. One may expect that these findings communicate themselves to the SFE results, as it will be discussed in the next section.

Table 3.3 – Density, viscosity and Hildebrand solubility parameter of CO_2 for the SFE conditions studied in this work.

Run	T (°C)	P (bar)	ρ (kg m^3)	μ (10^{-5} Pa s)	δ (MPa$^{0.5}$)
3.1	40	100	629.9	4.8	1.6
3.2	40	140	764.3	6.6	2.0
3.3	40	200	840.1	8.0	2.2
3.4	50	100	385.6	2.9	1.0
3.5	50	140	673.7	5.4	1.7
3.6	50	200	785.5	7.0	2.0
3.7	60	100	290.0	2.4	0.7
3.8	60	140	536.2	4.2	1.4
3.9	60	200	724.5	6.1	1.9

The viscosities of CO_2 were estimated using the empirical equation developed by Altunin and Sakhabetdinov [30]. In this expression, viscosity is a function of density and temperature. The calculated values are also compiled in Table 3.3. In the same range of pressure, the global increments of viscosity found at 40, 50 and 60 °C are 66.7, 141.4 and 154.2 %, respectively, which is similar to the previous density trend. It is worth noting that both properties influence the percolation of CO_2 along bed and the external mass transfer coefficients, with final impact upon SFE results.

The Hildebrand solubility parameters can be used as indicators of mutual solubility, taking into account the rule of thumb that miscibility will occur when their difference is small, e.g. $\delta_1 - \delta_2 < 1$. This principle can be applied reasonably well for solid-liquid and liquid-liquid

behavior, but it is not generally applicable to supercritical fluids. Although carbon dioxide is strictly non-polar, it has a large quadrupole that can interact with other polar liquids and solids. At higher pressures, the proximity between CO_2 and solute molecules is shortened, leading to the creation of substantial dipole (induced or not)–quadrupole interactions that explains the CO_2-philic character of many solutes. From the works of Giddings and coworkers [31-32] the following simple expression may be used to estimate δ as function of the critical pressure of CO_2, P_c, and the reduced density at temperature T and at the normal boiling point, T_{eb}:

$$\delta = 1.25 P_c^{1/2} \left(\rho_r / \rho_{r,eb} \right) \tag{1}$$

The Hildebrand solubility parameters for the SFE conditions of this work are shown in Table 3.3. Once again significant variations are observed at 60 °C (171.4 %) and 50 °C (100.0 %), against a modest jump of 37.5 % at 40 °C, when pressure increases from 100 to 200 bar.

The calculated values of ρ and δ anticipate that the solubilities of the compounds of interest in this study will change significantly with temperature and pressure. In order to interpret such behavior, the solubilities of pure ursolic and 3-acetylursolic acids in supercritical CO_2 will be estimated. From the isofugacity condition, $f_i^{solid}(T,P) = f_i^{SCF}\left(T,P,y_i^*\right)$, the well-known equilibrium relation is obtained [33]:

$$y_i^* = \frac{P_i^{sat}}{\phi_i^{SCF} P} \exp\left[\frac{V_i^{solid}\left(P - P_i^{sat}\right)}{\Re T} \right] \tag{2}$$

where y_i^* is solute solubility, $P_i^{sat}(T)$ is solute vapor pressure, $\phi_i^{SCF}\left(P,T,y_i^*\right)$ is the fugacity coefficient of the solute in supercritical phase, V_i^{solid} is the solute molar volume in solid state, and $\Re$ is the universal gas constant. The necessary molar volumes of the solid triterpenic acids were estimated from their densities with resort to RCS ChemSpider database [34].

The triterpenic acids vapor pressures were calculated using an integrated form of the Clausius-Clapeyron equation proposed by Sepassi et al. [35]:

$$\log P_i^{sat} = -\frac{\Delta S_m (T_m - T)}{2.3 \Re T} + \frac{\Delta C_{p,m}}{2.3 \Re}\left[\frac{T_m - T}{T} - Ln\frac{T_m}{T} \right] - \frac{\Delta S_b (T_b - T)}{2.3 \Re T} + \frac{\Delta C_{p,b}}{2.3 \Re}\left[\frac{T_b - T}{T} - Ln\frac{T_b}{T} \right] \tag{3}$$

which requires for each acid the boiling (T_b) and melting (T_m) temperatures, and the entropy of melting (ΔS_m), entropy of boiling (ΔS_b), heat capacity change on melting $(\Delta C_{p,m})$, and heat capacity change on boiling $(\Delta C_{p,b})$. The values of T_b and T_m, as well as critical constants T_c and P_c, were estimated by the group contribution method proposed by Marrero *et al.* [36]. The remaining latent properties were computed with subsidiary expressions proposed by Sepassi et al. [35]. This method has been selected in view of the accurate results achieved for 815 organic

compounds, ranging over 15 orders of magnitude, for which the absolute error is 0.18 log units, corresponding to a factor of 1.5.

With regard to the fugacity coefficient, the calculation was accomplished with the Peng-Robinson equation of state (EoS) [33]:

$$\ln \phi_i^{SCF} = -\ln(Z-B) - \frac{A}{B\sqrt{8}} \ln \left[\frac{Z+\left(1+\sqrt{2}\right)B}{Z+\left(1-\sqrt{2}\right)B} \right] + Z - 1 \qquad (4)$$

whose nomenclature follows that universally adopted in the literature. The necessary Pitzer acentric factors of the triterpenic acids were estimated from Lee-Kesler correlation using *Aspen Properties* Version 2006.5.

In Table 3.4, the estimated values of all previous properties are given. Moreover, the ratios of solubilities of pure ursolic and 3-acetylursolic acids are listed in Table 3.5 for adjacent pressures at fixed temperature. Two main trends can be detected: (i) y_i^* increments are more important at high temperatures: e.g., in the case of ursolic acid, such ratios are 7.8 and 1.8 at 40 °C, 137.7 and 3.6 at 50 °C, and 241.9 and 9.2 at 60 °C. (ii) The solubility ratios at constant temperature are smoother at higher pressures: at 40 °C this quotient is 7.8 when pressure jumps from 100 to 140 bar, but only 1.8 for the variation 140-200 bar; at 50 °C one gets 137.7 against 3.6, and at 60 °C they are 241.9 and 9.2. In the whole, these results embody and follow those trends presented earlier in Table 3.3 for density, viscosity and Hildebrand parameter.

Table 3.4 – Estimated values of boiling, melting and critical properties of two key triterpenic acids (ursolic and 3-acetylursolic) plus respective acentric factors.

	Ursolic	3-Acetylursolic
M (g mol^{-1})	456.7	498.37
V_i (cm^3 mol^{-1})	415.7	453.4
T_m (K)	565.15	503.27
T_b (K)	801.19	810.9
T_c (K)	949.07	962.67
P_c (bar)	11.9	11.2
V_c (cm^{3}mol^{-1})	1527.0	1648.2
w	0.918	0.968
$\Delta S_m \left(\mathrm{J\,mol^{-1}K^{-1}}\right)$	64.8	68.5
$\Delta S_b \left(\mathrm{J\,mol^{-1}K^{-1}}\right)$	91.2	91.0
$\Delta C_{pm} \left(\mathrm{J\,mol^{-1}K^{-1}}\right)$	64.8	68.5
$\Delta C_{pb} \left(\mathrm{J\,mol^{-1}K^{-1}}\right)$	-120.6	-122.6
$V_{eb} \left(\mathrm{cm^3 mol^{-1}}\right)$	618.7	670.3

The same analysis was performed with respect to the convective mass transfer coefficient, k_f. Taking into account empirical correlations of the type $Sh = \alpha \mathrm{Re}^{\beta} Sc^{\gamma}$, the ratio of k_f values is given by:

$$\frac{(k_\mathrm{f})_{P1}}{(k_\mathrm{f})_{P2}} = \left[\frac{(D_{12})_{P1}}{(D_{12})_{P2}}\right]^{1-\gamma} \left(\frac{\rho_1}{\rho_2}\right)^{\beta-\gamma} \left(\frac{\mu_1}{\mu_2}\right)^{\gamma-\beta} \tag{5}$$

If additionally the Wilke-Chang equation [41, 42] is adopted for the tracer diffusion coefficients, D_{12}, the proportionality $D_{12} \propto T/\mu$ is established and Eq. (5) simplifies to:

$$\frac{(k_\mathrm{f})_{P1}}{(k_\mathrm{f})_{P2}} = \left(\frac{T_1}{T_2}\right)^{1-\gamma} \left(\frac{\rho_1}{\rho_2}\right)^{\beta-\gamma} \left(\frac{\mu_1}{\mu_2}\right)^{2\gamma-\beta-1} \tag{6}$$

These ratios were estimated for isothermal conditions using $\beta = 0.8$ and $\gamma = 1/3$ [2]. These results are listed in Table 3.5. In the whole, they lie between 0.71 and 0.84, and increase with increasing pressure. With respect to temperature impact on these ratios, the values denote a minimum at 50 °C when considering 140/100 pressure step and a decreasing trend with increasing temperature between 200 and 140 bar. Nonetheless, such variations are not comparable, in terms of magnitude, to those found for the solubility ratios.

Table 3.5 – Ratios of convective mass transfer coefficients, solubilities, and mass transfer fluxes (for dilute solutions) computed at adjacent pressures and fixed temperature. Ursolic acid and 3-acetylursolic acid are the key triterpenoids of our SFE selected for the calculation.

$T(°C)$	Property ratio	Ursolic acid		3-Acetylursolic acid	
		$\frac{P_1}{P_2} = \frac{140}{100}$	$\frac{P_1}{P_2} = \frac{200}{140}$	$\frac{P_1}{P_2} = \frac{140}{100}$	$\frac{P_1}{P_2} = \frac{200}{140}$
40	$(k_f)_{P1}/(k_f)_{P2}$	0.77	0.84	0.77	0.84
40	$(y_i^*)_{P1}/(y_i^*)_{P2}$	7.8	1.8	9.7	1.9
40	$(N_i^\infty)_{P1}/(N_i^\infty)_{P2}$	7.3	1.7	9.1	1.7
50	$(k_f)_{P1}/(k_f)_{P2}$	0.64	0.80	0.64	0.80
50	$(y_i^*)_{P1}/(y_i^*)_{P2}$	137.7	3.6	233.3	4.2
50	$(N_i^\infty)_{P1}/(N_i^\infty)_{P2}$	154.0	3.4	260.8	3.9
60	$(k_f)_{P1}/(k_f)_{P2}$	0.71	0.76	0.71	0.76
60	$(y_i^*)_{P1}/(y_i^*)_{P2}$	241.9	9.2	423.4	12.0
60	$(N_i^\infty)_{P1}/(N_i^\infty)_{P2}$	317.6	9.5	555.8	12.3

The product $k_f\,\rho_{CO_2}\,y_i^*$ was also calculated, since it is proportional to the solute flux, N_i, from *Eucalyptus* bark to the supercritical solvent in the case of dilute solutions $\left(N_i^\infty\right)$. Since the external mass transfer flux is $N_i = k_f\left(y_{i,interface} - y_{i,bulk}\right)\rho_{CO_2}/M_{CO_2}$, and $y_{i,bulk} \cong 0$, then the ratio of fluxes at infinite dilution can be estimated by:

$$\frac{\left(N_i^\infty\right)_{P1}}{\left(N_i^\infty\right)_{P2}} = \frac{\left(k_f\,\rho_{CO_2} y_i^*\right)_{P1}}{\left(k_f\,\rho_{CO_2} y_i^*\right)_{P2}} \tag{7}$$

where it was additionally assumed that the interface concentration was equal to the solubility, i.e. $y_{i,interface} \cong y_i^*$.

The computed values for the same triterpenic acids (TTA) at adjacent pressures and constant temperature are shown in Table 3.5 and plotted in Figure 3.3. The graphs point out that if pressure increases from 100 to 140 bar, the fluxes enhance notoriously in comparison to the jump from 140 to 200 bar. Moreover, these leaps are much superior at high pressures, in accordance with previous results for other quantities. Despite the decrease of k_f ratios with rising pressure (see Table 3.5), the solute flux ratios are globally incremented due to the significant enhancement of the solubility ratios.

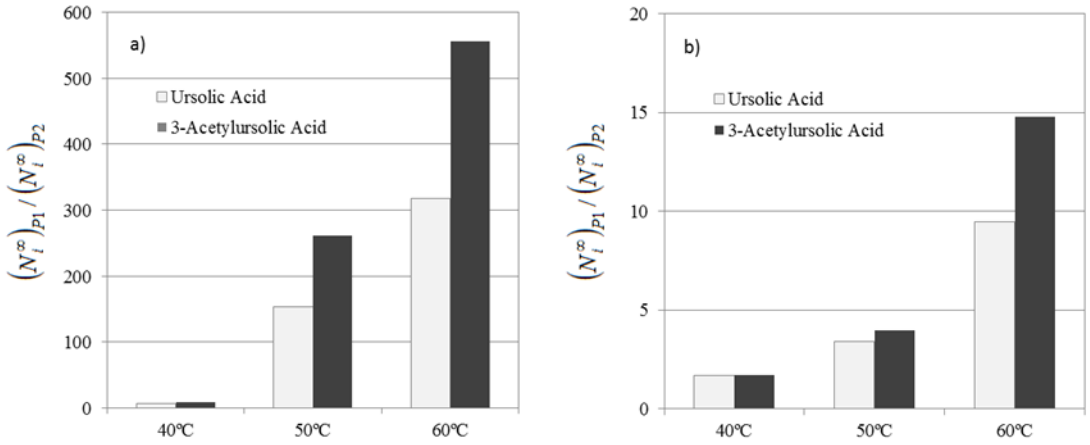

Figure 3.3 – Ratios of the mass transfer fluxes of two key triterpenic acids for the case of dilute solutions under isothermal conditions: $\left(N_i^\infty\right)_{P1}/\left(N_i^\infty\right)_{P2}$. (a) Adjacent pressures: $P_1 = 140$, $P_2 = 100$ bar; (b) Adjacent pressures: $P_1 = 200$, $P_2 = 140$ bar.

3.3.3 SFE OF *Eucaliptus globulus* BARK

The main objective of this work is to study the supercritical fluid extraction of *E. globulus* deciduous bark with CO_2 with particular emphasis on the global yields and on the individual extraction yields of the triterpenic acids of interest, whether acetylated or not.

Experiments were performed at three different temperatures (40, 50 and 60 °C) and pressures (100, 140 and 200 bar) at constant CO_2 mass flow rate (6 g min^{-1}) during 6 h. In Table 3.6 the results of the nine runs carried out in terms of extracted amounts by families and global yield (mg of solutes per 100 mg of bark) are shown. The labels of the nine runs correspond to the operating conditions identified in Table 3.1.

The global yields vary from 0.04 % to 0.77 % (see Table 3.6) when experimental conditions change from 60 °C/100 bar to 60 °C/200 bar, respectively. Such results can be explained by the dependence of the solvent power of CO_2 upon pressure and temperature. By increasing pressure, density increases and increments solubility, as δ values in Table 3.3 and Eq. (1) show. The temperature may impart an opposite effect, due to its positive influence upon solute vapor pressure and negative impact on CO_2 density.

Table 3.6 – Global and individual (per family of compounds) supercritical extraction yields of *E. globulus* deciduous bark. (Exp. conditions in Table 3.1).

Run	Extracted amounts by family (mg/kg_{bark})							Global Yield * (%)
	FA	LCAA	ST	TT total	Others	NI	ND	
3.1	532.8	448.3	236.8	978.3	81.8	133.9	269.2	0.27
3.2	240.6	296.4	245.7	1603.4	130.4	53.2	1771.8	0.43
3.3	568.5	375.4	237.5	2369.9	35.9	289.0	1868.5	0.57
3.4	189.1	131.1	46.6	215.6	68.1	79.4	187.9	0.09
3.5	268.7	314.0	275.8	1682.4	298.2	416.5	876.2	0.41
3.6	425.2	341.1	272.8	2827.1	95.2	231.5	1101.6	0.53
3.7	51.2	32.8	10.5	68.3	1.3	31.5	191.6	0.04
3.8	352.3	386.3	233.6	1015.3	210.1	159.2	270.1	0.26
3.9	603.3	579.6	334.8	2394.9	147.1	427.7	3223.5	0.77
Soxhlet†	514.9	936.7	557.0	7634.6	325.7	-	3165.3	1.31

FA – Fatty acids; LCAA – Long chain aliphatic alcohols; TT total – Total triterpenoids; NI – Nonidentified compounds; ND – Compounds not detected by GC-MS. ***** yield in mg of solutes per 100 mg of bark. †Taken from Table 3.2.

In order to detach the effects of the pressure and temperature upon the extraction yield, a tridimensional representation of the global yields as function of pressure and temperature is shown in Figure 3.4. It can be observed that, at constant temperature, the overall yield always increases with increasing pressure due to the solvent power behavior of CO_2 just described. It is noteworthy that at 100 and 140 bar an increase in temperature leads to a slight reduction of the extracted amounts. This fact may be essentially attributed to the higher sensitivity of CO_2 density to temperature in that range of pressures, which may be observed in Table 3.3. On the other hand, the increase of temperature at 200 bar does not imply the same trend, since a significant yield increase was reached at 60 °C. This is an example of a situation where the effect

of temperature is less direct, since it is the result of a balance between solute vapor pressure and CO_2 density (and so, solute fugacity coefficient).

In what concerns the impact of pressure in the extraction yields at 40 ºC, the results reveal an increase of 115 % from 100 bar to 200 bar. For the extractions carried out at 60 ºC, the extractable mass obtained is 18.3 times greater at 200 bar relatively to the 100 bar experiment.

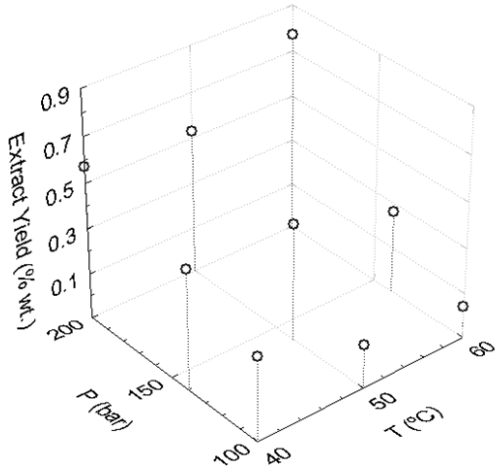

Figure 3.4 – Global yield of SFE of *Eucalyptus globulus* deciduous bark at different temperatures and pressures. (Data from Table 3.5 and exp. conditions in Table 3.1).

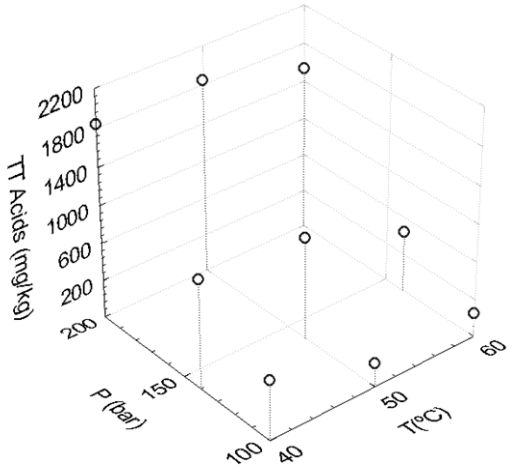

Figure 3.5 – Supercritical fluid extraction yields of TTA (mg / kg of bark) obtained at different conditions.

Once our target compounds are the triterpenic acids, their mass fractions in the extracts are individually listed in Table 3.7. The most abundant TTA in the nine extracts are betulonic, 3-acetyloleanolic and 3-acetylursolic acids. One particular evidence is that though the free TTA content is higher in the deciduous bark (see Table 3.2), their presence in the supercritical extracts was lower than their acetylated forms in all runs. Moreover at 100 bar and 40 ºC (Run 3.1) three of the free TTA were not even extracted, namely oleanoic, betulinic and ursolic acids, which is due to their different polarity in comparison to the remaining triterpenoids.

Moreover, it can be seen from Table 3.7 that the 3-acetylursolic acid is the molecule with the highest mass fraction in all extracts, reaching 21.3 % in Run 3.6 (50 ºC/200 bar). Once it can be easily hydrolyzed to ursolic acid, the potential content of the latter can amount up to 22.0 % prior to any purification steps. Nonetheless, the highest yield obtained (60 ºC/ 200 bar, 0.77 %; Table 3.6) is only 59 % of that achieved by dichloromethane Soxhlet extraction, which means that extraction time may be increased with advantage.

Table 3.7 – Concentrations (wt.%) of the major triterpenic acids obtained in the supercritical extracts of *Eucalyptus globulus* deciduous bark (Exp. conditions in Table 3.1).

Run	Mass fraction in extract (g/100 g of extract)					
	Betulonic	Oleanolic	Betulinic	Ursolic	3-Acetyloleanolic	3-acetylursolic
3.1	2.5	0.0	0.0	0.0	2.7	11.0
3.2	4.6	1.0	0.9	0.4	3.9	11.4
3.3	2.8	2.2	1.4	0.6	5.4	19.8
3.4	1.1	0.5	0.3	0.5	0.9	2.2
3.5	5.0	0.8	0.9	0.2	3.4	11.1
3.6	3.1	2.4	1.5	0.7	5.8	21.3
3.7	2.1	0.9	1.1	0.5	1.5	5.7
3.8	3.3	0.6	0.4	0.3	3.0	9.5
3.9	3.5	1.1	1.2	0.6	2.5	11.0

Considering our interest on the extractable TTA of *E. globulus* bark, the information concerning the overall extraction yields in Figure 3.4 should be combined with Figure 3.5 where their individual yields are plotted. Their removal in the low density region is particularly negligible and corroborates the small global yields given in Table 3.6, which means the extraction is not effective even to remove undesired compounds from the bark matrix. In turn, at higher pressures the overall yield increases and so does the amount of this family of compounds in the extract, a behavior that is in accordance not only with the increasing solvent power of the supercritical CO_2, approximately denoted by Hildebrand solubility parameter, but also with the increasing solubility ratios of the three key triterpenic acids presented in Table 3.5 and discussed in previous section. At this point one should recall that many solubility ratios reach scores of dozens and hundreds due to pressure increments.

Although the highest global yield was obtained at 200 bar and 60 °C (Run 3.9, 0.77 %), the most enriched extract in terms of TTA corresponds to Run 3.6 (200 bar / 50 °C). Figure 3.5 points out that, as predicted, at higher pressure the triterpenic acids were extracted in higher quantities. Hence, despite the overall yield of Run 3.9 is nearly 45.3 % higher than that of Run 3.6, the corresponding improvement on TTA yield of the latter over the former reaches 74.9 %.

In Figure 3.6, the yields of the free and acetylated TTA are graphed simultaneously against pressure and temperature. The graph reveals that the main differences between the nine extracts are mostly due to the quantities of the acetylated molecules rather than to the free ones. This fact can be explained by the higher polarity of free acids in relation to their acetylated forms, particularly if one takes into account their abundances in the bark. In fact, ursolic acid represents 16.87 wt.% of Soxhlet extract and 3-acetylursolic acid accounts for 13.27 wt.% (see Table 3.2), notwithstanding their contribution is changed in the final supercritical extracts (i.e., Table 3.7 and Figure 3.6).

From Figure 3.3 it is possible to justify the trends found in Figure 3.6. The limiting diluted mass flux ratios $\left(N_i^{\infty}\right)$ of 3-acetylursolic acid are always superior to those of ursolic acid, which means that under isothermal conditions the increasing pressure favors the acetylated form preferentially. This prediction reasoning corroborates the trend of the TTA yields patent in Figure 3.6 at fixed temperature.

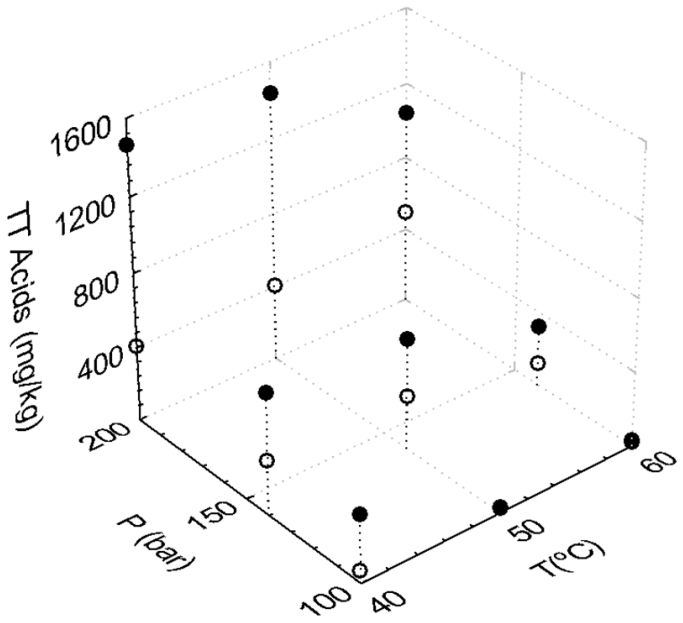

Figure 3.6 – Supercritical fluid extraction yields (mg / kg of bark) of free (filled dots) and acetylated (unfilled dots) TTA obtained at different conditions.

3.3 CONCLUSION

In this work the supercritical fluid extraction of *Eucalyptus globulus* deciduous bark using carbon dioxide at 40, 50 and 60 °C, and 100, 140 and 200 bar has been accomplished. The effect of the operating conditions upon the global extraction yields and on the individual yields of triterpenic acids has been analyzed and these results compared with conventional solvent extraction values.

Summarily, the global yields ranged from 0.04 to 0.77 wt.%, and the ursolic and 3-acetylursolic acids were the triterpenoids found most abundantly. In the region of low densities, most triterpenic acids have been weakly extracted. An important observation was that the acetylated TTA contribution imparted a large effect upon the extraction yields, as they appeared in large concentrations on the extracts independently of their absolute loadings in the bark. In the whole, the best operating conditions to maximize the extraction of triterpenic acids were 200 bar and 40 or 50 °C.

The experimental results are in agreement with predictions accomplished for the solubilities and mass transfer fluxes of ursolic and 3-acetylursolic acids that were chosen as key triterpenic acids in the process.

3.4 REFERENCES

[1] M.M.R. de Melo, E.L.G. Oliveira, A.J.D. Silvestre, C.M. Silva, Supercritical fluid extraction of triterpenic acids from *Eucalyptus globulus* bark, Journal of Supercritical Fluids, 70 (2012) 137-145.

[2] E.L.G. Oliveira, A.J.D. Silvestre, C.M. Silva, Review of kinetic models for supercritical fluid extraction, Chemical Engineering Research and Design, 89 (2011) 1104-1117.

[3] H. Sovová, R.P. Stateva, Supercritical fluid extraction from vegetable materials, Reviews in Chemical Engineering, 27 (2011) 79-156.

[4] O. Doker, U. Salgin, I. Sanal, U. Mehmetoglu, A. Calimli, Modeling of extraction of beta-carotene from apricot bagasse using supercritical CO_2 in packed bed extractor, Journal of Supercritical Fluids, 28 (2004) 11-19.

[5] K.S. Andrade, R.T. Goncalvez, M. Maraschin, R.M. Ribeiro-do-Valle, J. Martinez, S.R.S. Ferreira, Supercritical fluid extraction from spent coffee grounds and coffee husks: Antioxidant activity and effect of operational variables on extract composition, Talanta, 88 (2012) 544-552.

[6] H.M.A. Barbosa, M.M.R. de Melo, M.A. Coimbra, C.P. Passos, C.M. Silva, Optimization of the supercritical fluid coextraction of oil and diterpenes from spent coffee grounds using experimental design and response surface methodology, Journal of Supercritical Fluids, 85 (2014) 165-172.

[7] R.M.A. Domingues, E.L.G. Oliveira, C.S.R. Freire, R.M. Couto, P.C. Simões, C.P. Neto, A.J.D. Silvestre, C.M. Silva, Supercritical fluid extraction of *Eucalyptus globulus* bark – a promising approach for triterpenoids production, International Journal of Molecular Sciences, *13(6),* (2012) *7648-7662*.

[8] D.J.S. Patinha, R.M.A. Domingues, J.J. Villaverde, A.M.S. Silva, C.M. Silva, C.S.R. Freire, C. Pascoal Neto, A.J.D. Silvestre, Lipophilic extractives from the bark of *Eucalyptus grandis x globulus*, a rich source of methyl morolate: Selective extraction with supercritical CO_2, Industrial Crops and Products, 43 (2013) 340-348.

[9] B. Bozan, F. Temelli, Supercritical CO_2 extraction of flaxseed, Journal of the American Oil Chemists Society, 79 (2002) 231-235.

[10] D.S. Ivanov, R.R. Čolović, J.D. Lević, S.A. Sredanović, Optimization of supercritical fluid extraction of linseed oil using RSM, European Journal of Lipid Science and Technology, 114 (2012) 807-815.

[11] L. de Campos, F.V. Leimann, R.C. Pedrosa, S.R.S. Ferreira, Free radical scavenging of grape pomace extracts from Cabernet sauvingnon (*Vitis vinifera*), Bioresource Technology, 99 (2008) 8413-8420.

[12] A. Boszormenyi, S. Szarka, E. Hethelyi, I. Gyurjan, M. Laszlo, B. Simandi, E. Szoke, E. Lemberkovics, Triterpenes in traditional and supercritical-fluid extracts of *Morus alba* leaf and stem bark, Acta Chromatographica, 21 (2009) 659-669.

[13] A. de Lucas, E.M. de la Ossa, J. Rincon, M.A. Blanco, I. Gracia, Supercritical fluid extraction of tocopherol concentrates from olive tree leaves, Journal of Supercritical Fluids, 22 (2002) 221-228.

[14] A. de Lucas, J. Rincón, I. Gracia, Influence of operating variables on yield and quality parameters of olive husk oil extracted with supercritical carbon dioxide, Journal of the American Oil Chemists' Society, 79 (2002) 237-243.

[15] P. Benelli, C.A.S. Riehl, A. Smania, E.F.A. Smania, S.R.S. Ferreira, Bioactive extracts of orange (*Citrus sinensis* L. Osbeck) pomace obtained by SFE and low pressure techniques: Mathematical modeling and extract composition, Journal of Supercritical Fluids, 55 (2010) 132-141.

[16] M.G. Bernardo-Gil, L.M.C. Lopes, Supercritical fluid extraction of *Cucurbita ficifolia* seed oil, European Food Research and Technology, 219 (2004) 593-597.

[17] G. Perretti, E. Miniati, L. Montanari, P. Fantozzi, Improving the value of rice by-products by SFE, Journal of Supercritical Fluids, 26 (2003) 63-71.

[18] C.H. Wang, C.R. Chen, J.J. Wu, L.Y. Wang, C.M.J. Chang, W.J. Ho, Designing supercritical carbon dioxide extraction of rice bran oil that contain oryzanols using response surface methodology, Journal of Separation Science, 31 (2008) 1399-1407.

[19] G. Andrich, S. Balzini, A. Zinnai, V. De Vitis, S. Silvestri, F. Venturi, R. Fiorentini, Supercritical fluid extraction in sunflower seed technology, European Journal of Lipid Science and Technology, 103 (2001) 151-157.

[20] C. Devittori, D. Gumy, A. Kusy, L. Colarow, C. Bertoli, P. Lambelet, Supercritical fluid extraction of oil from millet bran, Journal of the American Oil Chemists' Society, 77 (2000) 573.

[21] M. Arshadi, A.J. Hunt, J.H. Clark, Supercritical fluid extraction (SFE) as an effective tool in reducing auto-oxidation of dried pine sawdust for power generation, RSC Advances, 2 (2012) 1806-1809.

[22] A. Rajaei, M. Barzegar, Y. Yamini, Supercritical fluid extraction of tea seed oil and its comparison with solvent extraction, European Food Research and Technology, 220 (2005) 401-405.

[23] W. Huang, Z. Li, H. Niu, D. Li, J. Zhang, Optimization of operating parameters for supercritical carbon dioxide extraction of lycopene by response surface methodology, Journal of Food Engineering, 89 (2008) 298-302.

[24] R.M.A. Domingues, M.M.R. de Melo, E.L.G. Oliveira, C.P. Neto, A.J.D. Silvestre, C.M. Silva, Optimization of the supercritical fluid extraction of triterpenic acids from *Eucalyptus globulus* bark using experimental design, Journal of Supercritical Fluids, 74 (2013) 105-114.

[25] S.A.O. Santos, J.J. Villaverde, C.M. Silva, C.P. Neto, A.J.D. Silvestre, Supercritical fluid extraction of phenolic compounds from *Eucalyptus globulus* Labill bark, Journal of Supercritical Fluids, 71 (2012) 71-79.

[26] R.M.A. Domingues, G.D.A. Sousa, C.S.R. Freire, A.J.D. Silvestre, C.P. Neto, *Eucalyptus globulus* biomass residues from pulping industry as a source of high value triterpenic compounds, Industrial Crops and Products, 31 (2010) 65-70.

[27] C.S.R. Freire, A.J.D. Silvestre, C.P. Neto, J.A.S. Cavaleiro, Lipophilic extractives of the inner and outer barks of *Eucalyptus globulus*, Holzforschung, 56 (2002) 372–379.

[28] K.S. Pitzer, D.R. Schreiber, Improving equation-of-state accuracy in the critical region - Equations for carbon-dioxide and neopentane as examples, Fluid Phase Equilibria, 41 (1988) 1-17.

[29] J.S. Gallagher, L. Haar, G.S. Kell, An Equation of State for Water, Abstracts of Papers of the American Chemical Society, 181 (1981) 12-Comp.

[30] V.V. Altunin, M. Sakhabetdinov, Viscosity of Liquid and Gaseous Carbon-Dioxide at Temperatures of 220-1300 K and Pressures up to 1200 Bar, Thermal Engineering, 19 (1972) 124-129.

[31] J.C. Giddings, M.N. Myers, L. McLaren, R.A. Keller, High pressure gas chromatography of nonvolatile species. Compressed gas is used to cause migration of intractable solutes, Science, 162 (1968) 67-73.

[32] L. McLaren, M.N. Myers, J.C. Giddings, Dense-gas chromatography of nonvolatile substances of high molecular weight, Science, 159 (1968) 197-199.

[33] J.R. Elliott, C.T. Lira, Introductory Chemical Engineering Thermodynamics, Prentice Hall, New York, 2012.

[34] ChemSpider, in, Royal Society of Chemistry, http://www.chemspider.com, Accessed in February 2012.

[35] K. Sepassi, P.B. Myrdal, S.H. Yalkowsky, Estimating pure-component vapor pressures of complex organic molecules: Part II, Industrial & Engineering Chemistry Research, 45 (2006) 8744-8747.

[36] J. Marrero, R. Gani, Group-contribution based estimation of pure component properties, Fluid Phase Equilibria, 183 (2001) 183-208.

4 EXPERIMENTAL OPTIMIZATION

The material presented in this chapter belong to three distinct publications of the author [1-3]. While the introductory remarks come from non-presented sections of the comprehensive review [1] already reported in Chapter 2, the results and discussion section was built from articles comprising the SFE optimization of spent coffee grounds (SCG) [2] and water hyacinth [3].

CHAPTER OUTLINE

4.1 INTRODUCTION

The accurate phenomenological modeling of processes involving natural biomass is complex and many times impossible to achieve because of the lack of necessary subsidiary data. A trend has been identified since 2000, involving the greater presence of statistical modeling such as design of experiments (DoE) in published articles. The DoE refers to statistical strategies that allow more precise and complete information to be obtained from an experimentally studied phenomenon with minimal number of assays and lowest material costs [4]. It is thus an efficient method that provides instructive data with minimum resources as counterpart.

A clear-cut picture regarding the use of DoE in SFE works is shown in Figure 4.1. Roughly one in five works from our database (547 publications) comprise design of experiments and two thirds of these involve response surface methodology (RSM). In terms of experimental designs types, there is a balance between Box-Behnken (BBD), Central Composite (CCD), Full Factorial and Fractional Factorial Designs, with a slight dominance of Box-Behnken and Central Composite, with 28 % and 26 %, respectively. Concerning the variables to be studied by these techniques, it was with no surprise that results showed pressure and temperature to have been chosen in 94 % and 92 % of the works, respectively. The third most chosen factor is time, which was present in 42 % of the works. Modifier concentration (c_{modifier}), particle diameter (d_{p}) and flow rate (Q) follow the latter with 20 %, 15 % and 13 %, respectively.

In Table 4.1 a selection of SFE works in which DoE was employed is listed. Notwithstanding the general use of the six variables mentioned above, works typically comprise designs with three factors having pressure and temperature as the commonest variables. Concerning the levels of variation, the majority of works applied three degrees of variation for factors, though two and four levels were also found. The number of factors and levels has a direct implication in the number of experiments and at the end plays a role in the DoE typology adopted.

With respect to DoE typologies, orthogonal tests (OT) enable factors assessment to be dealt independently despite having a common (dependent) test of significance [5]. They were initially developed to make DoE more applicable by reducing the number of experiments that full factorial designs require [6]. OT designs are prone to be saturated since the degrees of freedom for all effects are typically equal or close to the number of unique factor-level combinations included in the experiments [7]. In this sense, they allow the maximum number of factor-levels to be tested within the smallest setting of experiments. Application of orthogonal tests may be found in the works of Liu *et al.* with emblica [8], Xie *et al.* with *Patrinia villosa [9]*, and Cao and Ito with grape seed [10], among others that are also listed in Table 4.1.

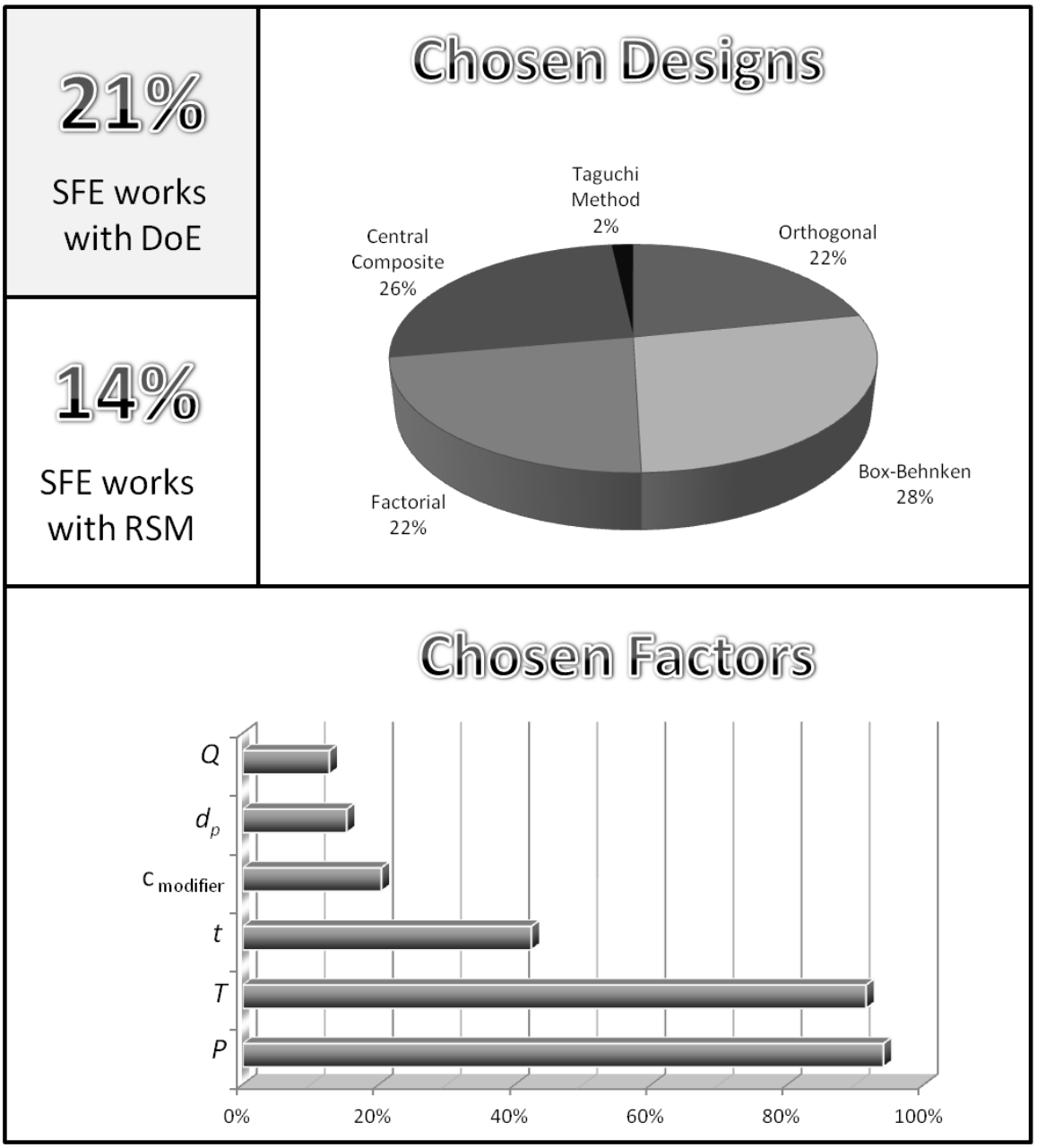

Figure 4.1 – Trends on the use of design of experiments (DoE) and response surface methodology (RSM) in SFE articles within 2000-2013, for a total of 547 publications considered.

Table 4.1 – SFE publications employing design of experiments (DoE) or response surface methodology (RSM) in the period 2000-2013.

Matrix	Variables				Factors	Levels	Runs	Features	Ref.
Alkanna tinctoria	P	T	Q	-	3	3	15	RSM, Box-Behnken	[11]
Allium cepa	P	T	t	-	3	3	17	RSM, Box-Behnken	[12]
Allium sativum	t	T	Solvent to sample ratio	Extractions number	4	3	27	RSM, Box-Behnken	[13]
Aloe vera	P	T	c_{modifier}	Q	4	3	9	Orthogonal array	[14]
Alpinia oxyphylla	P	T	t	-	3	3	15	RSM, Box-Behnken	[15]
Amaranthus paniculatus	P	T	t	d_{p}, w	5	2	67	Full Factorial	[16]
Angelica dahurica	P	T	Q	c_{modifier}	4	3	8	Orthogonal array	[17]
Anoectochilus roxburghii	P	T	c_{modifier}	-	3	3	9	Orthogonal array	[18]
Arbutus unedo	P	T	c_{modifier} .	-	3	3	17	RSM, Box-Behnken	[19]
Artemisia annua	P	T	Q	-	3	2	8	Full Factorial	[20]
Artemisia capillaris	P	Modifier Conc.	-	-	2	3	13	RSM, Central composite	[21]
Artemisia sieberi	P	T	t	c_{modifier}	4	3	9	Orthogonal array	[22]
Atractylode lancea	P	T	t	Q	3	4	9	Orthogonal array	[23]
Brassica napus	P	T	t	-	3	3	17	RSM, Box-Behnken	[24]
Bupleurum falcatum	P	T	t	c_{modifier}	4	3	9	Orthogonal array	[25]
Cajanus cajan	P	T	t	-	3	5	20	RSM, Central composite	[26]
Camellia sinensis	P	T	t	-	3	3	20	RSM, Central composite	[27]
Camellia sinensis	P	T	t	c_{modifier} , Ultrasonic Power	5	4	16	Orthogonal array	[28]
Cannabis sativa	P	T	d_{p}	-	3	3	15	RSM, Box-Behnken	[29]
Capsicum frutescens	P	$v_{\text{superficial}}$	-	-	2	3	12	Central composite	[30]
Capsicum frutescens	P	$v_{\text{superficial}}$	-	-	2	5	11	RSM, Central composite	[31]

Table 4.1 – SFE publications employing design of experiments (DoE) or response surface methodology (RSM) in the period 2000-2013 (cont.)

Catharanthus roseus	P	T	t	c_{modifier}	4	2	19	RSM, Fractional Factorial	[32]
Ceratonia síliqua	P	T	c_{modifier}	d_p	4	3	18	RSM, Central composite	[33]
Citrullus lanatus	P	T	Q	-	3	3	20	RSM, Central composite	[34]
Citrus grandis	P	T	t	-	3	3	17	RSM, Box-Behnken	[35]
Citrus paradisi	P	T	t	-	3	3	15	RSM, Box-Behnken	[36]
Citrus unshiu	P	t	c_{modifier}	-	3	3	15	RSM, Box-Behnken	[37]
Coffea Arabica	P	T	-	-	2	4	16	Full Factorial	[38]
Coffea spp.	P	T	c_{modifier}	-	3	3	15	RSM, Box-Behnken	[2]
Corylus avellana	P	T	Q	-	3	3	15	RSM, Box-Behnken	[39]
Corylus avellana	P	T	$v_{\text{superficial}}$	-	3	3	13	RSM, Fractional Factorial	[40]
Cratoxylum prunifolium	P	T	c_{modifier}	-	3	3	9	Orthogonal array	[41]
Cucurbita maxima	P	T	t	-	3	5	16	RSM, Central composite	[42]
Curcuma longa	P	T	Q	-	3	3	13	RSM, Box-Behnken	[43]
Curcurbita moschata	P	T	-	-	2	3	9	RSM, Central composite	[44]
Cydonia oblonga	P	T	Dynamic t	Static t, Modifier Conc.	5	3	35	RSM, Central composite	[45]
Cynanchum paniculatum	P	T	t	d_{p}	3	4	9	Orthogonal array	[46]
Diplotaenia cachrydifolia	P	T	c_{modifier}	-	3	3	15	RSM, Box-Behnken	[47]
Elaes guineensis	P	T	t	-	3	3	20	RSM, Central composite	[48]
Erythroxylum coca var. *coca*	P	T	c_{modifier}	Modifiers Ratio	4	3	33	RSM, Central composite	[49]
Eucalyptus globulus	Q	T	c_{modifier}	-	3	2	11	RSM, Full factorial	[50]
Eucalyptus globulus	P	T	c_{modifier}	-	3	3	27	RSM, Full factorial	[51]
Eugenia caryophyllata	P	T	d_{p}	-	3	3	9	Orthogonal array	[52]
Fructus Psoraleae	P	T	d_{p}	-	3	3	9	Orthogonal array	[53]
Garcinia mangostana	P	T	t	-	3	3	15	RSM, Box-Behnken	[54]
Ginkgo biloba	P	T	c_{modifier}	-	3	2	4	Orthogonal array	[55]

Table 4.1 – SFE publications employing design of experiments (DoE) or response surface methodology (RSM) in the period 2000-2013 (cont.)

Glycine variety	P	T	t	-	3	3	17	RSM, Box-Behnken	[56]
Gossypium varitety	P	T	t	-	3	3	15	RSM, Central composite	[57]
Helianthus annuus	P	T	Dryness	-	2	3	8	Full Factorial	[58]
Hippophae rhamnoides	P	T	t	-	3	3	17	RSM, Box-Behnken	[59]
Hippophae rhamnoids	P	T	t	-	3	3	17	RSM, Box-Behnken	[60]
Hyssopus officinalis	P	T	Dynamic t	Static t	4	4	25	Orthogonal array	[61]
Illicium verum	P	T	c_{modifier}	-	3	3	17	RSM, Box-Behnken	[62]
Jatropha curcas	P	T	Modifier/solid	-	3	1/3	8	RSM, Fractional Factorial	[63]
Lavandula angustifolia	P	T	t	-	3	3	15	RSM, Box-Behnken	[64]
Lavandula angustifolia	P	T	t	-	3	2	18	RSM, Central composite	[65]
Lavandula hybrida	P	T	t	Q	4	3	31	RSM, Central composite	[66]
Lepidium apetalum	P	T	T	Q	4	3-4	30	RSM, Central composite	[67]
Linum usitatissimum	P	T	Q	-	3	3	15	RSM, Box-Behnken	[68]
Linum usitatissimum	P	T	c_{modifier}		3	3	17	RSM, Box-Behnken	[69]
Linum usitatissimum	P	T	Q	-	3	5	18	RSM, Central composite	[70]
Maydis stigma	P	T	c_{modifier}	-	3	3	17	RSM, Box-Behnken	[71]
Mentha spicata	P	T	d_p	Q	5	4	16	Taguchi method	[72]
Mentha spicata	P	T	Q	-	3	3	20	RSM, Central composite	[73]
Microula sikkimensis	P	T	t	Q	4	3	9	Orthogonal array	[74]
Momordica charantia	P	T	t	-	3	3	15	RSM, Box-Behnken	[75]
Moringa oleifera	P	T	d_{p}	-	3	3	20	RSM, Central composite	[76]
Myrtus communis	P	T	c_{modifier}	-	3	3	16	RSM, Central composite	[77]
Nepeta pérsica	P	T	Dynamic t	Static t	4	5	25	Taguchi method	[78]
Nigella sativa	P	T	t	d_{p} Q, matrix dryness, flow direction	7	2	16	Fractional Factorial	[79]

Table 4.1 – SFE publications employing design of experiments (DoE) or response surface methodology (RSM) in the period 2000-2013 (cont.)

Nigella sativa	P	T	t	-	3	3	27	Full factorial	[80]
Olea europaea	P	T	t	d_p	4	3	26	Orthogonal array	[81]
Olea europaea	P	T	t	d_p	4	2	18	RSM, Full Factorial	[82]
Olea europaea	P	T	Q	-	3	3	15	Box-Behnken	[83]
Ophiopogon japonicas	P	T	t	$c_{modifier}$	4	3	9	RSM, Orthogonal array	[84]
Opuntia dillenii	P	T	t	-	3	4	16	RSM, Orthogonal array	[85]
Origanum majorana	P	T	-	-	2	3	11	RSM, Full Factorial	[86]
Origanum munituflorum	P	$T_{col\ bot}$	$T_{col\ top}$	Packing, $c_{modifier}$	5	2	8	RSM, Fractional Factorial	[87]
Patrinia villosa Juss	P	T	t	$c_{modifier}$	3	4	9	Orthogonal array	[9]
Phyllanthus emblica	P	T	t	$c_{modifier}$	4	3	9	Orthogonal array	[8]
Pistacia vera	P	Packing	$c_{modifier}$	-	3	2/4	26	RSM, Fractional Factorial	[88]
Prunus armeniaca	P	T	Q	$c_{modifier}$	4	3	27	RSM, Box-Behnken	[89]
Prunus armeniaca	P	T	$c_{modifier}$	-	3	5	20	Fractional Factorial	[90]
Prunus avium	P	T	$v_{superficial}$	-	3	3	13	RSM, Fractional Factorial	[91]
Prunus cerasus	P	T	t	Solid/Solvent ratio	4	3	27	RSM, Box-Behnken	[92]
Pueraria lobata	P	T	$c_{modifier}$	-	3	3	17	RSM, Box-Behnken	[93]
Punica granatum	P	T	Q	-	3	5	17	RSM, Central composite	[94]
Rosa Rubiginosa	P	T	t	-	3	3	13	RSM, Fractional Factorial	[95]
Salvia miltiorrhiza	P	T	t	Q	4	3	9	Orthogonal array	[96]
Satureja hortensis	P	T	t	$c_{modifier}$	4	3	10	Fractional factorial	[97]
Satureja hortensis	P	T	$c_{modifier}$		3	3	15	RSM, Box-Behnken	[97]
Scutellaria baicalensis	P	T	t	Modifier	4	3	9	Orthogonal array	[98]
Solanum lycopersicum	P	T	Q	-	3	3	17	RSM, Box-Behnken	[99]
Solanum lycopersicum	P	T	$c_{modifier}$	-	3	5	19	Central composite	[100]

Table 4.1 – SFE publications employing design of experiments (DoE) or response surface methodology (RSM) in the period 2000-2013 (conclusion)

Solanum lycopersicum	P	T	-	-	2	3	9	RSM, Full Factorial	[101]
Solanum lycopersicum	P	T	t	-	2	3	17	RSM, Central composite	[102]
Sophora flavescens	P	T	Q	c_{modifier}	4	3	9	Orthogonal array	[103]
Stevia rebaudiana	P	T	Modifier	-	3	3	15	RSM, Box-Behnken	[104]
Taraxacum officinale	P	T	-	-	2	3	11	RSM, Full Factorial	[105]
Thymbra spicata	P	T	t	-	3	3	15	RSM, Box-Behnken	[106]
Thymus zygis subsp. Sylvestris	P	T	t	-	3	3	13	RSM, Fractional Factorial	[107]
Tribulus terrestres	P	T	t	Q	4	5	31	RSM, Central composite	[108]
Trigonella foenum-graecum	P	T	t	-	3	5	20	RSM, Central composite	[109]
Triticum spp.	P	T	t	-	3	5	23	RSM, Central composite	[110]
Vetiveria zizanioides	P	T	t	-	3	5	19	RSM, Central composite	[111]
Vetiveria zizanioides	P	T	c_{modifier}	-	3	3	17	RSM, Central composite	[112]
Vitex agnus castus	P	T	-	-	2	3	11	Full Factorial	[113]
Vitis labrusca	P	T	c_{modifier}	-	3	4	16	Orthogonal array	[114]
Vitis vinifera	P	T	d_{p}	-	3	2/3	9	Orthogonal array	[10]
Vitis vinifera	ρ	T	Dynamic t	Static t Q, Modifier, c_{modifier} ,$T_{\text{restrictor}}$, T_{trap}, Solvent in trap V_{trap}, Packing	12	2	32	Fractional factorial	[115]
Xanthoceras sorbifolia	P	T	t	-	2	3	20	RSM, Central composite	[116]
Zingiber corallinum	P	T	t	c_{modifier}	4	4	16	Orthogonal array	[117]
Zingiber officinale	P	T	Modifier	-	3	2/3	12	Fractional Factorial	[118]

Central composite designs require at least five levels for each factor, which may be useful to confirm quadratic influences on the response, nevertheless they imply more trials to be carried out [119]. One strong advantage of CCD option is ensuring uniformity of precision within the experimental space, rather than in the central region of the response. This feature ensures protection against bias [120]. Examples of CCD employment in SFE works are provided by Danh *et al.* with vetiver (*Vetiveria zizanioides* L.) [111], Kassama *et al.* with tomato skin (*Solanum lycopersicum* L.) [100], and Mitra *et al.* with pumpkin seed (*Cucurbita maxima*) [42].

Box-Behnken may be preferable to CCD for two reasons: factors need only be varied over three levels and fewer runs are required [119]. The drawbacks of this design are essentially two: quadratic influences adequacy are not checked, and the variance of the response is assumed to be the same as center points variance [119], which is a pertinent issue when the conclusions focus on peripheral areas of experimental space rather than on middle. Table 4.1 presents several works using BBD, as the cases of SFE of flaxseed (*Linum usitatissimum*) from Özkal [68], olive (*Olea europaea* L.) pomace from Stavroulias and Panayiotou [83], spent coffee grounds from Barbosa et al. [2] or *Thymbra spicata* carried out by Sonsuzer *et al.* [106].

DoE arises frequently as part of Response Surface Methodology (RSM), since the latter comprises a package of statistical design and analysis tools implemented to determine how a response is affected by a set of quantitative variables in a specified region [119]. RSM typically involves the fitting of polynomial functions with linear and quadratic terms that have resemblance with the effects and interactions given by the DoE. The difference is that while DoE provides insights on positive and negative influence of each effect or interaction under study, RSM combines all effects according to their statistical significance and provide models (based only on the significant terms) that represent the experimental results within the experimental conditions ranges covered by the regression. In addition, this method provides useful 2D and 3D graphical means to visualize the behavior of the responses and to move easily interpret the results.

The aforesaid methods are worthwhile to optimize the operating conditions of processes towards the identification of maxima and minima in responses [120]. Being an experimental optimization technique, RSM sometimes allows a maximum or a minimum to be found in the margins of the variable values boundaries. In these cases further studies are required to optimize the response. Examples of this happening may be consulted in the works of de Lucas *et al.* [121] with olive (*Olea europaea* L.) husk oil or Özkal et. el [68] with flaxseed (*Linum usitatissimum*) oil. Nonetheless one should remember that apparatus limitations many times delimit the range of study for the chosen factors, specifically in the case of pressure. From the matrices point of view, temperature variations are many times hindered in the upper values in order to avoid the undesired thermal degradation of solutes. Figure 4.2 presents two cases where RSM results identified an inner set of optimized conditions (2A and 2B) and two cases

where further optimization would be necessary to reach and confirm an optimum zone (2C and 2D). Other works comprising RSM are compiled in Table 4.1.

To conclude, one may recall the extensive review of Franceschini and Macchietto on the state of the art of model-based design of experiments [122], where the authors stressed the importance of scientific community to keep fostering the use of DoE so it becomes a standard tool for experimentalists and industrial applications. While this message applies naturally to SFE, the thirteen years from 2000 year plainly confirm advances on this trend.

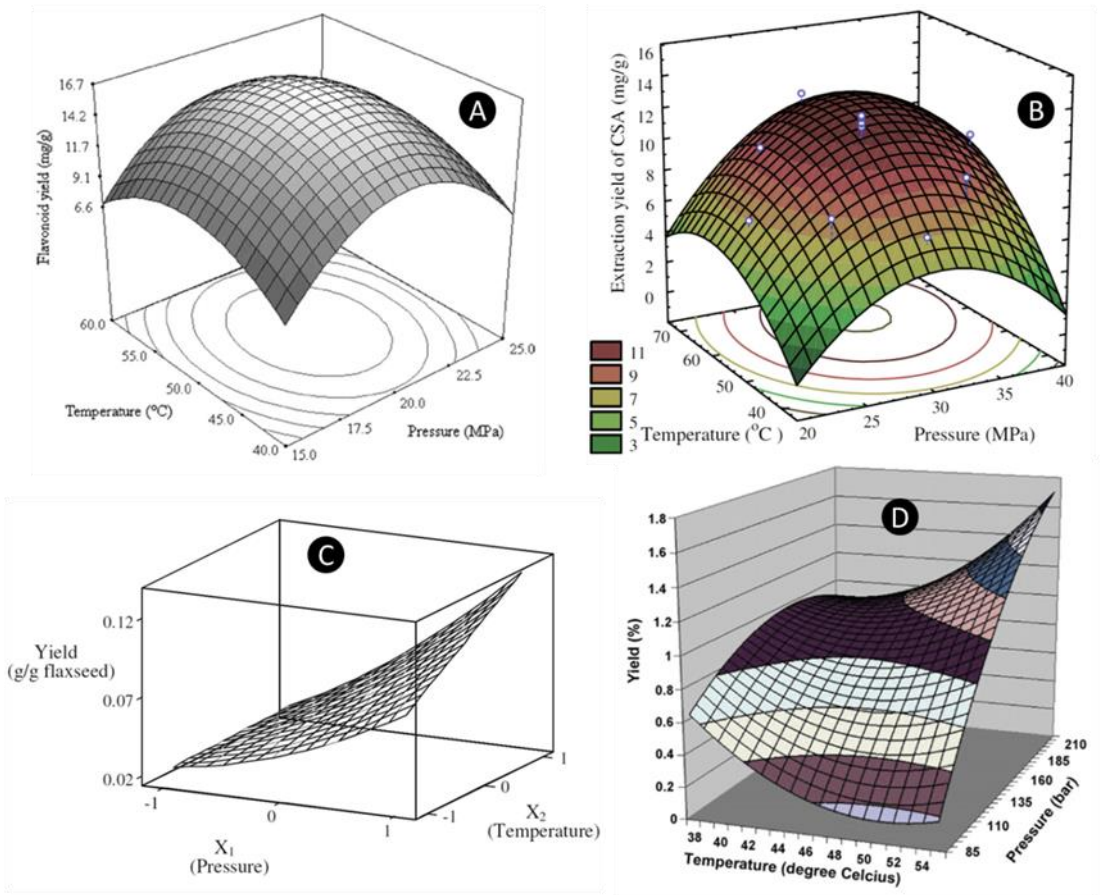

Figure 4.2 – Examples of RSM for the SFE yields of different species. A) flavonoid from SFE of *Pueraria lobata* [93] ; B) cajaninstilbene acid from pigeonpea (*Cajanus cajan*) [26]; C) oil from flaxseed (*Linum usitatissimum*) [68]; D) essential oil from vetiver (*Vetiveria zizanioides* L.) [111].

* * *

Accordingly, the experimental and modeling work hereafter presented can be systematized in two different studies of this thesis, as follows:

***Coffea* spp. study** – The work aims at the optimization of operating conditions of the supercritical fluid extraction of spent coffee grounds (SCG) using pure or modified CO_2, with particular emphasis on oil enrichment with diterpenes like kahweol, cafestol and 16-*O*-

methylcafestol. The analysis comprises the application of Box-Behnken design of experiments and response surface methodology, and involved three operating variables: pressure (140-190 bar), temperature (40-70 °C) and cosolvent (ethanol) addition (0-5 wt.%).

***Eichhornia crassipes* study –** The supercritical extraction of stalks and leaves of *Eichhornia crassipes* was carried out using pure and modified carbon dioxide. Preliminary results evidenced that the influence of temperature is weaker than pressure and ethanol content, and thus a design of experiments was performed in the ranges of 200-300 bar and 0.0-5.0 wt.% ethanol.

4.2 MATERIALS AND METHODS

4.2.1 RAW MATERIALS

Espresso spent coffee grounds (SCG) were obtained from a commercial batch of Delta Cafés Platina (Portugal) at the Department of Chemistry of University of Aveiro. The SCG samples were dried according to the ISO/DIS 11294-1993, following the method of oven drying at 105 °C for 8 h [123].

E. crassipes samples were obtained at Pateira de Fermentelos (40º 34' 31'' N, 8º 30' 57'' W), Aveiro, Portugal. The desired raw material, namely leaves and stalks, was separated from the remaining biomass and was initially air dried to remove the majority of the moisture. A mixture of these two morphological parts was produced under a known ratio comprising 65 wt.% of leaves and 35 wt.% of stalks, which is representative of the mass fraction proportions found naturally for this plant. Subsequently, the samples were submitted to a drying stage in a ventilated oven at 35 °C. The dried samples were then ground and further dried until no mass difference was achieved in order to quantify the biomass natural moisture.

4.2.2 CHEMICALS

Individual standards of kahweol, cafestol and 16–*O*–methylcafestol were purchased from LKT Laboratories Inc. All other reagents used were of analytical grade or higher available purity. Carbon dioxide was supplied with a purity of 99.95 % from Praxair or Air Liquide (Porto, Portugal).

Dichloromethane (99.99 %) was supplied by Fisher Scientific. Pyridine (99.8 %), hexadecanoic acid (99.9 %), nonadecan-1-ol (99 %), 5-cholesten-3β-ol (99 %) were supplied by Sigma-Aldrich. Trimethylsilyl chloride (99 %), tetracosane (99 %), hydrochloric acid (37 %) and N,O-bis(trimethylsilyl)trifluoroacetamide (99 %) were supplied by Fluka.

4.2.3 SOXHLET EXTRACTION

***Coffea* spp. study -** A sample of 45 g of SCG was loaded in a Soxhlet cartridge and extracted with *n*-hexane for 4 hours and 80 °C. At the end of extraction the solvent was recovered by rotary evaporation at 40 °C and the resulting oil was weighed. The results were expressed in mass percentage of dry residue and were used as reference for the supercritical fluid extractions. The extraction yield (η_{total}) is expressed in weight percentage as the quantity of oil ($w_{\text{SCG oil}}$) obtained from SCG (w_{SCG}):

$$\eta_{\text{total}}\ (\text{wt.}\%) = 100 \times \frac{w_{\text{SCG oil}}}{w_{\text{SCG}}} \quad (1)$$

***Eichhornia crassipes* study –** Soxhlet extractions with dichloromethane were performed in duplicate in order to establish a reference composition for the supercritical fluid extractions. Samples of approximately 16.6 g were placed in the Soxhlet cartridge and were submitted to a 6 hours extraction, after which the solvent was evaporated to dryness. The total sterols yield ($\boldsymbol{\eta_{\text{TotalSterols}}}$), individual yields ($\boldsymbol{\eta_{\text{i}}}$) and extracts concentrations (C_{i}) were calculated from the following relations:

$$\boldsymbol{\eta_{\text{TotalSterols}}}(\text{wt.}\%) = \frac{\boldsymbol{w_{\text{Sterols}}}}{\boldsymbol{w_{\text{biomass}}}} \times \mathbf{100} \quad (2)$$

$$\boldsymbol{\eta_{\text{i}}}(\text{wt.}\%) = \frac{\boldsymbol{w_{\text{i}}}}{\boldsymbol{w_{\text{biomass}}}} \times \mathbf{100} \quad (3)$$

$$\boldsymbol{C_{\text{i}}}(\text{wt.}\%) = \frac{\boldsymbol{w_{\text{i}}}}{\boldsymbol{w_{\text{extract}}}} \times \mathbf{100} \quad (4)$$

where $\boldsymbol{w_{\text{extract}}}$ is the mass of extract, $\boldsymbol{w_{\text{Sterols}}}$ is the mass of total sterols extracted, $\boldsymbol{w_{\text{i}}}$ is the mass of an individual extracted compound, and $\boldsymbol{w_{\text{biomass}}}$ is the mass of the dried biomass sample used in the experiment. The individual species focused were stigmasterol, cholesterol and β-sitosterol.

4.2.4 SUPERCRITICAL FLUID EXTRACTION

***Coffea* spp. study -** Supercritical fluid extractions were performed in an apparatus developed at Department of Chemistry of University of Aveiro. The scheme of process can be visualized on the publications of Passos *et al.* [124-125], together with the corresponding full description of the set up. Concisely, the CO_2 withdrawn from a container is primarily liquefied in a refrigerated bath and then pressurized by an air driven liquid pump to a high-pressure vessel. The solvent is brought to the extraction temperature by means of a long tubing coil placed inside the oven and the pressure is fixed in a forward pressure regulator. After percolating the seed bed, the extract stream passes through micrometering valves. The valves and the adjoining line are heated to prevent blocking up due to oil and CO_2 freezing, enabling the safe collection of extract in a separator.

In each run 60 g of SCG were introduced in the extraction vessel and a constant CO_2 mass flow rate of 12 g min^{-1} was applied. Extracts were collected in a recovery vessel with ethanol, where the effluent stream is submerged after extraction to avoid the loss of compounds. At the end of experiments, the ethanol of the recovery vessel was evaporated in a rotary evaporator. The results were expressed in weight percentage of dry biomass by Eq. (1).

***Eichhornia crassipes* study –** The SFE assays were accomplished in the same apparatus depicted in the Chapter 3 (see Section 3.2.3) and using the same method. In each run, an approximate load of 30 g of water hyacinth sample was introduced in the extractor.

4.2.5 EXTRACTS CHARACTERIZATION

***Coffea* spp. study -** Extracts were analysed in a HPLC equipment with a UV detector (Gilson) and a reverse-phase column (Spherisorb S10 ODS2 (C18), 25 cm × 4.6 mm). The mobile phase was a mixture of methanol/water (85:15, v/v) using a flow rate of 0.7 mL min^{-1} and detection wavelength of 220 nm, in agreement with the setting reported by Amorim *et al.* [126].

The total diterpenes content was determined by HPLC after saponification with KOH/ethanol, using diethyl ether for the solvent extraction of a 40 mg sample. Two additional washing steps with water were added to the procedure reported by Rafael *et al.* [127]. The identity of individual diterpenes was ensured by comparing their retention times with authentic standards. The quantification was made using external calibration curves of concentration *vs.* peak areas, whose coefficients of determination were higher than 0.99.

***Eichhornia crassipes* study –** Beforehand the GC-MS analysis, approximately 20 mg of each extracted sample were converted into its trimethylsilyl counterpart [128-129]. The procedure that was applied is as follows. Each dried sample was dissolved in 250 μL of pyridine containing 1 mg of tetracosane. The addition of 250 μL of N,O-bis(trimethylsilyl)trifluoroacetamide and 50 μL of trimethylsilyl chloride promotes the conversion of compounds with hydroxyl and carboxyl groups to trimethylsilyl (TMS) ethers and esters, respectively. This mixture was then maintained at 70 °C for 30 minutes its trimethylsilyl counterpart [128-129]. Finally, each extract was analyzed in duplicate with tetracosane as internal standard.

The analytical equipment used was a Trace Gas Chromatograph 2000 Series equipped with a Finnigan Trace MS mass spectrometer, using helium as carrier gas (35 cm s^{-1}), equipped with a DB-1 J&W capillary column (30 m × 0.32 mm i.d., 0.25 μm film thickness) and coupled

with an auto-sampler. The chromatographic conditions were as follows: initial temperature: 80 °C for 5 min; heating rate: 4 °C min^{-1}; final temperature: 285 °C for 10 min; injector temperature: 250 °C; transfer-line temperature: 290 °C; split ratio: 1:50. The MS was operated in the electron impact mode with electron impact energy of 70 eV and data collected at a rate of 1 scan s^{-1} over a range of m/z of 33–750. The ion source was maintained at 250 °C.

For the quantitative analysis, the instrument was calibrated with a pure reference compound representative of the family of compounds desired to quantify (β-sitosterol), relative to the internal standard. The response factor necessary to obtain the correct quantification of peak areas was calculated as a mean of six GC-MS runs.

4.2.6 DESIGN OF EXPERIMENTS (DOE) AND RESPONSE SURFACE METHODOLOGY (RSM)

The independent variables considered in the present work were codified according to the following expression:

$$X_k = \frac{x_k - x_0}{\Delta x_k} \tag{5}$$

where X_k is the codified value of the independent variable x_k, x_0 is its real value at the central point, and Δx_k is its step change.

Experimental results submitted to RSM analysis are usually well described by a second order polynomial function:

$$Y = \beta_0 + \sum_{i=1}^{k} \beta_i X_i + \sum_{i=1}^{k} \beta_{ii} X_i^2 + \sum_{i<j}^{k} \beta_{ij} X_i X_j \tag{6}$$

where Y is the studied response (whether η_{total}, C_{dit}, etc), β_0 is a constant, β_i are model coefficients linked to linear effects, β_{ii} are coefficients related to quadratic effects, and β_{ij} are coefficients for interaction effects.

***Coffea* spp. study –** In this work, the influence of three factors was studied, namely pressure (P), temperature (T), and ethanol concentration in the supercritical solvent (EtOH wt.%) using three different levels: 140-165-190 bar, 40-50-70 °C and 0-2.5-5.0 (wt.%), respectively (see Table 4.2). For this a Box–Behnken design (BBD) comprising fifteen experiments was chosen to study total extraction yield and diterpenes concentration in extracts (C_{dit}). In order to block the incidence of unknown and uncontrolled effects upon results (nuisance factor), randomization of experiments was accomplished.

Table 4.2 – Codification and levels of the three independent variables considered for Box–Behnken design of the *Coffea* spp. study.

Factor		Factor index (i) in Eq.(6)	Level correspondence		
			Low (-1)	Medium (0)	High (+1)
Pressure	P	1	140 bar	165 bar	190 bar
Temperature	T	2	40 °C	55 °C	70 °C
Ethanol content	EtOH	3	0 % (wt.)	2.5 % (wt.)	5.0 % (wt.)

STATISTICA software (version 5.1, StatSoft Inc., Tulsa, USA) was used for statistical treatment of the results. Analysis of variance (ANOVA) was employed to evaluate the statistically significant factors and interactions using Fisher's test and its associated probability p(F), while t-tests were performed to judge the significance of the correlated coefficients in each model. The determination coefficients, R^2, and their adjusted values, R^2_{adj}, were used to evaluate the adequacy of fit of the regression models. The determination coefficient for prediction, R^2_{pred}, was also employed to have an indication of the predictive aptitude of the regression model [130].

***Eichhornia crassipes* study** – In this work the previous methodology (DoE/RSM) was applied to $\boldsymbol{\eta}_{\mathbf{Total}}$, $\boldsymbol{\eta}_{\mathbf{TotalSterols}}$, and $\boldsymbol{\eta}_{\mathbf{i}}$ and C_{i} responses (where i refers to stigmasterol**,** cholesterol and β-sitosterol). Apart from the identification of the optima conditions, the statistical treatment has also the aim of (I) ranking the significant factors according to their respective impact on the response; (II) discard the non-significant contributions of the model; and (III) disclose whether each contribution acts towards the increase or decrease of the response variable.

A Full Factorial design of nine assays was adopted to study effects caused by two factors, pressure and ethanol content as modifier. These were studied with three levels of variation each: 200, 250 and 300 bar, and 0, 2.5 and 5.0 wt.%, respectively. Table 4.3 provides a summary of the experimental design adopted for the optimization study.

JMP software (version 8.0) was used for statistical treatment of the results. Accordingly, t-tests were applied to judge the significance of the estimated coefficients of the model.

Table 4.3 – Codification and levels of correspondence of the variables considered in the SFE of *E. crassipes* design of experiments.

Factor	Factor index (i) in Eq.(6)	Coded variable	Level of correspondence		
			-1	0	+1
Pressure (bar)	1	$X_{\mathrm{P}} = (P - 250)/50$	200	250	300
Ethanol content (wt.%)	2	$X_{\mathrm{EtOH}} = (\%_{\mathrm{EtOH}} - 2.5)/2.5$	0.0	2.5	5.0

4.3 RESULTS AND DISCUSSION

4.3.1 EXPERIMENTAL OPTIMIZATION OF *Coffea* spp.

Analysis of experimental results – Table 4.4 shows the experimental results of the Box-Behnken design assays. The total oil yield (η_{total}) ranged from 1.99 wt.% in Run 4.2 (140 bar, 70 °C, 2.5 wt.% EtOH) to 11.97 wt.% in Run 4.8 (190 bar, 55 °C, 5 wt.% EtOH). Concerning total diterpenes concentration in oil (C_{dit}), results ranged from 42.4 $\mathrm{mg\,g_{oil}^{-1}}$ in Run 4.2 (140 bar, 70 °C, 2.5 wt.% EtOH) to 107.44 4 $\mathrm{mg\,g_{oil}^{-1}}$ in Run 4.5 (140 bar, 55 °C, 0 wt.% EtOH). At first reading, results reveal that Run 4.2 provided both the lowest total yield and diterpenes concentration, and also that the maximum total yield (Run 4.8) was obtained at different conditions from those of the maximum diterpenic concentration (Run 4.5). These results emphasize the pertinence of the SFE optimization.A noteworthy aspect of the values from Table 4.5 is that, despite Soxhlet extraction yield is the highest (15.03 wt.%), all SFE runs led to extracts richer in diterpenes with the single exception of Run 4.2. Therefore, this anticipates the more selective character of SFE to obtain SCG oils richer in diterpenic compounds.

Table 4.4 – Results of SFE of spent coffee grounds samples used in the optimization work: total extraction yield (η_{total}, wt.%), and diterpenes concentration in extracts (C_{dit}, $\mathrm{mg\,g_{oil}^{-1}}$). Soxhlet results are also shown for comparison.

Run	P (bar)	T (°C)	EtOH (wt.%)	η_{total} (wt.%)	Concentration of Diterpenes ($\mathrm{mg\,g_{oil}^{-1}}$)			
					kahweol	cafestol	16 -*O*-methylcafestol	Total
4.1	140	40	2.5	10.21	27.83	18.98	10.64	57.45
4.2	140	70	2.5	1.99	14.63	9.21	18.63	42.47
4.3	190	40	2.5	11.66	25.77	17.66	9.83	53.26
4.4	190	70	2.5	8.74	30.85	20.61	11.48	62.94
4.5	140	55	0	4.61	47.56	32.06	27.82	107.44
4.6	140	55	5	8.79	27.59	18.80	10.13	56.52
4.7	190	55	0	9.16	27.81	24.40	22.36	74.57
4.8	190	55	5	11.97	26.45	17.92	9.44	53.81
4.9	165	40	0	8.98	40.50	29.53	17.56	87.59
4.10	165	40	5	11.60	24.21	17.31	14.32	55.84

4.11	165	70	0	1.93	40.00	27.09	27.30	94.39
4.12	165	70	5	8.94	32.92	23.04	10.80	66.76
4.13	165	55	2.5	10.62	29.37	20.87	12.18	62.42
4.14	165	55	2.5	10.52	28.68	20.27	11.12	60.07
4.15	165	55	2.5	9.97	30.23	22.33	12.32	64.88
Soxhlet with *n*-hexane				15.03	29.49	16.67	6.53	52.69

Analysis of statistical modeling results – The data from Table 4.5 were then submitted to RSM analysis in their coded form (Eqs. (5)) in order to assess individual and crossed interactions that influence each response, and to develop models based on the most influencing combination of factors. Table 4.6 presents the regression coefficients obtained for both responses studied (η_{total} and C_{dit}), wherein the bold marks highlight the significant coefficients at 95 % confidence level. The nonsignificant coefficients (*t*-test, $p > 0.05$) were purged from the full models (Eq. (6)) and, upon refitting and conversion to real variables (pressure, temperature, EtOH content), the reduced and uncodified models given by Eqs. (7) and (8) were obtained (see Table 4.6).

With regard to the goodness of fit of the reduced models, oil yield led to a high determination coefficient ($R^2 = 0.974$), while diterpenes concentration provided a smaller value, $R^2 = 0.875$. Moreover the short difference between R^2 and R^2_{adj} suggests a proper adequacy of reduced models to data. The good prediction capacity of the final models, given by the values of R^2_{pred} which are very similar to R^2_{adj}, is also an appreciable indicator, mainly if one takes into account that we are dealing with complex natural residues.

Table 4.5 – Regression coefficients of quadratic models of SFE of *Coffea* spp., fitted to the total extraction yield and total concentration of diterpenes in supercritical extracts. Bold values identify significant coefficients at 95 % confidence interval.

	η_{total} (wt.%)		C_{dit} (mg g_{oil}^{-1})	
	Regression coefficients	*t*-test *($p < 0.05$)*	Regression coefficients	*t*-test *($p < 0.05$)*
β_0	10.37	**<0.001**	62.4567	**<0.001**
β_1	1.99125	**0.003**	-2.4138	0.105
β_{11}	-0.725	0.058	-5.7446	**0.044**
β_2	-2.60625	**0.002**	1.5525	0.209
β_{22}	-1.495	**0.015**	-2.6821	0.165
β_3	2.0775	**0.004**	-16.3812	**0.003**
β_{33}	-1.0125	**0.039**	16.3704	**0.006**
β_{12}	1.325	**0.017**	6.165	**0.036**
β_{13}	-0.3425	0.189	7.5425	**0.024**
β_{23}	1.0975	**0.025**	1.03	0.482
R^2	0.990		0.898	
R^2_{adj}	0.973		0.714	

Table 4.6 – Reduced models of SFE of *Coffea* spp. for total extraction yield (η_{total}, wt.%) and total diterpenes concentration in extracts (C_{dit}, mg g_{oil}^{-1}). Units: T in °C, P in bar, and EtOH content in wt.%.

Reduced Model	R^2	R^2_{adj}	R^2_{pred}	Eq.
$\eta_{\text{total}} = 20.034651 - 0.114595\,P - 0.121893\,T - 0.01299\,\text{EtOH} - 0.006395\,T^2 - 0.153076\text{EtOH}^2 + 0.0035329\,P{\times}T + 0.29237\,T{\times}\text{EtOH}$	0.974	0.948	0.969	(7)
$C_{\text{dit}} = 51.46213 + 1.718733\,P - 2.68732\,T - 39.726\,\text{EtOH} - 0.00886\,P^2 + 2.652272\,\text{EtOH}^2 + 0.016424\,P{\times}T + 0.12068\,P{\times}\text{EtOH}$	0.875	0.806	0.871	(8)

Optimization of total extraction yield **-** Figure 4.3 presents a Pareto chart where all the studied factors and interactions are listed and evaluated in terms of their individual impact on results. The factors/interactions whose effect bars are shorter than the statistical significance boundary line (which delimits the region of statistically significance of $p > 0.05$) are considered non-significant. The color of the bars, white or black, indicate the type of influence brought about by each factor/interaction. Concerning η_{total}, results reveal that the influence of the three individual operating variables (P, T and EtOH content) are significant, being T the most important with a negative impact on the η_{total} response. The other two individual factors (P and EtOH content) exhibit a positive influence on the total extraction yield, as well as the $P\times T$ and $T\times\text{EtOH}$ interactions.

The individual P and T factors and their combination ($P\times T$) are physically related to important properties such as density, viscosity, diffusivity and solute vapor pressures (the last is only T-dependent. Considering that every variation of P and/or T induces changes on the referred fluid and solute properties, they are of a chief importance for the hydrodynamic, mass transfer and solubility phenomena that take place in the extraction. In view of this multiplicity of influences, pressure and temperature typically define in great extent the performance of SFE systems. Taking T as example, one knows that variations of this variable (at constant P) result in counteracting effects upon solubility since SC-CO_2 density (ρ) and vapor pressure of solutes ($P_{\text{i}}^{\text{sat}}$) exhibit contrary behaviors: when T is increased, ρ decreases while $P_{\text{i}}^{\text{sat}}$ increases. Upon examination of experimental data, it becomes evident that as T is increased, its negative effect due to density reduction prevails over the positive impact. With respect to ethanol addition, its positive influence on η_{total} (see Figure 4.3) is in agreement with expectations, as it increments the affinity of SC-CO_2 to more polar compounds [51].

The fitted response surface for η_{total} is given in Figure 4.4 for the two edge temperatures studied: 40 °C and 70 °C. The good quality of fitting anticipated by R^2 and R_{adj}^2 in Table 4.6 for this response can be visually confirmed through the closeness of reduced model surface and experimental data. Upon comparison of the surface plots shapes, very distinct profiles are observed for each temperature, namely: higher η_{total} values with a plateau-like profile (at 40 °C) *vs.* lower values with an inclined profile (at 70 °C). In this respect, the higher η_{total} values at 40 °C are in great agreement with the conclusion taken from Pareto chart (Figure 4.3), regarding the negative effect of T increments over total extraction yield. On the other hand, the surface plots reveal that the individual positive impact of pressure and cosolvent addition are stronger at 70 °C than at 40 °C, and also that the conjugation of higher values of P with EtOH content is particularly advantageous at the highest temperature (Figure 4.4.B*)* but negligible at the lowest one (Figure 4.4.A*)*.

Globally, the optimal conditions that maximize SCG extraction with SC-CO_2 are 190 bar/55 °C/5 wt.% EtOH, according to the reduced model ($\eta_{\text{total}} = 13.28$ wt.%).

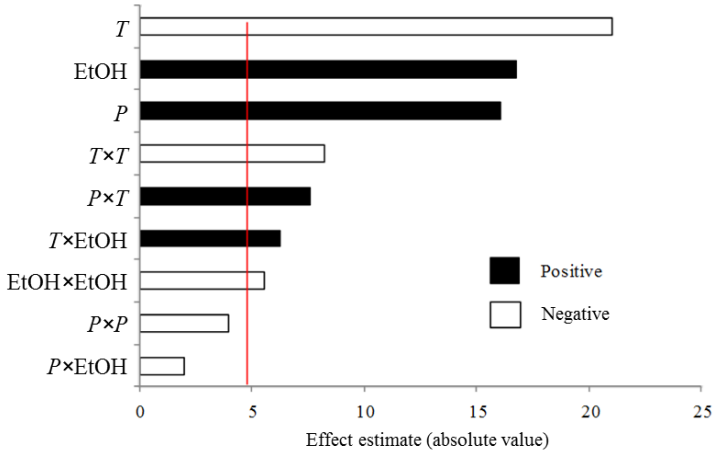

Figure 4.3 – Pareto diagram for the total extraction yield (η_{total}) of spent coffee grounds by supercritical fluid extraction. The vertical line defines the region of statistical significance (right side) at 95 % confidence interval.

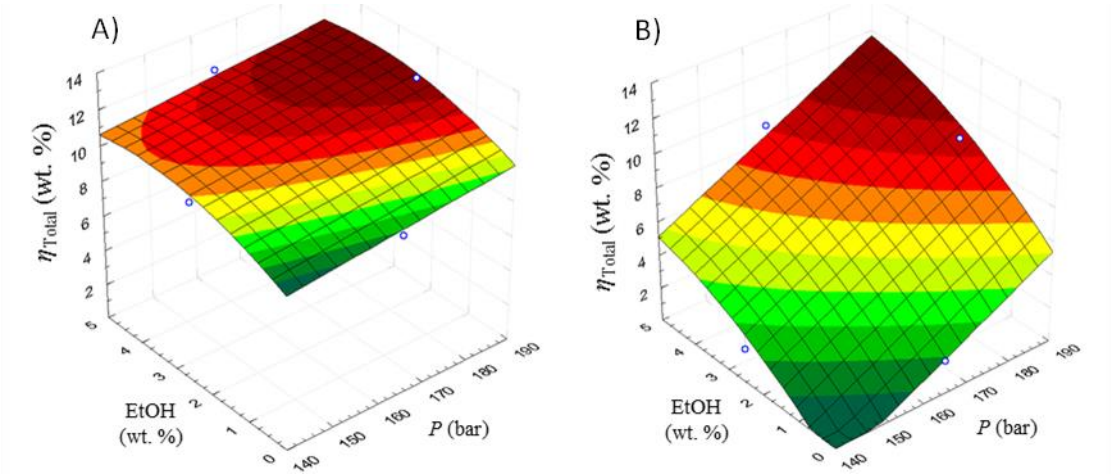

Figure 4.4 – Total extraction yield (η_{total}) results from extracts of spent coffee grounds obtained by supercritical fluid extraction. Data are graphed as function of pressure and ethanol content for the two edge temperatures: a) 40 °C and b) 70 °C.

Optimization of diterpenes concentration **-** The diterpenic compounds quantified in SCG extracts were cafestol, kahweol and 16-*O*-methylcafestol, either esterified or free. In this section, the statistical and regression treatment of the experimental data was similar to that implemented for the total extraction yield.

In consonance with expectations, the Pareto chart for this response (Figure 4.5) states that the modification of SC-CO_2 polarity through the addition of ethanol greatly influences C_{dit} values, as three (EtOH, $P\times T$, and $\mathrm{EtOH}\times\mathrm{EtOH}$) of the four factors/interactions involving cosolvent content confirmed statistically their importance in this case. Results show that its individual influence is predominantly negative, though it is compensated in lower degrees by the positive contributions of its quadratic parcel ($\mathrm{EtOH}\times\mathrm{EtOH}$) and its interaction with pressure ($P\times\mathrm{EtOH}$). Overall, experimental data clearly denote a negative impact of ethanol on diterpenes concentration (see Table 4.5), which must be due to the higher affinity of the modified supercritical solvent to other compounds of non-diterpenic nature. It is known that coffee diterpenes exhibit some polarity [131] and that pure SC-CO_2 has a poor affinity to such compounds. However, in view of the rich chemical composition of natural matrices, the decision of tuning solvent polarity with a modifier can sometimes lead to the removal of undesired compounds, obstructing thus the objective of maximizing the concentration of target molecules in the final extracts. Similarly in our study, the cosolvent increased the global yield though simultaneously reduced diterpenes concentration. The negative impact of ethanol content on C_{dit} can be fully disclosed in Figure 4.6, where C_{dit} is plotted for the minimum (0 wt.%) and maximum (5 wt.%) cosolvent addition percentages. The results are graphed using the same concentration scale, being therefore quite perceptible the difference in C_{dit} magnitudes for each case: 75-107 $\mathrm{mg\,g_{oil}^{-1}}$ for pure CO_2 extracts, against 45-75 $\mathrm{mg\,g_{oil}^{-1}}$ for assays with 5 % (wt.) modification.

With regard to the effects of P and T upon C_{dit}, the fitted model denotes that the temperature exhibits a soft impact on the results, while pressure acts differently depending on the ethanol content: it can make concentration vary up to 36 % (70 to 9 $\mathrm{mg\,g_{oil}^{-1}}$) when working with pure CO_2, while it can induce variations up to 60 % (45 to 7 $\mathrm{mg\,g_{oil}^{-1}}$) when 5 wt.% ethanol is introduced.

Hence, the operating conditions that provide the maximization of diterpenes concentration in SCG extracts (102.90 $\mathrm{mg\,g_{oil}^{-1}}$) arise as the combination of a lower pressure with no cosolvent addition, specifically 140 bar/40 °C/0 wt.% EtOH.

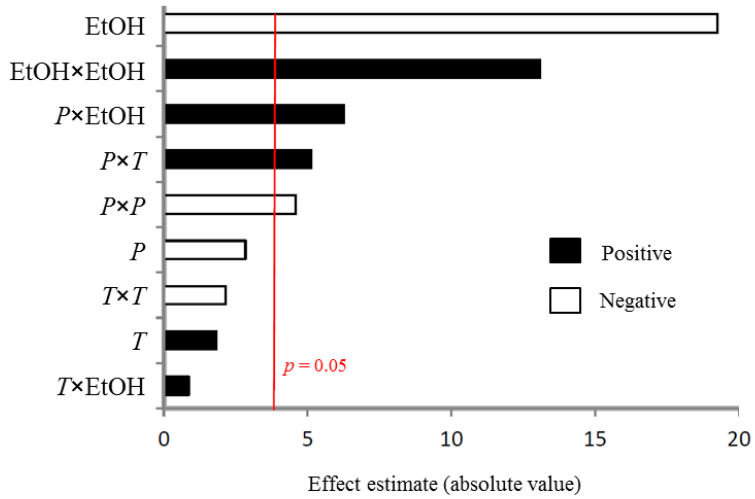

Figure 4.5 – Pareto diagram for the total diterpenes concentration (C_{dit}) in extracts of spent coffee grounds obtained by supercritical fluid extraction. The vertical line defines the region of statistical significance (right side) at 95 % confidence level.

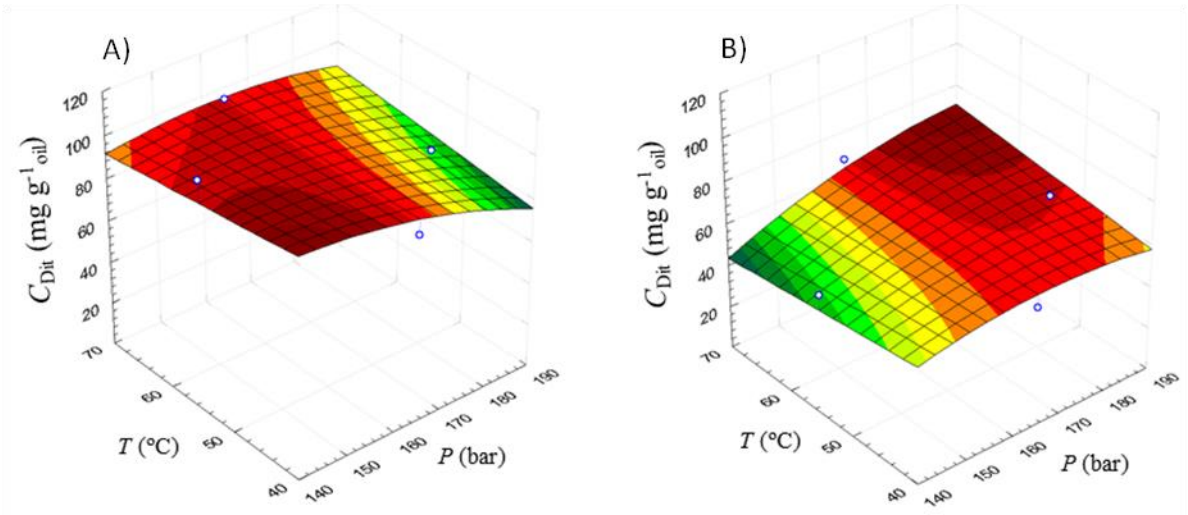

Figure 4.6 – Total diterpenes concentration (C_{dit}) in the supercritical extracts of spent coffee grounds. Results are graphed as function of pressure and temperature for the two edge cosolvent percentages: A) 0 wt.%, and B) 5 wt.%.

4.3.2 EXPERIMENTAL OPTIMIZATION OF *Eichhornia crassipes*

Analysis of the experimental results – At an initial stage, the characterization of the extracts obtained by conventional solid-liquid extraction and by SFE was assessed with the aim of quantifying and comparing both approaches. According to a previous work dichloromethane provides a selective uptake of the lipophillic fraction of the various morphological parts of *E. crasssipes [132]*, notwithstanding other solvents have been also chosen for the same purpose, such as *n*-hexane [133] and petroleum ether [134].

Figure 4.7 represents a typical GC-MS chromatogram of a dichloromethane Soxhlet extraction where the sterols retention times (RT) are outlined. Due to the vast amount and high concentration of stigmasterol present in the extract, and due to being a highly valuable compound, the overall sterol family was specifically emphasized in this work. The removal with dichloromethane led to a total yield of 1.9 wt.% with the total sterols fraction comprising 23.7 wt.% of the global extract. In addition, the individual concentrations of stigmasterol, cholesterol, β-sitosterol, and methylcholesterol in the extracts amount 15.55 %, 3.50 %, 2.98 % and 1.67 % (wt.), respectively. These Soxhlet extraction results will henceforth be taken as reference values along the SFE optimization of water hyacinth. For instance, Table 4.7 also provides the characterization of one SFE assay, namely Run 4.22, allowing a direct comparison between the two methods. In this sense, although the total extraction yield obtained by SFE for the selected conditions ($\boldsymbol{\eta_{Total}} = 0.75$ wt.%) is far lower than the value obtained by conventional Soxhlet ($\boldsymbol{\eta_{Total}} = 1.9$ wt.%), the supercritical method accomplishes a more selective extraction of the sterols family, with a purity of 36.6 wt.%, a value that is ca. 1.5 times higher than that achieved by Soxhlet.

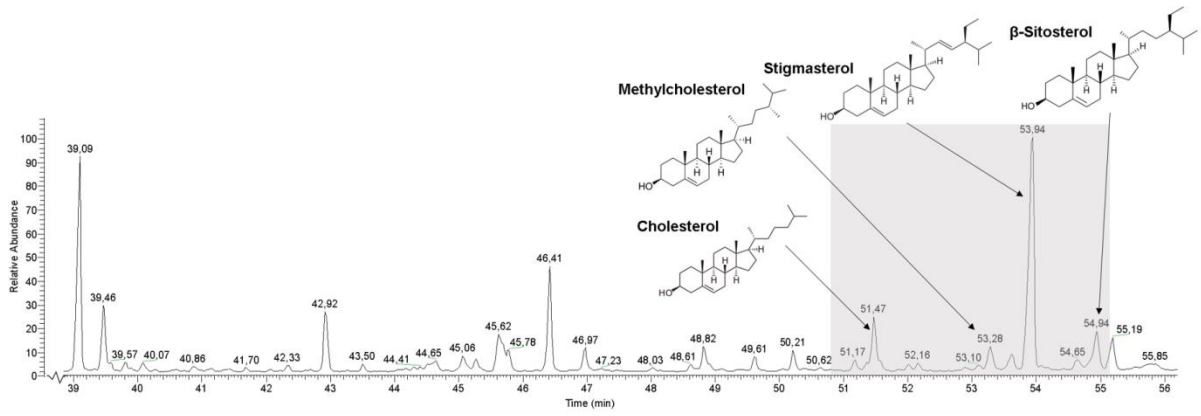

Figure 4.7 – GC–MS chromatogram of a dichloromethane extract of *E. crassipes*. The sterols of interest are found within the delimited region.

Table 4.7 – Identification and quantitative determination of sterols in the dichloromethane and supercritical CO_2 extracts of *E. crassipes*.

Peak	RT (min)	Compound	Soxhlet		SFE, Run 4.22 (300 bar, 0 wt.% EtOH)	
			$\boldsymbol{\eta_i}$ ($mg\ kg^{-1}_{biomass}$)	C_i (wt.%)	$\boldsymbol{\eta_i}$ ($mg\ kg^{-1}_{biomass}$)	C_i (wt.%)
1	51.47	Cholesterol	681.1	3.5 %	346.6	4.6 %
2	53.28	Methylcholesterol	325.0	1.7 %	177.5	2.4 %
3	53.94	Stigmasterol	3023.8	15.6 %	1889.0	25.1 %
4	54.94	β-sitosterol	579.9	3.0 %	339.2	4.5 %
Total Sterols ($mg\ kg^{-1}_{biomass}$)			4609.8	23.8 %	2752.3	36.6 %
(wt.%)			0.46 %		0.28 %	
Total Yield (wt.%)			1.90 %		0.75 %	

RT: Retention time (see Figure 4.7); EtOH: ethanol

Analysis of statistical modeling results – The experimental results of the extraction assays are displayed in Table 4.8. Six responses were evaluated simultaneously, these being total extraction yield (η_{Total}), total sterol extraction yield ($\eta_{TotalSterol}$), total sterol concentration ($C_{TotalSterol}$), and the individual concentration of stigmaterol, β-sitosterol and cholesterol in the extracts (C_{Stigm}, $C_{\beta-sitost}$ and $C_{cholest}$, respectively).

With regard to η_{Total}, the obtained yields ranged from 0.72 wt.% for the conditions of Run 4.16 [200 bar; 0 % ethanol] to 1.24 wt.% for the conditions of Run 4.24 [300 bar; 5.0 % ethanol], which correspond to 37 % and 65 % of the reference value given by the Soxhlet extraction (1.9 wt.%). In terms of $\eta_{TotalSterol}$, the absolute values of the later ranged from 0.24 wt.% in Run 4.19 [250 bar; 0.0% ethanol] to 0.35 wt.% in Run 4.23 [300 bar; 2.5 % ethanol], which represent 52 % and 76 % (wt.) of the sterols content established by the Soxhlet reference.

With the aim of investigating the main factors that influence the considered responses in this study, the experimental data was adjusted to a quadratic polynomial (of the form of Eq. (6)) and the Full Models (FM) obtained are displayed in Table 4.10 alongside the respective *p*-values regarding their statistical significance. In order to simplify the predictive model obtained, the coefficients that were statistically significant to the response ($p < 0.05$) were preserved and the experimental data points were re-fitted. Considering a general overview of fitting parameters, it is possible to assess the influence of each contribution towards each response. Regarding extraction yields, due to the positive signs of the β coefficients, all terms involving ethanol contribution (β_2, β_4 and β_5) act towards the increase of the response, whereas for the concentration responses the inverse scenario occurs. In practice, this implies that ethanol

Table 4.8 – Results of the SFE assays of *E.crassipes* performed for the purpose of the statistical optimization.

Run	P (bar)	%EtOH	η_{Total} (wt.%)	$\eta_{\text{TotalSterol}}$ (wt.%)	Concentration (wt.%)			
					$C_{\text{TotalSterol}}$ (wt.%)	C_{Stigm} (wt.%)	$C_{\beta-\text{sitost}}$ (wt.%)	C_{cholest} (wt.%)
4.16	200	0.0	0.72	0.25	35.02	24.90	3.91	4.12
4.17	200	2.5	0.90	0.30	33.17	22.19	4.19	4.74
4.18	200	5.0	1.17	0.31	27.92	18.96	3.62	3.63
4.19	250	0.0	0.78	0.24	31.12	22.70	3.67	3.54
4.20	250	2.5	0.88	0.32	36.32	24.76	4.33	4.89
4.21	250	5.0	1.25	0.34	27.28	18.49	3.52	3.48
4.22	300	0.0	0.75	0.28	36.63	25.14	4.52	4.61
4.23	300	2.5	0.90	0.35	38.26	26.35	4.74	4.89
4.24	300	5.0	1.24	0.30	24.35	17.59	2.97	2.50

EtOH: ethanol; Cholest: cholesterol; Stigm: stigmasterol; β-sistost: β-sitosterol;

Table 4.9 – Regression coefficients of the Full Model (FM) of the SFE of *E.crassipes*, including the individual significance for each response at a 95 % confidence interval, and the respective determination coefficient (bold values represent contributions that are statistically significant).

	Total extraction yield		Total sterol extraction yield		Sterol concentration							
					Total sterol		Stigmasterol		β-Sitosterol		Cholesterol	
	FM	p	FM	p	FM	p	FM	p	FM	p	FM	p
β_0	0.914	**<0.0001**	0.323	**0.0003**	35.258	**0.0005**	24.075	**0.0004**	4.316	**0.0004**	4.762	**0.0008**
β_1	0.0271	0.2170	0.00983	0.3722	0.521	0.695	0.506	0.5581	0.0885	0.542	-0.0803	0.695
β_2	0.225	**0.0010**	0.031	**0.0458**	-3.870	**0.0490**	-2.950	**0.0314**	-0.329	0.0840	-0.444	0.0972
β_{11}	-0.0307	0.3821	-0.0035	0.8435	0.983	0.6701	0.539	0.7136	0.155	0.537	0.115	0.745
β_{22}	0.0803	0.0758	-0.034	0.1279	-5.526	0.0774	-3.136	0.1	-0.718	**0.0488**	-1.192	**0.0343**
β_{12}	0.0231	0.3569	-0.00875	0.5023	-1.299	0.444	-0.401	0.6997	-0.309	0.145	-0.406	0.173
R^2	0.98		0.85		0.860		0.88		0.88		0.88	
R^2_{adj}	0.96		0.60		0.627		0.67		0.68		0.69	

increases the overall amount of extractives attained but such increment is mainly at the expenses of other compounds than the sought ones. As a result a dilution of the key compounds is prone to be achieved as more ethanol is added to the supercritical CO_2.

The coefficients of determination (R^2) and the adjusted coefficients of determination (R^2_{adj}), which aid in the understanding of the quality of the adjustment, are also displayed. Overall, every response provided R^2 higher than 0.85, being the highest for η_{Total}, attaining a value of 0.98. However, with the exception of η_{Total}, all the other responses exhibit R^2_{adj} values significantly lower than R^2, which indicates that the favourable goodness of fit attained in those responses is at the expenses of the various parameters of the full model.

Optimization of total extraction yield – In what concerns trends of η_{Total}, Figure 4.8(a) shows the surface of this response along pressure and ethanol content, being perceptible that the contribution of ethanol in the supercritical solvent mixture provides a higher impact than the overall effect of pressure. In fact, within the studied pressure values range (200-300 bar), relevant solvent properties such as density (ρ) and viscosity (μ) do not vary expressively: for instance, $\rho(300\text{ bar}, 50\text{ ºC}, 0.0\text{ wt.\% EtOH})/\rho(200\text{ bar}, 50\text{ ºC}, 0.0\text{ wt.\% EtOH}) = 1.1$ and $\mu(300\text{ bar}, 50\text{ ºC}, 0.0\text{ wt.\% EtOH})/\mu(200\text{ bar}, 50\text{ ºC}, 0.0\text{ wt.\% EtOH}) = 1.2$. (The SC-$CO_2$ density and viscosity were computed by the relationship proposed by Pitzer and Schreiber [135], and the empirical equation developed by Altunin and Sakhabetdinov [136], respectively). Although ethanol addition can affect per se the density and viscosity of the supercritical phase, Figure 4.8(a) evidences that jumps from 200 to 300 bar at either 2.5 or 5.0 wt.% EtOH are not more pronounced than without cosolvent, which reinforces the idea that, in practical terms, relevant properties of the supercritical CO_2 (or mixture) are not being considerably modified within the chosen pressure frame.

On the other hand, it has been noted that chemical forces due to specific solute-cosolvent interactions can be responsible for large solubility enhancements, rather than physical forces [137]. In fact, the increase of the supercritical medium polarity at constant pressure provided an extraction yield up to 1.6 times higher than the operation with pure SC-CO_2. Such evidence has been also reported for other biomass samples, as in the SFE optimization study of *Eucalyptus globulus* bark [51]. However, as has been mentioned above, the modification of the SC-CO_2 with ethanol favours majorly the solubilisation of more polar compounds, which may or may not be desirable if the extraction of specific target molecule/families (such as sterols) is objectively pursued.

Besides the general remark on how ethanol seems to be able to increase η_{Total}, it should be mentioned that different influence grades can be noticed between the range of values studied for this factor. Accordingly, the total extraction yield jumps observed between 0-2.5 wt.% EtOH

are visibly more modest than those observed for 2.5-5.0 wt.%. Such observation reveals the SFE process is sensitive to the amount of cosolvent that is being employed, suffering distinct enhancements depending on the chosen ranges. Such sensitivity should be considered under the light that the amount of hydrophilic extractives are 6.3-10.9 times greater than lipophilic extractives in *E. crassipes* [132]. Hence, the vast amount of polar extractives compared to the lipophilic fraction justifies the favourable evolution of η_{Total} with the increase of solvent polarity.

In the whole, the operating conditions that maximize the amount of extractives are 300 bar and 5.0 % ethanol. These should be compared with the specific performance of sterols uptake, which is the objective of the following subsections.

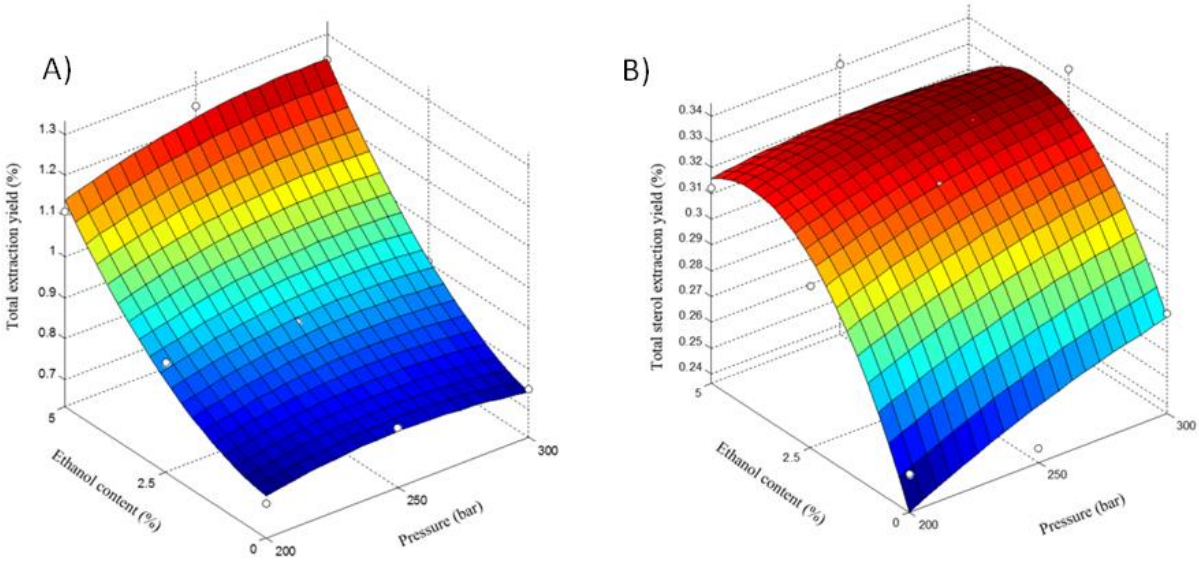

Figure 4.8 – Response surfaces plotting the effects of pressure and ethanol content over: A) total extraction yield, and B) Total sterols extraction yield. Temperature and CO_2 flow rate are fixed (50 °C and 7.5 g min^{-1}). Dots are experimental data, and surfaces are calculated by Eq. (6) with the coefficients of Table 4.9.

Optimization of total sterols extraction yield – Figure 4.B presents the extraction profile of sterols as function of ethanol content and pressure within the studied range of values for each factor. Despite η_{Total} and $\eta_{\text{TotalSterols}}$ visibly follow the same overall trend (i.e. major variations being caused by ethanol content than pressure), the profiles of both yields along the increase of ethanol concentration are distinct for the two responses. In fact, $\eta_{\text{TotalSterols}}$ exhibits a more pronounced increase when moving from 0 to 2.5 wt.% of cosolvent thanη_{Total} response does, but the opposite enhancement is verified within the jump of 2.5 to 5.0 wt.%. This evidence denotes that the uptake of sterols clearly benefits from a slight tuning of supercritical medium polarity as that caused by an addition of 2.5 % of ethanol, but that above this value no proportional advantage is noticed. Hence, operation with 5.0 wt.% ethanol represents a surplus of cosolvent that has no desirable consequences from a sterols removal point of view.

The advantageous way how ethanol can enhance sterols uptake would be undisputable if other compounds were not also present in the biomass samples to be extracted on a competitive basis. In fact, the addition of small quantities of ethanol can boost the molecular interactions between the supercritical solvent and polar compounds, increasing the removal rate of these. As a result significant amount of undesired components may also be recovered, which is not desirable in light of producing extracts with enriched fractions of sterol compounds. Hence, the sterols yield enhancement through cosolvent addition should be crossed with selectivity criteria, which, in practice, may be analysed finding optimum concentration regions for the sterols.

Optimization of sterols concentration – The last responses evaluated in this work are related to the sterols concentration in the extracts obtained under different operating conditions. Since, as a response, total sterols concentration is computed as the ratio between $\eta_{\mathrm{TotalSterol}}$ and η_{Total}, the trends observed for these functions may allow anticipating a given concentration profile. In this sense, the acknowledgement that ethanol influences more $\eta_{\mathrm{TotalSterol}}$ than η_{Total} with 2.5 wt.% ethanol, and the opposite is observed for 5.0 wt.% ethanol, suggests that the region of maximum concentration may be located at intermediate ethanol contents. Figure 4.9.A presents the overall sterols concentration profile along the studied range of operating conditions. As expected, a specific combination of operating conditions contributes to a more selective removal of sterols in contrast to the remaining undesirable compounds available in the biomass, those being 200-300 bar and 2.5 wt.% ethanol. Overall, the trend observed in the concentration profiles is in agreement with the discussion performed before, i.e. the conditions that maximize the sterol concentrations are those where the respective extraction yield achieves its plateau (see Figure 4.8). It is also worth to notice that since a vast amount of hydrophilic compounds are available, the milder ethanol conditions that allow a high removal of sterols are in fact favourable to the goal of having a maximum concentration of these compounds in the extracts. In fact, when 5.0 wt.% of cosolvent is introduced, the solubility of those polar extractives are significantly incremented, which reduces the concentration of our target family of sterols.

The existence of a clear optimum region for total sterols concentration in extracts triggered the interest to evaluate also the individual concentrations of the most representative sterols available in *E. crassipes* extract. Hence, in Figures 4.9.B, 4.9.C and 4.9.D one provides stigmasterol, β-sitosterol and cholesterol concentrations, respectively. These three molecules represent 93-96 % of the total sterols concentration of Figure 4.9.A. Besides, the individual responses considered gave the same maximum/minimum operating conditions arrangements, these being obtained at Runs 4.23 and 4.24 respectively. As observed in Figure 4.9.B, a similarity is noticeable between the concentration profiles of total sterols and stigmasterol. This is due to the fact the latter is the most representative sterol obtained from *E. crassipes*, accounting

individually 67-72 % of $C_{\mathrm{TotalSterol}}$ in SFE assays (see Table 4.8), while in Soxhlet it worths 66 % of the $C_{\mathrm{TotalSterol}}$. The very same profile is observed for cholesterol, showing that it shares in great extent with stigmasterol the sensitivity to the pressure and ethanol content conditions, notwithstanding its abundance represents only 11 wt.% of the sterols existing in the studied biomass (see Table 4.8).

A rather different profile was observed for β-sitosterol (Figure 4.9.C). As a matter of fact, this sterol evidences a greater sensitivity to pressure variations in the range of 200-300 bar than stigmasterol and cholesterol do. Accordingly, $C_{\beta-\mathrm{sitost}}$ is greatly enhanced by the jump to 300 bar, independently of the ethanol content that is chosen. However, the setting of an intermediate ethanol content (2.5 wt.%) is also preferable as the said enhancement reaches the maximum absolute concentration value on that region: 4.74 wt.%.

Taking into account the specificity of β-sitosterol in relation to the other occurring sterols, and also that it has been reported in several works [35–37] as the most abundant sterol present in vegetable biomass (not the case for *E. crassipes*), special attention should be paid when assuming β-sitosterol as representative of the behavior of other existing sterols, whose extraction might be of interest as well.

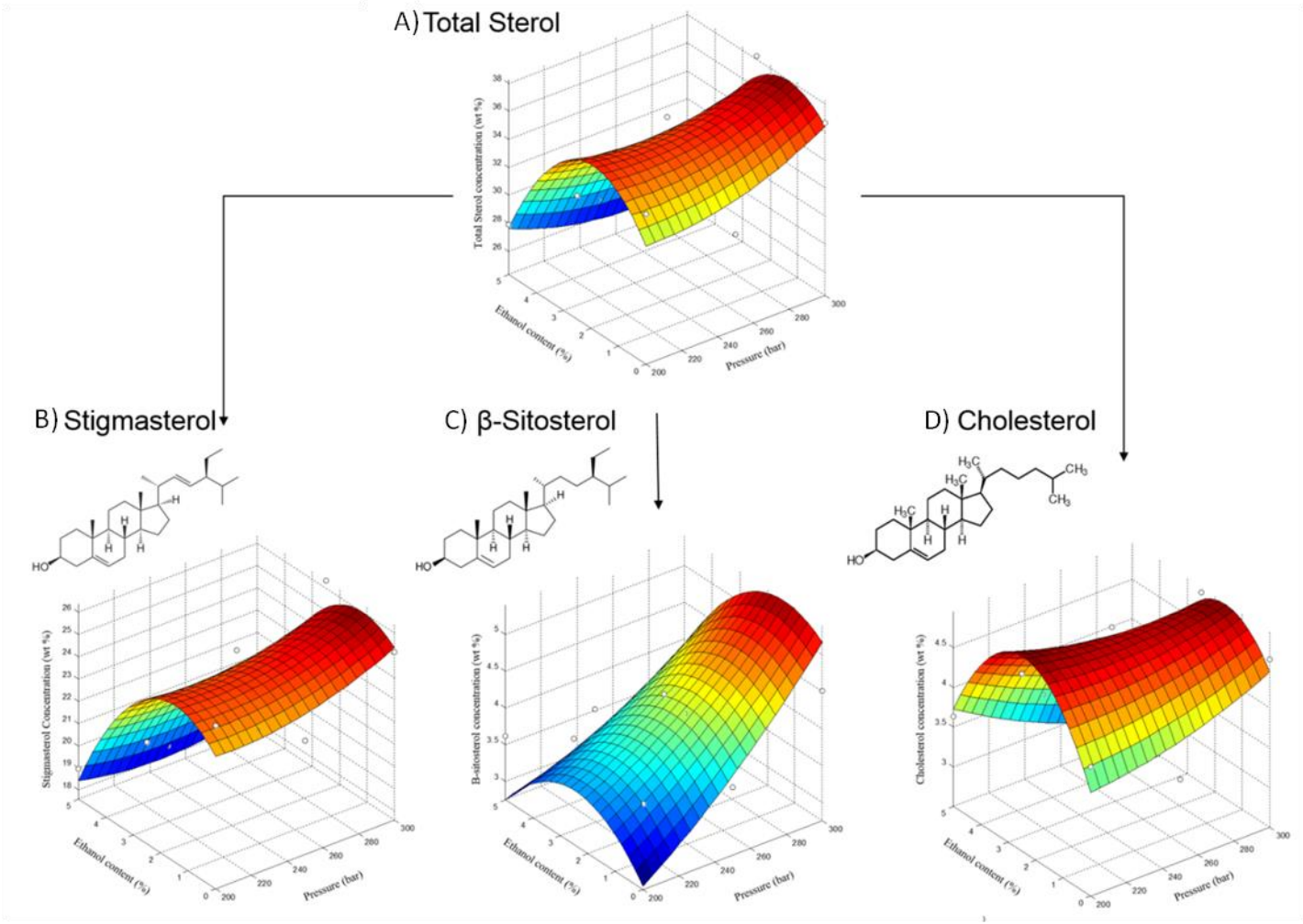

Figure 4.9 – Response surfaces showing the effects of pressure and ethanol content on the concentration of: A) total sterols, B) stigmasterol, C) β-sitosterol, and D) cholesterol. Dots are experimental data, and surfaces are given by the fitted models (Eq.(6) with the coefficients of Table 4.9), respectively.

4.4 CONCLUSIONS

***Coffea* spp. study -** In this work the optimization of the supercritical fluid extraction of spent coffee grounds (SCG) was carried out for three process variables, namely pressure (140-190 bar), temperature (40-70 ºC) and cosolvent (ethanol) content in the CO_2 stream (0-5 wt.%), using a Box-Behnken design of experiments and upon application of the response surface methodology.

The best conditions to maximize total extraction yield are 190 bar/55 ºC/5 wt.% EtOH, which lead to η_{Total}= 11.97 % ($g_{oil}/100\ g_{SCG}$). In terms of total concentration of diterpenic compounds in the supercritical extracts(C_{dit}), the optimized operating conditions are 140 bar/55 ºC/0 wt.% EtOH, providing C_{dit}= 107.44 mg g_{oil}^{-1}.

***Eichhornia crassipes* study –** The supercritical CO_2 extraction of a mixture of stalks and leaves of *E. crassipes* was carried out following a design of experiments where pressure (P) and ethanol content were the operating conditions to optimize over 200-300 bar and 0.0-5.0 wt.%, respectively. Upon application of a full factorial design of two factors and three levels, as well as the response surface methodology, total extraction yield (η_{Total}), stigmasterol yield (η_{Stigml}), total sterols concentration ($C_{TotalSterol}$), stigmasterol concentratio (C_{Stigm}), cholesterol concentration ($C_{cholest}$) and β–sitosterol concentrations ($C_{\beta-sitost}$) were modeled.

The optima conditions for η_{Total} were 250-300 bar and 5.0 wt.% ethanol, while for $\eta_{TotalSterol}$ were 300 bar and 2.5 wt.%. The latter conditions were also the most favorable to maximize $C_{TotalSterol}$, particularly C_{Stigm}. Under the referred optimum, η_{Total} = 1.25 wt.%, $\eta_{TotalSterol}$ = 0.35 wt.%, $C_{TotalSterol}$ = 38.26 wt.%, and C_{Stigm} = 26.35 wt.%. The comparative analysis of the impact of pressure and ethanol content on C_{Stigm}, $C_{cholest}$, and $C_{\beta-sitost}$ allowed to conclude that stigmasterol and cholesterol behave similarly, being particularly affected by ethanol content but not by pressure. On the other hand, β–sitosterol concentration in extracts exhibited a stronger dependence on pressure besides the influence of ethanol content.

In the whole, the reported results provide a pertinent contribution for the valorization of *E. crassipes* through the production of natural extracts with high contents of sterols, especially stigmasterol.

4.5 REFERENCES

[1] M.M.R. de Melo, A.J.D. Silvestre, C.M. Silva, Supercritical fluid extraction of vegetable matrices: Applications, trends and future perspectives of a convincing green technology, Journal of Supercritical Fluids, 92 (2014) 115-176.

[2] H.M.A. Barbosa, M.M.R. de Melo, M.A. Coimbra, C.P. Passos, C.M. Silva, Optimization of the supercritical fluid coextraction of oil and diterpenes from spent coffee grounds using experimental design and response surface methodology, Journal of Supercritical Fluids, 85 (2014) 165-172.

[3] P.F. Martins, M.M.R. de Melo, P. Sarmento, C.M. Silva, Supercritical fluid extraction of sterols from *Eichhornia crassipes* biomass using pure and modified carbon dioxide. Enhancement of stigmasterol yield and extract concentration, Journal of Supercritical Fluids, 107 (2016) 441-449.

[4] Z.R. Lazic, Design of Experiments in Chemical Engineering, John Wiley & Sons,Weinheim, , 2006.

[5] R. Mead, The Design of Experiments: Statistical Principles for Practical Applications, Cambridge University Press, Cambridge, 1990.

[6] R.K. Roy, Design of experiments using the Taguchi approach: 16 steps to product and process improvement, Wiley, USA, 2001.

[7] R.L. Mason, R.F. Gunst, J.L. Hess, Statistical Design and Analysis of Experi-ments: With Applications to Engineering and Science, Wiley, New Jersey, 2003.

[8] X. Liu, M. Zhao, J. Wang, W.E.I. Luo, Antimicrobial and antioxidant activity of emblica extracts obtained by supercritical carbon dioxide extraction and methanol extraction, Journal of Food Biochemistry, 33 (2009) 307-330.

[9] Y. Xie, J. Peng, G. Fan, Y. Wu, Chemical composition and antioxidant activity of volatiles from *Patrinia Villosa* Juss obtained by optimized supercritical fluid extraction, Journal of Pharmaceutical and Biomedical Analysis, 48 (2008) 796-801.

[10] X.L. Cao, Y.C. Ito, Supercritical fluid extraction of grape seed oil and subsequent separation of free fatty acids by high-speed counter-current chromatography, Journal of Chromatography A, 1021 (2003) 117-124.

[11] I.H. Akgun, A. Erkucuk, M. Pilavtepe, O. Yesil-Celiktas, Optimization of total alkannin yields of *Alkanna tinctoria* by using sub- and supercritical carbon dioxide extraction, Journal of Supercritical Fluids, 57 (2011) 31-37.

[12] C.L. Ye, Y.F. Lai, Supercritical CO_2 extraction optimization of onion oil using response surface methodology, Chemical Engineering & Technology, 35 (2012) 646-652.

[13] R. Li, W.-c. Chen, W.-p. Wang, W.-y. Tian, X.-g. Zhang, Extraction of essential oils from garlic (*Allium sativum*) using ligarine as solvent and its immunity activity in gastric cancer rat, Medicinal Chemistry Research, 19 (2010) 1092-1105.

[14] Q.H. Hu, Y. Hu, J. Xu, Free radical-scavenging activity of Aloe vera (*Aloe barbadensis* Miller) extracts by supercritical carbon dioxide extraction, Food Chemistry, 91 (2005) 85-90.

[15] H.Y. Ju, K.C. Huang, J.H. Chen, Y.C. Liu, C.M.J. Chang, C.C. Lee, C. Chang, C.J. Shieh, Optimization of the extraction of *Alpinia oxyphylla* essence oil in supercritical carbon dioxide, Journal of the American Oil Chemists Society, 87 (2010) 1063-1070.

[16] P. Bhattacharjee, D. Chatterjee, R.S. Singhal, Supercritical carbon dioxide extraction of squalene from *Amaranthus paniculatus*: Experiments and process characterization, Food and Bioprocess Technology, 5 (2012) 2506-2521.

[17] Q.H. Chen, P. Li, J. He, Z. Zhang, J. Liu, Supercritical fluid extraction for identification and determination of volatile metabolites from *Angelica dahurica* by GC-MS, Journal of Separation Science, 31 (2008) 3218-3224.

[18] L.Y. Huang, T.H. Zhong, T.W. Chen, Z. Ye, G.N. Chen, Identification of beta-sitosterol, stigmasterol and ergosterin in *A. roxburghii* using supercritical fluid extraction followed by liquid chromatography/atmospheric pressure chemical ioneization ion trap mass spectrometry, Rapid Communications in Mass Spectrometry, 21 (2007) 3024-3032.

[19] S. Akay, I. Alpak, O. Yesil-Celiktas, Effects of process parameters on supercritical CO_2 extraction of total phenols from strawberry (*Arbutus unedo* L.) fruits: An optimization study, Journal of Separation Science, 34 (2011) 1925-1931.

[20] S. Quispe-Condori, D. Sanchez, M.A. Foglio, P.T.V. Rosa, C. Zetzl, G. Brunner, M.A.A. Meireles, Global yield isotherms and kinetic of artemisinin extraction from *Artemisia annua* L leaves using supercritical carbon dioxide, Journal of Supercritical Fluids, 36 (2005) 40-48.

[21] C.-C. Yang, M.-R. Lee, S.-L. Hsu, C.-M.J. Chang, Supercritical fluids extraction of capillarisin from *Artemisia capillaris* and its inhibition of in vitro growth of hepatoma cells, The Journal of Supercritical Fluids, 42 (2007) 96-103.

[22] E. Ghasemi, Y. Yamini, N. Bahramifar, F. Sefidkon, Comparative analysis of the oil and supercritical CO_2 extract of *Artemisia sieberi*, Journal of Food Engineering, 79 (2007) 306-311.

[23] Q.H. Chen, P. Li, H.D. Yang, X.L. Li, J. Zhu, F.C. Chen, Identification of volatile compounds of *Atractylode lancea* Rhizoma using supercritical fluid extraction and GC-MS, Journal of Separation Science, 32 (2009) 3152-3156.

[24] K.W. Chan, M. Ismail, Supercritical carbon dioxide fluid extraction of *Hibiscus cannabinus* L. seed oil: A potential solvent-free and high antioxidative edible oil, Food Chemistry, 114 (2009) 970-975.

[25] Y. Sun, L. Wei, J. Wang, J. Bi, Z. Liu, Y. Wang, Z. Guo, Optimization of supercritical fluid extraction of saikosaponins from *Bupleurum falcatum* with orthogonal array design, Journal of Separation Science, 33 (2010) 1161-1166.

[26] Y. Kong, Y.J. Fu, Y.G. Zu, W. Liu, W. Wang, X. Hua, M. Yang, Ethanol modified supercritical fluid extraction and antioxidant activity of cajaninstilbene acid and pinostrobin from pigeonpea [*Cajanus cajan* (L.) Millsp.] leaves, Food Chemistry, 117 (2009) 152-159.

[27] Y.F. Wang, D. Sun, H. Chen, L.S. Qian, P. Xu, Fatty acid composition and antioxidant activity of tea (*Camellia sinensis* L.) seed oil extracted by optimized supercritical carbon dioxide, International Journal of Molecular Sciences, 12 (2011) 7708-7719.

[28] W.-Q. Tang, D.-C. Li, Y.-X. Lv, J.-G. Jiang, Extraction and removal of caffeine from green tea by ultrasonic-enhanced supercritical fluid, Journal of Food Science, 75 (2010) C363-C368.

[29] C. Da Porto, D. Voinovich, D. Decorti, A. Natolino, Response surface optimization of hemp seed (*Cannabis sativa* L.) oil yield and oxidation stability by supercritical carbon dioxide extraction, Journal of Supercritical Fluids, 68 (2012) 45-51.

[30] C. Duarte, M. Moldao-Martins, A.F. Gouveia, S. Beirao da Costa, A.E. Leitao, M.G. Bernardo-Gil, Supercritical fluid extraction of red pepper (*Capsicum frutescens* L.), Journal of Supercritical Fluids, 30 (2004) 155-161.

[31] A.F. Gouveia, C. Duarte, M.L.B. da Costa, M.G. Bernardo-Gil, M. Moldao-Martins, Oxidative stability of olive oil flavoured by *Capsicum frutescens* supercritical fluid extracts, European Journal of Lipid Science and Technology, 108 (2006) 421-428.

[32] A. Verma, K. Hartonen, M.L. Riekkola, Optimisation of supercritical fluid extraction of indole alkaloids from *Catharanthus roseus* using experimental design methodology-comparison with other extraction techniques, Phytochemical Analysis, 19 (2008) 52-63.

[33] M.G. Bernardo-Gil, R. Roque, L.B. Roseiro, L.C. Duarte, F. Girio, P. Esteves, Supercritical extraction of carob kibbles (*Ceratonia siliqua* L.), Journal of Supercritical Fluids, 59 (2011) 36-42.

[34] K.L. Nyam, C.P. Tan, O.M. Lai, K. Long, Y.B.C. Man, Optimization of supercritical CO_2 extraction of phytosterol-enriched oil from Kalahari melon seeds, Food and Bioprocess Technology, 4 (2011) 1432-1441.

[35] J.Z. He, P. Shao, J.H. Liu, Q.M. Ru, Supercritical carbon dioxide extraction of flavonoids from Pomelo (*Citrus grandis* (L.) Osbeck) peel and their antioxidant activity, International Journal of Molecular Sciences, 13 (2012) 13065-13078.

[36] J. Yu, D.V. Dandekar, R.T. Toledo, R.K. Singh, B.S. Patil, Supercritical fluid extraction of limonoids and naringin from grapefruit (*Citrus paradisi* Macf.) seeds, Food Chemistry, 105 (2007) 1026-1031.

[37] S. Lim, S.K. Jung, M.K. Jwa, Extraction of carotenoids from *Citrus unshiu* press cake by supercritical carbon dioxide, Food Sci Biotechnol, 12 (2003) 513 - 520.

[38] J.M.A. Araujo, D. Sandi, Extraction of coffee diterpenes and coffee oil using supercritical carbon dioxide, Food Chemistry, 101 (2006) 1087-1094.

[39] S.G. Ozkal, M.E. Yener, U. Salgin, U. Mehmetoglu, Response surfaces of hazelnut oil yield in supercritical carbon dioxide, European Food Research and Technology, 220 (2005) 74-78.

[40] M.G. Bernardo-Gil, J. Grenha, J. Santos, P. Cardoso, Supercritical fluid extraction and characterisation of oil from hazelnut, European Journal of Lipid Science and Technology, 104 (2002) 402-409.

[41] X.L. Cao, Y. Tian, T.Y. Zhang, Y. Ito, Supercritical fluid extraction of catechins from *Cratoxylum prunifolium* Dyer and subsequent purification by high-speed counter-current chromatography, Journal of Chromatography A, 898 (2000) 75-81.

[42] P. Mitra, H.S. Ramaswamy, K.S. Chang, Pumpkin (*Cucurbita maxima*) seed oil extraction using supercritical carbon dioxide and physicochemical properties of the oil, Journal of Food Engineering, 95 (2009) 208-213.

[43] G. Began, M. Goto, A. Kodama, T. Hirose, Response surfaces of total oil yield of turmeric (*Curcuma longa*) in supercritical carbon dioxide, Food Research International, 33 (2000) 341-345.

[44] J. Shi, C. Yi, X. Ye, S. Xue, Y. Jiang, Y. Ma, D. Liu, Effects of supercritical CO_2 fluid parameters on chemical composition and yield of carotenoids extracted from pumpkin, LWT - Food Science and Technology, 43 (2010) 39-44.

[45] B. Daneshvand, K.M. Ara, F. Raofie, Comparison of supercritical fluid extraction and ultrasound-assisted extraction of fatty acids from quince (*Cydonia oblonga* Miller) seed using response surface methodology and central composite design, Journal of Chromatography A, 1252 (2012) 1-7.

[46] Y.S. Sun, Z.B. Liu, J.H. Wang, W. Tian, H.Y. Zhou, L.X. Zhu, C.L. Zhang, Supercritical fluid extraction of paeonol from *Cynanchum paniculatum* (Bge.) Kitag. and subsequent isolation by high-speed counter-current chromatography coupled with high-performance liquid chromatography-photodiode array detector, Separation and Purification Technology, 64 (2008) 221-226.

[47] M. Khajeh, Optimisation of supercritical fluid extraction of essential oil components of *Diplotaenia cachrydifolia*: Box-Behnken design, Natural Product Research, 26 (2012) 1926-1930.

[48] R. Davarnejad, K.M. Kassim, A. Zainal, S.A. Sata, Supercritical fluid extraction of beta-carotene from crude palm oil using CO_2, Journal of Food Engineering, 89 (2008) 472-478.

[49] E. Talansier, M.E.M. Braga, P.T.V. Rosa, D. Paolucci-Jeanjean, M.A.A. Meireles, Supercritical fluid extraction of vetiver roots: A study of SFE kinetics, The Journal of Supercritical Fluids, 47 (2008) 200-208.

[50] S.A.O. Santos, J.J. Villaverde, C.M. Silva, C.P. Neto, A.J.D. Silvestre, Supercritical fluid extraction of phenolic compounds from *Eucalyptus globulus* Labill bark, Journal of Supercritical Fluids, 71 (2012) 71-79.

[51] R.M.A. Domingues, M.M.R. de Melo, E.L.G. Oliveira, C.P. Neto, A.J.D. Silvestre, C.M. Silva, Optimization of the supercritical fluid extraction of triterpenic acids from *Eucalyptus globulus* bark using experimental design, Journal of Supercritical Fluids, 74 (2013) 105-114.

[52] W. Guan, S. Li, R. Yan, S. Tang, C. Quan, Comparison of essential oils of clove buds extracted with supercritical carbon dioxide and other three traditional extraction methods, Food Chemistry, 101 (2007) 1558-1564.

[53] X. Wang, C. Li, Y. Wang, T.-X. Cai, *n*-Heptane isomerization over mesoporous MoOx and Ni–MoOx catalysts, Catalysis Today, 93–95 (2004) 135-140.

[54] A.S. Zarena, N.M. Sachindra, K.U. Sankar, Optimisation of ethanol modified supercritical carbon dioxide on the extract yield and antioxidant activity from *Garcinia mangostana* L., Food Chemistry, 130 (2012) 203-208.

[55] C. Yang, Y.R. Xu, W.X. Yao, Extraction of pharmaceutical components from *Ginkgo biloba* leaves using supercritical carbon dioxide, Journal of Agricultural and Food Chemistry, 50 (2002) 846-849.

[56] S. Jokic, Z. Zekovic, S. Vidovic, R. Sudar, I. Nemet, M. Bilic, D. Velic, Supercritical CO_2 extraction of soybean oil: process optimisation and triacylglycerol composition, International Journal of Food Science and Technology, 45 (2010) 1939-1946.

[57] P. Bhattacharjee, R.S. Singhal, S.R. Tiwari, Supercritical carbon dioxide extraction of cottonseed oil, Journal of Food Engineering, 79 (2007) 892-898.

[58] L. Casas, C. Mantell, M. Rodriguez, A. Torres, F.A. Macias, E.M. de la Ossa, Effect of the addition of cosolvent on the supercritical fluid extraction of bioactive compounds from *Helianthus annuus* L., Journal of Supercritical Fluids, 41 (2007) 43-49.

[59] L.D. Kagliwal, A.S. Pol, S.C. Patil, R.S. Singhal, V.B. Patravale, Antioxidant-rich extract from dehydrated seabuckthorn berries by supercritical carbon dioxide extraction, Food and Bioprocess Technology, 5 (2012) 2768-2776.

[60] L.D. Kagliwal, S.C. Patil, A.S. Pol, R.S. Singhal, V.B. Patravale, Separation of bioactives from seabuckthorn seeds by supercritical carbon dioxide extraction methodology through solubility parameter approach, Separation and Purification Technology, 80 (2011) 533-540.

[61] H. Kazazi, K. Rezaei, S.J. Ghotb-Sharif, Z. Emam-Djomeh, Y. Yamini, Supercriticial fluid extraction of flavors and fragrances from *Hyssopus officinalis* L. cultivated in Iran, Food Chemistry, 105 (2007) 805-811.

[62] G.L. Li, Z.W. Sun, L.A. Xia, J.Y. Shi, Y.J. Liu, Y.R. Suo, J.M. You, Supercritical CO_2 oil extraction from Chinese star anise seed and simultaneous compositional analysis using HPLC by fluorescence detection and online atmospheric CI-MS identification, Journal of the Science of Food and Agriculture, 90 (2010) 1905-1913.

[63] W.H. Chen, C.H. Chen, C.M.J. Chang, Y.H. Chiu, D. Hsiang, Supercritical carbon dioxide extraction of triglycerides from *Jatropha curcas* L. seeds, Journal of Supercritical Fluids, 51 (2009) 174-180.

[64] S.M. Ghoreishi, H. Kamali, H.S. Ghaziaskar, A.A. Dadkhah, Optimization of supercritical extraction of linalyl acetate from lavender via Box-Behnken design, Chemical Engineering & Technology, 35 (2012) 1641-1648.

[65] L.T. Danh, D.A.T. Ngo, T.N.H. Le, J. Zhao, R. Mammucari, N. Foster, Antioxidant activity, yield and chemical composition of lavender essential oil extracted by supercritical CO_2, Journal of Supercritical Fluids, 70 (2012) 27-34.

[66] S. Santoyo, S. Cavero, L. Jaime, E. Ibanez, F.J. Senorans, G. Reglero, Supercritical carbon dioxide extraction of compounds with antimicrobial activity from *Origanum vulgare* L.:

Determination of optimal extraction parameters, Journal of Food Protection, 69 (2006) 369-375.

[67] W. Xu, K.D. Chu, H. Li, L.D. Chen, Y.Q. Zhang, X.C. Tang, Extraction of *Lepidium apetalum* seed oil using supercritical carbon dioxide and anti-oxidant activity of the extracted oil, Molecules, 16 (2011) 10029-10045.

[68] S.G. Ozkal, Response surface analysis and modeling of flaxseed oil yield in supercritical carbon dioxide, Journal of the American Oil Chemists Society, 86 (2009) 1129-1135.

[69] L.M. Comin, F. Temelli, M.A. Saldana, Supercritical CO_2 extraction of flax lignans, Journal of the American Oil Chemists Society, 88 (2011) 707-715.

[70] B. Bozan, F. Temelli, Supercritical CO_2 extraction of flaxseed, Journal of the American Oil Chemists Society, 79 (2002) 231-235.

[71] J. Liu, S.Y. Lin, Z.Z. Wang, C.N. Wang, E.L. Wang, Y. Zhang, J.B. Liu, Supercritical fluid extraction of flavonoids from *Maydis stigma* and its nitrite-scavenging ability, Food and Bioproducts Processing, 89 (2011) 333-339.

[72] K. Ansari, I. Goodarznia, Optimization of supercritical carbon dioxide extraction of essential oil from spearmint (*Mentha spicata* L.) leaves by using Taguchi methodology, Journal of Supercritical Fluids, 67 (2012) 123-130.

[73] M. Bimakr, R.A. Rahman, A. Ganjloo, F.S. Taip, L.M. Salleh, M.Z.I. Sarker, Optimization of supercritical carbon dioxide extraction of bioactive flavonoid compounds from spearmint (*Mentha spicata* L.) leaves by using response surface methodology, Food and Bioprocess Technology, 5 (2012) 912-920.

[74] S. Lina, R. Fei, Z. Xudong, D. Yangong, H. Fa, Supercritical carbon dioxide extraction of *Microula sikkimensis* seed oil, Journal of the American Oil Chemists' Society, 87 (2010) 1221-1226.

[75] B. Shan, J.H. Xie, J.H. Zhu, Y. Peng, Ethanol modified supercritical carbon dioxide extraction of flavonoids from *Momordica charantia* L. and its antioxidant activity, Food and Bioproducts Processing, 90 (2012) 579-587.

[76] H.N. Nguyen, P.A.D. Gaspillo, J.B. Maridable, R.M. Malaluan, H. Hinode, C. Salim, H.K.P. Huynh, Extraction of oil from *Moringa oleifera* kernels using supercritical carbon dioxide with ethanol for pretreatment: Optimization of the extraction process, Chemical Engineering and Processing, 50 (2011) 1207-1213.

[77] E. Ghasemi, F. Raofie, N.M. Najafi, Application of response surface methodology and central composite design for the optimisation of supercritical fluid extraction of essential oils from *Myrtus communis* L. leaves, Food Chemistry, 126 (2011) 1449-1453.

[78] M. Khajeh, Y. Yamini, S. Shariati, Comparison of essential oils compositions of *Nepeta persica* obtained by supercritical carbon dioxide extraction and steam distillation methods, Food and Bioproducts Processing, 88 (2010) 227-232.

[79] M. Fullana, F. Trabelsi, F. Recasens, Use of neural net computing for statistical and kinetic modelling and simulation of supercritical fluid extractors, Chemical Engineering Science, 55 (2000) 79-95.

[80] Z. Solati, B.S. Baharin, H. Bagheri, Supercritical carbon dioxide (SC-CO_2) extraction of *Nigella sativa* L. oil using full factorial design, Industrial Crops and Products, 36 (2012) 519-523.

[81] A. de Lucas, J. Rincón, I. Gracia, Influence of operating variables on yield and quality parameters of olive husk oil extracted with supercritical carbon dioxide, Journal of the American Oil Chemists' Society, 79 (2002) 237-243.

[82] A. de Lucas, E.M. de la Ossa, J. Rincon, M.A. Blanco, I. Gracia, Supercritical fluid extraction of tocopherol concentrates from olive tree leaves, Journal of Supercritical Fluids, 22 (2002) 221-228.

[83] S. Stavroulias, C. Panayiotou, Determination of optimum conditions for the extraction of squalene from olive pomace with supercritical CO_2, Chemical and Biochemical Engineering Quarterly, 19 (2005) 373-381.

[84] C. Ma, G. Li, J. Zhang, Q. Zheng, X. Fan, Z. Wang, An efficient combination of supercritical fluid extraction and high-speed counter-current chromatography to extract and purify homoisoflavonoids from *Ophiopogon japonicus* (Thunb.) Ker-Gawler, Journal of Separation Science, 32 (2009) 1949-1956.

[85] W. Liu, Y.-J. Fu, Y.-G. Zu, M.-H. Tong, N. Wu, X.-L. Liu, S. Zhang, Supercritical carbon dioxide extraction of seed oil from *Opuntia dillenii* Haw. and its antioxidant activity, Food Chemistry, 114 (2009) 334-339.

[86] E. Vági, E. Rapavi, M. Hadolin, K. Vásárhelyiné Perédi, A. Balázs, A. Blázovics, B. Simándi, Phenolic and triterpenoid antioxidants from *Origanum majorana* L. herb and extracts obtained with different solvents, Journal of Agricultural and Food Chemistry, 53 (2005) 17-21.

[87] H. Kubat, U. Akman, O. Hortacsu, Semi-batch packed-column deterpenation of origanum oil by dense carbon dioxide, Chemical Engineering and Processing, 40 (2001) 19-32.

[88] A. Sheibani, H.S. Ghaziaskar, Pressurized fluid extraction of pistachio oil using a modified supercritical fluid extractor and factorial design for optimization, LWT - Food Science and Technology, 41 (2008) 1472-1477.

[89] S.G. Ozkal, M.E. Yener, L. Bayindirli, Response surfaces of apricot kernel oil yield in supercritical carbon dioxide, Lwt-Food Science and Technology, 38 (2005) 611-616.

[90] I.S. Sanal, E. Bayraktar, U.U. Mehmetoglu, A. Calimli, Determination of optimum conditions for SC-(CO_2 plus ethanol) extraction of beta-carotene from apricot pomace using response surface methodology, Journal of Supercritical Fluids, 34 (2005) 331-338.

[91] G. Bernardo-Gil, C. Oneto, P. Antunes, M.F. Rodrigues, J.M. Empis, Extraction of lipids from cherry seed oil using supercritical carbon dioxide, European Food Research and Technology, 212 (2001) 170-174.

[92] İ.H. Adil, M.E. Yener, A. Bayındırlı, Extraction of total phenolics of sour cherry pomace by high pressure solvent and subcritical Fluid and determination of the antioxidant activities of the extracts, Separation Science and Technology, 43 (2008) 1091-1110.

[93] L. Wang, B. Yang, X. Du, C. Yi, Optimisation of supercritical fluid extraction of flavonoids from *Pueraria lobata*, Food Chemistry, 108 (2008) 737-741.

[94] G. Liu, X. Xu, Q. Hao, Y. Gao, Supercritical CO_2 extraction optimization of pomegranate (*Punica granatum* L.) seed oil using response surface methodology, LWT - Food Science and Technology, 42 (2009) 1491-1495.

[95] J.M. Del Valle, S. Bello, J. Thiel, A. Allen, L. Chordia, Comparison of conventional and supercritical CO_2-extracted rosehip oil, Brazilian Journal of Chemical Engineering, 17 (2000) 335-348.

[96] L. Wang, Y. Song, Y. Cheng, X. Liu, Orthogonal array design for the optimization of supercritical fluid extraction of tanshinones from Danshen, Journal of Separation Science, 31 (2008) 321-328.

[97] M. Khajeh, Optimization of process variables for essential oil components from *Satureja hortensis* by supercritical fluid extraction using Box-Behnken experimental design, The Journal of Supercritical Fluids, 55 (2011) 944-948.

[98] Y. Chang, B. Liu, B. Shen, Orthogonal array design for the optimization of supercritical fluid extraction of baicalin from roots of *Scutellaria baicalensis* Georgi, Journal of Separation Science, 30 (2007) 1568-1574.

[99] C. Yi, J. Shi, S.J. Xue, Y.M. Jiang, D. Li, Effects of supercritical fluid extraction parameters on lycopene yield and antioxidant activity, Food Chemistry, 113 (2009) 1088-1094.

[100] L.S. Kassama, J. Shi, G.S. Mittal, Optimization of supercritical fluid extraction of lycopene from tomato skin with central composite rotatable design model, Separation and Purification Technology, 60 (2008) 278-284.

[101] E. Vági, B. Simándi, K.P. Vásárhelyiné, H. Daood, Á. Kéry, F. Doleschall, B. Nagy, Supercritical carbon dioxide extraction of carotenoids, tocopherols and sitosterols from industrial tomato by-products, Journal of Supercritical Fluids, 40 (2007) 218-226.

[102] W. Huang, Z. Li, H. Niu, D. Li, J. Zhang, Optimization of operating parameters for supercritical carbon dioxide extraction of lycopene by response surface methodology, Journal of Food Engineering, 89 (2008) 298-302.

[103] J.Y. Ling, G.Y. Zhang, Z.J. Cui, C.K. Zhang, Supercritical fluid extraction of quinolizidine alkaloids from *Sophora flavescens* Ait. and purification by high-speed counter-current chromatography, Journal of Chromatography A, 1145 (2007) 123-127.

[104] A. Erkucuk, I.H. Akgun, O. Yesil-Celiktas, Supercritical CO_2 extraction of glycosides from *Stevia rebaudiana* leaves: Identification and optimization, The Journal of Supercritical Fluids, 51 (2009) 29-35.

[105] B. Simándi, S.T. Kristo, Á. Kéry, L.K. Selmeczi, I. Kmecz, S. Kemény, Supercritical fluid extraction of dandelion leaves, The Journal of Supercritical Fluids, 23 (2002) 135-142.

[106] S. Sonsuzer, S. Sahin, L. Yilmaz, Optimization of supercritical CO_2 extraction of *Thymbra spicata* oil, The Journal of Supercritical Fluids, 30 (2004) 189-199.

[107] M. Moldao-Martins, A. Palavra, M.L.B. da Costa, M.G. Bernardo-Gil, Supercritical CO_2 extraction of *Thymus zygis* L. subsp *sylvestris* aroma, Journal of Supercritical Fluids, 18 (2000) 25-34.

[108] S.M. Ghoreishi, E. Bataghva, A.A. Dadkhah, Response surface optimization of essential oil and diosgenin extraction from *Tribulus terrestris* via supercritical fluid technology, Chemical Engineering & Technology, 35 (2012) 133-141.

[109] R. Yang, H. Wang, N. Jing, C. Ding, Y. Suo, J. You, *Trigonella foenum-graecum* L. seed oil obtained by supercritical CO_2 extraction, Journal of the American Oil Chemists' Society, 89 (2012) 2269-2278.

[110] N. Gelmez, N.S. Kincal, M.E. Yener, Optimization of supercritical carbon dioxide extraction of antioxidants from roasted wheat germ based on yield, total phenolic and tocopherol contents, and antioxidant activities of the extracts, Journal of Supercritical Fluids, 48 (2009) 217-224.

[111] L.T. Danh, R. Mammucari, P. Truong, N. Foster, Response surface method applied to supercritical carbon dioxide extraction of *Vetiveria zizanioides* essential oil, Chemical Engineering Journal, 155 (2009) 617-626.

[112] L.T. Danh, P. Truong, R. Mammucari, N. Foster, Extraction of vetiver essential oil by ethanol-modified supercritical carbon dioxide, Chemical Engineering Journal, 165 (2010) 26-34.

[113] D. Cossuta, B. Simándi, E. Vági, J. Hohmann, A. Prechl, É. Lemberkovics, Á. Kéry, T. Keve, Supercritical fluid extraction of *Vitex agnus* castus fruit, The Journal of Supercritical Fluids, 47 (2008) 188-194.

[114] K. Ghafoor, F.Y. AL-Juhaimi, Y.H. Choi, Supercritical fluid extraction of phenolic compounds and antioxidants from Grape (*Vitis labrusca* B.) seeds, Plant Foods for Human Nutrition, 67 (2012) 407-414.

[115] M. Palma, L.T. Taylor, B.W. Zoecklein, L.S. Douglas, Supercritical fluid extraction of grape glycosides, Journal of Agricultural and Food Chemistry, 48 (2000) 775-779.

[116] S. Zhang, Y.-G. Zu, Y.-J. Fu, M. Luo, W. Liu, J. Li, T. Efferth, Supercritical carbon dioxide extraction of seed oil from yellow horn (*Xanthoceras sorbifolia* Bunge.) and its anti-oxidant activity, Bioresource Technology, 101 (2010) 2537-2544.

[117] Y. Zhannan, L. Shiqiong, P. Quancai, Z. Chao, Y. Zhengwen, GC-MS analysis of the essential oil of coral ginger (*Zingiber corallinum* Hance) rhizome obtained by supercritical fluid extraction and steam distillation extraction, Chromatographia, 69 (2009) 785.

[118] K.C. Zancan, M.O.M. Marques, A.J. Petenate, M.A.M. Meireles, Extraction of ginger (*Zingiber officinale* Roscoe) oleoresin with CO_2 and co-solvents: a study of the antioxidant action of the extracts, Journal of Supercritical Fluids, 24 (2002) 57-76.

[119] J. Lawson, Design and analysis of experiments with examples of SAS, Taylor& Francis, USA, 2010.

[120] I. Forrest, W. Breyfogle, Implementing six sigma: Smarter solutions using statistical methods, John Wiley & Sons, New Jersey, 2003.

[121] A. de Lucas, J. Rincón, I. Gracia, Influence of operation variables on quality parameters of olive husk oil extracted with CO_2: Three-step sequential extraction, Journal of the American Oil Chemists' Society, 80 (2003) 181-188.

[122] G. Franceschini, S. Macchietto, Model-based design of experiments for parameter precision: State of the art, Chemical Engineering Science, 63 (2008) 4846-4872.

[123] A. Illy, R. Viani, Expresso Coffee - The chemistry of quality, London, 1995.

[124] C.P. Passos, R.M. Silva, F.A. Da Silva, M.A. Coimbra, C.M. Silva, Supercritical fluid extraction of grape seed (*Vitis vinifera* L.) oil. Effect of the operating conditions upon oil composition and antioxidant capacity, Chemical Engineering Journal, 160 (2010) 634-640.

[125] C.P. Passos, R.M. Silva, F.A. Da Silva, M.A. Coimbra, C.M. Silva, Enhancement of the supercritical fluid extraction of grape seed oil by using enzymatically pre-treated seed, Journal of Supercritical Fluids, 48 (2009) 225-229.

[126] I.S. Amorim, E.B. Ferreira, R.R. Lima, R.G.F.A. Pereira, Monte Carlo based test for inferring about the unidimensionality of a Brazilian coffee sensory panel, Food Quality and Preference, 21 (2010) 319-323.

[127] R.F. Rodrigues, A.K. Tashima, R.M.S. Pereira, R.S. Mohamed, F.A. Cabral, Coumarin solubility and extraction from emburana (*Torresea cearensis*) seeds with supercritical carbon dioxide, Journal of Supercritical Fluids, 43 (2008) 375-382.

[128] D.J.S. Patinha, R.M.A. Domingues, J.J. Villaverde, A.M.S. Silva, C.M. Silva, C.S.R. Freire, C. Pascoal Neto, A.J.D. Silvestre, Lipophilic extractives from the bark of *Eucalyptus grandis x globulus*, a rich source of methyl morolate: Selective extraction with supercritical CO_2, Industrial Crops and Products, 43 (2013) 340-348.

[129] R.M.A. Domingues, E.L.G. Oliveira, C.S.R. Freire, R.M. Couto, P.C. Simões, C.P. Neto, A.J.D. Silvestre, C.M. Silva, Supercritical fluid extraction of *Eucalyptus globulus* bark – a promising approach for triterpenoids production, International Journal of Molecular Sciences, *13(6),* (2012) *7648-7662*.

[130] D.C. Montgomery, Design and analysis of experiments, 5 ed., New York, 2001.

[131] R.C.E. Dias, S.T. Alves, M.d.T. Benassi, Spectrophotometric method for quantification of kahweol in coffee, Journal of Food Composition and Analysis, 31 (2013) 137-143.

[132] R.P. Silva, M.M.R. de Melo, A.J.D. Silvestre, C.M. Silva, Polar and lipophilic extracts characterization of roots, stalks, leaves and flowers of water hyacinth (Eichhornia crassipes), and insights for its future valorization, Industrial Crops and Products, 76 (2015) 1033-1038.

[133] P.S. Pião, L.M.X. Lopes, I.R. Nascimento, Esteróides e um nucleosídeo da macrófita fitoremediadora *Eicchornia crassipes* (Pontederiaceae), Araraquara, in, 2010.

[134] P.U. Rani, K. Jamil, Effect of water hyacinth leaf extract on mortality, growth and metamorphosis of certain pests of stored products, Insect Science and Its Application, 10 (1989) 327-332.

[135] K.S. Pitzer, D.R. Schreiber, Improving equation-of-state accuracy in the critical region - Equations for carbon-dioxide and neopentane as examples, Fluid Phase Equilibria, 41 (1988) 1-17.

[136] V.V. Altunin, M. Sakhabetdinov, Viscosity of Liquid and Gaseous Carbon-Dioxide at Temperatures of 220-1300 K and Pressures up to 1200 Bar, Thermal Engineering, 19 (1972) 124-129.

[137] C.D. Saquing, F.P. Lucien, N.R. Foster, Steric effects and preferential interactions in supercritical carbon dioxide, Industrial & Engineering Chemistry Research, 37 (1998) 4190-4197.

5 MEASUREMENT OF EXTRACTION CURVES

This chapter comprehends experimental results published by the author in three different articles [1-3], namely on the SFE of Quercus cerris cork [3], of Eichhornia crassipes biomass [2], and spent coffee grounds from Coffea spp. *[1]. These works focus the measurement of SFE curves of these natural matrices, including the profiles of target compounds found in each biomass sample.*

CHAPTER OUTLINE

5.1 INTRODUCTION

Extraction curves are vital for the correct assessment of SFE kinetics, as they allow the disclosure of different extraction regimes (characterized by distinct extraction rates) and thus the inspection of the mechanisms that govern the separation in different stages of the process.

If a low interstitial velocity (low flow rate) is chosen, the film resistance and/or the accumulation in the bulk may prevail over intraparticle diffusion and solubility issues, thus diminishing the rate of extraction by itself. On the other hand, if the extractor is being run under increasing interstitial velocities, the most representative limitations may become solubility and/or intraparticle diffusion. Nonetheless, high velocities may also lead to a misuse of SC-CO_2 that will then be spent in excess at the expenses of non-optimized utility and energy costs. This aspect is important to increase the economic viability of a SFE unit.

Figure 5.1 illustrates an optimization of flow rate by graphing cumulative curves of total extraction yield of *E. globulus* bark measured at 200 bar, 40 °C, with 5 % (wt.) of ethanol, for different CO_2 flow rates [4]: 6, 12 and 14 g min^{-1}. When Q_{CO2} is doubled from 6 to 12 g min^{-1} a relevant enhancement of the extraction rate is observed. An additional increase to 14 g min^{-1} shows no further significant yield enhancement. As a result, it was considered that 12 g min^{-1} is an optimized value for SFE flow rate since it originates an interstitial velocity that maximizes the rate of extraction while simultaneously minimizes utilities and energy costs. This is an elucidative example of a rational selection of a flow rate value.

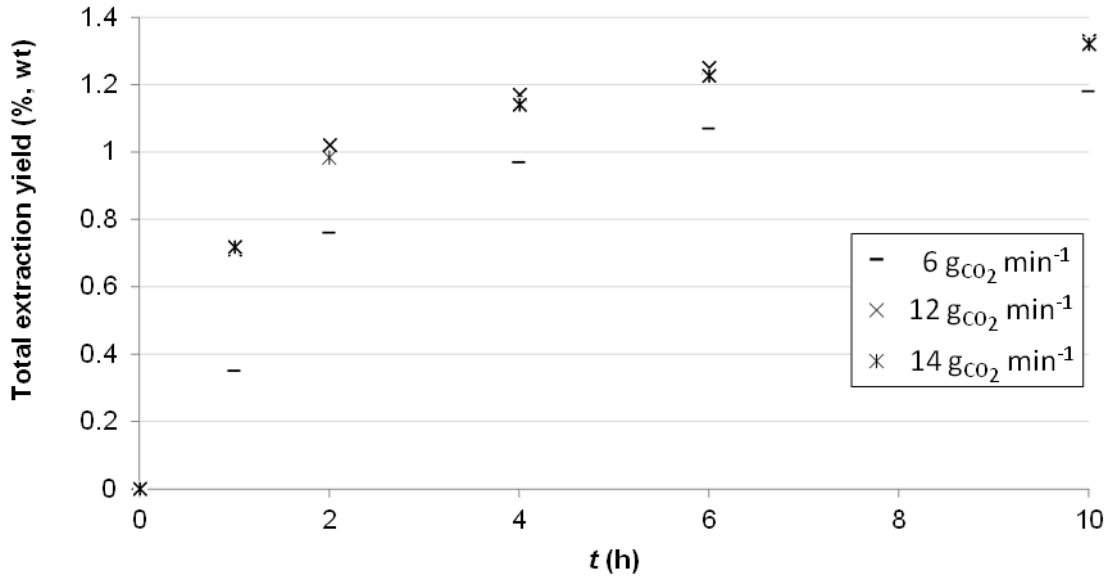

Figure 5.1 - Cumulative curves of total extraction yield of *E. globulus* bark at different CO_2 flow rates. Fixed conditions: 200 bar, 40 °C, 5 % (wt.) ethanol. Data taken from [4].

In fact, taking into account empirical correlations of the type $\mathrm{Sh} = \alpha\,\mathrm{Re}^{\beta}\mathrm{Sc}^{\gamma}$, the ratio of convective values (k_f) of runs *i* and *j* can be estimated in terms of fluid velocities (u) or mass flow rates (Q_{CO_2}) ratios by:

$$\frac{(k_f)_i}{(k_f)_f} = \left(\frac{u_i}{u_j}\right)^{\beta} = \left(\frac{Q_{CO_2,i}}{Q_{CO_2,j}}\right)^{\beta} \quad (1)$$

In some works $\beta = 0.8$ [5-8], for which the convective coefficients ratios reach 1.74 and 1.13 for 6-12 g min^{-1} and 12-14 g min^{-1} jumps, respectively. In both cases the increments of k_f are significant but in the second case no improvement was observed in the extraction yield which proves the elimination of the film. At this stage, the process gets centered on intraparticle diffusion and solutes solubility, and makes additional flow rate increments useless for the goal of extraction, as Figure 5.2 evidences.

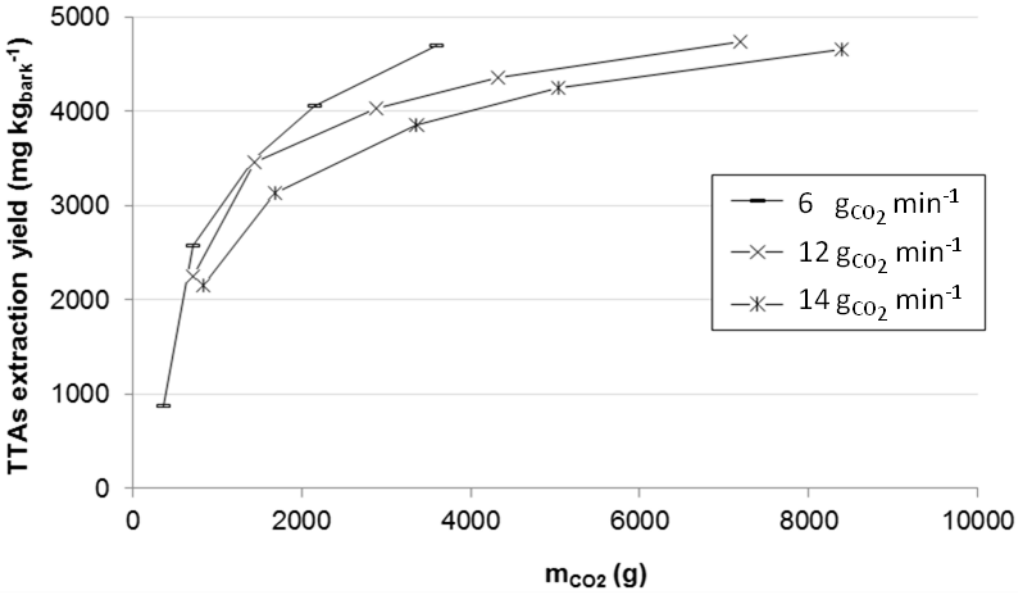

Figure 5.2 - Cumulative curves of triterpenic acids (TTAs) extraction yield of *E. globulus* bark plotted as function of mass of spent CO_2 for three different flow rates. Fixed conditions: 200 bar, 40 °C, 5 % (wt.) ethanol [4].

In light of the aforementioned remarks, this chapter is devoted to the experimental measurement of supercritical extraction curves, including the analysis of the impact of different operating conditions on the kinetic and cumulative profiles. The furnished curves are then revisited in the next chapter for modeling purposes, namely for phenomenological insights.

Accordingly, the experimental work presented in this chapter is systematized in three different studies, as follows:

***Quercus cerris* study** [3] – In this work, the supercritical fluid extraction of *Q. cerris* cork was carried out in order to measure cumulative curves for both total and friedelin extraction yields. The influence of particle size and ethanol (CO_2 modifier) content were assessed in the ranges of coarse particles to >80 mesh size, and 0–5 wt.%. For this, pressure, temperature, and flow rate were kept constant at 300 bar, 50 °C and 11 g min^{-1}.

***Eichhornia crassipes* study** [2] – In this article a preliminary study on the potential of SFE of *E. crassipes* as a privileged source of stigmasterol is presented, aiming at the analysis of the process sensitivity to temperature, cosolvent and run time conditions. In addition, taking advantage of the insights obtained through the optimization study presented in Chapter 4 of this thesis, SFE curves of *Eichhornia crassipes* were measured for different pressure (200, 250, and 300 bar), ethanol content (0 and 5 wt.%), and CO_2 flow rate (5.0, 7.5 and 10.0 g min^{-1}) conditions, and studied in terms of total (η_{total}) and stigmasterol ($\eta_{stigmasterol}$) extraction yields.

***Coffea* spp. study** [1] - Extraction curves were measured taking into account the trends unveiled by the design of experiments and response surface analysis (presented in Chapter 4), namely that ethanol does decrease diterpenes concentration, temperature exhibits a soft influence, and pressure is an important factor (lower values are desirable). Therefore, the selected operating conditions were the following: pure CO_2 at minimum and maximum pressures, 140 bar and 190 bar, respectively, and an intermediate temperature (55 °C).

5.2 MATERIALS AND METHODS

5.2.1 RAW MATERIALS

***Eichhornia crassipes* and *Coffea* spp. studies** – The raw materials used for this study are the same previously presented in Chapter 4, in section 4.2.1.

***Quercus cerris* study** – Bark was obtained from Kahramanmaras, Turkey, and was granulated with a hammer-type industrial mill. The resulting granules were separated by density difference in distilled water in 10 min mixing time. The floating fraction of cork-enriched granules (subsequently named cork) was dried, ground, and sieved according to the following particles sizes: coarse particles (<20 mesh), 20-40 mesh, 40-60 mesh, 60-80 mesh, and >80 mesh, which correspond to average diameters of >0.85, 0.64, 0.34, 0.22 and < 0.18 mm – see Figure 5.3. The bed densities of these samples are also given in Figure 5.3, and were determined by volumetric and gravimetric measurements to determine the volume occupied by a known mass of compressed cork sample. Soxhlet results using *Q. cerris* samples of 20-40 mesh and dichloromethane as solvent led to a total extraction yield of 4.02 wt.% and a friedelin yield of 1.05 wt.%.

In addition, the cellular morphology of the cork samples was assessed by SEM analysis using a Hitachi S4100 microscope. Previously to each analysis, aliquots of cork samples (with different particle sizes) were prepared with a gold/palladium (Au/Pd) alloy deposition. The SEM pictures are presented in Figure 5.4 for three decreasing particle sizes, i.e. coarse, 20-40 mesh and >80 mesh, using two degrees of magnification: 100x and 600x. Accordingly, the impact of grinding can be checked from the top to the bottom of Figure 5.4, with significant damaging of the external cell structures (depicted in micrographs on the left) being noticed as particles become smaller (depicted in micrographs on the right). The first relevant conclusion is the material exhibits broken cells at surface besides its internal intact cells. It has been shown that the region of open cells can outbound the surface layer [9], thus the fraction of broken cells (g) should better be obtained by fitting SFE curves, rather than by estimation of the surface layer volume [10] using SEM pictures.

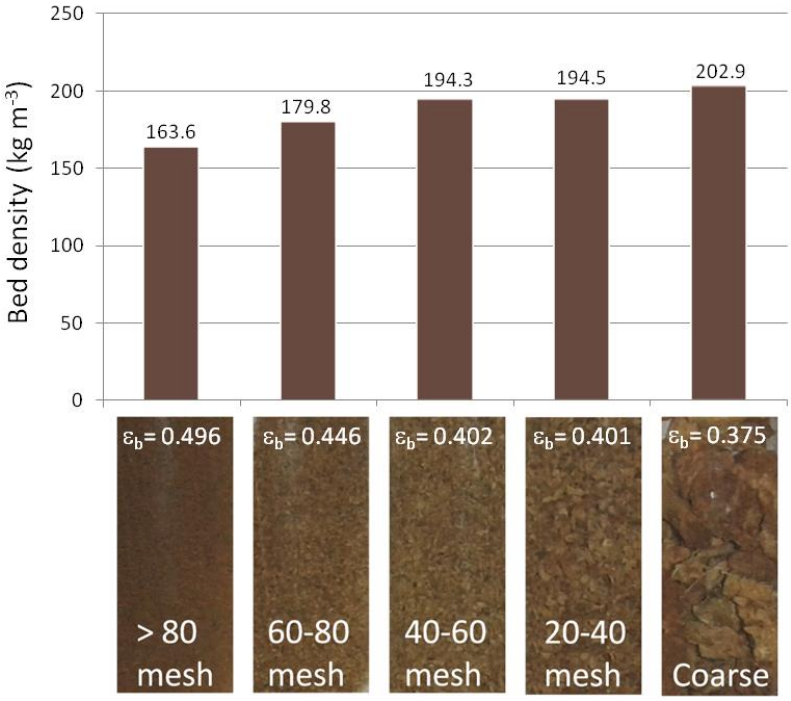

Figure 5.3 - Bed density, bed porosity, and visual aspect of cork samples with different ranges of particle size.

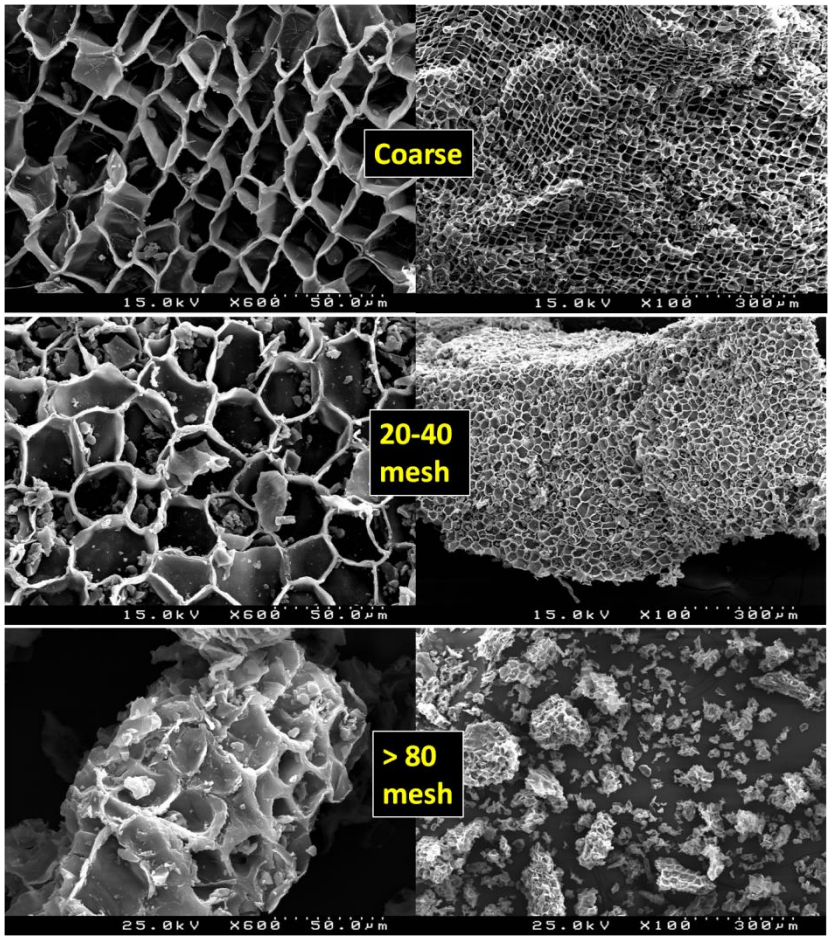

Figure 5.4 - SEM pictures of cork samples of different particle size before SFE.

5.2.2 CHEMICALS

***Quercus cerris* study –** Ursolic acid (98 % purity), betulinic acid (98 % purity), and oleanolic acid (98 % purity) were purchased from Aktin Chemicals (Chengdu, China); betulonic acid (95 % purity) was purchased from CHEMOS GmbH (Regenstauf, Germany); Pyridine (99 % purity), N,O-bis(trimethylsilyl)trifluoroacetamide (99 % purity), trimethylchlorosilane (99 % purity), and tetracosane (99 % purity) were supplied by Sigma Chemical Co. (Madrid, Spain). Ethanol (99.99 %) was supplied by Fisher Scientific. CO_2 (99.95 %) was supplied by Praxair (Porto, Portugal).

***Eichhornia crassipes* study –** These features are the same presented in section 4.2.2 (Chapter 4) for the study of this raw material.

***Coffea* spp. study -** A fatty acids methyl esters (FAME) mix (C8-C24) and methyl heptadecanoate ester were purchased from Supelco (Bellefonte, PA, USA). All other reagents used were of analytical grade or higher available purity. Carbon dioxide was supplied with a purity of 99.95 % from Praxair (Porto, Portugal).

5.2.3 SUPERCRITICAL FLUID EXTRACTION

***Quercus cerris* study –** In this work, SFE experiments were carried out using both pure and ethanol modified CO_2. The extraction was performed in a 0.5 L capacity Spe-ed™ apparatus (Applied Separations, USA) already presented in this thesis in section 3.2.3 (Chapter 3). The bed was held static through the usage of a metallic sponge on both free spaces of the extractor, together with a fine polymeric filter to ensure the particles remained in the bed.

The performed experiments and the respective operating conditions are summarized in Table 5.1. The determination of each experimental point of the various SFE curves was carried out hourly, followed by the replacement of the extract collector. In each run, an approximate load of 50 g of *Q. cerris* cork was introduced in the extractor. The densities of the supercritical fluid (SCF) are the following: 841.9 kg m^{-3} for Runs 5.1 to 5.5 (300 bar, 50 °C and 2.5 wt.% of EtOH) and 844.9 kg m^{-3} for Run 5.7 (300 bar, 50 °C and 5.0 wt.% of EtOH) interpolated from experimental data [11], and 839.0 kg m^{-3} for Run 5.6 (300 bar, 50 °C and 0 wt.% of EtOH), calculated from the relationship proposed by Pitzer and Schreiber [12]. These values are also listed in Table 5.1.

Table 5.1 – Experimental conditions of the SFE of *Q. cerris*. Pressure, temperature and flow rate were held constant in 300 bar, 50 °C and 11 $\mathrm{g\,min^{-1}}$.

Curve	w_{biomass} (g)	Particle size (mesh)	L_{b} (cm)	x_{EtOH} (wt.%)	ρ_{SCF} (kg m^{-3})
Run 5.1	45.71	> 80	5.7	2.5	841.9
Run 5.2	34.37	60-80	3.9	2.5	841.9
Run 5.3	45.72	40-60	4.8	2.5	841.9
Run 5.4	45.74	20-40	4.8	2.5	841.9
Run 5.5	45.74	Coarse	4.6	2.5	841.9
Run 5.6	45.71	20-40	4.8	0	839.0
Run 5.7	45.77	20-40	4.8	5.0	844.9

L_{b} = height of the extractor bed; x_{EtOH} = weight percentage of ethanol in the supercritical solvent (CO_2+EtOH); ρ_{SCF}= density of supercritical solvent, calculated by the model of Pitzer and Schreiber (pure CO_2) [12] and interpolated from experimental data of Pohler and Kiran (for CO_2 modified with ethanol) [11].

***Eichhornia crassipes* study –** The procedure was the same presented in section 4.2.2 (Chapter 4) for the optimization of the SFE of this raw material. In each run, an approximate load of 30 g of water hyacinth was introduced in the extractor. The bed was held static through the usage of a metallic sponge on both free space of the extractor, together with a fine polymeric filter to ensure the particles remained at the same position. The performed experiments and the respective operating conditions are summarized in Table 5.2. In addition,

the determination of each experimental point of the various SFE curves was carried out hourly, followed by the replacement of the extract collector.

Table 5.2 - Experimental conditions of the SFE runs performed in the work of SFE of *E. crassipes*. Temperature was held constant at 50 °C.

Curve	P (bar)	x_{EtOH} (wt.%)	$Q_{\mathrm{CO_2}}$ (g min^{-1})	Ref.
Run 5.8	250	0	5.0	This work
Run 5.9	250	0	7.5	This work
Run 5.10	250	0	10.0	This work
Run 5.11	200	0	7.5	This work
Run 5.12	250	5	7.5	This work
Run 5.13	300	5	7.5	[13]

***Coffea* spp. study -** The SFE experiments were carried out with carbon dioxide under semi-continuous operation in an apparatus built/assembled at the University of Aveiro. A detailed description of this equipment may be consulted elsewhere [14]. In each experiment, 60 g of dried raw material was placed inside the extractor, the flow rate used was 12 g_{CO2} min^{-1}, the temperature varied from 40 to 55 °C, and the pressure from 140 to 190 bar. The operating conditions are shown in Table 5.3, along with two runs taken from the literature [15].

It was considered acceptable to combine data from different sources because the contents of lipids and fatty acid profiles are comparable. Nevertheless they are distinguished as blocks, block A comprising Runs 5.14, 5.15, and 5.16 (this work), and block B comprising Runs 5.17 and 5.18 (data from [15]).

Table 5.3 – Operating conditions of the experiments performed in this work and taken from literature for comparison purposes.

	w_{SCG} (g)	Q_{CO2} (g min^{-1})	Q_{CO2} w_{SCG}^{-1} (h^{-1})	P (bar)	T (°C)	Ref.
Run 5.14	60	12	12	190	40	This work
Run 5.15	60	12	12	190	55	This work
Run 5.16	60	12	12	140	55	This work
Run 5.17	20	10	30	200	50	[15]
Run 5.18	20	10	30	300	50	[15]

For comparison purposes an extract of spent coffee grounds was firstly obtained by Soxhlet. An amount of 30.4 g of spent coffee grounds was placed inside the Soxhlet apparatus and treated with 300 mL of analytical grade *n*-hexane for 4 h. At the end the solvent was evaporated to

dryness and the extract was weighed and analyzed by GC–FID. The extraction was performed in triplicate.

5.2.4 EXTRACTS CHARACTERIZATION

***Quercus cerris* study –** Previously to the GC-MS analysis, approximately 20 mg of each extracted sample were converted into its trimethylsilyl (TMS) counterpart [16-17]. Each dried sample was firstly dissolved in 250 μL of pyridine containing 1 mg of tetracosane. The addition of 250 μL of N,O-bis(trimethylsilyl)trifluoroacetamide and 50 μL of trimethylsilyl chloride promotes the conversion of compounds with hydroxyl and carboxyl groups to TMS ethers and esters, respectively. This mixture was then maintained at 70 °C for 30 minutes [4]. Finally, each extract was analyzed in duplicate with tetracosane as internal standard.

***Eichhornia crassipes* study –** The procedure was the same presented in section 4.2.5 (Chapter 4) for the experimental optimization of the SFE of this raw material.

***Coffea* spp. study -** The tryacylglicerides content was determined by GC-FID by the sum of the amounts of the individual fatty acids methyl esters obtained after transesterification with sodium methoxide according to the methodology described by Passos et al. [14]. The compounds were identified by comparing their retention times with those of a commercial FAME mixture (C_8-C_{24}).

5.3 RESULTS AND DISCUSSION

5.3.1 *SFE* curves of *Quercus cerris*

Total extraction yield – The total extraction yield profiles (η_{total}) for *Q. cerris* cork of different particle sizes (Runs 5.1 to 5.5) and different cosolvent ratios (Runs 5.4, 5.6, and 5.7) are provided in Figures 5.5.A and 5.5.B, respectively. From the alignment of the cumulative yields at $t = 6$ h in Figure 5.5.A, one may notice an upwards trend of the datapoints according to the decrease of particle sizes. In fact, the lowest yield obtained after 6 hours of SFE belongs to the cork sample having the biggest particles (coarse), which attained 1.2 wt.%, against 2.8 wt.% for particle sizes >80 mesh (Run 5.1). Accordingly, from a total extraction yield perspective one may conclude that particle diameter induces significant jumps in the attainable yield values, and that these jumps have a correspondence with the decrease of particle sizes. Nevertheless, still at $t = 6$ h, a larger gap is noticed between Run 5.3 (40-60 mesh) and Run 5.2 (60-80 mesh), which denotes the existence of a threshold particle size (40-60 mesh) above which the enhancement of η_{total} is more pronounced. When thoroughly considered, the effect of the threshold particle size on the extraction curves is evident even for earlier times: for $t = 1$ h, datapoints are already sorted in two groups: one below 0.8 wt.% for Runs 5.3-5.5 (particle

sizes equal or greater than 40-60 mesh), and the other above this value, composed of Runs 5.1-5.2 (particle sizes equal to or lower than 60-80 mesh). Furthermore, from the second hour onwards, the shapes of the curves (and thus their gap) remain stable.

As far as the impact of ethanol content (x_{EtOH}, wt.%) on η_{total} is concerned, a yield rank is noticeable as higher ethanol contents are used. For instance, at $t = 5$ h, the extraction using 5.0 % ethanol (Run 5.7) yielded 2.2 wt.%, against 1.4 wt.% when using half of that percent (Run 5.4), and 0.9 wt.% without ethanol (Run 5.6). Nevertheless, the degree of the enhancements does not follow a linear dependence on the cosolvent addition: it is between 2.5 wt.% and 5.0 wt.% that a substantial gain of η_{total} is observed, particularly after the first hour of extraction.

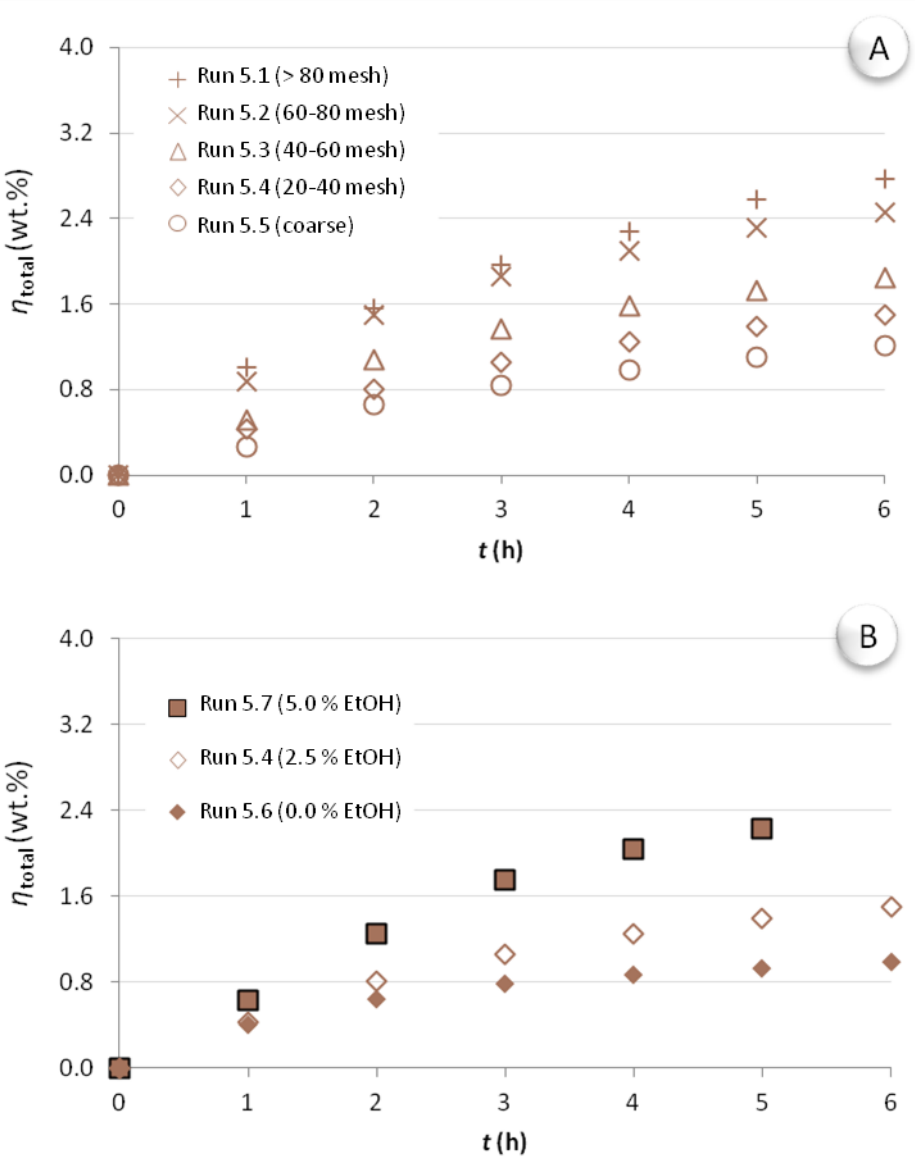

Figure 5.5 – Cumulative curves of total extraction yield (η_{total}) of *Q. cerris* biomass for: A) different particle size ranges at fixed 2.5 wt.% of ethanol; B) different cosolvent concentrations at fixed particle size range of 20-40 mesh. Pressure, temperature and flow rate were held constant in 300 bar, 50°C and 11 g min^{-1}.

Finally, the joint analysis of Figures 5.5.A and 5.5.B allow also drawing conclusions on how the grinding and the use of ethanol as cosolvent in SFE can be considered as alternative options in relation to each other:

(i) under SFE operating conditions of 300 bar, 50 °C and 11 $\mathrm{g\,min^{-1}}$, processing cork samples with 20-40 mesh without cosolvent (Run 5.6) is comparable to extracting non ground particles (coarse) with 2.5 wt.% of ethanol (Run 5.5);

(ii) for particles of 20-40 mesh, the performance associated to using 5.0 wt.% ethanol is comparable to processing cork particles of 60-80 mesh with 2.5 wt.% of ethanol;

Friedelin extraction yield – The friedelin extraction yield ($\eta_{\mathrm{friedelin}}$) profiles of the seven runs are graphed in Figure 5.6.A for different particles sizes, and in Figure 5.6.B for different x_{EtOH} values.

Likewise for η_{total} a correspondence was found between particle size and friedelin yield: the smaller the cork particles become, the faster the extraction goes and the higher the final yields are. Nevertheless, at $t = 6$ h a negligible yield difference is observed between the samples of 60-80 mesh and >80 mesh, being reached a maximum value of 0.68 wt.%. Lastly, results also evidence the non existence of a plateau within the six hours of experiment, which highlights that the practical depletion of this compound from biomass was not reached in any of the seven experiments, despite the eased access to extractives in the lower particle size samples.

With reference to the impact of ethanol on the uptake of friedelin, a linear proportion seems to prevail on the curves, with the increase of the yields being approximately proportional to the content of ethanol from the second hour on. For instance, at t =5 h, $\eta_{\mathrm{friedelin}} = 0.26$ wt.% for pure CO_2, 0.33 wt.% for 2.5 wt.% ethanol, and 0.43 wt.% for 5.0 wt.% ethanol. These correspond to the following ratios: $\eta_{\mathrm{friedelin}}\,(0\,\%\,\mathrm{EtOH})/\eta_{\mathrm{friedelin}}\,(2.5\,\%\,\mathrm{EtOH})$=0.79, and $\eta_{\mathrm{friedelin}}\,(5.0\,\%\,\mathrm{EtOH})/\eta_{\mathrm{friedelin}}\,(2.5\,\%\,\mathrm{EtOH}) = 1.30$, which, in other words, comprise -21 % and +30 % of the yields obtained with 2.5 % EtOH, respectively. Hence, one may conclude that:

(i) Avoiding ethanol when extracting samples of 20-40 mesh at 300 bar and 50 °C, 11 $\mathrm{g\,min^{-1}}$ produces a loss of friedelin uptake that is lower than if coarse particles are extracted with a supercritical mixture of 2.5 wt.% EtOH.

(ii) Doubling the amount of ethanol from 2.5 to 5.0 wt.% enhances less the productivity of the process than if the particles are milled to the next particle size interval, i.e. 40-60 mesh.

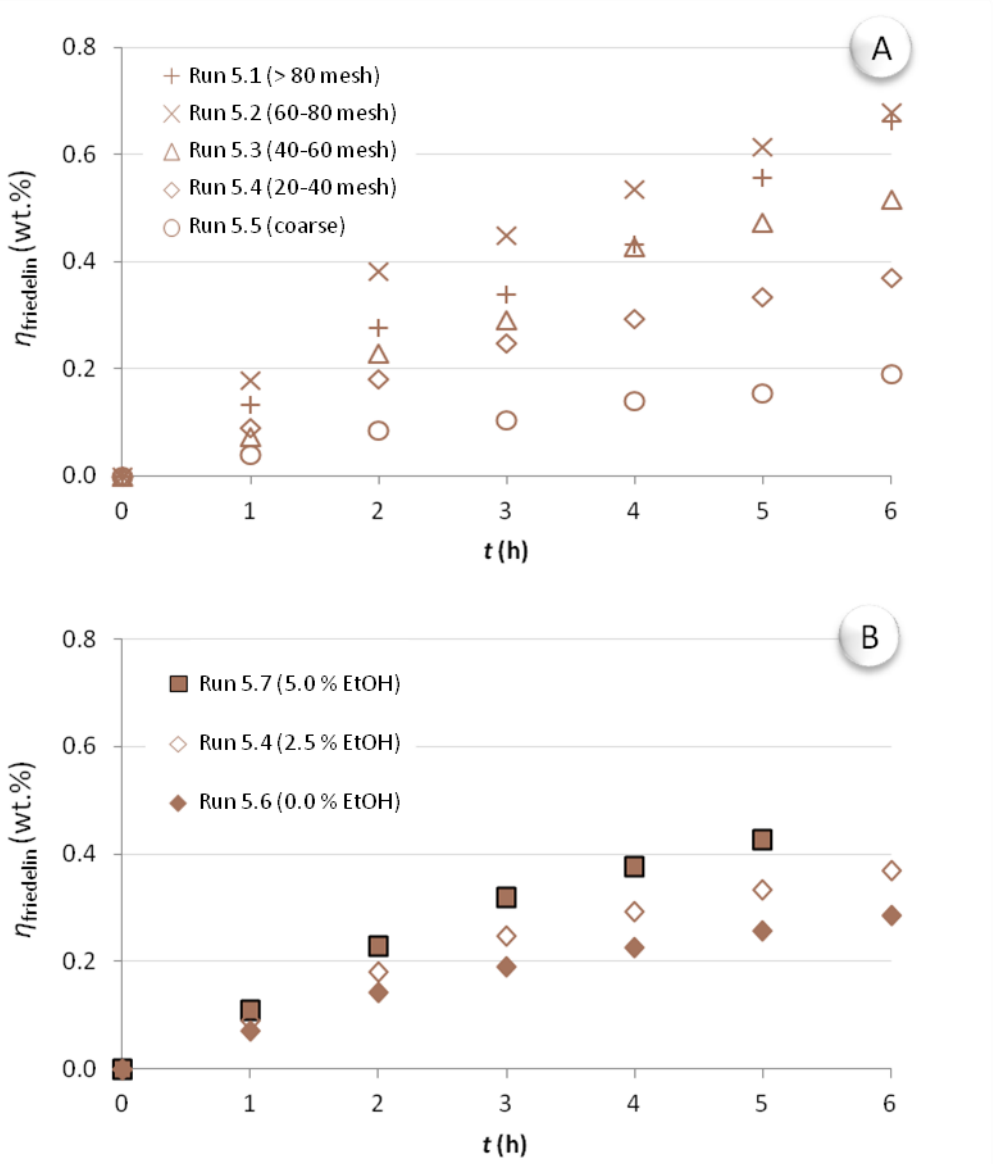

Figure 5.6 – Cumulative curves of friedelin extraction yield ($\eta_{friedelin}$) of *Q. cerris* biomass for: A) different particle size ranges at fixed 2.5 wt.% of ethanol; B) different cosolvent concentrations at fixed particle size range of 20-40 mesh. Pressure, temperature and flow rate were held constant in 300 bar, 50 °C and 11 g min^{-1}.

5.3.2 SFE CURVES OF *Eichhornia crassipes*

Total extraction yield curves – With reference to the generic extract uptake along time, Figure 5.7 illustrates the profiles of the assays performed in this work. Accordingly, Figure 5.7.A comprises Runs 5.8 to 5.10, which differ from each other only on flow rate values, and no cosolvent was used (see Table 5.2). On the other hand, in Figure 5.7.B two effects can be analyzed in contrast to Runs 5.8-5.10: the impact of changing the operating pressure (see Runs

5.9 and 5.11), and the impact of using ethanol as cosolvent (Runs 5.9 and 5.11, against Runs 5.12 and 5.13, see Table 5.2).

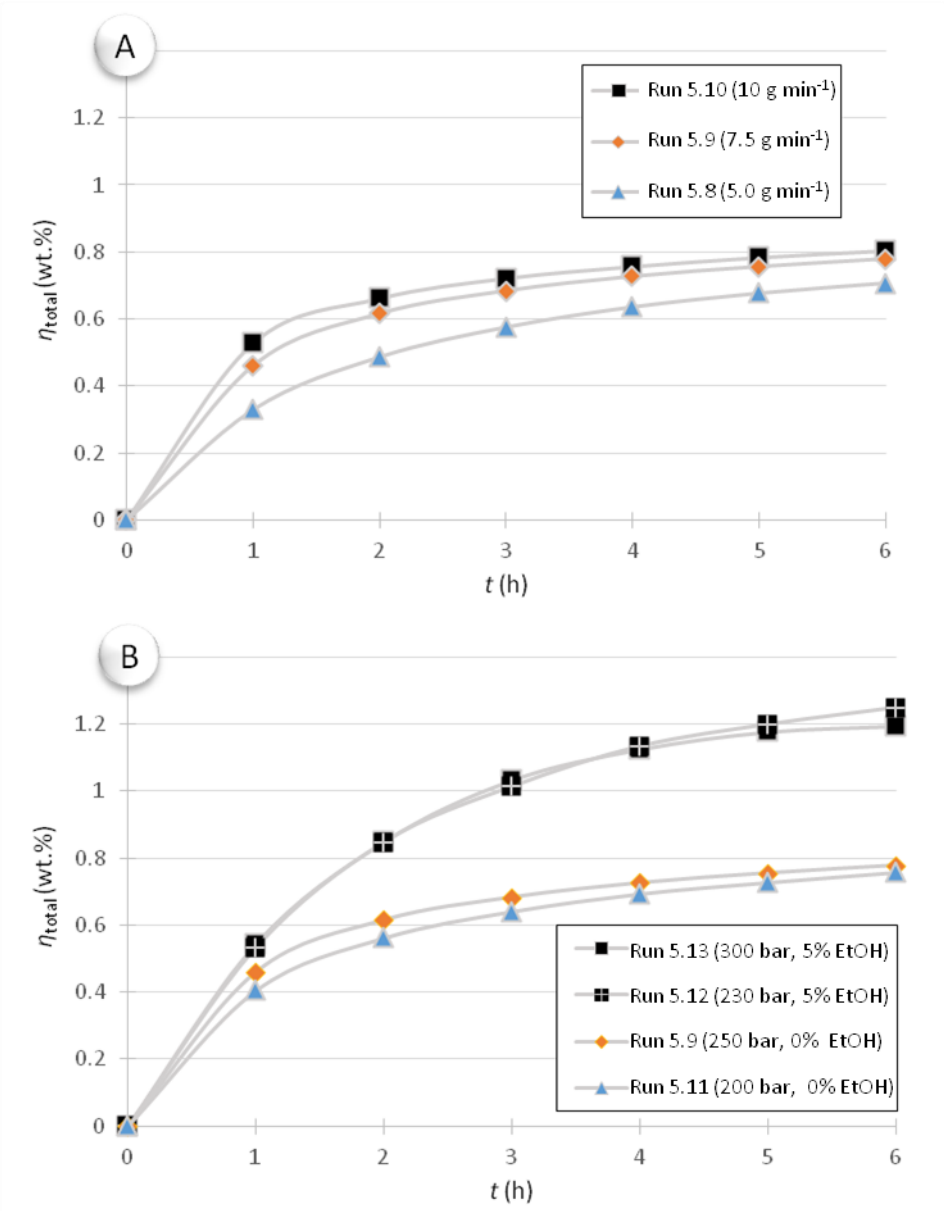

Figure 5.7 – Cumulative curves of total extraction yield (η_{total}) of *E. crassipes* biomass at: A) different flow rates for 250 bar and 0 wt.% ethanol; B) different pressures and/or ethanol content for 7.5 g min^{-1}. Curves are lines to guide the eyes; see experimental conditions in Table 5.2.

As far as the flow rate impact is concerned, a proportional increase of the extraction rate was noticed in the first hour as Q_{CO_2} was increased from 5.0 to 10.0 g min^{-1}. Hence, by the end of the experiments at $t = 6$ h, the η_{total} values attained were 0.706 wt.% (Run 5.8), 0.778 wt.% (Run 5.9), and 0.803 wt.% (Run 5.10).

Despite the advantageous extraction performance as the flow rate was increased, the jump between 5.0 and 7.5 $\mathrm{g\,min^{-1}}$ was greater than between 7.5 and 10.0 $\mathrm{g\,min^{-1}}$, which is in accordance with expectations, as the film resistance to mass transfer is progressively reduced as Q_{CO_2} increases. For instance, this has been observed in SFE experiments involving eucalypt bark [18], where an experimental study was performed by changing CO_2 flow rate from 6 $\mathrm{g\,min^{-1}}$ to 14 $\mathrm{g\,min^{-1}}$, and also on tomato skins [19], where the respective CO_2 flow rate change was from 1.5 mL $\mathrm{min^{-1}}$ to 4.5 mL $\mathrm{min^{-1}}$.

With reference to ethanol addition, Runs 5.12 and 5.13 show that, in relation to Run 5.9, they are able to increase total yield up to 60 % within the 6 hours of extraction, reaching up to $\eta_{\mathrm{total}} = 1.25$ wt.% (Run 5.12). An additional insight provided by Runs 5.12 and 5.13 comprise the fact that when using 5.0 % ethanol, a 50 bar variation in pressure from 250 to 300 bar imparts a negligible effect on the shape and magnitude of the extraction curve. On the other hand, Run 5.11 (200 bar/0 % EtOH/7.5 $\mathrm{g\,min^{-1}}$) gave rise to a curve that is intermediate between those of Run 5.8 (250 bar/0 % EtOH/5.0 $\mathrm{g\,min^{-1}}$) and Run 5.9 (250 bar/0 % EtOH/7.5 $\mathrm{g\,min^{-1}}$). Hence, one may conclude that decreasing the flow rate from 7.5 to 5.0 $\mathrm{g\,min^{-1}}$ has a greater impact on the extraction curves than decreasing pressure by 50 bar from 250 to 200 bar.

Stigmasterol extraction yield – With reference to the specific uptake of stigmasterol along time, Figure 5.8 illustrates the profiles of the six assays following the same division of Figure 5.7, namely, with Runs 5.8-5.10 being in Figure 5.8.A (where only flow rate values change and no cosolvent was used), and Runs 5.9 and 5.11-5.13 being in Figure 5.8.B (where the impacts of changing the operating pressure and of using ethanol as cosolvent can be noticed).

In general, identical insights concerning the impact of flow rate and pressure variations can be taken for η_{stigm}, where the final stigmasterol yields jump from 0.167 wt.% (Run 5.8) to 0.176 wt.% (Run 5.9) and then to 0.173 wt.% (Run 5.10). Once again a much larger difference is noticed between 5.0 and 7.5 $\mathrm{g\,min^{-1}}$ (Runs 5.8 and 5.9) than between 7.5 and 10.0 $\mathrm{g\,min^{-1}}$ (Run 5.9 and 5.10).

As far as the impact of ethanol is concerned, a great gain was noticed on the attained stigmasterol yields when using 5 % of ethanol. In fact, two yield plateaus were observed within the six runs: one at ca. $\eta_{\mathrm{stigm}} = 0.17$ wt.% for 0 % EtOH (Runs 5.8 to 5.11), and the other at 0.23 wt. % for 5.0 % ethanol (Runs 5.12 and 5.13). These results suggest that the attainable amount of extractives can be of very different ranges whether using cosolvent or not, which is a pertinent remark to model the experimental results.

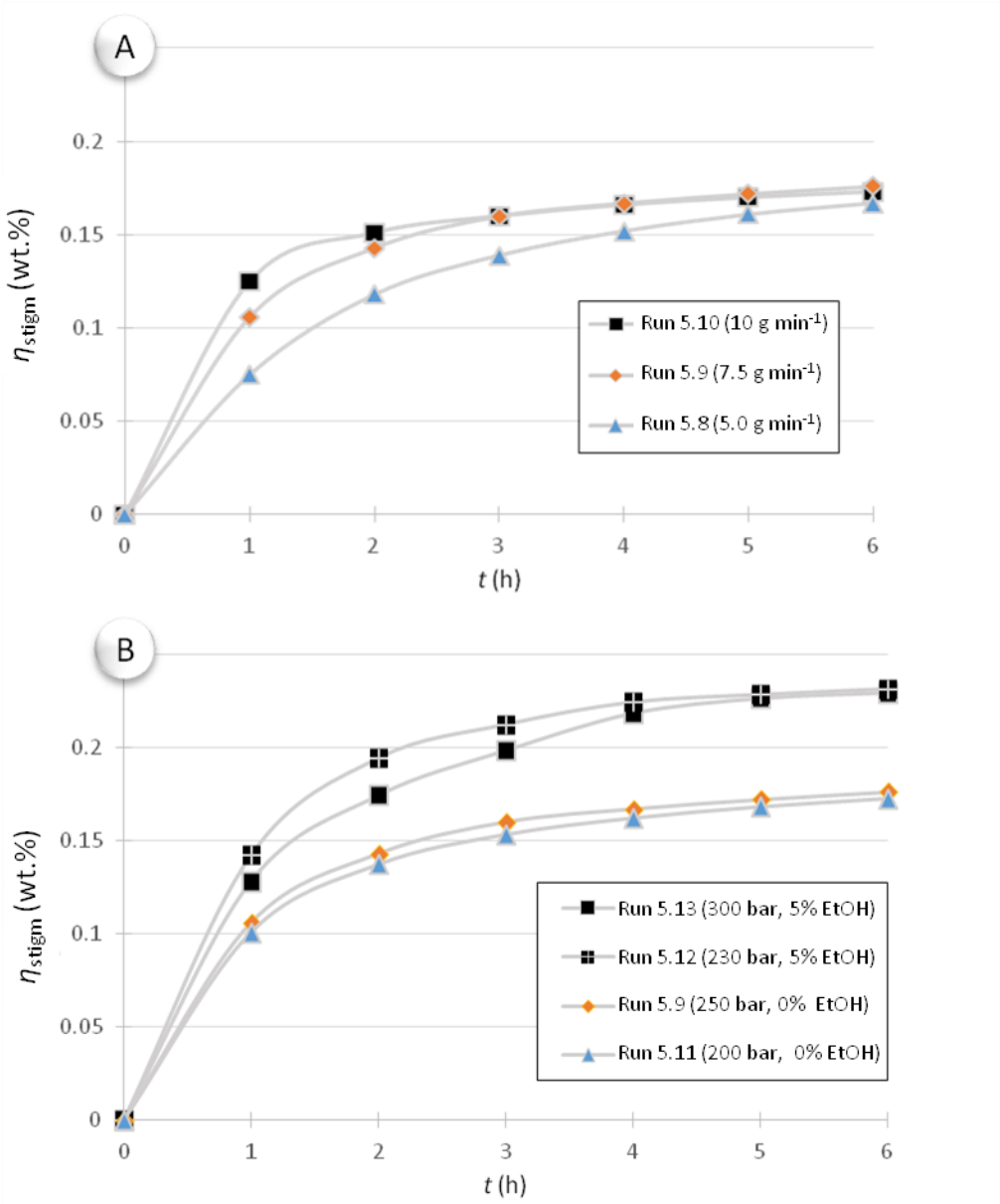

Figure 5.8 – Cumulative curves of stigmasterol extraction yield (η_{stigm}) of *E. crassipes* biomass at: A) different flow rates for 250 bar and 0 wt.% ethanol; B) at different pressures and/or ethanol content for 7.5 g min^{-1}. Curves are lines to guide the eyes; see experimental conditions in Table 5.2.

A particularity of η_{stigm} response in relation to η_{total} comprises the fact that, under an addition of 5.0 % (wt.) ethanol, the quickest way to remove stigmasterol from the *E. crassipes* matrix is at 250 bar rather than at 300 bar. However, it seems that such advantage is mainly for shorter extraction times (t=0-4 h), as the two series where ethanol was used (Runs 5.12 and 5.13) converged to an identical plateau after 6 h of uptake. Nevertheless, the said time advantage of working at 250 bar is a notable and advantageous behaviour as it is not simultaneously noticed for the total yield response under the same conditions (see Figure 5.7.B). As a result, a temporary selectivity gain window is observed for stigmasterol, which is a remarkable result in

light of the interest to produce stigmasterol enriched extracts. This observation reminds the one attained by Domingues et al. [18], who studied the production of triterpenic acids enriched extracts using SC-CO_2 from eucalypt bark samples at 200 bar and 5 wt.% ethanol, and observed a progressive selectivity gain along time in favour of the mentioned acids caused by a variation in temperature conditions from 40 °C to 60 °C.

Final remarks – As usual in the SFE of natural biomass [20], our previous optimization of operating conditions (P, T, wt.% of ethanol) on the SFE of *E. crassipes* was accomplished under a constant extraction time, i.e. t=6 h [21]. Owing to the notorious similarity of the yield responses of both Runs 5.12 and 5.13 (see Figures 5.7.A and 5.7.B), the referred selectivity gain window becomes unnoticed to the response surface methodology (RSM) method adopted for optimization. Hence, very distinct results and conclusions would be obtained if the optimization was carried out at t = 2 h instead. However, it is worth noting that η_{stigm} and η_{total} profiles at t = 2 h are still very different from the final values attained at t =6 h, which is for sure the reason for the typical selection of high extraction times assumed by researchers.

In this respect, Melo et al. [22] proposed a more appropriate analysis of a SFE process based on economic criteria using the whole extraction curves (presented in full detail in Chapter 8). It also relies on the application of RSM, but the optimized response is the Cost of Manufacturing (COM) rather than the extraction yield solely, which allows that the best experimental conditions are selected using yield *vs.* time information in conjunction with process costs and productivity indicators. For instance, it has been shown that the most competitive extraction times were as low as 1 h for gac oil [23], 1.1 h for tomato residues extracts [24], and 2 h for spent coffee grounds [22], independently of the final yields attained after longer times.

These insights show that kinetics is fundamental for processes involving SFE, which in turn reinforce the pertinence of carrying out modeling studies based on these data. This is the objective of the next section.

5.3.3 SFE CURVES OF *Coffea* spp.

Total extraction yield– Figure 5.9 presents the SFE curves measured at 190 bar/40 °C and 190 bar/55 °C plotted against time. The results are normalized by the Soxhlet extraction yield and graphed as function of time. The cumulative curves from Couto *et al.* [15] are also represented for comparison. In general all curves exhibit the typical trend found in the SFE of edible oils, i.e. a constant period of extraction followed by a second diffusional period. In this work, the registered curvatures evidence kinetic limitations to mass transfer, particularly in Runs 5.14, 5.15, 5.17.

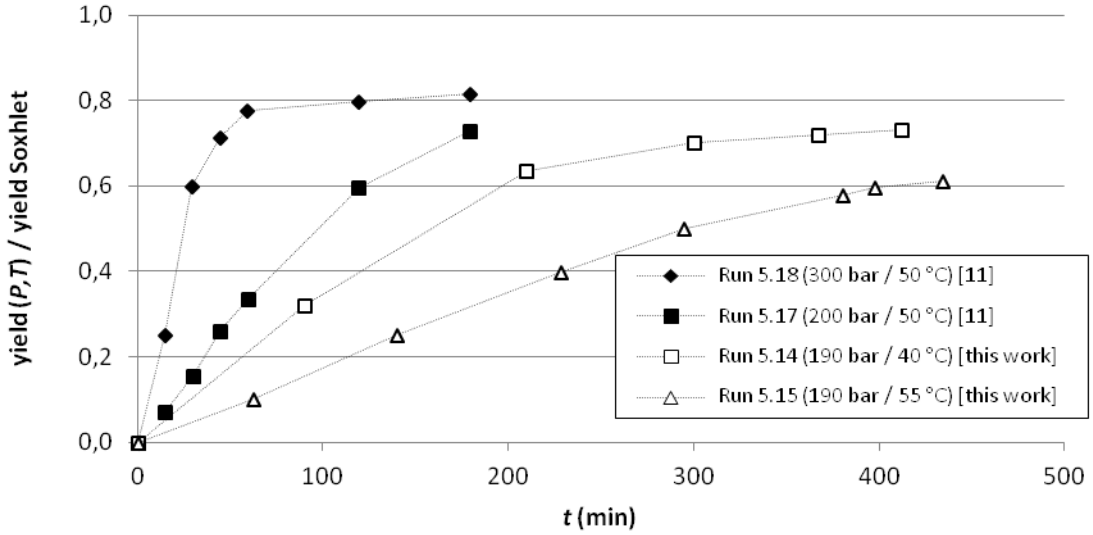

Figure 5.9 – SFE curves of spent coffee grounds (SCG) oil at different pressures and temperatures (see Table 5.3).

Considering that pressure, flow rate, and mass of SCG bed remained constant in our experiments (Runs 5.14 and 5.15), the different performances are due to the influence of temperature (40 °C *vs.* 55 °C). It is known that this variable is usually important in SFE processes owing to its impact on the solubility and diffusivity of compounds. Any increase in temperature generates two thermodynamic opposing effects – the positive influence upon solute vapor pressure and negative impact on CO_2 density – and also an effective diffusivity enhancement inside the particle. The external diffusion in the film may evidence a more complex dependence. The solute fluxes result obviously from the combination of these factors as it is analyzed in detail in the following.

The oil solubility (kg m^{-3}) can be estimated by the correlation of del Valle and Aguilera [25] as function of temperature (K) and SC-CO_2 density (kg m^{-3}) by:

$$y_s = \rho^{10.724} \exp\left(-\frac{18708}{T} + \frac{2186840}{T^2} + 40.361\right) \quad (2)$$

where density can be computed by the accurate equation of Pitzer and Schreiber [12]. The increment of the convective mass transfer coefficient (k_f) can be estimated by the correlation of Wakao and Funazkri [26]:

$$\mathrm{Sh} = 2.0 + 1.1\mathrm{Re}^{0.6}\mathrm{Sc}^{1/3} \quad (3)$$

Here the viscosity of SC-CO_2 was obtained by the equation of Altunin and Sakhabetdinov [27], and the diffusion coefficient (cm^2 s^{-1}) of triolein (taken as model molecule) was estimated by the very simple and accurate model of Magalhães *et al.* [28]:

$$D_{12} = T\left(\frac{a}{\eta_1} + b\right) \tag{4}$$

where T is in K, viscosity in cP, and triolein constants are $a = 6.34288\times10^{-9}$ and $b = 4.89262\times10^{-8}$. The effective diffusivities inside the biomass particles may be estimated taking into account their porosity (ϵ) and tortuosity (τ) by $D_{\text{eff}} = D_{12}\,\epsilon/\tau$. Finally, the oil flux from the matrix to the supercritical bulk can be predicted as a first approximation by its value at infinite dilution, i.e.:

$$N_{\text{oil}}^{\infty} = k_f\,\rho_{CO_2}\,(y_s - 0) \tag{5}$$

In Figures 5.10 and 5.11, the calculated results for the oil solubility, effective intraparticle diffusivity, convective mass transfer coefficient, and oil flux at infinite dilution are plotted. In order to evaluate the influence of the operating conditions upon each dependent variable, they are represented normalized by the same quantity at 190 bar/55 °C (Run 5.15), giving readers the opportunity to capture the enhancements over the reference values. In the case of Figure 5.10, the quantities corresponding to the experimental runs under analysis in this essay are superimposed.

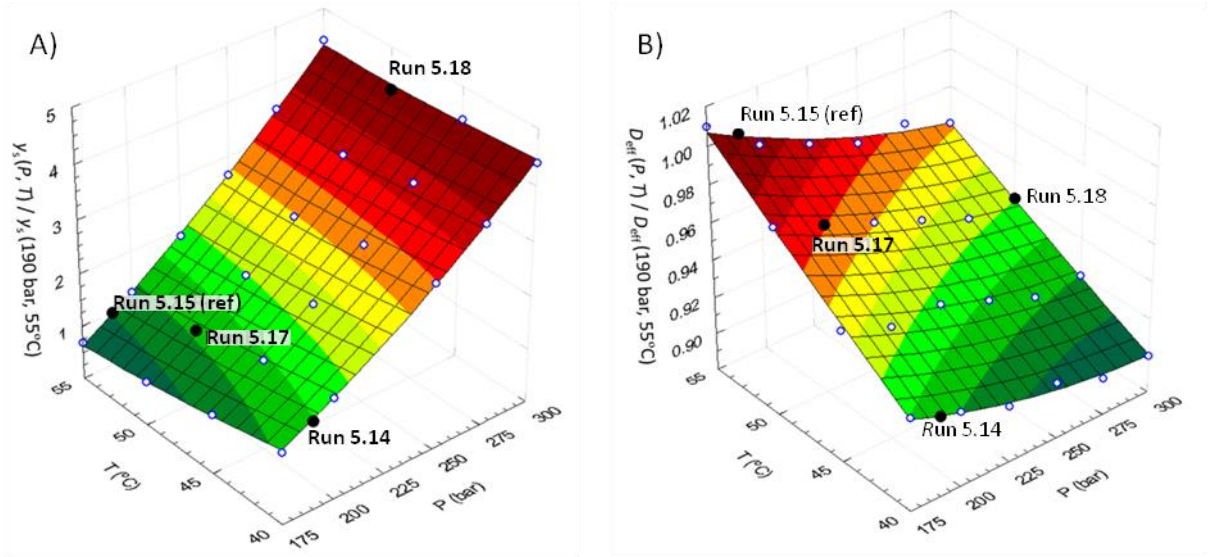

Figure 5.10 –A) normalized oil solubility computed by the expression proposed by del Valle and Aguilera [25]; B) normalized intraparticle effective diffusivities calculated on the basis of the correlation of Magalhães *et al.* [28], as functions of temperature and pressure.

From Figure 5.10.A it is evident that solubility favors largely Run 5.18 in comparison to Runs 5.14, 5.15 and 5.17, due to the chief effect of pressure; the y_s values increase like Run 5.15 < Run 5.17 < Run 5.14 << Run 5.18 (global absolute variation = 3.43 units). On the other hand, the kinetics inside the particles disclosed in Figure 5.10.B emphasize that the internal

limitations to mass transfer are equally important in all experiments, since there is not any major diffusivity jump (global variation = 0.08); however the increasing sequence of normalized D_{eff} is: Run 5.14 < Run 5.18 < Run 5.17 < Run 5.15. In terms of the normalized convective mass transfer coefficient, Figure 5.11.A points out the following behavior: Run 5.14 < Run 5.15 ≈ Run 5.18 < Run 5.17, though the global absolute variation is 0.25. Finally, the oil fluxes at infinite dilution plotted in Figure 5.11.B detach once again the importance of the pressure, since Run 5.15 < Run 5.14 ≈ Run 5.17 << Run 5.18 (global absolute variation = 2.96). As a result, the distinguishing factor behind the four experiments is the solubility enhancement observed which affects significantly the fluxes. Moreover all runs are equally affected by internal and/or external limitations to mass transfer. The experimental results of Figure 5.9 will be now analyzed on the light of these principles.

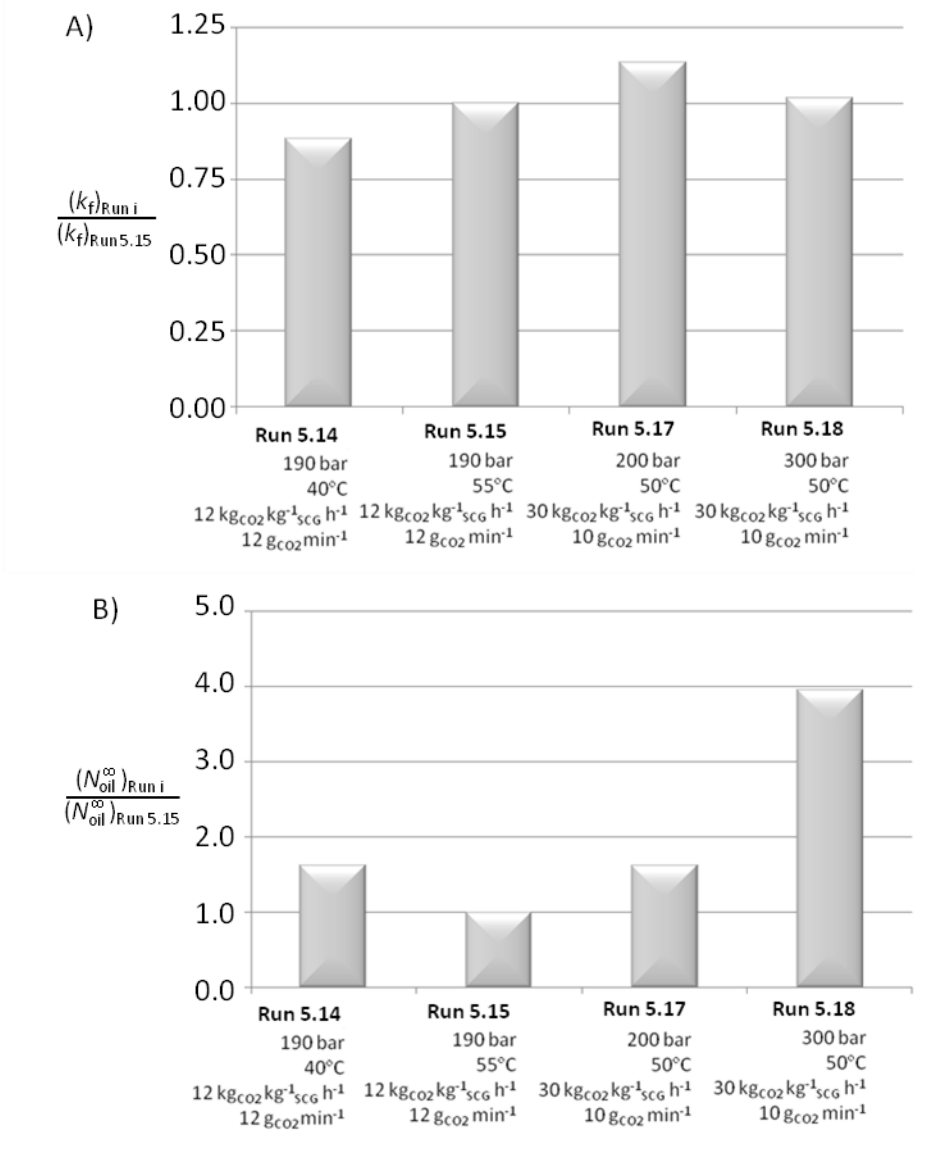

Figure 5.11 – A) normalized convective mass transfer coefficient calculated by the correlation of Puiggené *et al.* [29]; B) normalized oil removal fluxes in the limit of infinite dilute solutions.

Coming back to Figure 5.9, a temperature increase from 40 °C (Run 5.14) to 55 °C (Run 5.15) at 190 bar penalized the performance of the process, since the rate of extraction at 55 °C was delayed in comparison to the results at 40 °C. While Run 5.14 yields increased progressively until reaching 73 % of Soxhlet value, within the 7.2 h of the extraction curve at 190 bar/55 °C (Run 5.15), the highest yield attained was 61 %. These two assays denote a counterproductive effect of temperature on the process at this pressure, which is in great agreement with the indicative N_i^{∞} results for the two runs shown in Figure 5.11.b. In this case, the solubility increment compensates the negative effects of the internal and external mass transfer (confront Figure 5.11.A with Figures 5.10.B and 5.10.A.

The final yield achieved on Run 5.14 (190 bar/40 °C) is comparable to the value obtained by Couto *et al.* [15] on Run 5.17, at 200 bar/50 °C. On the other hand the extraction velocity from these authors is 60 % higher (measured by the slopes at short times), which apparently disagrees with the N_i^{∞} trend suggested in Figure 5.11.B. However taking into account that the space time of Run 5.17 is 40 % of Run 5.14, we are farther from the infinite dilute conditions, which means that the real flux in our case is inferior. This fact justifies the slope of curves 5.14 and 5.17 in Figure 5.9.

When considering the extraction curve 5.18 obtained at a harder pressure condition (300 bar) but same temperature (50 °C) of Run 5.17, the oil removal rate is visibly increased (3.6 times). In fact after 1 h of extraction the curve has already achieved a nearly flat region in the yield ratios range of 78-82 %. Such evidence unveils the great influence of pressure upon this SFE process, which is confirmed by the higher oil fluxes estimated by N_i^{∞} (see Figure 5.11.B): 1.62 *versus* 3.96. Once again the milestone effect is the solubility (see Figure 5.10.A) since the transport limitations are similar (see Figures 5.9.B and 5.10.A).

Tryacylglicerides profiles – The fatty acids profile along time of the SCG oil obtained by supercritical extraction in Run 5.15 (190 bar/55 °C) has been determined and is represented in Figure 5.12. The main fatty acids present in all the samples are linoleic acid (C18:2) and palmitic acid (C16:0), followed by oleic acid (C18:1) and stearic acid (C18:0). Other minor acids present in the extracts are linolenic (C18:3), and arachidic (C20:0) acids. Furthermore, Figure 5.12 shows that there is a small variation between the composition of individual supercritical extracts and that of Soxhlet. The global oil obtained by joining all SC extracts is also in good agreement with our Soxhlet and those reported in the literature for SCG [15, 30] (see Table 5.4). In general, literature results show that the fatty acids profile is independent of the raw material treatment (green *vs.* roasted), method of preparation (coffee brew *vs.* filtration), and also extraction method (Soxhlet *vs.* supercritical CO_2). The maximum yield of SCG oil obtained was 15.0 % of the SCG (dry weight) which is slightly lower when compared to Couto *et al.* [15] but higher when compared to Cruz *et al.* [30], all within an acceptable range.

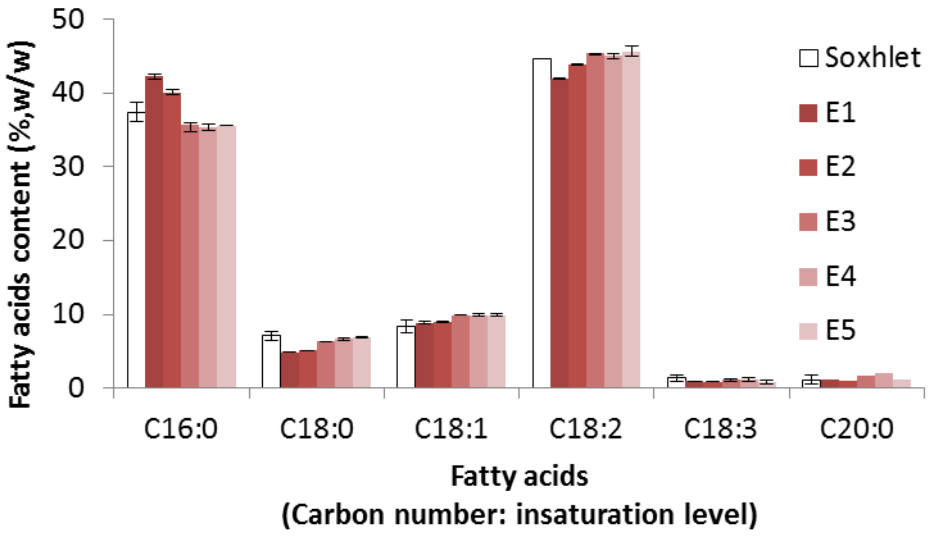

Figure 5.12 – Fatty acids profile of Soxhlet extracted SCG oil, and of the individual supercritical extracts E1 to E5 obtained at 190 bar/55 °C (Run 5.15 of Table 5.3 and Figure 5.9).

Table 5.4 – Extraction yields and fatty acids profiles obtained in this work and taken from literature. Data for SFE and Soxhlet extraction.

	This work		Couto *et al.* [15]		Cruz *et al.* [30]
Composition	Soxhlet (*n*-hexane)	SFE (Run 5.15)	Soxhlet (n-hexane)	SFE (Run 5.17)	Soxhlet (petroleum ether)
C16:0	37.37	37.48	46.22	36.19	32.8
C18:0	7.07	6.02	6.87	7.59	7.1
C18:1	8.31	9.53	8.63	11.24	10.3
C18:2	44.67	44.52	34.36	41.45	44.2
C18:3	1.42	0.99	1.39	0.86	1.5
C20:0	1.16	1.46	2.53	2.68	2.6
η (%)	15.0		18.3		12.5

Diterpenes profiles – The extraction curves of Runs 5.15 and 5.16 were measured taking into account the trends unveiled by the design of experiments and response surface analysis presented in Chapter 4, namely that ethanol does decrease diterpenes concentration, temperature exhibits a soft influence, and pressure is an important factor (lower values are desirable). Therefore, the selected operating conditions were the following: pure CO_2 at minimum and maximum pressures, 140 bar and 190 bar, respectively, and an intermediate

temperature (55 °C). These two curves allowed the diterpenes content of the cumulative extracts to be known and to be contrasted with the reference Soxhlet results.

Figure 5.13 presents C_{Dit} profiles as function of the spent mass of supercritical solvent. Very distinct profiles can be noticed both in terms of the shapes of curves, and on the concentration values attained. The remarkable selectivity advantages of SC-CO_2 upon diterpenes become clearly evident as the cumulative C_{Dit} results of the two runs overcome significantly the concentrations obtained by *n*-hexane extraction. In addition, the extraction curve measured at 140 bar/55 °C/0 wt.% EtOH (Figure 5.13.A) exhibits a parabolic shape that reaches a maximum value of 121 mg g_{oil}^{-1} at 5.7 kg_{CO2}, At this point, the C_{Dit} value obtained by SFE is 4.1 times greater than the reference from Soxhlet extraction. With regard to the measurements carried out at the maximum pressure, 190 bar, C_{Dit} begins with a concentration profile (first point) comparable to that of the 140 bar curve, but afterwards evolves to lower values but still superior to Soxhlet. In this case, the curve exhibits a point of highest concentration that reaches 95 mg g_{oil}^{-1} after spending 1.7 $kg_{CO2.}$ This value represents a concentration of 3.2 times of the *n*-hexane reference.

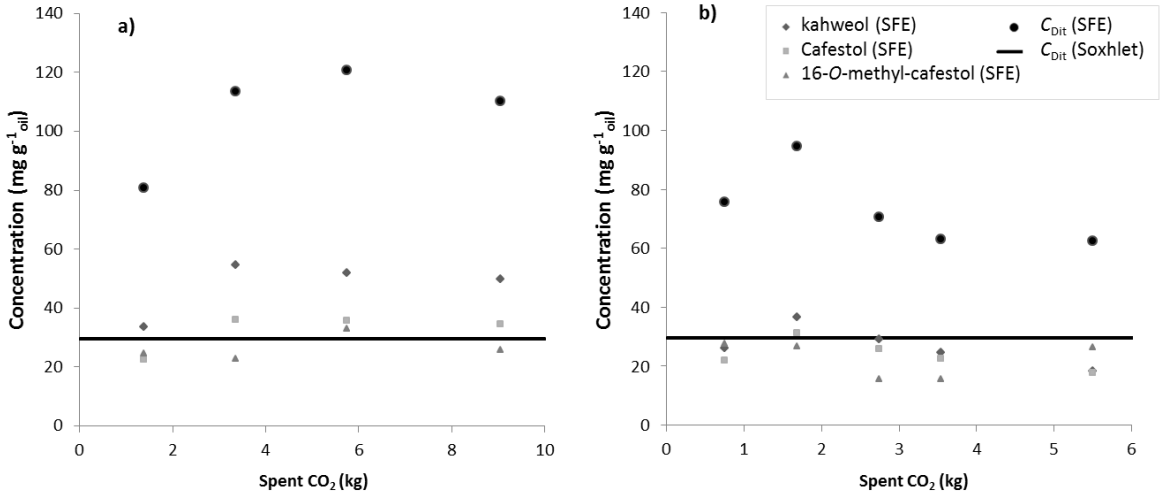

Figure 5.13 – Concentration of the most important diterpenes and total diterpenes in the supercritical cumulative extracts obtained along time, here expressed in terms of mass of spent CO_2. Operating conditions: A) 140 bar/55 °C (Run 5.16); B) 190 bar/55 °C (Run 5.17). Soxhlet results are also graphed as reference (horizontal line).

Concerning the individual profiles of the diterpenes, Figure 5.13 shows that their effective affinity to the SC-CO_2 seems to follow the same trend: kahweol appears as the most abundant, in accordance with its concentration in the matrix (recall Soxhlet results given in Table 4.5). With relation to cafestol and 16-*O*-methylcafestol, notwithstanding the latter exists in almost one third of the amount of the former (see Table 4.5), they are uptaken in equivalent

proportions in the supercritical extracts (see Figure 5.13). This must be intimately related with the fact that 16-*O*-methylcafestol is less polar than cafestol, which favours its affinity to pure CO_2 (see structural formulas in Table 2.1). It is worth noting that all three molecules contributed roughly equally to C_{Dit}.

In the whole, extraction curves using optimized operating conditions (particularly in the case of 190 bar, 55 °C and 0 wt.% EtOH) demonstrated the great selectivity advantages of the SC-CO_2 to produce SCG oil enriched in diterpenes. If it is true that such enhancement is obtained at expenses of a lower total extraction yield (in relation to Soxhlet results), it should be stressed that this trade-off seems to be highly favourable to SFE, as C_{Dit} increment is within 320-410 % while η_{Total} losses stay within 39-70 %.

5.4 CONCLUSIONS

***Quercus cerris* study –** SFE curves of *Q. cerris* cork were measured in a 0.5 L capacity unit, at 300 bar, 50 °C, and a CO_2 flow rate of 11 $\mathrm{g\,min^{-1}}$. The work focused on the impact of the particle size and cosolvent concentration on total extraction yield (η_{total}) and friedelin extraction yield ($\eta_{\mathrm{friedelin}}$). Extracts were analyzed by GC-MS.

Experimental results show that, for η_{total}, extracting cork samples of 20-40 mesh with pure CO_2 can be comparable to extracting coarse particles (<20 mesh) with CO_2 modified with 2.5 % of ethanol, and also that doubling the ethanol content to 5.0 %, the obtained, η_{total} is equivalent to further grinding the biomass to 60-80 mesh. For $\eta_{\mathrm{friedelin}}$ it was concluded that the addition of cosolvent is important to enhance the uptake of friedelin, but doubling its content from 2.5 to 5.0 wt.% EtOH enhances less the productivity than if the particles are further milled.

The study of selectivity to friedelin revealed that intermediate granulometries (20-40 mesh to 60-80 mesh) are advantageous, and that the addition of cosolvent can increase cumulative selectivity up to 1.2.

***Eichhornia crassipes* study –** The measurement of an extraction curve under optimized conditions (300 bar and 5.0 wt.% ethanol, at 50 °C) confirmed the reproducibility of experimental results, and also that sterols concentrations are higher in the first two hours of extraction but stabilize from the third hour of extraction onwards.

***Coffea* spp. study -** The measurement of extraction curves around preliminarily optimized conditions (140 bar/55 °C/0 wt.% EtOH and 190 bar/55 °C/0 wt.% EtOH) confirmed the good trends taken from the previous statistical analysis of Chapter 4, and revealed that SFE can

provide a C_{Dit} enhancement ranging from 320 to 410 % at the expenses of a η_{Total} loss within only 39-70 % in comparison to *n*-hexane extraction results.

5.5 REFERENCES

[1] H.M.A. Barbosa, M.M.R. de Melo, M.A. Coimbra, C.P. Passos, C.M. Silva, Optimization of the supercritical fluid coextraction of oil and diterpenes from spent coffee grounds using experimental design and response surface methodology, Journal of Supercritical Fluids, 85 (2014) 165-172.

[2] P.F. Martins, M.M.R. de Melo, P. Sarmento, C.M. Silva, Supercritical fluid extraction of sterols from *Eichhornia crassipes* biomass using pure and modified carbon dioxide. Enhancement of stigmasterol yield and extract concentration, Journal of Supercritical Fluids, 107 (2016) 441-449.

[3] M.M.R. de Melo, A. Şen, A.J.D. Silvestre, H. Pereira, C.M. Silva, Experimental and modeling study of supercritical CO_2 extraction of *Quercus cerris* cork: Influence of ethanol and particle size on extraction kinetics and selectivity to friedelin, Separation and Purification Technology, 187 (2017) 34-45.

[4] R.M.A. Domingues, M.M.R. de Melo, C.P. Neto, A.J.D. Silvestre, C.M. Silva, Measurement and modeling of supercritical fluid extraction curves of *Eucalyptus globulus* bark: Influence of the operating conditions upon yields and extract composition, Journal of Supercritical Fluids, 72 (2012) 176-185.

[5] E.L.G. Oliveira, A.J.D. Silvestre, C.M. Silva, Review of kinetic models for supercritical fluid extraction, Chemical Engineering Research and Design, 89 (2011) 1104-1117.

[6] C.S.G. Kitzberger, R.H. Lomonaco, E.M.Z. Michielin, L. Danielski, J. Correia, S.R.S. Ferreira, Supercritical fluid extraction of shiitake oil: Curve modeling and extract composition, Journal of Food Engineering, 90 (2009) 35-43.

[7] L.M.A.S. Campos, E.M.Z. Michielin, L. Danielski, S.R.S. Ferreira, Experimental data and modeling the supercritical fluid extraction of marigold (*Calendula officinalis*) oleoresin, Journal of Supercritical Fluids, 34 (2005) 163-170.

[8] N. Mezzomo, J. Martínez, S.R.S. Ferreira, Supercritical fluid extraction of peach (*Prunus persica*) almond oil: Kinetics, mathematical modeling and scale-up, Journal of Supercritical Fluids, 51 (2009) 10-16.

[9] L. Fiori, D. Basso, P. Costa, Supercritical extraction kinetics of seed oil: A new model bridging the 'broken and intact cells' and the 'shrinking-core' models, Journal of Supercritical Fluids, 48 (2009) 131-138.

[10] H. Sovová, Steps of supercritical fluid extraction of natural products and their characteristic times, Journal of Supercritical Fluids, 66 (2012) 73-79.

[11] H. Pohler, E. Kiran, Volumetric properties of carbon dioxide plus ethanol at high pressures, Journal of Chemical and Engineering Data, 42 (1997) 384-388.

[12] K.S. Pitzer, D.R. Schreiber, Improving equation-of-state accuracy in the critical region - Equations for carbon-dioxide and neopentane as examples, Fluid Phase Equilibria, 41 (1988) 1-17.

[13] M.M.R. de Melo, R.P. Silva, A.J.D. Silvestre, C.M. Silva, Valorization of water hyacinth through supercritical CO_2 extraction of stigmasterol, Industrial Crops and Products, 80 (2016) 177-185.

[14] C.P. Passos, R.M. Silva, F.A. Da Silva, M.A. Coimbra, C.M. Silva, Supercritical fluid extraction of grape seed (*Vitis vinifera* L.) oil. Effect of the operating conditions upon oil composition and antioxidant capacity, Chemical Engineering Journal, 160 (2010) 634-640.

[15] R.M. Couto, J. Fernandes, M.D.R.G. da Silva, P.C. Simões, Supercritical fluid extraction of lipids from spent coffee grounds, Journal of Supercritical Fluids, 51 (2009) 159-166.

[16] C.S.R. Freire, A.J.D. Silvestre, C.P. Neto, J.A.S. Cavaleiro, Lipophilic extractives of the inner and outer barks of *Eucalyptus globulus*, Holzforschung, 56 (2002) 372–379.

[17] M.M.R. de Melo, E.L.G. Oliveira, A.J.D. Silvestre, C.M. Silva, Supercritical fluid extraction of triterpenic acids from *Eucalyptus globulus* bark, Journal of Supercritical Fluids, 70 (2012) 137-145.

[18] R.M.A. Domingues, M.M.R. de Melo, C.P. Neto, A.J.D. Silvestre, C.M. Silva, Measurement and modeling of supercritical fluid extraction curves of Eucalyptus globulus bark: Influence of the operating conditions upon yields and extract composition, The Journal of Supercritical Fluids, 72 (2012) 176-185.

[19] U. Topal, M. Sasaki, M. Goto, K. Hayakawa, Extraction of Lycopene from Tomato Skin with Supercritical Carbon Dioxide: Effect of Operating Conditions and Solubility Analysis, Journal of Agricultural and Food Chemistry, 54 (2006) 5604-5610.

[20] M.M.R. de Melo, A.J.D. Silvestre, C.M. Silva, Supercritical fluid extraction of vegetable matrices: Applications, trends and future perspectives of a convincing green technology, Journal of Supercritical Fluids, 92 (2014) 115-176.

[21] P.F. Martins, M.M.R. de Melo, P. Sarmento, C.M. Silva, Supercritical fluid extraction of sterols from Eichhornia crassipes biomass using pure and modified carbon dioxide. Enhancement of stigmasterol yield and extract concentration, The Journal of Supercritical Fluids, 107 (2016) 441-449.

[22] M.M.R. de Melo, H.M.A. Barbosa, C.P. Passos, C.M. Silva, Supercritical fluid extraction of spent coffee grounds: Measurement of extraction curves, oil characterization and economic analysis, The Journal of Supercritical Fluids, 86 (2014) 150-159.

[23] P.F. Martins, M.M.R. de Melo, C.M. Silva, Gac oil and carotenes production using supercritical CO2: Sensitivity analysis and process optimization through a RSM–COM hybrid approach, The Journal of Supercritical Fluids, 100 (2015) 97-104.

[24] A.F. Silva, M.M.R. de Melo, C.M. Silva, Supercritical solvent selection (CO2 versus ethane) and optimization of operating conditions of the extraction of lycopene from tomato residues: Innovative analysis of extraction curves by a response surface methodology and

cost of manufacturing hybrid approach, The Journal of Supercritical Fluids, 95 (2014) 618-627.

[25] J.M. Del Valle, J.M. Aguilera, An improved equation for predicting the solubility of vegetable oils in supercritical carbon dioxide, Industrial & Engineering Chemistry Research, 27 (1988) 1551-1553.

[26] N. Wakao, T. Funazkri, Effect of fluid dispersion coefficients on particle-to-fluid mass transfer coefficients in packed beds, Chemical Engineering Science, 33 (1978) 1375-1384.

[27] V.V. Altunin, M. Sakhabetdinov, Viscosity of Liquid and Gaseous Carbon-Dioxide at Temperatures of 220-1300 K and Pressures up to 1200 Bar, Thermal Engineering, 19 (1972) 124-129.

[28] A.L. Magalhães, P.F. Lito, F.A. Da Silva, C.M. Silva, Simple and accurate correlations for diffusion coefficients of solutes in liquids and supercritical fluids over wide ranges of temperature and density, Journal of Supercritical Fluids, 76 (2013) 94-114.

[29] J. Puiggené, M.A. Larrayoz, F. Recasens, Free liquid-to-supercritical fluid mass transfer in packed beds, Chemical Engineering Science, 52 (1997) 195-212.

[30] R. Cruz, M.M. Cardoso, L. Fernandes, M. Oliveira, E. Mendes, P. Baptista, S. Morais, S. Casal, Espresso coffee residues: A valuable source of unextracted compounds, Journal of Agricultural and Food Chemistry, 60 (2012) 7777-7784.

6 KINETIC MODELING

This chapter is mainly devoted to modeling studies of the experimental results presented in Chapter 5. In the whole, it encompasses an introduction based on the comprehensive review on SFE of vegetal biomass from 2000 to 2013 [1], followed by the SFE studies for the mentioned biomasses (E. crassipes stalks and laves [2] and Q. cerris cork [3]).

CHAPTER OUTLINE

6.1 INTRODUCTION

In this section an overview of SFE modeling is provided, yet specific works on this subject were published by Oliveira et al. [4], Sovová et al. [5] and del Valle et al. [6]. It begins with some considerations regarding subsidiary thermodynamic and kinetic relations usually required by models (subsection 6.1.1), followed by the presentation of models based on their distinct complexity levels (6.2.2).

In general, SFE modeling analyses extraction curves from which kinetic and thermodynamic aspects of the processes are quantitatively obtained with great advantage for further upscaling and optimization studies as well as for economic assessments. Also in the scope of modeling subject, design of experiments and the response surface methodology have been adopted by SFE researchers as statistical methods that allow the disclosure of operating conditions impact on results and also comprise a way of describing experimental results when fundamental data is scarce or does not exist.

6.1.1 Subsidiary relations

Density (ρ) – SC-CO_2 density is perhaps the most important variable of the process from which experimental results are interpreted on first level, but also when more demanding calculations have to be performed. It can be obtained from thermodynamic tables [7] or a equations of state (EoS) such as the one from Pitzer and Schreiber [8]. When dealing with cosolvents such as ethanol, estimations can be achieved with resort to Peng-Robinson or other EoS plus mixing rules with adequate interaction parameters. Details are discussed by Pilavtepe and Yesil-Celiktas [9].

Viscosity (μ) – The viscosities of supercritical fluids are necessary for the prediction of diffusivities and mass transfer coefficients, and also for hydrodynamic studies. Predictive and correlation methods for dense fluids are listed by Reid et al. [10], Stephen and Lucas [11], Silva et al. [12], Monnery et al. [13], and Sovová and Prochazka [14]. Examples of such methods are Jossi, Stiel and Thodos [10], Altunin and Sakhabetdinov [15], and Vesovic and Wakeham [16].

Diffusivity (D_{12}) – The calculation of diffusivities is of major importance as this property is required to estimate: i) effective diffusivities (D_{eff}), and linear driving force coefficients (k_{LDF}); ii) convective mass transfer coefficients (k_{f}), via Sherwood (Sh), Reynolds (Re) and Schmidt (Sc) numbers; and iii) axial dispersion coefficients (D_{ax}), via Peclet (Pe), Reynolds and Schmidt numbers. Several models can be found in the literature for D_{12} calculation: the predictive expressions of Lai and Tan [17], Magalhães et al. [18], Vaz et al. [19-21], Wilke–Chang [10], Zhu et al.[22], and the correlations of Dymond [23], Funazukuri and Wakao [24], Liu et al. [25] and Magalhães and coworkers [26-33]. A worth noting feature concerning the application of various

models of Magalhães et al. is the fact that these authors provide spreadsheets for the estimation of D_{12}, which may be consulted in the supplementary material of the original papers [21, 26-27, 31].

Convective mass transfer coefficient (k_f) – Empirical relations of the type $\mathrm{Sh} = \alpha\ \mathrm{Re}^{\beta}\mathrm{Sc}^{\gamma}$ are generally employed and may be consulted in Oliveira et al.[4] and Sovová et al. [34]. Del Valle and de la Fuente [35] presented a comparison between experimental values of k_f in the SFE of oil seeds where an overestimation tendency of these methods at certain conditions is revealed.

Axial dispersion (D_{ax}) – Axial dispersion coefficients in supercritical fluids can be estimated by nondimensional correlations listed in the review of Oliveira et al. [4]. The simplest correlations set axial dispersion as function of Re, Sc, bed porosity (ε_b) and D_{12}, as it is the case of Wakao and Funazkri [36], Catchpole et al. [37] and Yu et al. [38]. In general, the axial dispersion is neglected when the rule of thumb $L_b > 50\ d_p$ is obeyed, where L_b is the length of the bed and d_p is the average diameter of biomass particles. However, even in such cases the axial dispersion term should not be eliminated from material balances in order to facilitate the numerical solution of the model.

Solubility (y_i^*) – Due to the fact that natural matrices contain several compounds from different chemical families, solubility predictions are many times hindered by the complexity of raw materials and the uncertainty of interactions between existing molecules. It is common practice to simplify the calculation approach either by considering the oil as a single entity or by considering one specific solute as the unique compound to be dissolved in SC-CO_2. In addition, solubility of edible oils is many times approximated using data from the first period of extraction of cumulative curves, more specifically using their slope for very low flow rates. It is worth noting this is only legitimate when SC-CO_2 gets saturated along bed. Mention and application of this procedure can be found in the work of Sovová [39].

The correlation (Eq. (1)) early proposed by Chrastil [40] for binary systems found great acceptance among researchers to estimate solubilities in SC-CO_2. It was conceived from the principle that solute-solvent solvation complexes exist under equilibrium, so that the solubility (y_i^*) is as function of solvent density (ρ_f) and temperature:

$$y_i^* = \rho_f^{k_1} \exp\left(\frac{a}{T} + b\right) \tag{1}$$

where k_1 is a parameter representing the average number of CO_2 molecules in the complex (also called association number), a_1 depends on vaporization and enthalpies of the solute, and b_1 is dependent on the solute molecular weight. To mention one example of application of this expression, Güçlü-Üstündağ and Temelli [41] used it to correlate the solubilities of several minor lipid components such as β-carotene, α-tocopherol, stigmasterol and squalene.

Two important empirical modifications of the seminal expression of Chrastil are worth noting, one from Adachi and Lu [42] and the other from Del Valle and Aguilera [43]. Del Valle and Aguilera introduced a temperature dependence on the heat of vaporization of solute, leading to a new expression that exhibits a quadratic temperature term:

$$y_i^* = \rho_{\mathrm{f}}^{k_1}\, exp\left(\frac{c}{T^2} + \frac{a}{T} + b\right) \tag{2}$$

This expression was correlated by the authors with solubility data of vegetable oils comprising triacylglycerides with 18 carbon atoms by treating the oil as a single entity. The proposed parameters are $k_1 = 10.724$, $a = -18708$, $b = -40.361$ and $c = 2186840$, for T given in K, and y_i^* and ρ_{f} given in $\mathrm{kg\ m^{-3}}$.

In a different approach, Adachi and Lu [42] assumed that the association number depends upon density rather than being a constant value. Hence, Eq. (1) gives rise to:

$$y_i^* = \rho_{\mathrm{f}}^{(c+d\,\rho_f+e\,\rho_f{}^2)}\, exp\left(\frac{a}{T} + b\right) \tag{3}$$

Several other expressions, from which some are improvements of the aforementioned ones, have been published in the literature. One may cite Mendez-Santiago and Teja [44], Sung and Shim [45], Bartle et al. [46], Kumar and Johnston [47], Yu et al. [48] , Gordillo et al. [49], and Garlapati and Madras [50] as examples.

With regard to ternary systems, i.e. involving cosolvents, González et al [51] proposed a modification to the Chrastil equation so that the influence of cosolvent is included in the calculations through a dependence on its mass concentration (y_{cosolv}), and by setting an association number also for the cosolvent (k'):

$$y_i^* = \rho_{\mathrm{f}}^{k}\, y_{\mathrm{cosolv}}{}^{k'}\, exp\left(\frac{a}{T} + b\right) \tag{4}$$

In addition, Mendez-Santiago and Teja [52] proposed an new semiempirical density-based model for ternary cosolvent systems which adds a cosolvent term to their original binary expression. The model was subjected to modification by Sauceau et al [53] who incorporated a Clausius–Clapeyron relation for the sublimation pressure and gave rise to a *T*-dependent term:

$$\frac{y_i\, P}{P^{std}} = exp\left[\frac{1}{T}\left(a + b\,\rho_{\mathrm{f}} + c\,y_{\mathrm{cosolv}} + d\,T\right)\right] \tag{5}$$

where *d* is a constant that in case of being null restitutes the Mendez-Santiago and Teja [52] expression for ternary systems; P^{std} is a constant value for pressure under standard conditions, 1 bar. Another modification to the Mendez-Santiago and Teja for ternary systems was published by Thakur and Teja [54]. Still for ternary (cosolvent) systems, Sovová [55] proposed an empirical

equation where solubility in a mixture of SC-CO_2 and cosolvent is given by a power function that relates the solubility in pure CO_2 (y^*_{i,CO_2}) with the cosolvent mass fraction (y_{cosolv}) as follow: $(y_{cosolv})^c$

$$y_i^* = y_{i,CO_2}^* + a\left(y_{i,CO_2}^*\right)^b (y_{cosolv})^c \quad (6)$$

where *a*, *b* and *c* are model constants to be fitted to experimental data.

The rigorous thermodynamic approach to predict solubilities of pure solids or liquids in a supercritical fluid (SCF) comprises the classical isofugacity condition that results in a well-known equilibrium relation, reliant on Poynting factor, solute vapor pressure (P_i^{sat}), fugacity coefficient of the solute in supercritical phase (ϕ_i^{SCF}), and molar volume of the pure solid or liquid (V_i^{solid}):

$$y_i^* = \frac{P_i^{sat}}{P\phi_i^{SCF}} exp\left[\frac{V_i^{solid}(P - P_i^{sat})}{\Re T}\right] \quad (7)$$

where $\Re$ is the universal gas constant. Considerations regarding the properties embodied in Eq. (7) are expressed in the following paragraphs.

With respect to P_i^{sat}, two strategies may be adopted for its calculation, which mostly depend on the available knowledge about the system under study:

i. For known systems, P_i^{sat} can be calculated by the Clapeyron equation, for which fusion properties of the solute and an adequate saturation curve are necessary. A more detailed description of this approach is given by Garnier et al. [56], who also provide a list of useful properties related the application of the Peng-Robinson (PR) EoS to solubility calculations for several solutes in SC-CO_2.
ii. For less known systems, P_i^{sat} may be obtained through an integrated form of the Clausius-Clapeyron equation [57], which demands solute boiling and melting temperatures, entropies and heat capacity changes, as well as the respective critical properties. For these, group contribution methods may be employed with advantage. An example of this type of calculation is provided in the work of de Melo *et al.* [58] for binary systems involving SC-CO_2 and triterpenic acids.

Concerning ϕ_i^{SCF}, it is computed by means of an equation of state such as PR-EoS or Redlich-Soave-Kwong EoS, among many other possibilities. Further aspects regarding the application of the PR-EoS may be found in both works of Garnier et al. [56] and Melo et al. [58]. A full compilation of works that employ EoS to model phase equilibria of solutes in supercritical media is provided by Ŝkerget et al. [59] or Díaz-Reinoso et al [60], including examples employing less common EoS options, such as the group contribution EoS, UNIFAC, the perturbed hard sphere chain EoS, the

quasi-chemical nonrandom lattice fluid, regular solution model with a Flory-Huggins term, and the multifluid nonrandom lattice fluid.

As far as V_i^{solid} is concerned, values may be obtained from available compilations of this property for several molecules [61-62], or, alternatively, from available databases such as RCS ChemSpider [63] that promptly provide predictions for a wide variety of chemical compounds.

Other works have been published with alternative thermodynamic emphasis. For instance, Su [64] recently proposed an approach to solubility modeling through a two-parameter expression developed from the regular solution model coupled with the Flory-Huggins equation. The correlative results from this equation are comparable to those obtained with three parameters semiempirical equations. In addition a semiempirical correlation based on regular solution theory that employs the Van der Walls EoS was early published by Ziger and Eckert [65].

6.1.2 Extraction models

Empirical models – When results are to be described by simple mathematical expressions, empirical models provide easy and prompt solutions. Expressions can be found in the literature that easily describe the shape of SFE curves such as Subra et al. [66] and Naik et al. [67] (see Table 6.1). These models are usually built in relation to the initial solute concentration in the matrix (x_0) and involve an adjustable parameter that may not allow any physical interpretation. Despite being able to provide reliable fittings, empirical models do not allow mass transfer coefficients to be determined and thus are of little aid for a deep understanding of the process, namely when scale-up objectives are targeted.

Table 6.1 – Empirical models for SFE processes.

Name	Ref	Expression	Eq.
Subra et al.	[66]	$\eta = x_0(1 - \mathrm{e}^{-\mathrm{K}t})$	(8)
		where, η is the extraction yield, t is time, x_0(is the concentration of the target species in the raw material expressed in the same units of η, and K is the model parameters related to the rate of extraction.	
Naik et al.	[67]	$\eta = x_0\left(\frac{t}{b+t}\right)$	(9)

Simplified models – The derivation of phenomenological models for SFE processes includes rate equations and mass balances to both supercritical fluid and solid phases, and require kinetic and

equilibrium data, and possibly some features of the physical structure of the matrix. Owing to the usual lack of information at both kinetics and equilibrium levels, and also to the implied complexity of natural matrices, simplified models providing approximate solutions have been published and adopted by research community. The application of simplified models to SFE results can provide useful hints regarding the limitations that prevail in a SFE process, which enable phenomena with insignificant importance to be discarded from future rigorous modeling.

Examples of simplified models have been proposed by Martínez et al. [68], Tan and Liou [69], and Gaspar [70], and Crank [71], among others (see Table 6.2). Their adequacy may be tested case-by-case upon fitting the proposed equations to experimental extraction curves. They normally embody one or two adjustable parameters (time or mass transfer related constants) and typically need at least the initial solute concentration in the biomass to be known.

The Logistic model (Eq. (10)), proposed by Martínez et al. [68], neglects axial dispersion and the accumulation in the bed, and assumes that the interfacial mass transfer only depends on the composition of the extract along the process. A logistic equation, usually applied to model population growth, is adopted to describe the variation of the extract composition along time. The Desorption model (Eqs. (11)-(13)) of Tan and Liou [69] assumes no accumulation in the bed and that the interfacial mass transfer of the extraction is well described by a first-order kinetic expression whose parameter k_d is the desorption constant. The Simple Single Plate model (Eq. (14)) (slab geometry) and the Diffusion model (Eq. (15)) (sphere particles) presented by Gaspar et al. [70] and Crank [71], respectively, assume also there is no accumulation in the bed nor film resistance to mass transfer, and that the process is governed by intraparticle diffusion.

Some simplified models have been derived for specific extraction periods, as is the case of Brunner [72] model (Table 6.2, Eq. (16)), which relates the outlet oil concentration with the solubility in SC-CO_2 during the first extraction period, when oil is essentially removed from the surface layers of the particles. This model is appropriate to constant rate extraction (CER) stages. In cases where the extraction curve exhibits more than one period, the complete solution is the combination of expressions upon the definition of characteristic times that delimit the transitions between such periods [73].

As an alternative approach, the previous specification of different extraction stages and further application of simplified expressions linked with the mass transfer mechanisms that prevail in each of them can be advantageous. Povh et al. [74] defined extraction regions in accordance with the model of Sovová [75] – i.e. constant extraction rate (CER) and falling extraction rate (FER) periods – and applied then straight lines in order to obtain the kinetic parameters related to that phenomenological model. The parameters were successfully confirmed by the corresponding values of Sovová.

Table 6.2 – Simplified models for SFE processes.

Name	Ref	Expression	Eq.
Logistic model	[68]	$\eta = \frac{X_0}{\exp(b\ t_{\mathrm{m}})}\left(\frac{1+\exp(b\ t_{\mathrm{m}})}{1+\exp[b\ (t_{\mathrm{m}}-t)]}-1\right)$	(10)
		where, η is the extraction yield, t is time, X_0 is the concentration of the target species in the raw material, and b and t_m are the two parameters of the model.	
Desorption model	[69]	$\eta = \frac{A}{k_d}[1-\exp(k_d\ \mathrm{B})]\times[\exp(-k_d\ t)-1]$	(11)
		$A = \frac{Q_{\mathrm{CO_2}}(1-\varepsilon_{\mathrm{b}})X_0\ \rho_s}{w_{\mathrm{b}}\ \varepsilon_{\mathrm{b}}\rho_{\mathrm{f}}}$	(12)
		$B = \frac{\varepsilon_b\ LS\rho_{\mathrm{f}}}{Q_{\mathrm{CO_2}}}$	(13)
		where $Q_{\mathrm{CO_2}}$ is the CO_2 mass flow rate, ε_b is the bed porosity, S is the extractor cross-sectional area, w_{b} is the mass of raw material in the extractor, ρ_{s} and ρ_{f} are the biomass and solvent densities, respectively.	
Simple Single Plate model	[70]	$\eta = X_0\left[1-\sum_{n=0}^{\infty}\frac{0.8}{(2n+1)^2}\exp\left(-\frac{D_{\mathrm{m}}(2n+1)^2\pi^2 t}{l^2}\right)\right]$	(14)
		where D_{m} is the solute diffusivity, and l the plate thickness.	
Diffusion model	[71]	$\eta = X_0\left[1-\frac{6}{\pi^2}\sum_{n=1}^{\infty}\frac{1}{n^2}\exp\left(-\frac{D_{\mathrm{m}}n^2\pi^2 t}{{R_p}^2}\right)\right]$	(15)
		where R_p is particle radius.	
Brunner	[72]	$\eta = \frac{y^* Q_{\mathrm{CO_2}}}{w_b}t\ \left[1-\exp\left(-\frac{k_{\mathrm{f}}a_0 w}{Q_{\mathrm{CO_2}}(1-\varepsilon_b)\rho_s}\right)\right]$	(16)
		where $\mathrm{a_0}$ is the specific surface area ($\mathrm{m^2 m^{-3}}$).	

Comprehensive phenomenological models – Despite the usefulness of simplified models for the collection of phenomenological insights about SFE processes, only far-reaching theoretical approaches allow the study of broader aspects that influence the separation performance. In this respect, topics like flow pattern, solute–matrix interactions, accumulation in the bed, axial dispersion, mass transfer resistances in series and/or in parallel may be mentioned.

Cocero and Garcia proposed a model [158] describing the SFE process through a fixed bed with plug flow, and linear equilibrium plus film resistance to mass transport. The set of material balances to both supercritical and solid phases plus equilibrium expression are given by:

$$\begin{cases} \varepsilon_b \dfrac{\partial y}{\partial t} = -u_i \dfrac{\partial y}{\partial z} - (k_\mathrm{f} a\ \ )(y - y^*) \\ (1-\varepsilon_b)\rho_\mathrm{s} \dfrac{\partial y_\mathrm{s}}{\partial t} = (k_\mathrm{f} a\ \ )(y - y^*) \\ y_\mathrm{s} = H\, y^* \end{cases} \tag{17}$$

where u_i (m h^{-1}) is the superficial velocity of the fluid phase, H is the solute partition coefficient, y_s (kg $\mathrm{kg}^{-1}_{\mathrm{biomass}}$) is the solute (pseudo-component) concentration in the biomass, y (kg m^{-3}) is the solute concentration in the fluid phase, y^* (kg m^{-3}) is the solute solubility in the supercritical phase, a (m^2 m^{-3}) is the specific external surface area, z (m) is the axial coordinate in the bed, ε_b is the bed porosity, t (h) is extraction time, ρ_s (kg m^{-3}) is the biomass (solid) density, k_f (m h^{-1}) is the convective mass transfer coefficient. For the integration, the initial conditions are $y = 0$ and $y_\mathrm{s} = X_0$ for $t = 0$, where X_0 is the original extractable solute amounts in the raw material, and the boundary condition is $y = 0$ at $z = 0$. The yield values are computed by material balance to the whole system as follows:

$$\eta(t) = \frac{Q_{\mathrm{CO_2}}}{\rho_{\mathrm{CO_2}} w_\mathrm{b}} \int_0^t y(t, z = L_\mathrm{b})\, dt \tag{18}$$

being L_b (m) the length of the extractor bed, $\rho_{\mathrm{CO_2}}$ the density of the CO_2, w_b the weight of biomass, and $Q_{\mathrm{CO_2}}$ the mass flow rate of SC-CO_2.

The broken plus intact cells (BIC) model proposed by Sovová [39, 75], the shrinking core model (SCM) from Goto et al. [76] or the combination of the latter two (SCM-BIC) as proposed by Fiori et al. [77] are perhaps the sound examples of SFE comprehensive modeling. The differences between those models rely on the conception of how extraction takes place in the solid phase. These models are summarized in Table 6.3.

Table 6.3 – Comprehensive phenomenological models for SFE processes: BIC= broken plus intact cells model, SCM = shrinking core model, SC-BIC = bridged model comprising shrinking core and broken plus intact cells concepts.

Model	Ref	Expression	Eq.
BIC	[39, 75]	$\begin{cases} \text{SC phase:} \quad \rho_\mathrm{f}\, \varepsilon \left(\dfrac{\partial y}{\partial t} + U \dfrac{\partial y}{\partial h}\right) = j_\mathrm{f} & (19) \\ \text{Broken cells:} \quad g\rho_\mathrm{f}(1-\varepsilon)\dfrac{\partial x_1}{\partial t} = j_\mathrm{s} - j_\mathrm{f} & (20) \\ \text{Intact cells:} \quad (1-g)\rho_\mathrm{s}(1-\varepsilon)\dfrac{\partial x_2}{\partial t} = -j_\mathrm{s} & (21) \end{cases}$	
		where y is the solute fluid phase concentration, x_1 and x_2 are the solute concentration in the broken and intact cells, respectively, g is the grinding efficiency, j_s is the flux from intact cells to broken cells, j_f is the flux from broken cells to SC solvent, U is the interstitial velocity, ρ_f is the solvent	

density, ρ_s is the solid density, ε is the bed porosity, t is time and h is the axial coordinate.

SCM [76]

$$\begin{cases} \text{SC phase: } \rho_f \varepsilon \left(\frac{\partial y}{\partial t} + U\frac{\partial y}{\partial h}\right) = j & (22) \\ \text{Solid phase: } \frac{D_{eff}}{r^2}\frac{\partial}{\partial r}\left(r^2 \frac{\partial y_{pores}}{\partial r}\right) = 0 & (23) \\ \text{and} \\ j = k_f a_p (y_{pores} - y) & (24) \end{cases}$$

where k_f is the convective mass transfer coefficient, a_p is the particle specific surface area, y_{pores} is the solute concentration in the pore network, D_{eff} is the effective diffusion coefficient and r is the radial coordinate in the particle.

SC-BIC [77]

$$\begin{cases} \text{SC phase: } \rho_f \varepsilon \left(\frac{\partial y}{\partial t} + U\frac{\partial y}{\partial h}\right) = j & (25) \\ \text{Solid phase: } \mathrm{j} = \frac{\partial V_{ex}}{\partial t} = 3\rho_f \frac{k}{R_p}\frac{y^* - y}{x_0} & (26) \\ k = f(\text{exhaustion model chosen}) & (27) \end{cases}$$

where V_{ex} is the volumetric exhaustion degree of the particle, x_0 is the concentration of the solute in the raw material, k is the overall mass transfer coefficient (varies along r), R_p is the particle radius, j is the flux from particles to solvent.

BIC model has been the most adopted approach in SFE modeling and is devoted to matrices submitted to milling in which two distinct structures are left to be extracted: cells with broken walls and intact cells. Accordingly, it considers that solutes removal can be driven by convection from broken (external) cells to the supercritical phase, and/or by diffusion from inner intact cells to the outer broken cells. According to this model, the extraction curves are divided in three regions, each one characterized by the dominance of specific or combined mass transfer mechanisms. In this sense, the initial period is named 'constant extraction rate' (CER), where the prevailing resistance is the external film diffusion and affects mostly accessible solutes on particles surface. The second period is called 'falling extraction rate' (FER) and combines the vanishing contribution of the convective term of CER with the increasingly important intraparticle diffusion of solutes from inner intact cells. Being an intermediate region, the noticeable outcome of this period is a progressive decrease of the oil flux as the accessible solute from broken cells reaches depletion and the internal diffusion from intact cells denotes an increasing relevance for the course of the whole process. The final period is the one with the slowest rate because the extraction is uniquely based on the transport of solutes from intact cells through diffusion. This period is known

as DC, which stands for 'diffusion controlled'. A summary of the mathematical formulation of BIC model is presented in Table 6.4 which contains an illustrative figure exhibiting the CER, FER and DC periods. Detailed reviews covering this issue, including all assumptions and examples of application, are provided by Oliveira et al. [4] and Huang et al. [78].

In a complementary study, Silva et al. [79] provided a comparison between numerical simulations of supercritical fluid extraction for two distinct cases: the original concept of broken plus intact cells where the internal mass transfer occurs in parallel or in series. The calculated results were compared with experimental data and showed similar performance. Later, Passos et al. [80] modeled the SFE of untreated and enzymatically pretreated grape seeds, being able to demonstrate that the fitted BIC model parameters do reflect the internal structure changes due to hydrolysis and grinding efficiency.

Following a different approach, the SCM assumes that there is a sharp dynamic boundary between the extracted and non-extracted regions of the particles, which moves towards the center as the extraction proceeds. The axial dispersion effect can be considered while radial dispersion is many times neglected if the extractor is of small diameter. Instead of relying on the concept of broken and intact cells, SCM simply assumes that the cells of the matrix have identical conditions in terms of structures and solutes concentration, and that solutes suffer an irreversible desorption from the matrix. As for BIC model, the full list of assumptions and examples of application of SCM can be consulted in the reviews of Oliveira et al. [4] and Huang et al. [78] .

The premise of considering a uniform structure for the matrix is a delicate one, as natural biomass can easily evidence variations on its microstructure due to being composed of different tissues/cells, but also owing to drying and pretreatment processes. It is known that attempts to enhance extraction yield through acoustic waves [81] or enzymatic hydrolysis [82] pretreatments can substantially modify the raw material, leading to fractions of cells with eased access to solutes in comparison to intact cells. Adding to this remark, both SCM and BIC model assume that all cells of the matrix, at initial conditions, contain solute. In fact, inert or already depleted cells can be present and in these cases the extractable part of the matrix represents a fraction of the whole biomass. The chance that part of the matrix does not contribute for the extraction is not enclosed in any of the two phenomenological models and could be a valuable enhancement for an improved interpretation of the SFE.

Finally, Fiori et al. [77] conceived a model that conjugates features of BIC model and SCM (SC-BIC model), and their combination of concepts provides novel representation possibilities for the particles exhaustion over time, enumerated by the authors as discrete, continuous and semi-continuous models for solid phase. These cases combine dynamic concentration boundary with the distinct extraction mechanisms due to matrix cells nonuniformities described by broken or intact

cells approach. The basic mathematical formulation of the SC-BIC models is given in Table 6.3. Broader considerations can be found in the original paper [77] and on subsequent reviews [4, 78].

In view of being the most employed model, the presentation of an integrated form of BIC is pertinent. In this sense, Table 6.4 illustrates the various extraction periods and corresponding algebraic equations to model SFE. Nimet et al. [83] applied this model to ten extraction curves of sunflower seeds, where $Z, W, r, y^*_{oil}, t_{\mathrm{CER}}, t_{\mathrm{FER}}, k_{\mathrm{s}}a$ and $k_f a$ are adjustable parameters. Working with palm oil, Jesus et al. [84] applied this integrated form of BIC to palm oil extraction curves, and set only $k_{\mathrm{s}}a$ and $k_f a$ as adjustable parameters

An example of extraction curves modeling is given in Figure 6.1 for the case of SFE of rosemary leaves (*Rosmarinus officinalis*). In this work, Carvalho *et al.* [85] present a study where three models from those mentioned above (Esquível *et al.* [86] , SCM and BIC model) are tested against flow rate and bed geometry variations. From the goodness of the fitting achieved, better results are given by Esquível e*t al.* equation, followed by BIC model whose representation was slightly better than SCM. Despite their results suggest the empirical model of Esquível *et al.* to be preferable, the nature of information that can be obtained by the two phenomenological models is of superior interest. In fact, they allow predictions for distinct operating conditions, being precious for ultimate scale-up studies where accurate simulations are fundamental. The extraction curves presented in Figure 6.1 provide also interesting information regarding the significant impact of flow rates on SFE results, as discussed in previous section, and raise geometric aspects into analysis.

By applying physical models to experimental data measured in beds with different height to diameter ($L_{\mathrm{b}}/D_{\mathrm{b}}$) ratios, Carvalho et al. [85] were able to infer how bed geometry influences relevant parameters like the period of constant extraction rate (t_{CER}) and global mass transfer coefficient. Yield results exhibit a noticeable enhancement when beds have larger length to diameter values, e.g. beds that favor length in comparison to diameter.

The compilation of SFE publications covered by the review of the author [1] found many examples of modeling. Table 6.5 provides a classification of papers with emphasis on modeling results. The type of approach employed is highlighted (whether empirical, simplified or comprehensive) as well as the designation of models employed. From Table 6.5 one can disclose that solubility modeling has been marginal in comparison to extraction curves studies, and also that BIC model is by far the most chosen to fit and interpret experimental results.

* * *

In the following sections, the two studies presented and discussed in Chapter 5 (Measurement of Extraction Curves) are revisited towards the kinetic modeling of the respective data. Hence, this chapter does not have a Materials and Methods section in the sense that all experimental data and respective experiments are the same previously presented (see Section 5.2).

Table 6.4 – Integrated form of the broken plus intact cells (BIC) model.

Model equations		Eq.
$w_{\text{oil}} = Q_{CO_2} y^*_{oil}\, t\, [1 - exp(-Z)]$	for $0 \le t \le t_{\text{CER}}$	(28)
$w_{\text{oil}} = Q_{CO_2} y^*_{oil}\, t\, [t - t_{\text{CER}} exp(Zm(t) - Z)]$	for $t_{\text{CER}} \le t \le t_{\text{FER}}$	(29)
$w_{\text{oil}} = w' \left\{ x_0 - \frac{y^*_{oil}}{W} \ln \left[1 + \left(\exp\left(\frac{W x_0}{y^*_{oil}} \right) - 1 \right) \exp\left(\frac{W Q_{CO_2}}{w'} (t_{\text{CER}} - t) \right) \text{g} \right] \right\}$	for $t \ge t_{\text{FER}}$	(30)

Complementary equations:

$$Z = \frac{k_{\text{f}} a\, w' \rho_{\text{f}}}{Q_{\text{CO}_2} \rho_{\text{b}}} \tag{31}$$

$$W = \frac{w' k_{\text{s}} a}{Q_{\text{CO}_2} (1 - \varepsilon)} \tag{32}$$

$$t_{\text{CER}} = \frac{(1 - g) w' x_0}{Q_{\text{CO}_2}\, y^*_{\text{oil}}\, Z} \tag{33}$$

$$t_{\text{FER}} = t_{\text{CER}} + \frac{w'}{W Q_{\text{CO}_2}} \ln \left[g + (1 - g) \exp\left(\frac{W x_0}{y^*_{\text{oil}}} \right) \right] \tag{34}$$

$$Zm\,(t) = \frac{Z\, y^*_{\text{oil}}}{W\, w'} \ln \left\{ \frac{1}{1 - g} \left[\exp\left(\frac{W Q_{CO_2}}{w'} (t - t_{\text{CER}}) \right) - g \right] \right\} \tag{35}$$

where w' is the solid mass in oil-free basis, ρ_{b} is the bed density, $k_{\text{f}} a$ is the solvent phase volumetric mass transfer coefficient, and $k_{\text{s}} a$ is the solid phase volumetric mass transfer coefficient.

Extraction periods scheme

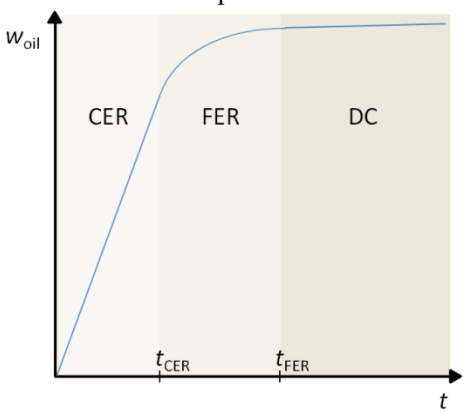

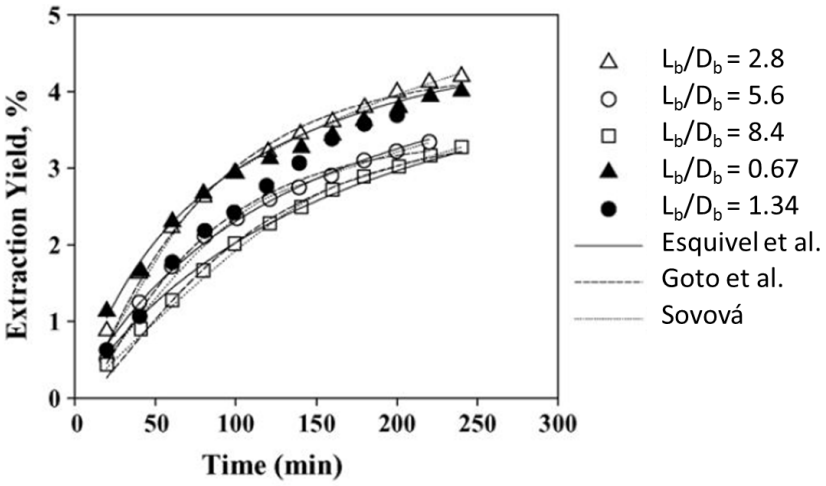

Figure 6.1 – Experimental and fitted extraction curves of rosemary leaves (*Rosmarinus officinalis*). Experiments performed at 300 bar, and 40 °C and different flow rates: (Δ, ○, ●, □) 8.33×10^{-5} kg s^{-1} , (▲) 5.25×10^{-5} kg s^{-1}. L_b is bed length and D_b bed diameter. Adapted from Carvalho *et al.* [85].

Table 6.5 – SFE publications that comprise modeling studies. Sol = solubility, Ext = extraction.

Matrix	Scope	Type of Model	Model	Ref.
Amaranth	Sol	Empirical	Chrastil [40]	[87]
	Sol	Empirical	Del-Valle and Aguilera Chrastil modification [43]	
	Ext	Simplified	Reverchon and Osseo [88]	
Aniseed	Ext	Comprehensive	Sovová [75]	[89]
Annatto	Ext	Comprehensive	Sovová [75]	[90]
Annato	Sol	Empirical	Splines	[91]
Apricot	Ext	Comprehensive	Sovová [75]	[92]
Artemisia annua L.	Ext	Comprehensive	Sovová [75]	[93]
	Ext	Simplified	Martínez et al [68]	
	Ext	Empirical	Esquível et al [86]	
Baccharis trimera	Ext	Comprehensive	Reverchon [94]	[95]
	Ext	Comprehensive	Sovová [75]	
Baccharis trimera	Ext	Simplified	Tan and Liou [69]	[96]
	Ext	Simplified	Brunner [72]	
	Ext	Comprehensive	Sovová [75]	
	Ext	Empirical	Esquível [86]	
Blac cumin	Ext	Statistical	Neural networks + Goto et al. [76]	[97]
Black pepper	Ext	Comprehensive	Sovová [75]	[98]
	Ext	Comprehensive	Ŝkerget and Knez [99]	
Borage, Primrose	Ext	Simplified	Hong [100]	[101]
	Ext	Simplified	Brunner [72]	

Canola, Sesame	Sol		BET	[102]
	Sol		Henry	
	Sol		Freundlich	
Cashew	Sol	EoS	Peng–Robinson	[103]
Cashew	Ext	Comprehensive	Mukhopadhyay [102]	[104]
	Ext	Comprehensive	Goto et al. [76]	
	Sol	Empirical	Chrastil [40]	
	Ext	Empirical	Subra et al. [66]	
Celery	Ext	Empirical	Naik et al. [67]	[105]
	Ext	Simplified	Reverchon and Osseo [88]	
	Ext	Comprehensive	Sovová [75]	
Chamomile	Ext	Comprehensive	Sovová [75]	[74]
Clove	Ext	Comprehensive	Adaptation of Goto et al [76]	[106]
	Ext	Comprehensive	Sovová [75]	
	Ext	Simplified	Martínez et al [68]	
Coffee	Ext		Araus [107]	[108]
Coffee	Ext	Comprehensive	Sovová [75]	[109]
	Ext	Simplified	Martínez et al [68]	
	Ext	Simplified	Crank [71]	
Cordia verbenacea	Ext	Simplified	Crank [71]	[110]
	Ext	Empirical	Naik et al. [67]	
	Ext	Simplified	Tan and Liou [69]	
	Ext	Comprehensive	Goto et al [76]	
	Ext	Comprehensive	Sovová [75]	
Cupuacu	Ext	Comprehensive	Sovová [75]	[111]
Fennel	Ext	Comprehensive	Sovová [75]	[112]
	Ext	Comprehensive	Goto et al. [76]	
	Ext	Simplified	Tan and Liou [69]	
Fig leaf gourd	Ext	Comprehensive	Sovová [75]	[113]
Ginger	Ext	Comprehensive	Sovová [75]	[114]
Ginger	Ext	Comprehensive	Sovová [75]	[68]
	Ext	Approximate	Martínez et al [68]	
Grape	Ext	Comprehensive		[80]
Grape	Ext	Comprehensive		[79]
Hazelnut	Sol	Empirical	Chrastil [40]	[115]
	Ext		Andrich et al. [63]	
Hazelnut, Walnut	Ext	Comprehensive	Sovová [75]	[116]
Hypericum caprifoliatum	Ext	Simplified	Tan and Liou [69]	[117]
	Ext	Comprehensive	Reverchon [94]	
	Ext	Comprehensive	Sovová [75]	
Hyssop	Ext	Comprehensive	Sovová [39]	[118]
Jalapeño	Ext	Comprehensive	Sovová [75]	[119]
Lavender	Ext	Comprehensive	Akgun [117]	[120]

Marigold	Ext	Comprehensive	Sovová [75]	[121]
Marigold	Ext	Comprehensive	Sovová [75]	[122]
	Ext	Simplified	Martínez et al [68]	
	Ext	Simplified	Tan and Liou [69]	
	Ext	Simplified	Gaspar et al. [70]	
	Ext		Reverchon [94]	
Marigold	Sol	Empirical	Chrastil [40]	[123]
Neem	Ext	Comprehensive	Goto et al [76]	[124]
Neem	Ext	Comprehensive	Goto et al [76]	[125]
Nutmeg	Ext	Comprehensive	Sovová [75]	[126]
	Ext	Comprehensive	Goto et al [76]	
Orange	Ext	Comprehensive	Sovová [75]	[127]
Oregano	Ext	Simplified	Adaptation from Bartle et al [128]	[70]
	Ext	Simplified	Gaspar et al. [70]	
Oregano	Ext	Statistical/Empirical	Stepwise regression	[129]
Palm	Ext	Comprehensive	Sovová [75]	[130]
Paprika	Ext	Comprehensive	Sovová [75]	[131]
Parsley	Ext	Simplified	Reverchon and Osseo [88]	[132]
	Ext		Naik et al. [67]	
	Ext	Comprehensive	Sovová [75]	
	Ext	Comprehensive	Adaptation from Sovová [75]	
Peach	Ext	Comprehensive	Sovová [75]	[133]
	Ext	Simplified	Martínez et al [68]	
	Ext	Simplified	Crank [71]	
	Ext	Simplified	Campos et al. [122]	
	Ext	Simplified	Kitzberger et al. [134]	
Pupunha	Ext	Simplified	Tan and Liou [69]	[135]
Rapeseed	Ext	Comprehensive	Goto et al [76]	[136]
Red pepper	Ext		Peker et al. [665]	[137]
Rice	Ext	Simplified	Brunner [72]	[138]
Rosemary	Ext	Simplified	Crank [71]	[85]
	Ext	Comprehensive	Sovová [75]	
	Ext	Comprehensive	Goto et. Al. [76]	
	Ext	Empirical	Esquível et. al. [86]	
	Ext	Simplified	Tan and Liou [69]	
	Ext	Simplified	Martínez et al [68]	
Rosemary	Ext	Comprehensive	Sovová [75]	[139]
Sacha inchi	Sol	Empirical	Chrastil [40]	[140]
Safflower	Ext	Comprehensive	Sovová [75]	[141]
Schisandra chinensis			Straight lines	[142]
Shiitake mushroom	Ext	Comprehensive	Sovová [75]	[134]
	Ext	Simplified	Martínez et al. [68]	
	Ext	Simplified	Tan and Liou [69]	
	Ext	Simplified	Crank [71]	
	Ext	Comprehensive	Goto et al. [76]	
	Ext	Empirical	Esquível et al. [86]	

Spanish sage	Ext	Comprehensive	Sovová [75]	[143]
Spearmint	Ext	Comprehensive		[144]
Stevia	Ext	Comprehensive	Sovová [75]	[145]
Sunflower	Ext	Approximate	Andrich et al [63]	[146]
	Sol	Empirical	Chrastil [40]	
	Sol	Empirical	del Valle and Aguilera [43]	
	Sol	Empirical	Yu et al [48]	
Sunflower	Ext	Comprehensive	Sovová [75]	[147]
	Ext	Comprehensive	Catchpole [148]	
Sunflower	Ext	Comprehensive		[149]
Thyme	Ext	Comprehensive	Goto et al [76]	[150]
Thyme	Ext	Simplified	Reverchon et al. [151]	[152]
Tomato	Ext	Simplified	Brunner [72]	[153]
Tomato	Sol	Empirical	Chrastil [40]	[154]
Turmeric	Ext	Simplified	Tan and Liou [69]	[155]
Valerian	Ext	Comprehensive		[156]
Vetiver	Sol	EoS	Peng-Robinson	[157]

6.2 MODELING

6.2.1 SFE CURVES OF *Eichhornia crassipes*

Aiming at the disclosure of the dominant mechanisms of the SFE process, the extraction curves measured at lab scale were studied with simple expressions:

i) two models that exclusively focus on intraparticle diffusion, namely the Diffusion model for spherical particles [159] (DFM) and the Single Simple Plate model (SSPM) for slab geometry [70];

ii) A model applied by Cocero and Garcia [158] that conjugates linear SC-CO_2/solid equilibrium (i.e., solute-matrix interaction exists) and film resistance, henceforth called LEFM;

iii) a more comprehensive modeling approach, the integrated broken plus intact cells (BIC) model, which can be employed with advantage to obtain richer insights about the global mass transfer phenomenon, including kinetics, thermodynamics and biomass features.

6.2.2 SFE CURVES OF *Quercus cerris*

With the aim of studying the impact of the operating conditions on the kinetics, thermodynamics, and selectivity of the SFE, the integrated broken plus intact cells (BIC) model was applied to the

extraction curves measured at lab scale. BIC model was initially proposed by Sovová [75, 160] and has been the most adopted approach in SFE phenomenological modeling [4, 161].

6.3 RESULTS AND DISCUSSION

6.3.1 SFE OF *Eichhornia crassipes*

Simplified models – The three models based on the simplest assumptions (LEFM, DFM and SSPM) were used to represent the six SFE runs. Driven by the noticeable distinct plateaus evidenced by the experimental data depending on the usage (Runs 5.12-5.13) or not (Runs 5.8-5.10) of cosolvent, two X_0 adjustable parameters were admitted for each model.

Concerning the fitting of DFM and SSPM, which rely solely on intraparticle diffusion mechanism, Runs 5.8 to 5.10 shared the same D_m since P and T are constant on those assays. As for Runs 5.11 to 5.13, individual fittings of D_m were accomplished since changes in pressure and/or ethanol content affect the diffusion coefficients. The fitting parameters were, in these cases, $D_m/{L_p}^2$ and X_0 for SSPM, and $D_m/{R_p}^2$ and X_0 for DFM. In the case of LEFM the volumetric convective mass transfer coefficient ($k_\mathrm{f}a$) was fitted individually to each data series, while the equilibrium partition coefficient (H) was grouped for each fixed set of (P, T, ethanol content) conditions, i.e. four H parameters were used for the six Runs (note that X_0 is the third parameters as mentioned above).
The overall results achieved by the simplified models are reported in Table 6.6 for η_total and in Table 6.7 for η_stigm, together with the average deviations (AARD) and the determination coefficients (R^2) of the fittings. In addition, the experimental data and calculated results of η_total are plotted in Figure 6.2 for Runs 5.8 to 5.10. In turn, Figure 6.3 illustrates the fittings attained for η_stigm for Runs 5.11 and 5.12.

With regard to η_total, equivalent fittings were attained by SSPM, DFM, and LEFM. Taking the joint AARDs, the overall values range from 3.43 % for Runs 5.12-5.13 (using SSPM) to 7.89 % for Runs 5.8-5.11 (using DFM). In terms of the determination coefficients, all curves exhibited scores above 97 %. It is worth noting that two distinct X_0 intervals were obtained as expected in advance for experiments with and without ethanol, namely: 0.00760-0.00829 $\mathrm{kg\,kg^{-1}}$ (for Runs 5.8-5.11) and 0.01270-0.01694 (for Runs 5.12-5.13). This finding is naturally related to the solubility enhancement caused by cosolvent addition, which increases the affinity of the supercritical mixture to the polar solutes of the biomass. Accordingly the optimized X_0 values refer to extracts of quite distinct chemical composition, reason why their direct comparison may have no strict equivalent basis. A final remark on LEFM model comprises the capability of correctly predicting the trend of $k_\mathrm{f}a$ increment as $Q_{\mathrm{CO_2}}$ is increased. In fact, a great jump was observed between Run 5.8 and Run

Table 6.6 – LEFM, SSPM and DFM adjusted parameters and fitting indicators applied to experimental η_{total} data.

Exp.	LEFM						SSPM					DFM				
	X_0 (kg kg^{-1})	H	$k_f a$ (h^{-1})	R^2 (%)	AARD (%)		X_0 (kg kg^{-1})	$D_m/{L_p}^2$ (h^{-1})	R^2 (%)	AARD (%)		X_0 (kg kg^{-1})	$D_m/{R_p}^2$ (h^{-1})	R^2 (%)	AARD (%)	
Run 5.8	0.00760	0.4347	0.1287	99.91	7.77	5.73	0.00829	0.0537	99.68	14.24	7.31	0.00829	0.0507	0.9856	22.70	7.89
Run 5.9			0.2549	98.29	4.22				99.78	2.77				0.9994	1.92	
Run 5.10			0.3015	97.03	6.74				99.13	8.36				0.9991	4.14	
Run 5.11		0.5919	0.2760	98.87	4.21			0.0458	99.25	1.51			0.0398	0.9981	2.77	
Run 5.12	0.01270	1.1455	0.4243	99.78	4.60	6.78	0.01410	0.0342	99.84	2.43	3.43	0.01694	0.0170	0.9960	4.41	5.37
Run 5.13		0.8135	0.4225	99.98	8.95			0.0330	99.60	4.03			0.0148	0.9941	6.33	

Table 6.7 – LEFM, SSPM and DFM adjusted parameters and fitting indicators applied to experimental η_{stigm} data.

Exp.	LEFM						SSPM					DFM				
	X_0 (kg kg^{-1})	H	$k_f a$ (h^{-1})	R^2 (%)	AARD (%)		X_0 (kg kg^{-1})	$D_m/{L_p}^2$ (h^{-1})	R^2 (%)	AARD (%)		X_0 (kg kg^{-1})	$D_m/{R_p}^2$ (h^{-1})	R^2 (%)	AARD (%)	
Run 5.8	0.00171	0.2729	0.0935	99.91	7.35	5.04	0.00176	0.0616	99.28	10.08	5.84	0.00182	0.0424	98.95	12.19	6.00
Run 5.9			0.1626	99.26	5.27				99.88	3.91				99.86	3.70	
Run 5.10			0.1996	97.86	4.27				98.60	6.55				98.95	6.44	
Run 5.11		0.7657	0.4575	99.01	3.28			0.0605	99.94	1.15			0.0409	99.20	1.66	
Run 5.12	0.0023	0.6813	0.4327	99.61	4.87	7.38	0.00237	0.0684	99.89	1.06	3.13	0.00241	0.0443	99.73	3.24	2.63
Run 5.13		1.5265	0.3278	99.05	9.89			0.0554	99.98	5.02			0.0423	99.88	2.02	

5.9 ($k_f a = 0.1287\ h^{-1}$ *vs.* $k_f a = 0.2549\ h^{-1}$, respectively), which corroborates the trends discussed in Section 5.3.2 about the evolution of the extractions curves. The coefficient for Run 5.10 is closer to the one of Run 5.9, which means that, in practice, the film resistance could have been eliminated.

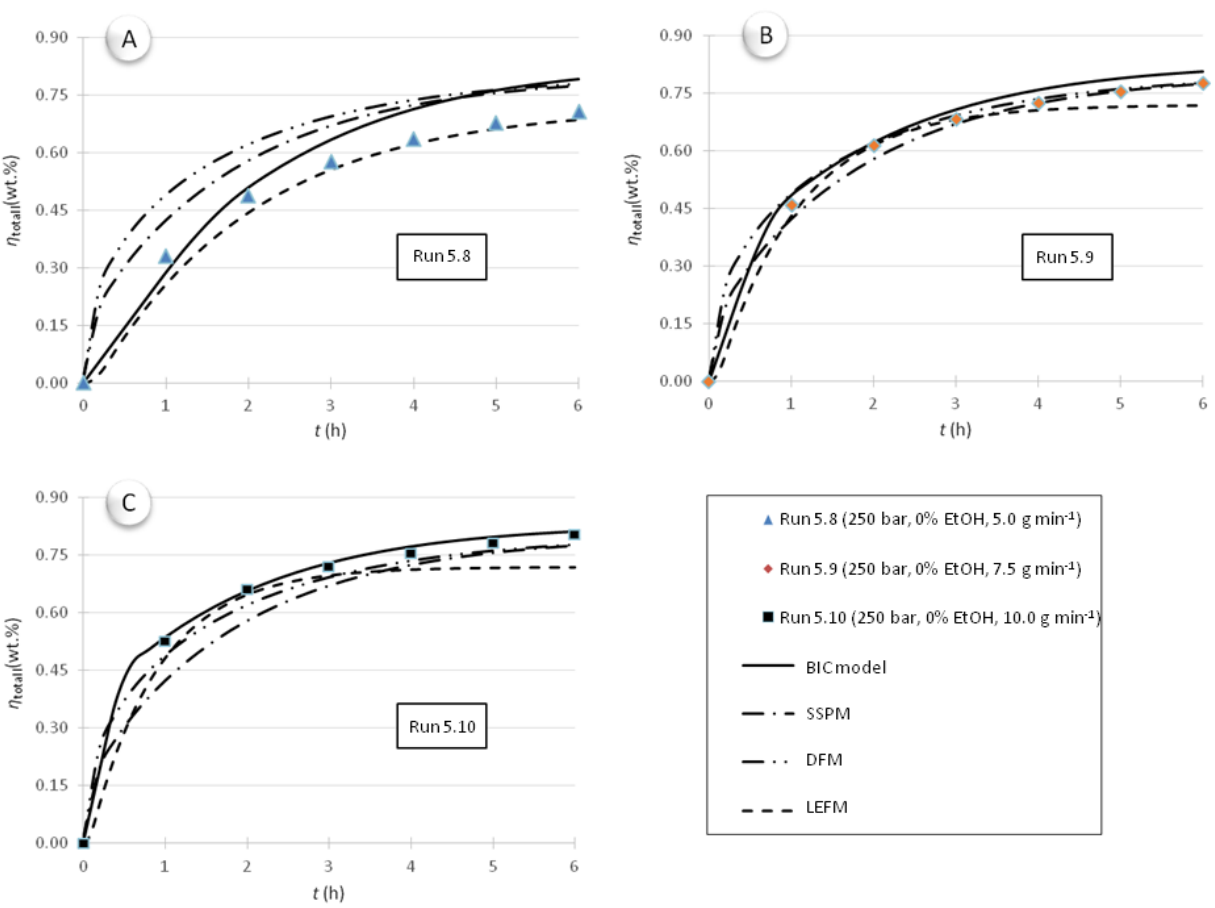

Figure 6.2 - Total yield of SFE of *E. crassipes* along time for 250 bar, 0 wt.% ethanol and $Q_{CO_2} = 5.0\ g\ min^{-1}$ (Run 5.8); 250 bar, 0 wt.% ethanol and $Q_{CO_2} = 7.5\ g\ min^{-1}$ (Run 5.9); and 250 bar, 0 wt.% ethanol and $Q_{CO_2} = 10.0\ g\ min^{-1}$ (Run 5.10. Lines: modeling results achieved by Eqs. (14), (15), (26) to (34).

With respect to the intraparticle diffusion models (SSPM and DFM), they exhibited a better global representation of the experimental η_{total} curves (comparing to LEFM) when cosolvent was used (Runs 5.11-5.12) than in the pure CO_2 assays (Runs 5.8-5.11). In addition, SSPM led to AARD values slightly lower than DFM: 3.43 % vs. 5.37 % for Runs 5.12 and 5.13, and equivalent for Runs 5.8 to 5.11 (7.31 % vs. 7.89 %, respectively). Hence, these results suggest a similar adequacy of both particle geometries. It is worth noting the individual AARDs obtained by SSPM and DFM for Run 5.8 are clearly higher than the remaining ones: 14.24 % against 1.51-8.36 % (SSPM), and 22.70 % against 1.92-6.33 % (DFM). This highlights the existence of important external transport limitations when working at the superficial velocity of Run 5.8, which is in accordance with the values of the fitted $k_f a$ of LEFM discussed above. This implies that the optimized D_m values of

SSPM and DFM for Runs 5.8-5.11 may be underestimated because $D_m/{L_p}^2$ and $D_m/{R_p}^2$ appear as lumped kinetic parameters of Eqs. (14) and (15).

With relation to η_{stigm}, identical conclusions can be drawn regarding the equivalent fitting adequacy of the three simplified models: LEFM (AARD=5.73-6.78 %), SSPM (AARD=3.43-7.31 %), and DFM (AARD=5.37-7.89 %). A noteworthy feature of SSPM comprises the higher values of the intraparticle diffusion coefficients of stigmasterol in relation to the overall extracts. In fact, the fitted $D_m/{L_p}^2$ of stigmasterol is 0.0616 h^{-1}/0.0537 h^{-1} = 1.2 times greater in the case of Runs 5.8 to 5.10, 1.3 in Run 4, 2.0 in Run 5.12, and 1.7 in Run 5.13. Such superiority confirms a kinetic selectivity for stigmasterol in relation to the remaining extractable compounds, which is in agreement with exploratory results already published on SFE of *E. crassipes* [162]. Nevertheless, the same modeling results also suggest a kinetic selectivity gain through the reduction of pressure, namely 1.2 (250 bar, Runs 5.8 to 5.10) < 1.3 (200 bar, Run 5.11), and an optimum value as ethanol is progressively added: 1.2 (0 wt.% Ethanol, Runs 5.8 to 5.10) < 2.0 (5.0 wt.% Ethanol, Run 5.12). This has been experimentally demonstrated elsewhere (see Chapter 4, Section 4.3.3) [163].

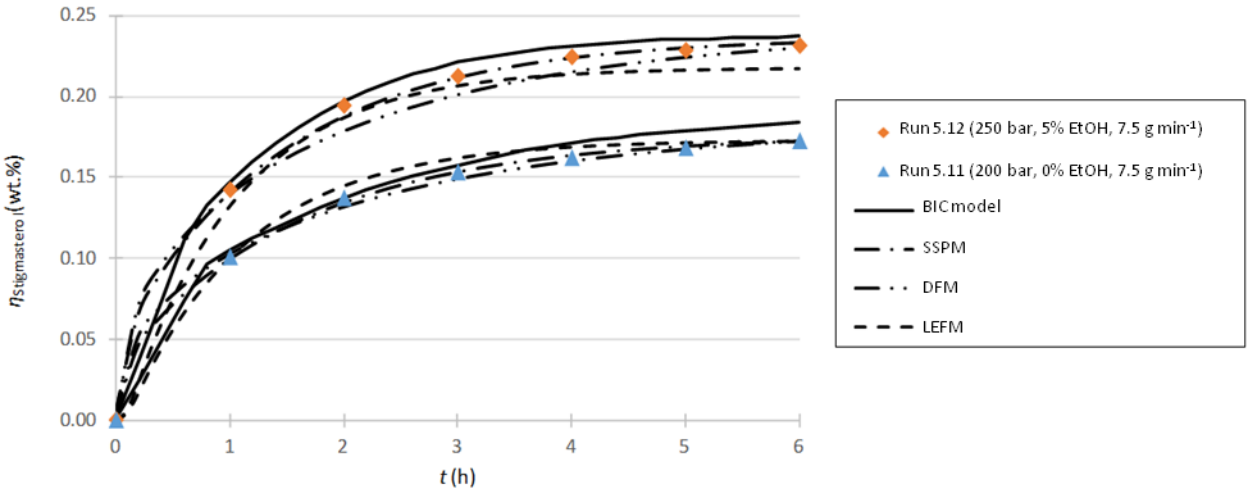

Figure 6.3 – Stigmasterol extraction yield of SFE of *E. crassipes* along time for 200 bar, 0 wt.% ethanol and $Q_{CO_2} = 7.5\ g\ min^{-1}$ (Run 5.11); and 250 bar, 5 wt.% ethanol and $Q_{CO_2} = 7.5\ g\ min^{-1}$ (Run 5.13) Lines: modeling results achieved by Eqs. (14), (15), (26) to (34).

Broken plus intact cells (BIC) model - With regard to the application of this comprehensive model, the six experimental runs were simultaneously used for fitting η_{total} and for fitting η_{stigm}. The overall results are given in Table 6.8 for η_{total} and in Table 6.9 for η_{stigm}, particularly the correlated parameters: X_0, solubility (y^*), broken cells fraction (g), volumetric convective mass transfer coefficient ($k_f a$), and volumetric intact cells mass transfer coefficient ($k_s a$).

Table 6.8 – BIC model adjusted parameters and fitting indicators applied to experimental η_{total} data.

Exp.	Fitted Parameters					AARD(%)		Extraction periods	
	$k_s a$ (h^{-1})	$k_f a$ (h^{-1})	y^*	g	X_0 (kg kg^{-1})			t_{CER} (h)	t_{FER} (h)
Run 5.8	0.3158	1.375	0.000411	0.507	0.00830	10.65	4.20	0.9317	1.9967
Run 5.9		4.455				3.83		0.2874	0.9534
Run 5.10		17.49				1.62		0.0732	0.5555
Run 5.11		2.857	0.000411			4.65		0.5533	1.3979
Run 5.12	0.2795	33.16	0.000398		0.0128	5.14		0.0741	1.3427
Run 5.13		25.90	0.000418			3.96		0.0859	1.3353

Table 6.9 – BIC model parameters and fitting indicators applied to experimental η_{stigm} data.

Exp.	Fitted Parameters					AARD(%)		Extraction periods	
	$k_s a$ (h^{-1})	$k_f a$ (h^{-1})	y^*	g	X_0 (kg kg^{-1})			t_{CER} (h)	t_{FER} (h)
Run 5.8	0.3034	1.798	0.0001130	0.592	0.00191	5.11	4.02	0.5753	1.4692
Run 5.9		50.40				3.20		0.0205	0.5729
Run 5.10		114.66				5.67		0.0090	0.4069
Run 5.11		62.41	0.0000826			4.50		0.0238	0.8100
Run 5.12	0.5325	33.78	0.0001310		0.00238	3.16		0.0356	0.7453
Run 5.13		17.74	0.0000914			5.64		0.0877	1.1389

As noticeable in both tables, several of the five adjusted parameters are shared by two or more experimental runs. In fact only g was held constant for the six assays, since all biomass was submitted to the same grinding process and was uniformly divided in various samples for subsequent SFE. Therefore, as variations on the broken cells fraction are not expected to occur within this study, only one degree of freedom was left for the six assays. In addition, X_0 and $k_s a$ were shared by runs following a criterion of whether cosolvent was used (Runs 5.12 and 5.13) or not (Runs 5.8 to 5.11). This decision took into account the previous insights from simplified models results, particularly in relation to X_0. Moreover, the solubilities were grouped based on the different combinations of CO_2 pressure + ethanol content, which implied that Runs 5.8 to 5.10 possess only a single parameter. Finally, an individual convective coefficient was adjusted for each experimental run as this factor is influenced by pressure, flow rate, and/or ethanol content. In view of the simultaneous fitting of the model, an overall AARD was calculated for each response, being attained AARD= 4.20 % for η_{total}, and 4.02 % for η_{stigm}.

Despite the fact that the broken cells fractions (g) was fitted once to each response, the values were 0.507 (based on η_{total} data) and 0.592 (based on η_{stigm} data), which represents deviations of only 9.2 % from their average. As far as X_0 is concerned, the BIC model results led to quite distinct values depending on the usage of ethanol as cosolvent: 0.00830 kg kg^{-1} (0 wt.% ethanol) *vs.* 0.01280 kg kg^{-1} (5.0 wt.% ethanol) for η_{total}, and 0.00191 kg kg^{-1} *vs.* 0.00238 kg kg^{-1} for η_{stigm}, respectively. Since these results are different between each other and also distinct from the reference Soxhlet values ($\eta_{\text{total}} = 0.0190$ kg kg^{-1} and $\eta_{\text{stigm}} = 0.0030$ kg kg^{-1} using dichloromethane [163]) it should be pondered if it is realistic to assume that the absolute content of extractives typically determined by Soxhlet is applicable to SFE processes. The same finding has been already reported in the literature [164-166]. One may cite, for instance, the SFE of eucalypt bark ($\eta_{\text{total}} = 0.0150$ using dichloromethane in a Soxhlet *vs.* $\eta_{\text{total}} = 0.0120$ kg kg^{-1} for SFE [164]); and *Quercus cerris* cork ($\eta_{\text{total}} = 0.0402$ kg kg^{-1} using dichloromethane in a Soxhlet *versus* $\eta_{\text{total}} = 0.0113$ kg kg^{-1} for SFE [166]). Such yield assumption may have a significant impact on the goodness of the fittings achieved by the models adopted to describe experimental curves, as well as it may distort the magnitude of other parameters at the expenses of providing the best possible fitting.

With reference to the volumetric convective coefficients ($k_f a$), the BIC model was able to provide increasing parameters for the progressive flow rate increments of Runs 5.8 to 5.10, which is qualitatively correct. As has been mentioned above, when the parameters of both η_{total} and η_{stigm} responses are compared, one verifies that the kinetic selectivity advantage discussed before is once again confirmed: the obtained $k_f a$ is 1.31 greater (for η_{stigm} in relation to η_{total}) in the case of Run 5.8, and 11.3, 40.1, 21.8, 1.02 and 0.68 for Runs 5.9 to 5.13, respectively. From these ratios one may infer how the kinetic selectivity to stigmasterol can be favored by the proper selection of flow rate (5.0 g min^{-1} is much worse than 7.5 and 10.0 g min^{-1}), the usage of a lower pressure (200 bar), and through the avoidance or a moderate usage of ethanol, which breaks the natural SC-

CO_2 selectivity appetence due to the polarity tuning. Nevertheless, all these remarks should be crossed with the impact of the pressure and ethanol content on solubility. In fact, while for the bulk extract the solubility values were similar (from 0.000398 to 0.000411), variations in the order of magnitude were attained for stigmasterol, with the major reductions being observed in Run 5.13, where 300 bar and 5.0 wt.% ethanol provided a 23.6 % lower y^* than for Runs 5.8 to 5.10. Likewise 200 bar and 0 wt.% ethanol (Run 4) provided a 26.9 % lower y^* than for Runs 1 to 3. In opposition, the combined conditions of 5.0 wt.% ethanol and 250 bar showed to cause an increase of 15.9 % in y^*. For these reasons, one may conclude that the aforementioned selectivity advantage is being driven by kinetic rather than by solubility enhancements.

Since one of the premises of the BIC model is related to the existence of three periods of extraction, implying distinct removal rates and resistances to mass transport, the characteristic times t_{CER} (end time of constant extraction rate period) and t_{FER} (end time of falling extraction rate period) were calculated from the fitted parameters (Eqs. (32) and (33)), being reported in Tables 6.8 and 6.9 for each response. With regard to t_{CER}, it is noteworthy how the increase of flow rate led to a decrease of t_{CER} values in both η_{total} and η_{stigm}. For instance, in η_{total} the pace of this decrease was 0.9317 h > 0.2874 h > 0.0732 h for Runs 5.8 to 5.10, respectively. Besides this decrease in t_{CER}, a shortening of t_{FER} was also correspondingly noticed: 1.9967 h > 0.9534 h > 0.5555 h. Accordingly, still for η_{total}, one gets: $t_{\mathrm{FER}} - t_{\mathrm{CER}} = 1.065$ h for Run 5.8, 0.6660 h for Run 5.9, and 0.4823 h for Run 5.10, which implies that from the lowest flow rate (Run 5.8) to the highest one (Run 5.10) the process evolves quickly from the initial maximum rate extraction period to a point where the extraction is governed solely by intraparticle diffusion ($t > t_{\mathrm{FER}}$). These findings rely on the fact that from Runs 5.8 to 5.10 the characteristic time for film diffusion $(d_{\mathrm{p}}/k_{\mathrm{f}})$ is decreasing because the increment of flow rate reduces the thickness of the boundary layer around biomass particles, which subsequently enhances k_{f}.

Despite t_{CER} and t_{FER} were commented for η_{total}, the same reasoning can also be applied to η_{stigm} and the same trends discussed above can be confirmed. In any case, it is worth noting that for η_{stigm} the values of t_{CER} and t_{FER} are even smaller than those for η_{total}. Hence, the extraction periods for stigmasterol removal seem to suffer an anticipation in relation to the generic extract removal, which suggests that shorter extraction times tend to favor the enhanced extraction of this sterol in relation to the uptake of other extractives, thus reducing the operating costs of a future commercial SFE unit.

6.3.2 SFE CURVES OF *Quercus cerris*

Broken plus intact cells (BIC) model - With reference to the application of the integrated broken plus intact cells (BIC) model to this matrix, the experimental η_{total} and $\eta_{\text{friedelin}}$ data were modeled at the same time. This decision was driven by the fact that grinding and bed related parameters are common to several runs of both functions, and thus their fitting should simultaneously take into account all measured curves. In practice, this led to adjusting 14 extraction curves at the same time, with one g parameter for each grinding degree: >80 mesh, 60-80 mesh, 40-60 mesh, 20-40 mesh, and coarse particles (<20 mesh), according to the following restriction. With the objective of reducing the number of adjusted parameters, the following fitting relation is assumed:

$$g\left(d_{\text{p}}\right) = \frac{g_1}{d_{\text{p}}} + g_2 \tag{36}$$

where d_{p} is the average particle size of the biomass, in mesh units.

Moreover runs for equal $P - T - x_{\text{EtOH}}$ conditions must have the same solubility constant. This implied that, for each response (total yield or friedelin yield), three y^* values were considered: one for Runs 5.1 to 5.5, one for Run 5.6 and one for Run 5.7. The same decision was adopted regarding the practical absolute extractives content (X_0), based on realistic considerations already discussed elsewhere in the literature [2, 164-166]. Finally, the transport coefficients, namely film ($k_{\text{f}}a$) and intraparticle volumetric ($k_{\text{s}}a$) coefficient, were fitted independently to each curve and each response in light of the fact they depend on both $P - T - x_{\text{EtOH}}$ conditions and average particle sizes.

The modeling results are furnished in Tables 6.10 and 6.11, where it can be noticed that overall deviations (AARD) remained as low as 4.43 % for η_{total} and 4.25 % for $\eta_{\text{friedelin}}$. Despite these values, higher deviations were observed in some assays, with emphasis to Run 5.5, the one involving coarse particles, which scored AARD values of 13.72 % and 9.58 %, respectively. The quality of the fittings can be visually checked in Figures 6.4 and 6.5, for Runs 5.1 to 5.7 and both responses. It is clear how the BIC model describes correctly the trends of the experimental data, and also how the different extraction rate periods become more perceptible observing the predicted yields of each response.

With respect to the fraction of broken cells, g, the fitted constants were $g_1 = -3.5455$ and $g_2 = 0.7832$, which means g values between 0.43 (Run 5.5, coarse particles) and 0.74 (Run 5.1, >80 mesh). Due to Eq. (36), coherent results were obtained, namely progressively higher g values as cork cells became more disrupted, and thus more accessible to the supercritical solvent medium.

As far as X_0 is concerned, the magnitudes of their values suggested different insights depending on the considered yield. For instance, in the case of η_{total}, a greater value of X_0 was obtained for assays involving ethanol, namely 0.0340 kg kg^{-1}, against 0.0170 kg kg^{-1} for pure CO_2. Simultaneously, the values of X_0 for $\eta_{\text{friedelin}}$ suggest that the practical content of friedelin in the samples also increase if ethanol is used: 0.0074 kg kg^{-1}, when operating with ethanol (Runs 5.1-5.5 and 5.7) *vs.* 0.0046 kg kg^{-1} if not.

Also related to ethanol content are the fitted solubility values, y^*, for the total extract. The modeling results show that this cosolvent is able to increase the global y^* from 0.0098 (value for pure CO_2) to 0.0152 (for 5.0 wt.%), with the intermediate content of ethanol (2.5 wt.%) scoring closer to the value of pure CO_2. Concerning friedelin solubility, the fitted values for pure CO_2 and 2.5 wt.% ethanol are close to each other, ranging from 0.0019 to 0.0020, respectively, jumping then to 0.0033 when CO_2 is further modified to 5.0 wt.% of ethanol.

Table 6.10 – BIC model results for total extraction yield (η_{total}) of *Q. cerris*.

Exp.	Particle size (mesh)	x_{EtOH} (wt.%)	$k_f a$ (h^{-1})	y^*	$g^{(*)}$	$k_s a$ ($10^{-2}\ \text{h}^{-1}$)	X_0 (kg kg^{-1})	AARD (%)
Run 5.1	> 80	2.5	0.333	0.0076	0.74	13.2	0.0340	0.98
Run 5.2	60-80	2.5	0.293	"	0.73	5.96	"	2.97
Run 5.3	40-60	2.5	0.197	"	0.71	6.64	"	2.83
Run 5.4	20-40	2.5	0.130	"	0.67	2.93	"	5.72
Run 5.5	Coarse	2.5	0.087	"	0.43	6.10	"	13.72
Run 5.6	20-40	0.0	0.106	0.0098	0.67	6.16	0.0170	2.61
Run 5.7	20-40	5.0	0.117	0.0152	"	12.9	0.0340	1.71
Total								4.43

(*)This column of g values was computed from Eq. (36). g was fitted simultaneously to η_{total} and $\eta_{\text{friedelin}}$ data giving rise to g_1= -3.5455 mesh and g_2 = 0.7832.

Table 6.11 – BIC model results for friedelin extraction yield ($\eta_{\text{friedelin}}$) of *Q. cerris*.

Exp.	Particle size (mesh)	x_{EtOH} (wt.%)	$k_f a$ (h^{-1})	y^*	$g^{(*)}$	$k_s a$ ($10^{-2}\ \text{h}^{-1}$)	X_0 (kg kg^{-1})	AARD (%)
Run 5.1	> 80	2.5	0.147	0.0020	0.74	13.9	0.0074	6.49
Run 5.2	60-80	2.5	0.240	"	0.73	10.2	"	1.36
Run 5.3	40-60	2.5	0.136	"	0.71	14.5	"	5.40
Run 5.4	20-40	2.5	0.115	"	0.67	4.77	"	3.30
Run 5.5	Coarse	2.5	0.045	"	0.43	14.1	"	9.58
Run 5.6	20-40	0.0	0.096	0.0019	0.67	8.48	0.0046	1.36
Run 5.7	20-40	5.0	0.089	0.0033	"	9.56	0.0074	1.89
Total								4.25

(*)This column of g values was computed from Eq. (36). g was fitted simultaneously to η_{total} and $\eta_{\text{friedelin}}$ data giving rise to g_1= -3.5455 mesh and g_2 = 0.7832.

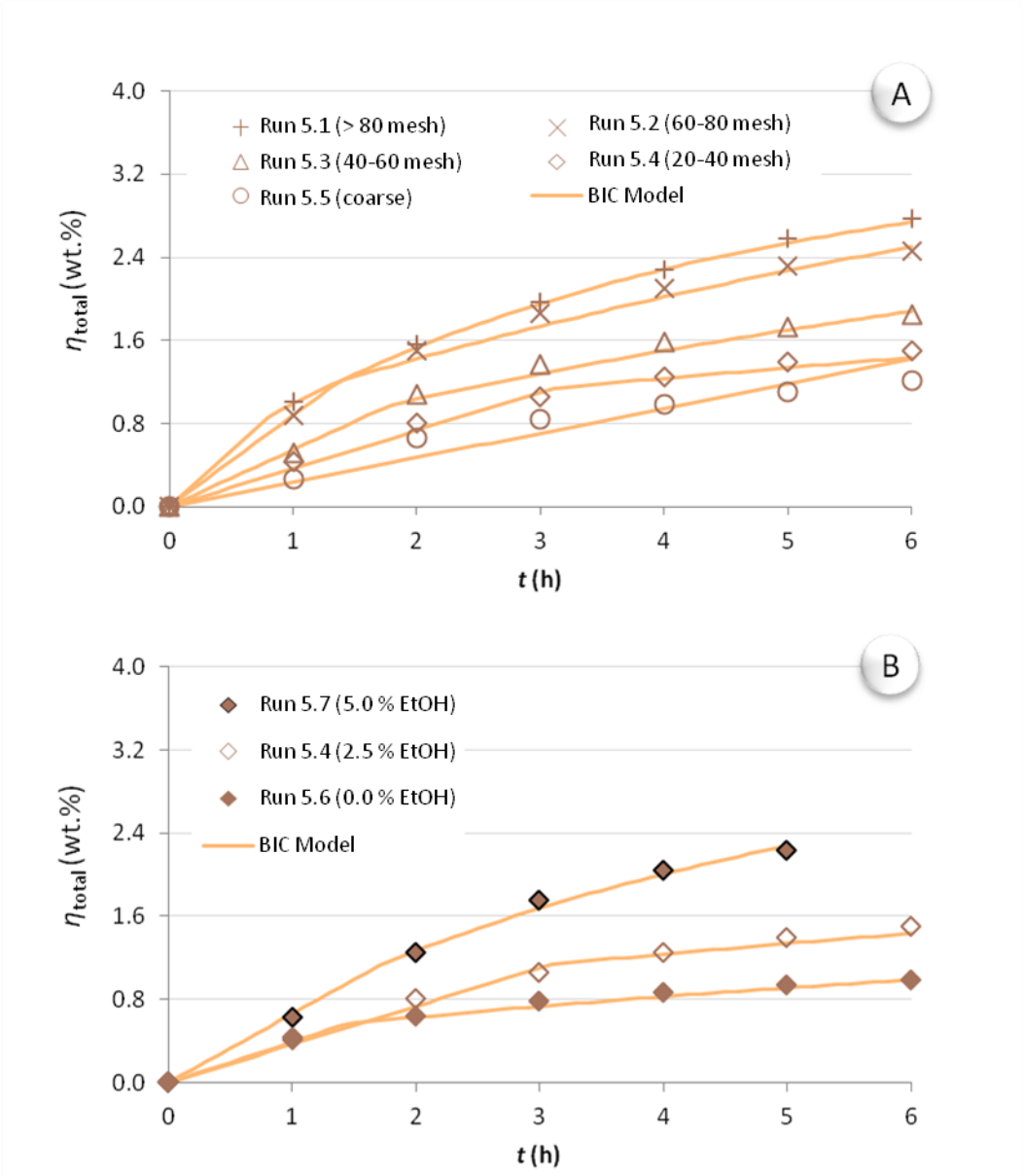

Figure 6.4 – Cumulative curves of total extraction yield (η_{total}) of *Q. cerris* biomass for: A) different particle size ranges at fixed 2.5 wt.% of ethanol; B) different cosolvent concentrations at fixed particle size range of 20-40 mesh. Pressure, temperature and flow rate were held constant in 300 bar, 50 °C and 11 g min^{-1}. Symbols: experimental data; lines: modeling results.

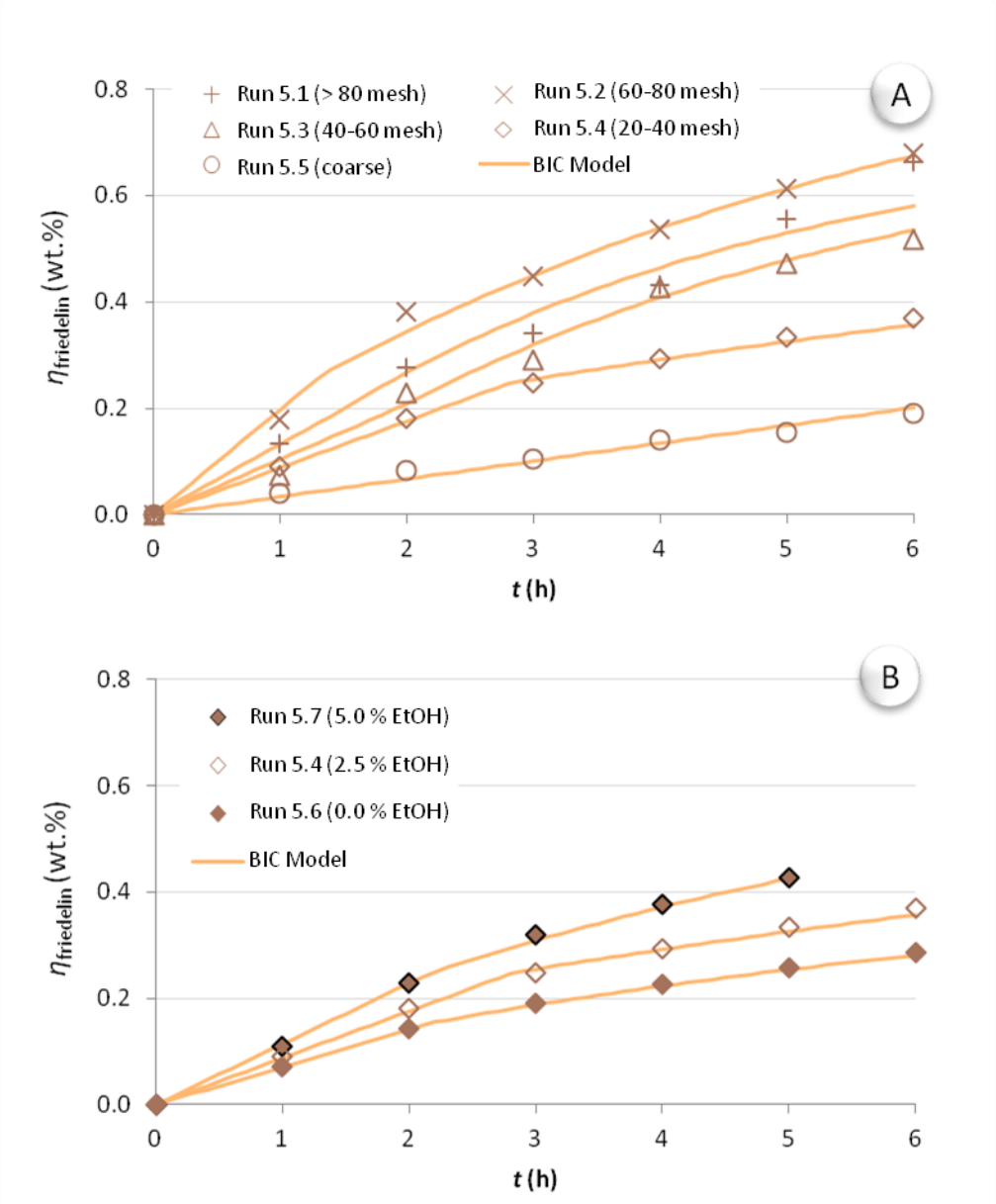

Figure 6.5 – Cumulative curves of friedelin extraction yield ($\eta_{friedelin}$) of *Q. cerris* biomass for: A) different particle size ranges at fixed 2.5 wt.% of ethanol; B) different cosolvent concentrations at fixed particle size range of 20-40 mesh. Pressure, temperature and flow rate were held constant in 300 bar, 50 °C and 11 g min^{-1}. Symbols: experimental data; lines: modeling results.

With respect to the film mass transfer coefficients ($k_f a$), the impact of ethanol content seems negligible in comparison to the effect of particle size. Accordingly, for η_{total} response and assays sharing the same average particle sizes (Runs 5.4, 5.6 and 5.7; 20-40 mesh), the attained $k_f a$ values range from 0.106 to 0.130 h^{-1}, while between particles sizes under the same ethanol modification (Runs 5.1 to 5.5; 2.5 wt.% EtOH) this parameter changes from 0.087 h^{-1} to 0.333 h^{-1} . Similar trends are observed for $\eta_{\text{friedelin}}$. These results can be crossed with the dimensionless correlations for convective mass transfer coefficient of the type $\text{Sh} = \alpha \text{Re}^{\beta} \text{Sc}^{\gamma}$, where α, β and γ are constants. For two assays involving the same $P - T - x_{\text{EtOH}}$ and flow rate conditions but different particle sizes, this relation gives rise to:

$$\frac{(k_f)_{d_{p.1}}}{(k_f)_{d_{p,2}}} = \left(\frac{d_{p.1}}{d_{p.2}}\right)^{\beta-1} \tag{37}$$

Moreover, taking into account that the adjusted parameters in BIC model were $k_f a$ (having h^{-1} units) and that the surface-area-to-volume ratio is $a = 3/d_p$ for spherical particles, the previous ratio can be further manipulated into:

$$\frac{(k_f a)_{d_{p,1}}}{(k_f a)_{d_{p,2}}} = \left(\frac{d_{p,1}}{d_{p,2}}\right)^{\beta-2} \tag{38}$$

As a result, assuming that β = 0.8 [4], for a jump like those between 20-40 mesh (Run 5.4) to 60-80 mesh (Run 5.2), a score of $(k_f a)_{60-80\ \text{mesh}}/(k_f a)_{20-40\ \text{mesh}} = 3.5$ can be anticipated. If computed using the adjusted parameters, the respective ratio scores $0.293/0.130 = 2.3$ for η_{total} and $0.240/0.115 = 2.1$ for $\eta_{\text{friedelin}}$. Notwithstanding the introduced approximation of perfect spheres and the accuracy of the dimensionless correlations, such ratios evidence the significant increase of the film mass transfer coefficient when average particle size decreases.

In terms of the internal transport, and again for η_{total}, advantageous $k_s a$ values were attained for the assays having the highest amount of ethanol (5.0 wt.%) or the lowest particle size (> 80 mesh), which scored 0.129 h^{-1} and 0.132 h^{-1}, respectively. Likewise observed for $k_f a$, the values of $k_s a$ reveal a greater dependence on particle size: a variation from 0.0293 to 0.132 h^{-1} was attained for the 2nd highest (Run 5.4) and smallest (Run 5.1) particle size assays, respectively. Hence, these results clearly indicate that particle size considerably penalize the rate of removal of solutes from the interior of the biomass particles. In order to interpret these trends in light of existing knowledge, the observed behavior of $k_s a$ might be checked against the expression of the linear driving force (LDF) mass transfer coefficient (k_{LDF}, h^{-1}) given by [167]:

$$k_{\text{LDF}} = 15\ \frac{D_e}{R_p^2} \tag{39}$$

where D_e is the effective solute diffusivity and $R_\mathrm{p} = d_\mathrm{p}/2$ is particle radius. Likewise done for $k_\mathrm{f}a$, this equation can be manipulated for two assays involving the same $P - T - x_\mathrm{EtOH}$ and flow rate conditions but different particle sizes, resulting in the following ratio:

$$\frac{(k_\mathrm{LDF})_{d_\mathrm{p,1}}}{(k_\mathrm{LDF})_{d_\mathrm{p,2}}} = \left(\frac{d_\mathrm{p,2}}{d_\mathrm{p,1}}\right)^2 \tag{40}$$

Owing to the fact that k_LDF has a correspondence to $k_\mathrm{s}a$, a jump like that between 20-40 mesh (Run 5.4) and 60-80 mesh (Run 5.2) is expected to score 8 using Eq. (40). Accordingly, if computed through the adjusted $k_\mathrm{s}a$ the same ratio scores 2.0 for η_total, and 2.1 for $\eta_\mathrm{friedelin}$. Although the LDF model has been derived for adsorption processes and its validity requires that the intraparticle concentration profiles are well developed (parabolic) [167-168], the above mentioned results clearly show that our experimental trend is in accordance with theory.

Analysis of extraction periods – The objective of this section is to disclose the results of characteristic extraction periods defined by the BIC model: CER, FER and DC (as described in Table 6.4), with a special emphasis on the former. In this respect, Figure 6.6 presents the predicted lengths of each period for the bulk extract, being graphically organized in terms of particle size (Figure 6.6.A) and ethanol content of the supercritical solvent (Figure 6.6.B).

To begin with, results clearly show a decrease of CER period as the particle size of cork samples becomes smaller. Globally, CER period duration is shortened from more than 6 h (Run 5.5, coarse particles) to 0.8 h (Run 5.1, >80 mesh). It is known that grinding plays an important role on the accessibility of supercritical solvent to the extractives, leading to a faster uptake of these. On the other hand, the most favourable extraction times for industrial SFE processes are usually in the vicinity of the CER period end [169-171]. Moreover, it is frequently found in semi-continuous operation with beds in parallel that the minimum switching time between cycles (to decompress, unload and reload the biomass, and repressurize) is about 1 h [172-173]. Taking this into account the CER time of Run 5.1 (>80 mesh) falls below this value, implying that the process will enter in the DC period before finishing the preparation of the second bed.

With regard to the impact of the cosolvent, modeling results show that the CER period can be shortened also through the use of pure SC-CO_2 (under identical $P - T$ and particle size conditions), leading to only 1.4 h (Run 5.6). In contrast, the assay for 5.0 wt.% (EtOH) exhibited a shorter CER period in relation to 2.5 wt.%, scoring in turn 1.7 h. In general, it should be noted that the duration of the CER period is not conclusive regarding how much extractives can be attained. For this reason, Figure 6.7 presents quantitative data specifically for CER period and bulk extract (η_total), opening the way to a full assessment of the impact of the different operating conditions during this period. Accordingly Figure 6.7.A presents the extraction rates (left side axis, depicted in grey) and accumulated yields by the end of CER period (right side axis, depicted in orange) for

different cork particle size ranges, and Figure 6.7.B shows the same data but for different x_{EtOH} values.

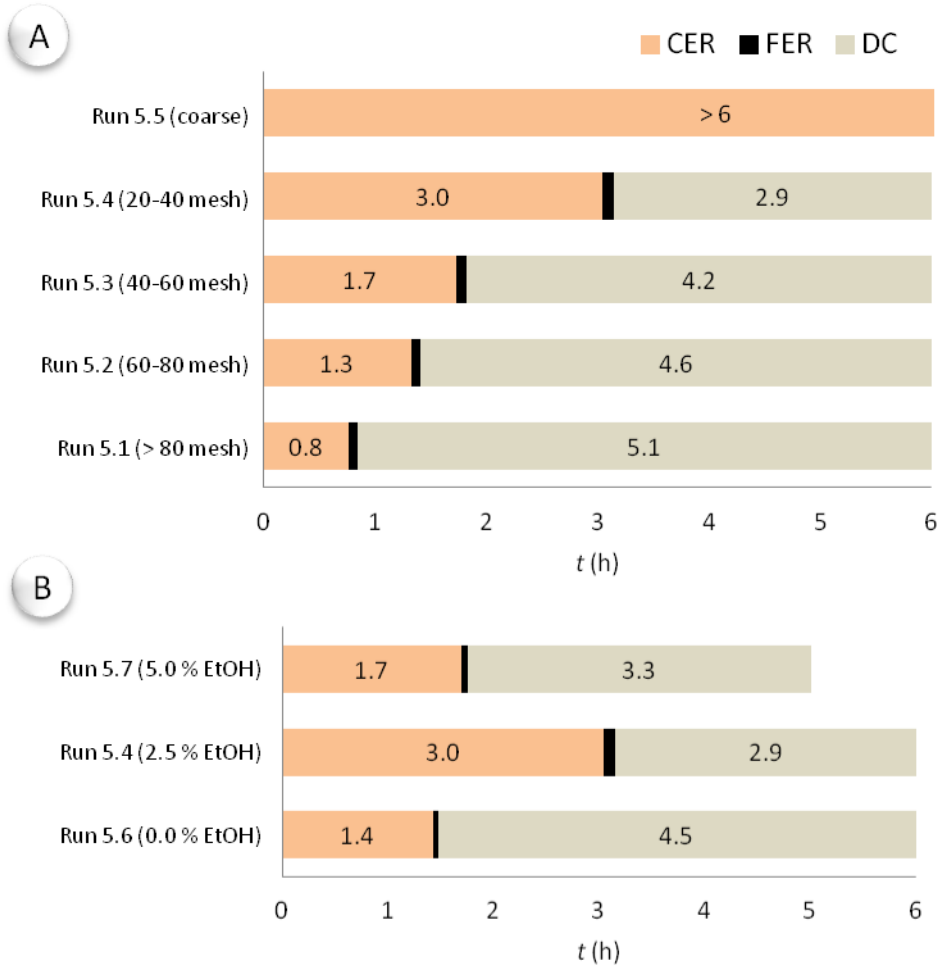

Figure 6.6 – Lengths of the BIC model extraction periods for the bulk extract as function of: A) different particle size ranges at fixed 2.5 wt.% of ethanol (Runs 5.1 to 5.5); B) different cosolvent concentrations at fixed particle size range of 20-40 mesh (Runs 5.4, 5.6 and 5.7). Pressure, temperature and flow rate were held constant in 300 bar, 50 °C and 1 g min^{-1}. (CER - constant extraction rate period; FER - falling extraction rate period, DC - diffusion controlled period).

As expected, the rates of extraction during the CER period follow a trend imposed by the particle sizes which is clearly visible from the slopes in Figures 6.4.A: greatly ground particles (from Run 5.5 to 5.1) enable higher extraction rates, from 0.1 to 1.1 wt.% h^{-1} , respectively. Accordingly, while in theory when particles become small enough the process reaches a maximum ruled by solubility limitations, such was not noticed in any of the runs, especially between Runs 5.1 and 5.2, those involving the smallest particle sizes. Nevertheless, the assay where coarse particles were employed (Run 5.5) exhibits an extraction rate that is one order of magnitude lower than those of the assay with the smallest particles (Runs 5.1), thus showing its extended t_{CER} (see Figure 5) is due the slow kinetics of the process. Remember that for this assay, $k_{\mathrm{f}}a$ reached the smallest value of all experiments, 0.087 h^{-1} (see Table 6.10). Nevertheless, the pronounced extension of CER

period (in relation to DC) in the SFE curve involving coarse particles (5.5) demands caution when taking phenomenological conclusions or insights for that assay. Finally it should be noted that Run 5.2 (60-80 mesh) and Run 5.3 (40-60 mesh) seem to provide a productivity trade off between the effort of grinding particles and the extension the extraction process can be operated under constant extraction rate. This becomes evident by the η_{total} accumulated by the end of CER period: 1.1 % and 1.0 %, respectively.

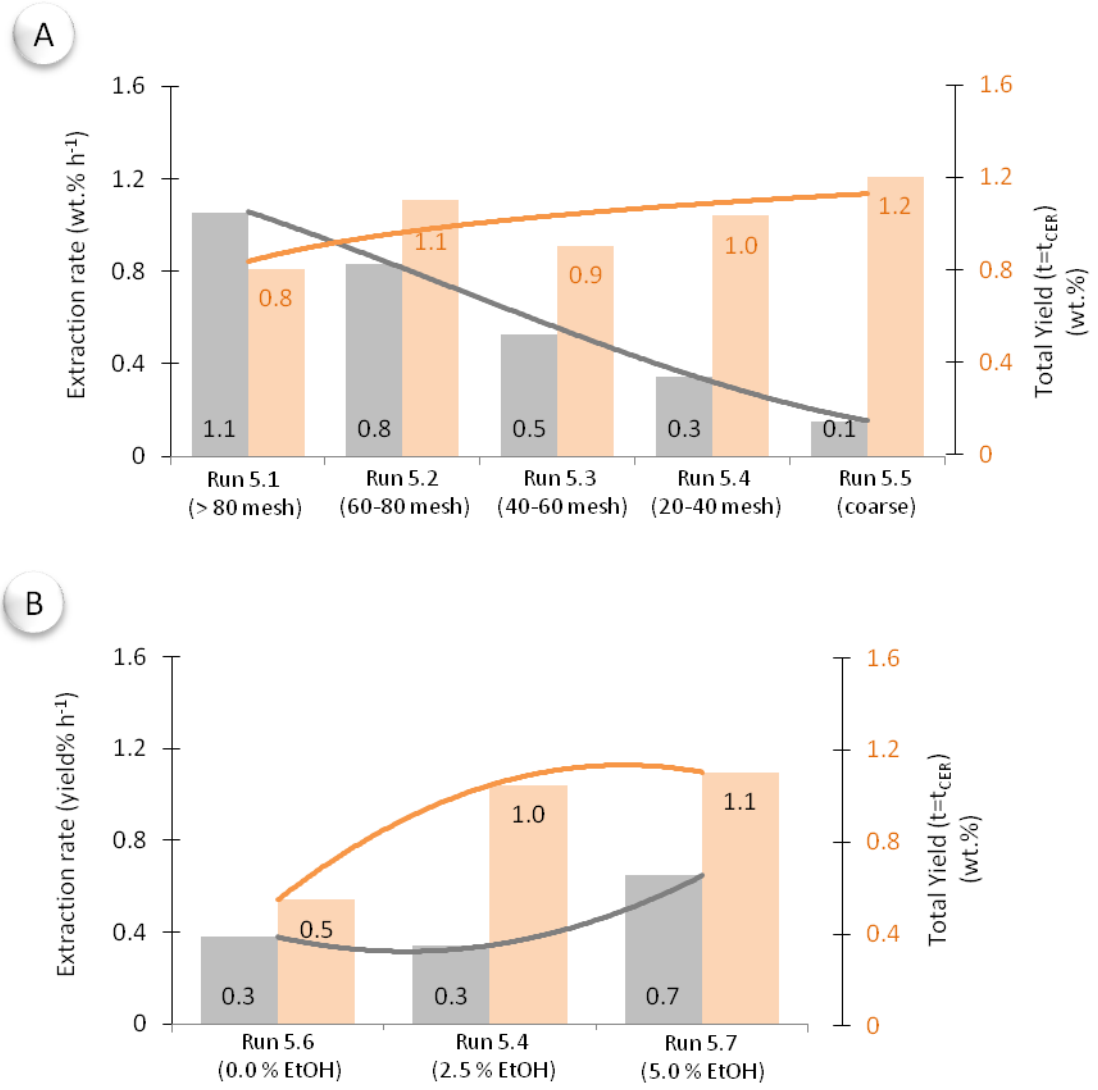

Figure 6.7 – Modelled extraction rates and yields of bulk extract (η_{total}) at the end of CER period as function of: A) different particle size ranges at fixed 2.5 wt.% of ethanol (Runs 5.1 to 5.5); B) different cosolvent concentrations at fixed particle size range of 20-40 mesh (Runs 5.4, 5.6 and 5.7). Pressure, temperature and flow rate were held constant in 300 bar, 50 °C and 11 g min^{-1}.

With reference to the impact of ethanol addition on the extraction rate, two key behaviors can be observed in Figure 6.7 for Runs 5.7 or 5.6 in relation to Run 5.4. The first one is that the doubling of ethanol addition to 5.0 wt.%, from Run 5.4 to Run 5.7 leads to more than a doubling of

extraction rate on these essays (from 0.3 to 0.7 wt.% h^{-1} respectively) but not a change in accumulated yield, i.e. 1.0-1.1 wt.%. Secondly, when cut to 0 wt.% EtOH, the accumulated yield by the end of CER period is shortened to half (0.5 wt.% in Run 5.6 *vs.* 1.0 wt.% in Run 5.4), but the extraction rate remains constant at 0.3 wt.% h^{-1}.

Globally, the commented results show that resort to a cosolvent might favor not only the accumulated amounts of extract at the end of the CER period, but also the kinetics of the process (extraction rate). Nevertheless, such dual enhancing effect seems to depend on the amount of ethanol that is chosen for the extraction. In addition, the same results also evidence that the milling of the biomass plays a decisive role on the extraction rate during the CER period, but seems to not affect the accumulated yields at the end of that period.

Selectivity to Friedelin – Selectivity enhancements cannot be confounded with higher extraction yield of target compounds. For instance, it is common that the usage of a cosolvent may increase total yield not only at the expenses of greater extraction of target compounds but also due to a higher uptake of non-target extractives [163, 174]. Taking into account the target compounds may be non-uniformly distributed in the biomass (i.e., may occur preferentially in outer layers or in specific inner locations like vacuoles) [150, 175-176] the selectivity can be also affected by changes in particle size besides solvent state ($P - T - x_{\mathrm{EtOH}}$) and kinetic conditions (i.e., equilibrium and kinetic selectivities).

Taking advantage of the experimental and modeling results presented above, friedelin selectivities were calculated along time using cumulative yields, aiming at the disclosure of the impact of pressure, temperature, cosolvent content, particle size and time on the uptake of this target compound. For the calculation of the selectivity to friedelin, $\alpha_{\mathrm{f,nf}}$, the experimental yields (η_{total} and $\eta_{\mathrm{friedelin}}$) of each assay and the extractives content for both responses ($X_{0,\mathrm{total}}$ and $X_{0,\mathrm{friedelin}}$) were used, as follows:

$$\alpha_{\mathrm{f,nf}}(\boldsymbol{t}) = \frac{\eta_{\mathrm{friedelin}}(t)\times\left[X_{0,\mathrm{non-friedelin}} - \eta_{\mathrm{non-friedelin}}(t)\right]}{\eta_{\mathrm{non-friedelin}}(t)\times\left[X_{0,\mathrm{friedelin}} - \eta_{\mathrm{friedelin}}(t)\right]} \tag{41}$$

where

$$\eta_{\mathrm{non-friedelin}}(t) = \eta_{\mathrm{total}}(t) - \eta_{\mathrm{friedelin}}(\boldsymbol{t}) \tag{42}$$

$$X_{0,\mathrm{non-friedelin}} = X_{0,total} - X_{0,\mathrm{friedelin}} \tag{43}$$

and subscripts f and nf stand for friedelin and non-friedelin molecules, respectively.

In this respect, Figure 6.8 illustrates the computed selectivities towards friedelin along extraction time, as function of particle size range (Figure 6.8.A) and ethanol content of the supercritical solvent (Figure 6.8.B). At first sight, it is noticeable that in four of the seven assays it was possible

to reach $\alpha_{f,nf}$ values above 1. This means that, depending on the chosen extraction times, friedelin was removed with advantage over all the other compounds (labeled as non-friedelin). While desirable, this clearly depicts the challenge of obtaining extracts enriched in target molecules, thus reinforcing the importance of optimizing the operating conditions of SFE. In fact, results show that particle sizes can change selectivities during the first hour from 0.45 (>80 mesh) to 1.01 (60-80 mesh) which, in other words, represents an enhancement of 124 % in the value of $\alpha_{f,nf}$. The attained results clearly point to an advantage of operating with intermediate granulometries instead of coarse particles or too ground particles (> 80 mesh), which is amplified if extraction times are augmented.

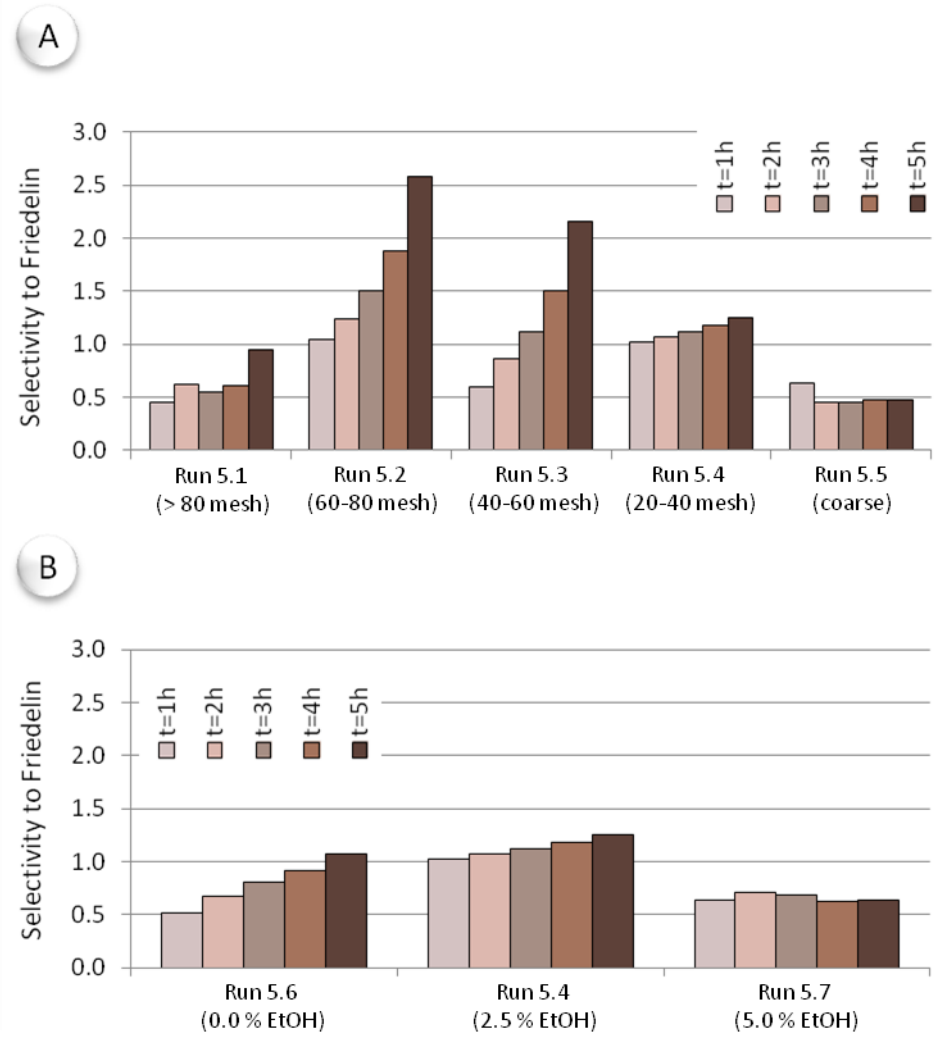

Figure 6.8 – Cumulative selectivity to friedelin, $\alpha_{f,nf}$, along extraction time as function of: A) different particle size ranges at fixed 2.5 wt.% of ethanol (Runs 5.1 to 5.5); B) different cosolvent concentrations at fixed particle size range of 20-40 mesh (Runs 5.4, 5.6 and 5.7). Pressure, temperature and CO_2 flow rate were held constant at 300 bar, 50 °C and 11 g min^{-1}.

With regard to cosolvent concentration, the respective profile is evident in Figure 6.8.B, with the lowest range of values being for 5.0 wt.% EtOH and the highest for 2.5 wt.% EtOH. Based on the five hour bars, the jumps for these concentrations ratios are such that $\alpha_{f,nf}(2.5\,\%\,EtOH)$ is 1.2

times higher than $\alpha_{f,nf}(0.0\,\%\,EtOH)$, and $\alpha_{f,nf}(5.0\,\%\,EtOH)$ is 2.0 times lower than $\alpha_{f,nf}(2.5\,\%\,EtOH)$. With this pace, it becomes clear that the use of ethanol as cosolvent is able to boost the selectivity to friedelin, but also that intermediate amounts are desirable for such enrichment, otherwise the selectivity gain can be lost due to the abundant removal of non-target extractives available in the biomass. A similar trend was reported also by Martins et al [163] for the SFE of stigmasterol from *Eichhornia crassipes,* by Barbosa et al [177] for diterpenes from spent coffee grounds, and by Domingues et al. [175] for triterpenic acids from *Eucalyptus globulus* bark.

As far as the impact of time is concerned, Run 5.2 ($x_{EtOH} = 2.5$ wt.%, 60-80 mesh) and Run 5.3 ($x_{EtOH} = 2.5$ wt.%, 40-60 mesh) exhibit increasing selectivity profiles along time. The former shows a constant pace evolution of $\alpha_{f,nf}$ from 1.05 (t = 1 h) to 1.88 (t = 4 h), and then a final jump to 2.58 (t= 5 h), being the latter the highest selectivity value attained in this study. Nevertheless, it is known that as the extraction time is extended, the absolute amounts being recovered become very small, leading these selectivity gains to progressive lose importance in the context of the accumulated extract.

6.4 CONCLUSION

***Eichhornia crassipes* study –** The results achieved by simplified models (LEFM, DFM and SSPM) suggest both intraparticle diffusion (assumed in DFM and SSPM) and film diffusion (assumed in LEFM) play a role in the resistance to mass transfer that dominates the SFE. In this respect, DFM and SSPM scored lower deviations (AARD values from 2.63 to 5.37 %) in assays where cosolvent was employed, and LEFM when working with pure CO_2 (AARD values from 5.04 to 5.73 %).

The application of the broken plus intact cells (BIC) model to the six experimental runs at the same time allowed to represent data with AARD = 4.20 % (η_{total}) and 4.02 % (η_{stigm}), and to get instructive insights on the process. The adjusted maximum stigmasterol yield was 0.191 % with pure SC-CO_2, and 0.238 % (wt.) using ethanol as cosolvent. Results also evidence that the characteristic extraction periods finish earlier for stigmasterol yield response, than for the overall extraction yield, which confirm that shorter times are preferable to produce stigmasterol enriched extracts from *E. crassipes*.

In the whole, these experimental and modeling results confer a deeper understanding of the phenomena intrinsic to the SFE of *E. crassipes*, and represent a supportive study towards future scale-up assays.

***Quercus cerris* study –** Upon the application of the broken plus intact cells (BIC) model to the 14 experimental runs at the same time, the fitting errors (AARD) were only 4.43 % (η_{total}) and 4.25 % ($\eta_{\text{friedelin}}$), being the highest deviations observed for coarse cork particles. Modeling results showed that the cosolvent addition does not lead to significant kinetic advantages in relation to pure SC-CO_2 , as under comparable particle size conditions the convective mass transfer coefficients ($k_f a$) ranged only from 0.106 to 0.130 h^{-1} (for η_{total} response). Nevertheless greater kinetic advantages were observed for intraparticle diffusion ($k_s a$), but only for ethanol addition of 5 wt.%. Finally modeling allowed also to confirm that the initial extraction rates are higher for smaller particles, that intermediate particle (40-60 mesh to 60-80 mesh) provide a rate *vs.* yield favorable compromise, and that the extraction rate in the initial period (CER) is two times greater for 5.0 % EtOH. However, the accumulated yield in that period is roughly the same as for 2.5 % EtOH (for η_{total}).

The study of selectivity to friedelin revealed that intermediate granulometries (40-60 mesh to 60-80 mesh) are advantageous, and that the crossed effect of cosolvent addition and particle size can boost cumulative selectivity up to 2.6.

In the whole, this work furnishes pertinent arguments on how particle size, ethanol content and CO_2 flow rate conditions can affect the production of friedelin-enriched extracts by supercritical fluid extraction.

6.5 REFERENCES

[1] M.M.R. de Melo, A.J.D. Silvestre, C.M. Silva, Supercritical fluid extraction of vegetable matrices: Applications, trends and future perspectives of a convincing green technology, Journal of Supercritical Fluids, 92 (2014) 115-176.

[2] M.M.R. de Melo, P.F. Martins, A.J.D. Silvestre, P. Sarmento, C.M. Silva, Measurement and modeling of supercritical fluid extraction curves of *Eichhornia crassipes* for enhanced stigmasterol production: Mechanistic insights of the process, Separation and Purification Technology, 163 (2016) 189-198.

[3] M.M.R. de Melo, A. Şen, A.J.D. Silvestre, H. Pereira, C.M. Silva, Experimental and modeling study of supercritical CO_2 extraction of *Quercus cerris* cork: influence of ethanol and particle size on extraction kinetics and selectivity to friedelin, Separation and Purification Technology, (submitted).

[4] E.L.G. Oliveira, A.J.D. Silvestre, C.M. Silva, Review of kinetic models for supercritical fluid extraction, Chemical Engineering Research and Design, 89 (2011) 1104-1117.

[5] H. Sovovà, R.P. Stateva, Supercritical fluid extraction from vegetable materials, Reviews in Chemical Engineering, 27 (2011) 79-156.

[6] J.M. del Valle, J.C. de la Fuente, D.A. Cardarelli, Contributions to supercritical extraction of vegetable substrates in Latin America, Journal of Food Engineering, 67 (2005) 35-57.

[7] S. Angus, B. Amstrong, K.M. De Reuck, Internation Thermodynamic Tables of the Fluid State: Carbon Dioxide, Pergamon Press, Oxford, 1976.

[8] K.S. Pitzer, D.R. Schreiber, Improving equation-of-state accuracy in the critical region - Equations for carbon-dioxide and neopentane as examples, Fluid Phase Equilibria, 41 (1988) 1-17.

[9] M. Pilavtepe, O. Yesil-Celiktas, Mathematical modeling and mass transfer considerations in supercritical fluid extraction of Posidonia oceanica residues, The Journal of Supercritical Fluids, 82 (2013) 244-250.

[10] R.C. Reid, J.M. Prausnitz, B.E. Poling, The Properties of Gases & Liquids, 5th ed., McGraw-Hill Professional, New York, 2001.

[11] K. Stephan, K. Lucas, Viscosity of Dense Fluids, Plenum Press, Lafayette, 1979.

[12] C.M. Silva, H. Liu, Modelling of transport properties of hard sphere fluids and related systems, and its application, in: A. Mulero (Ed.) Theory and Simulation of Hard Spehere Fluids and Related Systems, Lecture Notes in Physics 753, Springer, Berlin, 2008, pp. 383-501.

[13] W.D. Monnery, W.Y. Svrcek, A.K. Mehrotra, Viscosity: A critical review of practical predictive and correlative methods, The Canadian Journal of Chemical Engineering, 73 (1995) 3-40.

[14] H. Sovova, J. Prochazka, Calculations of compressed carbon dioxide viscosities, Industrial & Engineering Chemistry Research, 32 (1993) 3162-3169.

[15] V.V. Altunin, M. Sakhabetdinov, Viscosity of Liquid and Gaseous Carbon-Dioxide at Temperatures of 220-1300 K and Pressures up to 1200 Bar, Thermal Engineering, 19 (1972) 124-129.

[16] V. Vesovic, W.A. Wakeham, Prediction of the viscosity of fluid mixtures over wide ranges of temperature and pressure, Chemical Engineering Science, 44 (1989) 2181-2189.

[17] C.-C. Lai, C.-S. Tan, Measurement of molecular diffusion coefficients in supercritical carbon dioxide using a coated capillary column, Industrial & Engineering Chemistry Research, 34 (1995) 674-680.

[18] A.L. Magalhães, R.V. Vaz, R.M.G. Gonçalves, F.A. Da Silva, C.M. Silva, Accurate hydrodynamic models for the prediction of tracer diffusivities in supercritical carbon dioxide, Journal of Supercritical Fluids, 83 (2013) 15-27.

[19] R.V. Vaz, A.L. Magalhães, C.M. Silva, Improved Stokes–Einstein based models for diffusivities in supercritical CO_2, Journal of the Taiwan Institute of Chemical Engineers, 45 (2014) 1280-1284.

[20] R.V. Vaz, A.L. Magalhães, C.M. Silva, Improved hydrodynamic equations for the accurate prediction of diffusivities in supercritical carbon dioxide, Fluid Phase Equilibria, 360 (2013) 401-415.

[21] R.V. Vaz, A.L. Magalhães, C.M. Silva, Prediction of binary diffusion coefficients in supercritical CO_2 with improved behavior near the critical point, Journal of Supercritical Fluids, 91 (2014) 24-36.

[22] Y. Zhu, X. Lu, J. Zhou, Y. Wang, J. Shi, Prediction of diffusion coefficients for gas, liquid and supercritical fluid: application to pure real fluids and infinite dilute binary solutions based on the simulation of Lennard–Jones fluid, Fluid Phase Equilibria, 194–197 (2002) 1141-1159.

[23] H.B.E. Dymond, E. Vogel, W.A. Wakeham, V. Vesovic, M.J. Assael, Theory—Dense Fluids, Cambridge University Press, Cambridge, 2005.

[24] T. Funazukuri, N. Wakao, AiChe Annual Meeting, (1993).

[25] H. Liu, C.M. Silva, E.A. Macedo, New equations for tracer diffusion coefficients of solutes in supercritical and liquid solvents based on the Lennard-Jones fluid model, Industrial & Engineering Chemistry Research, 36 (1997) 246-252.

[26] A.L. Magalhães, F.A. Da Silva, C.M. Silva, Free-volume model for the diffusion coefficients of solutes at infinite dilution in supercritical CO_2 and liquid H_2O, Journal of Supercritical Fluids, 74 (2013) 89-104.

[27] P.F. Lito, A.L. Magalhães, J.R.B. Gomes, C.M. Silva, Universal model for accurate calculation of tracer diffusion coefficients in gas, liquid and supercritical systems, Journal of Chromatography A, 1290 (2013) 1-26.

[28] A.L. Magalhães, F.A. Da Silva, C.M. Silva, New models for tracer diffusion coefficients of hard sphere and real systems: Application to gases, liquids and supercritical fluids, Journal of Supercritical Fluids, 55 (2011) 898-923.

[29] A.L. Magalhães, F.A. Da Silva, C.M. Silva, New models for tracer diffusion coefficients of hard sphere and real systems: Application to gases, liquids and supercritical fluids, The Journal of Supercritical Fluids, 55 (2011) 898-923.

[30] A.L. Magalhães, F.A. Da Silva, C.M. Silva, New tracer diffusion correlation for real systems over wide ranges of temperature and density, Chemical Engineering Journal, 166 (2011) 49-72.

[31] A.L. Magalhães, F.A. Da Silva, C.M. Silva, Tracer diffusion coefficients of polar systems, Chemical Engineering Science, 73 (2012) 151-168.

[32] A.L. Magalhães, P.F. Lito, F.A. Da Silva, C.M. Silva, Simple and accurate correlations for diffusion coefficients of solutes in liquids and supercritical fluids over wide ranges of temperature and density, Journal of Supercritical Fluids, 76 (2013) 94-114.

[33] A.L. Magalhães, S.P. Cardoso, B.R. Figueiredo, F.A. Da Silva, C.M. Silva, Revisiting the Liu–Silva–Macedo model for tracer diffusion coefficients of supercritical, liquid, and gaseous systems, Industrial & Engineering Chemistry Research, 49 (2010) 7697-7700.

[34] H. Sovová, R.P. Stateva, Supercritical fluid extraction from vegetable materials, Reviews in Chemical Engineering, 27 (2011) 79-156.

[35] J.M. Del Valle, J.C. De La Fuente, Supercritical CO_2 extraction of oilseeds: Review of kinetic and equilibrium models, Critical Reviews in Food Science and Nutrition, 46 (2006) 131-160.

[36] N. Wakao, T. Funazkri, Effect of fluid dispersion coefficients on particle-to-fluid mass transfer coefficients in packed beds, Chemical Engineering Science, 33 (1978) 1375-1384.

[37] O.J. Catchpole, R. Bernig, M.B. King, Measurement and correlation of packed-bed axial dispersion coefficients in supercritical carbon dioxide, Industrial & Engineering Chemistry Research, 35 (1996) 824-828.

[38] D. Yu, K. Jackson, T.C. Harmon, Dispersion and diffusion in porous media under supercritical conditions, Chemical Engineering Science, 54 (1999) 357-367.

[39] H. Sovová, Mathematical model for supercritical fluid extraction of natural products and extraction curve evaluation, Journal of Supercritical Fluids, 33 (2005) 35-52.

[40] J. Chrastil, Solubility of solids and liquids in supercritical gases, Journal of Physical Chemistry, 86, (1982) 3016–3021.

[41] Ö. Güçlü-Üstündağ, F. Temelli, Correlating the solubility behavior of minor lipid components in supercritical carbon dioxide, Journal of Supercritical Fluids, 31 (2004) 235-253.

[42] Y. Adachi, B.C.Y. Lu, Supercritical fluid extraction with carbon dioxide and ethylene, Fluid Phase Equilibria, 14 (1983) 147-156.

[43] J.M. Del Valle, J.M. Aguilera, An improved equation for predicting the solubility of vegetable oils in supercritical carbon dioxide, Industrial & Engineering Chemistry Research, 27 (1988) 1551-1553.

[44] J. Méndez-Santiago, A.S. Teja, The solubility of solids in supercritical fluids, Fluid Phase Equilibria, 158–160 (1999) 501-510.

[45] H.-D. Sung, J.-J. Shim, Solubility of C. I. Disperse Red 60 and C. I. Disperse Blue 60 in supercritical carbon dioxide, Journal of Chemical & Engineering Data, 44 (1999) 985-989.

[46] K.D. Bartle, A.A. Clifford, S.A. Jafar, G.F. Shilstone, Solubilities of solids and liquids of low volatility in supercritical carbon dioxide, Journal of Physical and Chemical Reference Data, 20 (1991) 713-756.

[47] S.K. Kumar, K.P. Johnston, Modelling the solubility of solids in supercritical fluids with density as the independent variable, Journal of Supercritical Fluids, 1 (1988) 15-22.

[48] Z.-R. Yu, B. Singh, S.S.H. Rizvi, J.A. Zollweg, Solubilities of fatty acids, fatty acid esters, triglycerides, and fats and oils in supercritical carbon dioxide, Journal of Supercritical Fluids, 7 (1994) 51-59.

[49] M.D. Gordillo, M.A. Blanco, A. Molero, E. Martinez de la Ossa, Solubility of the antibiotic Penicillin G in supercritical carbon dioxide, The Journal of Supercritical Fluids, 15 (1999) 183-190.

[50] C. Garlapati, G. Madras, Solubilities of solids in supercritical fluids using dimensionally consistent modified solvate complex models, Fluid Phase Equilibria, 283 (2009) 97-101.

[51] J.C. González, M.R. Vieytes, A.M. Botana, J.M. Vieites, L.M. Botana, Modified mass action law-based model to correlate the solubility of solids and liquids in entrained supercritical carbon dioxide, Journal of Chromatography A, 910 (2001) 119-125.

[52] J. Mendez-Santiago, A.S. Teja, Solubility of solids in supercritical fluids: Consistency of data and a new model for cosolvent systems, Industrial & Engineering Chemistry Research, 39 (2000) 4767-4771.

[53] M. Sauceau, J.J. Letourneau, D. Richon, J. Fages, Enhanced density-based models for solid compound solubilities in supercritical carbon dioxide with cosolvents, Fluid Phase Equilibria, 208 (2003) 99-113.

[54] R. Thakur, R.B. Gupta, Rapid expansion of supercritical solution with solid cosolvent (RESS−SC) process: Formation of griseofulvin nanoparticles, Industrial & Engineering Chemistry Research, 44 (2005) 7380-7387.

[55] H. Sovová, Solubility of ferulic acid in supercritical carbon dioxide with ethanol as cosolvent, Journal of Chemical & Engineering Data, 46 (2001) 1255-1257.

[56] S. Garnier, E. Neau, P. Alessi, A. Cortesi, I. Kikic, Modelling solubility of solids in supercritical fluids using fusion properties, Fluid Phase Equilibria, 158–160 (1999) 491-500.

[57] K. Sepassi, P.B. Myrdal, S.H. Yalkowsky, Estimating pure-component vapor pressures of complex organic molecules: Part II, Industrial & Engineering Chemistry Research, 45 (2006) 8744-8747.

[58] M.M.R. de Melo, E.L.G. Oliveira, A.J.D. Silvestre, C.M. Silva, Supercritical fluid extraction of triterpenic acids from *Eucalyptus globulus* bark, Journal of Supercritical Fluids, 70 (2012) 137-145.

[59] M. Škerget, Ž. Knez, M. Knez-Hrnčič, Solubility of solids in sub- and supercritical fluids: A review, Journal of Chemical & Engineering Data, 56 (2011) 694-719.

[60] B. Díaz-Reinoso, A. Moure, H. Domínguez, J.C. Parajó, Supercritical CO_2 extraction and purification of compounds with antioxidant activity, Journal of Agricultural and Food Chemistry, 54 (2006) 2441-2469.

[61] S. Vafai, B.D. Drake, R.L. Smith, Solid molar volumes of interest to supercritical extraction at 298 K: atropine, berberine hydrochloride hydrate, brucine dihydrate, capsaicin, ergotamine tartrate dihydrate, naphthalene, penicillin V, piperine, quinine, strychnine, theobromine, theophylline, and yohimbine hydrochloride, Journal of Chemical & Engineering Data, 38 (1993) 125-127.

[62] S.N. Vaidya, G.C. Kennedy, Compressibility of 18 molecular organic solids to 45 kbar, Journal of Chemical Physics, 55 (1971) 987-992.

[63] ChemSpider, in, Royal Society of Chemistry, http://www.chemspider.com, Accessed in February 2012.

[64] C.-S. Su, Correlation and estimation of solubilities of fatty acids in supercritical carbon dioxide using solution model approach, Journal of Supercritical Fluids, 81 (2013) 79-85.

[65] D.H. Ziger, C.A. Eckert, Correlation and prediction of solid-supercritical fluid phase equilibriums, Industrial & Engineering Chemistry Process Design and Development, 22 (1983) 582-588.

[66] P. Subra, S. Castellani, P. Jestin, A. Aoufi, Extraction of β-carotene with supercritical fluids: Experiments and modelling, Journal of Supercritical Fluids, 12 (1998) 261-269.

[67] S.N. Naik, H. Lentz, R.C. Maheshwari, Extraction of perfumes and flavours from plant materials with liquid carbon dioxide under liquid—vapor equilibrium conditions, Fluid Phase Equilibria, 49 (1989) 115-126.

[68] J. Martinez, A.R. Monteiro, P.T.V. Rosa, M.O.M. Marques, M.A.A. Meireles, Multicomponent model to describe extraction of ginger oleoresin with supercritical carbon dioxide, Industrial & Engineering Chemistry Research, 42 (2003) 1057-1063.

[69] C.-S. Tan, D.-C. Liou, Modeling of desorption at supercritical conditions, Aiche Journal, 35 (1989) 1029-1031.

[70] F. Gaspar, T. Lu, R. Santos, B. Al-Duri, Modelling the extraction of essential oils with compressed carbon dioxide, Journal of Supercritical Fluids, 25 (2003) 247-260.

[71] J. Crank, The Mathematics of Diffusion, 2 ed., Clarendon Press, Oxford, England, 1975.

[72] G. Brunner, Mass transfer from solid material in gas extraction, Berichte der Bunsengesellschaft für physikalische Chemie, 88 (1984) 887-891.

[73] H. Sovová, Steps of supercritical fluid extraction of natural products and their characteristic times, Journal of Supercritical Fluids, 66 (2012) 73-79.

[74] N.P. Povh, M.O.M. Marques, M.A.A. Meireles, Supercritical CO_2 extraction of essential oil and oleoresin from chamomile (*Chamomilla recutita* [L.] Rauschert), Journal of Supercritical Fluids, 21 (2001) 245-256.

[75] H. Sovová, Rate of the vegetable oil extraction with supercritical CO2—I. Modelling of extraction curves, Chemical Engineering Science, 49 (1994) 409-414.

[76] M. Goto, B.C. Roy, T. Hirose, Shrinking-core leaching model for supercritical-fluid extraction, Journal of Supercritical Fluids, 9 (1996) 128-133.

[77] L. Fiori, D. Basso, P. Costa, Supercritical extraction kinetics of seed oil: A new model bridging the 'broken and intact cells' and the 'shrinking-core' models, Journal of Supercritical Fluids, 48 (2009) 131-138.

[78] Z. Huang, X.-h. Shi, W.-j. Jiang, Theoretical models for supercritical fluid extraction, Journal of Chromatography A, 1250 (2012) 2-26.

[79] C.M. Silva, C.P. Passos, M.A. Coimbra, F.A. Da Silva, Numerical simulation ofsupercritical extraction processes, Chemical Product and Process Modeling 4, Article 9, 2009.

[80] C.P. Passos, M.A. Coimbra, F.A. Da Silva, C.M. Silva, Modelling the supercritical fluid extraction of edible oils and analysis of the effect of enzymatic pre-treatments of seed upon model parameters, Chemical Engineering Research and Design, 89 (2011) 1118-1125.

[81] N. Hasan, B. Farouk, Mass transfer enhancement in supercritical fluid extraction by acoustic waves, Journal of Supercritical Fluids, 80 (2013) 60-70.

[82] C.P. Passos, R.M. Silva, F.A. Da Silva, M.A. Coimbra, C.M. Silva, Enhancement of the supercritical fluid extraction of grape seed oil by using enzymatically pre-treated seed, Journal of Supercritical Fluids, 48 (2009) 225-229.

[83] G. Nimet, E.A. da Silva, F. Palú, C. Dariva, L.d.S. Freitas, A.M. Neto, L.C. Filho, Extraction of sunflower (*Heliantus annuus* L.) oil with supercritical CO_2 and subcritical propane: Experimental and modeling, Chemical Engineering Journal, 168 (2011) 262-268.

[84] A.A. Jesus, L.C. Almeida, E.A. Silva, L.C. Filho, S.M.S. Egues, E. Franceschi, M. Fortuny, A.F. Santos, J. Araujo, E.M.B.D. Sousa, C. Dariva, Extraction of palm oil using propane, ethanol and its mixtures as compressed solvent, Journal of Supercritical Fluids, 81 (2013) 245-253.

[85] R.N. Carvalho Jr, L.S. Moura, P.T.V. Rosa, M.A.A. Meireles, Supercritical fluid extraction from rosemary (*Rosmarinus officinalis*): Kinetic data, extract's global yield, composition, and antioxidant activity, The Journal of Supercritical Fluids, 35 (2005) 197-204.

[86] M.M. Esquível, M.G. Bernardo-Gil, M.B. King, Mathematical models for supercritical extraction of olive husk oil, The Journal of Supercritical Fluids, 16 (1999) 43-58.

[87] D. Westerman, R.C.D. Santos, J.A. Bosley, J.S. Rogers, B. Al-Duri, Extraction of Amaranth seed oil by supercritical carbon dioxide, Journal of Supercritical Fluids, 37 (2006) 38-52.

[88] E. Reverchon, L.S. Osseo, Modelling the supercritical extraction of basil oil, in: M. Perrut, G. Brunner (Eds.) Third International Symposium on Supercritical Fluids, 1994.

[89] V.M. Rodrigues, P.T.V. Rosa, M.O.M. Marques, A.J. Petenate, M.A.A. Meireles, Supercritical extraction of essential oil from aniseed (*Pimpinella anisum* L) using CO_2: Solubility, kinetics, and composition data, Journal of Agricultural and Food Chemistry, 51 (2003) 1518-1523.

[90] B.P. Nobre, R.L. Mendes, E.M. Queiroz, F.L.P. Pessoa, J.P. Coelho, A.F. Palavra, Supercritical carbon dioxide extraction of pigments from *Bixa orellana* seeds (experiments and modeling), Brazilian Journal of Chemical Engineering, 23 (2006) 251-258.

[91] C.L.C. Albuquerque, M.A.A. Meireles, Defatting of annatto seeds using supercritical carbon dioxide as a pretreatment for the production of bixin: Experimental, modeling and economic evaluation of the process, Journal of Supercritical Fluids, 66 (2012) 86-95.

[92] S.G. Ozkal, M.E. Yener, L. Bayindirli, Mass transfer modeling of apricot kernel oil extraction with supercritical carbon dioxide, Journal of Supercritical Fluids, 35 (2005) 119-127.

[93] S. Quispe-Condori, D. Sanchez, M.A. Foglio, P.T.V. Rosa, C. Zetzl, G. Brunner, M.A.A. Meireles, Global yield isotherms and kinetic of artemisinin extraction from *Artemisia annua* L leaves using supercritical carbon dioxide, Journal of Supercritical Fluids, 36 (2005) 40-48.

[94] E. Reverchon, Mathematical modeling of supercritical extraction of sage oil, Aiche Journal, 42 (1996) 1765-1771.

[95] R.M.F. Vargas, E. Cassel, G.M.F. Gomes, L.G.S. Longhi, L. Atti-Serafini, A.C. Atti-Santos, Supercritical extraction of carqueja essential oil: Experiments and modeling, Brazilian Journal of Chemical Engineering, 23 (2006) 375-382.

[96] D.C.M.N. Silva, L.F.V. Bresciani, R.L. Dalagnol, L. Danielski, R.A. Yunes, S.R.S. Ferreira, Supercritical fluid extraction of carqueja (*Baccharis trimera*) oil: Process parameters and composition profiles, Food and Bioproducts Processing, 87 (2009) 317-326.

[97] M. Fullana, F. Trabelsi, F. Recasens, Use of neural net computing for statistical and kinetic modelling and simulation of supercritical fluid extractors, Chemical Engineering Science, 55 (2000) 79-95.

[98] C. Perakis, V. Louli, K. Magoulas, Supercritical fluid extraction of black pepper oil, Journal of Food Engineering, 71 (2005) 386-393.

[99] M. Škerget, Ž. Knez, Modelling high pressure extraction processes, Computers & Chemical Engineering, 25 (2001) 879-886.

[100] I.K. Hong, S.W. Rho, K.S. Lee, W.H. Lee, K.P. Yoo, Modeling of soybean oil bed extraction with supercritical carbon dioxide, Korean Journal of Chemical Engineering, 7 (1990) 40-46.

[101] P. Kotnik, M. Skerget, Z. Knez, Kinetics of supercritical carbon dioxide extraction of borage and evening primrose seed oil, European Journal of Lipid Science and Technology, 108 (2006) 569-576.

[102] M. Mukhopadhyay, Natural extracts using supercritical carbon dioxide, USA, CRC Press, 2000.

[103] W.B. Setianto, S. Yoshikawa, R.L. Smith, H. Inomata, L.J. Florusse, C.J. Peters, Pressure profile separation of phenolic liquid compounds from cashew (*Anacardium occidentale*) shell with supercritical carbon dioxide and aspects of its phase equilibria, Journal of Supercritical Fluids, 48 (2009) 203-210.

[104] R.N. Patel, S. Bandyopadhyay, A. Ganesh, Extraction of cashew (*Anacardium occidentale*) nut shell liquid using supercritical carbon dioxide, Bioresource Technology, 97 (2006) 847-853.

[105] I. Papamichail, V. Louli, K. Magoulas, Supercritical fluid extraction of celery seed oil, Journal of Supercritical Fluids, 18 (2000) 213-226.

[106] T. Hatami, M.A.A. Meireles, G. Zahedi, Mathematical modeling and genetic algorithm optimization of clove oil extraction with supercritical carbon dioxide, The Journal of Supercritical Fluids, 51 (2010) 331-338.

[107] K. Araus, E. Uquiche, J.M. del Valle, Matrix effects in supercritical CO_2 extraction of essential oils from plant material, Journal of Food Engineering, 92 (2009) 438-447.

[108] R.M. Couto, J. Fernandes, M.D.R.G. da Silva, P.C. Simões, Supercritical fluid extraction of lipids from spent coffee grounds, Journal of Supercritical Fluids, 51 (2009) 159-166.

[109] K.S. Andrade, R.T. Goncalvez, M. Maraschin, R.M. Ribeiro-do-Valle, J. Martinez, S.R.S. Ferreira, Supercritical fluid extraction from spent coffee grounds and coffee husks: Antioxidant activity and effect of operational variables on extract composition, Talanta, 88 (2012) 544-552.

[110] S. Quispe-Condori, M.A. Foglio, P.T.V. Rosa, M.A.A. Meireles, Obtaining beta-caryophyllene from *Cordia verbenacea* de Candolle by supercritical fluid extraction, Journal of Supercritical Fluids, 46 (2008) 27-32.

[111] A.A. de Azevedo, U. Kopcak, R. Mohamed, Extraction of fat from fermented Cupuaçu seeds with supercritical solvents, Journal of Supercritical Fluids, 27 (2003) 223-237.

[112] L.S. Moura, R.N. Carvalho, M.B. Stefanini, L.C. Ming, M.A.A. Meireles, Supercritical fluid extraction from fennel (*Foeniculum vulgare*): global yield, composition and kinetic data, Journal of Supercritical Fluids, 35 (2005) 212-219.

[113] M.G. Bernardo-Gil, M. Casquilho, M.M. Esquivel, M.A. Ribeiro, Supercritical fluid extraction of fig leaf gourd seeds oil: Fatty acids composition and extraction kinetics, Journal of Supercritical Fluids, 49 (2009) 32-36.

[114] K.C. Zancan, M.O.M. Marques, A.J. Petenate, M.A.M. Meireles, Extraction of ginger (*Zingiber officinale* Roscoe) oleoresin with CO_2 and co-solvents: a study of the antioxidant action of the extracts, Journal of Supercritical Fluids, 24 (2002) 57-76.

[115] S.G. Ozkal, U. Salgin, M.E. Yener, Supercritical carbon dioxide extraction of hazelnut oil, Journal of Food Engineering, 69 (2005) 217-223.

[116] M.G. Bernardo-Gil, M. Casquilho, Modeling the supercritical fluid extraction of hazelnut and walnut oils, Aiche Journal, 53 (2007) 2980-2985.

[117] Akgun, M. , Investigation of thermodynamic and transport properties in supercritical fluid extraction, Yildiz Technical University, Instanbul, Turkey, 1999.

[118] E. Langa, J. Cacho, A.M.F. Palavra, J. Burillo, A.M. Mainar, J.S. Urieta, The evolution of hyssop oil composition in the supercritical extraction curve: Modelling of the oil extraction process, Journal of Supercritical Fluids, 49 (2009) 37-44.

[119] J.M. del Valle, M. Jimenez, J.C. de la Fuente, Extraction kinetics of pre-pelletized Jalapeno peppers with supercritical CO_2, Journal of Supercritical Fluids, 25 (2003) 33-44.

[120] M. Akgun, N.A. Akgun, S. Dincer, Extraction and modeling of lavender flower essential oil using supercritical carbon dioxide, Industrial & Engineering Chemistry Research, 39 (2000) 473-477.

[121] Y. Gao, B. Nagy, X. Liu, B. Simándi, Q. Wang, Supercritical CO_2 extraction of lutein esters from marigold (*Tagetes erecta* L.) enhanced by ultrasound, The Journal of Supercritical Fluids, 49 (2009) 345-350.

[122] L.M.A.S. Campos, E.M.Z. Michielin, L. Danielski, S.R.S. Ferreira, Experimental data and modeling the supercritical fluid extraction of marigold (*Calendula officinalis*) oleoresin, Journal of Supercritical Fluids, 34 (2005) 163-170.

[123] L. Danielski, L.M.A.S. Campos, L.F.V. Bresciani, H. Hense, R.A. Yunes, S.R.S. Ferreira, Marigold (*Calendula officinalis* L.) oleoresin: Solubility in SC-CO2 and composition profile, Chemical Engineering and Processing: Process Intensification, 46 (2007) 99-106.

[124] D. Mongkholkhajornsilp, S. Douglas, P.L. Douglas, A. Elkamel, W. Teppaitoon, S. Pongamphai, Supercritical CO_2 extraction of nimbin from neem seeds - a modelling study, Journal of Food Engineering, 71 (2005) 331-340.

[125] A. Ajchariyapagorn, T. Kumhom, S. Pongamphai, S. Douglas, P.L. Douglas, W. Teppaitoon, Predicting the extraction yield of nimbin from neem seeds in supercritical CO_2 using group contribution methods, equations of state and a shrinking core extraction model, Journal of Supercritical Fluids, 51 (2009) 36-42.

[126] S. Machmudah, A. Sulaswatty, M. Sasaki, M. Goto, T. Hirose, Supercritical CO_2 extraction of nutmeg oil: Experiments and modeling, Journal of Supercritical Fluids, 39 (2006) 30-39.

[127] A. Berna, A. Tarrega, M. Blasco, S. Subirats, Supercritical CO_2 extraction of essential oil from orange peel; effect of the height of the bed, Journal of Supercritical Fluids, 18 (2000) 227-237.

[128] K.D. Bartle, A.A. Clifford, S.B. Hawthorne, J.J. Langenfeld, D.J. Miller, R. Robinson, A model for dynamic extraction using a supercritical fluid, Journal of Supercritical Fluids, 3 (1990) 143-149.

[129] H. Kubat, U. Akman, O. Hortacsu, Semi-batch packed-column deterpenation of origanum oil by dense carbon dioxide, Chemical Engineering and Processing, 40 (2001) 19-32.

[130] L.F. de França, M.A.A. Meireles, Modeling the extraction of carotene and lipids from pressed palm oil (*Elaes guineensis*) fibers using supercritical CO_2, Journal of Supercritical Fluids, 18 (2000) 35-47.

[131] B. Nagy, B. Simandi, Effects of particle size distribution, moisture content, and initial oil content on the supercritical fluid extraction of paprika, Journal of Supercritical Fluids, 46 (2008) 293-298.

[132] V. Louli, G. Folas, E. Voutsas, K. Magoulas, Extraction of parsley seed oil by supercritical CO_2, The Journal of Supercritical Fluids, 30 (2004) 163-174.

[133] N. Mezzomo, J. Martínez, S.R.S. Ferreira, Supercritical fluid extraction of peach (*Prunus persica*) almond oil: Kinetics, mathematical modeling and scale-up, Journal of Supercritical Fluids, 51 (2009) 10-16.

[134] C.S.G. Kitzberger, R.H. Lomonaco, E.M.Z. Michielin, L. Danielski, J. Correia, S.R.S. Ferreira, Supercritical fluid extraction of shiitake oil: Curve modeling and extract composition, Journal of Food Engineering, 90 (2009) 35-43.

[135] M.E. Araújo, N.T. Machado, L.F. Franca, M.A.A. Meireles, Supercritical extraction of pupunha (*Guilielma speciosa*) oil in a fixed bed using carbon dioxide, Brazilian Journal of Chemical Engineering, 17 (2000) 297-306.

[136] J.C. Germain, J.M. del Valle, J.C. de la Fuente, Natural convection retards supercritical CO_2 extraction of essential oils and lipids from vegetable substrates, Industrial & Engineering Chemistry Research, 44 (2005) 2879-2886.

[137] E. Uquiche, J.M. del Valle, J. Ortiz, Supercritical carbon dioxide extraction of red pepper (*Capsicum annuum* L.) oleoresin, Journal of Food Engineering, 65 (2004) 55-66.

[138] L. Danielski, C. Zetzl, H. Hense, G. Brunner, A process line for the production of raffinated rice oil from rice bran, Journal of Supercritical Fluids, 34 (2005) 133-141.

[139] O. Bensebia, D. Barth, B. Bensebia, A. Dahmani, Supercritical CO_2 extraction of rosemary: Effect of extraction parameters and modelling, Journal of Supercritical Fluids, 49 (2009) 161-166.

[140] L.A. Follegatti-Romero, C.R. Piantino, R. Grimaldi, F.A. Cabral, Supercritical CO_2 extraction of omega-3 rich oil from Sacha inchi (*Plukenetia volubilis* L.) seeds, The Journal of Supercritical Fluids, 49 (2009) 323-329.

[141] X.J. Han, L.M. Cheng, R. Zhang, J.C. Bi, Extraction of safflower seed oil by supercritical CO_2, Journal of Food Engineering, 92 (2009) 370-376.

[142] H. Sovová, L. Opletal, M. Bártlová, M. Sajfrtová, M. Křenková, Supercritical fluid extraction of lignans and cinnamic acid from *Schisandra chinensis*, The Journal of Supercritical Fluids, 42 (2007) 88-95.

[143] E. Langa, G.D. Porta, A.M.F. Palavra, J.S. Urieta, A.M. Mainar, Supercritical fluid extraction of Spanish sage essential oil: Optimization of the process parameters and modelling, The Journal of Supercritical Fluids, 49 (2009) 174-181.

[144] K.H. Kim, J. Hong, A mass transfer model for super- and near-critical CO_2 extraction of spearmint leaf oil, Separation Science and Technology, 37 (2002) 2271-2288.

[145] S.K. Yoda, M.O.M. Marques, A.J. Petenate, M.A.A. Meireles, Supercritical fluid extraction from *Stevia rebaudiana* Bertoni using CO_2 and CO_2+water: extraction kinetics and identification of extracted components, Journal of Food Engineering, 57 (2003) 125-134.

[146] G. Andrich, S. Balzini, A. Zinnai, V. De Vitis, S. Silvestri, F. Venturi, R. Fiorentini, Supercritical fluid extraction in sunflower seed technology, European Journal of Lipid Science and Technology, 103 (2001) 151-157.

[147] H.K. Kiriamiti, E. Rascol, A. Marty, J.S. Condoret, Extraction rates of oil from high oleic sunflower seeds with supercritical carbon dioxide, Chemical Engineering and Processing, 41 (2002) 711-718.

[148] B.M. King, T.R. Bott, Extraction of natural products using near-critical solvents, Blackie Academic & Professional,, 1-2 (26) (1993) 209–227.

[149] U. Salgin, O. Doker, A. Calimli, Extraction of sunflower oil with supercritical CO_2: Experiments and modeling, Journal of Supercritical Fluids, 38 (2006) 326-331.

[150] S.A.B.V. de Melo, G.M.N. Costa, R. Garau, A. Casula, B. Pittau, Supercritical CO_2 extraction of essential oils from *Thymus vulgaris*, Brazilian Journal of Chemical Engineering, 17 (2000) 367-371.

[151] E. Reverchon, G.D. Porta, F. Senatore, Supercritical CO_2 extraction and fractionation of lavender essential oil and waxes, Journal of Agricultural and Food Chemistry, 43 (1995) 1654-1658.

[152] Z. Zeković, Ž. Lepojević, A. Tolić, Modeling of the thyme-supercritical carbon dioxide extraction system. I. The influence of carbon dioxide flow rate and grinding degree of thyme, Separation Science and Technology, 36 (2001) 3459-3472.

[153] E. Vági, B. Simándi, K.P. Vásárhelyiné, H. Daood, Á. Kéry, F. Doleschall, B. Nagy, Supercritical carbon dioxide extraction of carotenoids, tocopherols and sitosterols from industrial tomato by-products, Journal of Supercritical Fluids, 40 (2007) 218-226.

[154] U. Topal, M. Sasaki, M. Goto, K. Hayakawa, Extraction of lycopene from tomato skin with supercritical carbon dioxide: Effect of operating conditions and solubility analysis, Journal of Agricultural and Food Chemistry, 54 (2006) 5604-5610.

[155] A.L. Chassagnez-Mendez, N.C.F. Correa, L.F. Franca, N.T. Machado, M.E. Araujo, A mass transfer model applied to the supercritical extraction with CO_2 of curcumins from turmeric rhizomes (*Curcuma longa* L), Brazilian Journal of Chemical Engineering, 17 (2000) 315-322.

[156] I. Zizovic, M. Stamenić, J. Ivanović, A. Orlović, M. Ristić, S. Djordjević, S.D. Petrović, D. Skala, Supercritical carbon dioxide extraction of sesquiterpenes from valerian root, The Journal of Supercritical Fluids, 43 (2007) 249-258.

[157] T.M. Takeuchi, P.F. Leal, R. Favareto, L. Cardozo-Filho, M.L. Corazza, P.T.V. Rosa, M.A.A. Meireles, Study of the phase equilibrium formed inside the flash tank used at the separation step of a supercritical fluid extraction unit, The Journal of Supercritical Fluids, 43 (2008) 447-459.

[158] M.J. Cocero, J. García, Mathematical model of supercritical extraction applied to oil seed extraction by CO2+saturated alcohol — I. Desorption model, The Journal of Supercritical Fluids, 20 (2001) 229-243.

[159] J. Crank, The Mathematics of Diffusion, 2nd ed., Oxford University Press, USA, 1980.

[160] H. Sovová, Mathematical model for supercritical fluid extraction of natural products and extraction curve evaluation, The Journal of Supercritical Fluids, 33 (2005) 35-52.

[161] M.M.R. de Melo, R.M.A. Domingues, A.J.D. Silvestre, C.M. Silva, Extraction and purification of triterpenoids using supercritical fluids: From lab to exploitation, Mini-Reviews in Organic Chemistry, 11 (2014) 362-381.

[162] M.M.R. de Melo, R.P. Silva, A.J.D. Silvestre, C.M. Silva, Valorization of water hyacinth through supercritical CO_2 extraction of stigmasterol, Industrial Crops and Products, 80 (2016) 177-185.

[163] P.F. Martins, M.M.R. de Melo, P. Sarmento, C.M. Silva, Supercritical fluid extraction of sterols from *Eichhornia crassipes* biomass using pure and modified carbon dioxide. Enhancement of stigmasterol yield and extract concentration, Journal of Supercritical Fluids, 107 (2016) 441-449.

[164] R.M.A. Domingues, M.M.R. de Melo, C.P. Neto, A.J.D. Silvestre, C.M. Silva, Measurement and modeling of supercritical fluid extraction curves of *Eucalyptus globulus* bark: Influence of the operating conditions upon yields and extract composition, Journal of Supercritical Fluids, 72 (2012) 176-185.

[165] L. Fiori, Grape seed oil supercritical extraction kinetic and solubility data: Critical approach and modeling, Journal of Supercritical Fluids, 43 (2007) 43-54.

[166] A. Şen, M.M.R. de Melo, A.J.D. Silvestre, H. Pereira, C.M. Silva, Prospective pathway for a green and enhanced friedelin production through supercritical fluid extraction of *Quercus cerris* cork, Journal of Supercritical Fluids, 97 (2015) 247-255.

[167] J.P.S. Aniceto, C.M. Silva, Preparative Chromatography: Batch and Continuous, in: Analytical Separation Science, Wiley-VCH Verlag GmbH & Co. KGaA, 2015.

[168] C.H. Liaw, J.S.P. Wang, R.A. Greenkorn, K.C. Chao, Kinetics of fixed-bed adsorption: A new solution, Aiche Journal, 25 (1979) 376-381.

[169] P.F. Martins, M.M.R. de Melo, C.M. Silva, Techno-economic optimization of the subcritical fluid extraction of oil from Moringa oleifera seeds and subsequent production of a purified sterols fraction, The Journal of Supercritical Fluids, 107 (2016) 682-689.

[170] N.C.M.C.S. Leitão, G.H.C. Prado, P.C. Veggi, M.A.A. Meireles, C.G. Pereira, *Anacardium occidentale* L. leaves extraction via SFE: Global yields, extraction kinetics, mathematical modeling and economic evaluation, The Journal of Supercritical Fluids, 78 (2013) 114-123.

[171] P.I.N. Carvalho, J.F. Osorio-Tobón, M.A. Rostagno, A.J. Petenate, M.A.A. Meireles, Techno-economic evaluation of the extraction of turmeric (Curcuma longa L.) oil and ar-turmerone using supercritical carbon dioxide, The Journal of Supercritical Fluids, 105 (2015) 44-54.

[172] L. Fiori, Supercritical extraction of grape seed oil at industrial-scale: Plant and process design, modeling, economic feasibility, Chemical Engineering and Processing: Process Intensification, 49 (2010) 866-872.

[173] J.M. del Valle, Extraction of natural compounds using supercritical CO_2: Going from the laboratory to the industrial application, Journal of Supercritical Fluids, 96 (2015) 180-199.

[174] R.M.A. Domingues, M.M.R. de Melo, E.L.G. Oliveira, C.P. Neto, A.J.D. Silvestre, C.M. Silva, Optimization of the supercritical fluid extraction of triterpenic acids from *Eucalyptus globulus* bark using experimental design, Journal of Supercritical Fluids, 74 (2013) 105-114.

[175] R.M.A. Domingues, E.L.G. Oliveira, C.S.R. Freire, R.M. Couto, P.C. Simões, C.P. Neto, A.J.D. Silvestre, C.M. Silva, Supercritical fluid extraction of *Eucalyptus globulus* bark – a promising approach for triterpenoids production, International Journal of Molecular Sciences, *13(6),* (2012) *7648-7662*.

[176] G. Brunner, Gas Extraction, Chapter 8, New York, 1994.

[177] H.M.A. Barbosa, M.M.R. de Melo, M.A. Coimbra, C.P. Passos, C.M. Silva, Optimization of the supercritical fluid coextraction of oil and diterpenes from spent coffee grounds using experimental design and response surface methodology, Journal of Supercritical Fluids, 85 (2014) 165-172.

7 SCALE-UP

This chapter is devoted to present and discuss scale-up studies of SFE in the last years based on the comprehensive review of the author covering research works from 2000 to 2013 [1], and to report an experimental scale-up study [2] comprising experiments of SFE of Eucalyptus globulus performed at three different scales: 0.5, 5.0 and 80 L.

CHAPTER OUTLINE

7.1 INTRODUCTION

As an alternative technology competing with the conventional solvent extraction that has a long history of application in industry, some promising SFE works have been matter of upscaling studies. For a process to reach an adequate scale-up level, it is expected that it has been previously assessed upon optimization of operating conditions, selection of preferable extraction times from yield *vs.* time curves, and modeling of the same curves in order to disclose extraction mechanisms that characterize the rate of solutes removal from biomass.

When SFE research approaches exploitation scenarios, it is highly recommendable that the process variables have been previously analyzed with attention at lab scale. Nonetheless, it is common practice to find empirical scale-up studies and units working under conditions optimized for distinct biomass species and target molecules. Such procedure can lead to erroneously scaled-up units.

With respect to scale-up criteria, SFE upscaling should obey rules regarding geometric, physical and chemical relationships, which are to be kept unchanged intentionally according to the mechanism that drives the process. Such carefulness ensures more accuracy when comparing results obtained at different scales, and also assures that these results are phenomenologically consistent. In this sense, there is a different adequate relationship for each type of limitation governing the SFE process. Four criteria may be listed:

i. When solubility limits the process, the mass of spent SC solvent per mass bed raw material ($w_{CO_2}\, w_b{}^{-1}$) should be kept constant [3];

ii. When intraparticle diffusion is the major limitation, the ratio of SC solvent flow rate to mass of bed raw material ($Q_{CO_2}\, w_b^{-1}$) should be kept constant [3];

iii. When both limitations are relevant, $w_{CO_2}\, w_b{}^{-1}$, and $Q_{CO_2}\, w_b^{-1}$ values should be held constant [3];

iv. An alternative approach is to fix both $w_{CO_2}\, w_b{}^{-1}$ and $Q_{CO_2}\, w_b^{-1}$, and fix also a dimensionless number such as Re. This may imply changing particle size of the raw material, since variables like *P* and *T* cannot be changed [4];

A fifth criterion should also be mentioned which rather than being directly based in mass transfer or equilibrium arguments, concerns geometric similarity issues. In this respect, the option to fix the ratio of bed length and bed diameter (L_b/D_b) can also be found in literature for upscaling SFE processes [5-6].

It is worth noting that besides the choice of proper upscaling criteria results may still not be confirmed at higher scales as a consequence of irrelevant phenomena at smaller scales that

become non-negligible at higher scales [7]. The aggregation of biomass and channeling are two illustrative examples that must be cited in this respect. For this reason, checking of modeling results at two scales is essential to confirm the reliability of the obtained results [8].

Figure 7.1 presents an example of scale-up studies performed following two of the aforementioned relationships for SFE of peach almond (*Prunus persica*) oil [4] and results are also fitted with BICM. In the reported case, distinct agreement observations arose from the application of criteria (*ii)* and (i*v).* In fact, the scale-up experiment performed under a fix ratio of flow rate and mass of raw material (*ii*) led to good results, while the establishment of Re number and the two ratios proposed in (*iv)* exhibited higher deviations. Despite this dissonance, such results can be useful for the SFE process by taking the visible deviations as opportunities to check the scale-up assumptions and to reinterpret extraction phenomena mechanisms. Nevertheless, such approach is only recommended when scale-up experiments are not too costly, or when the upscaling is performed in smaller units, closer to lab scale than to industrial reality.

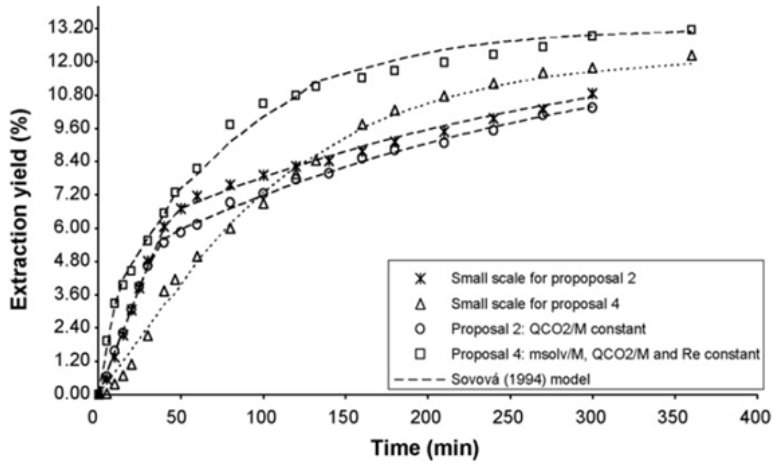

Figure 7.1 – Experimental and modeled extraction curves of different scale-up criteria SFE experiments and their respective small scale curves from peach (*Prunus persica*) almond. Plot retrieved from [4].

The bed geometry may influence SFE processes, a statement that is particularly prone to concern when SFE studies involve different extractors at different scales. Taking this into account, Carvalho Jr. *et al.* [9] devised two expressions that relate working conditions (SC-CO_2 flow rate, Q, and bed weight, w_b) at different bed geometries (diameter, D_b, and length L_b):

$$\frac{Q_2}{Q_1} = \left(\frac{w_{b2}}{w_{b1}}\right)^2 \times \frac{L_{b1}}{L_{b2}} \times \frac{D_{b_1}}{D_{b_2}} \quad (1)$$

and

$$\frac{Q_2}{Q_1} = \left(\frac{w_{b2}}{w_{b1}}\right)^2 \times \frac{L_{b1}}{L_{b2}} \times \left(\frac{D_{b_1}}{D_{b_2}}\right)^3 \quad (2)$$

where Eq. (1) is specially devoted to cases where the total amount of extractable solute (X_0) is determined from experiments using different SFE units, and Eq. (2) allows one to calculate a flow rate that ensures the same kinetic behavior between two SFE units.

In a very instructive study, del Valle et al. [10] evaluated the influence of scale on the SFE of rosehip seeds, in which 1 L and 2.6 L capacity units were used to undertake the experiments. They started by fitting a two-period model (based on solubility dominance at the onset and intraparticle diffusion limitations at the end of extraction) to the 1 L assays, which was considered to represent data adequately. However, for the runs carried out in the 2.6 L extractor the model failed to describe the profiles, particularly along the curvature branches. Several possibilities were raised to explain the lack of fit of the model, namely: i) transport of solute through CO_2 recycling stream; ii) axial dispersion in the supercritical phase; and iii) flow heterogeneity in the bed. The authors performed then a sensitivity analysis through model simulations, by varying the inlet oil concentration, axial dispersion coefficient, and solvent interstitial velocity (solid lines in Figure 7.2). It is noticeable that the three variables influence the process towards the experimental data. In addition, the occurrence of a heterogeneous flow inside the extractor was undoubtedly the factor that most efficiently improved the representation of the measured data. Despite the usefulness of the model to disclose the physical phenomena guiding the SFE, only new experiments could allow, in their case, the elucidation of whether the discrepancies between model and data in the 2.6 L extractor were due to only one of the factors or to their conjugation.

Other scale-up works are listed in Table 7.1, such as the one of Kotnik et al. [11] who worked with a 60 mL and 4 L vessels for the extraction of chamomile (*Matricaria chamomilla*) flowers, that of Lu et al. [12] who reported the SFE of *Pteris semipinnata* L. in a 20 L pilot scale extractor, or that of Ranalli *et al.* [13] who performed SC-CO_2 extractions of carrot (*Daucus carota* L.) root oil in 5 L pilot extractor. Special attention should be paid to the work of Han et al [14], who successfully attempted the upscaling of the SFE of safflower seed with a jump from a 0.5 to 260 L extractor using $Q_{CO_2}\, w_b^{-1}$ as scale-up criterion. Alternatively, Fullana et al. [15] presented an alternative approach to scale-up based on the use of neural networks, which allows addressing upscaling within few requirements regarding kinetics information. It is also included in Table 7.1 our work on *Eucalyptus globulus* that is the core of this chapter.

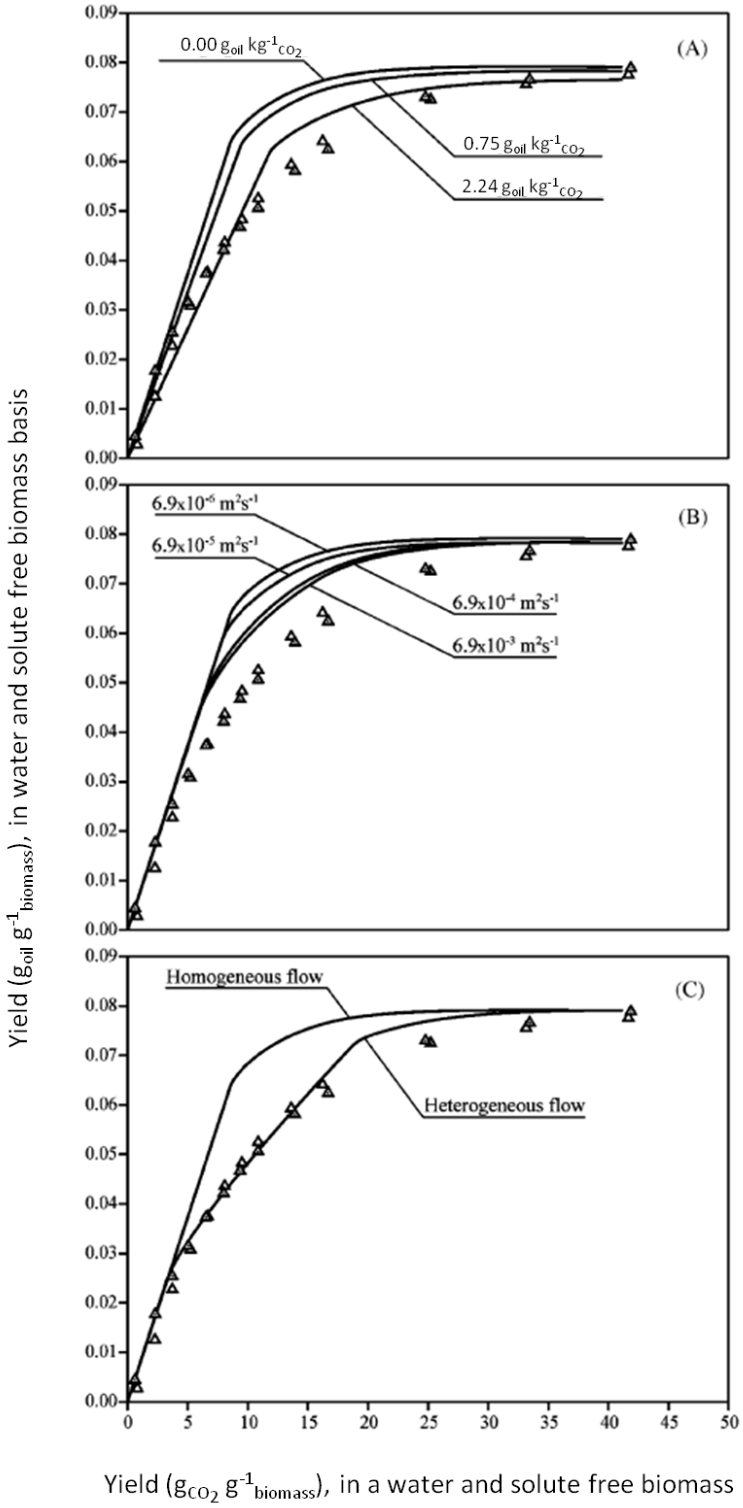

Figure 7.2 – Sensitivity analysis of the simulated extraction yield of roll milled rosehip seeds (0.1 mm size) as a function of specific solvent mass in 2.6 L plant experiments with 200 g min^{-1} of CO_2 at 40 °C and 300 bar: A) effect of the oil concentration at the extractor inlet; B) effect of the axial dispersion coefficient inside the bed; C) effect of the non-uniformity of solvent flow (i.e. the presence of an outer annular region of high interstitial velocity, and an inner circular region of lower interstitial velocity). Symbols represent experimental data. Figure retrieved from [10].

Table 7.1 – Higher scale and scale-up studies on SFE compiled by the author in the period *from* 2000 to 2013 [1].

Matrix	Scales	Unit capacity	Scale-up criteria	Ref
Allium cepa L.	Intermediate	5 L		[16]
Bixa orellana L.	Lab	0.007 L		[17]
	Lab	0.029 L	$w_{CO_2}\, w_b{}^{-1}$	
Carthamus tinctorius	Lab	0.5 L		[14]
	Pilot	260 L	$Q_{CO_2}\, w_b^{-1}$	
Citrus sinensis	Lab	0.5 L		[7]
	Intermediate	5 L	$w_{CO_2}\, w_b{}^{-1}$ and $Q_{CO_2}\, w_b^{-1}$	
Daucus carota L.	Intermediate	5 L		[13]
Eucalyptus globulus *	Lab	0.5 L		[2]
	Intermediate	5.0 L	$Q_{CO_2}\, w_b^{-1}$	
	Pilot	80.0 L	$Q_{CO_2}\, w_b^{-1}$	
Eugenia caryophillus	Lab	0.006 L		[18]
	Lab	0.280 L	$v_{superficial}$	
	Lab	0.280 L	$t_{residence,\ CO2}$	
Glycine variety	Lab	0.2 L		[6]
	Intermediate	5 L	L_b / D_b	
	Intermediate	5 L	$Q_{CO_2}\, w_b^{-1}$	
Helianthus annuus L.	Intermediate	2 L		[19]
Helianthus annuus L.	Lab	0.01 L		[5]
	Intermediate	1.2 L	$\approx L_b$ / D_b	
Matricaria chamomilla	Lab	0.060 L		[11]
	Intermediate	5 L		
Origanum vulgare L.	Intermediate	2 L		[20]
Thymus zygis	Intermediate	2L		
Salvia officinalis	Intermediate	2 L		
Rosmarinus officinalis	Intermediate	2 L		
Pinus brutia	Lab	0.3 L		[21]
	Intermediate	6.5 L	$Q_{CO_2}\, w_b^{-1}$	
Pteris semipinnata L.	Intermediate	20 L		[12]
Sophora flavescens	Lab	0.01L		[22]
	Lab	1 L		
Tanacetum parthenium	Lab	0.06		[23]
	Intermediate	4 L		
Thymus vulgaris L.	Intermediate	10.3 L		[24]
Thymus vulgaris L.	Intermediate	5 L		[25]
Triticum spp.	Lab	0.01 L		[26]
	Intermediate	4 L	$w_{CO_2}\, w_b{}^{-1}$	
Vitis vinifera L.	Lab	0.01 L		[27]
	Intermediate	2 L		
Vitis vinifera L.	Lab	0.3 L		[28]
	Intermediate	5.1 L	$w_{CO_2}\, w_b{}^{-1}$	

* Accomplished by the author and part of this thesis.

In general, scale-up that targets big jumps in extractor dimensions embodies a research path that begins with an initial exploratory lab experiment and which reaches scale studies after being matter of working conditions optimization and modeling. A significant volume of resources (time, material, human) is required to accomplish such research path, reason why preliminary economic assessments are sometimes carried out to foresee the gross viability of the process. When process remains promising and scale-up stage is overcome with success, the process has finally reached the point of being studied under deeper economic assessments.

* * *

In the following section, the SFE of *Eucalyptus globulus* deciduous bark is accomplished with SC-CO_2 modified with ethanol (cosolvent) in extractors of 0.5, 5.0 and 80 L, taking into account relevant information from previous essays [29-31]. Accordingly, scale-up experiments performed in the facilities of University of Aveiro and Natex [32] are presented and discussed. Several extraction curves are measured together with the TTAs concentration in the extracts along time. Modeling is also accomplished, being fundamental to identify the prevailing mass transfer mechanism and establish the appropriate scale up-criterion. At the end, this work is intended to provide reliable arguments to demonstrate SFE as a valid technical solution to produce valuable natural extracts from such an abundant vegetable residue.

7.2 MODELING

Aiming at the disclosure and confirmation of the dominant mechanisms of the SFE process, the extraction curves measured at lab scale can be modeled with simple expressions based on distinct assumptions: i) a model combining equilibrium (taken as solubility in the supercritical solvent) plus external film resistance published by Brunner [33], hereafter denoted by SFM; ii) a model proposed by Cocero and Garcia [34] that conjugates linear equilibrium (i.e., solute-matrix interaction exists) and film resistance, henceforth called LEFM; iii) two models that exclusively focus on intraparticle diffusion, namely the Diffusion model for spherical particles [35] (DFM) and the Single Simple Plate model (SSPM) for slab geometry [36].

The goodness of the fit of the models is quantified in this work by the average absolute relative deviation (AARD) defined by:

$$\mathrm{AARD}(\%) = \frac{100}{n}\sum_{i=1}^{n}\left|\frac{\eta_{\mathrm{total,i}}^{\mathrm{calc}} - \eta_{\mathrm{total,i}}^{\mathrm{exp}}}{\eta_{\mathrm{total,i}}^{\mathrm{exp}}}\right| \tag{3}$$

where n is the number of points of the cumulative curve, $\eta_{\mathrm{total,i}}^{\mathrm{calc}}$ and $\eta_{\mathrm{total,i}}^{\mathrm{exp}}$ are the calculated and experimental total extraction yields of point i, respectively.

All the models used in this work were previously presented in Chapter 6 of this thesis.

7.3 MATERIALS AND METHODS

7.3.1 RAW MATERIALS

Deciduous bark of *E. globulus* was randomly harvested from a 20-year-old clone plantation cultivated in Eixo (40º37'13.56''N, 8º34'08.43''W), region of Aveiro, Portugal. The bark was then dried in an oven at 40 ºC during approximately 72 h, reaching final moisture content between 2 and 5 wt.%, milled to granulometry lower than 2 mm, and stored in hermetically sealed bags until use. The deciduous bark was selected as substrate since it is mostly outer bark, favoring the TTAs concentration. It is worth noting the abundance of TTAs is much higher in the outer bark of *E. globulus* than in the inner bark [37].

7.3.2 CHEMICALS

Nonacosan-1-ol (98% purity) and β-sitosterol (99% purity) were purchased from Fluka Chemie (Madrid, Spain); ursolic acid (98% purity), betulinic acid (98% purity), and oleanolic acid (98% purity) were purchased from Aktin Chemicals (Chengdu, China); betulonic acid (95% purity) was purchased from CHEMOS GmbH (Regenstauf, Germany); palmitic acid (99% purity), dichloromethane (99% purity), pyridine (99% purity), bis(trimethylsilyl)trifluoroacetamide (99% purity), trimethylchlorosilane (99% purity), and tetracosane (99% purity) were supplied by Sigma Chemical Co. (Madrid, Spain). Carbon dioxide was supplied with a purity of 99.95% from Praxair (Porto, Portugal).

7.3.3 SUPERCRITICAL FLUID EXTRACTION

The SFE assays were carried out in three different apparatus (0.5, 5.0 and 80.0 L; see Figure 7.3). The experimental conditions presented in Table 7.2 were chosen attending to preceding studies performed at lab scale. These included optimization of the most relevant operating conditions, namely pressure, temperature, cosolvent concentration and flow rate [29, 31]. The lab scale experiments were performed in a 0.5 L unit whose full description and operation is provided elsewhere [29]. The intermediate scale (5.0 L) and pilot scale (80.0 L) experiments were carried out in Natex facilities [32].

7.3.4 EXTRACTS CHARACTERIZATION

Extracts were analyzed by GC–MS. About 20 mg of each dried extract were trimethylsilylated according to the literature [30, 38]. Two aliquots of each extract were analyzed in triplicate, being the reported results the average of the measurements (less than 5% variation between injections of the same aliquot and between aliquots of the same sample). The GC–MS analyses were performed using tetracosane as internal standard, in a Trace Gas Chromatograph 2000

Series equipped with a Finnigan Trace MS mass spectrometer, using helium as carrier gas (35 cm s^{-1}), equipped with a DB-1 J&W capillary column (30 m × 0.32 mm i.d., 0.25 μm film thickness). The chromatographic conditions were as follows: initial temperature: 80 °C for 5 min; temperature rate: 4 °C min^{-1}; final temperature: 285 °C for 10 min; injector temperature: 250 °C; transfer-line temperature: 290 °C; split ratio: 1:50. The MS was operated in the electron impact mode with electron impact energy of 70 eV and data collected at a rate of 1 scan s^{-1} over a range of m/z of 33–750. The ion source was maintained at 250 °C.

Table 7.2 – Experimental conditions of the SFE runs included in this work. Pressure and temperature are held constant in 200 bar and 40 °C, respectively.

Exp.	Scale (L)	Mass of bark (kg)	Ethanol content (wt.%)	$Q_{CO_2}\, w_{bark}^{-1}$ ($kg_{CO2}\, h^{-1}\, kg^{-1}{}_{bark}$)$^{++}$	Extractor geometry^{+++} L_b / D_b
Run 7.1	0.5	0.0703	2.5	10	1.6
Run 7.2*	0.5	0.0700	5.0	10	1.6
Run 7.3	5.0	0.900	2.5	10	6.1
Run 7.4	5.0	0.900	5.0	10	6.1
Run 7.5	80.0	13.7	2.5	10	4.1

* Experiment taken from ref. [29]; $^{++}$ ratio between the mass flow rate of CO_2 and the mass of bark inside extractor. $^{+++}L_b$ is the bed length, and D_b is the bed diameter.

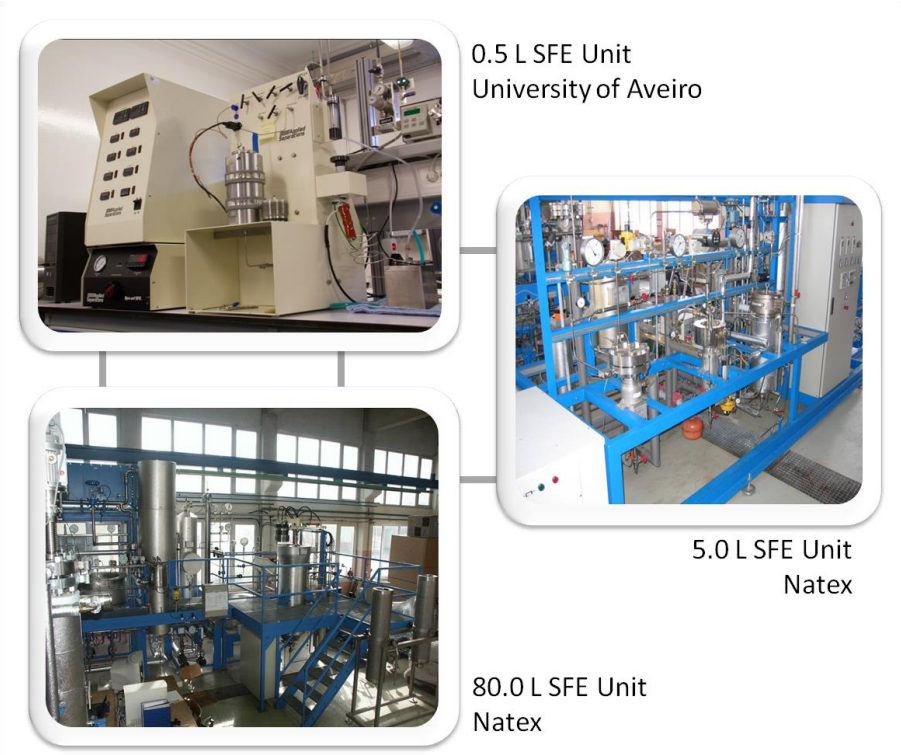

Figure 7.3 – Supercritical fluid extraction units used in the scale-up study of this work.

7.4 RESULTS AND DISCUSSION

The experimental and modelling results obtained in this work are discussed in the following three subsections. The first one comprehends the measurement and modelling of extraction curves at lab scale, from which the appropriate scale-up criterion is disclosed. The subsequent subsections are devoted to the scale-up of the process (based on the previously established criterion) using 2.5 wt.% and 5.0 wt.% ethanol, respectively.

7.4.1 EXPERIMENTAL AND MODELLING RESULTS AT LAB SCALE. SCALE-UP CRITERION

Experimental Results - With regard to the experimental results (Figure 7.4), they confirm the impact of the ethanol addition to enhance the overall extraction rate and, thus, the cumulative yields achieved along time. While an overlapping of both runs is observed within the first hour of extraction, where a linear increase is quite acceptable, Run 7.2 (5 wt.% ethanol) exhibits higher extraction rate from this point until the end of the experiment. For instance the last point of Run 7.1 was measured at 6.5 h, for which the total yield is 20 % lower than that of Run 7.2 (interpolated for the same time). The justification for this behavior is the concentration of ethanol in the system, which enhances the rate of solute removal due to solubility increment, since all remaining operating conditions and equipment geometry are the same [31, 38-39].

Despite the fact that the cumulative yields are still increasing after 6 h of extraction, the removal rates in the final stage of the experiments are considerably low in relation to their respective magnitudes at the onset of the process. Such behavior dues naturally to the diminution of the mass transfer driving force along the semi-continuous process. Nonetheless, when the extraction rate starts to decay in early periods of the experiment – which happens in the case of SFE of *Eucalyptus* bark – that may reveal the existence and influence of limitations to mass transfer, mainly inside the particle [1, 40-43]. The study and disclosure of these resistances can be achieved with the aid of distinct models, upon checking how different assumptions adjust to the experimental data [1, 29]. This issue is addressed in the following paragraphs of this subsection.

Modeling Results - The models listed in Section 7.2 were applied to Runs 7.1 and 7.2, being the respective results plotted in Figure 7.4 along with experimental data. Their optimized parameters and computed average deviations are compiled in Table 7.3.

With regard to the SFM (see Table 6.2), the results achieved by fitting the kinetic parameter k_1 to the set of points of each assay are very weak, as the large deviations found for Run 7.1 (AARD = 49.8 %) and Run 7.2 (AARD = 40.9 %) demonstrate (see Table 7.3). This is also

evident from Figure 7.4, where these linear plots do not follow the real experimental trends of both cumulative curves along time. Such linear behavior can be expected when abundant extractable material/solute is available to compensate the mass transfer limitations in order to ensure a constant period of extraction [1, 40, 42-44]. This is in great agreement with comprehensive models that set the initial period of extraction as the most suitable for an extraction rate defined by solubility and external mass transfer resistance [1, 44].

When linear equilibrium plus film resistance premises (LEFM) are tested with experimental results, the fittings exhibit a significant improvement in comparison to the SFM: deviations between 29.2 % and 40.3 % are obtained, which represent ca. 10 % less than those for SFM. Nevertheless it should be stressed that in the LEFM two parameters were adjusted rather than one, which should be taken into account also for the interpretation of the better goodness of fit performances revealed by this model. In any case, the results are still poor in terms of extraction curves representation.

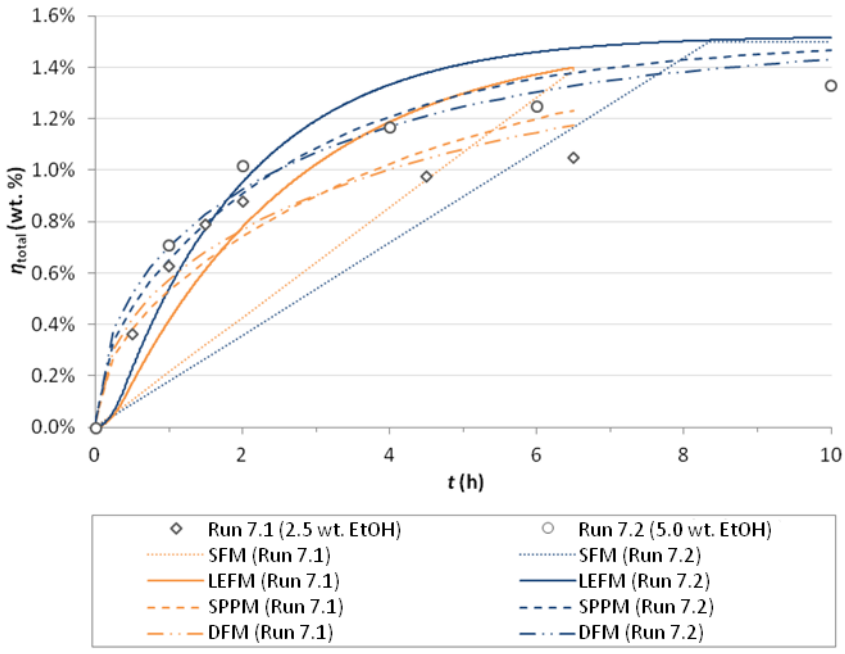

Figure 7.4 – Total extraction yield of *E. globulus* bark against time for 200 bar, 40 °C, 12 $g_{CO_2} min^{-1}$, and two ethanol (EtOH) concentrations (2.5 and 5.0 wt.%). Lines: modeling results.

As far as pure intraparticle diffusion based models are concerned – namely SSPM and DFM – the results confirmed the greater adequacy of this assumption for the SFE of *E. globulus* bark, in agreement with previous studies [29]. In fact, these expressions provide deviations between 3.7 % and 11.8 %, being the lowest errors attained by the DFM (i.e. for spherical particles) with AARD = 3.7 % and 10.1 %. In this work, the SSPM (slab geometry) is also adopted in the calculations since (milled) bark is a natural biomass without a strict geometry.

In the whole, modeling clearly highlights the major role played by intraparticle diffusion in relation to the solubility/linear equilibrium plus external resistance pair of assumptions. This insight is valuable for a proper selection of the scale-up criterion to be adopted [1, 3] which is discussed in the following.

Table 7.3 – Modeling of the cumulative curves of total extraction yield of *E. globulus* bark (Runs 7.1 and 7.2 of Table 7.2). Results were obtained for the solubility plus film model (SFM), linear equilibrium plus film model (LEFM), Simple Single Plate model (SSPM), and Diffusion model (DFM).

Run	SFM		LEFM			SSPM		DFM	
	k $(\mathrm{g}/(100\,\mathrm{g}_{\mathrm{bark}}.\mathrm{h}))$	AARD (%)	H	$k_{\mathrm{g}}a$ (h^{-1})	AARD (%)	$D_{\mathrm{m}}\delta^{-2}$ (h^{-1})	AARD (%)	$D_{\mathrm{m}}R^{-2}$ (h^{-1})	AARD (%)
7.1	0.002138	49.8	4.472	0.4477	40.3	0.0234	11.8	0.0163	10.1
7.2	0.001798	40.9	2.383	0.3178	29.2	0.0359	6.8	0.0261	3.7

Scale-up Criterion - Before moving to the experiments at higher scales (5.0 and 80.0 L) it is necessary to establish an appropriate scale-up criterion. The well-known criteria are those presented in Section 7.1. The selection of one of these criteria is driven by the mass transfer mechanisms that prevail in the SFE process under study. By holding constant the adequate scale-up parameters it is expected that the transfer of scale will not fail due to a wrong interpretation of the kinetics of the process. However, other factors may also restrict the performance of the scale-up, such as the geometries of extractors, channeling, biomass aggregation, which may become more visible in higher scale operation [7, 10].

Taking into account the greater suitability of the models based on intraparticle diffusion (DFM and SSPM), the appropriate scale-up establishes that the ratio between flow rate and biomass weight is constant. The value of $Q_{\mathrm{CO_2}}\, w_{\mathrm{bark}}^{-1} = 10$ $\mathrm{kg_{CO2}\ h^{-1}\ kg^{-1}_{bark}}$ listed in Table 7.2 arises as consequence of the flow rate optimized in a previous work (12 g $\mathrm{min^{-1}}$) [45], and is adopted in this work for the experiments carried out in the 5.0 L unit (Runs 7.3 and 7.4) and 80.0 L unit (Run 7.5).

7.4.2 SCALE-UP STUDIES AT 200 bar / 40 ºC / 2.5 wt.% ETHANOL

This study involved experiments performed at lab (0.5 L), intermediate (5.0 L) and pilot (80.0 L) scales, which correspond to Runs 7.1, 7.3 and 7.5 of Table 7.2. The curves of total yield and TTAs concentration in the extracts are plotted in Figures 7.5 and 7.6 respectively. Despite the geometric differences between the three units (from Table 7.2: $L_b/D_b = 1.6,$ 6.1 and 4.1), the η_{total} results exhibit a very concordant trend. Slower extraction rates in both higher scale assays are observed, which may be attributed to the associated inferior interstitial velocities inside the higher extractors, as a direct consequence of the higher L_b/D_b ratios of these units. Nonetheless, one can see that after 4 h this splitting essentially disappears since the driving force to mass transfer decreases continuously as extraction proceeds, and because all curves tend to the same maximum yield ($\eta_{total} \rightarrow X_0 = 1.5$ wt.%). It is also worth noting that Run 7.5 evidences a constant period of extraction between 0 and 1 h, as it is pointed out above for the lab scale run.

With reference to the concentration of TTAs in the supercritical extracts (Figure 7.6), the cumulative values measured along time are close and their trends can be considered very similar. A noteworthy aspect concerns the fact that the differences in bed geometries do not affect this response as affect η_{total}, which reveals that the delay in the extraction yields is not accompanied by selectivity changes of the supercritical solvent along time. Within the three runs, the process takes 1 hour to reach a concentration of TTAs above 30 wt.% and then remained in the range of 30 % and 45 %.

Globally these results detach that the scale-up criterion for the SFE of *Eucalyptus globulus* deciduous bark has been properly identified. It is important to highlight that this scale-up is tested with experiments involving a significant jump of 160 (= 80.0 L / 0.5 L) in the extractor volume. In the literature such ratios frequently lie between 10 and 100 [1]. One may cite the works by Yesil-Celiktas et al. [21], Jokic et al. [6], Cretnik et al. [23], Ling et al. [22], etc, who adopted variations of 21, 25, 67, and 100, respectively, in the extractor volume.

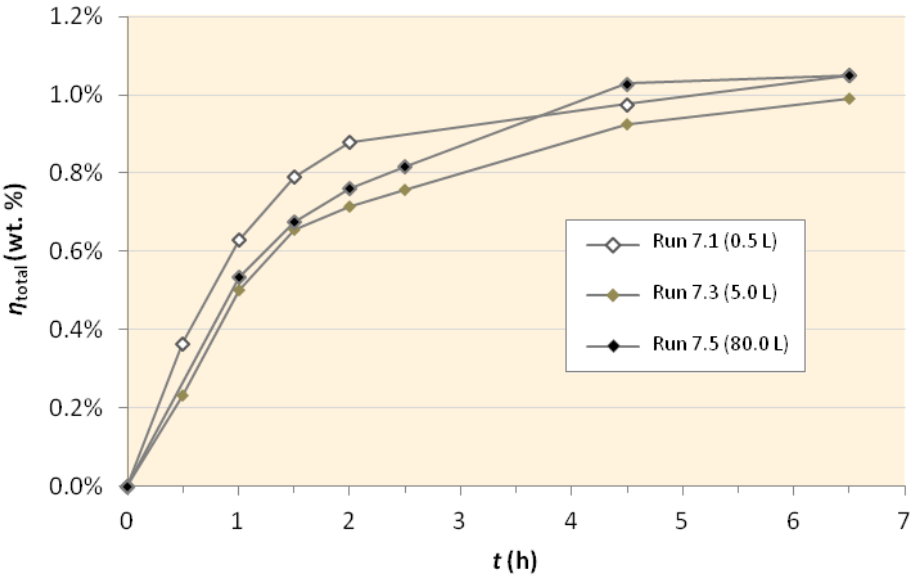

Figure 7.5 – Cumulative curves of total extraction yield of *E. globulus* deciduous bark at lab (0.5 L), intermediate (5.0 L) and pilot (80.0 L) scales. Operating conditions: 200 bar, 40 °C, 2.5 wt.% ethanol and $Q_{CO_2}\ w_{bark}^{-1}$= 10 h^{-1}. (Curves are lines to guide the eyes).

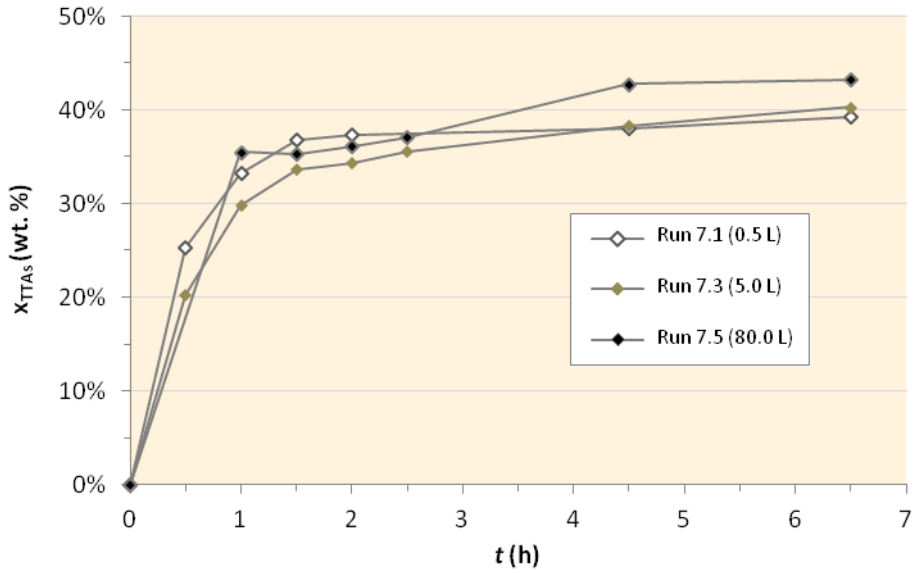

Figure 7.6 – Cumulative concentration of TTAs in the supercritical extracts of *E. globulus* deciduous bark measured at lab (0.5 L), intermediate (5.0 L) and pilot (80.0 L) scales. Operating conditions: 200 bar, 40 °C, 2.5 wt.% ethanol and $Q_{CO_2}\ w_{bark}^{-1}$= 10 h^{-1}. (Curves are lines to guide the eyes).

7.4.3 SCALE-UP STUDIES AT 200 bar/ 40 ºC / 5.0 wt.% ETHANOL

As far as the upscaling of Run 7.2 is concerned, technical limitations related to the amounts of ethanol do not allow a large jump to the pilot scale, i.e. from 0.5 to 5.0 L and then to 80.0 L as in the previous case. Accordingly, the total yield results and the cumulative concentration of TTAs in extracts are plotted in Figures 7.7 and 7.8, respectively, for the lab (Run 7.2; 0.5 L) and intermediate (Run 7.4; 5.0 L) units.

The measured η_{total} values revealed a great resemblance of the two runs during the first hour of extraction, followed by a slight deviation up to ca. 6 h, which may be once again linked to the lower interstitial velocity inside the 5.0 L extractor. In this case, $L_b/D_b = 6.1$ while for the lab equipment it is only 1.6 (see Table 7.2). Besides the great concordance in terms of total extraction yield, the respective cumulative x_{TTAs} curves exhibit a similar behaviour also, with the higher scale assay approaching a stable value around $x_{\text{TTAs}} = 39$ wt.% against 35 wt.% for 0.5 L. In the literature, differences registered at different scales are frequently reported, and most of the times linked to geometric variations of the equipment utilized and to the natural variability of biomass. For instance, the relevant scale-up results published by Yesil-Celiktas et al. on SFE of pine bark [21], who presented total catechin concentrations 31 % higher in the 6.5 L scale at 200 bar/60 °C /3 % ethanol, in relation to the corresponding run at 0.3 L scale.

In an overview of the scale-up experiments of sections 7.4.2 and 7.4.3, one may detach that there is a common feature between them: for $t > 1.5$ h, the purities found at lab scale are essentially constant or increase very slowly (≈39 % in Run 7.1 and 36 % in Run 7.2), while at higher scales they exhibit an increasing profile (from 34 % to 40 % in Run 7.3, 35 % to 43 % in Run 7.5, and 31 % to 39 % in Run 7.4).

While from a scientific and technical perspective positive outcomes are achieved with the increment of the TTAs concentration upon the employment of higher contents of ethanol (i.e., 5.0 wt.% in spite of 2.5 wt.%), direct counterpart consequences at economic level should also be taken into account, because the usage of ethanol makes SFE processes more expensive. On the other hand, if the final commercial interest of this process is an enriched mixture of TTAs, a recent patent focusing the solid-liquid extraction (with organic solvents) and purification of TTAs from *Eucalyptus* bark embodies a rather feasible way to reach final TTAs contents around 98.5 wt.%, independently of the starting point being TTAs mixtures of 30 or 40 wt.% [46]. In this sense, the final word on the most suitable path for the SFE extracts will demand, firstly, an accurate definition of the final application of the product and, secondly, an economic evaluation in which the impact of extraction time and ethanol usage upon total yield and TTAs concentration is adequately scored [47]. Such work is, however, beyond the scope of this article.

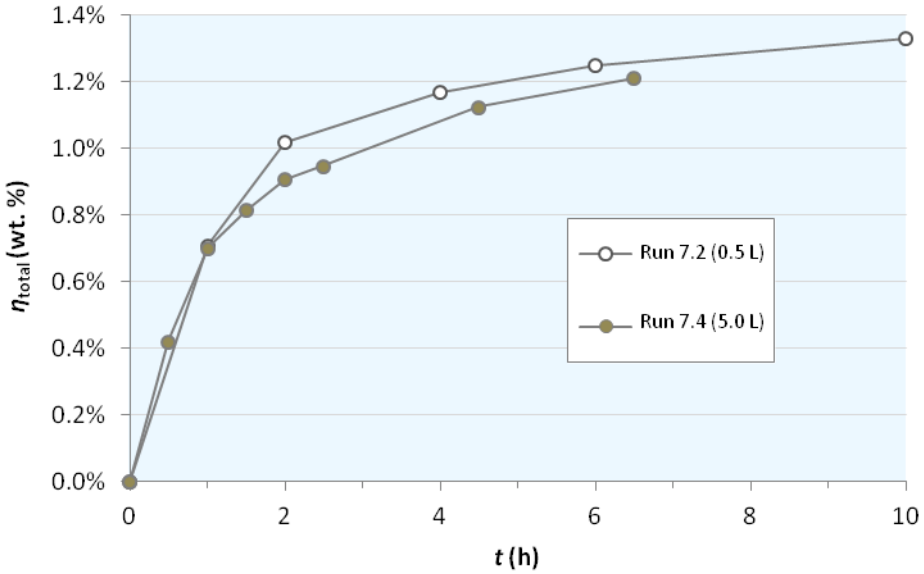

Figure 7.7 – Cumulative curves of total extraction yield of *E. globulus* bark at lab (0.5 L) and intermediate (5.0 L) scales. Operating conditions: 200 bar, 40 °C, 5.0 wt.% ethanol and $Q_{CO_2}\ w_{bark}^{-1}$= 10 h^{-1}. (Curves are lines to guide the eyes).

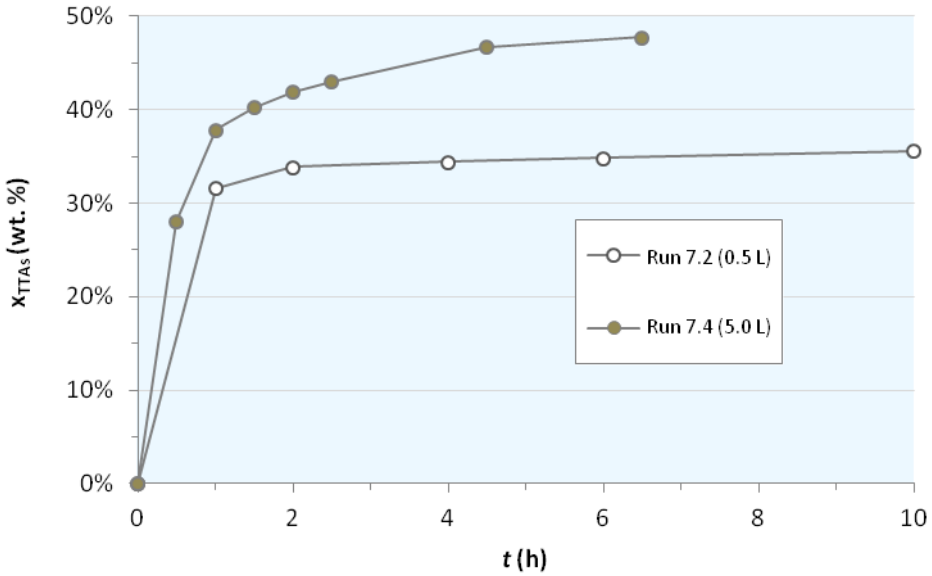

Figure 7.8 – Cumulative concentration of TTAs in the supercritical extracts of *E. globulus* bark measured at lab (0.5 L) and intermediate (5.0 L) scales. Operating conditions: 200 bar, 40 °C, 5.0 wt.% ethanol and $Q_{CO_2}\ w_{bark}^{-1}$= 10 h^{-1}. (Curves are lines to guide the eyes).

7.5 CONCLUSION

In this work scale-up studies of the SFE of *E. globulus* deciduous bark are presented, supported by previous research on the subject, mainly the optimization of the operating conditions, i.e. pressure, temperature, ethanol content, and CO_2 flow rate. The experiments are carried out at three different scales: 0.5, 5.0 and 80.0 L.

The modeling of the measured lab scale extraction curves confirm that the intraparticle diffusion is the most important resistance of the process, since models based on this assumption provide good results, with average deviations between 3.7 % and 11.8 %. The recommended scale-up criterion in such case is the constancy of the ratio between solvent flow rate and biomass weight, which in this case is equal to 10 h^{-1}.

The upscaling studies are performed for two operating conditions, (200 bar, 40 °C, 2.5 wt.% ethanol and 200 bar, 40 °C, 5.0 wt.% ethanol), for which the extraction curves obtained at lab, intermediate and pilot scales evidence good agreement in terms of extraction yield and triterpenic acids concentration in extracts. The differences observed in some periods of the extraction may be explained by the geometric differences of the three extractors. In the whole, these experiments legitimate the validity of the adopted scale-up criterion, and provide valuable evidence to support the technical viability of the SFE for future exploitation at commercial scales.

7.6 REFERENCES

[1] M.M.R. de Melo, A.J.D. Silvestre, C.M. Silva, Supercritical fluid extraction of vegetable matrices: Applications, trends and future perspectives of a convincing green technology, Journal of Supercritical Fluids, 92 (2014) 115-176.

[2] M.M.R. de Melo, R.M.A. Domingues, M. Sova, E. Lack, H. Seidlitz, F. Lang Jr, A.J.D. Silvestre, C.M. Silva, Scale-up studies of the supercritical fluid extraction of triterpenic acids from Eucalyptus globulus bark, The Journal of Supercritical Fluids, 95 (2014) 44-50.

[3] M. Perrut, Supercritical fluid applications: Industrial developments and economic issues, Industrial & Engineering Chemistry Research, 39 (2000) 4531-4535.

[4] N. Mezzomo, J. Martínez, S.R.S. Ferreira, Supercritical fluid extraction of peach (*Prunus persica*) almond oil: Kinetics, mathematical modeling and scale-up, Journal of Supercritical Fluids, 51 (2009) 10-16.

[5] L. Casas, C. Mantell, M. Rodriguez, A. Torres, F.A. Macias, E.J.M. de La Ossa, SFE kinetics of bioactive compounds from *Helianthus annuus* L., Journal of Separation Science, 32 (2009) 1445-1453.

[6] S. Jokic, B. Nagy, Z. Zekovic, S. Vidovic, M. Bilic, D. Velic, B. Simandi, Effects of supercritical CO_2 extraction parameters on soybean oil yield, Food and Bioproducts Processing, 90 (2012) 693-699.

[7] A. Berna, A. Tarrega, M. Blasco, S. Subirats, Supercritical CO_2 extraction of essential oil from orange peel; effect of the height of the bed, Journal of Supercritical Fluids, 18 (2000) 227-237.

[8] M. Perrut, J.Y. Clavier, M. Poletto, E. Reverchon, Mathematical modeling of sunflower seed extraction by supercritical CO_2, Industrial & Engineering Chemistry Research, 36 (1997) 430-435.

[9] R.N. Carvalho Jr, L.S. Moura, P.T.V. Rosa, M.A.A. Meireles, Supercritical fluid extraction from rosemary (*Rosmarinus officinalis*): Kinetic data, extract's global yield, composition, and antioxidant activity, The Journal of Supercritical Fluids, 35 (2005) 197-204.

[10] J.M. del Valle, O. Rivera, M. Mattea, L. Ruetsch, J. Daghero, A. Flores, Supercritical CO_2 processing of pretreated rosehip seeds: effect of process scale on oil extraction kinetics, The Journal of Supercritical Fluids, 31 (2004) 159-174.

[11] P. Kotnik, M. Skerget, Z. Knez, Supercritical fluid extraction of chamomile flower heads: Comparison with conventional extraction, kinetics and scale-up, Journal of Supercritical Fluids, 43 (2007) 192-198.

[12] Y. Lu, B. Zhu, K. Wu, Z. Gou, L. Li, G.G. Chen, L. Cui, N. Liang, Analysis of operation conditions for a pilot-scale supercritical CO_2 extraction of diterpenoid from *Pteris semipinnata* L, Asia-Pacific Journal of Chemical Engineering, 7 (2012) 777-782.

[13] A. Ranalli, S. Contento, L. Lucera, G. Pavone, G. Di Giacomo, L. Aloisio, C. Di Gregorio, A. Mucci, I. Kourtikakis, Characterization of carrot root oil arising from supercritical fluid carbon dioxide extraction, Journal of Agricultural and Food Chemistry, 52 (2004) 4795-4801.

[14] X.J. Han, L.M. Cheng, R. Zhang, J.C. Bi, Extraction of safflower seed oil by supercritical CO_2, Journal of Food Engineering, 92 (2009) 370-376.

[15] M. Fullana, F. Trabelsi, F. Recasens, Use of neural net computing for statistical and kinetic modelling and simulation of supercritical fluid extractors, Chemical Engineering Science, 55 (2000) 79-95.

[16] B. Simandi, A. Sass-Kiss, B. Czukor, A. Deak, A. Prechl, A. Csordas, J. Sawinsky, Pilot-scale extraction and fractional separation of onion oleoresin using supercritical carbon dioxide, Journal of Food Engineering, 46 (2000) 183-188.

[17] C.L.C. Albuquerque, M.A.A. Meireles, Defatting of annatto seeds using supercritical carbon dioxide as a pretreatment for the production of bixin: Experimental, modeling and economic evaluation of the process, Journal of Supercritical Fluids, 66 (2012) 86-95.

[18] T. Hatami, M.A.A. Meireles, G. Zahedi, Mathematical modeling and genetic algorithm optimization of clove oil extraction with supercritical carbon dioxide, The Journal of Supercritical Fluids, 51 (2010) 331-338.

[19] L. Casas, C. Mantell, M. Rodriguez, A. Torres, F.A. Macias, E.J.M. de la Ossa, Supercritical fluid extraction of bioactive compounds from sunflower leaves with carbon dioxide and water on a pilot plant scale, Journal of Supercritical Fluids, 45 (2008) 37-42.

[20] T. Fornari, A. Ruiz-Rodriguez, G. Vicente, E. Vazquez, M.R. Garcia-Risco, G. Reglero, Kinetic study of the supercritical CO_2 extraction of different plants from Lamiaceae family, Journal of Supercritical Fluids, 64 (2012) 1-8.

[21] O. Yesil-Celiktas, F. Otto, S. Gruener, H. Parlar, Determination of extractability of pine bark using supercritical CO_2 extraction and different solvents: optimization and prediction, Journal of Agricultural and Food Chemistry, 57 (2009) 341-347.

[22] J.Y. Ling, G.Y. Zhang, Z.J. Cui, C.K. Zhang, Supercritical fluid extraction of quinolizidine alkaloids from *Sophora flavescens* Ait. and purification by high-speed counter-current chromatography, Journal of Chromatography A, 1145 (2007) 123-127.

[23] L. Čretnik, M. Škerget, Ž. Knez, Separation of parthenolide from feverfew: performance of conventional and high-pressure extraction techniques, Separation and Purification Technology, 41 (2005) 13-20.

[24] S.S. Petrovic, J. Ivanovic, S. Milovanovic, I. Zizovic, Comparative analyses of the diffusion coefficients from thyme for different extraction processes, Journal of the Serbian Chemical Society, 77 (2012) 799-813.

[25] B. Simandi, V. Hajdu, K. Peredi, B. Czukor, A. Nobik-Kovacs, A. Kery, Antioxidant activity of pilot-plant alcoholic and supercritical carbon dioxide extracts of thyme, European Journal of Lipid Science and Technology, 103 (2001) 355-358.

[26] M. Eisenmenger, N.T. Dunford, F. Eller, S. Taylor, J. Martinez, Pilot-scale supercritical carbon dioxide extraction and fractionation of wheat germ oil, Journal of the American Oil Chemists Society, 83 (2006) 863-868.

[27] X.L. Cao, Y.C. Ito, Supercritical fluid extraction of grape seed oil and subsequent separation of free fatty acids by high-speed counter-current chromatography, Journal of Chromatography A, 1021 (2003) 117-124.

[28] J.M. Prado, I. Dalmolin, N.D.D. Carareto, R.C. Basso, A.J.A. Meirelles, J.V. Oliveira, E.A.C. Batista, M.A.A. Meireles, Supercritical fluid extraction of grape seed: Process scale-up, extract chemical composition and economic evaluation, Journal of Food Engineering, 109 (2012) 249-257.

[29] R.M.A. Domingues, M.M.R. de Melo, C.P. Neto, A.J.D. Silvestre, C.M. Silva, Measurement and modeling of supercritical fluid extraction curves of *Eucalyptus globulus* bark: Influence of the operating conditions upon yields and extract composition, Journal of Supercritical Fluids, 72 (2012) 176-185.

[30] M.M.R. de Melo, E.L.G. Oliveira, A.J.D. Silvestre, C.M. Silva, Supercritical fluid extraction of triterpenic acids from *Eucalyptus globulus* bark, Journal of Supercritical Fluids, 70 (2012) 137-145.

[31] R.M.A. Domingues, M.M.R. de Melo, E.L.G. Oliveira, C.P. Neto, A.J.D. Silvestre, C.M. Silva, Optimization of the supercritical fluid extraction of triterpenic acids from

Eucalyptus globulus bark using experimental design, Journal of Supercritical Fluids, 74 (2013) 105-114.

[32] Natex, Extraction Plants, Accessed in 2014, www.natex.at, in.

[33] G. Brunner, Mass transfer from solid material in gas extraction, Berichte der Bunsengesellschaft für physikalische Chemie, 88 (1984) 887-891.

[34] M.J. Cocero, J. García, Mathematical model of supercritical extraction applied to oil seed extraction by CO2+saturated alcohol — I. Desorption model, The Journal of Supercritical Fluids, 20 (2001) 229-243.

[35] J. Crank, The Mathematics of Diffusion, 2 ed., Clarendon Press, Oxford, England, 1975.

[36] F. Gaspar, T. Lu, R. Santos, B. Al-Duri, Modelling the extraction of essential oils with compressed carbon dioxide, Journal of Supercritical Fluids, 25 (2003) 247-260.

[37] R.M.A. Domingues, D.J.S. Patinha, G.D.A. Sousa, J.J. Villaverde, C.M. Silva, C.S.R. Freire, A.J.D. Silvestre, C. Pascoal Neto, *Eucalyptus* biomass residues from agro-forest and pulping industries as sources of high-value triterpenic compounds, Cellulose Chemistry and Technology, 45 (2011) 475-481.

[38] R.M.A. Domingues, E.L.G. Oliveira, C.S.R. Freire, R.M. Couto, P.C. Simões, C.P. Neto, A.J.D. Silvestre, C.M. Silva, Supercritical fluid extraction of *Eucalyptus globulus* bark – a promising approach for triterpenoids production, International Journal of Molecular Sciences, *13(6),* (2012) *7648-7662*.

[39] M.M.R. de Melo, R.M.A. Domingues, A.J.D. Silvestre, C.M. Silva, Extraction and purification of triterpenoids using supercritical fluids: From lab to exploitation, Mini-Reviews in Organic Chemistry, 11 (2014) 362-381.

[40] C.P. Passos, M.A. Coimbra, F.A. Da Silva, C.M. Silva, Modelling the supercritical fluid extraction of edible oils and analysis of the effect of enzymatic pre-treatments of seed upon model parameters, Chemical Engineering Research and Design, 89 (2011) 1118-1125.

[41] H. Sovová, Mathematical model for supercritical fluid extraction of natural products and extraction curve evaluation, Journal of Supercritical Fluids, 33 (2005) 35-52.

[42] C.M. Silva, C.P. Passos, M.A. Coimbra, F.A. Da Silva, Numerical simulation ofsupercritical extraction processes, Chemical Product and Process Modeling 4, Article 9, 2009.

[43] L. Fiori, D. Basso, P. Costa, Supercritical extraction kinetics of seed oil: A new model bridging the 'broken and intact cells' and the 'shrinking-core' models, Journal of Supercritical Fluids, 48 (2009) 131-138.

[44] H. Sovová, R.P. Stateva, Supercritical fluid extraction from vegetable materials, Reviews in Chemical Engineering, 27 (2011) 79-156.

[45] F. Esmaeilzadeh, H. As'adi, M. Lashkarbolooki, Calculation of the solid solubilities in supercritical carbon dioxide using a new G^{ex} mixing rule, The Journal of Supercritical Fluids, 51 (2009) 148-158.

[46] R.M.A. Domingues, C.S.R. Freire, A.J.D. Silvestre, C.P. Neto, C.M. Silva, Method for obtaining an extract rich in triterpenic acids from *Eucalyptus* barks, PAT 106278, 2012,

[47] M.M.R. de Melo, A.J.D. Silvestre, C.M. Silva, Supercritical fluid extraction of oil and bioactive compounds from grape residues: experimental optimization, modeling and economic evaluation, in: J.S. Câmara (Ed.) Grapes: Production, Phenolic Composition and Potential Biomedical Effects, Nova Publisher, 2014.

8 TECHNO-ECONOMIC ANALYSIS

This chapter is devoted to the economic analysis of SFE based on a comprehensive review from 2000 to 2013 [1], and to present integrally four studies on the subject focusing the SFE of Moringa seed [2], spent coffee grounds [3], tomato residues [4], and gac fruit [5].

CHAPTER OUTLINE

8.1 INTRODUCTION

Despite its ultimate position within the necessary research background that confirms the technical potential of a specific SFE process and encourages further advances towards commercial application, economic assessment results provide valuable insights even at earlier stages of research, when decisions regarding operating conditions, matrix pretreatments and/or cosolvent addition can be pondered and dealt in time. However, owing to the fact that economic assessments easily reflect inadequate decisions based on previous optimization, modeling and scale-up, one should aim to have a reliable knowledge of the process when performing this type of studies. For instance, the capital cost of a SFE process is not linear with pressure, as some equipment components are available in discrete steps [6], and for this reason misleading conclusions upon economic viability can be taken. In addition, from the point of view of incomes, the scale of production can influence the market prices from the side of an excessive offer leading to saturation and decline of profits.

With regard to the types of operation scheme, it has been shown that continuous operation is the one that generally minimizes the total costs, but the difference to batch extraction is not significant enough to justify the continuous approach, at least for large-scale operation [7]. The main reason is the larger amount of energy needed to introduce and remove the biomass at separate locations necessary in continuous operation, in comparison to the time-sequenced operation steps in a conventional batch system [7]. For this reason most of the commercial units that inspire new economic studies comprise semi-continuous operation, reliant on a succession of batches.

A very pertinent question for a proper economic evaluation relies on the main objective of the SFE process, namely if it is of low volume / high value type or high volume / low value scenario. This issue is connected to the aspects discussed in Section 3. In fact, the motivation of the work should be clear at economic level, so that the real product can be undoubtedly identified: whether valuable compounds diluted/mixed in oils/extracts, or ordinary bulk extracts/oils with no other features than the fact of being natural mixtures obtained by a green separation technology. In the first case, the solutes concentration may be the key variable to the viability of the process while, in the second, the success may be reliant on the capacity to obtain high extraction yields in short times.

Most of the economic assessment studies on SFE address cases where bulk extracts/oils are the goal of the process. In this sense, low attention has been paid to the impact of the concentrations/purities of the final extracts. Such fact is somehow misleading because much of the research of last years has been centered on the enhancement of specific bioactive molecules in SC-CO_2 extracts. For instance, the enrichment of extracts/oils is the most invoked reason to justify the frequent usage of cosolvents. The inclusion of modifiers can only be judged if, at the

end of the process, the final product is priced taking into account its eventual enriched composition. The purpose of the SFE technology is not merely to make possible more productive separations in comparison to other reference methods, but also to produce extracts/oils with precious enrichments on fractions comprising interesting compounds. In this sense, the field demands a more properly scoring of the added-value provided by the SFE technology in relation to bulk essential oils, because the economics of the process should reflect two specificities of this technology: 1) lower extraction yields may exhibit interesting selectivity gains as counterpart; 2) both composition and extraction yield vary with time and upon modifications in other operating conditions. As a result, economic viability can be seen as an optimized trade-off between the concomitant variations of yield and concentration, from the income side, and the investment and operation expenditures, from the fixed and variable costs, respectively.

In order to emphasize the significant differences of approaching SFE to maximize extraction yields or to produce extracts enriched in target molecules, the following figures should be analysed: Figure 8.1 shows market quotations of essential oils (obtained by steam distillation), and Figure 8.2 illustrates the market prices of target molecules of some SFE works from Table S1 (recall Chapter 2), when sold with high purities (>70 %). It is worth noting that these prices were not obtained for bulky purchasing and certainly exhibit deviations from industrial trade reality. Nevertheless, the reported data were obtained from few suppliers, which means that all values are on the same comparison basis, namely European market.

As can be observed, the majority of the essential oils reported in Figure 8.1 have quotations between 25 and 150 € kg^{-1}. The most expensive examples were found for chamomile, vetiver and black peper, with prices varying from 288 to 454 € kg^{-1}. These values arise from an already existing market whose oils are produced by technologies like steam distillation or hydrodistillation. The green label of both SFE and water-based separations suggests that these quotations are also suitable for economic analysis of SFE processes. Nonetheless this equivalence neglects the real value of the enriched extracts that supercritical solvents may obtain. For this reason, one could expect a worthier quotation for the SFE oils when they exhibit enhanced concentrations of target compounds. For instance, Barbosa et al. [8] showed that the content of anticarcinogenic diterpenoids (cafestol, kawheol, and 16-*O*-methylcafestol) in the oil obtained by SC-CO_2 extraction of spent coffee grounds more than trebles that of the oil produced by solid-liquid extraction using dichloromethane. Such selectivity gain should be taken into account so that the SFE is fairly pondered at economic level.

Another clearcut example of the necessity to bring reasonable prices to the economic assessment of supercritical separations is provided by eucalypt, in the sense it has the lowest prices among those reported in Figure 8.1 (23 € kg^{-1}). However, from the outer bark of

eucalypt, one can obtain extracts with concentrations of ursolic and betulinic acids as high as 27 % (wt) [9-12]. Upon checking the valuable prices of both molecules in high purity supply contexts (values higher than 6×10^5 € kg^{-1} – see Figure 8.2), a more consistent price should be associated to such product. These remarks on extracts/oils prices are of vital importance for the viability of SFE projects, and though literature has no other solutions than to adopt essential oil quotations, these simplistic comparisons are many times misleading in view of the superior quality of some products achieved with supercritical solvents.

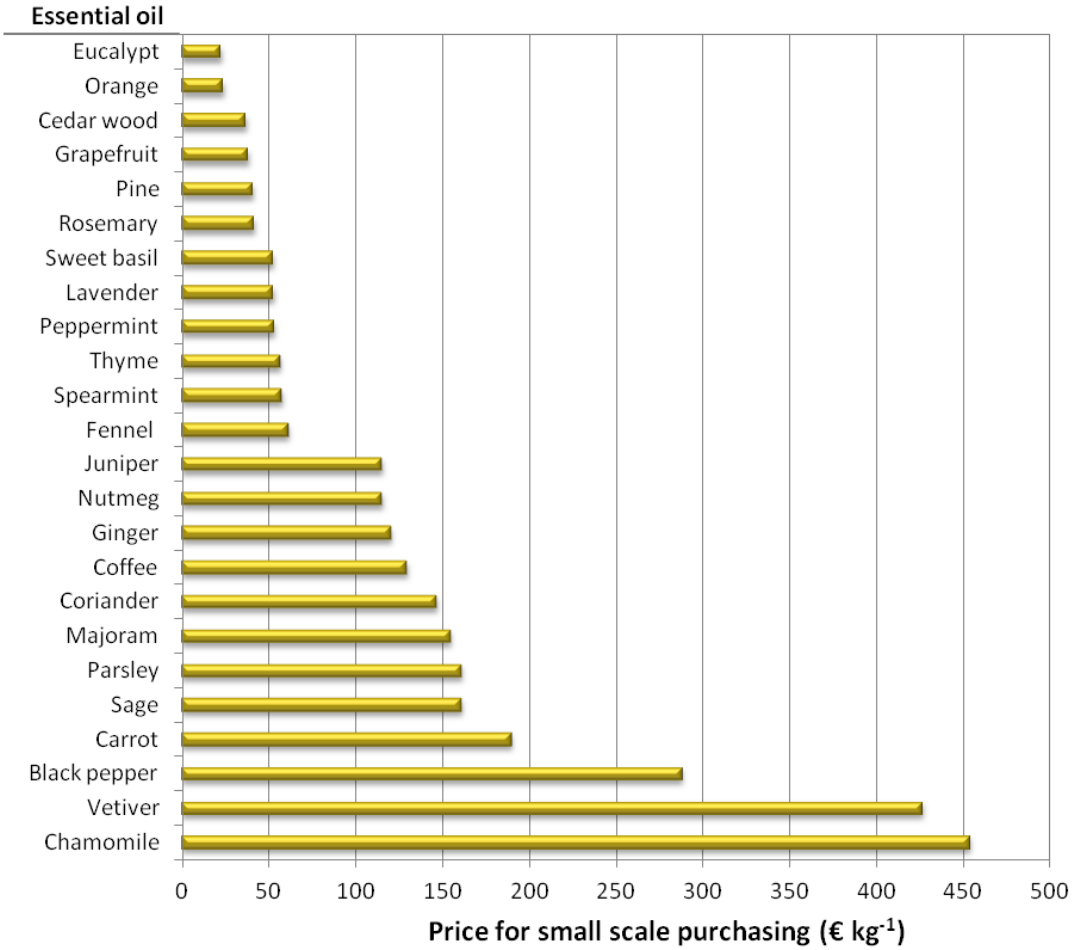

Figure 8.1 – Commercial quotations (for small scale purchasing) of some essential oils. Data taken from one European supplier [13], with exception of coffee oil [14].

When the overall purpose of the SFE process is to enhance the profitability of an already existing process by means of using raw material spare parts or by including a SFE step to concentrate in the final product (or remove from it) a minor constituent, the process economics may benefit from the availability of raw materials, utilities and labor resources. Such industrial context can be sufficient to ensure viability, as raw material purchasing and transport costs can be eliminated from the calculations. For instance, Leal *et al.* [15] concluded that the cost of raw material of the SFE of sweet basil (*Ocimum basilicum*) represented 80 % of the process costs, prevailing over energy or utility costs. One example of a SFE research that has been studied in

complementation to a main industrial process is the extraction of *Eucalyptus globulus* bark, which is the dominant species in Portuguese pulp and paper industry. In this context, the SFE of triterpenic acids from *E. globulus* bark can take advantage from the readiness of raw material and the existence of utilities in the mill, two important synergies to enhance the process economics.

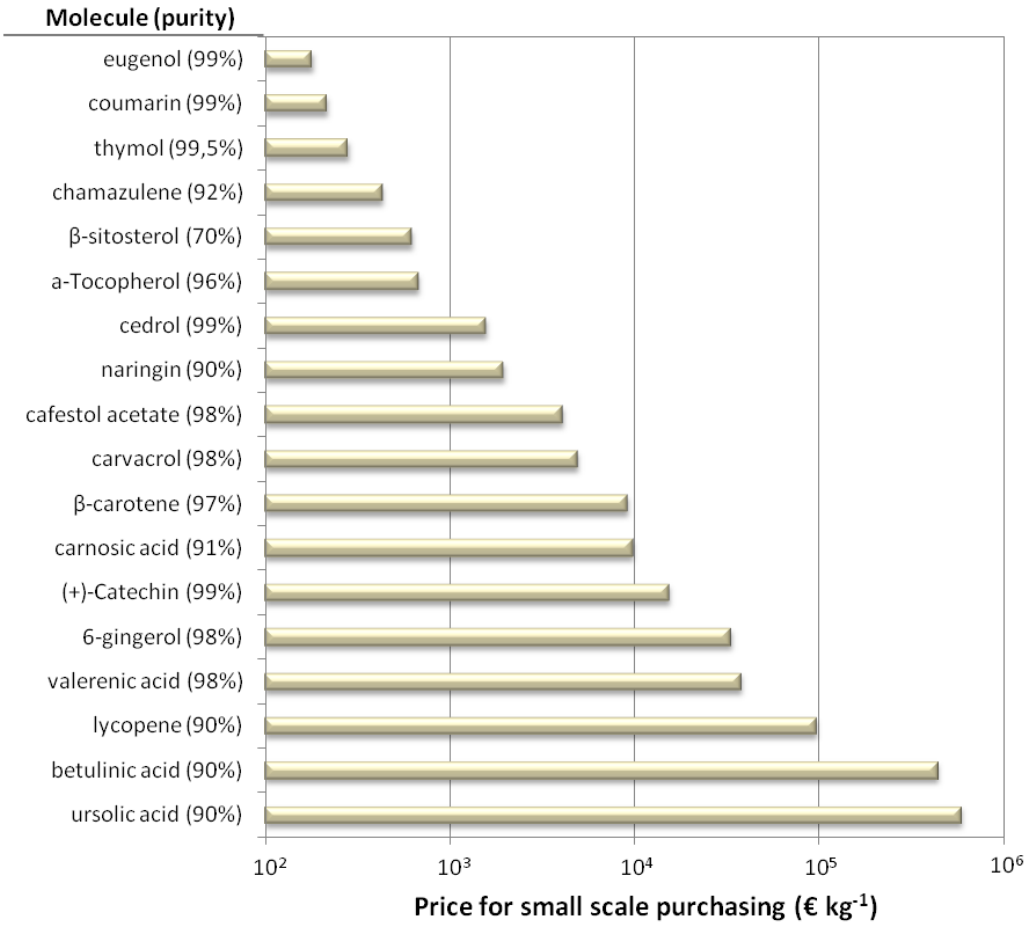

Figure 8.2 – Commercial quotations (for small scale purchasing) of some of SFE target compounds. Data were taken from one European supplier [16] and are presented in logarithmic scale.

When considering fixed costs, labor parcel is a non-negligible variable due to the semi-continuous character of SFE processes and the resulting need to periodically handle raw-material at the onset and end of each extraction cycle. This variable communicates intimately with the duration of extraction, since the shorter the extraction cycles are, the greater the human handling needs become. In addition, the duration of extraction cycles has a chief influence on productivity and therefore on economic viability, since it is advisable to work during the constant extraction rate (CER) period (recall the figure in Table 6.4), which implies to replace the (almost) exhausted biomass inside extractor by a virgin one in spite of keeping the process running on the falling extraction rate (FER –see Table 6.4) period. These

considerations require semi-continuous operation involving arrangements of several beds in series or in parallel [3, 17-21].

At industrial level, the time needed to unload, reload and pressurize an extractor may not be negligible if dealing with processes involving low extraction times. Melo et al [3] addressed this issue in detail, by performing an economic study of SFE of spent coffee (*Coffea* spp.) grounds. This is a key factor that shall be correctly tackled to boost the productivity and profitability of SFE units.

With respect to the SC-CO_2 modification with organic solvents, it is frequently exploited without the full acknowledgement of the economic impact this option may represents. The inclusion of cosolvents may influence licensing, since then SFE plants lose their innocuous character upon explosion, fire and pollution hazards that pure CO_2 ensures. On the other hand, the employment of cosolvents brings an additional source of raw material costs, and requires extra equipment to be purchased, such as a liquid pumps, independent tubing lines, and units for their subsequent recovery/purification. In view of the semi-continuous nature of SFE processes, the choice of plant layouts is also a relevant matter. Assessments typically consider layouts with 2-3 beds in parallel or series. The final decision should reflect a deal between investment costs, cycle duration, labor costs and profitability [3, 17-21]. Economic analyses provide key answers to this issue.

Most research found in literature regarding the economics of SFE process relies on the methodology of Turton *et al.* [22] which sets the cost of manufacturing (COM) as a function of investment cost (FCI), labor cost (COL), utility cost (CUT), waste treatment cost (CWT) and raw material cost (CRM), using the following relation:

$$\mathrm{COM} = 0.304\,\mathrm{FCI} + 2.73\mathrm{COL} + 1.23(\mathrm{CUT} + \mathrm{CWT} + \mathrm{CRM}) \quad (1)$$

Since total investment is usually expressed upon an annual depreciation rate (e.g. 10 % per year), FCI is time-dependent and demands an analogous correspondence on the other terms of Eq. (1). In this way, the resulting COM value will then represent the sum of fixed and variable costs on a yearly basis.

Once COM value itself has no connection with production, many times it is combined with annual production to determine the specific production cost (US$ per mass of product). By stipulating a market value for the supercritical extract, net income calculations can be accomplished and lead to a fuller disclosure regarding the economy of the process:

$$\text{Annual Net Income} = \text{Annual Revenue} - \mathrm{COM} \quad (2)$$

The determination of both annual revenue and COM terms require that a simulation of the production is performed with all the optimized operating conditions (*P, T, t, Q)* and other variables and parameters, some of them established by the researcher. In Table 8.1 these input data are listed for analysis.

Table 8.1 – List of assumptions necessary for an economic assessment of a SFE process.

General	1. Unit working period (h per day and h per year); 2. Number of workers *per* unit extractor; 3. Scale-up criterion; 4. Minimum pressure in the separator (extract collection vessel); 5. Required time to unload, load and pressurize one extractor; 6. Definition whether CO_2 is lots in each full decompression or not; 7.Bed density; 8. Bed porosity; 9 Market price of SFE extract; 10. Matrix initial moisture; 11. Dried matrix heat capacity;
FCI	12. Annual depreciation rate; 13. SFE unit price;
COL	14. Labor cost;
CUT	15. Electricity cost; 16. Steam cost;
CWT	17. Waste treatment cost;
CRM	18. Matrix drying cost; 19. Matrix milling cost; 20. Other matrix pretreatment cost; 21. Make-up CO_2 purchasing price.

A key variable is the price of the SFE unit, whose impact on the process economics is substantial. Some useful rules and information can be used, such as the formula proposed by Lack et al. [23], for units comprising three extractors operating up to 550 bar, that sets FCI as function of extractors volume ($V_{\text{extractor}}$):

$$\text{FCI} = 1.0162 \ln(V_{\text{extractor}}) - 4.9147 \quad (3)$$

where $V_{\text{extractor}}$ is the total extraction volume, in L, and FCI is given in million euros.

In alternative, the expression from Peters and Timmerhaus [24] allows FCI to be estimated from the already known cost of another unit, as long as the annually processed raw material (w), whatever it might be, is compensated:

$$\mathrm{FCI}_2 = \mathrm{FCI}_1 \left(\frac{w_2}{w_1}\right)^{0.6} \tag{4}$$

A similar but more accurate expression was proposed by Perrut [25], who replaced w by the pair $V_{extractor}$ and Q, and corrected the exponent:

$$\mathrm{FCI}_2 = \mathrm{FCI}_1 \left(\frac{V_{\mathrm{extractor}_1} Q_2}{V_{\mathrm{extractor}_2} Q_1}\right)^{0.24} \tag{5}$$

Attending to recent literature works, prices of SFE units have been estimated as 1.2-2 M$ (US) for 2×0.5 m^3 extractors [26] or 2 M$ (US) for units comprising 2×0.4 m^3 extractors and also a flash tank, CO_2 reservoir, condenser, one pump, and a heat exchanger [17].

In what concerns CUT, CWT and CRM it is necessary to perform simulations to solve the mass and energy balances for the operating conditions of the SFE unit under analysis. The choices of SuperPro Design® [17, 27-28] and Aspen Plus® [3, 29] may be cited as the most popular simulators that can be adopted for this purpose.

Studies on the economics of SFE processes have been addressed in literature by several authors in the last years. Some examples are presented in the following for illustration. Working on SFE of sweet basil (*Ocimum basilicum*), Leal et al. [15] used COM methodology to cross the concomitant impact of different pressures and cosolvent (water) contents on the costs of manufacturing. They showed the minimum costs to be nearly 48 US$ $kg^{-1}_{product}$ for operation at 300 bar and 20 % water addition, and that the highest COM values to be for 300 bar operation and 1% water addition, 1049 $\mathrm{US\$\,kg^{-1}_{product}}$. Danielski et al. [30] carried out an economic analysis on their SFE work with rice (*Oryza sativa* L.) bran (by-product of rice processing) followed by a stage of oil deacidification. They showed the production costs of the combined unit were competitive when contrasted with the commercial prices of rice bran oil. Pereira and Meireles [18] performed an economic analysis on their SFE work with rosemary (*Rosmarinus officinalis*), fennel (*Foeniculum vulgare*) and anise (*Pimpinella anisum*) essential oils. They adopted COM methodology and focused specifically cost estimation rather than profitability. Figure 8.3 presents the main results of their essay. Applying the COM approach to the extraction of essential oils by steam distillation from the same matrices, Pereira and Meireles proved SFE to lead to COM values 1.8-2.5 times inferior.

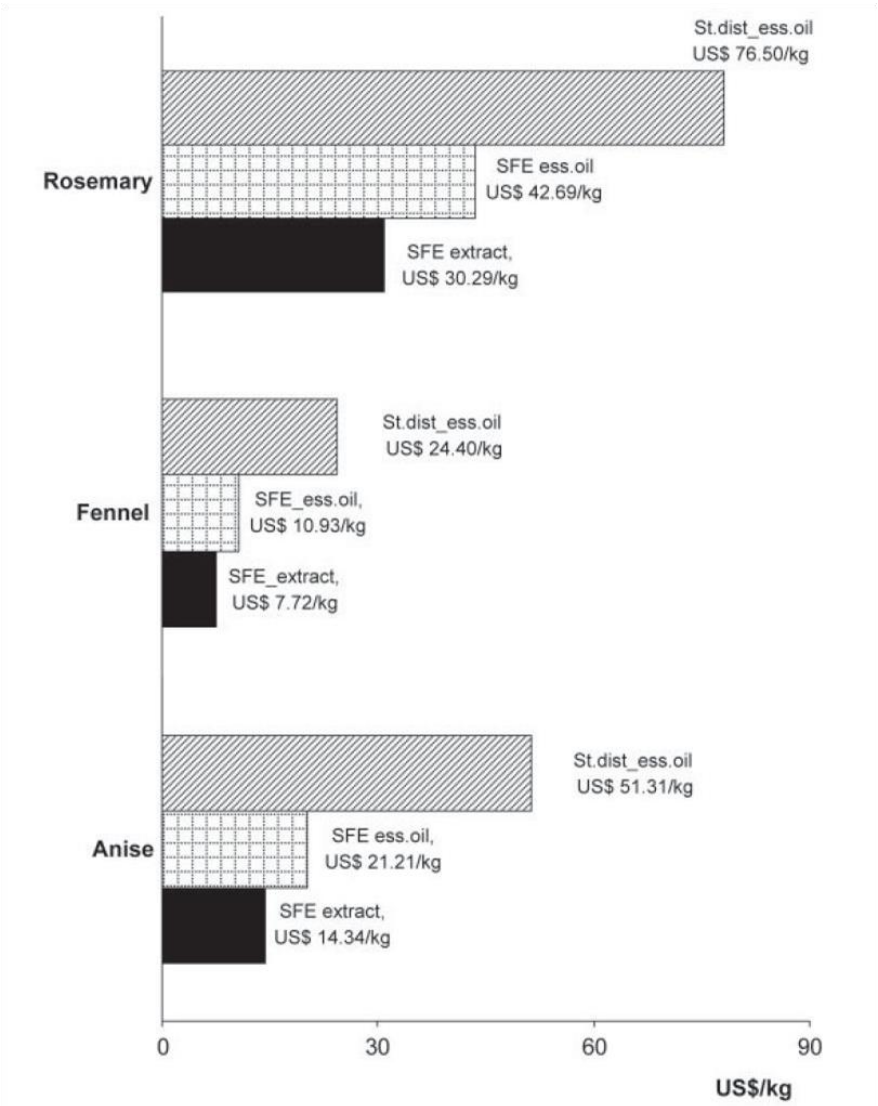

Figure 8.3 – Comparison of COM values for the extraction of rosemary, fennel, and anise extracts. Bars represent extract and essential oil obtained by SFE, and essential oil obtained by steam distillation [18].

* * *

In the following sections, four different studies are presented and discussed on the topic of techno-economics of SFE of vegetal biomass samples. These are:

- SFE of moringa seeds (Study I);
- SFE of spent coffee grounds (Study II);
- SFE of tomato residues (Study III);
- SFE of gac fruit (Study IV).

In the case of Study II, the experimental work (extraction and characterization) was accomplished in this work altogether with the techno-economic analysis. For the others, data

were retrieved from the literature. Moreover, for the case of Study III, theoretical calculations on solubility of the target compound (lycopene) were accomplished to support discussion.
Finally, despite sharing the same context (biorefinery) and extraction technology (SFE), each of the four studies present their own specificities, not only in terms of the expectable production scales, but also regarding pretreatments and posttreatments that might suit or enhance the objectives of the respective processes.

8.2 METHODS

8.2.1 STUDY I – SFE OF MORINGA SEEDS [2]

Oil solubility estimation - In order to better understand the physical and economical characteristics of a SFE process, the rate-controlling step must be identified. The latter can range from solubility limitations to film resistance or even to internal diffusion resistance. When dealing with vegetable oils present in high concentrations inside solid matrices, the oil solubility in the sub/supercritical medium is the typical governing factor behind the rates at which the process takes place. For this reason its measurement or estimation can provide useful information about the kinetics of the extraction [31].

Zhao et al. [32] measured the solubility of *Moringa oleifera* oil at 200-500 bar and 60-100 °C. The experimental data obtained were adjusted by the Peng-Robinson equation of state and three density based expressions (Chrastil [33], del Valle and Aguilera [34], and Adachi and Lu [35]). Among these four options, the Chrastil equation modified by del Valle and Aguilera was the one that best fitted the experimental data. Therefore, the estimation of moringa oil solubility in $SC-CO_2$ within the operating conditions studied in this work was accomplished using del Valle and Aguilera modification, as follows:

$$y_i^* = \rho_f^{k_1} \exp\left(\frac{c}{T^2} + \frac{a}{T} + b\right) \quad (6)$$

where y_i^*(kg m^{-3}) is the extract solubility, ρ_f (kg m^{-3}) is the solvent density, T is the absolute temperature, k_1 is the association number, and the constants a, b and c are related to the thermal effects involved in the solubilization process. The model parameters were adjusted to experimental data and the respective values are $k_1 = 7.22$, $a = -2.3\times10^4$K, $b = 3.31\times10^6$ and $c = -8.17$ K^2.

Supercritical fluid extraction - The SFE experiments considered for this study are based on pilot scale data published by Ruttarattanamongkol et al. [36]. These authors investigated the process of extraction using carbon dioxide as a solvent under near-critical and supercritical conditions in the pressure ranges from 150 to 350 bar, and the temperature ranges from 25 to

35 °C at the fixed flow rate of 20 $\mathrm{kg\,h^{-1}}$. A brief description of the extraction curves attained by these researchers in their work is furnished in Section 8.3.1.

Response Surface Methodology (RSM) - In relation to the optimization of variables from a process towards a desired response, RSM is a statistical method that discloses the several relations, either direct or crossed, between the process independent variables and the response obtained, i.e. the dependent variable. This method also unveils which parameters are in fact statistically significant, allowing thus the neglecting of the non-significant ones. At the end, the model obtained translates a relation of the significant contributions with the final response, allowing therefore an optimum region to be identified. This technique has been widely applied in SFE of vegetable matrices, such as grapes [37], spent coffee [8], eucalypt [11], etc. Nonetheless, RSM is typically used to optimize productivity responses such as extraction yield, rather than being used to enhance the economic performance of a SFE process. That is the purpose of RSM-COM hybrid approach [4] which was adopted for the present study.

In terms of selection of process factors for the optimization, previous SFE data of moringa seed were taken into account [36], where it was shown that the influence of temperature (T) is much less significant than the effect of pressure(P) and extraction time (t) over the studied ranges of experimental conditions. For that reason, the optimization study was performed at fixed T in order to unveil the best (P, t) conditions that minimize COM of the moringa oil ($\mathrm{COM_{oil}}$). In this work, the experimental design adopted uses 2 factors and a mix of 3 and 4 levels of correspondence, totalizing 12 experimental points. Pressure was studied at 150, 250 and 350 bar, whereas extraction time spanned four levels, these being 1.3, 2.0, 2.7 and 3.4 h. In Table 8.2 the summary of the design of experiments adopted is presented, including the codification of the independent variables.

Table 8.2 – Codifications and levels of correspondence of the variables used in the optimization study.

Factor	Variable	Codified variable	Level of correspondence				
			-1	-0.33	0	0.33	1
pressure (bar)	P	$X_\mathrm{P} = (P - 250)/100$	150	-	250	-	350
extraction time (h)	t	$X_\mathrm{t} = (t - 2.35)/1.05$	1.3	2.0	-	2.7	3.4

In order to obtain the contributions of the linear, pure quadratic and crossed effects of the process parameters selected above, the following polynomial relation was adopted:

$$\mathrm{COM} = \beta_0 + \beta_1 \times \mathrm{X_P} + \beta_2 \mathrm{X_P^2} + \beta_3 \times \mathrm{X_P} \times \mathrm{X_t} + \beta_4 \times \mathrm{X_t} + \beta_5 \times \mathrm{X_t^2} \qquad (7)$$

where the β coefficients are the model parameters from which the influence of the various effects is pondered and ranked. In the particular case of this work, COM studies were applied to the production of oil ($\mathtt{COM}_{\mathtt{oil}}$) and sterols mixture ($\mathtt{COM}_{\mathtt{sterols}}$).

For the statistical treatment of the experimental results, JMP® software (version 8.0) was used. *t*-tests were performed in order to judge the individual significance of the estimated coefficients of the model. Finally, the goodness of the fit was assessed from the values of the coefficient of determination and its adjusted version (R^2 and R^2_{adj}, respectively).

Economic analysis - The overall process considered in this work encompasses a total of three stages: a pretreatment step comprising milling and drying units, the SFE extraction unit, and a purification unit, with the following features:

(i) The milling is accomplished in a hammer mill for crushing the seeds, which is able to reduce the average particle size down to 5-47 μm. The nominal power of the unit is 145 kW, and an estimated price is 230 k€. The drying unit consists of one belt drying system and is devoted to the reduction of the moisture content from a natural moisture value of 12.34 % [38] to 5.88 % [36], where steam and electricity are the necessary utilities for this purpose. The predicted investment needed for such solution can be as high as 0.35 M€ [5], which makes the drying stage to demand an investment that amounts 11.5 % of the one required for the SFE stage.

(ii) The SFE unit consists of two extraction vessels of 1 m^3 capacity each (the size was chosen in accordance with the typical availability of the biomass), one CO_2 storage tank, one pump, a heat exchanger, a condenser, a set of valves, and a separator. Being the key stage of the process, the whole unit demands an investment of 3.05 M€, which accounts for 82.8 % of the investment;

(iii) The purification unit consists of a distillation column to be operated under vacuum and sized in accordance with the oil production capacity of the SFE unit. The investment cost (FCI) for the fractionation column was estimated by the method proposed by *Turton et al.* [22], which considers the cost of equipment as a function of the operating pressure, materials of construction and geometrical characteristics of the unit. Accordingly, the investment cost for the purification unit amounts only 0.3 % of that required for the SFE stage.

Regarding the operation of the SFE unit, a ratio of one employee per extractor was adopted, as well as 24 hours operation per day, during 330 days per year. Furthermore, it was considered that only one extraction cycle takes place at a given time, implying that while one extractor is running the remaining extractor is being prepared (it is assumed the time needed to unload, load and pressurize one extractor is 1 h). Since two extraction cycles do not occur simultaneously, the extractor in preparation must always wait for the end of the ongoing cycle

in order to start. Regarding the separation/collecting vessel, a minimum pressure of 45 bar was admitted, and a temperature of 40 °C was chosen in accordance to the reference study considered [36]. The costs of utility consumption were obtained from Aspen Plus® 7.3 simulations of the SFE process, as presented in Figure 8.4.

Beyond the cost of manufacturing, the overall net income should also be considered for a more complete assessment of the economic performance of the integrated unit, since the revenues of the process may (or may not) compensate higher costs of production and/or oscillations in production volumes. Regarding the pricings of the oil and sterols mixture, conservative values were considered for both products, being these 30 and 350 € kg^{-1}, respectively.

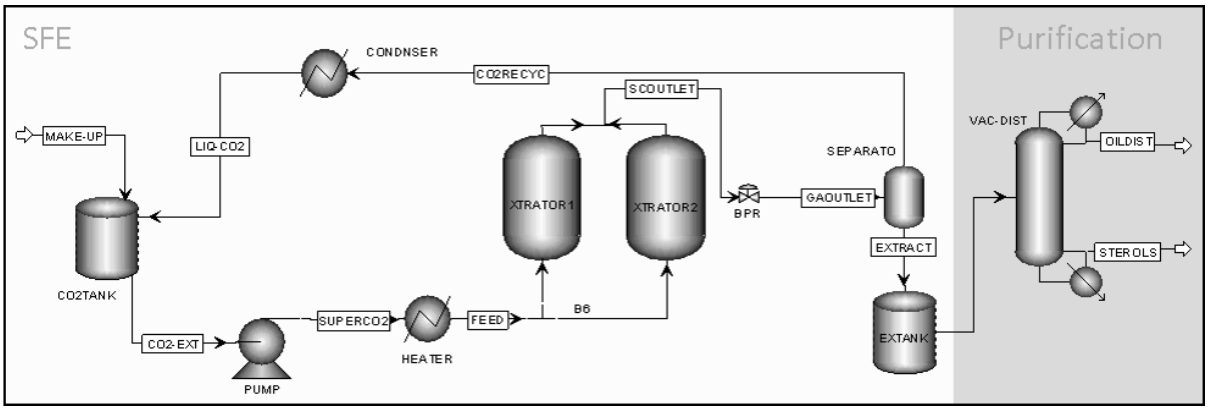

Figure 8.4 – Process flowsheet used for the estimation of the costs related to utilities consumption in the integrated process. The drying stage is not represented.

Project and simulation in Aspen Plus® - The recovery of phytosterols from vegetable and tall oils is a well-known goal, for which several process strategies are described in patents literature [39]. The most typical methods range from adsorptive [40-41] to chemical reaction [42], and also thermodynamic fractioning [43] natures.

In this work the removal of sterols by high vacuum distillation was adopted following Clark et al. patent [43], which briefly encompasses a column operating between 240 °C and 196 °C at 0.004 bar. These values fall in the temperatures ranges typically employed in postreatment steps of oils such as deodorization [43], being thus compatible with thermal processing already used in the vegetable oils industry.

With respect to the feed composition, a representative stream was adopted based on the characterization of the raw material present in reference [36]. Accordingly for the simulations, the stream comprehended the following compounds: oleic acid (85 %, w/w), palmitic acid

(7.3 %), and stearic acid (7.4 %) for the fatty acid fraction, and stigmasterol (0.05 %) and beta-sitosterol (0.2 %) for the sterol fraction of the extract.

The purification process of Clark et al. [43] was adapted to the SFE of ben oil under study, and Aspen Plus® version 7.3 was used to simulate the distillation column towards the desired separation. The NRTL model was the thermodynamic expression chosen in the calculations. The first steps of the purification approach comprised the preliminary design of the column for the aforementioned feed composition and operating conditions. The study revealed that a column with 5 theoretical stages, a diameter of 1 meter, a distillate-to-feed ratio of 0.9981, and a reflux ratio five times greater than the minimum (conservative heuristic rule) is able to produce sterols with purity up to 89.4 wt.% (bottom product).

8.2.2 STUDY II – SFE OF SPENT COFFEE GROUNDS [3]

Supercritical fluid extraction - The experimental procedure used for this study are the same presented in Chapter 5 in section 5.2.3 for the study of this raw material, namely assays 5.14 and 5.18 (recall Table 5.3, in Chapter 5).

Economic analysis - The list of assumptions that support our economic assessment results is presented in Table 8.3. All data regarding utilities costs were obtained from simulations of the SFE process in Aspen Plus® (version 7.3).

8.2.3 STUDY II – SFE OF TOMATO RESIDUES [4]

Equilibrium calculations: lycopene solubility - Lycopene solubility in supercritical carbon dioxide was estimated in order to provide useful arguments for an enriched understanding of the experimental and economic results of this work. The adopted approach is similar to that used for the estimation of ursolic acid in a previous study of SFE of *Eucalyptus globulus* bark [9]. Accordingly, the solubility was computed from the well-known isofugacity condition relation:

$$y_i^* = \frac{P_i^{sat}}{\emptyset_i^{SCF} P} \exp\left[\frac{V_{\mathrm{i}}^{solid}\left(P - P_i^{sat}\right)}{\Re T}\right] \tag{8}$$

where i is the solute (lycopene), y_i^* is solute solubility, $P_i^{sat}(T)$ is solute vapor pressure, $\emptyset_i^{SCF}(P, T, y_i^*)$ is the fugacity coefficient of the solute in supercritical phase, V_{i}^{solid} is the solute molar volume in solid state, $\Re$ is the universal gas constant, P is pressure, and T is temperature.
In brief, $P_i^{sat}(T)$ was calculated using an integrated form of the Clausius-Clapeyron equation proposed by Sepassi et al. [44] that depends on the knowledge of boiling (T_{b}) and melting (T_{m})

temperatures. The latter two, as well as the critical temperature (T_c) , were computed from the group contribution method proposed by Marrero *et al.*[45]. With regard to the fugacity coefficient, $\emptyset_i^{SCF}(P,T,y_i^*)$, the calculation was accomplished with the Peng-Robinson Equation of State (PR-EoS) [9, 46-47]. Other latent lycopene properties such as boiling and melting heat capacities and entropies changes ($\Delta C_{p,b}, \Delta C_{p,m}, \Delta S_m, \Delta S_b$, respectively) were computed with subsidiary expressions proposed by Sepassi et al. [44]. All the necessary equations are compiled in Table 8.4.

Table 8.3 - List of assumptions of the economic analysis of the SFE of spent coffee grounds.

General	- Unit working period: 24 h per day, 330 days per year. - Number of workers *per* extractor = 1. - Scale-up criterion: solvent flow rate per mass of SCG in the extractor $Q_{CO2}\, w_{SCG}^{-1}$ - Minimum pressure in the separator (extract collection vessel) = 45 bar. - Required time to unload, load and pressurize 1 extractor (t_{prep}): 1 h - Whenever the extraction time is inferior to the preparation time ($t < t_{prep} =$ 1h), the unit is switched off. - The CO_2 losses in each full decompression correspond to the mass of CO_2 inside the extractor at 45 bar and 40 °C. - SCG bed density = 400 kg m^{-3}. - SCG bed porosity = 0.8. - Exchange ratio €/$US (on May 2013) = 0.766 - Market price of coffee oil = 130 € kg^{-1} [48] (in ref. [49], a large value of 194 € kg^{-1} is reported. We adopted the lower one for a conservative analysis of the process.) - SCG initial moisture = 60.7 % (wt) [50] - Dried SCG heat capacity = 1.434 kJ kg^{-1} $°C^{-1}$ [51]
FCI	- Annual depreciation rate = 10 % - SFE units prices: (i) 1.5 M€ for a unit comprising two 0.4 m^3 extractors as presented by Rosa and Meireles [52]; (ii) 2.3 M€ for a three-extractors unit each with 0.4 m^3 of capacity, calculated by the expression proposed by Lack *et al.* [23]; (iii) 3.2 M€ for a three-extractors unit each with 1.0 m^3 of capacity, calculated by the expression proposed by Lack *et al.* [23].
COL	- Labor cost = 10 € h^{-1} $worker^{-1}$
CUT	- Cost of electricity = 50 € MWh^{-1} - Cost of steam = 1.53 € ton^{-1}
CWT	- Cost of waste treatment = 0 €
CR	- Cost of spent coffee grounds drying = 0.016 € kg^{-1}_{SCG} - Cost of CO_2 = 800 € ton^{-1}

Economic analysis - Different assumptions were established, being all presented in Table 8.5. Besides these, all data regarding utilities costs were obtained by Aspen Plus® (version 7.3) simulations of the SFE process.

The commercial plant that was considered for the economic study comprises three modules: 1 filter press unit for the primary reduction of the biomass moisture from 82.5 % to 30 % (wt.)

Table 8.4 – List of equations utilized for the calculation of the fugacity coefficient and vapor pressure of lycopene needed in Eq. (8).

Equation *	Ref.	Eq.#
$\mathrm{Ln}\phi_i^{SCF} = -\mathrm{Ln}(Z-B) - \frac{A}{B\sqrt{8}}\mathrm{Ln}\left[\frac{Z+\left(1+\sqrt{2}\right)B}{Z+\left(1-\sqrt{2}\right)B}\right] + Z - 1$	[9, 46-47]	(9)
$\mathrm{Log}P_{\mathrm{i}}^{\mathrm{sat}} = -\frac{\Delta S_{\mathrm{m}}(T_{\mathrm{m}}-T)}{2.3\Re T} + \frac{\Delta C_{\mathrm{p,m}}}{2.3\Re}\left[\frac{T_{\mathrm{m}}-T}{T} - Ln\frac{T_{\mathrm{m}}}{T}\right] - \frac{\Delta S_{\mathrm{b}}(T_{\mathrm{b}}-T)}{2.3\Re T} + \frac{\Delta C_{\mathrm{p,b}}}{2.3\Re}\left[\frac{T_{\mathrm{b}}-T}{T} - Ln\frac{T_{\mathrm{b}}}{T}\right]$	[44]	(10)
$T_{\mathrm{b}} = T_{\mathrm{b}_0} exp\left(\sum_i N_i T_{\mathrm{b1}_i} + \sum_j M_j T_{\mathrm{b2}_j} + \sum_k O_k T_{\mathrm{b3}_k}\right)$	[45]	(11)
$T_{\mathrm{c}} = T_{c_0} exp\left(\sum_i N_i T_{\mathrm{c1}_i} + \sum_j M_j T_{\mathrm{c2}_j} + \sum_k O_k T_{\mathrm{c3}_k}\right)$	[45]	(12)
$P_{\mathrm{c}} = P_{c_4} + \left(P_{c_5} + \sum_i N_i P_{\mathrm{c1}_i} + \sum_j M_j P_{\mathrm{c2}_j} + \sum_k O_k P_{\mathrm{c3}_k}\right)^{-0.5}$	[45]	(13)
$V_{\mathrm{c}} = V_{c_0} + \sum_i N_i T_{\mathrm{c1}_i} + \sum_j M_j T_{\mathrm{c2}_j} + \sum_k O_k T_{\mathrm{c3}_k}$	[45]	(14)
$\Delta S_m = 56.5 - 19.2\, Log\,(\sigma) + 9.2\tau$	[44]	(15)
$\Delta S_b = 86 + 0.4\tau + 1421\ \mathrm{HBP}$	[44]	(16)
$\Delta C_{\mathrm{p}_m} = \Delta S_m$	[44]	(17)
$\Delta C_{\mathrm{p_b}} = -56 - 4\tau - 40\ \mathrm{HBP}$	[44]	(18)

* Nomenclature: τ is the molecular flexibility number; σ is the molecular symmetry parameter; HBN is the hydrogen bond density number; HBP is the hydrogen bonding parameter; $M, O, P_{c1}, P_{c2}, P_{c3}, P_{c4}, P_{c5}\ V_{c0}, V_{c1}, V_{c2}, V_{c3}, T_{c0}, T_{c1}, T_{c2}, T_{c3}, T_{\mathrm{b0}}, T_{\mathrm{b1}}, T_{\mathrm{b2}}, T_{\mathrm{b3}}$ are group contribution parameters of the method.

The commercial plant that was considered for the economic study comprises three modules: 1 filter press unit for the primary reduction of the biomass moisture from 82.5 % to 30 % (wt.) through the consumption of power, 1 belt drying system for the subsequent reduction of moisture from 30 % to 4.6 % (wt.) that demands both steam and electricity utilities, and, finally, one SFE unit with two extractors of 1 m^3 intended to work alternately. The estimated price for the pretreatment modules is 0.35 M€, and the anticipated price for the full SFE unit is 2.6 M€. For the particular case of supercritical ethane, it is known that hazardous locations require special precautions, such as explosion proof equipment and wiring. Such installations

reach two to three times the cost of similar installations in nonharzardous (e.g. general-purpose) location [53]. In this sense, a three-fold price of SFE unit (7.8 M€) was used in order to take into account the hazardous character imposed by the usage of ethane.

Concerning the SFE unit, a daily operation of 24 hours and an annual activity of 330 days were assumed. For such activity one employee per extractor is necessary, which results in the

Table 8.5 – List of assumptions of the economic analysis of the SFE of tomato wastes.

General	- Unit working period: 24 h per day, 330 days per year. - Number of workers *per* extractor = 1. - Scale-up criterion: solvent flow rate per mass of dried biomass in the extractor $(Q_{CO_2}\, w_{biomass}^{-1})$ - Minimum pressure in the separator (extract collection vessel) = 45 bar. - Required time to unload, load and pressurize extractor (t_{prep}): 1 h - Maximum number of extractors in operation: 1 for a scheme of 2 extractors in parallel; - Maximum number of extractors under unload/load/repressurization = 1 - Whenever the extraction time is inferior to the previous preparation time (1 h), the unit is switched off until the next cycle. - The fluid losses in each full decompression correspond to the mass of fluid inside the extractor at 45 bar and 40 °C. - Bed porosity = 0.8 - Exchange ratio $US/€ (on July 2014) = 0.736 - Biomass initial moisture = 82.5 % (wt.) [54] - Tomato heat capacity = 4.0 kJ kg^{-1} $°C^{-1}$
FCI	- Annual depreciation rate = 10 % - Price of a two-extractor of 1 m^3 capacity SFE unit: 2.6 M€ - Price of a two-extractor of 1 m^3 capacity SFE unit for an hazardous solvent: 7.9 M€ - Price of tomato waste drying unit: 0.35 M€
COL	- Labor cost = 10 € $h^{-1}worker^{-1}$
CUT	- Cost of electricity = 50 € MWh^{-1} - Cost of steam = 1.53 € ton^{-1} - Drying costs comprise the utilities necessary for the reduction of tomato moisture from 82.5 % to 4.6 % (wt.)
CWT	- Cost of waste treatment = 0 €
CRM	- Cost of CO_2 = 800 € ton^{-1} - Cost of ethane = 941 € ton^{-1}

constant presence of two workers: one to control the extraction itself, and the other devoted to the preparation of the resting extractor for the next cycle of extraction. Based on insights from commercial units [3, 55-56], a 1 h period was defined as the required time for the preparation stage. The latter comprises full decompression of the extractor with the depleted bed, removal

of the latter, introduction of virgin biomass, and subsequent unit pressurization up to the desired extraction pressure. In addition, only one extraction cycle takes place at a given time, which implies that the extractor under preparation must always wait for the end of the ongoing extraction cycle to start its own cycle. In case the extraction time is shorter than the time required for the preparation of the resting extraction, the unit is shut down and the consumption of utilities is suspended.

With respect to the minimum pressure of the system, a value of 45 bar was specified. This is the low pressure needed for extract collection, which is performed at extractor outlet. Such pressure should be low enough to allow the precipitation of the solutes due to solvent expansion, but not so low to avoid excessive compressing costs. However, there is an additional subtle point that must be taken into account. In a previous economic study on the SFE of spent coffee grounds [3] it was shown that, from the point of view of COM, 45 bar is realistic and very appropriate. The reason is that it largely influences the amount of CO_2 that is lost in each full decompression at the end of each cycle, which thus reflects on the magnitude of costs of the raw material (CRM) parcel.

Response Surface Methodology (RSM) - This technique has been broadly employed in SFE of vegetable biomass, being examples of its application the works on olive [57-58], eucalypt [11], spent coffee [8, 59], or vetiver [60-61]. However, it is typically used to optimize productivity indicators such as extraction yields rather than economic indicators like COM or net income. In this work, RSM was applied with this second objective.

An experimental design comprising three factors and a mix of three and four levels was adopted, totalizing 36 experiments. Pressure and temperature were studied with three levels of variation each: $P = 300, 400 \text{ and } 500$ bar, and $T = 70, 80 \text{ and } 90$ °C. On the other hand, spent CO_2 was studied in four equidistant levels: $w_{CO_2} = 25, 50, 75 \text{ and } 100 \ \mathrm{kg_{CO_2} kg_{sample}^{-1}}$. In this case four levels were fixed to represent more accurately the hard nonlinear behavior of some of the extraction curves analyzed in this work (as it is evident below in Figure 8.26). In Table 8.6 a summary of the experimental design adopted for the COM study is provided.

Table 8.6 – Codification and levels of the independent variables used in the COM optimization of SFE of tomato wastes.

Factor	Variable	Variable	Level Correspondence				
			-1	-0.333	0	+0.333	+1
Pressure (bar)	P	X_P	300	-	400	-	500
Temperature (°C)	T	X_T	70	-	80	-	90
Spent CO_2 ($\mathrm{kg_{CO_2} kg_{sample}^{-1}}$)	w_{CO_2}	$X_{w_{CO_2}}$	25	50	-	75	100

In view of the interest to disclose linear, quadratic and crossed sources of influence, a corresponding quadratic polynomial was adopted:

$$\mathbf{COM} = \boldsymbol{\beta_0} + \boldsymbol{\beta_1 X_P} + \boldsymbol{\beta_2 X_T} + \boldsymbol{\beta_3 X_{wCO2}} + \boldsymbol{\beta_4 X_P^2} + \boldsymbol{\beta_5 X_T^2} + \boldsymbol{\beta_6 X_{wCO2}^2} + \boldsymbol{\beta_7 X_P X_T} + \boldsymbol{\beta_8 X_P X_{wCO2}} + \boldsymbol{\beta_9 X_T X_{wCO2}} \quad (19)$$

where the β_i coefficients are the model parameters from which the different influence contributions are pondered and ranked. For the regression, factors were coded according to the level correspondence provided in Table 8.6.

JMP® software (version 8.0) was used for statistical treatment of the results. Accordingly, *t*-tests were applied to judge the significance ($\beta_i \neq 0$) of the estimated coefficients of the model. The determination coefficient, R^2, and its adjusted version, R^2_{adj}, were used to evaluate the goodness of the fit of the regression model.

8.2.4 STUDY IV – SFE OF GAC FRUIT [5].

Economic analysis - As referred in the introduction, RSM-COM optimization approach uses an economic based response to model the performance of the whole SFE process (including drying pretreatment). For each of the parcels of Eq. (1), different assumptions were established, being presented in Table 8.7.

With reference to the commercial plant, the proposed capacity of the SFE unit (two 0.4 m^3 extractors) was chosen in view of the outputs of existing farms of gac fruit, being therefore compatible with typical production rates. For the drying unit, an identical technical solution as the one proposed for SFE of tomato waste [4] was employed: one filter press unit for the primary reduction of the biomass moisture from 80 % to 30 % (wt.) through the consumption of electric energy, and one belt drying system for the subsequent reduction of moisture from 30 % to 7 % (wt.), demanding both steam and electric energy. In the whole, the full process (extraction plus drying) requires an investment of 2.95 M€ (see FCI in Table 8.7).

As far as the SFE unit is concerned, a ratio of one employee per extractor was adopted (i.e. two workers always present during the unit operation), as well as a daily operation of 24 h during 330 days per year. In addition, one hour was adopted as the time necessary for preparation stage (t_{prep}), which comprises full decompression of the extractor with the depleted bed, removal of the latter, introduction of a new biomass load, and subsequent unit pressurization up to the desired extraction pressure. The assumed preparation time value has been also admitted by other SFE researchers [29, 62]. Moreover, only one extraction cycle takes place at a given time, which implies that the extractor under preparation must always wait for the end of the ongoing extraction cycle to start its own cycle. For this reason, in the eventual case the extraction time

is shorter than the preparation time of the resting extractor, the unit is shut down and the consumption of utilities is suspended.

All data regarding utilities costs were obtained by Aspen Plus® (version 7.3) simulations of the SFE process, using RK-Aspen as the thermodynamic model. A flowsheet of the proposed unit is exhibited in Figure 8.5, with the extractors in central position ("XTRACTOR" and "XTRACTOR2" labels), and CO_2 storage reservoir ("CO2TANK"), pumping and heating on the left. On the right side of the extractors, the decompression valve ("BPR") is used to impose the intended extract collection vessel ("SEPARATO") pressure (45 bar, see Table 8.7). The gaseous CO_2 leaving the separator flows then to a condenser ("CONDENSE") that promotes phase change to liquid state and further storage in "CO2TANK", which has also an additional inlet stream comprising make-up CO_2 to cope with solvent losses.

Table 8.7 – List of assumptions of the economic analysis of the SFE of gac oil.

General	- Unit working period: 24 h per day, 330 days per year; - Number of workers *per* extractor = 1; - Scale-up criterion: solvent mass per mass of dried biomass in the extractor $(w_{CO_2}\ w_{biomass}^{-1})$; - Extract collection vessel pressure = 45 bar; - Required time to unload, load and pressurize extractor: t_{prep} = 1 h; - Maximum number of extractors in operation: 1 for a scheme of 2 extractors in parallel; - Maximum number of extractors under unload/load/repressurization = 1; - Whenever the extraction time is inferior to the previous preparation time (1 h), the unit is switched off until the next cycle; - The fluid losses in each full decompression at the end of each cycle is the mass of CO_2 inside the extractor at 45 bar and 40 °C; - Bed porosity = 0.8; - Exchange ratio $US/€ (on October 2014) = 0.7917; - Biomass initial moisture = 80 % [63] ;
FCI	- Annual depreciation rate = 10 %; - Price of a two-extractor of 0.4 m^3 capacity SFE unit: 2.6 M€; - Price of a drying unit: 0.35 M€;
COL	- Labor cost = 10 € $h^{-1}worker^{-1}$;
CUT	- Cost of electricity = 50 € MWh^{-1}; - Cost of steam = 1.53 € ton^{-1}; - Drying costs comprise the utilities necessary for the reduction of gac aryl moisture from 80 % to 7 % (wt.) ;
CWT	- Cost of waste treatment = 0 €;
CRM	- Cost of CO_2 = 800 € ton^{-1};

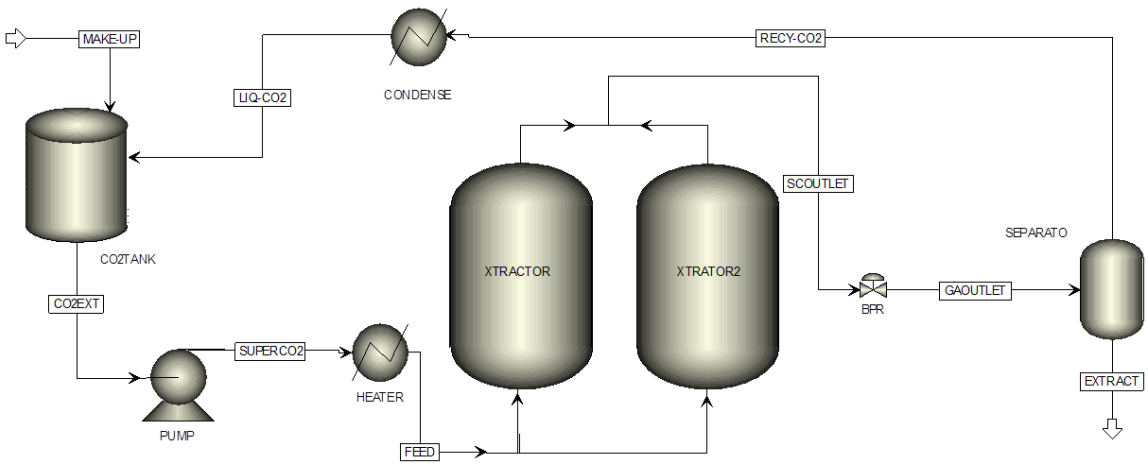

Figure 8.5 – SFE unit flowsheet of the simulation in Aspen Plus® (version 7.3), used for the calculation of utilities and energy consumption under different operating conditions. The drying unit is not shown for simplicity.

Response Surface Methodology (RSM) - An experimental design comprising three factors (P, T, t) and a mix of two and four levels was adopted, totalizing 24 experiments. Pressure was studied with two levels of variation (200 and 400 bar), temperature with three levels (40 , 50 and 60 °C), and extraction time with four equidistant levels (0.5, 1.0, 1.5 and 2.0 h). Table 8.8 provides a summary of the experimental design adopted for the RSM-COM optimization study.

In view of the interest to disclose linear, quadratic and crossed sources of influence, a multivariate second-degree polynomial was adopted according to:

$$\mathrm{COM} = \beta_0 + \beta_1 X_\mathrm{P} + \beta_2 X_\mathrm{T} + \beta_3 X_t + \beta_4 X_\mathrm{T}^{\,2} + \beta_5 X_\mathrm{t}^{\,2} + \beta_6 X_\mathrm{P} X_\mathrm{T} + \beta_7 X_\mathrm{P} X_t + \beta_8 X_\mathrm{T} X_t \qquad (20)$$

where the β_i coefficients are the model parameters from which the individual monomial contributions are pondered and ranked. For the regression, the three factors were coded according to the level correspondence provided in Table 8.8.

JMP® software (version 8.0) was used for statistical treatment of the results. Accordingly, t-tests were applied to judge the significance of the fitted coefficients of the model for a 95% confidence level. The coefficient of determination, R^2, and its adjusted version, R^2_{adj}, were used to evaluate the goodness of fit of the regression model.

Table 8.8 – Codification and levels of the three independent variables considered in the RSM-COM optimization gac fruit study.

Factor	Variable	Codified Variable	Level Correspondence between variables and codified variables				
			-1	-0.333	0	+0.333	+1
Pressure (bar)	P	$X_{\mathrm{P}} = \frac{P - 300}{100}$	200	-	-	-	400
Temperature (°C)	T	$X_{\mathrm{T}} = \frac{T - 50}{10}$	40	-	50	-	60
Time (h)	t	$X_{\mathrm{t}} = \frac{t - 1.25}{0.750}$	0.5	1.0	-	1.5	2.0

8.3 RESULTS AND DISCUSSION

8.3.1 STUDY I – SFE OF MORINGA SEEDS [2]

Brief description of the SFE curves - The proposed integrated process comprising drying pretreatment, SFE and vacuum distillation is based on the experimental SFE data obtained by *Ruttarattanamongkol et al.* [36], namely SFE curves measured for conditions of pressure and temperature ranging from 150 to 350 bar and 25 to 35 °C, respectively – Figure 8.6. The seeds were previously de-hulled, ground into a powder and sieved through 1 mm screening size. The sub/supercritical extraction assays were performed in a pilot plant of Natex Prozesstechnologie (Ternitz, Austria) with capacity of 2 L and a load of 850 g of biomass per run. The system includes an extraction column, a vessel for extract collection (separator), a CO_2 storage tank, a heat exchanger, a piston pump and pressure reduction valve. The CO_2 flow rate was maintained at 20 $\mathrm{kg\,h^{-1}}$ for each extraction run, which corresponds to a flow rate/biomass weight ratio of 25.53 $\mathrm{h^{-1}}$, and the temperature inside the separator was fixed at 40 °C. With regard to sterols quantification, Gas Chromatography-Mass Spectrometry (GC-MS) was employed to assess their concentration in the moringa oil samples.

In Table 8.19 a summary of operating conditions (temperature, flow rate, pressure) of the selected SFE curves is reported, including the estimated oil solubility for the various conditions using Eq.(6). In addition, the minimum $\mathrm{COM_{oil}}$ among the extraction times studied is reported, as well as the respective oil production under the conditions of the said minimum $\mathrm{COM_{oil}}$.

In terms of overall trends, Table 8.9 is quite clear: oil solubility increases as pressure is increased, leading to a consequent enhancement in oil production and a decrease in the cost of manufacturing of moringa oil. The course of these trends will be object of statistical confirmation, embodied in the RSM-COM analysis.

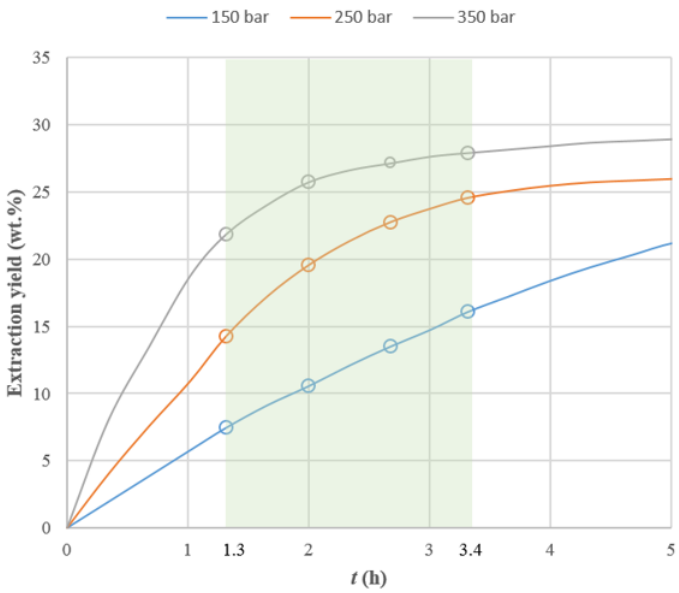

Figure 8.6 – Experimental extraction curves of moringa oil, where the shaded area represents the time interval covered by the RSM-COM analysis of this work. Data taken from [36].

Table 8.9 - Compilation of experimental values used in the RSM-COM optimization, minimum $\mathrm{COM}_{\mathrm{oil}}$ obtained for each value of P and the respective production and solubility.

T (°C)	Flow rate ($\mathrm{kg_{CO_2}\,h^{-1}}$)	P (bar)	Oil solubility ($\mathrm{g_{oil}\,L_{CO_2}^{-1}}$)	Min $\mathrm{COM}_{\mathrm{oil}}$ (€ $\mathrm{kg_{oil}^{-1}}$)	Oil Production @ Min $\mathrm{COM}_{\mathrm{oil}}$ ($\mathrm{kg_{oil}\,year^{-1}}$)
30	20	150	1.92	6.52	163 320
		250	3.56	3.81	329 586
		350	5.10	2.64	558 870

Screening of the significant factors - The RSM-COM approach under discussion is specifically focused on oil, which means the purification expenses to obtain the sterols fraction were left out of these calculations. In this sense, the bulk oil directly produced by the SFE unit was taken as the product into which $\mathrm{COM_{oil}}$ refers to.

Upon building a regression of $\mathrm{COM_{oil}}$ as function of the process variables, a screening was performed in order not only to evaluate the significance of each effect upon the generic model and to discard the non-significant ones, but also to disclose their impact (positive or negative) on the cost of manufacturing.

In Figure 8.7 the Pareto diagram concerning the fitted model is presented, being the relative impacts on $\mathrm{COM_{oil}}$ hierarchized from highest contribution (bottom of the graphic) to the lowest

contributions (top of the graphic). Observing each variable individually, pressure is clearly the most significant factor, either linearly (P), quadratically (P^2) or crossed with time ($P{\times}t$). Moreover, this contribution accounts for more than 45 % of the weight on the response, being therefore the governing term in the process. While it is known that higher pressures imply greater utilities consumption (in this work they increase 32 % when passing from 150 to 350 bar), the Pareto chart evidences that these expenses do not prevail along pressure increments, since an overall cheapening of the extraction process is reported along P. Remarkably, the linear effect of pressure is the only effect that acts in favor of the economy of the process, i.e. leads to lower $\mathrm{COM_{oil}}$ values. Such behavior has been also reported in the SFE of lycopene [4] and gac oil [5]. The remaining contributions ($t, t^2, P{\times}t$ and P^2) increase $\mathrm{COM_{oil}}$, being P^2 the second most important effect after P, followed by the crossed contribution between pressure and time ($P{\times}t$).

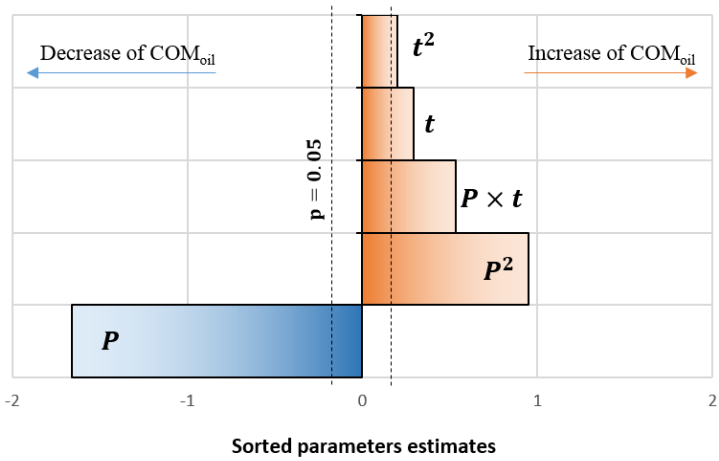

Figure 8.7 – Statistical analysis of the impact of different factors and interactions upon $\mathrm{COM_{oil}}$. Dashed lines delimit the region of no statistical significance for a 95% confidence interval.

The diminution of $\mathrm{COM_{oil}}$ with the increase of pressure can be interpreted in light of the oil solubility dependence reported in Table 8.9. The sensitivity of a SFE process to solubility variations becomes more relevant when dealing with biomass of high oil contents (typically the case of the commodity edible oils), since saturation of the sub/supercritical phase is prone to be reached at extractor outlet. Under such circumstances, the oil uptake typically resembles a straight line from the beginning of the SFE onwards, giving rise to the well-known first period of extraction. Since pressure increments increase SC-CO_2 density, which in turn imparts a power law driven increase on the solubility (from Eq. (6), $y_i^* \propto \rho_f^{k_1}$), the higher the P the more the overall process productivity is increased, which is highly advantageous for SFE economy.

With regard to the effects imparted by extraction time, the strongest influence of this factor on $\mathrm{COM_{oil}}$ takes place setting P as moderator (i.e. $P{\times}t$), which means that the way the time affects the process costs depends on the selected value of pressure. This result is in agreement with the observations taken from Figure 8.6 in the sense that: i) at 150 bar, increasing time is advantageous in the shadowed region since the extraction rate keeps constant. The linear shape

of this cumulative curve ensures that productivity is proportional to the extraction time; ii) at 250 and 350 bar the rate suffers a progressive decrease along time, making the process less productive after 1.3 h of extraction. This is due to the significant enhancement of solubility at higher pressures, which increases the driving force to mass transfer and thus the overall extractives fluxes, that rapidly exhausts the biomass bed. In this way, one easily reaches the second period of extraction (ruled by intraparticle diffusion) where productivity is not proportional to the extraction time.

Optimization of the SFE process - Taking into account that all factors ($t, t^2, P\times t$ and P^2) are statistically significant to $\mathrm{COM_{oil}}$ for a 95% confidence interval, all them were maintained in the response surface model. The final uncoded equation is given by:

$$\mathrm{COM_{oil}} = 0.0000949\times P^2 + 0.00506\times P\times t - 0.0759\times P + 0.179\times t^2 - 1.90\times t + 17.5 \qquad (21)$$

where $\mathrm{COM_{oil}}$ is expressed in $€\,\mathrm{kg_{oil}^{-1}}$, P in bar, and t in h. In order to visualize the individual effects imparted by pressure and time, and their conjugated contribution to $\mathrm{COM_{oil}}$, a graphical representation of Eq. (21) is plotted in Figure 8.8. In a first general view, the $\mathrm{COM_{oil}}$ values range from 7.4 $€\,\mathrm{kg_{oil}^{-1}}$ at 150 bar and 1.3 h, to 2.8 $€\,\mathrm{kg_{oil}^{-1}}$ at 350 bar and the same extraction time, and at a constant temperature of 30 °C.

Within the plotted $[P, t]$ frame of Figure 8.8, the optima operating conditions are the combination of highest pressure (350 bar) and shortest extraction time (1.3 h), which corresponds to a total of 6010 extraction cycles. In addition, the fact that the smallest value of t is responsible for both the maximum and minimum $\mathrm{COM_{oil}}$ is an indicator that pressure is in fact the key factor of $\mathrm{COM_{oil}}$.

Since oil solubility increases with increasing pressure, the time required to produce an equal amount of extract (at fixed solvent flow rate) is naturally lower at higher P. Additionally, an operation under quicker extraction cycles allows the number of batches per year to be increased, which enhances the annual oil production. Taking into consideration that $\mathrm{COM_{oil}}$ is indexed to the amount of oil obtained, higher productivity gives rise also to a decrease in the costs of production.

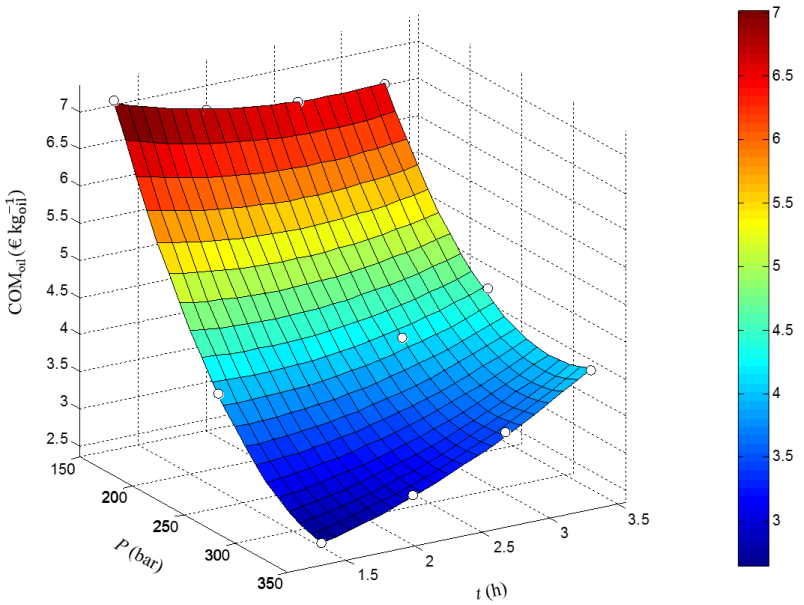

Figure 8.8 - COM_{oil} as function of pressure and extraction time. Symbols are calculated results, and the response surface model is Eq. (21).

With regard to the market attractiveness of the reported COM_{oil} values, since moringa oil fatty acid profile is similar to those of high value edible oils (high concentration of oleic and behenic acids) [36], its price can attain values as high as 50 € kg_{oil}^{-1} [64]. Nonetheless, even adopting a more conservative market price of 30 € kg_{oil}^{-1} - as it was done for the net income calculations in this work - the proposed process provides competitive results towards the commercialization of this oil.

Integrated process with sterols purification - Sterols are a complementary high value fraction of moringa oil that could be exploited as a second independent product of the SFE process, rather than minor components with negligible added value for the bulk oil. Owing to the higher market value of sterols in relation to ben oil, the integration of a sterols purification step after the SFE stage could add more value to the whole process. This was the principle behind studying the inclusion of a purification stage.

As far as the assessment of the process costs for the two products is concerned, they were estimated with the same COM expression used previously (see Eq. (1)), but with the following nuances: (i) COM_{oil} comprises the FCI, CUT, COL costs of the upstream stages of moringa bulk oil production, namely the drying biomass and the subcritical extraction; (ii) $COM_{sterols}$ comprehends not only the FCI, CUT and COL costs specifically related to the purification goal, but also all the costs implied in the previous production of bulk moringa oil. In practice:

$$\mathrm{COM}_{\mathrm{sterols}} = \mathrm{COM}_{\mathrm{oil}} + \text{Purification stage costs (FCI, CUT, COL)} \quad (22)$$

While it is clear from the previous topics that the economic attractiveness of sterols isolation depends on the cumulative costs of three stages (drying + SFE + purification), four scenarios involving the operation of the integrated process have been analyzed in this work, by combining different number of workers with distinct production arrangements. In Table 8.10 the results achieved for the four cases considered are summarized, being the reference scenario a production case where no purification stage exists at all (i.e. only drying + SFE are assumed).

Since the expansion of the process through the introduction of additional units forces the re-arrangement of the work plan of the plant, an additional full-time worker may be necessary to cope with the operation of the distillation column (2nd Scenario). In alternative, one may consider rearranging the production so that the two workers of the reference case can deal both with extraction and purification stages at the expenses of stopping the extraction unit during one day a week, and using that day to purify the oil obtained in the previous six days (3rd Scenario). Finally, the last possibility comprises the ideal situation where the distillation unit can be operated one day a week in parallel to the SFE unit (which in turn operates 7 days per week), with same number of workers of the reference case (4th scenario).

Due to the relatively low amounts of purified sterols obtained from the purification unit (a maximum of 1.9 $\mathrm{ton\,year^{-1}}$), a continuous operation may be not necessary [65]. Hence, a batch or semi-batch distillation was chosen for the sterols isolation, which opened the way for the different scenarios concerning when and how to operate this unit.

Before discussing the performance of $\mathrm{COM}_{\mathrm{sterols}}$ for each scenario, it is worthwhile to note that $\mathrm{COM}_{\mathrm{oil}}$ is only affected when less days of production are established for the SFE unit, which happens in the 3rd scenario. In the latter, $\mathrm{COM}_{\mathrm{oil}}$ jumps to 2.96 $€\,\mathrm{kg_{oil}^{-1}}$, which represents a cost of production 6.8 % greater than the reference value (2.76 $€\,\mathrm{kg_{oil}^{-1}}$). Furthermore, such constraints on the time devoted to the SFE operation impose a much more significant impact on annual production, which is reduced by 15.8 % in the case of the 3rd scenario. This drops the overall net income of the process by 12.7 % in relation to the reference value of 15.22 $\mathrm{M€\,year^{-1}}$ of the 1st case.

Concerning $\mathrm{COM}_{\mathrm{sterols}}$, 2nd and 4th scenarios represent opposite realities in terms of human resources synergies for an integrated process like the one considered. In fact, when an extra worker is specifically allocated to the purification process, $\mathrm{COM}_{\mathrm{sterols}}$ jumps to 23.29 $€\,\mathrm{kg_{sterols}^{-1}}$. If this extra worker is not hired to cope only with the purification stage, $\mathrm{COM}_{\mathrm{sterols}}$ is decreased by 77.9 %, amounting 5.60 $€\,\mathrm{kg_{sterols}^{-1}}$. Owing to the lower cost of production, the 4th scenario is

the one that leads to the highest net income values, namely 15.87 M€ $year^{-1}$. This clearly underlines the advantages of considering an integrated process involving a sharing of human resources (4th scenario) in relation to two processes requiring independent human resources (2nd scenario), answering thus to the opportunity to bridge SFE with posttreatment that increase the added-value of the bulk extracts or oils produced.

Table 8.10 – Economic performance of the integrated process (drying + SFE + purification) for several scenarios: assumptions and calculated results.

Scenario	Workers per shift	SFE	Purification stage	COM (€ kg^{-1})	Production (ton $year^{-1}$)	Net income (M€ $year^{-1}$)
1st case (Ref.)	2 (for SFE)	7 days/week	-	Oil = 2.76	Oil = 558.9	15.22
2nd case	2+1 (for SFE + for Purification)	7 days/week	1 day/week	Oil = 2.76 Sterols = 23.3	Oil = 558.9 Sterols = 1.9	15.84
3rd case	2 (for SFE + Purification)	6 days/week	1 day/week	Oil = 2.96 Sterols = 5.60	Oil = 470.8 Sterols = 1.6	13.28
4th case	2 (for SFE + Purification)	7 days/week	1 day/week	Oil = 2.76 Sterols = 5.23	Oil = 558.9 Sterols = 1.9	15.87

Furthermore, an important insight also verified in other RSM-COM work [4] is that the arrangements that minimize the cost of manufacturing may not always be the most favorable conditions to maximize the profits of the process, since the annual net income relies also on the production volumes attained, and also on the market prices of the products in question.

In the whole, the analysis presented in this section shows that the purification approach of the bulk moringa oil towards the production of a secondary enriched sterols stream with almost 89.4 % purity can be accomplished with advantage as a downstream stage of the SFE unit. Due to the fact sterols represent very low fractions of the oil, the economic performance of purification is able to enhance the overall process net income only up to 4.3 % (4th scenario). This percentage is fully due to the specific valorization of the 0.25 % fraction that sterols represent in the bulk moringa oil, which is a remarkable outcome.

8.3.2 STUDY II – SFE OF SPENT COFFEE GROUNDS [3]

Selection of SFE curves and extraction times - In view of the objective to perform an economic evaluation of this SFE process, the selection of the operating conditions was based on the normalized cumulative curves of Figure 8.9. Runs 5.14 and 5.18 were chosen for this purpose: 190 bar/40 °C and 300 bar/50 °C (see Table 5.3 and Figure 8.9).

To perform the comparative economic evaluation, the extraction time should be held constant in each case. The specification of this variable is very important because it defines the moment when an extracted bed should be replaced by a virgin one, and through this definition aspects like utilities, SCG processed or energy costs are also affected. In this essay it corresponds to the transition from the period when process is being mostly controlled by external mass transfer limitations and the period when intraparticle diffusion starts to be dominant, which can be determined by the intersection of the straight lines fitting both regimes (see Figure 8.19). The times obtained are 0.7 h and 3.8 h for 300 bar/50 °C and 190 bar/40 °C runs, respectively.

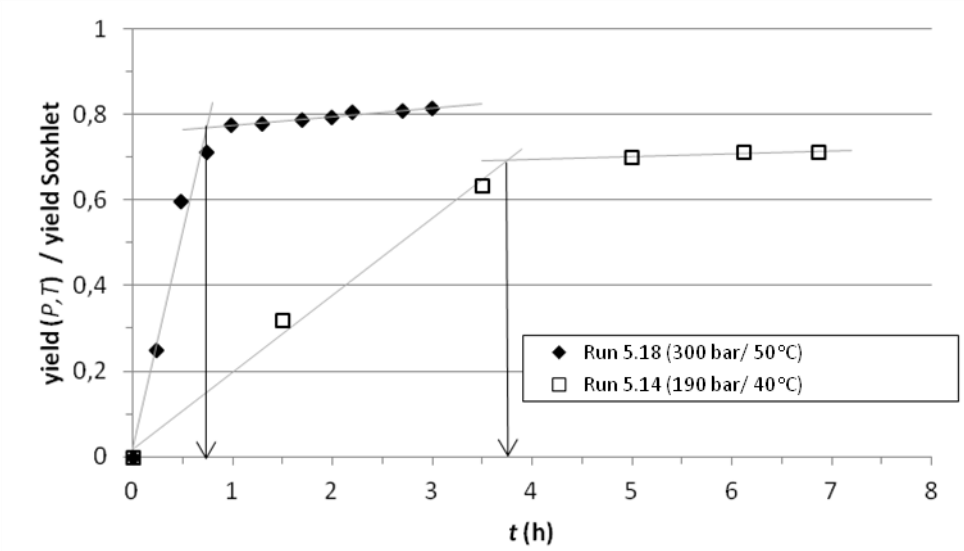

Figure 8.9 – SFE curves of spent coffee grounds (SCG) of experiments 5.14 and 5.18 of Table 5.3, and determination of their extraction times.

Economic evaluation - The economic assessment of the SFE of the SCG oil based on the data of Figure 8.9, and Tables 8.3 was accomplished after fitting the extraction time.

A SFE unit comprising two 0.4 m^3 extractors (see Table 8.3) was chosen to compare the performances of the two SFE conditions considered (Runs 5.14 and 5.18). Figure 8.10 presents the COM_{oil} and the annual SCG oil production expected in each circumstance. In what concerns COM_{oil}, it may be observed there are significant differences between the two cases. While the

lower pressure case (190 bar/40 °C, Run 5.14) leads to a COM_{oil} of 642 k€ year^{-1}, at 300 bar and 50 °C it reaches 951 k€ year^{-1}. To better understand the nature of these very distinct COM_{oil} values, Figure 8.11 provides the partition of COM_{oil} values in their respective fractions, namely, investment (FCI), labor (COL), utility (CUT), waste treatment (CWT), and raw material (CRM) costs – see Eq. (1).

While FCI + COL absolute costs are exactly the same in both cases, (the SFE unit and the work load is the same), the CUT + CRM parcels increase significantly, passing from 25 % of COM_{oil} in Run 5.14 to 50 % of COM_{oil} in Run 5.18. Such increase is a direct consequence of the severer conditions of pressure (300 bar) and temperature (50 °C), and of the higher number of batches being processed annually in view of the shorter extraction time (0.7 h). The more the batches processed the higher the amount of CO_2 that is lost due to full decompression steps which increases the make-up costs of CO_2. Moreover, shorter extraction cycles also imply higher costs of repressurization (CUT) and, also, a higher cost regarding the drying of the raw material (CUT).

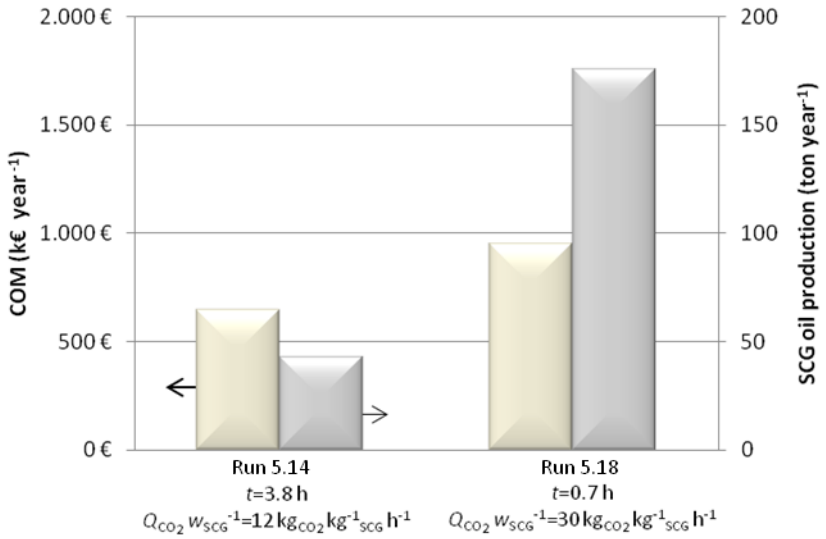

Figure 8.10 – Oil cost of manufacturing (COM_{oil}) and oil production for two 0.4 m^3 extractors in parallel, at 190 bar, 40 °C, t = 3.8 h, $Q_{CO2}\ w_{SCG}^{-1}$ =12 $kg_{CO2}\ kg^{-1}{}_{SCG}\ h^{-1}$, and 300 bar, 50 °C, t = 0.7 h, $Q_{CO2}\ w_{SCG}^{-1}$ = 30 $kg_{CO2}\ kg^{-1}{}_{SCG}\ h^{-1}$, respectively.

If the economic assessment was based only on COM values, one would be tempted to opt towards the situation that leads to lower process costs. This is the drawback of using this methodology as single tool to evaluate the economic attractiveness of a process. Accordingly, if productivities are also taken into account for each case, one may disclose that the differences between the performances of the two cases are even greater than those of the COM values, as shown in Figure 8.12. While SFE case with severer conditions (300 bar/50 °C/30 $kg_{CO2}\ kg^{-1}{}_{SCG}\ h^{-1}$) lead to a COM_{oil} 1.5 times greater, it also leads to an annual production 4.1 times greater, which reflects the great impact of the higher extraction rate advantages observed in Figure 8.9.

As a result, the expected annual production at 300 bar, 50 °C and t = 0.7 h is 176 ton of SCG oil, while at 190 bar, 40 °C and t = 3.8 h, it is set on 43 ton. Furthermore if the COM_{oil} and production results are combined in terms of a net income calculation, which is shown in Figure 8.12, economic viability can be fully unveiled. Notwithstanding the fact that the two cases lead to a positive economic viability, the choice upon the fastest extraction case (300 bar, 50 °C, t = 0.7 h) represents 4.4 times the net income of the less productive case, reaching 21.9 M€ year^{-1}. It is worthwhile to stress that in this case the viability of the process is highly supported by the larger productivity in view of the high commercial value of SCG oil, which thus pay the higher costs resulting from the harder extraction conditions implied.

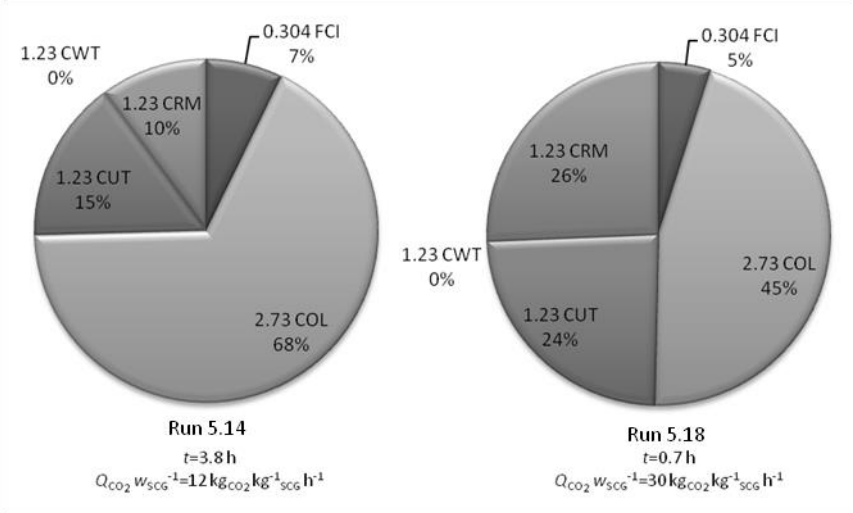

Figure 8.11 – Parcels (%) of the COM_{oil} values (see Eq. (1)) for the SFE units working at 190 bar, 40 °C, t = 3.8 h, $Q_{CO2}\, w_{SCG}^{-1}$ = 12 $kg_{CO2}\, kg^{-1}{}_{SCG}\, h^{-1}$ and 300 bar, 50 °C, t = 0.7 h, $Q_{CO2}\, w_{SCG}^{-1}$ = 30 $kg_{CO2}\, kg^{-1}{}_{SCG}\, h^{-1}$ respectively. In both cases there are two extractors of 0.4 m^3 working in parallel.

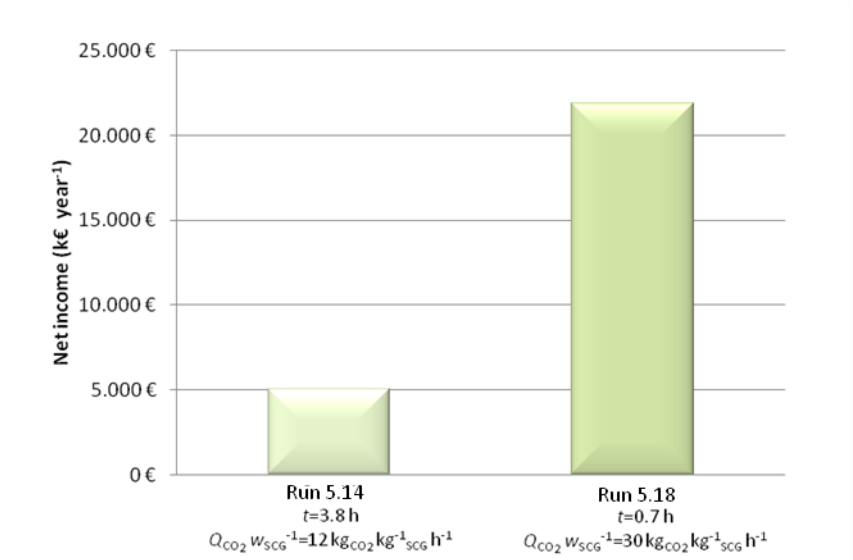

Figure 8.12 – Net Income for two 0.4 m^3 extractors in parallel at 190 bar, 40 °C, t = 3.8h, $Q_{CO2}\, w_{SCG}^{-1}$ = 12 $kg_{CO2}\, kg^{-1}{}_{SCG}\, h^{-1}$, and 300 bar, 50 °C, t = 0.7 h, $Q_{CO2}\, w_{SCG}^{-1}$ = 30 $kg_{CO2}\, kg^{-1}{}_{SCG}\, h^{-1}$, respectively.

Sensitivity analysis: extraction time and SFE unit capacity - It is worthwhile to check how $\mathrm{COM_{oil}}$, productivity and net income behave when some chief process parameters are changed. Furthermore, if the SFE unit layout is changed, the conjugation of different equipment, raw material, labor and utilities costs with the corresponding variations on productivity and thus product revenues may be meaningfully different. The same is true for extraction time, which largely influences the overall process net income, as previously discussed. The sensitivity analysis of this section is based on the best case studied before, namely SFE extraction curve at 300 bar, 50 °C and $Q_{CO2}\, w_{SCG}^{-1}$=30 $kg_{CO2}\, kg^{-1}{}_{SCG}\, h^{-1}$ (Run 5.18).

Figure 8.13 presents $\mathrm{COM_{oil}}$ as a function of extraction time for each of the three SFE unit configurations referred in Table 8.3. Values for time of extraction equal to zero are provided to disclose the impact of investment (FCI) and operational labor (COL) costs, which represent the process fixed costs. The $\mathrm{COM_{oil}}$ values exhibit a similar trend in all cases, namely, they increase up to a maximum and then start to decrease: the maxima are 2 h for 3 extractors and 1 h for 2 extractors. For an arrangement of N extractors in parallel, such maxima correspond to:

$$t\,(\mathrm{COM_{oil,\ max}}) = (N-1)\times t_{\mathrm{prep}} \tag{27}$$

where t_{prep} is the time required for the preparation of an extractor (unload, load and pressurization). The growing sections of Figure 8.13 are due to the increment of utilities cost (CUT) while their diminishing is attributed to the fall of CRM. Without loss of generality, this is clearly illustrated in Figure 8.14 for the case of 3 extractors of 1 m^3.

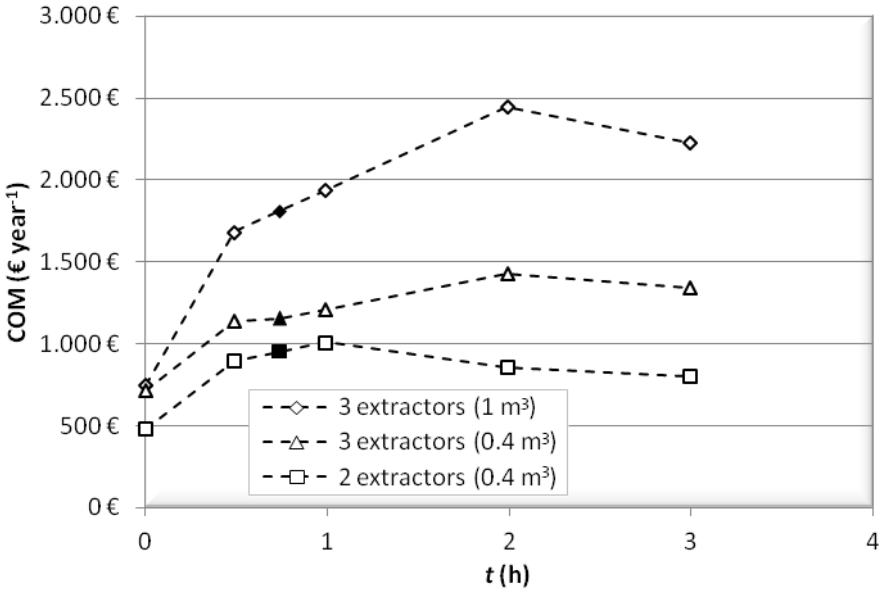

Figure 8.13 – Oil cost of manufacturing ($\mathrm{COM_{oil}}$) of spent coffee grounds (SCG) as function of extraction time per cycle, at 300 bar, 50 °C, $Q_{CO2}\, w_{SCG}^{-1}$ = 30 $kg_{CO2}\, kg^{-1}{}_{SCG}\, h^{-1}$ (Run 5.18), for different SFE unit configurations.

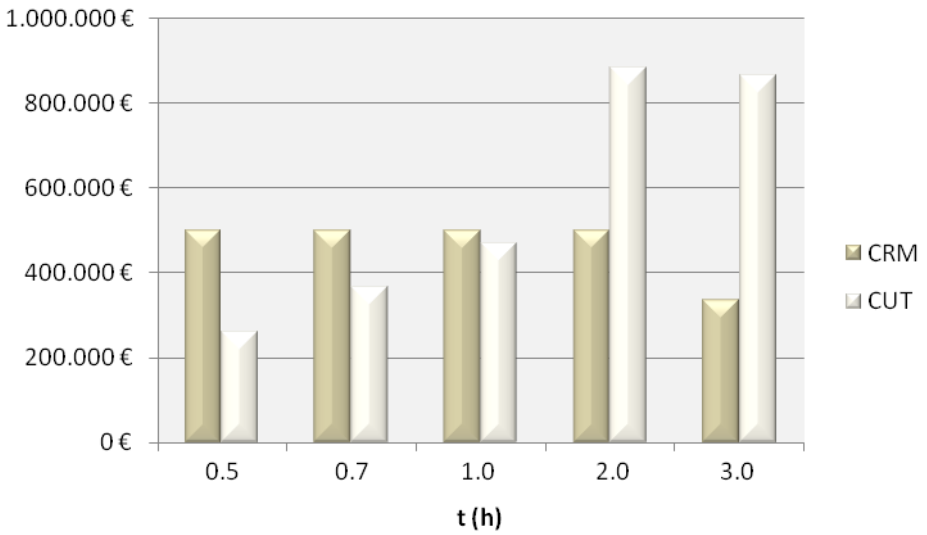

Figure 8.14 – Utility (CUT) and raw material (CRM) costs against extraction time for the SFE of spent coffee grounds (SCG) oil at 300 bar, 50 °C, $Q_{CO2}\ w_{SCG}^{-1}$ = 30 $kg_{CO2}\ kg^{-1}{}_{SCG}\ h^{-1}$ (Run 5.18) for unit layout comprising 3 extractors of 1 m^3 in parallel.

In Figure 8.15 the SCG oil production is plotted against extraction time. It is evident the differences found for the three arrangements, as their maxima lie between 177 and 454 ton $year^{-1}$. However, the most significant feature is the overlapping of the 3×0.4 m^3 and 2×0.4 m^3 arrangements for extraction times lower than 1 h, since in this period the process is controlled by the preparation time, t_{prep} = 1 h.

Net income values are presented in Figure 8.16 as function of extraction time for the different SFE unit arrangement. Given all the assumptions of Table 8.3, the net income is positive for any extraction time and layout considered. The shape of the net income profiles is quite similar to the annual production profiles (Figure 8.15), because the expected revenues from the produced oil are rather high in comparison to the respective costs of manufacturing (COM_{oil}). The maximum values for each unit are 56 M€ for 3 extractors of 1 m^3 and t = 2 h, 22 M€ for 3 extractors of 0.4 m^3 and t = 2 h, and 22 M€ for 2 extractors of 0.4 m^3 and t = 1 h. Within the interval between t = 0.7 h (time established from extraction curve – see Figure 8.9) and $t(COM_{oil,\ max})$, the net income profile slightly increases, while outside it decreases sharply instead.

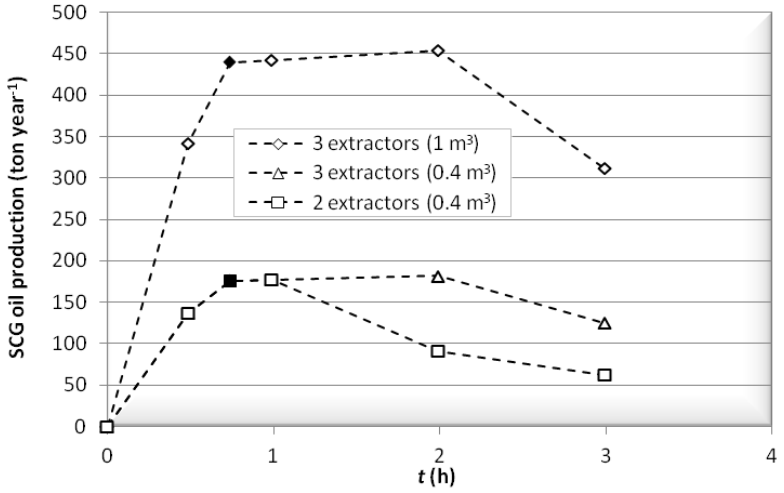

Figure 8.15– Annual production of spent coffee grounds (SCG) oil as function of extraction time, at 300 bar, 50 °C, $Q_{CO2}\ w_{SCG}^{-1}$ = 30 $kg_{CO2}\ kg^{-1}{}_{SCG}\ h^{-1}$ (Run 5.18), for different SFE unit configurations.

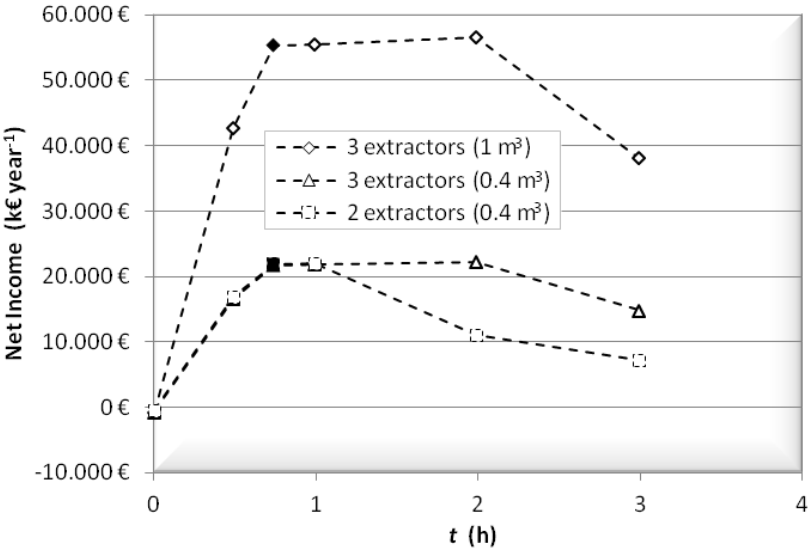

Figure 8.16 – Net income of spent coffee grounds (SCG) oil as function of extraction time, at 300 bar, 50 °C, $Q_{CO2}\ w_{SCG}^{-1}$ = 30 $kg_{CO2}\ kg^{-1}{}_{SCG}\ h^{-1}$ (Run 5.18), for different SFE unit configurations.

Sensitivity analysis: minimum pressure of the system - Besides time and extractors arrangement, another working parameter that also affects COM_{oil} is the minimum pressure in the separator where the extract precipitates, by means of the mass of CO_2 that is lost in each batch and through the energy needed for heating and cooling. In this respect, a sensitivity analysis is provided in Figure 8.17 for an arrangement of 2 extractors with 0.4 m^3, where *P, T, t* and $Q_{CO2}\ w_{SCG}^{-1}$ conditions were held constant (300 bar, 50 °C, 0.7 h and 30 $kg_{CO2}\ kg^{-1}{}_{SCG}\ h^{-1}$, respectively) while the separator pressure was varied from 40 to 65 bar. The effect upon COM_{oil} is very important – with variations between -3.4 to +18.2 % - and it reflects the nonlinear variation of CO_2 density with pressure. Furthermore, if the pressure in the separator is decreased to 40 bar, COM_{oil} value is reduced 3.4 %, a substantial saving. The implication of

this result relies in the balance between the less CO_2 that is lost in every full decompression to atmospheric pressure, and utilities necessary to pressurize the unit to 300 bar. Considering the increasing trend observable in Figure 8.17, results show that the impact of losing more CO_2 penalizes more the COM_{oil} value than the corresponding energy savings reduce its value. In addition, if 65 bar rather than 45 bar are used in the separator, the system will lead to a COM_{oil} value that is 18.2 % higher. If one takes into account that 25 bar (the range of *P* values in Figure 8.17) in a process that operates at 300 bar may seem inoffensive, results reveal that such variable is in fact quite influential in the final costs.

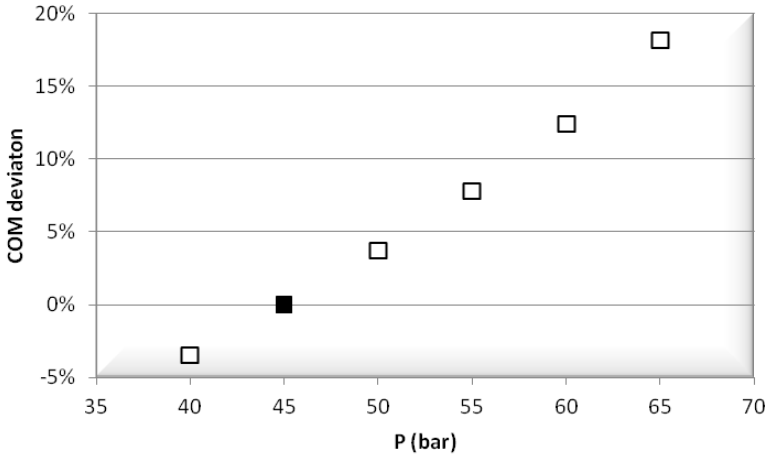

Figure 8.17 – Variation of cost of manufacturing (COM_{oil}) as function of the separator pressure (reference = 45 bar). Data for SFE at 300 bar, 50 °C, t = 0.7 h, $Q_{CO2}\ w_{SCG}^{-1}$ = 30 kg_{CO2} $kg^{-1}{}_{SCG}$ h^{-1} (Run 5.18). The corresponding densities are 83.9, 97.8, 113.2, 130.2, 149.4 and 171.6 kg m^{-3}.

8.3.3 STUDY III – SFE OF TOMATO RESIDUES [4]

Brief description of the SFE curves - With respect to the SFE results necessary for the optimization of COM, experimental data were taken from the work of Topal et al. [66], who measured extraction curves for pressures of 300, 400 and 500 bar, and temperatures of 70 , 80 and 90 °C. These authors tested different CO_2 flow rates and ensured that 2.5 mL min^{-1} (measured at pump condition) was high enough to eliminate the external film resistance to mass transfer and the accumulation in the bed. Therefore, the flow rate was considered already established for this process, and we only had to analyze the influence of pressure, temperature and mass of spent solvent. Concerning the raw material, dried tomato skin samples were used in amounts between 3.9 and 7.0 g per experiment. The maximum lycopene content of samples was determined by Soxhlet extraction using chloroform, and was identified as 1.13 g per kg of dry tomato skin. The lycopene concentrations were measured by HPLC analysis equipped with

UV-visible detector [66]. In view that drying skins were used, it was referred that lycopene was extracted from tomato skin with negligible degradation at the optimum conditions and that the amount extracted comprised 94 % of the total carotenoid content of the sample [66].

The comparison between supercritical ethane and supercritical carbon dioxide was based on the studies of Nobre et al [54, 67], who measured extraction curves for both solvents at the same pressure and temperature, namely 300 bar and 60 °C. In their case, industrial wastes were used as raw material, with initial moisture content of 82.5 % (wt.) that was then reduced to 4.6 % (wt.) prior to the SFE assays.

The most relevant information regarding the extraction curves analyzed in this work is compiled in Table 8.11, together with the most important results calculated for each curve, namely, the minimum COM and the corresponding lycopene production. These values are discussed in detail below.

Table 8.11 – Experimental extraction curves considered in this work together with calculated minimum $\mathrm{COM_{oil}}$ and lycopene production values.

Run	Tomato sample	SC Solvent	P (bar)	T (°C)	Q (10^{-3}kg min^{-1})	min(COM) (k€ kg$^{-1}_{\mathrm{lycopene}}$)	Lycopene Production @min(COM) (kg year^{-1})	Ref.
8.1	skin	CO_2	300	70	2.4	4.2	803	[66]
8.2	skin	CO_2	300	80	2.4	3.5	974	[66]
8.3	skin	CO_2	300	90	2.4	2.6	1310	[66]
8.4	skin	CO_2	400	70	2.4	2.9	1549	[66]
8.5	skin	CO_2	400	80	2.4	2.6	1735	[66]
8.6	skin	CO_2	400	90	2.4	1.9	2451	[66]
8.7	skin	CO_2	500	70	2.4	2.7	1649	[66]
8.8	skin	CO_2	500	80	2.4	2.2	3553	[66]
8.9	skin	CO_2	500	90	2.4	1.8	4317	[66]
8.10	industrial wastes	CO_2	300	60	0.59	17.8	177.8	[54]
8.11	industrial wastes	Ethane	300	60	0.27	10.9	432.2	[67]

Equilibrium calculations: lycopene solubility - Aiming at a better disclosure of the lycopene affinity to carbon dioxide, equilibrium calculations based on the Peng-Robinson EoS were performed following the method described in section 8.2.3 (Eqs. (8)-(18)). The necessary properties for these estimations are presented in Table 8.12, being part of them reported for

the first time in the literature. The main objective of these calculations was the interpretation of the SFE data under analysis in the following sections.

As far as lycopene solubility is concerned, Figure 8.18 plots ratios of this variable in relation to a reference condition arbitrarily defined as 300 bar and 70 °C, which is linked to the minimum values of $P-T$ operating conditions selected in our economic study. As a result, the graphed surface of solubility ratio unveil how lycopene dissolves in supercritical CO_2 (SC-CO_2) for pressures up to 500 bar and temperatures up to 90 °C in relation to the reference condition.

Table 8.12 – Properties necessary for the estimation of the lycopene solubility in SC-CO_2.

Property	Value	Ref.
M (g mol^{-1})	456.7	-
V_i (cm^{3}mol^{-1})	415.7	[68]
T_m (K)	565.15	[69]
T_b (K)	801.19	This work
T_c (K)	949.07	This work
P_c (bar)	11.9	This work
V_c (cm^{3}mol^{-1})	1527.0	This work
w (Pitzer acentric factor)	0.827	[70]
ΔS_m (J mol^{-1}K^{-1})	153.6	This work
ΔS_b (J mol^{-1}K^{-1})	91.6	This work
$\Delta C_{p\,m}$ (J mol^{-1}K^{-1})	153.6	This work
$\Delta C_{p\,b}$ (J mol^{-1}K^{-1})	-112.0	This work

Several insights may be stressed from Figure 8.18, and perhaps the most pertinent one relies on the degree of variation of lycopene solubility within the $P-T$ range considered: ratios can be as different as 1.0 (reference condition) and 16.7 (500 bar, 90 °C). From an individual variable perspective, changes in pressure or temperature affect significantly solubility, being the most significant jumps particularly for pressures equal or greater than 400 bar and temperatures from 80 °C on. Nevertheless, the most substantial increase of the lycopene solubility in SC-CO_2 is given by combined increase of pressure and temperature. Accordingly, while the lowest ratio is found for the minimum pressure and temperature (300 bar and 70 °C), the maximum solubility ratio is found for the maximum values of the $P-T$ variables, namely 500 bar and 90 °C.

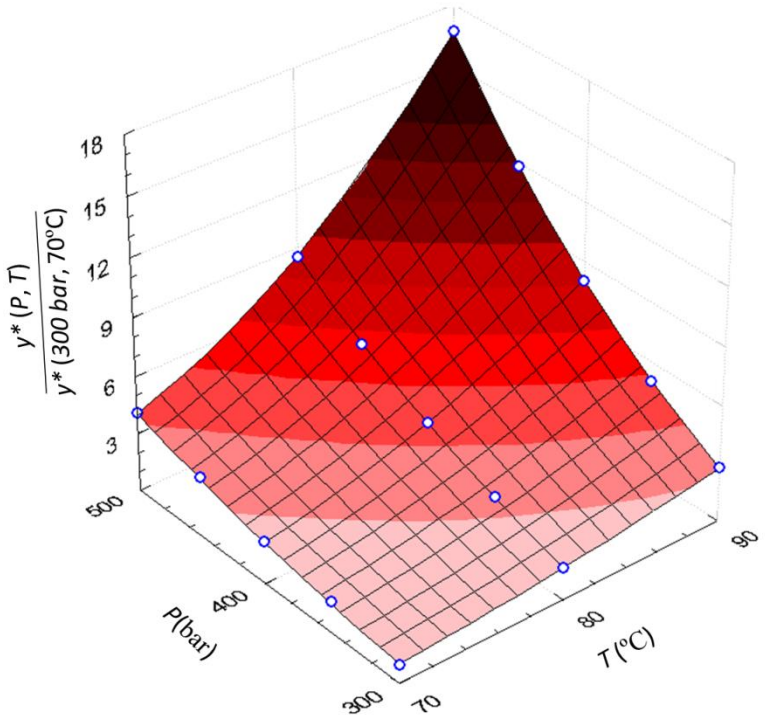

Figure 8.18 – Ratio between the lycopene solubility in SC-CO_2 at $P-T$ and its value at 300 bar and 70 °C (reference condition).

With respect to the temperature influence over the lycopene solubility, a worth noting feature should be referred. In this case, y_i^* is a monotonically increasing function of T, which means that the positive and exponential contribution of the lycopene vapour pressure dominates over the negative effect associated to the CO_2 density reduction that penalizes solvent capacity. With relation to the pressure influence, the calculated results are in agreement with expectations since increments on P increase the CO_2 density, always favoring solubility.

It is important to emphasize that the calculated solubility results are only valid for this binary system. The specific case of SFE of tomato residues comprise, among other compounds, the co-removal of fatty acids, which have been referred as enhancers of the lycopene pigment extraction from the vegetable samples [71]. Therefore, despite Figure 8.18 suggests great alterations in the affinity of lycopene to the SC-CO_2, within this range of pressure and temperature, the additional impact of other extractives can be of significant importance for an accurate thermodynamic understanding of the process.

Screening of the significant factors - The first important achievement of RSM comprises the screening of the relevant effects governing the SFE. Accordingly, Figure 8.19 presents a discrimination of the regression parameters ranked from lowest (top of the graph) to highest (bottom of the graph) influence upon the response (bottom of the graph). Since each regression parameter is related to one specific effect – linear, quadric or crossed – the interpretation of

Figure 8.19 goes beyond the mathematical meaning of the model, being suitable for the screening of these effects on the economics of the SFE process.

The two most impacting effects on COM are pressure and temperature, which influence the response in the most desirable direction, viz. the decrease of the lycopene production costs. Despite both P and T have contributions toward the lowering of COM, the pressure is quite more influential, with an impact 1.3 times greater than that of temperature. In light of the major influence of these variables, one should refer the great agreement between these results and those shown in Figure 8.18 for the solubility of lycopene in SC-CO_2.

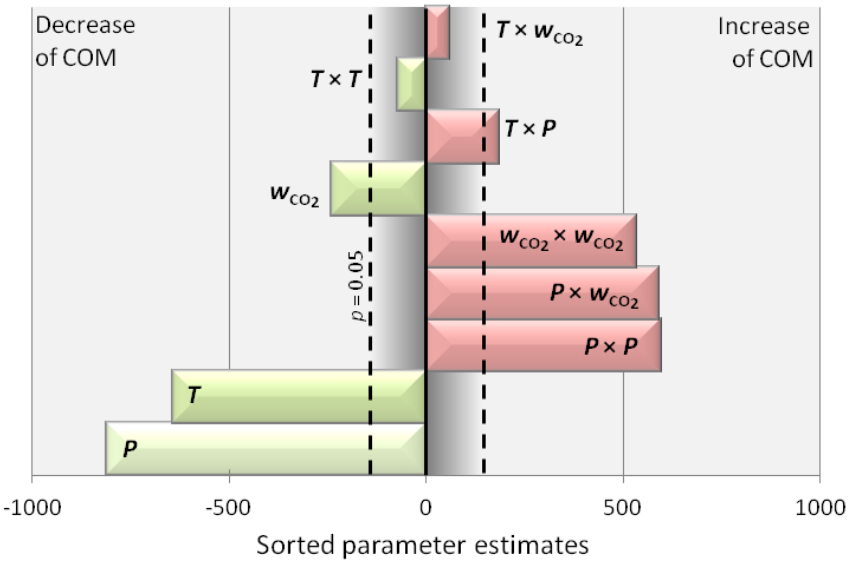

Figure 8.19 – Statistical impact of the different factors and interactions upon the COM response. Bars inside the dashed region are not statistically significant with 95 % confidence level.

The third most influential effect on $\mathrm{COM_{oil}}$ is the square of the pressure. Being a positive contribution, this effect leads to a curvature with tendency to exhibit a minimum zone. Nevertheless, according to Figure 8.19, the $P \times P$ effect is about 36 % weaker than the linear impact of P. For this reason, the parabolic profile imparted by the quadratic term is softened by the expressive linear dependence on P.

The synergistic combination of pressure and spent mass of CO_2 ($P \times w_{CO_2}$) is the fourth most important effect on COM, exhibiting a similar impact to that of $P \times P$ in terms of magnitude and trend. Taking into account that the spent CO_2 is proportional to the extraction time ($w_{CO_2} \propto t_{ext}$), both P and w_{CO_2} are naturally interlinked since preferable COM values are obtained for lower extraction times when higher pressures are used, or higher extraction times if pressure is kept in low solubility regions. With relation to the positive contribution to COM, note that t_{ext}

or w_{CO_2} influences directly the costs associated to the cycles of operation due to make-up CO_2 and biomass pretreatment. Besides, whenever the extraction tends to the maximum yield, any increment of t_{ext} or w_{CO_2} is counterproductive as the additional solute removal is low while the operating costs remain the same. Accordingly, a trade-off between these costs and lycopene production enhancement defines the preferable extraction time. In conclusion, considering that a proper selection of both P and w_{CO_2} is key to boost the SFE productivity and economic performance, there is no surprise about the significant impact of the $P \times w_{CO_2}$ interaction shown in Figure 8.19.

Despite the linear w_{CO_2} effect is relevant *per se*, its square, $w_{CO_2} \times w_{CO_2}$, is even more significant. Such parabolic behaviour reflects the trade-off that is inevitably established for this factor: i) During the first period of extraction, the extension of w_{CO_2} (i.e. t_{ext}) may be explored with interest as it increases the extraction yield proportionally. ii) Nonetheless, when the biomass is getting exhausted, increasing w_{CO_2} is counterproductive as the extraction rate starts to be controlled by intraparticle diffusion.

With regard to the seventh significant effect, the $T \times P$ interaction is only slightly beyond the threshold limits of 5 % marked in Figure 8.19, thus its influence on COM response is very soft in comparison to the previous ones. With relation to the remaining effects, the 95 % confidence level analysis pointed $T \times T$, and $P \times w_{CO_2}$ as not significant to explain COM variations. Hence these terms were purged from the original RSM regression, being the data refitted to 6 parameters. The reduced and uncoded final model holds a determination coefficient $R^2 = 0.939$ and an adjusted determination coefficient $R^2_{adj} = 0.923$. It is given by:

$$\begin{aligned} \mathrm{COM} = {} & 2393.6 - 643.13\left(\frac{T-80}{10}\right) - 809.92\left(\frac{P-400}{100}\right) - 238.69\left(\frac{w_{CO_2}-62.5}{37.5}\right) \\ & + 587.77\left(\frac{P-400}{100}\right)^2 + 533.20\left(\frac{w_{CO_2}-62.5}{37.5}\right)^2 \\ & + 594.57\left(\frac{P-400}{100}\right)\left(\frac{w_{CO_2}-62.5}{37.5}\right) + 182.09\left(\frac{T-80}{10}\right)\left(\frac{P-400}{100}\right) \end{aligned} \quad (28)$$

It is worth noting that R^2_{adj}, that takes into account both R^2 and the degrees of freedom, is similar to its corresponding R^2. It is known that when R^2_{adj} and R^2 differ considerably the model is prone to include nonsignificant terms, which was not our case.

Analysis of significant effects - Owing to the confirmation of pressure and temperature as the major sources of influence upon COM, four surface graphs were plotted in Figure 8.20 to analyse the performances of COM in the edge P and T conditions.

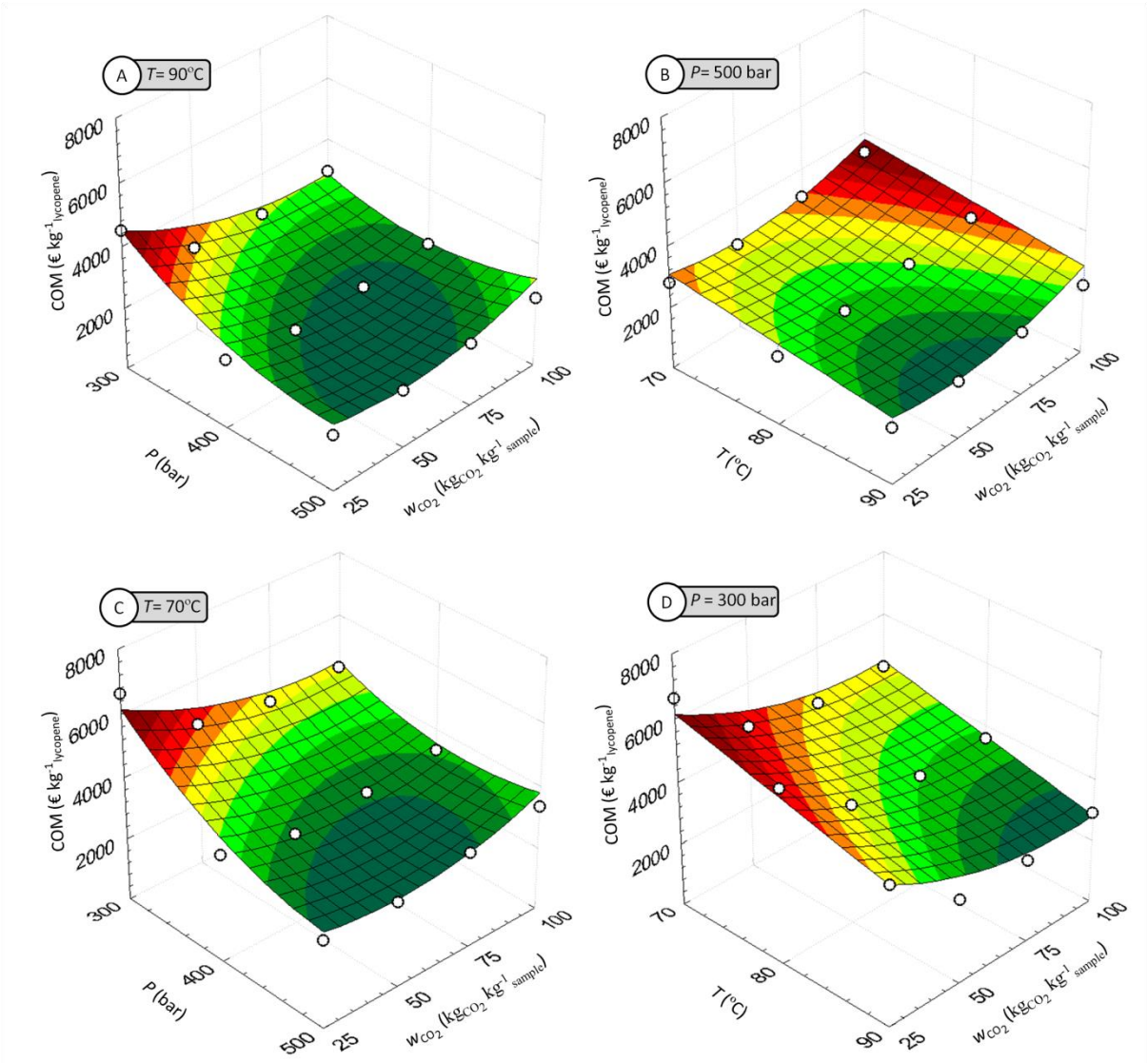

Figure 8.20 - COM values as function of (A) spent mass of CO_2 and pressure for T = 90 °C, and (B) spent mass of CO_2 and temperature for P = 500 bar. Points, experimental data; surfaces, Eq. (28).

In the range of $P - T - w_{CO_2}$ studied, the COM values vary from 1.8 to 6.6 k€ per kilogram of lycopene produced, which is a wide margin of variation that reinforces the importance of a correct selection of the SFE operating conditions. The lowest COM values were attained when a conjugation of highest P, highest T and lowest w_{CO_2} was observed (see Figures 8.20A or 8.20B). On the other hand, the most expensive operation arose for a combination of lowest P, lowest T and lowest w_{CO_2}, i.e. 300 bar, 70 °C and 25 $kg_{CO_2} kg_{sample}^{-1}$ (see Figures 8.20C or 8.20D).

When the plot of Figure 8.20A is inspected carefully (T = 90 °C), not only the substantial influence of P to decrease COM becomes clear, but also its linear/quadratic behavior in

different w_{CO_2} regions is evident: at low extraction times ($w_{CO_2} = 25\ kg_{CO_2} kg_{sample}^{-1}$), COM decreases slightly nonlinearly as pressure increases; on the other hand, at higher extraction times ($w_{CO_2} = 100\ kg_{CO_2} kg_{sample}^{-1}$), the quadratic influence of pressure overcomes the linear effect discussed above, leading to a minimum between 400 and 500 bar.

The plot in Figure 8.20B, for the highest pressure ($P = 500$ bar), allows a visual confirmation of the temperature influence upon COM, namely a negative linear impact that is roughly identical for all w_{CO_2} values considered. This was expected in advance since Figure 8.18 highlights that the lycopene solubility is very positively sensible to temperature at high pressures, which means that the vapor pressure increment dominates over the CO_2 density decrease [23,35].

Despite representing less favorable COM situations, the plots of Figures 8.20C and 8.20D are useful to reinforce the chief role played by pressure. In fact, at $T = 70$ °C (Figure 8.20C) some COM values are still competitive (e.g., values between 2.7 and 2.8 k€ $kg_{lycopene}^{-1}$), but only near 500 bar. The importance of high pressures to ensure low costs of manufacturing becomes evident through Figure 8.20D, which is plotted for 300 bar. In comparison to the remaining three graphs, the relative high position of this surface is markedly evident.

Optimum COM conditions - Independently of the existence of a single minimum in the COM function, it is desirable to detach a region of low costs of manufacturing since we are dealing with a natural biomass. For this reason, the four most interesting experimental points of our COM optimization study were picked and plotted in Figure 8.21 for more careful discussion. These points range only from 1.8 and 2.0 k€ $kg_{lycopene}^{-1}$, which represent a variation of 10 % between the lowest (500 bar/90 °C/$25\ kg_{CO_2} kg_{sample}^{-1}$) and the highest (400 bar/90 °C/$75\ kg_{CO_2} kg_{sample}^{-1}$) COM value. If the economic assessment of this SFE process is exclusively focused on the COM response, one neglects for sure the importance of annual production, which will be a decisive indicator in this case. In order to tackle this issue, the lycopene annual production is plotted in Figure 8.21 overlapped to the corresponding COM values.

When the lycopene production of the four most attractive COM datapoints are compared, one discloses that the same SFE unit produces annually between 1731 and 4316 $kg_{lycopene}$, which represents a global variation of 249 % for 10 % of COM reduction. Fortunately the operating conditions for the lowest COM (i.e., 500 bar/90 °C/$25\ kg_{CO_2} kg_{sample}^{-1}$) are also the same for the highest productivity, which is very promising for an eventual commercial application. In the case of Runs 8.9 (second bar) and 6 (third bar), both COM and productivity are equivalent, but in Run 8.6 (fourth bar) the productivity dropped to 1731 $kg_{lycopene}\ year^{-1}$ while the COM is practically the same. The key aspect behind these insights is the extraction time, which is also appended to Figure 8.21 (values between 1.1 and 2.5 h), as lower times increase the number of processed batches. Notwithstanding being only the fourth most important effect for COM, extraction time (through w_{CO_2}) is of utmost importance when productivity is assessed. In

conclusion, Run 8.9 with $w_{CO_2} = 25\ kg_{CO_2}kg_{sample}^{-1}$ ($t_{ext} = 1.1$ h) is in fact linked to the best SFE operating conditions.

Owing to the approach followed in this work, where COM analysis is combined with a statistical optimization method (RSM), it was possible to determine an optimum COM value for each extraction curve considered. In this respect, Figure 8.22 presents the nine cumulative curves used in this work, in which the specific region covered by the economic analysis ($25\ kg_{CO_2}kg_{sample}^{-1} \leq w_{CO_2} \leq 100\ kg_{CO_2}kg_{sample}^{-1}$) is highlighted. Furthermore, the various optima found were also marked in Figure 8.22, with the objective to point out the best CO_2 consumption for each curve, and a dashed line linking them was also drawn. Despite the great resemblance between the extraction curves of Figure 8.22 for 400 and 500 bar, (in opposition to the performances observed at 300 bar), their minimum COM values still correspond to a w_{CO_2} difference of 13-28 $kg_{CO_2}kg_{sample}^{-1}$, which in turn imply extraction cycles 31-56 min longer in the case of $P = 400$ bar.

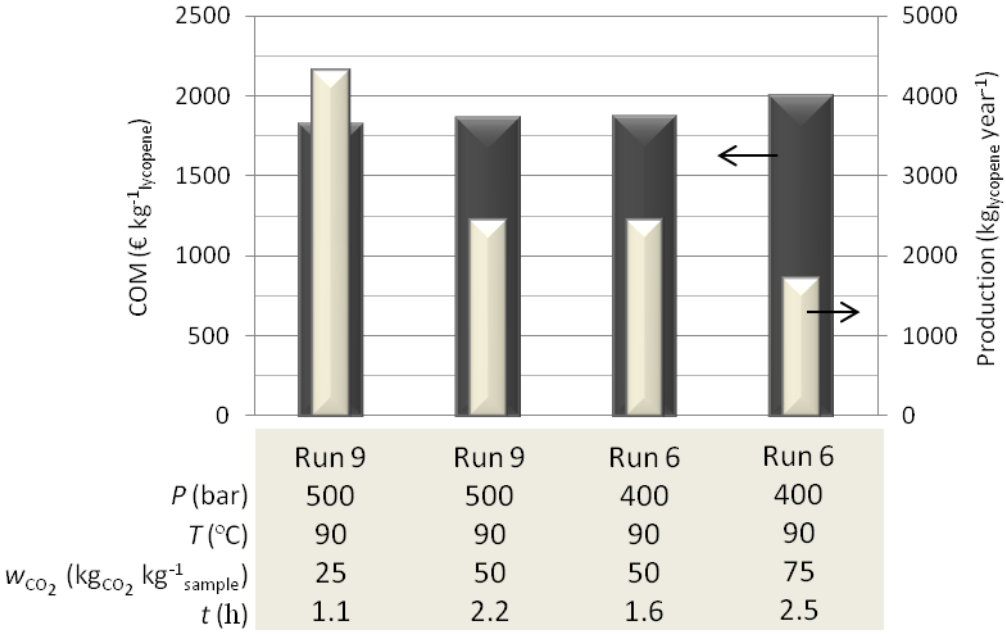

Figure 8.21 – Lowest COM values obtained from the optimization study, together with their corresponding annual production of lycopene.

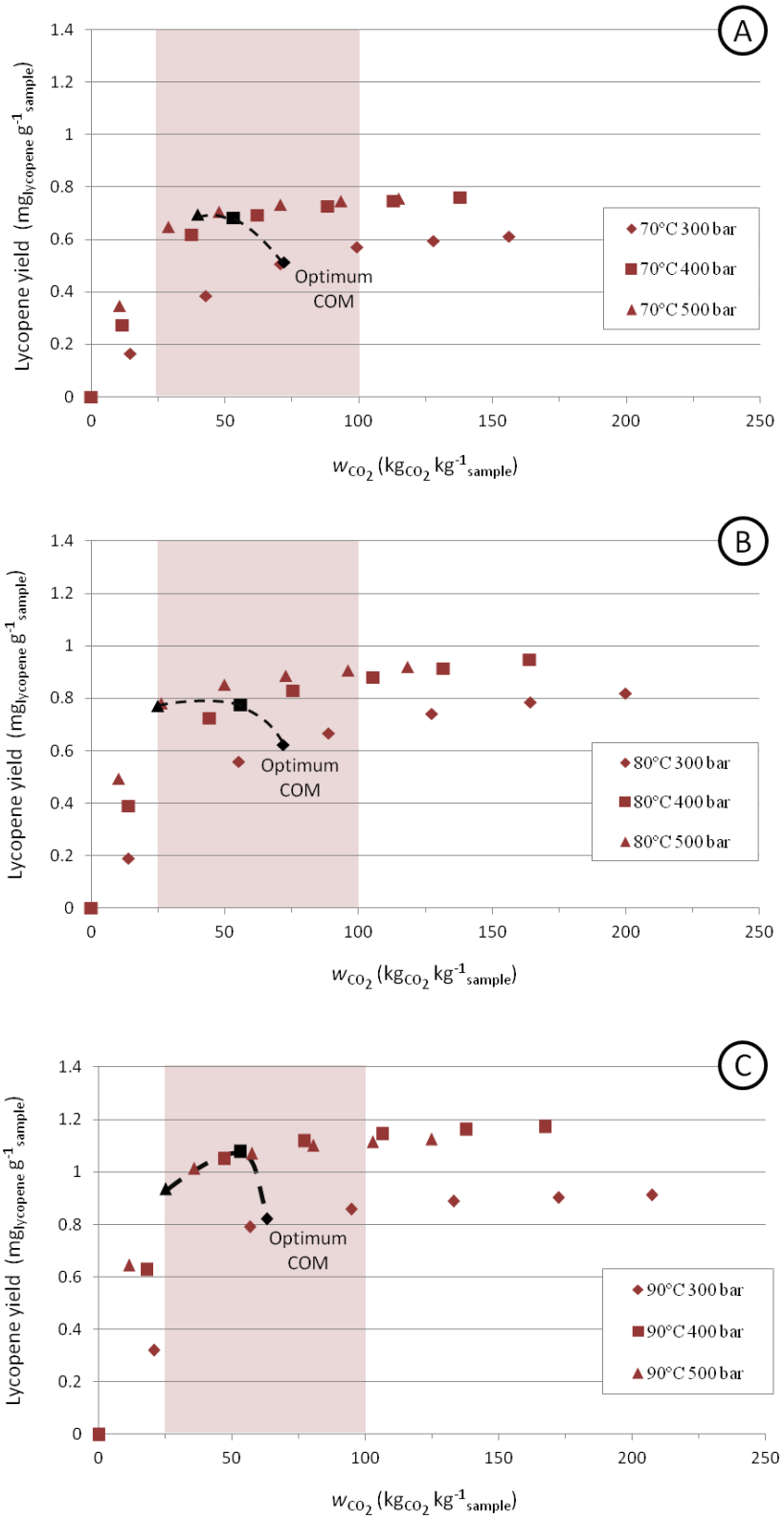

Figure 8.22 – Supercritical extraction curves, and line of optimum COM values. Runs 8.1-8.9 of Table 8.11 for tomato skins.

A noteworthy aspect of our approach concerns the scientific and reliable way it allows the detection of optimum COM values in extraction curves. Whenever two very defined periods of

extraction are present, which occurs in the SFE of edible oils [72-73], the best extraction time is easily determined empirically from the intersection of the tangent lines to both periods of extraction (e.g., [3, 52]). Nonetheless, if the first period of extraction is absent or if the plateau corresponding to the maximum extraction yield is not well defined, which happens here with the curves at 300 bar/70 °C (Figure 8.22A) and 300 bar/80 °C (Figure 8.22B), such empirical determination is not accurate or even unsuitable. Most notably, even in the most simple and evident case of edible oils cited above, the best operating time after an economic analysis can be changed from that originally determined from the method of straight lines intersection [1, 3]. Taking all these arguments into account, it may be emphasized that the methodology proposed in this work (RSM-COM) answers the core objective of identifying rigorously the best COM of a SFE process.

Supercritical ethane as an alternative to supercritical CO_2 - Even though carbon dioxide is the prevalent solvent for the SFE of vegetable biomass, several authors have devoted their research also to ethane. Examples of research works using supercritical ethane and vegetable raw materials are found for cocoa beans [74], Cupuaçu seeds [75], and orange peel oil [76].

Owing to the existence of a study on the SFE of tomato residues with SC-ethane, our economic analysis was extended to this alternative. Accordingly, Nobre et al [54, 67] measured extraction curves at fixed $P-T$ conditions (300 bar and 60 °C) using SC-CO_2 and SC-ethane in the separation of industrial tomato wastes (see Table 8.11). Based on their results, the optimum extraction times were determined, along with COM and productivity, being the respective results listed in Table 8.11 and plotted in Figure 8.23. As far as we know, a comparison between these two solvents from an economic perspective for the same application has not been reported in the literature.

The main insight from the economic analysis is suggested by the larger bars of Figure 8.23A, which stand for the COM of each process: the SC-ethane option leads to COM = 10900 € $kg^{-1}_{lycopene}$ against 17800 € $kg^{-1}_{lycopene}$ for the SC-CO_2. Such ample magnitude recommends a further inspection on the reasons for this, for which the discrimination of the COM parcels provided in Figure 8.23B can bring some light. Accordingly, when four parcels of COM (see Eq. (1) and Table 8.5) are compared in an annual basis, it becomes clear that working with SC-ethane is in fact more expensive. While labor cost (COL) is the same in both cases, the carbon dioxide process is considerably cheaper in terms of investment (FCI), utilities (CUT) and raw material (CRM) annual costs.

As far as the investment cost is concerned, the penalization of unit price for ethane due to being a hazardous solvent is visible in Figure 8.23B, despite the small magnitude of the FCI bars in

comparison to the other parcels. The fact that the explosion proof seems not to be an important hindrance to the economic performance of the process, it becomes a remarkable insight favoring the utilization of inflammable solvents (or even cosolvents) such as ethane, propane, ethanol, etc., among SFE technology.

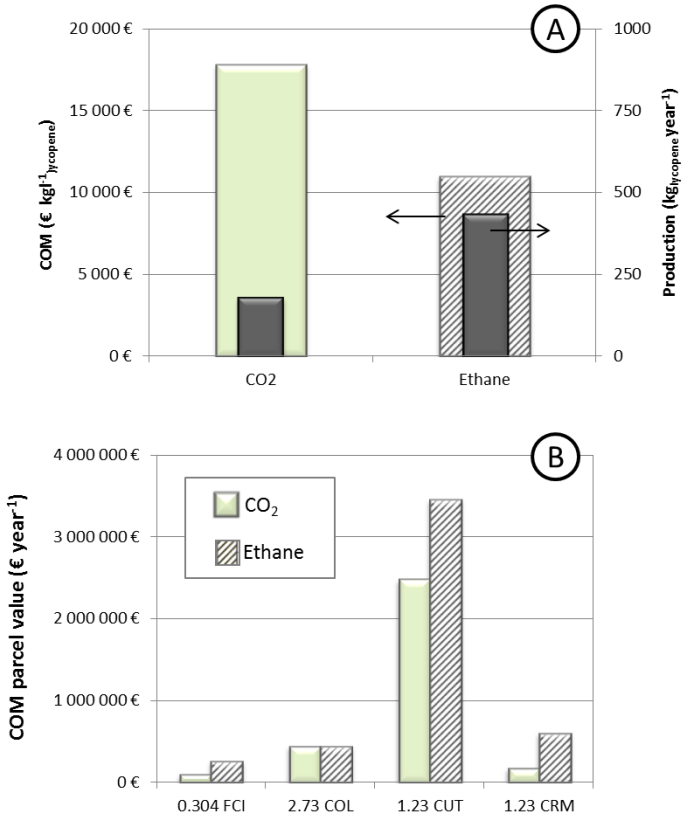

Figure 8.23 – Supercritical fluid extraction using carbon dioxide or ethane as solvent: (A) COM values and annual lycopene production; (B) structure of the different COM parcels (see Eq.(1)) for a year time basis. Operating conditions: CO_2 (300 bar, 60 °C, t_{ext} = 1.5 h), ethane (300 bar, 60 °C, t_{ext} = 1.0 h).

It is worth noting that both CUT and CRM parcels are strongly linked to the extraction time and that the latter is quite distinct in both cases: t_{ext} = 1.0 h for ethane and t_{ext} = 1.5 h for CO_2. As consequence, the number of batches in the case of ethane is 50% greater, thus requiring higher biomass pretreatment costs (included in CUT). This is the key factor for the higher CUT parcel computed for ethane, and it should be credited as such because the sole operation (pumps and heating/cooling requirements) using SC-ethane is, in fact, cheaper than that working with SC-CO_2. It is the higher volume of processed raw material in the case of SC-ethane that makes its CUT parcel 1.4 times higher.

In what concerns the higher CRM value, the number of annual batches (through extraction time) plays once again a decisive role in the performance observed for this parcel. Shorter

processes imply more solvent lost in each full decompression from the minimum pressure of the system (i.e. 45 bar, see Table 8.5) to ambient pressure. In the case of ethane, not only the frequency of full decompressions is greater, due to the shorter cycles of the extractor, but also the amount of ethane lost at 45 bar is greater due to its higher density in comparison to CO_2 under the same pressure. On top of this, the higher cost of ethane in relation to carbon dioxide (941 *vs.* 800 € ton^{-1}) contributes to the higher value exhibited by CRM parcel in the ethane case.

Attending to the two previous paragraphs, it is clear that the ethane advantage cannot arise from savings at annual costs level. Since the reported COM values are ratios between costs and lycopene production, in an annual basis, the answer must lie on the denominator. Consequently, Figure 8.23.A answers to this argument through the thin bars, which represent the annual production in both cases: the SC-ethane provides an annual production 2.4 times greater than CO_2, which is high enough to significantly decrease COM.

As a final remark to this comparative solvent analysis, it should be referred that the optimization presented and discussed above revealed that the performance of CO_2 at 300 bar is considerably worse than that at 500 bar in terms of COM values. Also, it should be taken into account that the tomato residues employed in both studies are distinct: tomato skins for the Run 8.1-8.9, and tomato industrial wastes (a mixture of pulps, skins, seeds) for Runs 10-11.

While a proper comparison between ethane and carbon dioxide demands a larger and common range of operating conditions, the particular pressure and temperature used in this study is *a priori* technically unfavorable to carbon dioxide. Despite more competitive operating conditions for SC-CO_2 could lead to other conclusions, the available data for this economic assessment suggests that ethane is advantageous for the SFE of lycopene from industrial tomato wastes, even considering a three-fold more expensive price of the SFE unit due to the explosion proof requirement imposed by ethane.

8.3.4 STUDY IV – SFE OF GAC FRUIT [5]

Brief description of the SFE curves - The RSM-COM optimization study carried out in this work was centered in the experimental data provided by Tai et al. [77], who measured SFE curves under different P,T and $Q_{CO_2}/w_{\text{biomass}}$ conditions. The $Q_{CO_2}/w_{\text{biomass}}$ is the ratio of CO_2 mass flow rate to biomass weight, which is equivalent to a weight hourly space velocity (WHSV); it will henceforth be called specific CO_2 flow rate. Their experiments were performed in a 0.056 L SFE apparatus, using 5 g of gac aril powder in each individual assay. As far as the SFE of carotenes from gac aril are concerned, the extracts content was determined by

absorbance at a wavelength of 450 nm, using β-carotene as standard. This method is described in greater detail in the work of Chuang and Brunner [78].

Table 8.13 summarizes the experimental conditions ($P, T, Q_{CO_2}/w_{biomass}$) of the extraction curves used in this assay (Runs 8.12-8.20), and presents our calculated best production costs for gac oil and carotenes in each run, within the 0.5-2.0 h time frame studied, as well as the respective production under that conditions.

Screening effects and optimization of conditions for COM_{oil} values - The first stage of the work comprised the screening of the linear, quadratic and crossed effects o P, T and t regarding COM_{oil}, aiming at (i) ranking the significant ones according to their relative impact, (ii) discarding the irrelevant ones, (iii) disclosing the positive or negative influence of each effect on COM. Figure 8.24 presents a Pareto chart with the screening results regarding COM_{oil}.

Pressure is the most influential factor on COM_{oil}, either individually (P), or crossed with temperature ($P \times T$) and with time ($P \times t$). Contrarily to the former terms, increments of $P \times t$ increase COM_{oil} values (undesirable effect), a behaviour that is also observed for the quadratic contribution of time ($t \times t$). In addition, the latter is the second most influent among the contributions studied. On the other hand, the screening shows that ($T \times t$) and ($T \times T$) are not statistically significant for COM_{oil}.

Upon an inspection of the three most important bars of the Pareto chart plotted in Figure 8.24, it is evident the prevailing importance of P and t factors, whether independently or combined, in relation to temperature. In great resemblance to what was observed for SFE of lycopene from tomato residues using RSM-COM approach [4], the linear effect of P assumes a dominant role on the decrease of COM_{oil} (desirable effect), and therefore higher values of pressure cheapen the process. Despite high pressures represent essentially higher utilities costs, P plays a chief role in the extraction rate and maximum yield of the SFE curves, being able to enhance process productivity and thus decrease COM_{oil}, as the latter is the ratio between the annual costs and the oil amount produced in the same time frame.

With regard to the effect of time, its quadratic term ($t \times t$) is only slightly less influent than P. Being a term of second degree it implies the profiles along t are quadratic and, besides this, the positive sign associated to this parcel reflects a curvature profile with a minimum COM_{oil} value (positive second derivative). This trade-off result is rather comprehensible since extraction time affects the process economics through two antagonistic sides. If on the one hand it establishes the number of batches processed each year and thus raw material drying and also make-up CO_2 costs, on the other hand it influences productivity, namely the attained extraction yields, as process kinetics is different for every (P, T) pair chosen. For the discussed reasons, one can

Table 8.13 – Extraction curves considered and some results in the 0.5-2.0 h time frame: experimental conditions, calculated minimum $\mathrm{COM_{oil}}$ and $\mathrm{COM_{carotenes}}$ values, and the respective annual productions. Data taken from [77].

Run	Scope of the study			Experimental conditions			Oil extraction		Carotenes extraction	
	$\mathrm{COM_{oil}}$ optimization	$\mathrm{COM_{carotenes}}$ calculation	$Q_{CO_2}/W_{biomass}$ analysis	P (bar)	T (°C)	$Q_{CO_2}/W_{biomass}$ ($kg_{CO_2}\ h^{-1} kg_{biomass}^{-1}$)	Min. $\mathrm{COM_{oil}}$ (€ kg_{oil}^{-1})	Production* ($ton_{oil}\ year^{-1}$)	Min. $\mathrm{COM_{carotenes}}$ (€ $kg_{carotenes}^{-1}$)	Production* ($kg_{carotenes}\ year^{-1}$)
8.12	✓			200	40	70	11.99	71.99	-	-
8.13	✓			400	40	70	8.11	110.73	-	-
8.14	✓	✓		200	50	70	15.05	50.77	2560	280
8.15		✓		300	50	70	8.00	109.86	930	950
8.16	✓	✓	✓	400	50	70	7.98	112.40	790	1130
8.17	✓			200	60	70	21.90	32.59	-	-
8.18	✓	✓	✓	400	60	70	7.98	111.81	1160	770
8.19			✓	400	60	50	8.51	101.47	-	-
8.20			✓	400	60	90	8.31	111.40	-	-

*under the respective minimum $\mathrm{COM_{oil}}$ or $\mathrm{COM_{carotenes}}$ conditions;

expect that an optimum intermediate extraction time should be found for $\mathrm{COM_{oil}}$ for each (P,T) considered.

As far as temperature is concerned, the studied range of 40-60 °C belongs to the typical T values used in SFE of vegetable biomass [1], and perhaps its lower impact on results (T bars vs. P and/or t bars) reflects a more appropriate choice of this variable *a priori*. Like t, temperature can affect the process in both costs and productivity fronts. However, the screening results reveal that the individual influence of temperature is as important for $\mathrm{COM_{oil}}$ as the covariation of T and P. In fact these two terms (T and $P{\times}T$) null each other in terms of the way they impact $\mathrm{COM_{oil}}$.

Based on the Pareto chart, the negligible contributions for a significance level of 0.05 were discarded from the statistical modeling, namely $T{\times}t$ and $T{\times}T$ terms. The final reduced uncoded model is given by:

$$\begin{aligned}\mathrm{COM_{oil}} = {} & 0.02714{\times}P + 1.198{\times}T - 41.44{\times}t + 0.05755 \\ & {\times}P{\times}t - 0.003030{\times}T{\times}P + 8.738{\times}t^2 + 6.560\end{aligned} \tag{29}$$

where the units of $\mathrm{COM_{oil}}$, $P,T,$ and t are € $\mathrm{kg_{oil}^{-1}}$, bar, °C and h, respectively, and for which the coefficient of determination is $R^2 = 0.928$ and the adjusted coefficient of determination is $R^2_{\mathrm{adj}} = 0.890$.

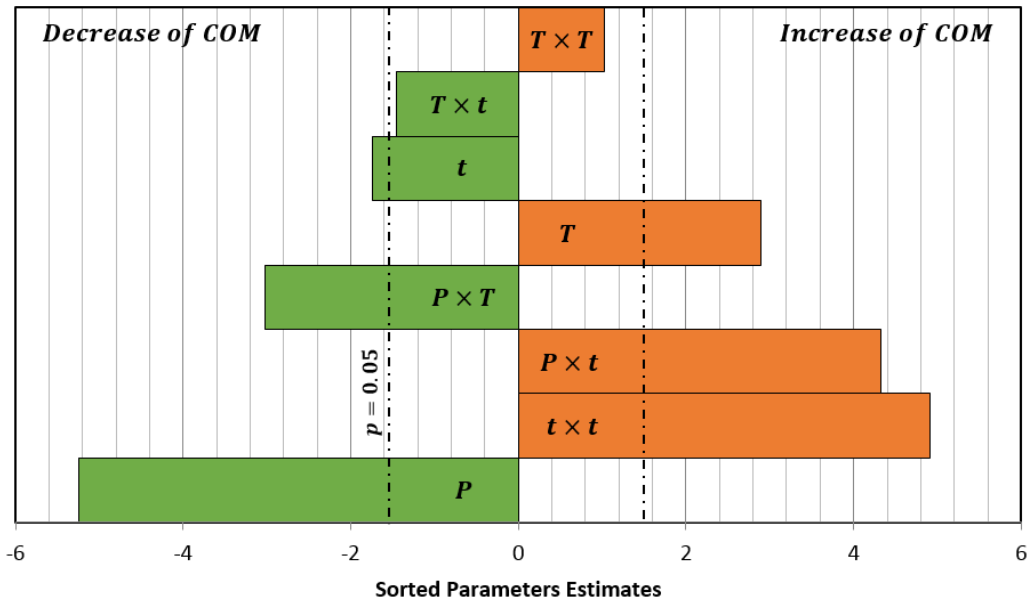

Figure 8.24 – Statistical impact of the different factors and interactions upon $\mathrm{COM_{oil}}$ response. Bars inside the dashed region are not statistically significant for a 95% confidence interval.

Figure 8.25 presents four response surfaces obtained by Eq. (29), where the importance of a good selection of (P,T,t) conditions is quite evident from the relative degree of variation

observed between COM_{oil} results. Taking into account that the same COM_{oil} axis scale was used for each plot, the rather different COM_{oil} values in each graph can be visually compared. Accordingly, the highest COM_{oil} value is attained for lowest pressure, shortest time and maximum temperature (viz. 200 bar, 0.5 h, and 60 °C), where $COM_{oil} = 41$ € kg_{oil}^{-1} (see Figures 8.25B and 8.25C). On the other hand the minimum value of COM is placed at the highest P, intermediate t and maximum T (viz. 400 bar, 1 h, and 60 °C) where $COM_{oil} = 8$ € kg_{oil}^{-1} (see Figures 8.25B and 8.25D).

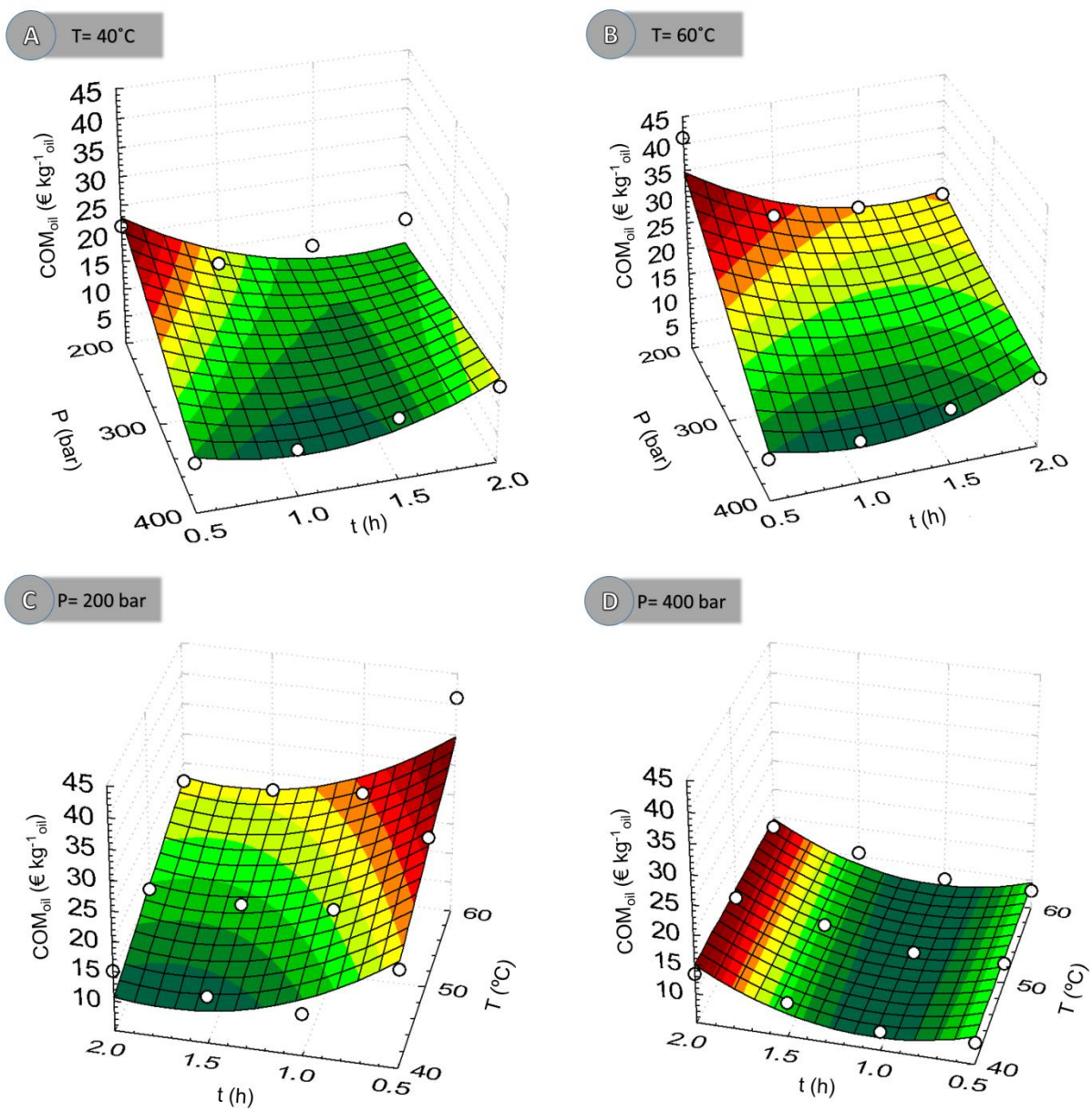

Figure 8.25 – COM_{oil} as function of (A) P and t at T= 40 °C; (B) P and t at T= 60 °C; (C) T and t at P = 200 bar; (D) T and t at P = 400 bar. Points represent COM_{oil} values computed from experimental data; surfaces are calculated by Eq. (29).

Looking at $\mathrm{COM_{oil}}$ evolution along P axes, decreasing ramp profiles towards higher P values are noticeable in Figures 8.25A and 8.25B. These are visual confirmations of the larger bar of the Pareto chart of Figure 8.25 regarding the impact of P and $P{\times}T$. Hence, under the most favorable pressure (400 bar; Figure 8.25D), the variation of $\mathrm{COM_{oil}}$ is narrower. In fact, in this plot the maximum $\mathrm{COM_{oil}}$ worths 13 € $\mathrm{kg_{oil}^{-1}}$ for $t = 2$ h and $T = 60°\mathrm{C}$, and the minimum is 8 € $\mathrm{kg_{oil}^{-1}}$ for $t = 1$ h and $T = 60$ °C. This result is naturally associated to the expected increment of CO_2 solvent power with increasing pressure. According to the works of Giddings and collaborators [79-80], the following simple expression may be used to estimate the solvent power of carbon dioxide via its Hildebrand solubility parameter (δ):

$$\delta = 1.25 P_c^{1/2} \left(\rho_r / \rho_{r,eb} \right) \tag{30}$$

where P_c is critical pressure, ρ_r is reduced density, and $\rho_{r,eb}$ is reduced density at normal boiling point. It is clear that high pressures give rise to high densities, and thus to high solubilities.

With reference to the graphical behavior of $\mathrm{COM_{oil}}$ *vs.* t, the expected quadratic profiles are noticeable in any of the four surfaces of Figure 8.25, with minimum $\mathrm{COM_{oil}}$ values located at $t = 1$ h whatsoever the $P - T$ values considered. On the other hand, upon inspection of maximum $\mathrm{COM_{oil}}$ regions of each graph, one can disclose that they rely on combinations of extraction time and pressure, which is in agreement with the $P{\times}t$ contribution (see Figure 8.25). While under low P values the maximum $\mathrm{COM_{oil}}$ is observed at shorter times ($t = 0.5$ h), the increase of P leads to maximum $\mathrm{COM_{oil}}$ values being relocated to the regions where extraction cycles have 2 h of duration (see Figures 8.25C and 8.25D). The results are in agreement with our expectations because: (i) at low pressure the solvent power of CO_2 is lower, therefore, increasing the extraction time becomes benefic for the process; (ii) at high pressure the solubility is higher, which means there is no gain when extraction time is continuously raised, because biomass is quickly exhausted. Time is capital during the first period of extraction, but essentially adverse in economic terms in the second period. This is particularly evident in the case of SFE of edible oils [72, 81-85].

For the assessment of the graphical influence of temperature, it is worth noting that this factor has an important impact when the operation is set at the lowest pressure (i.e. out of the preferable P), but becomes almost of negligible importance at maximum P. In this sense, upon holding constant the best pressure (400 bar), and allowing variations on T and t (see Figure 8.25D), the reduced individual influence of T is promptly perceived (Figure 8.25D). On the contrary, Figure 8.25C evidences the importance of T at $P = 200$ bar, particularly when short cycles are considered. These observations are easily interpreted, because at high pressure the influence of temperature upon oil solubility is weaker. At 200 bar, δ ranges from 7.3 to 6.3 $\mathrm{MPa^{0.5}}$, for T between 40 and 60 °C, while at 400 bar the previous range is only 8.3 – 7.7 $\mathrm{MPa^{0.5}}$.

As a final remark, it is pertinent to refer that gac oil is currently traded at 5-200 € kg_{oil}^{-1} [86], depending on its quality. Hence, considering that a SFE based process provides a product with high quality and a green label, COM_{oil} values ranging from 8 to 41 € kg_{oil}^{-1} are rather compatible with current market prices. Nevertheless, optimization may be of decisive importance to ensure the economic robustness of the process.

Sensitivity analysis of COM_{oil} to specific flow rate - Considering that the SC-CO_2 flow rate is one of the most important parameters to specify within SFE technology (it affects not only the expenses of running the process but also productivity) it is of major relevance to study the overall dependence of COM_{oil} on $Q_{CO_2}/W_{biomass}$. Hence, a sensitivity analysis of the impact of the specific flow rate on COM_{oil} was performed at 400 bar and 50 °C for $Q_{CO_2}/W_{biomass}$ values of 50, 70 and 90 $kg_{CO_2}\ h^{-1}\ kg_{biomass}^{-1}$, and using the same extraction times considered above, i.e. 0.5, 1.0, 1.5, 2.0 h. The reason for using T=50 °C rather than 60 °C (the best T) dues to the availability of experimental data for the proposed study (see Table 8.13). Nonetheless, the conclusions are the same because, as has been shown, the influence of temperature is very weak at 400 bar.

Figure 8.26 represents the evolution of the COM_{oil} with extraction time for the specific flow rates analysed. For 50 $kg_{CO_2}\ h^{-1}\ kg_{biomass}^{-1}$, the trend is clearly convex with a minimum for t=1.0 h. In contrast, for both 70 and 90 $kg_{CO_2}\ h^{-1}\ kg_{biomass}^{-1}$, the minimum COM_{oil} is still observed at 1.0 h, but both profiles are essentially monotonic functions. The highest production cost is observed at t = 2.0 h and $Q_{CO_2}/W_{biomass}$ = 90 $kg_{CO_2}\ h^{-1}\ kg_{biomass}^{-1}$, reaching 13 € kg_{oil}^{-1}. On the other hand, the lowest COM_{oil} is found for the ($P, T, Q_{CO_2}/W_{biomass}$) conditions reported in before, i.e. 400 bar, 1.0 h and 70 $kg_{CO_2}\ h^{-1}\ kg_{biomass}^{-1}$, amounting 8 € kg_{oil}^{-1}.

In order to evaluate theCOM_{oil} sensitivity to $Q_{CO_2}/W_{biomass}$ at distinct extraction times, it is necessary to recall that different t values imply different number of batches being processed by the SFE unit. The increase of this number is accompanied with larger CO_2 make-up costs (affecting the CRM parcel in Eq. (1)) and the utility-drying costs (CUT in Eq. (1)). As a result, decreasing t for fixed $Q_{CO_2}/W_{biomass}$ not only increases utilities consumption but also the costs of raw material. If, in turn, $Q_{CO_2}/W_{biomass}$ is changed instead of t, its increase affects the COM_{oil} only through an increase of the utilities consumption, due to pumping and heating/condensation of CO_2. Therefore, the combination of shorter t and higher $Q_{CO_2}/W_{biomass}$ values is expected to be the worst scenario for COM_{oil} attending to both CUT and CRM contributions. Nonetheless, since productivity also matters for COM_{oil} when expressed as € kg_{oil}^{-1}, these cost trends may be softened or sharpened due to the shapes of extraction curves.

As it is known, flow rate increments induce productivity enhancements only until a threshold limit, after which the SFE process becomes solely dependent on intraparticle kinetics. In fact,

such increments reduce the film resistance to mass transfer until vanishing it completely after a certain Biot number is attained. Remember $\mathrm{Biot} \equiv (k_\mathrm{f}\,\overline{d_\mathrm{p}})/D_\mathrm{eff}$, where k_f is the convective mass transfer coefficient, $\overline{d_\mathrm{p}}$ is the mean particle diameter, and D_eff is the effective diffusivity in the particle. While at fixed P and T the film resistance can be reduced by increasing $Q_{\mathrm{CO_2}}/W_\mathrm{biomass}$ (which increases k_f), the intraparticle kinetics relies on variables like particle size (diffusion length) and internal structure of the biomass (porosity and tortuosity, as a first approximation). Accordingly, the results for $Q_{\mathrm{CO_2}}/W_\mathrm{biomass}$ variations from 70 to 90 $\mathrm{kg_{CO_2}\,h^{-1}\,kg_{biomass}^{-1}}$ presented in Figure 8.26 reflect the said diminution of the film resistance importance in relation to internal limitations.

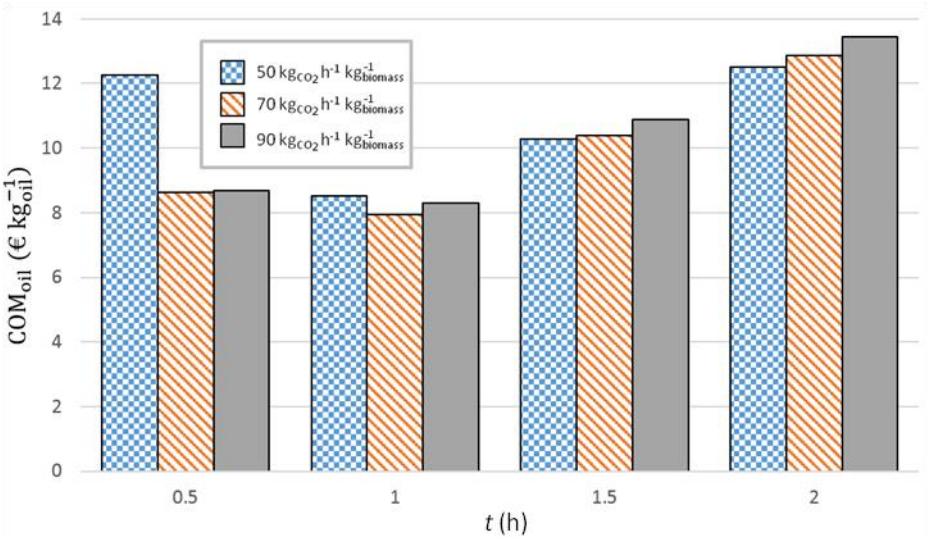

Figure 8.26 – Evolution of the $\mathrm{COM_{oil}}$ along time at P = 400 bar and T = 50 °C, for different specific flow rates.

Production costs of carotenes from gac aril - As gac fruit is known to have a high content of carotenes in its aril, a study on the cost of manufacturing with respect to these compounds was deemed worthy and pertinent.

Profiles of $\mathrm{COM_{carotenes}}$ along extraction time for different (P,T) conditions are plotted in Figure 8.27. Although each of the three variables must be taken into consideration in order to reach the optimum operating point (lowest $\mathrm{COM_{carotenes}}$), it is clear that P once again exhibits the highest impact upon the overall choice of process conditions, particularly under short cycle operation (t = 0.5 h) where it can increase $\mathrm{COM_{carotenes}}$ up to 12 times, under the same T (50 °C). Depending on the chosen combinations of (P,T,t), carotenes production costs can range from 755 $€\,\mathrm{kg_{carotenes}^{-1}}$ for 400 bar, 50 °C and 1.0 h , to 10900 $€\,\mathrm{kg_{carotenes}^{-1}}$, at 200 bar, 50 °C and 0.5 h.

Taking into account solely the contribution of pressure for the optimized t=1 h (obtained above regarding RSM-COM), the $\mathrm{COM_{carotenes}}$ between 300 and 400 bar worths 946 $€\,\mathrm{kg_{carotenes}^{-1}}$ and

755 $€\,kg^{-1}_{carotenes}$, respectively. This means that lowering the pressure by 100 bar implies a production of carotenes that is 25 % more expensive. In addition, out of the optimum extraction time zone, the economic gap between these two pressures modifies, particularly if the SFE cycles are made shorter. For instance, at $t = 0.5$ h the referred reduction of 100 bar imparts a 235 % more expensive process. For $t = 1.5$ and 2.0 h the variations are only 20% and 22 %, respectively.

Within the examination of $COM_{carotenes}$ for optimum (P,T) conditions (i.e. 400 bar and 50 °C), the trend along time is identical to the one observed previously in the study of the extraction of bulk gac oil. However, such trend is not observed in the case of $P = 200$ bar, for which maximum t is the preferable option, as it lowers $COM_{carotenes}$ up to 4 times in relation to $t =$ 0.5 h.

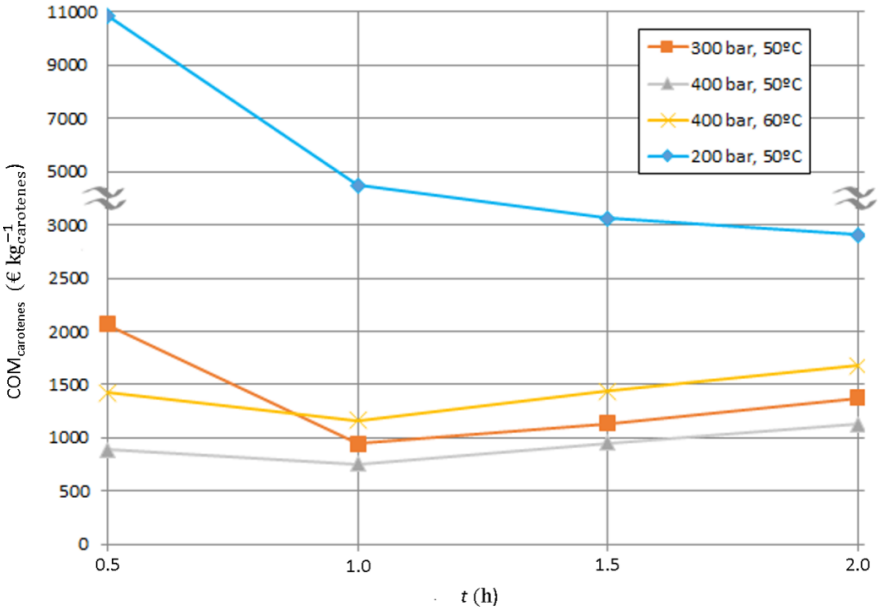

Figure 8.27 – $COM_{carotenes}$ along extraction time for different (P,T) conditions.

With reference to the impact of temperature on $COM_{carotenes}$, its contribution seems to affect the absolute values attained but not the trend along time. In this respect, one should point the similarity of the profiles attained at 400 bar/50 °C and 400 bar/60 °C. A noteworthy remark concerning temperature influence on the overall SFE process comprises the fact that the best (P,t) values for COM_{oil} (400 bar/60 °C) do not correspond to the preferable operating conditions to minimize the cost of manufacturing of carotenes: less 10 °C is preferable for a minimized $COM_{carotenes}$.

In the whole, the COM results regarding oil production and uptake of carotenes seem in this case to be almost synchronized (400 bar and 1 h, but T is the exception), which reinforces the role played by the optimization carried out in this study towards choosing adequate operating conditions in processes of this kind. Moreover, the production cost of 755 $€\,kg^{-1}_{carotenes}$ seems

not an unbearable economic hurdle at least considering reported quotations of lycopene and β–carotene (small scale purchasing reality), ranging from 10^4 to 10^5 € kg^{-1} for individual purities greater than 90 % [4, 87]. The most competitive $COM_{carotenes}$ achieved in this work provide enough economic margin to devise and match a posterior purification stage of the supercritical extracts of gac aril, which can be of chemical [88-89] or adsorptive [90] nature.

8.4 CONCLUSION

SFE of Moringa seeds – A techno-economic study encompassing the production of edible oil and an independent fraction of sterols from *Moringa oleifeira* seeds was accomplished using the RSM-COM approach. The integrated process comprehends the preliminary drying of the biomass, then its subcritical fluid extraction, and finally the separation of sterols from the bulk oil.

While temperature (30 °C) and flow rate (20 $kg\,h^{-1}$) remained constant in the study, but the pressure (P) and extraction time (t) conditions were optimized within the ranges of 150-350 bar and 1.3-3.4 h, respectively. The sterols purification was assessed through a simulation of a vacuum distillation (reported in the literature) using Aspen Plus®.

The statistical screening of effects showed that P is the variable with prevailing impact on the decrease of COM_{oil} values, and that time is important when crossed with pressure. Hence, the optima conditions for a minimized cost of manufacturing are 350 bar and 1.3 h, where COM_{oil}=2.76 € kg_{oil}^{-1} using a SFE unit comprising two extractors of 1 m^3 capacity.

Upon the inclusion of a downstream vacuum distillation stage, several cases were studied and the most profitable one comprises the sharing of human resources between the SFE (operating 7 days a week) and the distillation unit (operating 1 day a week), giving rise to an annual production of 558.9 tons of oil and 1.9 tons of sterols, and an estimated net income of 15.87 M€ $year^{-1}$.

In the whole, this study attests that the proposed integrated process for the coproduction of high quality edible oil and a mixture of sterols with 89.4 wt.% purity is feasible and benefits from labor cost synergies. The estimated positive economic performance of the process opens the way for further attempts to implement the biorefinery concept through a green technology such as sub/supercritical fluid extraction.

SFE of spent coffee grounds – The supercritical fluid extraction of spent coffee grounds (SCG) oil was studied in this work by measuring extraction curves at different conditions,

followed by oil characterization, modeling and economic analysis. Results were deeply compared with data from the literature. Under the range of experimental conditions covered, the final extraction yields lie within 0.61–0.81 of *n*-hexane Soxhlet values.

The obtained SFE oils are rich in linoleic and palmitic acids (44.5 and 37.5 %) with profiles comparable to Soxhlet results (44.7 and 37.4 %) and are in agreement with the values reported in the literature. Moreover the triacylglycerides profiles remain uniform along the supercritical extraction.

A preliminary economic evaluation involving two assays from the four experiments under analysis revealed that 300 bar/50 °C/30 kg_{CO2} kg^{-1}_{SCG} h^{-1} are the most advantageous operating conditions, independently of the unit arrangement considered. For a set-up of 3 beds of 1 m^3, the production evolves like 0–439–454–311 ton $year^{-1}$ for 0–0.7–2.0–3.0 h of extraction. If extraction time is held in 2 h, the cost of manufacturing (COM) is 2.4 M€ $year^{-1}$ and the process net income reaches 56 M€ $year^{-1}$, which is a very promising result.

Through a sensitivity analysis, it was shown that an accurate definition of the separator vessel pressure has a significant impact on COM value, and that a 25 bar difference in this parameter can lead to a COM increase of 18.2 %.

SFE of tomato residues – In this work the economics of the SFE of lycopene from tomato wastes was analyzed by the RSM-COM approach. In this way an accurate procedure for the determination of the best operating conditions in terms of final costs of production is available in contrast to conventional approaches. The variables under analysis were pressure, temperature and spent CO_2 (or, equivalently, extraction time).

Through a statistical screening of effects, both pressure and temperature were confirmed as the chief sources of influence upon COM, which agrees with the estimated trend of the lycopene solubility in SC-CO_2. Increasing these variables cheapens the process, being the influence linear on *T* but linear plus quadratic on *P*. Spent CO_2 (and thus extraction time) is also significant, imparting a parabolic effect on COM and a crossed interlink with pressure.

The experimental COM values ranged from 1.8 to 6.6 k€ per kilogram of lycopene produced, and the best operating conditions were 500 bar/90 °C/25 $kg_{CO_2} kg^{-1}_{sample}$. Among the (P, T, w_{CO_2}) conditions that provide costs of manufacturing close to the best COM, very distinct annual production values were achieved: they varied up to 249 % against 10 % of COM variation. This fact should be taken into account for a final establishment of the SFE operation.

The screening of the best supercritical solvent (ethane *versus* carbon dioxide) was also studied at 300 bar and 60 °C. With SC-ethane higher extraction rates were observed, giving rise to shorter extraction cycles and thus greater annual productivity and lower COM. Nonetheless, under these (P, T) conditions the carbon dioxide is far from its best performance as solvent.

SFE of gac fruit – The optimization of a gac oil production process combining a drying pretreatment line and a SFE unit was performed using the RSM-COM approach. This method provided an accurate way of determining the best pressure (P), temperature (T), and extraction time (t) for the minimization of the cost of manufacturing (COM) regarding gac oil and also carotenes production.

The statistical screening of relevant factors showed that the linear increase of P plays the biggest role in the decrease of $\mathrm{COM_{oil}}$, followed by a quadratic effect imposed by t, which gives rise to a minimum $\mathrm{COM_{oil}}$ region. The crossed effect of extraction time and pressure comprise the third most influent contribution.

With regard to the optimization of the SFE of gac oil, the minimum $\mathrm{COM_{oil}}$ is attained at 400 bar, 60 °C and 1 h, amounting 8 $€\,\mathrm{kg_{oil}^{-1}}$. This value shows that the combined drying and SFE units are not only technically but also economically feasible in terms of market, since gac oil is currently traded at 30-50 $€\,\mathrm{kg_{oil}^{-1}}$ (in low amount orders).

The assessment of production cost of carotenes extraction from gac aryl pointed to $\mathrm{COM_{carotenes}}$ from 755 to 10900 $€\,\mathrm{kg_{carotenes}^{-1}}$, for the operating conditions of 400 bar/50 °C /1.0 h and 200 bar/50 °C/0.5 h, respectively. The lowest value of $\mathrm{COM_{carotenes}}$ is also bearable from a market perspective, as pure carotenes are traded between 10^4 and $10^5 €\,\mathrm{kg^{-1}}$ and the best results reported allow an economic margin to devise final purification.

The sensitivity analysis of specific flow rate ($Q_{\mathrm{CO_2}}/W_{\mathrm{biomass}}$) on the production cost of gac oil showed that at optimum extraction time ($t = 1$ h) the best $Q_{\mathrm{CO_2}}/W_{\mathrm{biomass}}$ is $70\,\mathrm{kg_{CO_2}\,h^{-1}\,kg_{biomass}^{-1}}$. The study revealed also that film diffusion limitations are significant at lower specific flow rate.

In the whole, the outcomes of this study fully support the exploitation of gac oil (and naturally occurring carotenes) from gac aryl through a green process like supercritical fluid extraction.

8.5 REFERENCES

[1] M.M.R. de Melo, A.J.D. Silvestre, C.M. Silva, Supercritical fluid extraction of vegetable matrices: Applications, trends and future perspectives of a convincing green technology, Journal of Supercritical Fluids, 92 (2014) 115-176.

[2] P.F. Martins, M.M.R. de Melo, C.M. Silva, Techno-economic optimization of the subcritical fluid extraction of oil from Moringa oleifera seeds and subsequent production of a purified sterols fraction, The Journal of Supercritical Fluids, 107 (2016) 682-689.

[3] M.M.R. de Melo, H.M.A. Barbosa, C.P. Passos, C.M. Silva, Supercritical fluid extraction of spent coffee grounds: Measurement of extraction curves, oil characterization and economic analysis, Journal of Supercritical Fluids, 86 (2014) 150-159.

[4] A.F. Silva, M.M.R. de Melo, C.M. Silva, Supercritical solvent selection (CO_2 *versus* ethane) and optimization of operating conditions of the extraction of lycopene from tomato residues: Innovative analysis of extraction curves by a response surface methodology and cost of manufacturing hybrid approach, The Journal of Supercritical Fluids, 95 (2014) 618-627.

[5] P.F. Martins, M.M.R. de Melo, C.M. Silva, Gac oil and carotenes production using supercritical CO_2: Sensitivity analysis and process optimization through a RSM–COM hybrid approach, The Journal of Supercritical Fluids, 100 (2015) 97-104.

[6] E.J. Beckman, Supercritical and near-critical CO_2 in green chemical synthesis and processing, The Journal of Supercritical Fluids, 28 (2004) 121-191.

[7] G. Brunner, Applications of Supercritical Fluids, in: J.M. Prausnitz, M.F. Doherty, R.A. Segalman (Eds.) Annual Review of Chemical and Biomolecular Engineering, Vol 1, 2010, pp. 321-342.

[8] H.M.A. Barbosa, M.M.R. de Melo, M.A. Coimbra, C.P. Passos, C.M. Silva, Optimization of the supercritical fluid coextraction of oil and diterpenes from spent coffee grounds using experimental design and response surface methodology, Journal of Supercritical Fluids, 85 (2014) 165-172.

[9] M.M.R. de Melo, E.L.G. Oliveira, A.J.D. Silvestre, C.M. Silva, Supercritical fluid extraction of triterpenic acids from *Eucalyptus globulus* bark, Journal of Supercritical Fluids, 70 (2012) 137-145.

[10] R.M.A. Domingues, M.M.R. de Melo, C.P. Neto, A.J.D. Silvestre, C.M. Silva, Measurement and modeling of supercritical fluid extraction curves of *Eucalyptus globulus* bark: Influence of the operating conditions upon yields and extract composition, Journal of Supercritical Fluids, 72 (2012) 176-185.

[11] R.M.A. Domingues, M.M.R. de Melo, E.L.G. Oliveira, C.P. Neto, A.J.D. Silvestre, C.M. Silva, Optimization of the supercritical fluid extraction of triterpenic acids from *Eucalyptus globulus* bark using experimental design, Journal of Supercritical Fluids, 74 (2013) 105-114.

[12] R.M.A. Domingues, E.L.G. Oliveira, C.S.R. Freire, R.M. Couto, P.C. Simões, C.P. Neto, A.J.D. Silvestre, C.M. Silva, Supercritical fluid extraction of *Eucalyptus globulus* bark – a promising approach for triterpenoids production, International Journal of Molecular Sciences, *13(6),* (2012) *7648-7662*.

[13] Essential Oils Direct, http://www.essentialoilsdirect.co.uk/, Accessed in March 2014.

[14] New Directions Aromatics, http://www.newdirectionsaromatics.ca, Accessed in December 2013.

[15] P.F. Leal, N.B. Maia, Q.A.C. Carmello, R.R. Catharino, M.N. Eberlin, M.A.A. Meireles, Sweet basil (*Ocimum basilicum*) extracts obtained by supercritical fluid extraction (SFE): Global yields, chemical composition, antioxidant activity, and estimation of the cost of manufacturing, Food and Bioprocess Technology, 1 (2007) 326.

[16] Sigma-Aldrich, http://www.sigmaaldrich.com/, Accessed in March 2014.

[17] J.M. Prado, I. Dalmolin, N.D.D. Carareto, R.C. Basso, A.J.A. Meirelles, J.V. Oliveira, E.A.C. Batista, M.A.A. Meireles, Supercritical fluid extraction of grape seed: Process scale-up, extract chemical composition and economic evaluation, Journal of Food Engineering, 109 (2012) 249-257.

[18] C.G. Pereira, M.A.A. Meireles, Economic analysis of rosemary, fennel and anise essential oils obtained by supercritical fluid extraction, Flavour and Fragrance Journal, 22 (2007) 407-413.

[19] C.L.C. Albuquerque, M.A.A. Meireles, Defatting of annatto seeds using supercritical carbon dioxide as a pretreatment for the production of bixin: Experimental, modeling and economic evaluation of the process, Journal of Supercritical Fluids, 66 (2012) 86-95.

[20] D.T. Santos, P.C. Veggi, M.A.A. Meireles, Optimization and economic evaluation of pressurized liquid extraction of phenolic compounds from jabuticaba skins, Journal of Food Engineering, 108 (2012) 444-452.

[21] C.G. Pereira, M.A.A. Meireles, Supercritical fluid extraction of bioactive compounds: Fundamentals, applications and economic perspectives, Food and Bioprocess Technology, 3 (2010) 340-372.

[22] R. Turton, R.C. Bailie, W.B. Whiting, J.A. Shaeiwitz, Analysis, synthesis and design of chemical processes, 2 ed., Prentice Hall, Upper Saddle River, 2003.

[23] E. Lack, T. Gamse, R. Marr, Separation Operations and Equipment, in: A. Bertucco, G. Vetter (Eds.), Elsevier, Amsterdam, The Netherlands, 2001.

[24] M. Peters, T. K., Plant Design and Economic for Chemical Engineering, 5th ed., McGraw-Hill Book Company, London, 2003.

[25] M. Perrut, Supercritical fluid applications: Industrial developments and economic issues, Industrial & Engineering Chemistry Research, 39 (2000) 4531-4535.

[26] A.C. Aguiar, J.V. Visentainer, J. Martínez, Extraction from striped weakfish (*Cynoscion striatus*) wastes with pressurized CO_2: Global yield, composition, kinetics and cost estimation, The Journal of Supercritical Fluids, 71 (2012) 1-10.

[27] A.M. Farías-Campomanes, M.A. Rostagno, M.A.A. Meireles, Production of polyphenol extracts from grape bagasse using supercritical fluids: Yield, extract composition and economic evaluation, The Journal of Supercritical Fluids, 77 (2013) 70-78.

[28] N.C.M.C.S. Leitão, G.H.C. Prado, P.C. Veggi, M.A.A. Meireles, C.G. Pereira, *Anacardium occidentale* L. leaves extraction via SFE: Global yields, extraction kinetics, mathematical modeling and economic evaluation, The Journal of Supercritical Fluids, 78 (2013) 114-123.

[29] L. Fiori, Supercritical extraction of grape seed oil at industrial-scale: Plant and process design, modeling, economic feasibility, Chemical Engineering and Processing: Process Intensification, 49 (2010) 866-872.

[30] L. Danielski, C. Zetzl, H. Hense, G. Brunner, A process line for the production of raffinated rice oil from rice bran, Journal of Supercritical Fluids, 34 (2005) 133-141.

[31] H.K. Kiriamiti, E. Rascol, A. Marty, J.S. Condoret, Extraction rates of oil from high oleic sunflower seeds with supercritical carbon dioxide, Chemical Engineering and Processing: Process Intensification, 41 (2002) 711-718.

[32] S. Zhao, D. Zhang, An experimental investigation into the solubility of *Moringa oleifera* oil in supercritical carbon dioxide, Journal of Food Engineering, 138 (2014) 1-10.

[33] J. Chrastil, Solubility of solids and liquids in supercritical gases, Journal of Physical Chemistry, 86, (1982) 3016–3021.

[34] J.M. Del Valle, J.M. Aguilera, An improved equation for predicting the solubility of vegetable oils in supercritical carbon dioxide, Industrial & Engineering Chemistry Research, 27 (1988) 1551-1553.

[35] Y. Adachi, B.C.Y. Lu, Supercritical fluid extraction with carbon dioxide and ethylene, Fluid Phase Equilibria, 14 (1983) 147-156.

[36] K. Ruttarattanamongkol, S. Siebenhandl-Ehn, M. Schreiner, A.M. Petrasch, Pilot-scale supercritical carbon dioxide extraction, physico-chemical properties and profile characterization of Moringa oleifera seed oil in comparison with conventional extraction methods, Industrial Crops and Products, 58 (2014) 68-77.

[37] K. Ghafoor, J. Park, Y.-H. Choi, Optimization of supercritical fluid extraction of bioactive compounds from grape (*Vitis labrusca* B.) peel by using response surface methodology, Innovative Food Science & Emerging Technologies, 11 (2010) 485-490.

[38] Cambodia Tree Seed Project, Seed Testing Reports: Moringa oleifera, 2002.

[39] P. Fernandes, J.M.S. Cabral, Phytosterols: Applications and recovery methods, Bioresource Technology, 98 (2007) 2335-2350.

[40] J.T. Barder, S.P. Johnson, Adsorption separation of sterols from tall oil pitchwith carbon adsorbent, US 4849112 A, 1989.

[41] J.T. Barder, Purification of sterols with activated carbon as adsorbent andchlorobenzene as desorbent, US 4882065 A, 1989.

[42] P. Alastri, Method for the concentration and separation of sterols, US 6160143A, 2000.

[43] J.P. Clark, A.D. Jimmy, G.G. Wilson, Purification of sterols by distillation, US3879431 A, 1975.

[44] K. Sepassi, P.B. Myrdal, S.H. Yalkowsky, Estimating pure-component vapor pressures of complex organic molecules: Part II, Industrial & Engineering Chemistry Research, 45 (2006) 8744-8747.

[45] J. Marrero, R. Gani, Group-contribution based estimation of pure component properties, Fluid Phase Equilibria, 183 (2001) 183-208.

[46] J.R. Elliott, C.T. Lira, Introductory Chemical Engineering Thermodynamics, Prentice Hall, New York, 2012.

[47] D.-Y. Peng, D.B. Robinson, A New Two-Constant Equation of State, Industrial & Engineering Chemistry Fundamentals, 15 (1976) 59-64.

[48] N.D. Aromatics, Coffee Essential Oil, December 2013, Available from:http://www.newdirectionsaromatics.ca.

[49] L. Natural Sourcing, Roasted Coffee Oil, December 2013, Available from: http://www.fromnaturewithlove.com/product.asp?product id=OILCOFFEEROASTED.

[50] C.P. Passos, M.A. Coimbra, Microwave superheated water extraction of polysaccharides from spent coffee grounds, Carbohydrate Polymers, 94 (2013) 626-633.

[51] Home-Barista.com, 14 December. Available from: http://www.home-barista.com.

[52] P.T.V. Rosa, M.A.A. Meireles, Rapid estimation of the manufacturing cost of extracts obtained by supercritical fluid extraction, Journal of Food Engineering, 67 (2005) 235-240.

[53] K.L. Mulholland, J.A. Dyer, Solvent selection in: Pollution Prevention, American Institute of Chemical Engineers,, New York, 1999, pp. 151-152.

[54] B.P. Nobre, A.F. Palavra, F.L.P. Pessoa, R.L. Mendes, Supercritical CO_2 extraction of trans-lycopene from Portuguese tomato industrial waste, Food Chemistry, 116 (2009) 680-685.

[55] Natex, Extraction Plants, Accessed in 2014, www.natex.at, in.

[56] M.M.R. de Melo, R.M.A. Domingues, M. Sova, E. Lack, H. Seidlitz, F. Lang Jr, A.J.D. Silvestre, C.M. Silva, Scale-up studies of the supercritical fluid extraction of triterpenic acids from Eucalyptus globulus bark, The Journal of Supercritical Fluids, 95 (2014) 44-50.

[57] S. Stavroulias, C. Panayiotou, Determination of optimum conditions for the extraction of squalene from olive pomace with supercritical CO_2, Chemical and Biochemical Engineering Quarterly, 19 (2005) 373-381.

[58] A. de Lucas, J. Rincón, I. Gracia, Influence of operation variables on quality parameters of olive husk oil extracted with CO_2: Three-step sequential extraction, Journal of the American Oil Chemists' Society, 80 (2003) 181-188.

[59] J.M.A. Araujo, D. Sandi, Extraction of coffee diterpenes and coffee oil using supercritical carbon dioxide, Food Chemistry, 101 (2007) 1087-1094.

[60] L.T. Danh, R. Mammucari, P. Truong, N. Foster, Response surface method applied to supercritical carbon dioxide extraction of *Vetiveria zizanioides* essential oil, Chemical Engineering Journal, 155 (2009) 617-626.

[61] L.T. Danh, P. Truong, R. Mammucari, N. Foster, Extraction of vetiver essential oil by ethanol-modified supercritical carbon dioxide, Chemical Engineering Journal, 165 (2010) 26-34.

[62] J.M. del Valle, Extraction of natural compounds using supercritical CO_2: Going from the laboratory to the industrial application, Journal of Supercritical Fluids, 96 (2015) 180-199.

[63] S. Parks, M. Nguyen, D. Gale, C. Murray, Assessing the Potential for a Gac (*Cochinchin gourd*) Industry in Australia, in: Australian Government Publication No. 13/060, Australian Government Publication, 2013.

[64] Lala Essential Oil, Moringa Oil—Carrier Oils, 2015,.

[65] J.M. Douglas, Conceptual Design of Chemical Processes, McGraw-Hill, Singapore, 1988.

[66] U. Topal, M. Sasaki, M. Goto, K. Hayakawa, Extraction of lycopene from tomato skin with supercritical carbon dioxide: Effect of operating conditions and solubility analysis, Journal of Agricultural and Food Chemistry, 54 (2006) 5604-5610.

[67] B.P. Nobre, L. Gouveia, P.G.S. Matos, A.F. Cristino, A.F. Palavra, R.L. Mendes, Supercritical extraction of lycopene from tomato industrial wastes with ethane, Molecules, 17 (2012) 8397.

[68] ChemSpider, in, Royal Society of Chemistry, http://www.chemspider.com, Accessed in February 2012.

[69] A. Estrella, J.F. López-Ortiz, W. Cabri, C. Rodríguez-Otero, N. Fraile, A.J. Erbez, J.L. Espartero, I. Carmona-Cuenca, E. Chaves, A. Muñoz-Ruiz, Natural lycopene from *Blakeslea trispora*: all-trans lycopene thermochemical and structural properties, Thermochimica Acta, 417 (2004) 157-161.

[70] S. Varona, A. Braeuer, A. Leipertz, Á. Martín, M.J. Cocero, Lycopene solubility in mixtures of carbon dioxide and ethyl acetate, The Journal of Supercritical Fluids, 75 (2013) 6-10.

[71] M.H. Zuknik, N.A. Nik Norulaini, A.K. Mohd Omar, Supercritical carbon dioxide extraction of lycopene: A review, Journal of Food Engineering, 112 (2012) 253-262.

[72] C.P. Passos, R.M. Silva, F.A. Da Silva, M.A. Coimbra, C.M. Silva, Supercritical fluid extraction of grape seed (*Vitis vinifera* L.) oil. Effect of the operating conditions upon oil composition and antioxidant capacity, Chemical Engineering Journal, 160 (2010) 634-640.

[73] C.P. Passos, M.A. Coimbra, F.A. Da Silva, C.M. Silva, Modelling the supercritical fluid extraction of edible oils and analysis of the effect of enzymatic pre-treatments of seed upon model parameters, Chemical Engineering Research and Design, 89 (2011) 1118-1125.

[74] M.D.A. Saldana, R.S. Mohamed, P. Mazzafera, Extraction of cocoa butter from Brazilian cocoa beans using supercritical CO_2 and ethane, Fluid Phase Equilibria, 194 (2002) 885-894.

[75] A.A. de Azevedo, U. Kopcak, R. Mohamed, Extraction of fat from fermented Cupuaçu seeds with supercritical solvents, Journal of Supercritical Fluids, 27 (2003) 223-237.

[76] S. Raeissi, S. Diaz, S. Espinosa, C.J. Peters, E.A. Brignole, Ethane as an alternative solvent for supercritical extraction of orange peel oils, Journal of Supercritical Fluids, 45 (2008) 306-313.

[77] H.P. Tai, K.P.T. Kim, Supercritical carbon dioxide extraction of Gac oil, Journal of Supercritical Fluids, 95 (2014) 567-571.

[78] M.-H. Chuang, G. Brunner, Concentration of minor components in crude palm oil, The Journal of Supercritical Fluids, 37 (2006) 151-156.

[79] J.C. Giddings, M.N. Myers, L. McLaren, R.A. Keller, High pressure gas chromatography of nonvolatile species. Compressed gas is used to cause migration of intractable solutes, Science, 162 (1968) 67-73.

[80] L. McLaren, M.N. Myers, J.C. Giddings, Dense-gas chromatography of nonvolatile substances of high molecular weight, Science, 159 (1968) 197-199.

[81] C.P. Passos, R.M. Silva, F.A. Da Silva, M.A. Coimbra, C.M. Silva, Enhancement of the supercritical fluid extraction of grape seed oil by using enzymatically pre-treated seed, Journal of Supercritical Fluids, 48 (2009) 225-229.

[82] H. Sovová, Rate of the vegetable oil extraction with supercritical CO_2—I. Modelling of extraction curves, Chemical Engineering Science, 49 (1994) 409-414.

[83] H. Sovová, R.P. Stateva, Supercritical fluid extraction from vegetable materials, Reviews in Chemical Engineering, 27 (2011) 79-156.

[84] L. Fiori, V. Lavelli, K.S. Duba, P.S.C. Sri Harsha, H.B. Mohamed, G. Guella, Supercritical CO_2 extraction of oil from seeds of six grape cultivars: Modeling of mass transfer kinetics and evaluation of lipid profiles and tocol contents, The Journal of Supercritical Fluids, 94 (2014) 71-80.

[85] L. Fiori, D. Basso, P. Costa, Supercritical extraction kinetics of seed oil: A new model bridging the 'broken and intact cells' and the 'shrinking-core' models, Journal of Supercritical Fluids, 48 (2009) 131-138.

[86] Alibaba Group, December 2014, Available from http://www.alibaba.com/.

[87] Sigma-Aldrich, March 2014, Available from http://www.sigmaaldrich.com.

[88] C. Chang, Y. Shen, C.M. Chang, Y.C. Shen, Method for preparing purity beta-carotene nano powder from Dunaliella salina capable, in: TW201300157-A,2011.

[89] L. Wan, Y. Zhang, D. Yao, Method for purifying carotene in chenopodium album,in: CN103058905-A, 2012.

[90] Z. Tong, L. Fang, Method for purifying lycopene, in: CN2005198592, 2007.

9 CONCLUSION

From an academic point of view, research on SFE has evolved and diversified since the early works on 1970 and 1980 decades, when this technology appeared vigorously as a promising bet for the upcoming years. Up to now, despite all progress achieved, wide implementation SFE technology is still to emerge, though the massive contribute of many researchers along years towards its consolidation.

The significant progress on this field is better disclosed if the yearly expectations of Rizvi at al. [1] are revisited. They stressed in 1986 that SFE was suffering technical restrictions imposed by the lack of knowledge concerning the complexity of natural substrates, which could be overcome with the development of reliable predictive models. Thirteen years later Smith et al. [2] still presented SFE as an immature technology still lacking robustness, as operational problems were prone to arise as consequence of the results being too matrix dependent.

Based on this thesis, one can assure that last decades have seen great advances for which full characterization and quantification of supercritical extracts, assessment of kinetic and equilibrium aspects, phenomenological modeling and optimization of operating conditions using statistical tools like DOE and RSM are elucidating examples. An important weakness is still found regarding fundamental research on the SFE of natural biomass so that the solutes-matrix interactions can be better understood and correctly taken into account by reliable predictive models.

Despite many SFE works lead to no further contribution than extracts production and their subsequent characterization, this dissertation emphasizes that SFE field has been fed with intermediate research (e.g., optimization of operating conditions or modeling) and by scale-up and economic studies that place investigation very close to industrial partners.

Apart from the specific insights disclosed in the previous chapters, the experimental and modeling work performed in this thesis led to the following conclusions:

- Eucalypt (*Eucalyptus globulus*) bark: whether pure or modified with ethanol, SC-CO_2 was able to remove triterpenic acids, and the measurement and modeling of extraction curves under optimum conditions (200 bar, 40 ºC and 2.5-5.0 wt.% of ethanol) pointed the ratio between solvent flow rate and biomass weight as the appropriate scale-up criterion of the process. With this criterion, a successful experimental scale-up was achieved at three scales: 0.5, 5.0, and 80 L.
- Turkish oak (*Quercus cerris*) cork: bulk extracts containing ca. 35 wt.% of friedeline were successfully produced by SFE and the extraction curves were modeled. The selectivity

to friedeline can reach up to 2.5 through a correct selection of particle size, cosolvent (ethanol) amounts and extraction time.

- Water hyacinth (*Eichhornia crassipes*) leaves and stalks: stigmasterol enriched extracts were obtained for shorter times (<1 h). The optimized conditions for total extraction yield were 250–300 bar and 5.0 wt.% ethanol, while for sterols were 300 bar and 2.5 wt.%.
- Tomato (*Solanum lycopersicum*) wastes: both carbon dioxide and ethane can be used as supercritical solvents to produce an essential oil that is rich in lycopene. The viability of the SFE was demonstrated, but while ethane led to greater productivity, further research is needed to define which one is preferable on a global basis.
- Gac (*Momordica. cochinchinensis*) fruit: it may be a promising and economically viable source of carotenes when produced by SFE at 400 bar, 70-90 $kg_{CO_2} kg_{biomass}^{-1} h^{-1}$, during 0.5-1.0 h.
- Moringa (*Moringa oleifera*) seeds: a techno-economic analysis unveiled that a well designed integrated process combining SFE and vacuum distillation allows the simultaneous production of an essential oil and a sterols enriched extract with 89.4 % concentration.
- Spent coffee (*Coffea* spp.) grounds: the oil produced by SFE is up to 4.1 times richer in diterpenes than *n*-hexane extracts, and a highly profitable process may be expected at commercial level.

To conclude, the extensive compilation and critical systematization of works provided by this thesis document the substantial advances that SFE field has been achieving as a result of intense, progressive and multidisciplinary research. Since 2000 the field has burst in terms of new biomass species, investigation of extracts enrichment and molecules isolation, and in the required tools and background knowledge necessary to reach a final degree where the feasibility of SFE implementation is expected. Through research, SFE has reached new industrial sectors into which there used to be weak ties. It is the case of pulp and paper industry and the recent election of supercritical CO_2 as a breakthrough technology for the 2050 world, attributed by the Confederation of European Paper Industries (CEPI) [3].

REFERENCES

[1] S.S.H. Rizvi, J.A. Daniels, A.L. Benado, J.A. Zollweg, Supercritical fluid extraction - Operating principles and food applications, Food Technology, 40 (1986) 57-64.
[2] R.M. Smith, Supercritical fluids in separation science - the dreams, the reality and the future, Journal of Chromatography A, 856 (1999) 83-115.
[3] CEPI, Unfold the Future - The Two Team Project, Confederation of European Paper Industries Brussels, 2013.

10 FUTURE WORK

The cumulative knowledge achieved in the SFE field has provided substantial progress on analytical, engineering, scale-up and economic issues regarding implementation of SFE processes at industrial level. Nevertheless, as Brunner [1] noted, much of the SFE research is not structured in a way that allows the design of a pathway from feedstock to products. In this sense, improvements are expected in upcoming years in order to enhance the quality of the research in the field on a cradle-to-gate perspective.

An important weakness is still found regarding fundamental research on the SFE of natural biomass so that the solutes-matrix interactions can be better understood and modeled. From a comprehensive observation, thermodynamic/equilibrium is still a field where further research is recommended, namely on the fundamental modeling of solutes in SC-CO_2, modified or not with cosolvents. While this observation embodies an effective opportunity for further consolidation of SFE research, scale-up is perhaps the second area where there is a substantial margin for deeper experimental work. Many authors limit the scale-up to slight volume or capacity jumps, placing their studies closer to lab scale than to a real commercial scale. As long as research comprises lab and real pilot units, together with reliable modeling and scale-up criteria, the uncertainty associated with natural biomass may be left behind, and the supercritical technology may reach an effective consolidation for industry. In addition, the combination of more comprehensive scale-up works with economic assessment studies would foster a clearer perception of the techno-economic appeal of SFE.

Beyond the aforementioned items, that can attenuate current sources of uncertainty for the SFE processes themselves, the knowledge of extracts price is frequently a source of uncertainty that can hinder their correct economic assessments. Taking into account the novelty of some active principles or their relatively niche dimension market, the establishment of a price for an extract can be so influential that a whole SFE process viability can be strongly penalized or unrealistically overestimated *per se*, independently of other aspects. Given that SFE many times allows the enhancement of target species concentration in extracts, SFE selectivity advantages for the quality of a final extract can only be fully disclosed upon a proper estimation of its market price for different compositions. As long as extract prices for distinct solutes concentration are known, the economic evaluation of SFE matched with purification techniques can be rigorously accomplished. In the whole, this argument highlights combined and hybrid processes embodying SFE to provide extracts with higher quality (higher market values).

Despite many SFE works lead to no further contribution than extracts production and their subsequent characterization, this thesis emphasizes that SFE field has been fed with intermediate research (e.g., optimization of operating conditions or modeling) and by scale-up and economic studies that place investigation very close to industrial partners. From industry side, there is still some hesitancy on a widespread implementation of supercritical technology both to new raw materials and well known ones, despite the number of patents filled every year in this area. In this respect, Machado et al. [2] published some data concerning patents from 1974 to 2012, where a substantial raise is observed since 2000, being the maximum in 2012, with 61 documents deposited. Some of these documents cover specific classes of bioactive compounds, such as the triterpernoids, including ursolic, oleanolic and betulinic acids [3]. Finally, food and agricultural sector represents one third of the SFE patent applications [2], which can be taken as a sign of the strong interlink between the biomass valorization opportunities and the biorefinery concept, which can be implemented in the neighbourdhood of bigger and already established processes.

REFERENCES

[1] G. Brunner, Applications of Supercritical Fluids, in: J.M. Prausnitz, M.F. Doherty, R.A. Segalman (Eds.) Annual Review of Chemical and Biomolecular Engineering, Vol 1, 2010, pp. 321-342.

[2] B.A.S. Machado, C.G. Pereira, S.B. Nunes, F.F. Padilha, M.A. Umsza-Guez, Supercritical fluid extraction using CO_2: Main applications and future perspectives, Separation Science and Technology, 48 (2013) 2741-2760.

[3] M.M.R. de Melo, R.M.A. Domingues, A.J.D. Silvestre, C.M. Silva, Extraction and purification of triterpenoids using supercritical fluids: From lab to exploitation, Mini-Reviews in Organic Chemistry, 11 (2014) 362-381.